STRESS-STRAIN BEHAVIOUR OF GRANULAR SOILS UNDER MONOTONIC AND CYCLIC LOADING CONDITIONS

by

Seid Majdeddin Mir Mohammad Hosseini

B.Sc., M.Sc.

A thesis submitted in fulfilment of the requirements for the degree of Doctor of Philosophy

Department of Civil Engineering

The University of Leeds

June 1987


بسم الله الرحمن الرحيم

In the Name of God the Compassionate, the Merciful

ACKNOWLEDGEMENTS

The author wishes to extend his appreciation to all those who contributed in any way towards the completion of this dissertation.

He wishes to express his appreciation and gratitude to Dr. R.D. Mackey and Dr. T.W. Cousens under whose supervision , guidance and encouragement this work was carried out.

The author wishes to acknowledge the technicians of the civil engineering department for their assistance and technical support in setting up and developing the testing equipment used in this research.

I also wish to thank the Ministry of Culture and Higher Education of the Islamic Republic of Iran under whose encouragement and financial support this work was carried out.

Finally I would like to express my appreciation to my family and my parent for their patience and continuous encouragement.

ABSTRACT

The stress-strain behaviour of granular soils under monotonic and cyclic loading conditions and small lateral strains was studied in this work. A simple cubic triaxial apparatus (SCTA), originally developed at Leeds University for monotonic stress-strain studies of sand under controlled and small lateral strains, was used in this investigation. The three principal stresses and strains can be independently controlled and measured in this apparatus. The SCTA was modified and further developed to allow cyclic stress-strain studies of granular soils to be Performed.

To increase the stress-strain data available on granular soils similar tests to those previously carried out on the medium sand , were performed on fine and coarse sands under monotonic loading conditions. The samples tested were cubic of 150 mm side length and prepared with ranges of initial porosities in a dry condition.

To study the cyclic stress-strain behaviour of sand at small strains, a series of new tests on similar cubic samples of the medium sand were performed under cyclic loading conditions. Cyclic loads with different frequencies , amplitudes and number of cycles were applied and the samples were prepared dry at the loosest and densest conditions.

Values of the coefficients of active pressure , earth pressure at rest , constrained secant modulus, Young's modulus and Poisson's ratio for the fine , medium and coarse sandswere obtained and compared for different conditions. The relationships between vertical and lateral stresses are found and the volume change behaviour of sands in different conditions are studied. Finally some comparisons are made between the results obtained from monotonic and cyclic loading conditions.

CONTENTS

NOTATION

a, a2, a3, A	Constant parameters
b, b2, b3, B	Constant parameters
c, C	Constant parameters
Cc	Compression index
d	Dimension of the cubic sample
d_{10}	Particle diameter of which 10% of the soil is finer
D	Constrained secant modulus
Dr	Relative density
e	Void ratio
E, Et	Young's modulus
f1, f2	Constant parameters
g	Constant parameter
k, k1, k2	Constant parameters
K	Ratio of lateral stress to vertical stress
Ko	Coefficient of earth pressure at rest
Ka (Kap, Kat)	Coefficient of active earth pressure (from plane strain tests, from triaxial tests)
Kr	Rankine ratio=$\tan^2(45+\varphi/2)$
m	Constant parameter
M	Initial tangent modulus
n	porosity
n_i	initial porosity
n_{cv}	Critical porosity (at constant volume of the sample)
n_o	Porosity of sample due to compression in Ko condition
n_p	Porosity after the sample is strained in the plane strain test
n_t	Porosity after the sample is strained in the triaxial test
Pa	atmospheric pressure (1 kg/cm^2)
r1, r2, r3	Ratios of maximum principal stress to the stress levels at which unloading commences
V	Total volume of the sample
ΔV, dV	Change in the volume
$\Delta V/V$	Volumetric strain
$(\Delta V/V)o$	Volumetric strain of the sample due to compression in Ko condition
$(\Delta V/V)p$	Volumetric strain due to straining the sample in the plane strain condition
$(\Delta V/V)t$	Volumetric strain due to straining the sample in the triaxial condition
Δ, δ	Change, e.g. $\Delta\sigma$
γx, γy, γz	shear strain in the x, y and z directions
ε	Normal strain
$\varepsilon_1, \varepsilon_2, \varepsilon_3$	Principal normal strains
εv	Vertical strain
εve	Elastic part of the vertical strain
εvp	plastic part of the vertical strain
$\varepsilon vmax.$, $\varepsilon vmin.$	Maximum and minimum values of the vertical strain over a cycle of load
εh	Lateral strain in triaxial tests
$\varepsilon h1$, $\varepsilon h2$	Lateral strains in each lateral direction

	for a cubic sample
ε_{vp}, ε_{1p}	Vertical strain due to straining the sample in plane strain test (cyclic, monotonic tests)
ε_{vt}, ε_{1t}	Vertical strain due to straining the sample in triaxial test (cyclic, monotonic tests)
ν	Poisson's ratio
σ, $(\overline{\sigma})$	Normal stress (effective)
σ_x, σ_y, σ_z	Normal stresses in the x, y, z directions
σ_1, σ_2, σ_3	Principal stresses
σ_{3p}	Minor principal stress in plane strain tests
σ_h	Average of the lateral stresses
σ_{ho}	Average of the lateral stresses in Ko conditions
σ_{ht}	Average of the lateral stresses in triaxial tests
σ_v	Vertical stress in cyclic tests
$\sigma_{vmax.}$, $\sigma_{vmin.}$	Maximum and minimum values of σ_v in a cycle of load
σ_{h1}, σ_{h2}	Lateral stresses on the sides of a cubic sample in cyclic tests
$\sigma_{h1max.}$, $\sigma_{h1min.}$	Maximum and minimum values of σ_{h1} over a load cycle
$\sigma_{h2max.}$, $\sigma_{h2min.}$	Maximum and minimum values of σ_{h2} over a load cycle
$\sigma_{homax.}$, $\sigma_{homin.}$	Maximum and minimum values of σ_{ho} over a load cycle
σ_{hp}	Lateral stress in the direction of straining of the sample in cyclic plane strain tests
τ	Shear stress on a given plane
τ_x, τ_y, τ_z	Shear stresses on the x, y, z planes
φ	Angle of internal friction
φ_{cv}, φ_u	Peak, residual angles of internal friction
φ_f	Semi-empirical value of φ between φ_u and φ_{cv}

CHAPTER ONE

INTRODUCTION AND LITERATURE REVIEW

1.1 INTRODUCTION

To solve many problems in soil engineering it is usually necessary to predict the amount of deformation resulting from the application of a specific load to ensure that ground movements are acceptable. For this reason an understanding of the stress-strain relationship of soils is vital. However, due to the particulate and multiphase nature of the soil, the response of a soil to a change in load is highly complex. From a practical point of view, it is desirable to adopt comparatively simple laboratory tests to measure the properties needed for analysis. Difficulties arise because the stress-strain behaviour of a soil is strongly influenced by many parameters such as confining pressure and stress path. The stress- strain behaviour of soils also depends on a number of other factors including such things as type of soil, voids ratio, water content, soil fabric, drainage conditions, stress history and duration of loading.

Although for convenience standard approaches using elasticity theory assume the modulus of elasticity and Poisson's ratio of a soil to be constant, soils are not perfectly elastic and display non-linear elastic-plastic behaviour. Simple elastic approaches are in many instances

unrealistic as the plastic properties of the soil are ignored. Increasing attention has been focussed on obtaining more satisfactory formulations of stress-strain relationships for both cohesive and non-cohesive soils that incorporate such things as inelasticity, strain hardening and stress dependency. The behaviour of soil is more complicated if, after the initial loading, unloading and subsequent reloading occurs. One illustration of this is the progressive settlement of granular soils under successive loading-unloading-reloading cycles due to the plastic strain component. The other component is elastic deformation which is recoverable in each cycle [1]. Nevertheless, the precise relationship between these two types of deformation, whether the progressive component levels off after a number of load cycles ,the influence of the initial conditions of the sand sample on its response and the effect of the stress or strain path on the behaviour of the sand are among the problems that still require clarification. This ideally would be done by carrying out a series of accurate and comprehensive investigations under controlled conditions.

The two main types of soils ,cohesive (clays) and non-cohesive (granular including sands), both display the type of behaviour described above. However, the work in this dissertation is limited to the study of granular soils. As a full and extensive review of experimental stress-strain studies and test apparatus has been carried out recently by El-Gammel[22] at Leeds University, only a brief summary of experimental and theoretical studies of both static and cyclic loading conditions of granular soils directly rele-

vant to this investigation is given below.

1.2 REVIEW OF EXPERIMENTAL WORK

1.2.1 MONOTONIC LOADING

In the earliest experimental stress-strain studies of granular soils the intention was usually to investigate the applicability of elasticity theory. This theory describes the stress-strain behaviour of perfect elastic materials which obey Hookes'law. Timoshenko [4] defines elasticity as "the property by which a body returns to its original shape after removal of the load". The properties of a perfect elastic material are independent of the orientation of the principal axes and only two constants (E, the modulus of elasticity and ν, Poisson's ratio) are required to express the stress- strain relationships:

$$\varepsilon_x = \frac{\sigma x}{E} - \frac{\nu}{E}(\sigma_y + \sigma_z) \qquad (1.1)$$

$$\gamma_{xy} = \frac{(1+\nu)}{E}\tau_{xy} \qquad (1.2)$$

The suggestion that the theory of elasticity seemed to be applicable to the behaviour of a loose cohesionless granular medium was first put forward by Boussinesq [37]. Boussinesq in his studies of stress distribution used Hookes' law and considered sand as an ideal elastic ,isotropic,homogenous and semi-infinite material. Since sand is a very complex material these and other similar

solutions, because of their simplicity, could not represent the real behaviour of the material.

Fopl[15] carried out some classic laboratory tests and measured the surface deformations of a sand mass at different points around a circular loaded area. He found that the results were not consistent with those Boussinesq [54] obtained for the case of an elastic semi -infinite material. Since then many experiments have been performed in order to study the stress distributions in sand. It has been found that the increase in stress in a soil mass due to a surface load increment is not so spread out as is the case within an elastic material and usually it is remarkably concentrated around the vertical loading axis.

Griffith [3] and Frohlich [53] in their expression for the stress distribution in sand suggested a new experimental factor which could give a better explanation of the behaviour of the sand. It was suggested that when the value of the factor is 3 the material would act as an elastic-solid, homogeneous and semi-infinite. If it equals 4, the sand will behave as a solid semi-infinite material in which the modulus of elasticity increases in direct proportion to the depth. Wilson and Sutton [5], in order to obtain a better understanding of stress distributions within a sand mass, decided to insert some measurement devices in the sand. They performed a series of standard triaxial tests in which $\sigma_2 = \sigma_3$. The results were compared with those obtained assuming perfect elastic behaviour. Assuming that the sand consists of elastic spherical particles in as loose a packing as possible, they proposed:

$$\varepsilon = C\sigma^{(2/3)} \qquad (1.3)$$

Where C is an experimental constant.

Jakobson [6] in his experimental studies of the stress-strain behaviour of sand accepted the assumption of Wilson and Sutton, but assumed the spheres were not perfectly elastic. As a result the stress-strain equation becomes:

$$\varepsilon = C\sigma^{(a)} \qquad (1.4)$$

Where C and a are both experimental constants. The above equation was in good agreement with the experimental data (figure 1.1) and the two constants were found to be:

$$\varepsilon = 0.608 \times 10^{-3}\sigma^{0.612} \quad (kg/cm^2) \qquad (1.5)$$

The values of C and a are not the same for all experiments but the differences are not great.

These experimental stress-strain studies of sand were followed by tests performed by Janbu [7]. Data were obtained from triaxial tests performed under constant principal stress ratios ($K=\sigma_3/\sigma_1$). Results suggested that the tangent modulus of the stress-strain curve ($M=d\sigma_1/d\varepsilon_1$) be used for relating the vertical strains to the vertical stresses. Consequently the following incremental expression for increasing vertical stress from $\overline{\sigma_1}$ to $\overline{\sigma_1'}$ was derived:

$$\varepsilon_1 = \left(\frac{1}{m \cdot a}\right)\left[\left(\bar{\sigma}_1' / P_a\right)^a - \left(\bar{\sigma}_1 / P_a\right)^a\right] \qquad (1.6)$$

Where: ε_1 = vertical strain

P_a = reference stress = 1 atmosphere = 1 Kg./cm^2

$\bar{\sigma}_1'$ = effective vertical stress = $\bar{\sigma}_1 + \Delta\bar{\sigma}_1$

m = modulus number

a = stress exponent

Pa has been employed to make the equation dimensionless. Janbu measured m and a for different sands experimentally. In 1965 Janbu [9] completed his studies of stress-strain relationships in a joint work with Hjeldness. This study indicated that m and a change with changing principal stress ratio . The variations of vertical strain and tangent modulus versus vertical stress under different conditions are replotted in figures 1.2 and 1.3.

These experimental equations concerning the stress-strain behaviour of granular soils did not cover all the factors affecting the response of sand e.g. intermediate stress and non-axisymmetric test conditions. Consequently more experimental studies on different aspects of the behaviour of sand were carried out by many researchers. El-Sohby in 1969 [14] assumed that the deformation of a mass of sand under a specific loading condition might be considered as made up of two separate components. The first is the elastic component which takes place due to the elastic deformation of the individual particles and depends upon the compressibility of the grains. The second is the sliding or plastic component which occurs because of the relative movements of

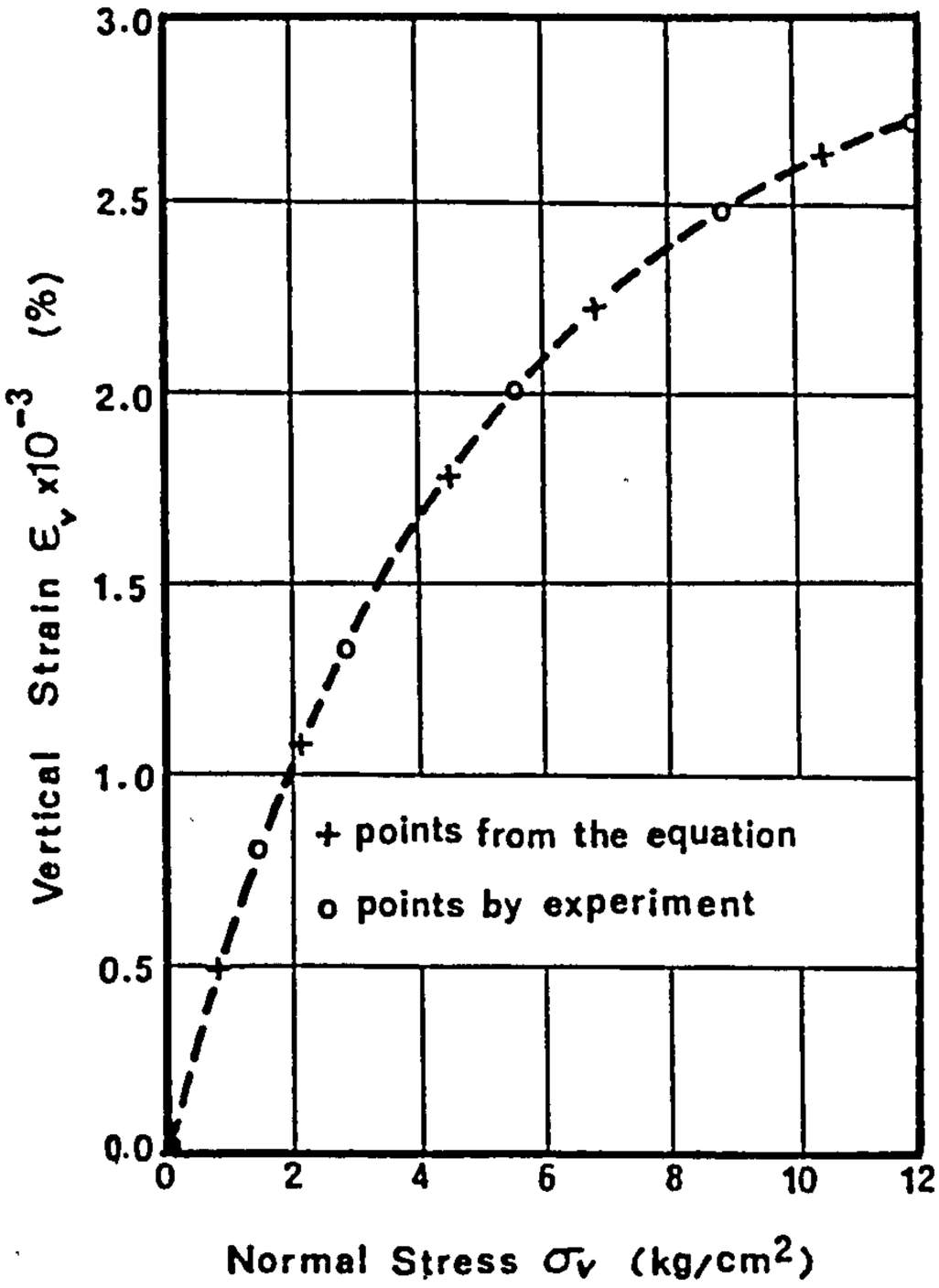

FIGURE1.1 The experimental and theoretical relationship between ε_v and σ_v
(El-Gammel 22, after Jakobson 6)

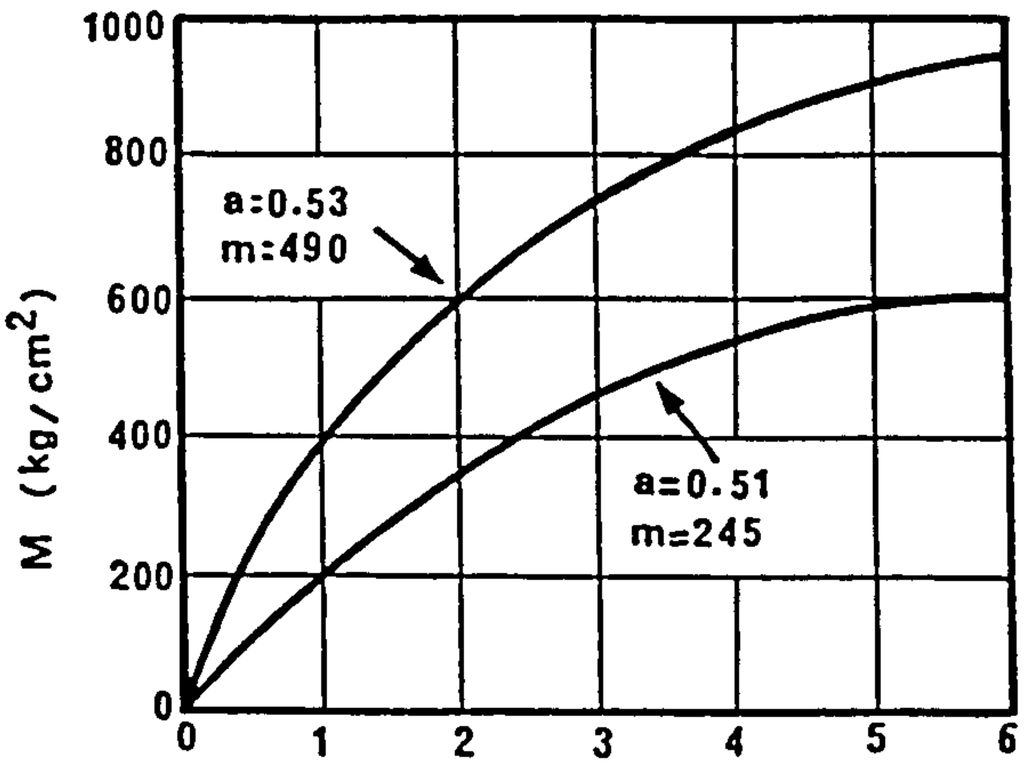

FIGURE1.2 Variation of the tangent modulus with the vertical stress.

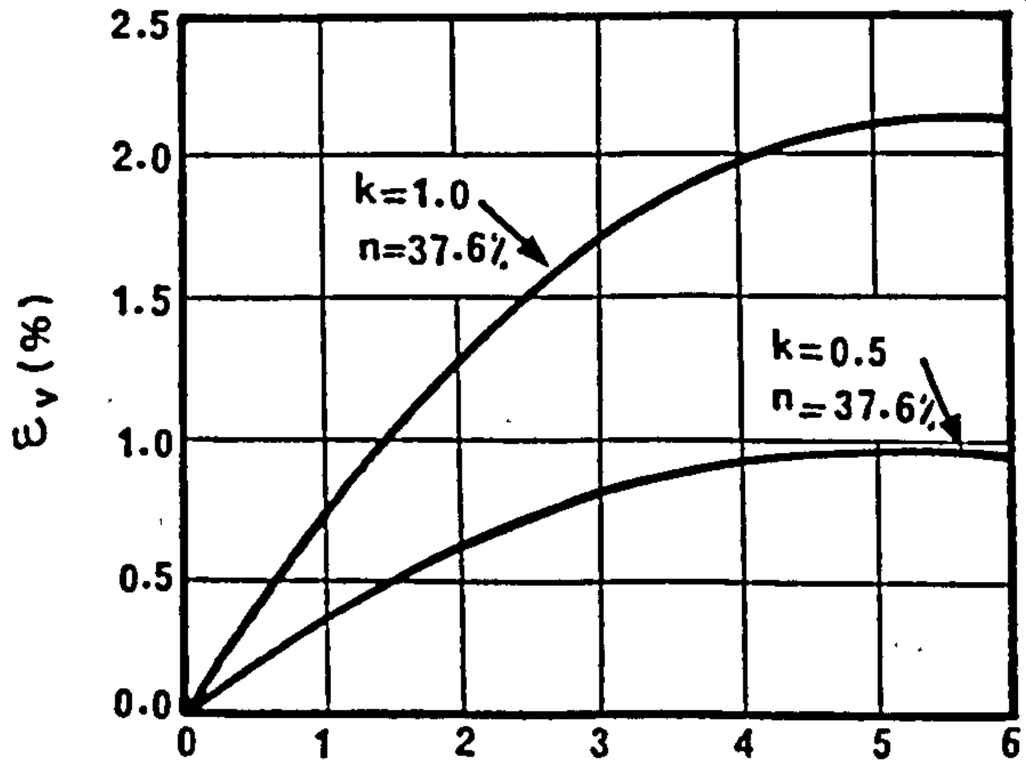

FIGURE1.3 Variation of the vertical strain with the vertical stress.

(El-Gammel 22, after Janbu and Hjeldnes 9)

the particles and is related to the shear forces developed within the mass. Therefore, while the first component of deformation may be approached by studying the elastic behaviour of the individual particles, the second component has to be studied in terms of the laws governing friction between solid bodies, which emphasises the importance of separating the two components. Nevertheless other researchers, e.g. Dantu [52], and Ko and Scott [55], found that the deformations of sand under all-round pressures are almost elastic, particularly if the samples are dense and subjected to a number of successive cycles of repeated loads. Ko and Scott [12] elsewhere in their experimental studies loaded a sample made by packing equal spheres. They calculated the deformation of each sphere due to the forces acting on the contact surface and compared these to the total deformation of the mass in order to examine the deformational behaviour of granular soils. However, it was concluded that the direct application of the behaviour of packings of equal spheres to explain the behaviour of granular materials was not possible. The results of some more realistic tests [56] showed that under certain conditions solutions based on linear elasticity might be helpful but that these were not accurate where the sand is anisotropic or if it behaves non-linearly. However Huang [57] noted that these solutions could be applicable for non-linear elastic materials if their moduli of elasticity were considered to vary with the applied stress.

In 1968 Holubec [13] proposed an incremental elastic solution which included a combination of non-linear and anisotropic properties of materials. He pointed out that the

study of the stress-strain behaviour of cohesionless soils has shown that they behave as elastic work-hardening plastic materials. This means that when a cohesionless soil is subjected to a load, both elastic and plastic deformations are probable. Thus any strain increment may be divided into elastic and plastic components and in this case both elastic and plastic theories are applicable. Yet the plastic behaviour of sand could not be explained completely by this incremental elastic solution. Coon and Evans [58] described the stress-strain behaviour of sand in a general incremental form. The inherent anisotropic property of sand due to the assumption of non-linearity could be included. In their studies they found that neither linear elastic nor ideal plastic models are adequate expressions for the behaviour of granular soils under general conditions.

A more comprehensive study of the stress-strain behaviour of sand was carried out by El-Gammel[22] in 1984. After a series of tests on cubic samples (150 mm size) of medium size Leighton Buzzard sand, under different conditions of initial porosity and confinement, he concluded that the variation of elastic and plastic deformations not only depends on the level of vertical stress, but on the porosity of the sample as well. He observed that as the porosity of the sand decreases, both the elastic and plastic strains decrease but the rate of the decrease of the plastic deformations is greater than that of elastic ones. El-Gammel during some true triaxial tests found that a sharp decrease in the lateral stresses take place due to application of small lateral deformations. In some cases this decrease was re-

ported as more than 40% at lateral strains of about 0.3%. The effect of the intermediate principal stress was studied and significant changes in the stress-strain behaviour of samples due to this factor were obtained. He found the lateral stress induced in the triaxial strain condition is about 30% greater than that in plane-strain condition under the same conditions of initial porosity and vertical stress.

Although many important factors affecting the stress-strain behaviour of sand were taken into account in this piece of research, there is no evidence as to whether particle size will have a major influence on the overall behaviour. Neither is it known whether the information obtained from the study on the medium sand can be used for other kinds of granular materials. One of the aims of the current investigation is to clarify these problems by conducting similar tests on cohesionless soils of other sizes.

1.2.2 CYCLIC LOADING

The majority of the experimental stress-strain studies carried out on granular soils to date have involved monotonic loading conditions. However the limitations of stress-strain analyses based on solely monotonic test data and the wide occurrence of cyclic loading in practice e.g. on offshore structures, reciprocating machine foundations, earthquake vibrations, transient vibration induced by atomic or nuclear explosions, and pile driving vibrations etc, has resulted in cyclic studies becoming increasingly important. Many researchers have concentrated their cyclic studies on

simulating critical field loading conditions and have tried to reproduce some specific phenomena like liquefaction of sand or other failure mechanisms, hysteresis damping etc, which usually involves a large amount of strain. However, without fundamental information on the stress-strain characteristics of sand and its inherent properties, especially when the range of allowed movements is small, as occurs in many field conditions, a reliable and clear interpretation and anticipation of sand behaviour under general cyclic loading conditions is not possible.

If sand behaves like an elastic material it should return to its initial shape on unloading [4]. Reloading the sample will cause precisely the same pattern of deformation as before and in this case successive loading-unloading-reloading cycles will give exactly the same results as each other. If the behaviour is not elastic, hysteresis loops will develop in the stress-strain plots and some irrecoverable strain will occur. This fact indicates how important the role of the cyclic test is when the inherent characteristics and stress-strain behaviour of a specimen are under investigation.

A large number of researchers dealing with the stress-strain behaviour of soils have found that after unloading sand samples the strains induced do not disappear completely and some irrecoverable deformations remain (El-Sohby [14], Holubec [13], Ko and Scott [12], Lade and Duncan [18], Pyke [1] , Drucker et al. [59], Shaw [44], Ting [45], El-Gammel [22]). The relationship between elastic and plastic deformations may be obtained by applying cycles of load

to the sample. In this case the trend of variations of these two components of deformation will also be obtained. Holubec [13], while confirming the elastic-plastic behaviour of sand , stated that during reloading the samples showed approximately linear elastic behaviour. Lade and Duncan [18] in their studies indicated that both elastic and plastic deformations occur from the beginning of the loading of cohesionless soils. The plastic strain is initially smaller than the elastic strain but as the vertical stress increases the plastic strains dominate. However, during the application of several load cycles to the sand sample the elastic and plastic deformations may be determined more clearly. Drucker, Gibson, and Henkel [60] in their studies on granular soils concluded that these materials behave as elastic-work hardening-plastic ones which become stiffer as the loading cycles continue. In a similar investigation carried out on coarse Ottawa sand by Poorshasb, Holubec, and Sherbourne [61] it was reported that the behaviour of this kind of sand is far from the idealised model which considers it to be an elastic work- hardening plastic material. This conclusion was also reached by Barden and Khayatt [62] in their studies on dense and loose samples of fine sand. Although it has been clearly observed from the general stress-strain behaviour of sand subjected to cycles of loads, that the elastic and plastic deformations occur in each cycle with a decreasing rate of plastic strain and constant values of elastic strain in different cycles [133] the elastic work- hardening plastic theory is not sufficiently advanced to cover the whole response of the sand in these conditions. Typical

stress-strain curves during several cycles of loading on Monterey coarse sand in an oedometer test carried out by Seaman et.al [133], are shown in figure 1.4. Seaman et.al also state that during the first 10 to 50 cycles, a small amount of permanent strain resulted from each cycle and finally a stable hysteresis loop was obtained, involving little or no additional permanent strain for each cycle of loading.

In some cases the lack of accurate and reliable experimental data governing all major factors influencing the stress-strain behaviour of sand has made it difficult to obtain comprehensive solutions. As a result experiments were carried out in this area. Burley et.al [19] showed that the behaviour of granular media subjected to first loading was found to be consistent with the equations which Daniel [63] had proposed after conducting true triaxial tests. These equations will be presented in the theoretical review (section 1.3). They concluded that at low values of strain the hysteresis loop due to unloading-reloading cycles might be considered comparatively small, and that at this stage the stress-strain behaviour of the sample could perhaps, as a first approximation, be represented by a straight line. However as cycling continues at higher strain levels the hysteresis loop becomes larger, presumably due to greater slip of the particles. Therefore it is not acceptable to approximate the whole unloading portion as linear because significant errors will be introduced. In 1978 Kii [20] continued the work carried out by Daniel and Burley et.al. He studied the stress-strain behaviour of sand in both cubic and rec-

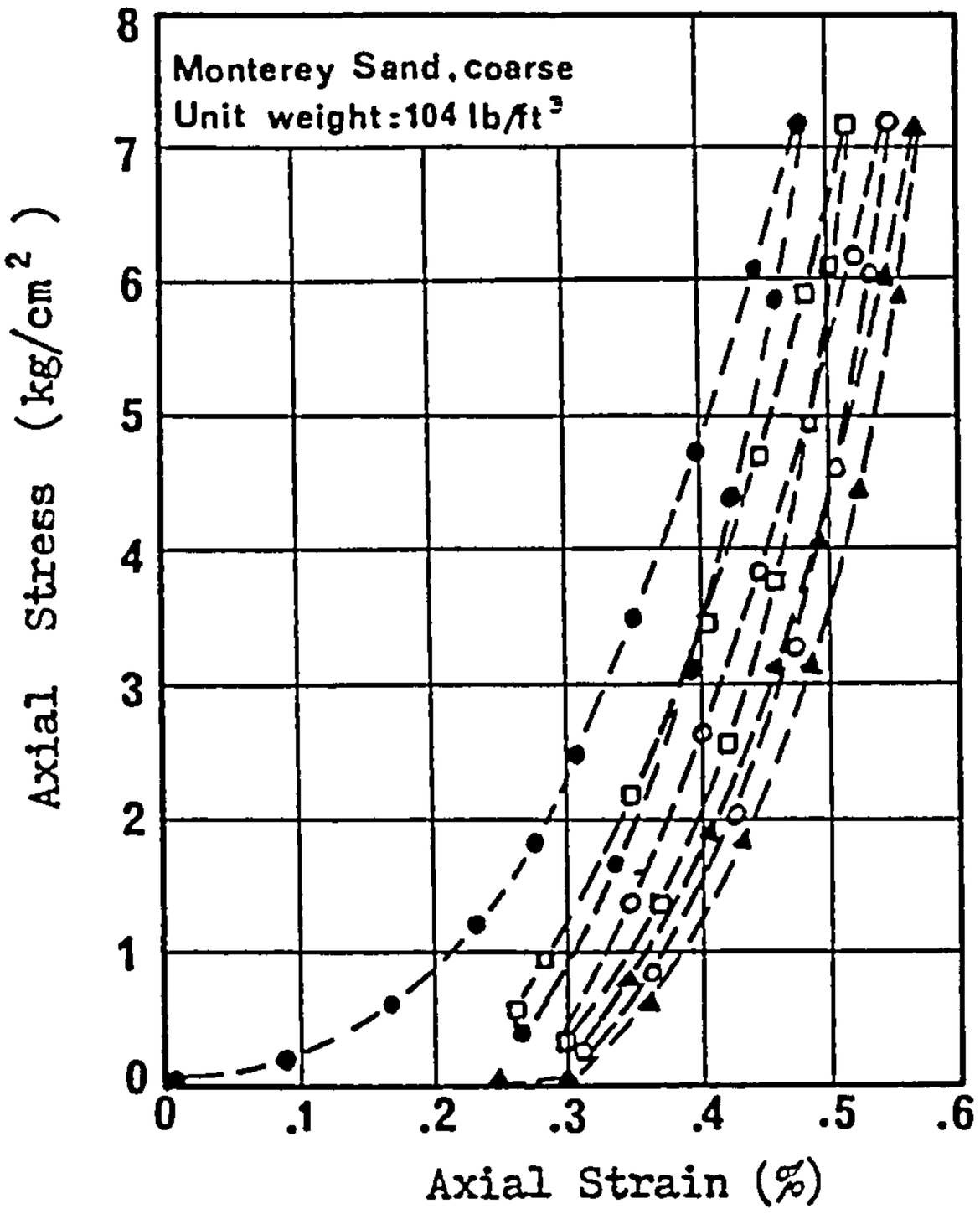

FIGURE 1.4 Stress-Strain curves during several cycles of loading in oedometer tests.

(Seaman et al., 1963)

tangular cells subjected to different and independent triaxial stresses. The specimens were tested under both incremental loads to failure and cyclic loads up to 5 cycles. He developed the stress-strain formula suggested by Daniel and further modified by Burley et.al (shown in section 1.3). The results of the experiments fitted his equation acceptably. Kii conducted a series of tests to study whether sand is an elastic work-hardening plastic material and attempted to obtain a comprehensive theory covering both elastic and plastic behaviour of sand. The results from cyclic loading showed large plastic deformations during unloading from levels of stress greater than 75% of the failure stress to lower levels of stress. This was then followed by linear elastic reloading until approximately 50% of the failure stress was reached, after which reloading becomes more plastic, finishing up at a slightly higher stress than the virgin loading curve. He also found that granular soils of medium density usually dilate on approaching failure. A typical stress-strain curve under independent triaxial stresses and cyclic loading (5 cycles) is shown in figure 1.5.

However the deformations induced in the sand samples under a few load cycles may not be the same as those induced when the number of load cycles increases. Shaw [44], during a series of repeated loading tests on granular soils, states that the materials exhibit two distinct types of deformation; the elastic which is recoverable and the permanent (plastic) which is the build up of irrecoverable strain over a number of load applications (figure 1.6). He also introduced the concept of a threshold value for the stress-path

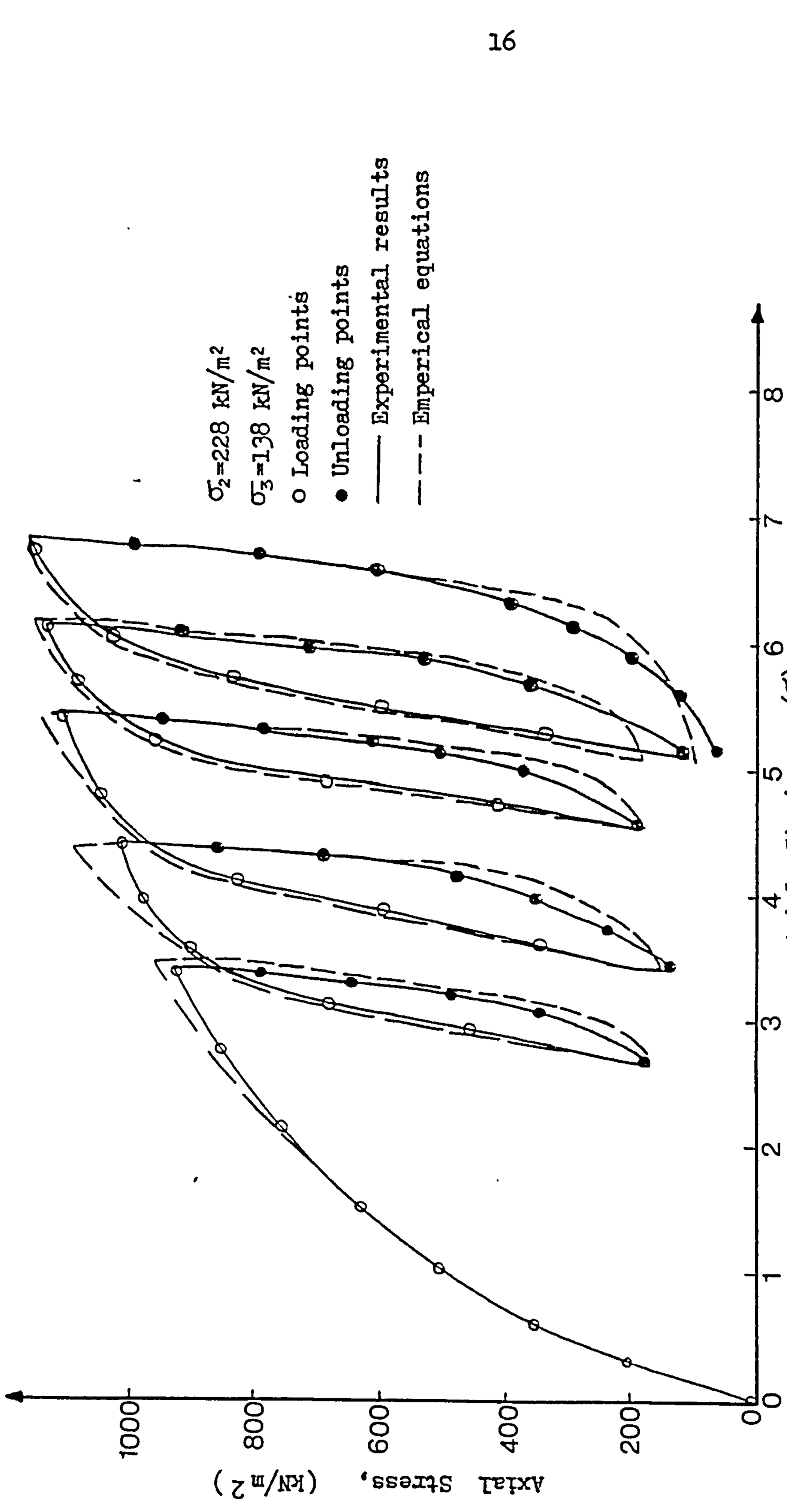

FIGURE 1.5 Stress-strain relationships under independent triaxial stresses and repeated loading (Kli 1978,20)

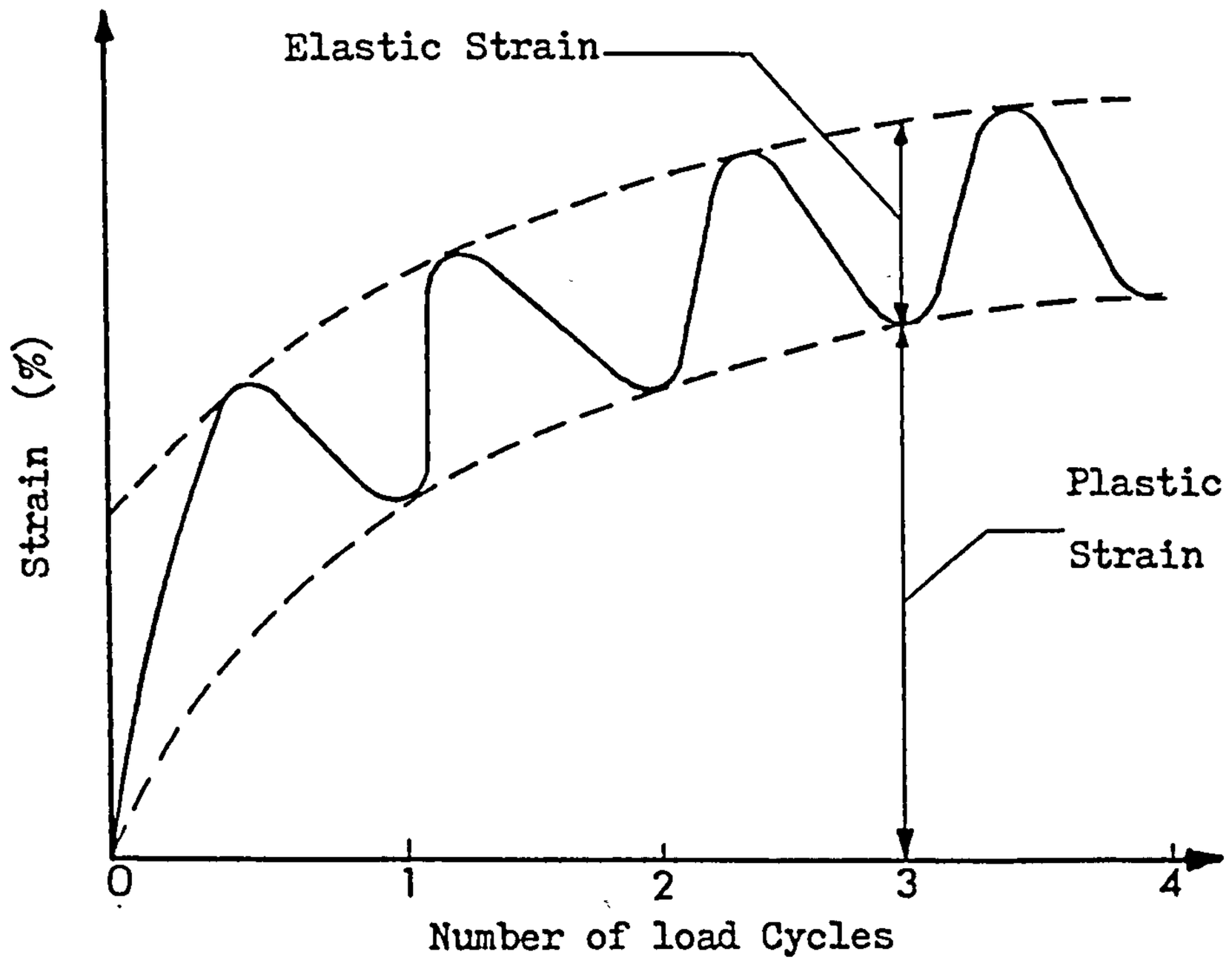

FIGURE 1.6 Components of Strain in the repeated load triaxial tests.

(Shaw 1980, 44)

above which large permanent shear strains develop, although the stress-path is still below the failure envelope. The elastic strains were found to stabilize after several hundred cycles of load for stress-states below the threshold value. He emphasises that above the threshold value the elastic strain behaviour is erratic. Permanent deformations of sand due to cyclic loading have also been studied by many investigators, but there is conflicting evidence on whether or not equilibrium is reached. Shackel [64] (1973) concluded "that much more research is needed into the problem of characterizing the non-recoverable behaviour of granular materials".

The other notable phenomenon that occurs in some cases of cyclic loadings on sand is large decrease in voids ratio compared to other static or low frequency cyclic loading. This large volume decrease is sometimes broadly described as compaction of the material [Pyke, 37] although this is not an appropriate term. Silver and Seed [34] found that the vertical strain due to so called compaction, during a series of cyclic tests on dry sand, was not significantly affected by the value of the vertical stress and was dependent on the shear stress amplitude induced in the sample at shear strains exceeding 0.05%. The cyclic shear strain which deforms the sample, allowing particles to move into a denser packing, may well be a fundamental parameter in determining the volume change behaviour of cohesionless soils under cyclic loading conditions. This has been confirmed by Pyke [65] and Youd [66] who showed that cyclic shearing is most effective in causing densification. Nevertheless Silver and

Seed [34] in their experimental studies have shown that compaction in cyclic simple shear tests is a function of the relative density and previous strain history as well as of the magnitude of the cyclic shear strain. The compaction per cycle decreases with an increasing number of load cycles. It was found, somewhat surprisingly, that for a given cyclic shear strain the amount of compaction was independent of the vertical stress. Youd [66] has confirmed these findings and shown that the compaction in simple shear tests is independent of frequency for both dry and drained saturated samples. Initial shear strains and overconsolidation have both been found to reduce the amount of compaction [Pyke, 65]. However, it is not quite clear what contribution the inherent characteristics of the sand make to the compaction of the material under cyclic loading compared to the contribution due to the conditions under which it is tested. Pyke shows the amount of compaction in cyclic triaxial tests increases with an increase in the confining pressure but that it is independent of the vertical stress in cyclic simple shear tests.

Some other aspects of the deformation behaviour of sand under cyclic loading conditions have been studied and discussed by a number of researchers.

Larew and Leonards [27] performed some cyclic triaxial tests on fine granular soils and found a critical level of cyclic deviator stress above which deformation continues to increase until failure occurs. For levels less than this critical value, the deformation remained constant. They suggested that the ratio of the critical stress level to the

static deviator stress at failure in a conventional triaxial test may be taken as a measure of the strength reduction due to the effect of cyclic loading. However, Seed and his co-workers [23] in their cyclic studies on silt found another factor affecting the deformation of the samples. They state that the deformation depends on the number of stress applications and is independent of frequency within the frequency range of 3 to 20 load applications per minute.

Although in recent years a lot of research has been carried out on sand behaviour under cyclic loading conditions, such as those reported on the liquefaction of saturated sand by Finn and Atkinson [67], [68], most researchers have investigated only limited aspects of sand response under cyclic loading and the lack of a general and fundamental investigation of stress-strain behaviour before failure is quite evident. The most recent piece of research attempted in this area is that by El-Gammel [22] in 1984 which concentrates mainly on monotonic loading. He performed a few loading-unloading-reloading tests on medium size Leighton Buzzard sand, which while confirming the elastic work-hardening plastic behaviour of sand, emphasised that a series of basic and comprehensive cyclic tests is still required to obtain an accurate and reliable understanding of the stress-strain behaviour of sand under different loading conditions.

1.3 REVIEW OF THEORETICAL WORK

Before 1960 mathematical models for the stress-strain relationships of sand were usually derived by considering the sand as a semi-infinite elastic material and only

vertical stresses and strains were taken into account, e.g. the models proposed by Wilson and Sutton [5], Jackobson [6], and Janbu [7]. As a result the expressions could only be applied under certain conditions and a comprehensive theory capable of describing the stress-strain behaviour of sand under general conditions of three dimensional stresses and strains did not exist. In 1963 Kondner and Zelasko [10] proposed a non-linear stress-strain relationship of hyperbolic form which included the principal stresses and was applicable to both sands and clays as follows:

$$\sigma_1 - \sigma_3 = \frac{\varepsilon_1}{a + b\varepsilon_1} \qquad (1.7)$$

Where: σ_1 =the major principal stress

σ_3 =the minor principal stress(= σ_2)

ε_1 =the strain in the major principal direction

and a and b =constants to be found experimentally.

Kondner et.al [10] deduced their equation from conventional triaxial test results, yet in some cases it did not fit the actual stress-strain curve. Using experimental data from conventional triaxial tests other researchers such as Hansen [11], Desai [69], Breth, Schuter and Pise [70] also derived stress-strain equations in which the intermediate principal stress was assumed to be equal to the minor principal stress. Among them Hansen [11] developed Kondners' work [10] by proposing two additional functional representations:

$$\sigma_1 - \sigma_3 = \left[\frac{\varepsilon_1}{a_2 + b_2 \varepsilon_1} \right]^{\frac{1}{2}} \qquad (1.8)$$

$$\sigma_1 - \sigma_3 = \frac{(\varepsilon_1)^{1/2}}{a_3 + b_3 \varepsilon_1} \qquad (1.9)$$

Equation 1.8 allows for the possibility of parabolic variations of stress-strain curves at small strains. Equation 1.9 is an alternative form to account for the maximum value of $\sigma_1 - \sigma_3$ for a finite strain, i.e. it is suitable when the curve shows a decrease after a peak stress has been reached. Hansen [11] used data from Kondners' work [10] and compared the stresses obtained from equations 1.7, 1.8, and 1.9. He observed that if the stress-strain curve is initially linear, equation 1.7 is suitable, if it is initially parabolic, equation 1.8 will probably be better, and if it exhibits work softening, equation 1.9 should be used. Although Hansens' equations give a better prediction of the stress- strain curves than that suggested initially by Kondner and Zelasko [10] , they were not yet able to express the relationships between principal stresses and strains when they were imposed on a sand sample independently.

Daniel [63] by conducting true triaxial tests, in which the three principal stresses can be applied independently, produced the following stress-strain relationship for granular materials

$$\sigma_1 = \frac{1}{Kr} \sqrt{\sigma_2 \sigma_3} \, (1 - A e^{B \varepsilon_1}) \qquad (1.10)$$

Where: σ_1 , σ_2 , and σ_3 = the principal stresses

ε_1 = the major principal strain

Kr = the Rankine ratio

and A and B are constants to be found experimentally.

He has also produced a generalized principal stress-strain relationship of the following type which is of an incremental nature and applicable to dry granular media subjected to first loading:

$$\delta\varepsilon_1 = \frac{\delta\sigma_1}{k(\sigma_1 - 1/kr\sqrt{\sigma_2\sigma_3})} - (2 - \frac{\sigma_1}{\sigma_2})(\frac{a}{\sigma_1/kr - \sigma_3} - \frac{b}{\sigma_1/kr})\delta\sigma_3$$

$$- \frac{\sigma_3}{\sigma_1}(\frac{a}{\sigma_3/kr - \sigma_2} - \frac{b}{\sigma_3/kr})\delta\sigma_2 \qquad (1.11)$$

Where: σ_1 , σ_2 , and σ_3 = principal stresses.

ε_1 , ε_2 , and ε_3 = principal strains.

$\delta\sigma_1$, $\delta\varepsilon_1$, etc. = a small increment of the quality concerned.

Kr = Rankine ratio.

and k, a, and b are constants to be found experimentally.

There are similar equations for $\delta\varepsilon_2$ and $\delta\varepsilon_3$. If the condition of $\sigma_1 = \sigma_2 = \sigma_3$ is applied to Daniels' equations, a relationship close to that suggested by Kondner is derived which means in the simplified case Daniels' equations give the same results as Kondners'. Burley et.al [19] continued

experimental and theoretical studies on granular soils and developed Daniels' work [63] to find some empirical equations for both the loading and unloading portions of a complete cycle of load. They derived more accurate incremental equations for the first loading of sand than Daniels', as follows:

$$\delta\varepsilon_1 = \frac{\delta\sigma_1}{K1\left(\frac{\sqrt{\sigma_2\sigma_3}}{Kr} - \sigma_1\right)} - \frac{\delta\sigma_2}{K2\frac{\sigma_1}{\sigma_3}\left(\frac{\sqrt{\sigma_3\sigma_1}}{Kr} - \sigma_2\right)}$$

$$- \frac{\delta\sigma_3}{K2\frac{\sigma_1}{\sigma_2}\left(\frac{\sqrt{\sigma_1\sigma_2}}{Kr} - \sigma_3\right)} \qquad (1.12)$$

Where k1 and k2 are constants which can be found experimentally. These equations are similar to Daniels' but give more consistent results. Burley et al(1975) also derived the following incremental equations which satisfactorily predicted the behaviour of a specimen during the unloading sequence:

$$\delta\varepsilon_1 = \frac{\exp(-r_3\sigma_1/\sqrt{\sigma_2\sigma_3})}{f1\sqrt{\sigma_2\sigma_3}}\delta\sigma_1 - \frac{\exp(-r_2\sigma_2/\sqrt{\sigma_3\sigma_1})}{f2(\sigma_3/\sigma_1)^g\sqrt{\sigma_1\sigma_3}}\delta\sigma_2$$

$$- \frac{\exp(-r_1\sigma_3/\sqrt{\sigma_2\sigma_1})}{f2(\sigma_2/\sigma_1)^g\sqrt{\sigma_2\sigma_1}}\delta\sigma_3 \qquad (1.13)$$

Where: f1, f2, and g are constants to be found experimentally

r1, r2, and r3 = the ratios of ultimate principal stresses to the stress levels at which the unloading commences.

Burley et.al in their studies found that the response of the sample on reloading after the application of the first cycle could be represented by linear elastic behaviour, so they suggested the following equations to represent the reloading characteristics:

$$\delta\varepsilon_1 = \frac{\varepsilon_{11i} - \varepsilon_{11f}}{\sigma_{1i} - \sigma_{1f}}\delta\sigma_1 - \frac{\varepsilon_{12i} - \varepsilon_{12f}}{\sigma_{2i} - \sigma_{2f}}\delta\sigma_2$$

$$- \frac{\varepsilon_{13i} - \varepsilon_{13f}}{\sigma_{3i} - \sigma_{3f}}\delta\sigma_3 \qquad (1.14)$$

Where ε_{12i}, ε_{12f}, etc. are the strains in the major principal direction due to the loading in the intermediate principal direction at the beginning and end of the unloading-reloading cycle respectively.

These equations, although useful for samples subjected to cyclic loading in the special conditions under which Burley et.al carried out their experiments, due to their incremental nature are too complicated and difficult for general use unless processed by computer. Furthermore stress-strain theories based entirely on assumed incremental elastic behaviour have certain short-comings for the prediction of soil response at high stress-levels due to domination of plastic strains at these levels.

The theories of plasticity have been applied to cohesionless soils by many researchers. The three basic requirements for a plastic stress-strain theory are as follows [Hill and Mendelson, 71]:

(1) There must exist a yield surface

(2) A flow rule is also required

(3) A work-hardening law is needed.

Drucker, Gibson and Henkel [60], Rowe [72], Roscoe et.al [17], Duncan and Lade [18], Khosla and Wu [73], Vesic and Clough [74], Scofield and Wroth [75], Atkinson and Bransby [76], Kirkpatrick [77], Vermeer [78], Naylor [79], Scott [80], Sandler and Diamagio [16], etc, are amongst those who have used the theories of plasticity in examining the behaviour of sand and who have developed plasticity models, details of which are described in their publications. Among the two most widely used are those known as the stress-dilatancy theory and critical state soil model (C.S.S.M), both of which merit presentation here.

Rowe [72] developed the stress-dilatancy relationships from studies of the interaction between spherical particles. From considerations of energy input and output of the mass, relationships between the strain increment ratio and the stress ratios were derived for the conditions of triaxial compression, triaxial extension, and plane-strain. The theory does not consider elastic strain and is therefore most accurate at high stress levels where plastic strain dominates. Several important concepts of plasticity theory are expressed in the stress-dilatancy relationships and they provide valuable insight into the stress-strain behaviour of

sand.

Roscoe and his co-workers [17] originally developed the critical state soil model using experimental evidence from axisymmetric tests (triaxial compression and consolidation) on remolded clay. Based on the concept of the flow rule and plastic potential from plasticity theory, the C.S.S.M. model was developed using simple curve fitting procedures. Finally simple functions for the plastic potential and the hardening law were suggested for the specific conditions of triaxial compression and plane-strain. The theory has been extended to sand in simple shear [Wroth and Bassett 81] and triaxial compression [Poorooshasb et.al, 61].

The stress-dilatancy theory and the critical state soil mechanics model demonstrate that elements of real sand behaviour can be modelled relatively well within the realm of elasticity and plasticity theories.

Treating the soil as an elastic plastic work-hardening material, Roscoe et al. [82] proposed a theoretical model in which the yield surface consists of a "critical state line" and "bullet shaped" expanding cap, while Sandler and Diamagio [16] offered another model comprising the generalized Mohr-Coulomb yield surface with an expanding elliptical cap. In both models the stress-strain relationships are developed on the principle of energy conservation during straining of a soil sample and the caps are functions of volumetric strain. The capabilities of these two models were later examined by Khosla [35] in his studies of the impact of stress -path on the static and cyclic response of sand. He found that the critical state model over-estimated the

strains, while the other model could effectively predict the plastic strains for both static and cyclic loading. Nevertheless near the failure envelope the experimental points fell below the theoretical yield surface and large deviation from normality took place.

The stress-dilatancy theory of Rowe [72] was used as a basis to derive a relationship between stresses and strains, assuming sand is a particulate material consisting of rigid groups of compacted particles by Barden and Khayatt [83]. Using this theory based on the principle of maximum energy conservation between particles, they expressed the stress-dilatancy for the triaxial compression tests as follows.

$$\frac{\sigma_1}{\sigma_3} = (1 - \frac{dv}{d\varepsilon_1}) \tan^2 (45 + \frac{\varphi_f}{2}) \qquad (1.15)$$

Where: σ_1 and σ_3 = major and minor principal stresses.

dV = a small change in the volume of the specimen.

$d\varepsilon_1$ = a small change in the major principal strain.

and φ_f = a semi-empirical angle which must lie between the upper limit of φ_{cv} and the lower limit of φ_u (ultimate value).

For the analysis of triaxial extension tests ($\sigma_1 = \sigma_2 > \sigma_3$) the theory was extended by them to give:

$$\frac{\sigma_1}{\sigma_3} = \frac{1}{(1 - \frac{dv}{d\varepsilon_3})} \tan^2 (45 + \frac{\varphi_f}{2}) \qquad (1.16)$$

And for the plane-strain test ($\varepsilon_2 = 0$) it can be demonstrated that:

$$\frac{\sigma_1}{\sigma_3} = (1 - \frac{dv}{d\varepsilon_1}) \tan^2 (45 + \frac{\varphi_f}{2}) \qquad (1.17)$$

It is seen that the triaxial compression and plane-strain tests have identical equations. Although these equations can effectively represent the stress-strain behaviour of cohesionless soils, particularly when high levels of vertical stress are involved, they cannot be used for elastic deformations because they neglect elastic strains. Also, in cases where there is a high degree of interlocking in a highly compact assembly the principle of maximum energy transmission may not apply because there may be a lack of freedom of motion between particles [Horne, 84].

Analytical works, using plasticity theory for modelling sand behaviour under different monotonic and cyclic loading conditions have also been put forward and developed by other researchers. The most recent work in this area is that carried out by Bardet [85] in 1985. In this piece of research he applied the theory of plasticity to sand and offered a behavioural model representing both monotonic and cyclic responses. However the model still does not accurately predict the response of soils to cyclic conditions and is restricted to describing conventional triaxial tests. Apart from these points the initial requirements of the model, which needs eight material constants to be specified,

make it too complex for common use in routine practice.

Despite much theoretical study of sand behaviour under different loading conditions, each model proposed has its disadvantages. Therefore in order to derive a comprehensive model, more work is required in this area. The simplicity of such a model is as important as its accuracy and comprehensiveness.

1.4 REVIEW OF TESTING APPARATUS

The strength and deformation characteristics of soils are generally measured by means of conventional apparatus among which the most common types are confined compression (oedometer), direct shear box and isotropic compression apparatus. In recent years new devices developed from conventional apparatus, which are highly sophisticated and capable of conducting soil tests into new areas, have become available. Completely new pieces of apparatus have also been developed.

The oedometer apparatus which is the simplest device used to study the volumetric stress-strain relationships of soils under Ko conditions (figure 1.7) suffers from side friction when vertical strain occurs [86]. This apparatus, which is usually used for consolidation studies of cohesive soils, cannot be employed for other purposes and has limited usage in laboratory studies.

There has been wider application of direct shear apparatus in stress-strain and strength characterization of soils (figure 1.8). The relationships between shear stress and strain and also vertical and shear stresses can be

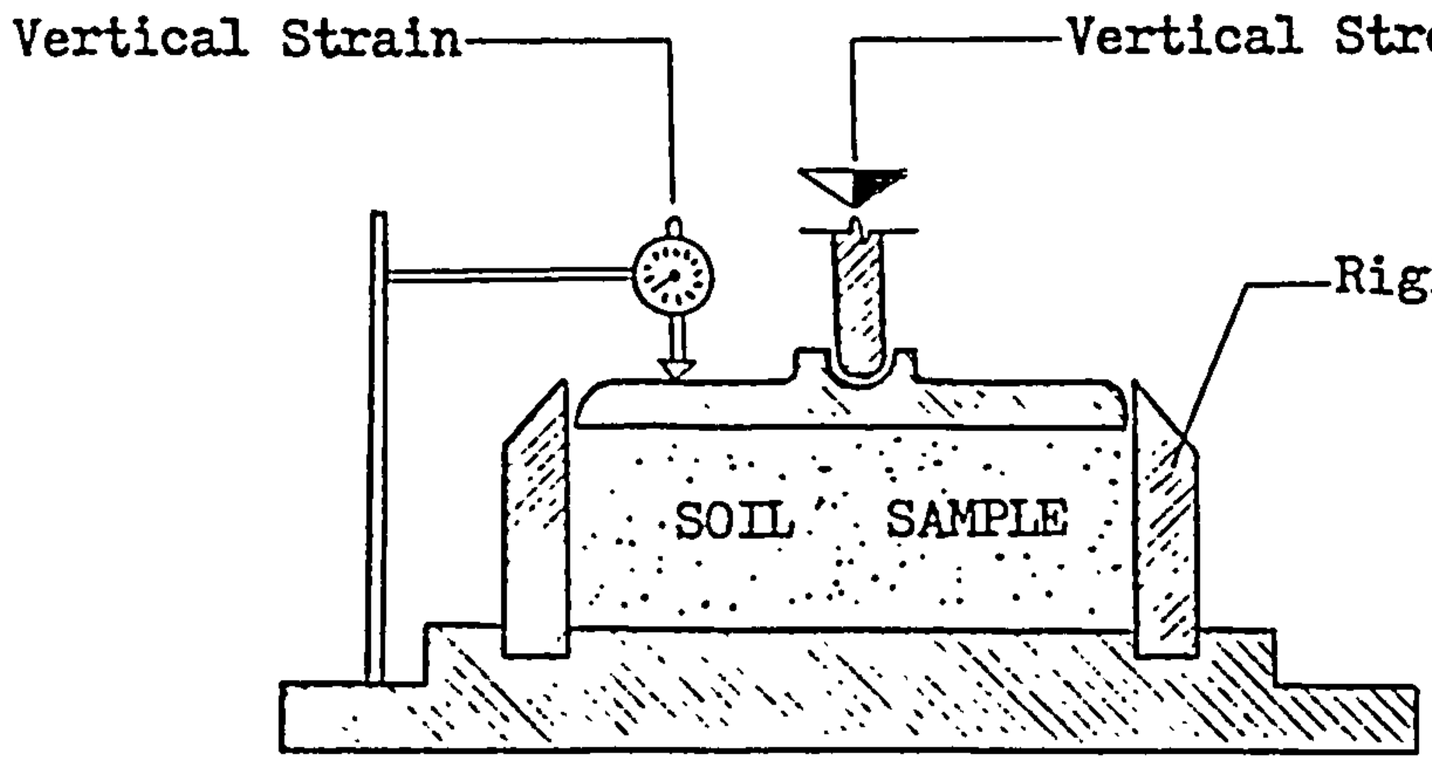

FIGURE 1.7 Schematic Diagram of a simple oedometer.

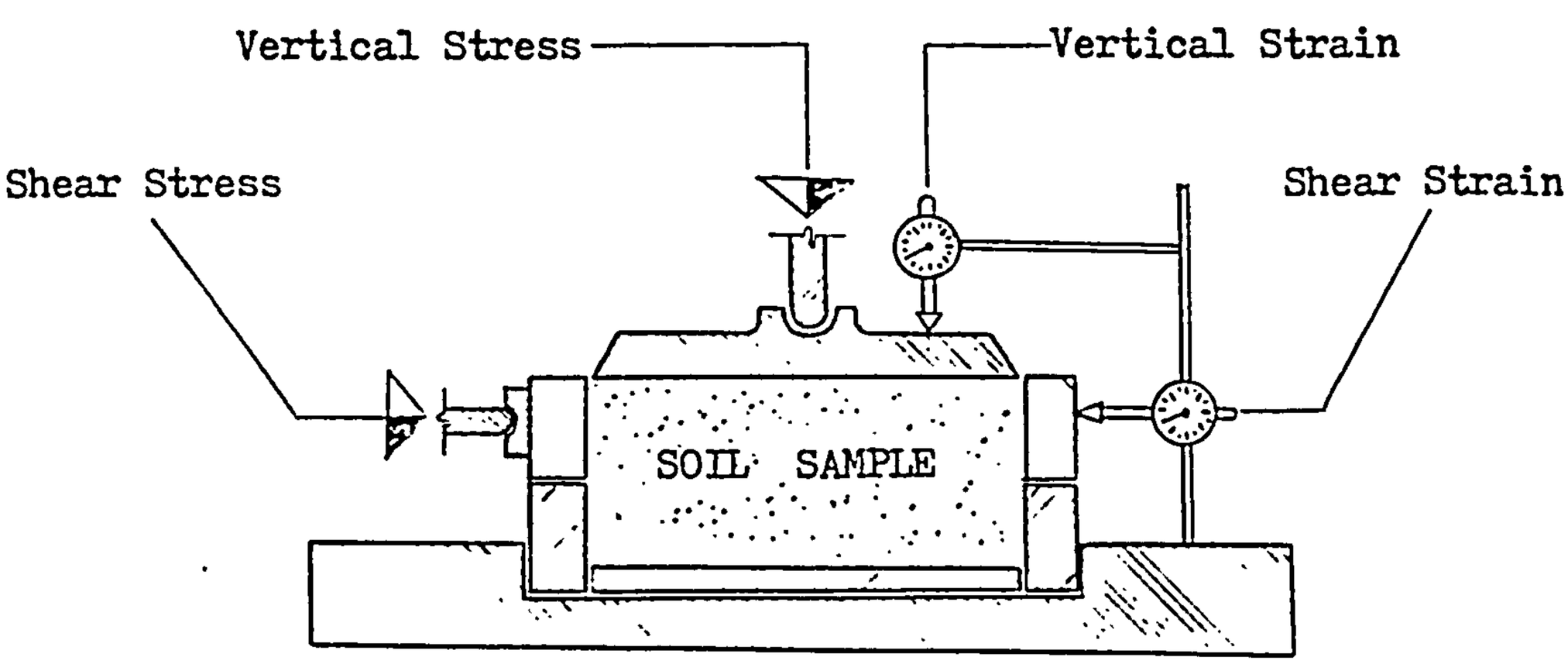

FIGURE 1.8 Schematic Representation of a Direct Shear Apparatus

studied easily. Peak strength and residual strength of the soil can be determined. The direct shear box has been greatly developed by the Norwegian Geotechnical Institute [87]. In this development, the original rectangular samples confined by rigid boundaries. were replaced by cylindrical specimens surrounded by wire reinforced rubber membranes (figure 1.9) so that the undrained strength can be measured using this apparatus. As the stress distribution in the sample is unknown the results may be doubtful, but they are closer to the field conditions than confined drained shear tests. Later, two types of shear apparatus were developed in which the axes of principal stresses and strains can be rotated to any desired angle. In the first one hollow cylindrical specimens under internal and external radial pressure are subjected to torsion loadings which, of course, are very complicated [Broms and Gasbarian, 88]. The second shear apparatus was developed by Roscoe et.al [89]. In this device lateral deformations of a cuboid specimen are prevented by stiff metal walls. The sides parallel to the direction of the shear deformations are fixed relative to the base and the cap while the other two sides are attached to the cap and the base by hinges (figure 1.10). The volumetric and shear strains can be measured under plane strain conditions while the non-uniformity of the sample is minimized. However it is too complicated to be used for routine tests. Another kind of shear apparatus which was developed at the University of London, has flexible boundaries and is able to perform plane strain shear tests [Arthur et.al 90]. It has been used to study the stress-strain behaviour and strength ani-

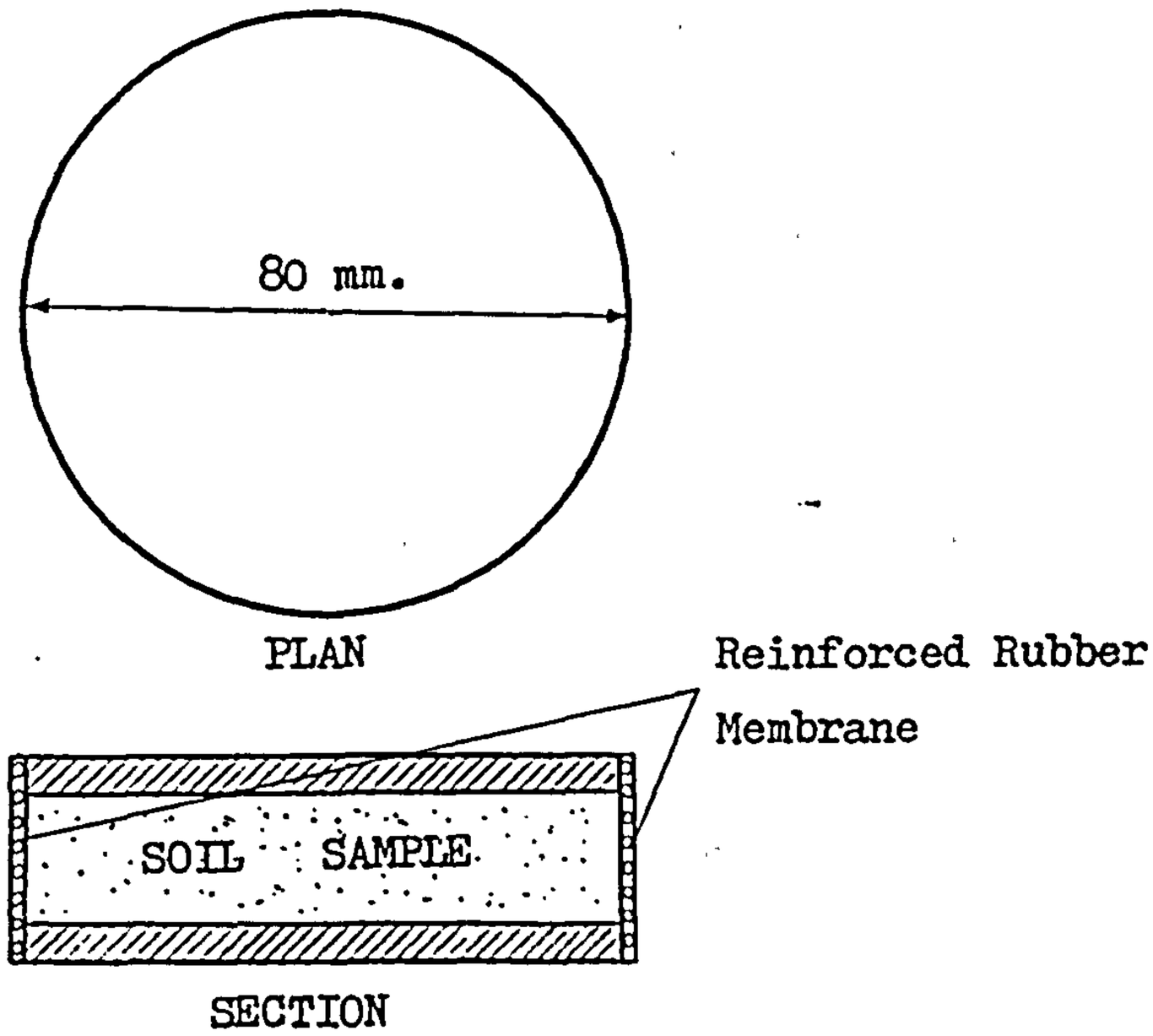

FIGURE 1.9 Schematic Sketch of Norwegian Geotechnical Institute Direct Simple Shear Apparatus.

(Bjerrum and Landva 1966)

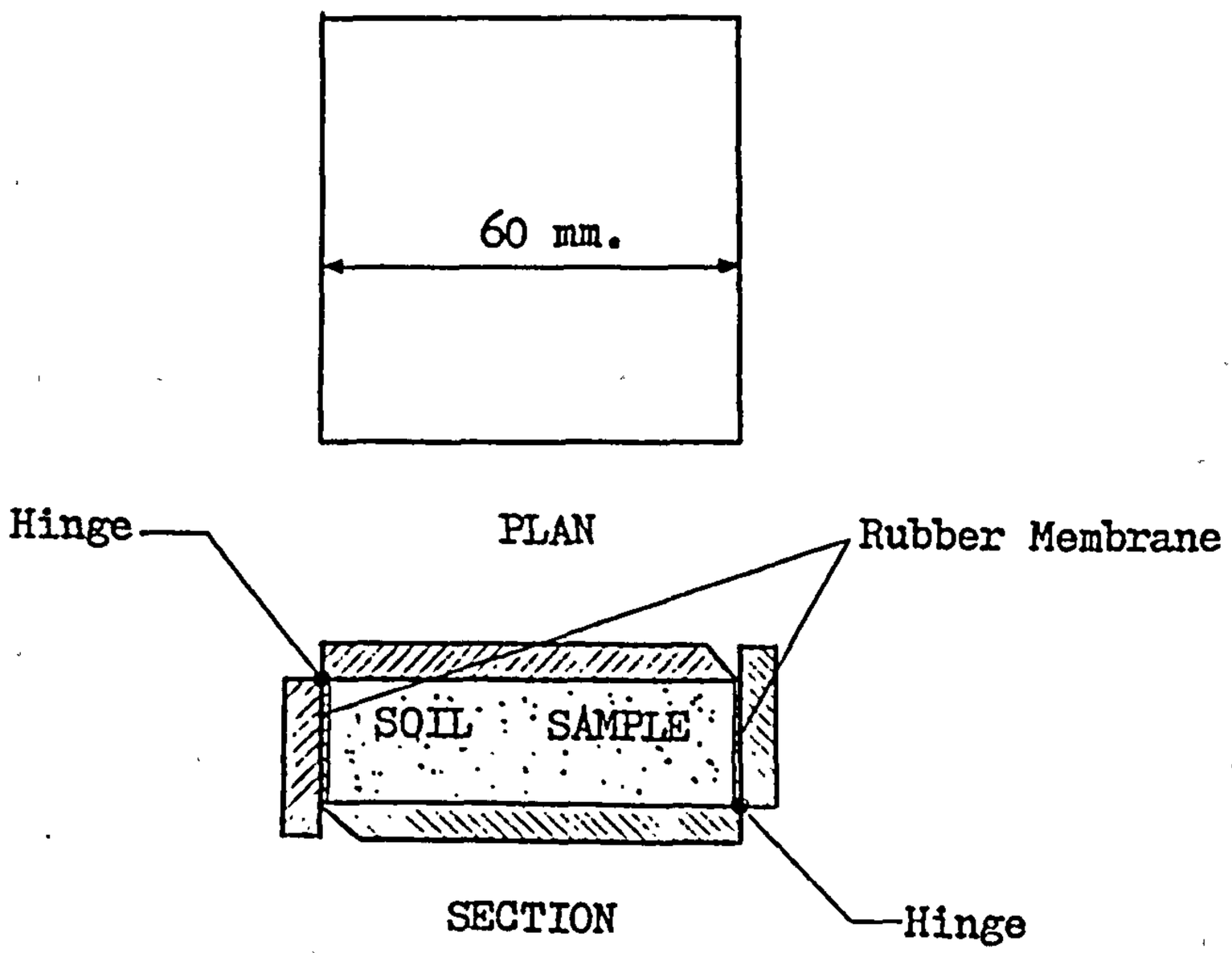

FIGURE 1.10 Schematic Sketch of the Cambridge University Direct Simple Shear Apparatus.

(Roscoe et al. 1953)

sotropy in sand and can monitor the rotation of principal axes. It is called the "Directional Shear Cell". Later a similar shear apparatus called the "Directional Shearing Cell", was developed by Rodriguez et.al [91]. They were able to study loose sand under large strains to failure without inducing non-uniformity within the sample. They showed that deformations induced in the sample should not be restricted by rigid boundaries for good results. Nevertheless, providing such a complicated boundary condition may limit the apparatus to plane strain conditions.

In general, using the shear apparatus usually causes an imposed failure plane in the soil specimen which is normally far from that which would occur in practice.

Another type of laboratory testing apparatus for stress-strain studies and the measurement of basic soil parameters is the conventional triaxial equipment (figure 1.11). It is the most popular and versatile of soil tests. Using this apparatus, cylindrical specimens of soil under a three dimensional stress field can be tested either in compression or extension. The compression triaxial test is the most common type. The specimen in this case is subjected to failure by increasing the axial stress under a constant value of confining pressure. In the extension triaxial test the axial stress is decreased till it falls below the confining pressure and as a result failure takes place. This type of triaxial test is comparatively difficult to perform compared to the compression test. Henkel and Bishop [92] in their laboratory studies concentrated on this equipment, extensively developed it and demonstrated its potential to

provide different stress or strain paths for testing dry, saturated, and partially saturated samples. Nevertheless, there are still some criticisms, most of which can be summarized as follows [Reads, 93]:

a) For accurate tests the effect of friction between loading shaft and the chamber must be taken into account.

b) The rigid plates which are normally placed at the two ends of the samples may restrain them and cause some non-uniformity in the specimen.

c) The rotation of the principal axes is not possible and as a result the isotropic properties of soils can not be studied.

d) Two of the principal stresses are always equal and the influence of the intermediate principal stress cannot be investigated.

Since the conventional triaxial apparatus is adequate for testing soil only when there are axisymmetric stress conditions, it cannot be applied to other cases when some degree of non-axisymmetry in stresses is involved. As a result the conventional triaxial apparatus is restricted to a few practical situations. This major limitation has caused many researchers to design new pieces of apparatus capable of applying true triaxial conditions (figure 1.12). Some of these devices have been able to allow rotation of principal axes in addition to applying different and independent principal stresses and strains. The early true triaxial apparatus were mechanically complicated and the tests results were questionable due to friction between sample and rigid platens [94, 6, 95, 63]. In recent years they have been devel-

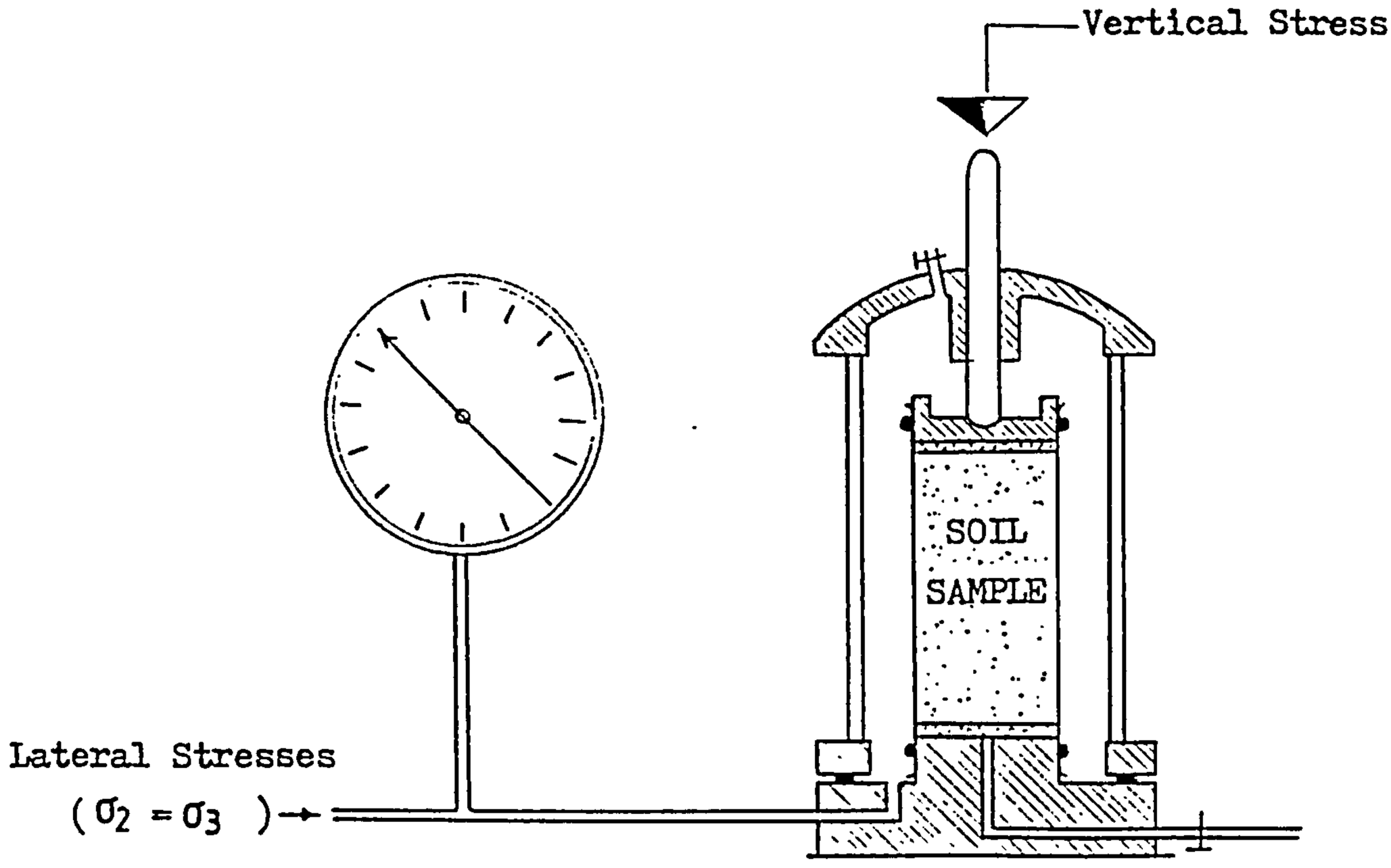

FIGURE 1.11 Diagrammatic Layout of the Conventional Triaxial Apparatus.

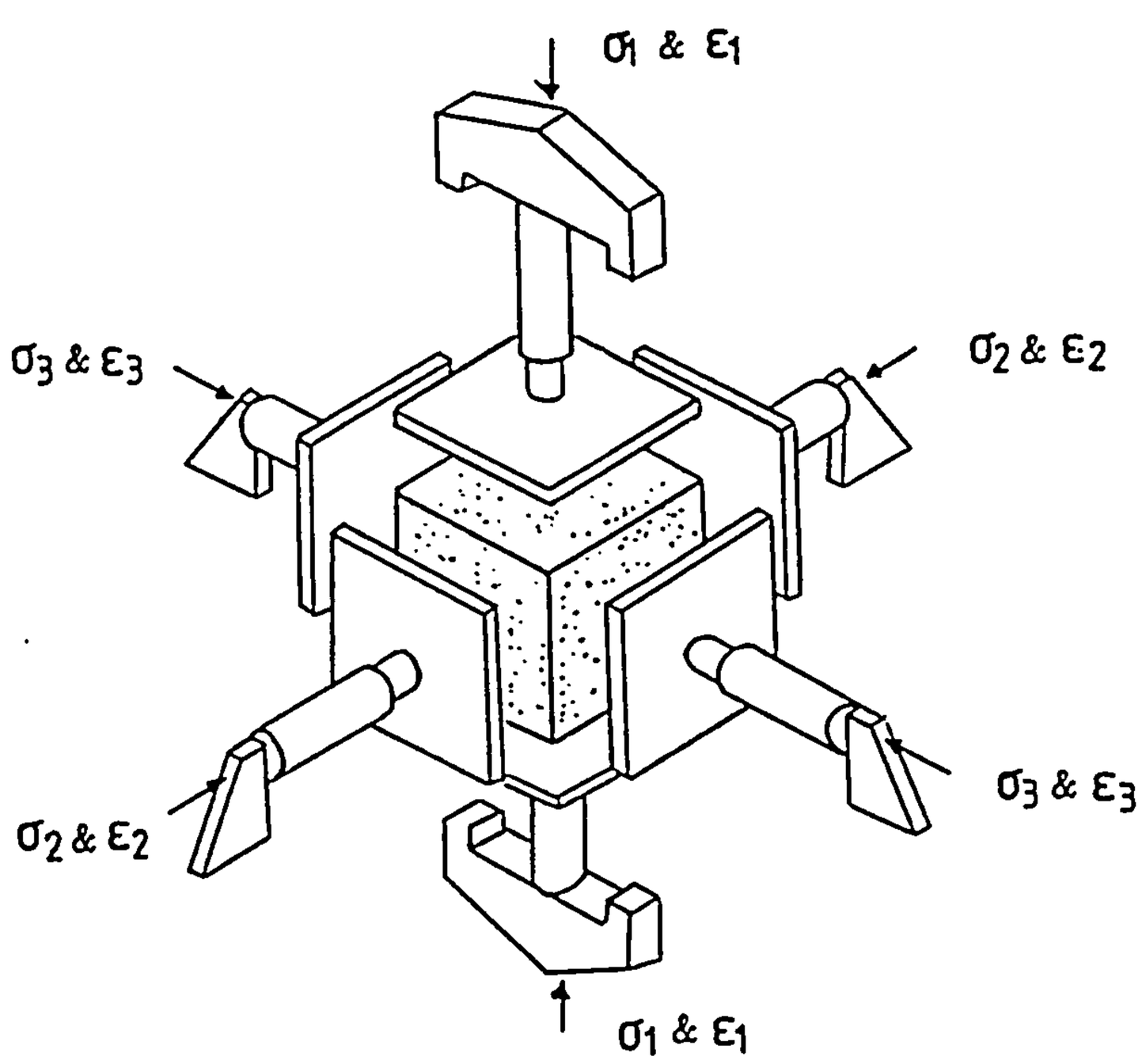

FIGURE 1.12 Schematic Representation of a True Triaxial Apparatus (with fully rigid boundaries).

oped significantly so that the stresses and strains acting upon a cuboidal sample can be independently monitored and accurately measured [96, 97, 98, 93, 99].

The true triaxial apparatus can be categorized on the basis of their boundary conditions into three different groups. The first one includes those providing principal stresses and strains by means of rigid platens (figure 1.12), like those used by Daniel [63], Hambly [100], Pearce [101], Gudehus [102], Wood [103], Fardis and Frydman [104], and Kii [20]. In this group of true triaxial apparatus which are basically designed for strain-controlled tests, the six faces of the cuboidal soil samples are surrounded by three pairs of parallel rigid platens. The principal stresses and strains which are normally produced by mechanical, pneumatic, hydraulic or combined systems, are transferred to the specimen through these rigid platens. This type of the true triaxial apparatus is relatively easy to construct. The principal strains can be applied uniformly and measured accurately. Also different, complicated and predetermined strain paths can be easily modelled. Apart from this, load cells and other measurement devices can be accommodated in the loading platens. Nevertheless, they suffer from some problems which can be summarized as follows [Sture and Desai 105]:

a) It is difficult to monitor the uniformity of the stresses induced in the sample.

b) It is difficult to apply predetermined stress-paths on the sample.

c) The interference of the loading platens takes

place at large multiaxial strain states.

d) The apparatus is usually large and the operation is normally complicated.

The second group of true triaxial apparatus have fully flexible boundaries (figure 1.13). Such devices have been employed by Bell [106], Ko and Scott [108], Lomize et.al [110], Arthur and Menzies [111], Lewin [113], Ko and Masson [114], Sture and Desai [105], Yamada and Ishihara [116], Berends and Ko [117], Rodriguez et.al [91].

This type of true triaxial apparatus can perform stress-controlled tests. The general design feature of this kind of triaxial device is flexible bags filled with compressed air or liquid over all the faces of the cuboidal specimen. The principal stresses acting upon the three pairs of soil faces can be independently monitored by controlling the amount of pressure produced inside each pair of flexible bags. In order to prevent interference between different bags when their inside pressures are not equal they are contained inside rigid space frames in some cases [108]. Green [118], Arthur and Menzies [119], and Bell [120] pointed out that the rigid frame may cause an edge restraint which may result in the stress-strain curves being steeper than would otherwise be the case and also in higher strengths. Although this type of apparatus has the great advantages of applying uniform stresses over the faces of cuboidal soil samples and following complicated and predetermined stress-paths easily, they are more difficult than the first group to construct. Sture and Desai [105] mentioned the main criticisms facing this type of true triaxial apparatus as follows:

a) Interference may occur at boundaries unless proper precautions are taken.

b) It is difficult to maintain the uniformity of the strains induced in the samples particularly when they are large.

d) Performing plane-strain tests requires some special corrections of stress states normal to plane to prevent any undesirable strain.

e) Accommodating pore water pressure facilities and measurement devices is difficult.

The last group of true triaxial apparatus are those with combinations of rigid and flexible boundaries (figure 1.14), such as the equipment used by Shibata and Karube [121], Lenoe [122], Young and Mckyes [123], Green [97], Sutherland and Mesdary [124], Dyson [98], Ramamurthy and Rawat [127], Barden and Proctor [126], Lade and Duncan [128], Green and Reads [129], and Samashekar [130]. In this kind of triaxial equipment various conditions of flexible and rigid and rigid-lubricated boundaries have been used. The vertical principal stress is normally applied through the rigid platens at the cap and base of the cuboidal sample. As far as the lateral stresses are concerned, usually one of them is applied by a cell pressure acting upon the specimen and the other one is provided by a special flexible or rigid system accommodated inside the chamber where the sample is contained. In some cases both lateral stresses have been applied by two pairs of similar flexible systems independently. The overall chamber has been abandoned in these cases [Rawat and Ramamurthy, 131].

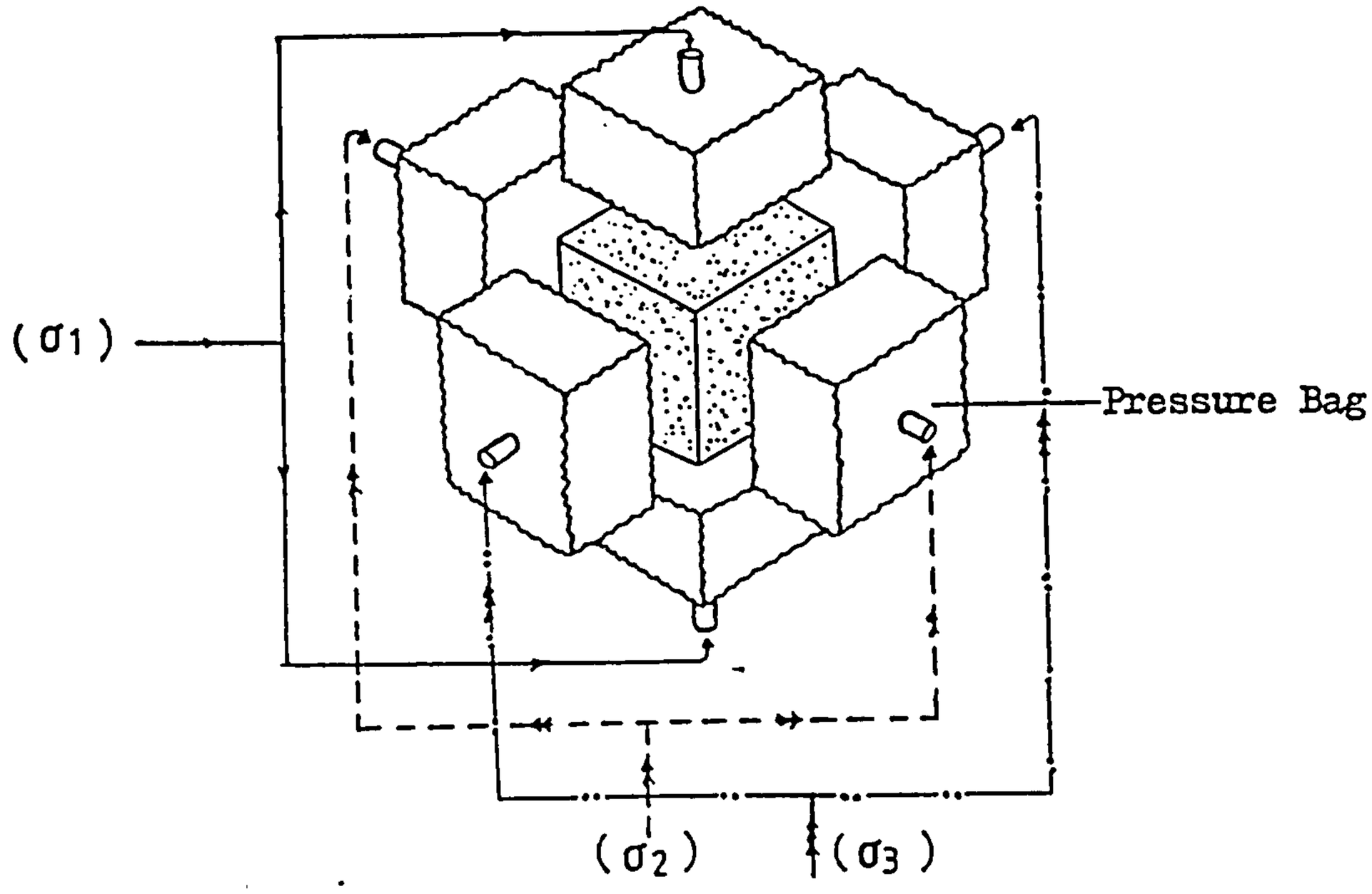

FIGURE 1.13 Schematic Representation of a True Triaxial Apparatus with fully flexible boundaries.

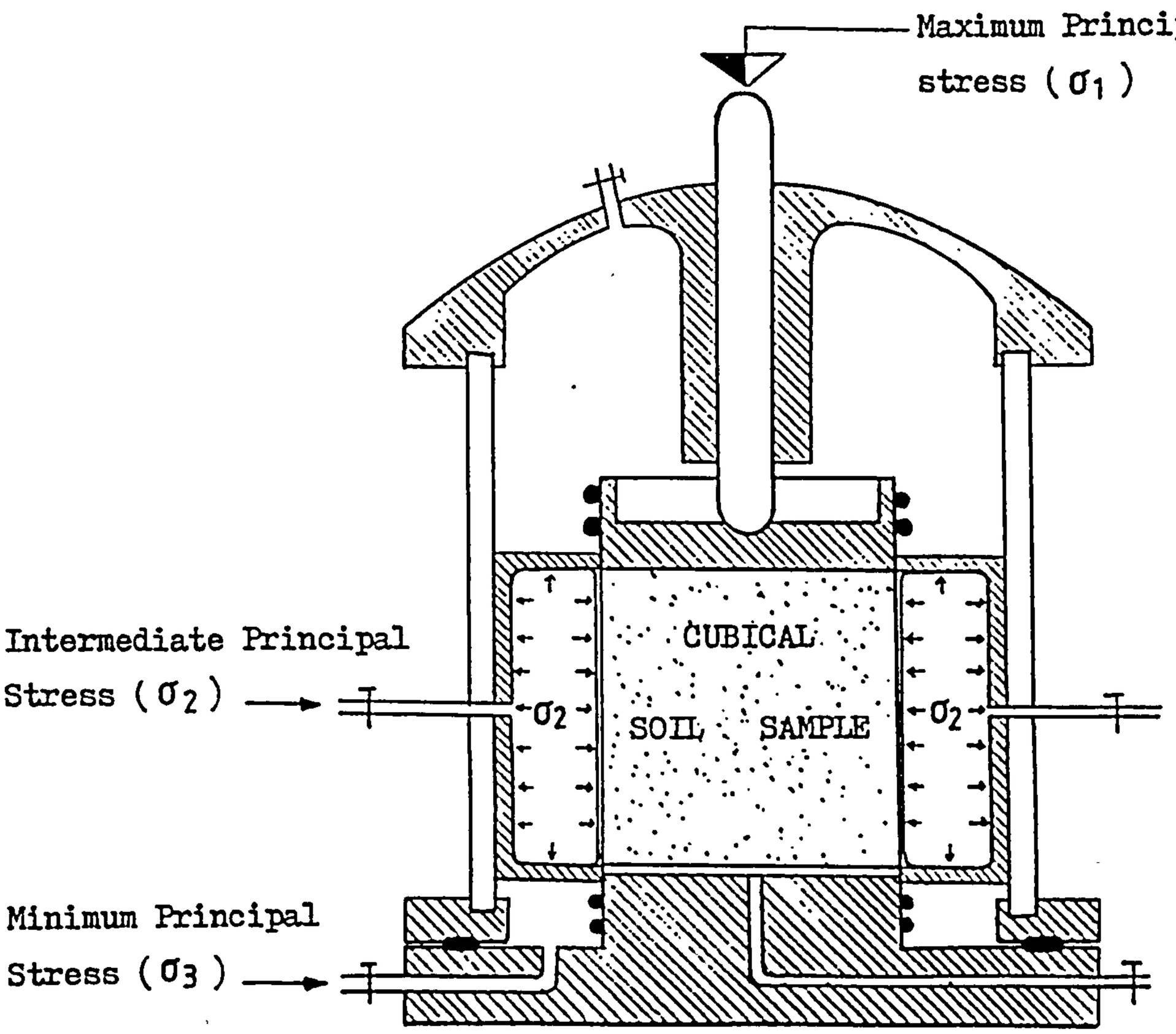

FIGURE 1.14 Schematic Sketch of a True Triaxial Apparatus with combination of rigid and flexible boundaries.

Boundary interference in this group can usually be avoided if the rigid boundary is used in the compressive deviator load direction, and the stress-controlled flexible boundary to the extension deviater direction. Also stress or strain paths can easily be applied provided a predetermined selection of specimen orientation with respect to the apparatus axes is allowed. Furthermore plane-strain tests can be performed and pore water pressure measurement devices can easily be accommodated. Nevertheless, they still suffer from some important disadvantages which are listed below [Sture and Desai, 105]:

a) It is usually impossible to apply complicated predetermined stress or strain paths.

b) The uniformity of stress and strain fields in directions normal to the rigid and flexible boundaries cannot be guaranteed.

c) Near boundaries usually heterogeneous stress and strain fields occur.

d) These apparatus are usually large.

e) The operation is usually extremely complicated.

In recent years a true triaxial apparatus with fully rigid boundaries has been developed at the soil mechanics laboratory of Leeds University [El-Gammel, 22] which is able to apply three independent principal stresses and strains on cubic sand samples of 150 mm size. Most disadvantages facing this type of true triaxial apparatus (mentioned before), have been eliminated for stress-strain studies of cohesionless soils over small ranges of strain under strain-controlled conditions. This apparatus was used in the current in-

vestigation after some modifications. A brief description of design principles and full explanations of essential modifications carried out, are presented in the next chapter.

1.5 SUMMARY AND CONCLUSION

It is essential to know the stress-strain behaviour of a soil in order to find solutions to soil engineering problems. Its importance was well recognised when Roscoe requested a change in outlook on the subject and that engineers stop concentrating only on the shear strength of soils and start to think in terms of their stress-strain behaviour [132].

The stress-strain behaviour of cohesionless soils has been studied by many researchers. A lot of empirical information has been obtained. However as the conditions under which the experimental studies are carried out has a great effect on the tests results, it is sometimes difficult to compare the results of different investigations. Yet the non-linearity and elastic-plastic characteristics of sand have been confirmed by most investigators. Other aspects still require more accurate and thorough studies in order that they be clarified.

Since most practical projects usually involve small deformations of the soil mass, stress-strain data at small strains are critical. By gathering sufficient information in this area the number of tests required to solve the problems in each case can be reduced. Although there is much information obtained from numerous tests on medium size sand [22] which shows a sharp decrease in stresses due to small

lateral strains less than 0.3%, it is not yet clear if the behaviour of all kinds of sands will be similar and if particle size has a major effect. Due to a lack of experimental evidence in this area a series of tests on sands with other sized particles is required.

The cyclic stress-strain behaviour of sand has increasingly been the subject of interest and study, not only because of its wide applications in soil engineering projects, but also to allow an insight into the inherent characteristics of cohesionless materials. Many researches have concentrated on this area and it has been confirmed that when a sample of granular soil is subjected to cyclic loadings, recoverable and irrecoverable deformations take place. While the first is usually related to the elastic properties of the particles the second is attributed to the sliding deformations of the mass and normally builds up as the number of load cycles increases. The majority of investigators have focussed their cyclic studies directly on particular phenomenon such as failure mechanisms, liquefaction, hysteresis damping, etc. As a result there is not enough information to completely identify the fundamental properties of sand . Further basic experiments are needed to rectify this.

The type of testing apparatus used is one of the important factors in laboratory studies. An adequate testing device should not only be able to simulate the field conditions but ensure the accuracy and simplicity of the test as well. Several testing apparatus have been used for experimental stress-strain studies of soils. In the early stages

their abilities were limited and they had many disadvantages. They range in type from simple oedometers to highly sophisticated triaxial apparatus. The true triaxial equipment which has been designed and used by many researchers has the great advantage of applying three independent principal stresses to soil samples and hence can provide a better approximation to actual field conditions in the laboratory. Although there are still some criticisms of this new kind of triaxial apparatus, in the absence of a perfect one, and taking special care when using them, they are the best devices for stress-strain studies under three dimensional stress states in the laboratory.

1.6 OBJECTIVES OF THIS INVESTIGATION

The majority of stress-strain experiments carried out so far concern the behaviour of sand at high levels of stress and large deformations leading to failure. Consequently the peak stress and strength of the material have been the focus of attention. However, when a practical problem in the field is being considered, small deformations due to low levels of vertical stresses are most likely and the behaviour of soil before failure is of great interest.

Since the stress-strain behaviour of medium size sand at low levels of static loads has already been studied [El-Gammel,22], the present project aims in part to investigate the effect of particle size on the stress-strain behaviour of granular soils by conducting similar tests on two other sizes (coarse and fine) of the same type of sand. The other objective of this research is to study the cyclic

stress-strain behaviour of the sand by performing a series of cyclic tests on medium size Leighton Buzzard sand at the same levels of vertical stress under controlled lateral strain conditions.

The apparatus used in the investigation is the simple cubic true triaxial apparatus (SCTA) developed at the soil mechanics laboratory of Leeds University. The specimens tested are all cubic of 150 mm dimension but with different initial porosities. Details of the objectives of this research for each loading area are as follows.

1.6.1 MONOTONIC LOADINGS

A series of detailed tests were to be performed on very fine and coarse sands under static loading in order to

- Determine the stress-strain behaviour under confined, plane strain, and triaxial strain conditions.
- Study the effect of porosity, vertical and intermediate principal stresses on sand behaviour.
- Study the variations of lateral stresses under different stress-strain conditions.
- Obtain a clearer idea of the interparticle behaviour of the sand.
- Study the effect of the particle size on the stress-strain behaviour of cohesionless soils.

1.6.2 CYCLIC LOADING

Medium sand samples were to be tested under cyclic vertical principal stress conditions to investigate

- The cyclic stress-strain behaviour under confined, plane strain, and triaxial strain conditions.

- The influence of the frequency, amplitude, and the number of loading cycles on the stress-strain behaviour of the sand.

- The effect of the porosity of the sample on the cyclic behaviour.

- The elastic and plastic behaviour of the sand under successive loading cycles.

- The variations of lateral stresses under different stress-strain conditions.

- The inherent characteristics and interactions between particles, and finally

- to compare cyclic and monotonic loading behaviour of the sand.

All these tests are to be carried out at small lateral strains. In chapter two the simple cubic true triaxial apparatus (SCTA) is explained and the essential modifications and developments carried out, described. Testing materials and sample preparation techniques are described in chapter three. In chapter four the results of static tests on both coarse and fine sands are given and in chapter five the results of cyclic experiments on medium sand. The behaviour of sand under monotonic loading conditions and the interpretation of the tests results are discussed in chapter six. In chapter seven the behaviour of sand under cyclic loading conditions is discussed and some comparisons between tests results under monotonic and cyclic loading conditions are presented. Finally conclusions and recommendations for further research are given in chapter eight.

CHAPTER TWO

THE EXPERIMENTAL EQUIPMENT

2.1 INTRODUCTION

The apparatus used in this investigation is a true triaxial apparatus which was developed at Leeds University originally for static loading conditions. The lateral strain is controlled in two horizontal directions and the lateral stress in these directions is measured. The stress in the third direction (vertical) is also controlled and the strain in this direction is measured.

These test conditions can be applied to a sample either by using different internal and external radial pressures on a hollow cylindrical specimen or by loading cuboidal samples in such a way that different and independent stresses act upon their three sets of parallel faces. The first technique is comparatively complicated so the second was selected by El-Gammel [22] and a simple cubic triaxial apparatus(SCTA) was developed which allowed the testing of cubic samples under monotonic loading conditions. The apparatus was originally designed to study the behaviour of sand in small strains and under working vertical stresses rather than failure stresses. As one objective of this investigation was the study of the behaviour of sand under cyclic loading conditions the rig had to be modified. A full description of the SCTA is given by El-Gammel in chapter four

of his dissertation. The design principles and structural details of the SCTA are presented briefly in the following section. The necessary modifications to the sample container and development of the loading system are also fully described.

2.2 DESCRIPTION OF THE SIMPLE CUBIC TRIAXIAL APPARATUS (SCTA)

The details of the SCTA as used by El-Gammel [22] are shown in figure 2.1. It consists of a steel sample container of inside dimensions 150x150x150 mm. The internal faces of the container are covered with a very smooth material(poly-tetra-fluoro-ethylene, PTFE), which is then coated with a thin layer of silicon grease and sheets of thin rubber membrane(0.26 mm thick) to eliminate shear stresses as far as possible. Two of the container's side walls are fixed and the other two are moveable. The two fixed walls are firmly connected to each other, bolted and pinned in position to the rigid base. To ensure their rigidity appropriate stiffeners are fitted behind them. The two moveable walls are free to slide laterally on the base. A guide shaft of 15 mm diameter is connected to the centre of the outer face of each free wall. It passes through a linear bearing and terminates in a load cell which measures the total load carried by the free wall. The load cell forms a link between the guide shaft and a driven shaft which controls lateral movement, using a fine screw thread. The driven shaft terminates in a handle which can be rotated to move the wall inwards and outwards a controlled amount. The base of the sample container and the other parts of the

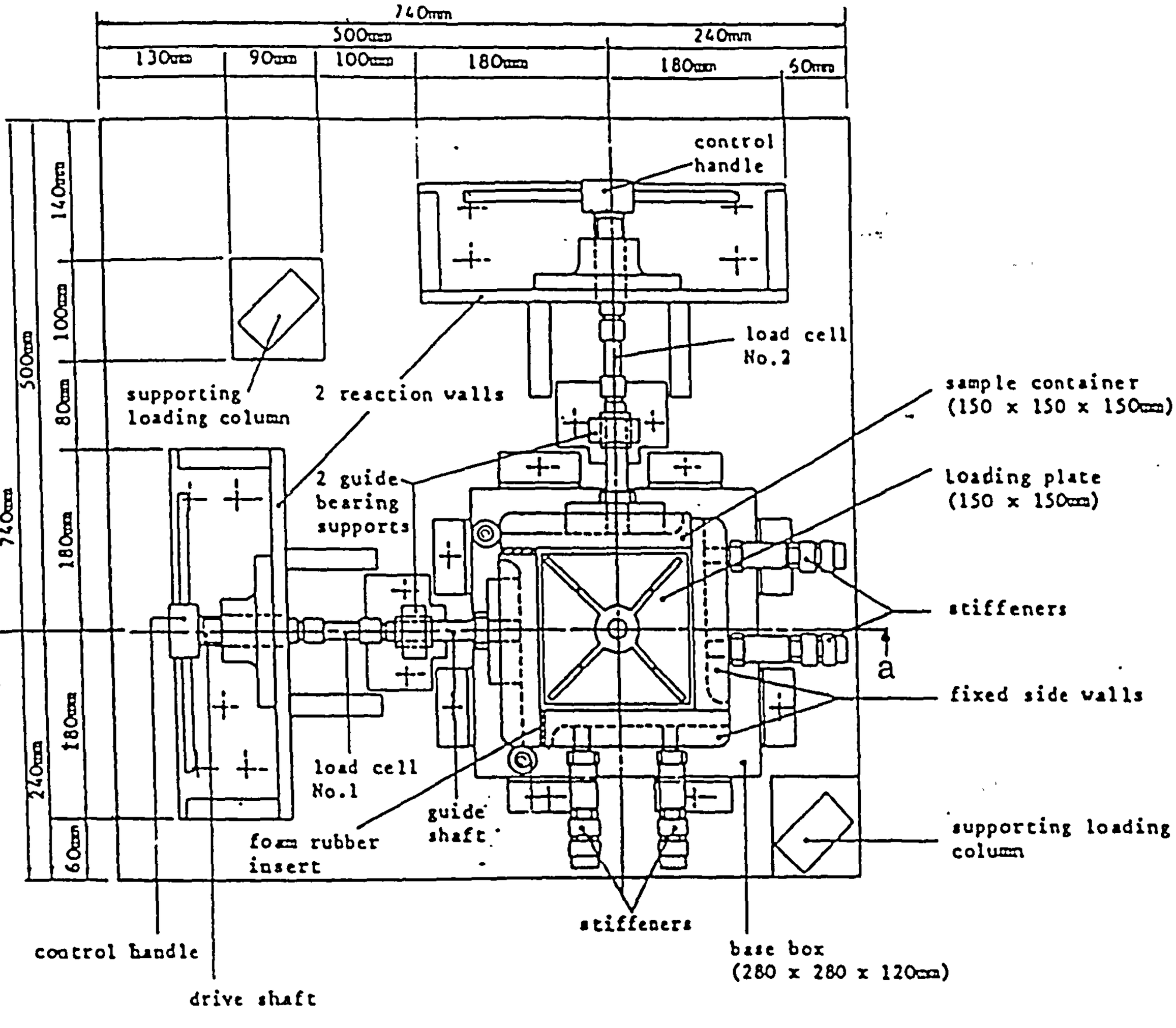

PLAN

dimensions in mm.

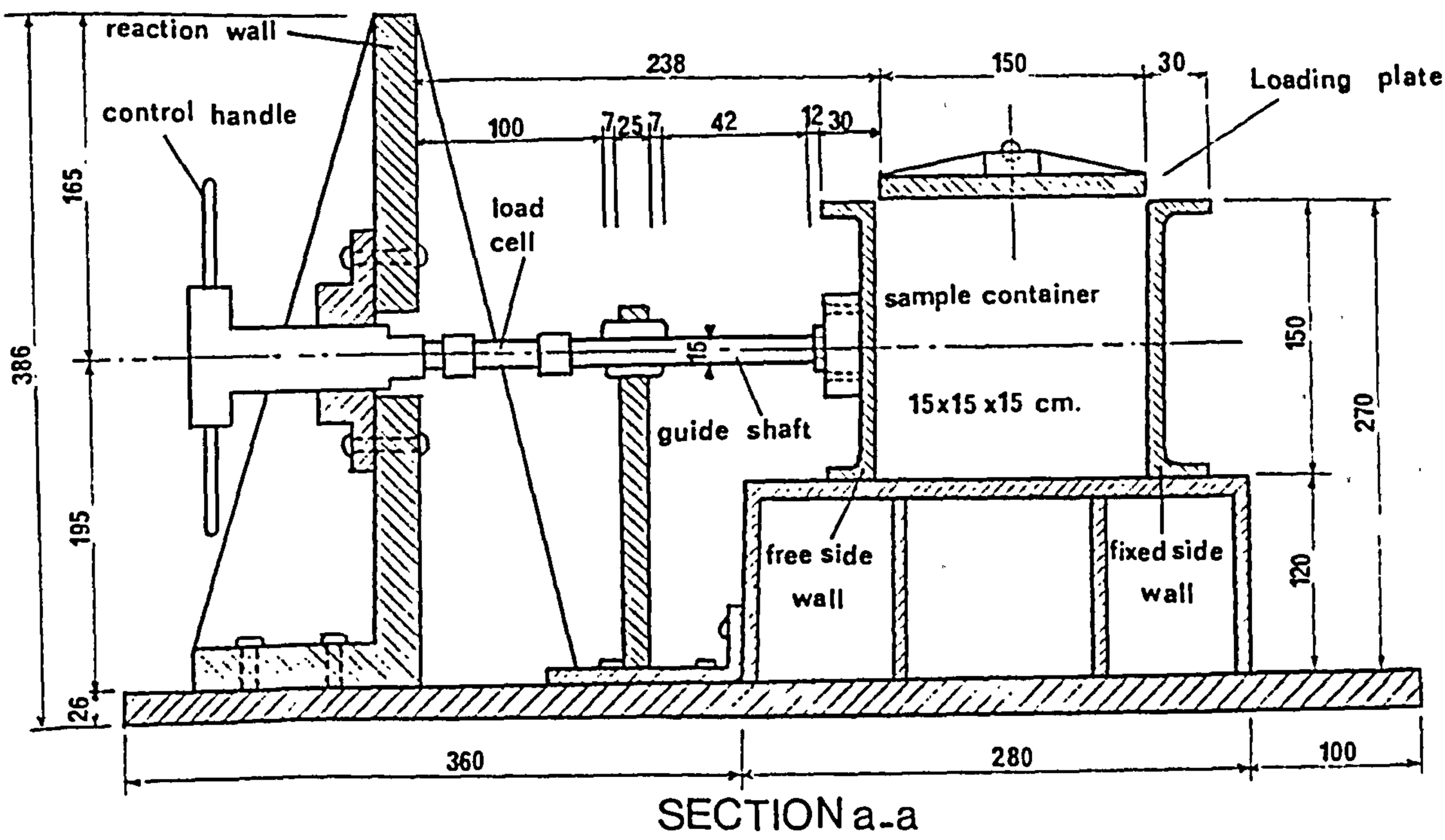

SECTION a-a

FIGURE 2.1 Details of the SCTA (El-Gammel 1984, 22)

apparatus are fixed on a thick steel plate of 740x740x26 mm dimensions.

The original loading system of the SCTA consisted of a simple lever arm, with a loading ratio of 20, which was loaded with dead weights. This lever arm system applied a vertical load to the loading plate of the SCTA via a ball bearing.

2.3 SPECIFICATIONS FOR THE MODIFIED SCTA

The SCTA described above was originally designed to study the stress-strain behaviour of sand under monotonic loading conditions. It had to be modified in order to perform cyclic loading experiments. The basic design requirements of the apparatus for the current investigation are as follows:

a) it should be capable of applying a principal stress system to the sample i.e. shear stresses on the faces should be zero.

b) the stress-strain conditions should be uniform and known in the sample.

c) the test rig should be able to apply and measure very small strains on the sample i.e. 0.01% vertical strain and 0.001% lateral strain increments.

d) the rig should be simple to construct and operate and be suitable for testing different grades of sand.

e) sufficient control of boundary conditions should be possible so that confined, plane strain and, triaxial tests can be carried out.

f) the loading system should be capable of applying both incremental monotonic and cyclic loads up to 450

kN/m^2.

The friction between the sand and faces of the container is reduced to a minimum level by using PTFE coated with silicon grease and a thin layer of natural rubber (0.26mm thick). The angle of wall friction was measured in the shear box apparatus under simulated test conditions and was found to be quite small. The maximum angle of friction measured was 3.5 degrees.

Applying different strain paths on the specimen using a cubic true triaxial apparatus is usually achieved by moving the four side walls of the sample container. In the SCTA for the sake of simplicity in construction and testing operations two of the vertical faces are fixed to the base and the other two are free to move, by which means the lateral strains are applied to the sample.

The maximum vertical stress that can be applied to the sample is 450 kN/m^2 which is equivalent to a 10 kN vertical load. This value was selected as being representative of reasonably high stress levels in practice and also is the highest value that could be applied using reasonably priced and readily available pneumatic systems that would allow cyclic loading. Investigation showed that to exceed this level for cyclic loading would entail the use of very expensive electro-magnetic loading systems. According to Reads [93] a vertical stress of 450 kN/m^2 should not cause appreciable crushing of the particles.

In order to study the behaviour of sand under working conditions (before failure occurs) the samples are subjected to small values of lateral strains (less than

0.75%). These strains are applied to the specimens in incremental steps of 0.033%. The uniformity of the strains of the sample and the accuracy of the apparatus in applying and measuring stresses and strains are fully discussed and explained in section 2.5.

2.4 OUTLINE DESCRIPTION OF THE MODIFIED SCTA

The general view of the SCTA after all modifications is shown in figure 2.2. Development of a new loading system and modifications of other parts of the SCTA were necessary. A detailed description of the loading system, measurement devices, and the data acquisition system is given in sections 2.6 and 2.7.

The main problems associated with the apparatus which had to be considered were:

a) friction on the faces of the sample container,

b) escape of sand from the container,

c) stiffness of the container,

d) stability of the free walls,

e) control of the lateral movements of the free walls,

f) the performance of the loading system.

Although friction between the sand and faces of the container is not zero (3.5 degrees maximum), it is not thought to be large enough to cause significant shear stresses, and therefore it can be assumed that practically the sample is under principal stress conditions. The escape of sand from the corners of the free walls was stopped by using 30 mm wide narrow pieces of very compressible rubber strip inside the gaps.

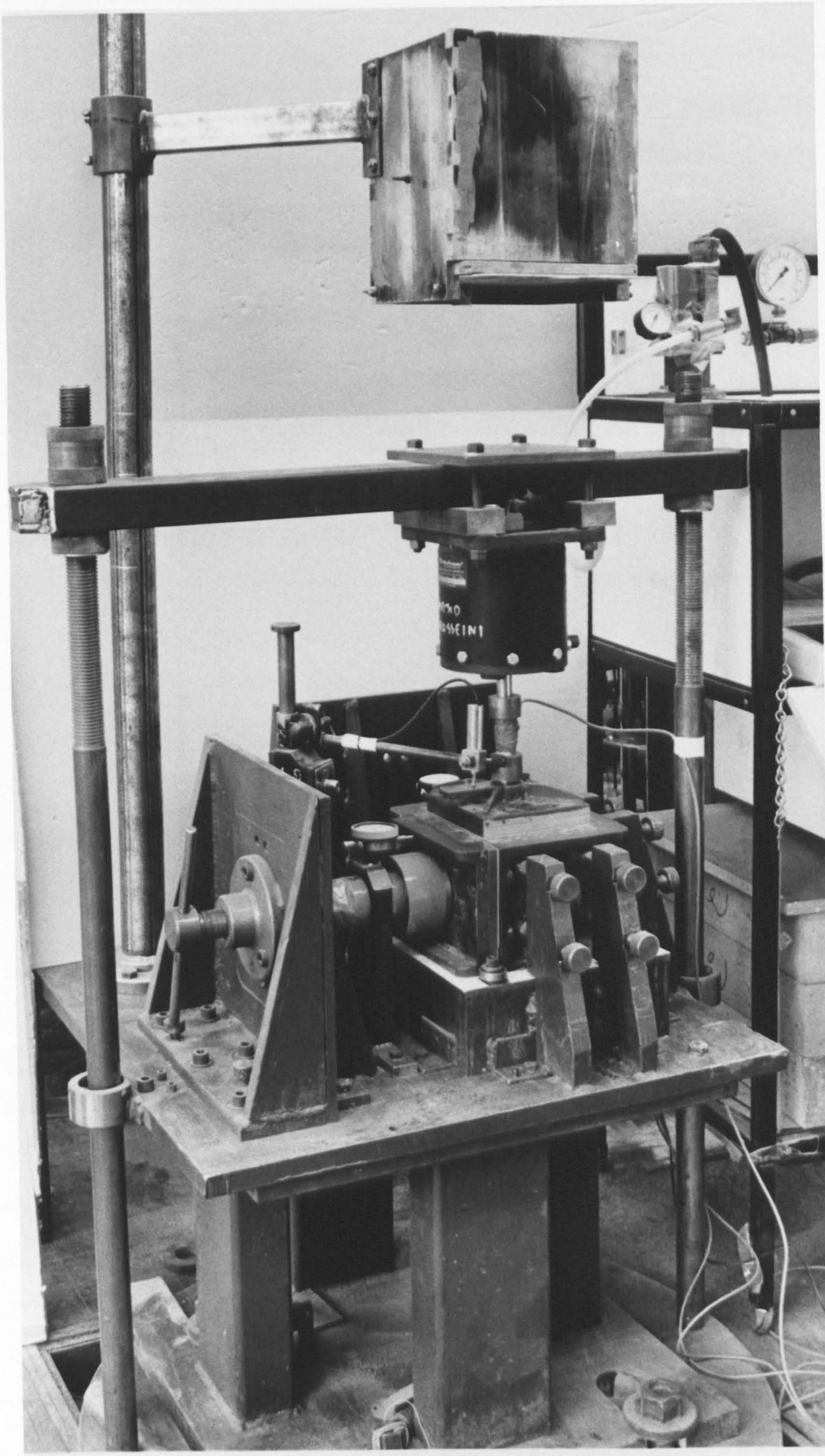

FIGURE 2.2 The SCTA modified for both monotonic and cyclic tests.

The next three areas(c,d,and,e) could potentially give rise to significant errors and required modifications which are described in section 2.5. The performance of the loading system and the method of controlling the new loading unit for producing different loading patterns are given in section 2.6.2.

2.5 ALTERATION OF THE SAMPLE CONTAINER

Since all parts of the original SCTA excluding the loading system were to be used in this investigation, an overall assessment of the performance of the equipment was carried out. The two fixed walls of the sample container were found to be sufficiently rigid and no measureable movements were observed. However the moveable walls and loading plate of the container seemed to suffer undesirable displacements. The amount of error and possible distortion of results introduced by these movements made modification of the container necessary.

2.5.1 DEFORMATION AND MOVEMENT OF THE FREE SIDE WALLS

The moveable walls of the sample container have to be rigid and capable of being fixed in their positions after being set to a particular constraint condition (e.g, confined, plane strain or triaxial strain). This is in order to preserve the uniformity of the specimen and the accuracy of the test. During initial checks the rigidity of these walls appeared to be low, .. and so further measurements were taken. Dial gauges were mounted at the top, middle and bottom of each free wall (three in each horizontal line) on their outer faces which measured the amount of movement at

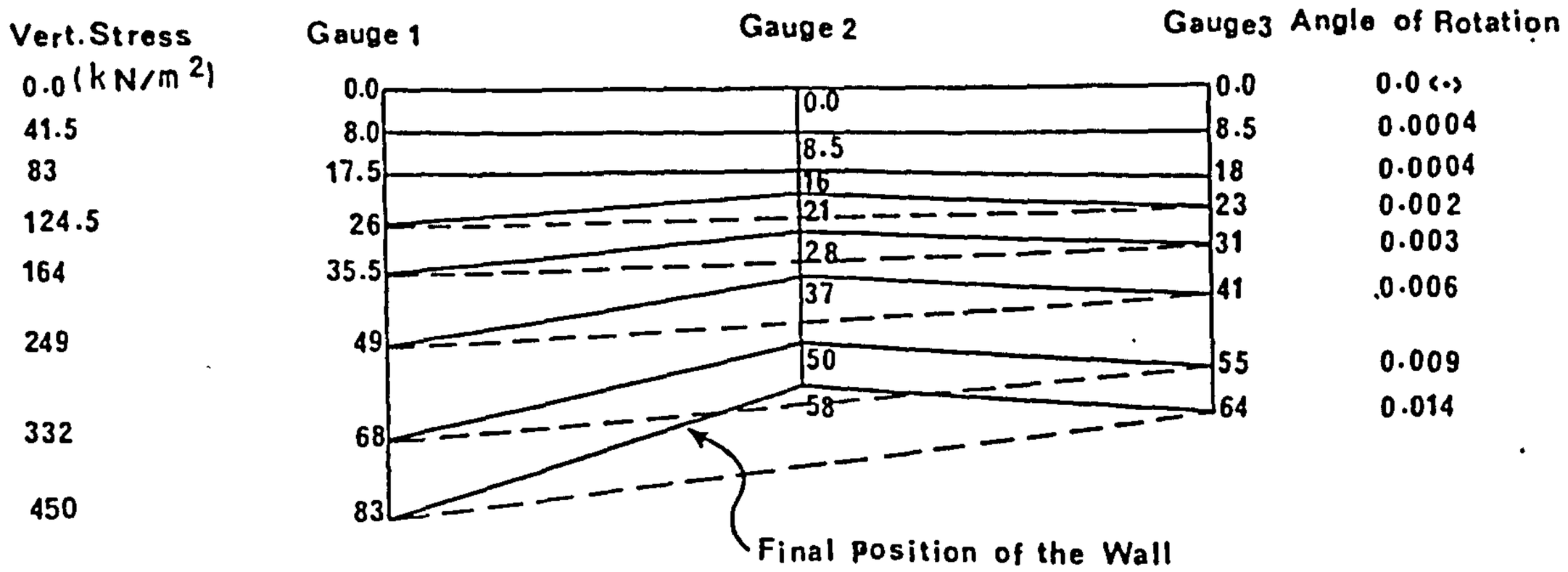

(gauge reading x.002 mm)

FIGURE 2.3 Typical deformation of the top edge of the free side walls under different vertical stresses.

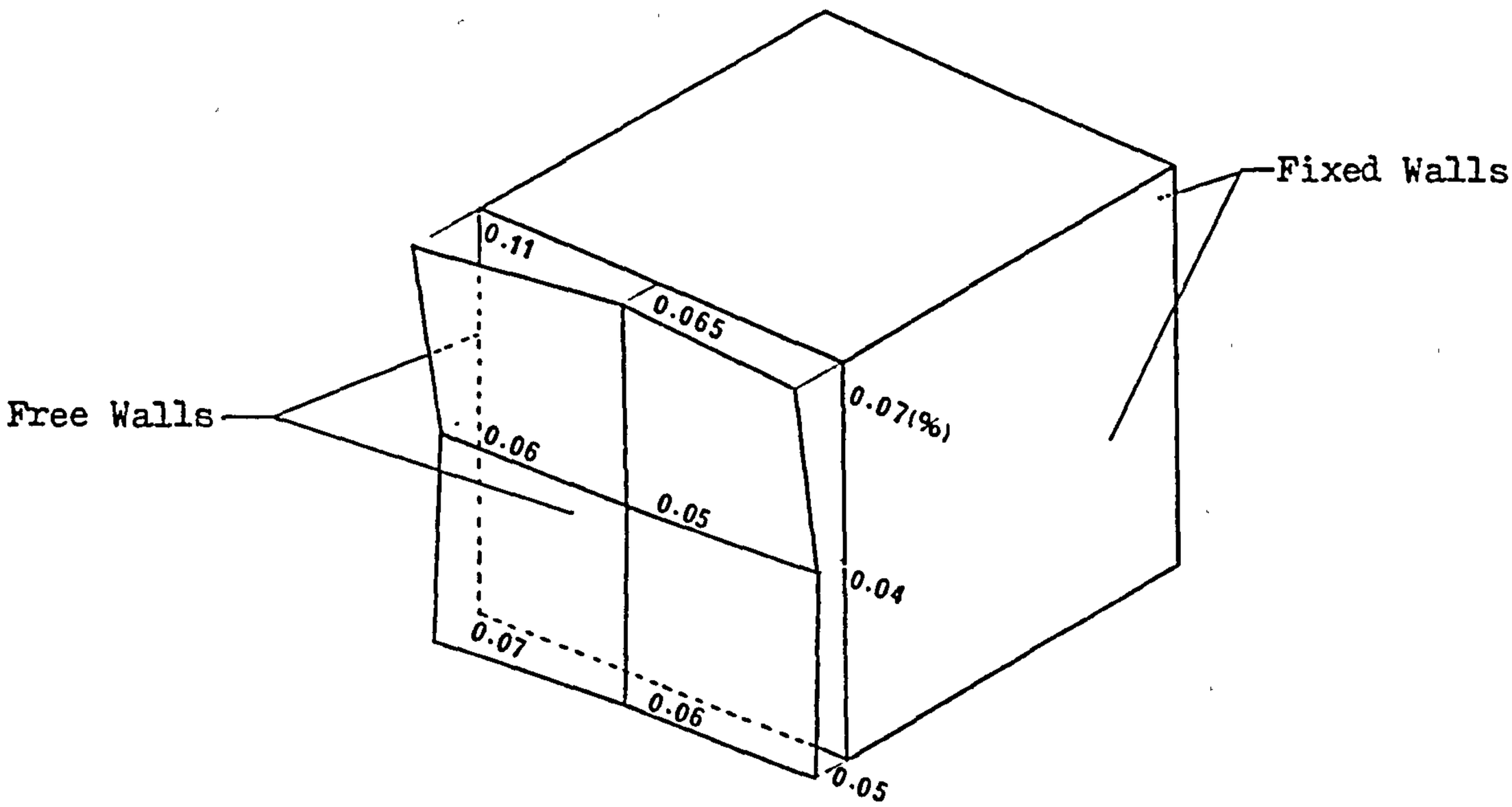

FIGURE 2.4 Strains induced due to deformation of the free side wall under maximum vertical stress before modification.

each point. The free side walls were set for confined (no-lateral strain) conditions and the container was filled with sand. During application of the vertical stress in steps up to the maximum value (450 kN/m^2) the movements of each face were recorded. Typical results for the top line of the wall under different vertical stresses and for all nine points under maximum vertical stress are shown in figures 2.3 and 2.4 respectively.

From figure 2.3 it can be seen that under small vertical stresses of up to 80 kN/m^2 nothing significant happens but as the load increases the wall tends to bend about its central support and to rotate about the right hand edge which is adjacent to the fixed side wall. Under maximum vertical stress both bending and rotation of the wall is quite clear. Figure 2.4 shows the resulting strains at the nine measurement points and the overall deformation of the wall is quite evident.

Although the values of the strains are small, El-Gammel [22] during his studies found sharp decreases in lateral stresses due to small lateral strains and that the main part of this variation took place before the lateral strain exceeded 0.2%. Therefore the uniformity of the lateral strains, which is one of the important advantages of this kind of true triaxial apparatus, can no longer be claimed.

In order to eliminate these errors it was necessary to identify their main sources. It is clear from the figures that the free walls not only bend about their centres but also rotate along their nearest edges to the fixed walls. While the first motion is mainly due to the elastic-

ity of the wall, the second may be attributed to the tolerance between the bearing and the guide shaft, which is connected rigidly to the wall, and also to the stiffness of the shaft. Therefore additional steel stiffening plates with the same dimensions and 12 mm thick were pinned to the interior faces of the free walls and the bending of the free faces was reduced significantly. The rotation of the free walls was more difficult to deal with. As the guide shaft transmits the total force on each wall to the load cell on the one hand it should not be too tight a fit inside the bearing to minimise any friction but on the other hand, too much tolerance will allow side movements of the shaft and accordingly movement of the wall. Therefore the amount of tolerance between the shaft and the support bearing has to be made as small as possible bearing in mind these restraints.

For these reasons the length of the support bearing was nearly doubled (from 39 mm to 65 mm) to keep the shaft in line more accurately. Also, the diameter of the shaft was increased from 15 mm to 30 mm to support the wall more rigidly and finally the support bearing was rebuilt to accommodate the new guide shaft with optimum tolerance.

A series of checking tests similar to those performed initially were carried out after the modifications. As the results show, in figure 2.5, the deformation of the free walls was reduced to an acceptable level and has no significant effect on the uniformity of the lateral strains.

2.5.2 DEFORMATION OF THE LOADING PLATE

The vertical load is transmitted to the sample via a loading plate on top of the specimen. The loading plate

was originally stiffened with webs and provided with a socket at its centre to accommodate a ball bearing. Before modifications of the free side walls, under vertical load the loading plate was tilting towards the corner of the container where the two moveable walls meet each other. This did not occur after the stiffening of the free walls. The only important factor therefore that needed to be controlled to avoid tilting was the initial position of the loading plate i.e. great care had to be taken to set it up horizontally.

The other problem associated with the loading plate was bending under high vertical load. Four dial gauges were mounted at its four corners and its vertical movements were recorded while the vertical load was increased to its maximum. It was found that as the vertical stress increased the loading plate tended to bend in a non-uniform manner. Figure 2.6 gives typical results of a test and although a large part of the overall movement is due to compressibility of the sand the bending of the plate, according to the differential movement of its corners, is quite clear under maximum load.

The bending of the top plate was reduced by increasing its thickness in a similar fashion to the modification of the side walls. A steel plate with the same dimensions and 15 mm in thickness was bolted and pinned firmly to the loading plate which reduced the amount of the bending effectively (fig 2.6). Details of the modified parts of the of the apparatus are shown in figure 2.7.

2.6 THE NEW LOADING SYSTEM

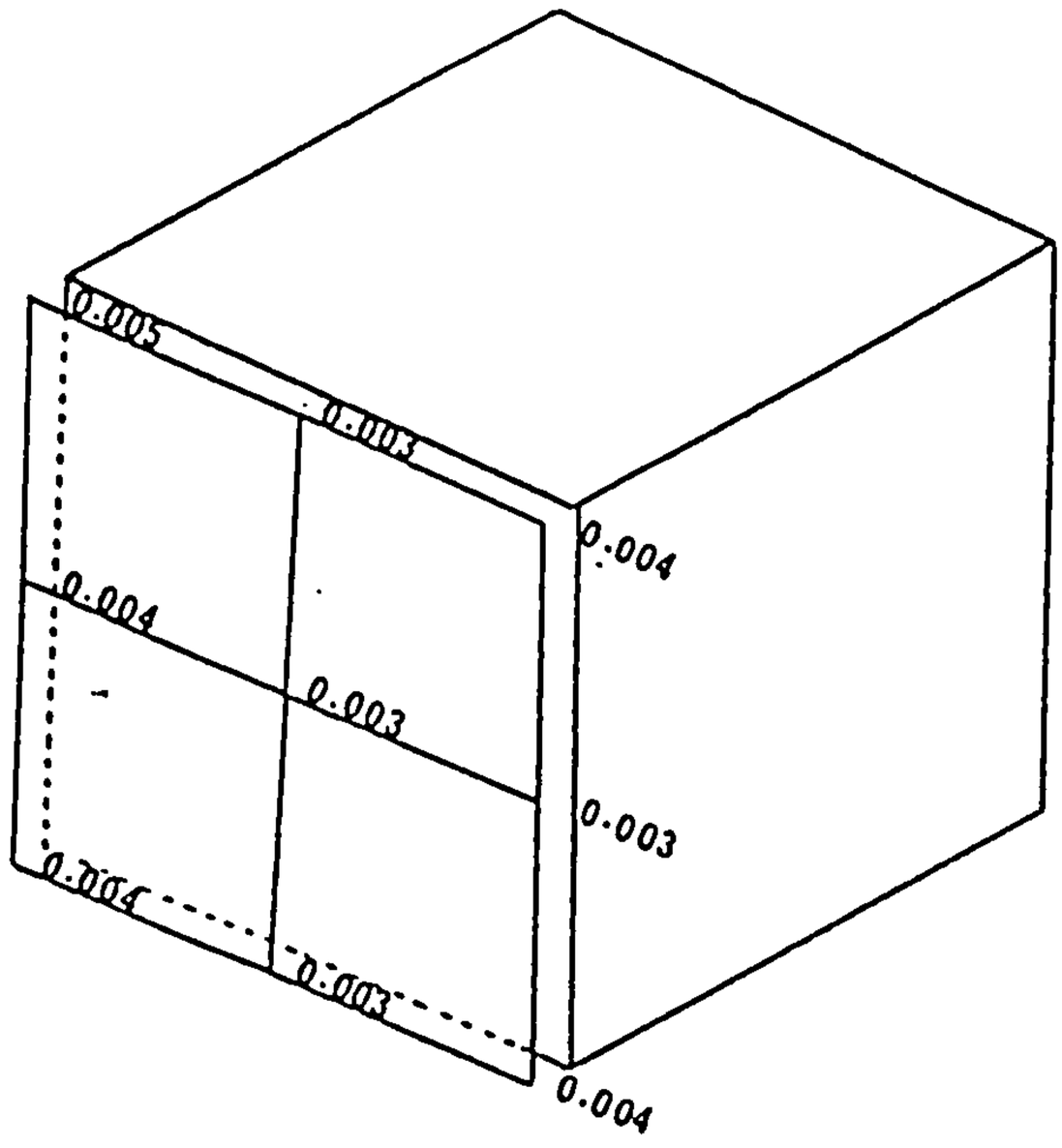

FIGURE 2.5 The lateral strains due to distortion of the free side wall under maximum vertical stress after modification.

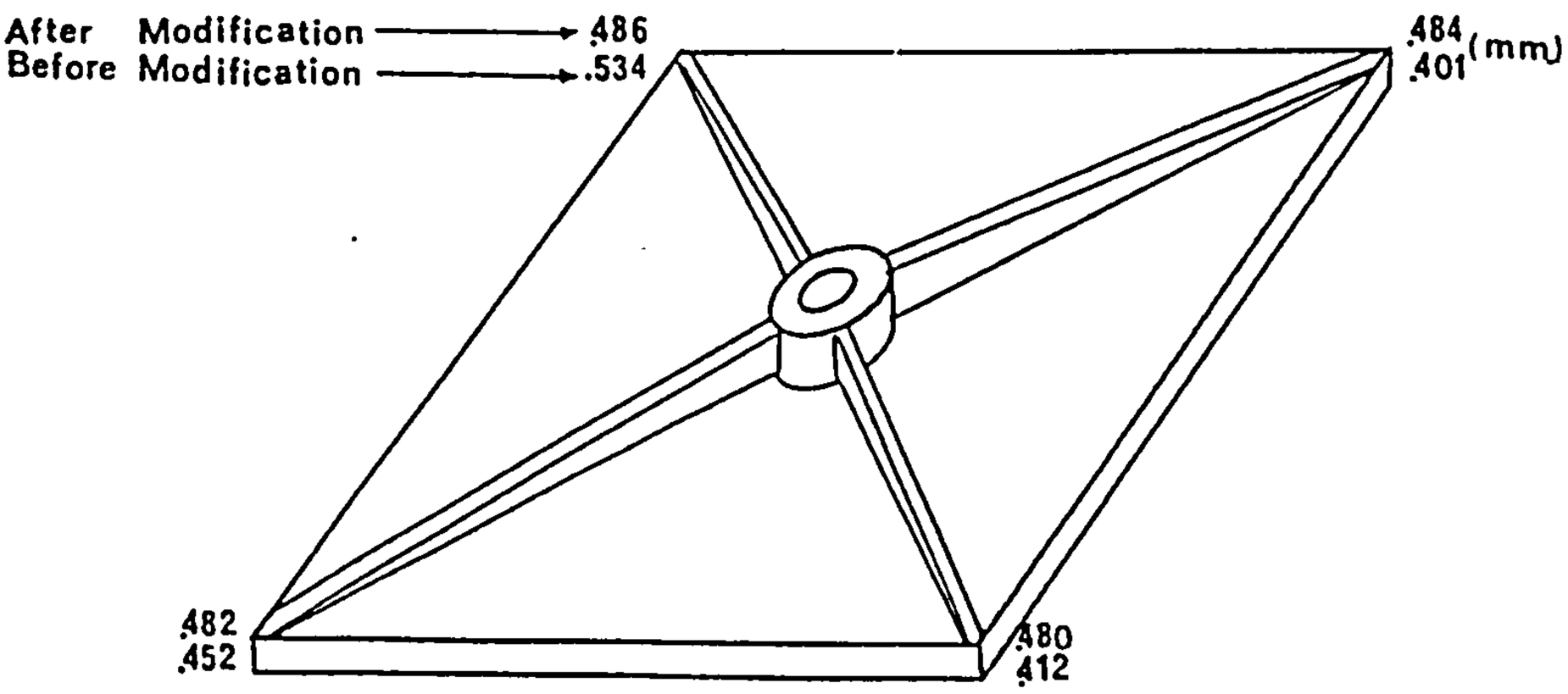

FIGURE 2.6 Variations in the vertical movement of the loading plate at its four corners under maximum vertical stress before and after modification.

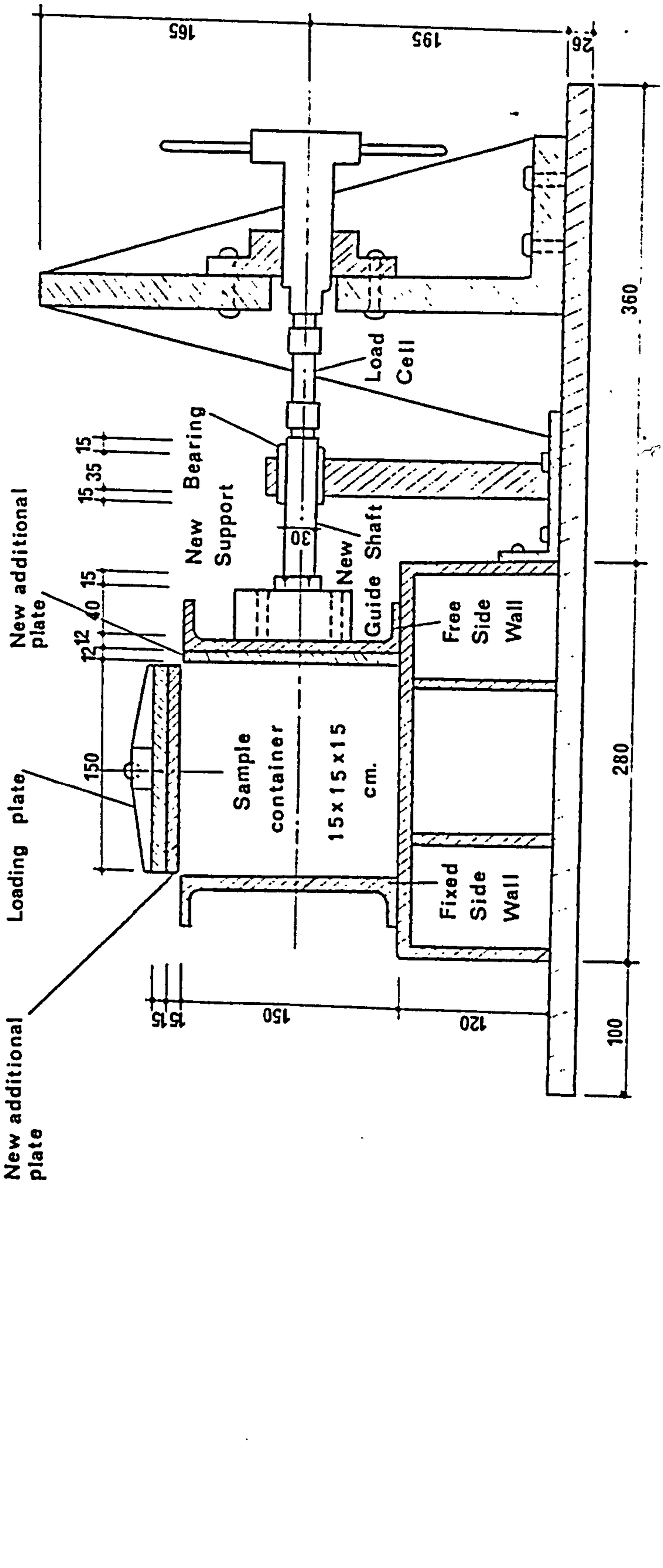

FIGURE 2.7 Cross-section of the modified SCTA.
(dimensions in mm)

As the main objective of this research was to obtain experimental data of monotonic and cyclic stress-strain behaviour of sand, the original loading system of the SCTA which was able to provide only a simple loading pattern had to be replaced by a new one capable of applying both monotonic and cyclic loads.

Different techniques can be used to provide cyclic loading e.g. mechanical, hydraulic, electrical, pneumatic, or a combination of these systems. The requirements for a versatile loading system capable of providing different loading patterns which was also easy to construct and operate coupled with the fact that a permanent compressed air supply existed in the laboratory suggested the use of a computer controlled pneumatic loading system as the most suitable for this research project. This system can be divided into the air cylinder (loading) and control sections which are explained below.

2.6.1 THE AIR CYLINDER AND SUPPORT FRAME

The vertical load is provided by a very low friction loss pneumatic cylinder. In the type selected a rolling diaphragm inside the cylinder is loaded by compressed air. The pressure acting upon the diaphragm is transmitted via a shaft. If the pressure is removed the shaft will return due to reaction of a return spring inside the chamber. Therefore altering the pressure of the compressed air will result in reciprocal movements of the shaft providing a cyclic loading capability.

As the maximum pressure of compressed air in the laboratory is 690 kN/m^2 (100 psi), to provide a vertical load

of 10 kN, equivalent to maximum vertical stress of 450 kN/m^2 on the sample, a cylinder with an effective area of 145 cm^2 was needed. A spring return air cylinder with a 155 cm^2 (24 sq.inch) effective area manufactured by Bellofram was used. The external dimensions of the cylinder are 200 mm height and 150 mm diameter.

The cylinder is mounted above the sample over the centre line of the container on a steel frame which consists of two solid steel rods, 40 mm diameter, acting as columns, and a box section of 90x50x6 mm as the beam which is designed to carry the maximum force with low deflections. The air cylinder can be lowered to touch the loading plate by moving the beam down along the threaded parts of the columns. Since the sand is deposited inside the container by a raining technique(see chapter 3) the beam also has to be moved to the side during this stage. For this reason it is slotted on one side which enables the beam to rotate about the other side and so be moved from its position above the sample container.

As the original base plate of the apparatus was not large enough to accommodate the loading frame a new larger circular base plate of 30 mm thickness was put under original one and the loading frame was rigidly fixed to this new plate. In order to additionally stiffen the columns they are supported by two adjustable braces approximately half way along their length. The air cylinder and loading frame are shown in figure 2.8.

2.6.2 THE LOAD CONTROLLING SYSTEM

The pressure of the compressed air sent to the

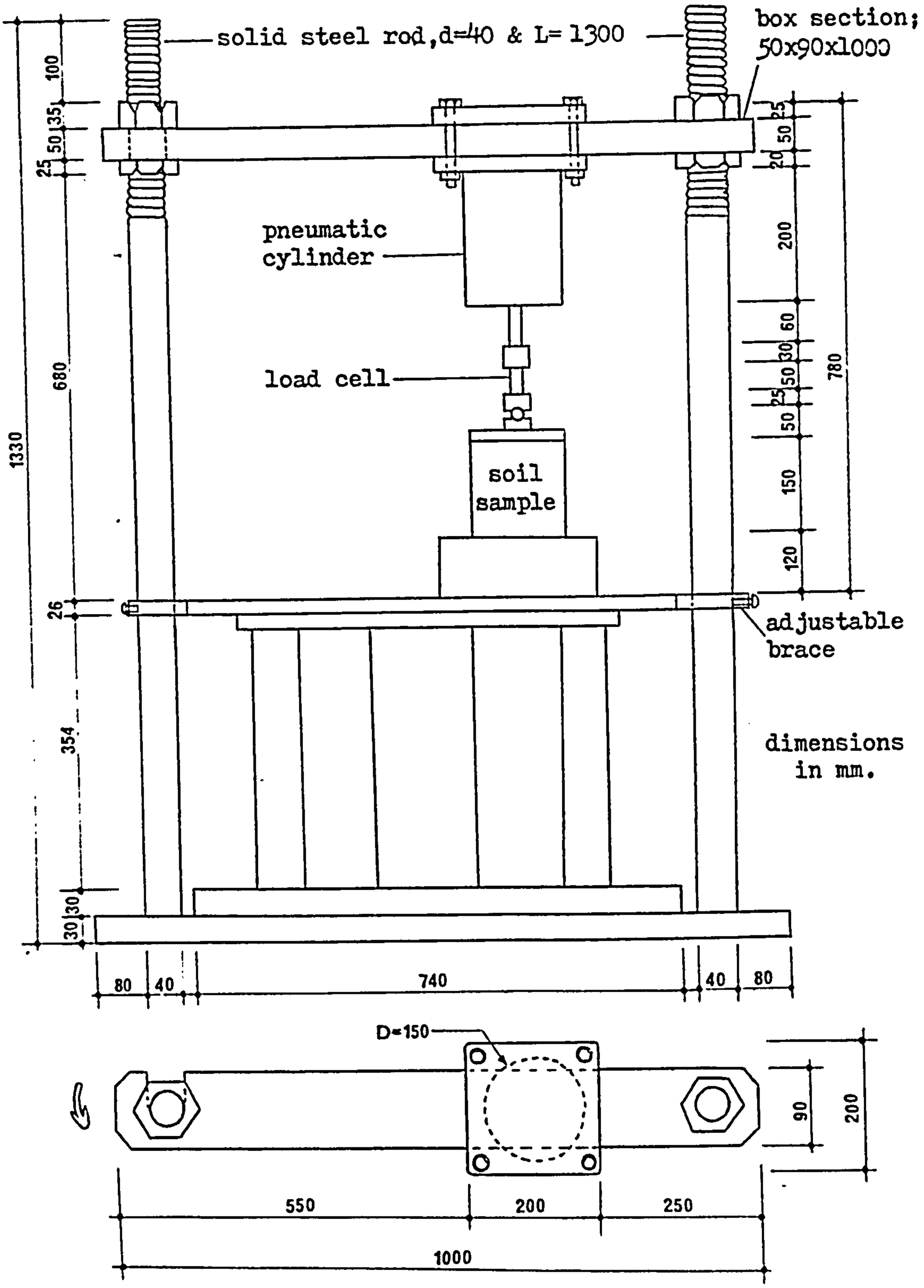

The beam of the loading frame (plan).

FIGURE 2.8 A simplified diagram of the air cylinder and loading frame.

pneumatic cylinder is controlled by an electro-pneumatic converter and a micro-computer. The converter used in this system is a digital electro-pneumatic 100D model, manufactured by John Watson & Smith Ltd. It consists of two main parts. The first part is an electronic interface which receives the digital signal (0 to 255, for changing the air pressure from 0 to the maximum) from the computer and converts it to an analogue signal. The second part is a mechanical device which regulates the pressure of the compressed air. This is done by passing the air through a nozzle against which a controlling diaphragm suspended in a magnetic field, is acting. The space between the nozzle and diaphragm is adjusted by altering the magnetic field which is controlled by the digital input.

The signals for the converter are generated using a BBC micro-computer. The frequency, amplitude and number of the cycles are controlled by software. The fastest cyclic load with a maximum 450 kN/m^2 peak produced by this system is 0.1 Hz. In fact cycles with frequencies greater than 0.1 Hz. can be produced but their maximum amplitude is reduced. This is due to the time required for the pneumatic cylinder and the mechanical part of the converter to respond i.e. it is due to the time needed for sufficient flow of air to occur to cause the required pressure and also for the air to exhaust. A special computer programme was written by which almost any shape of loading diagram can be produced e.g. sinusoidal, rectangular, triangular, etc. Monotonic loads can be applied to the samples using this loading programme or manually. Typical sinusoidal loads with the maximum am-

plitude obtained are illustrated in figure 2.9. A schematic diagram of the new loading system is shown in figure 2.10.

The performance of the loading system was examined under different patterns of loads and the stability of the applied loads over a period of time was checked. The vertical stresses were applied to the sample in increments of 10 kN/m^2 and the loading was continued up to the maximum level of the vertical stress (450 kN/m^2). Cyclic loads with different shapes, frequencies and amplitudes were also produced and examined at this stage. The loading system was found to operate well for the ranges of frequencies below 0.1 Hz and the vertical load was stable over time. A constant pressure loss of 10 kN/m^2 (1.5 psi) in the converter was found which of course did not affect the results because the ultimate vertical load applied to the sample was measured using a load cell directly connected to the specimen.

2.7 THE MEASUREMENT DEVICES

Measurement is one of the most sensitive and critical operations in experimental studies and it is here that errors are likely to occur. For this reason great care was taken in selecting instrumentation and calibrating it. In the SCTA the normal stresses and strains on the boundaries of the sample had to be measured.

2.7.1 STRAIN MEASUREMENT AND CONTROL DEVICES

As the samples were tested under lateral strain-controlled conditions the two horizontal lateral strains were monitored by two dial gauges fixed at the top of the support bearing. To apply a lateral strain the handles of

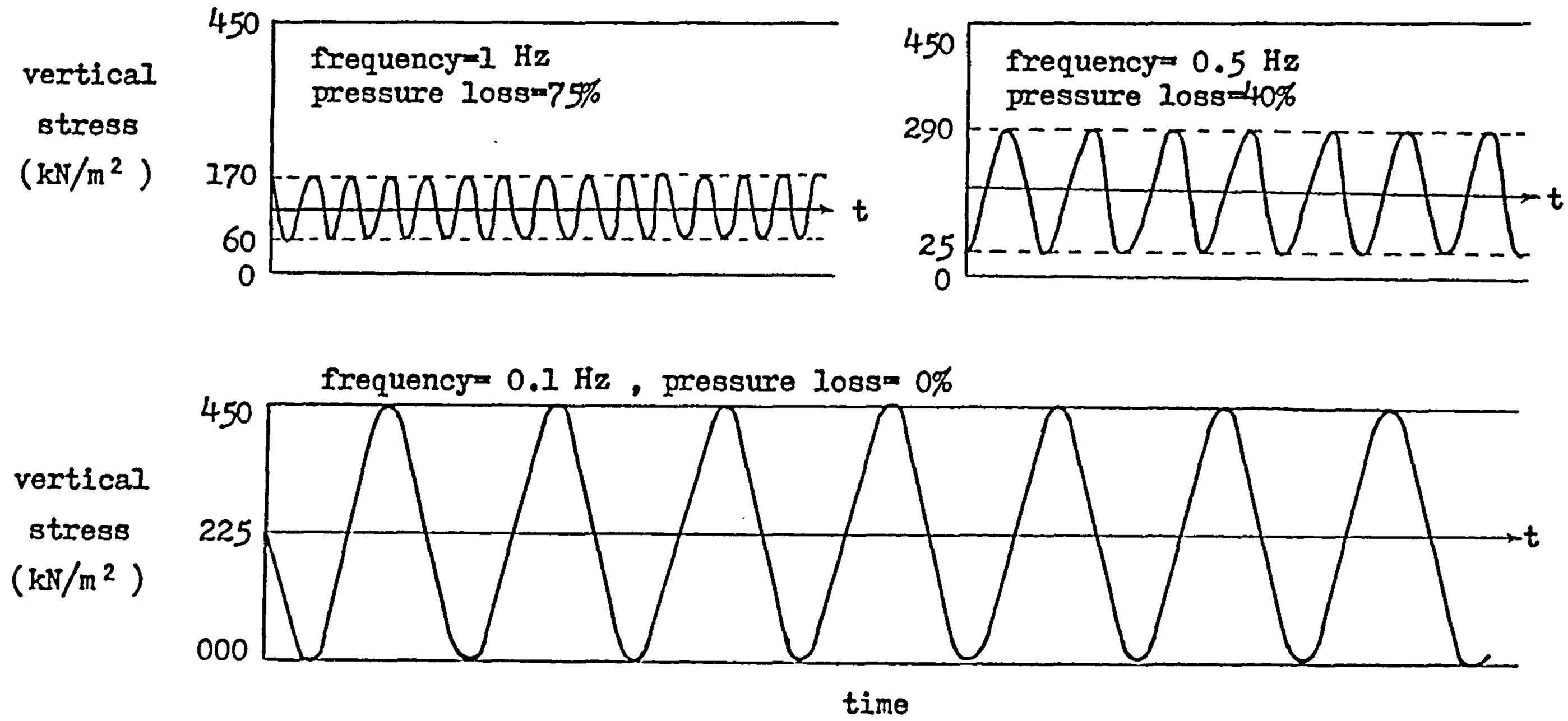

FIGURE 2.9 Maximum cyclic loads with different frequencies provided by the new loading system

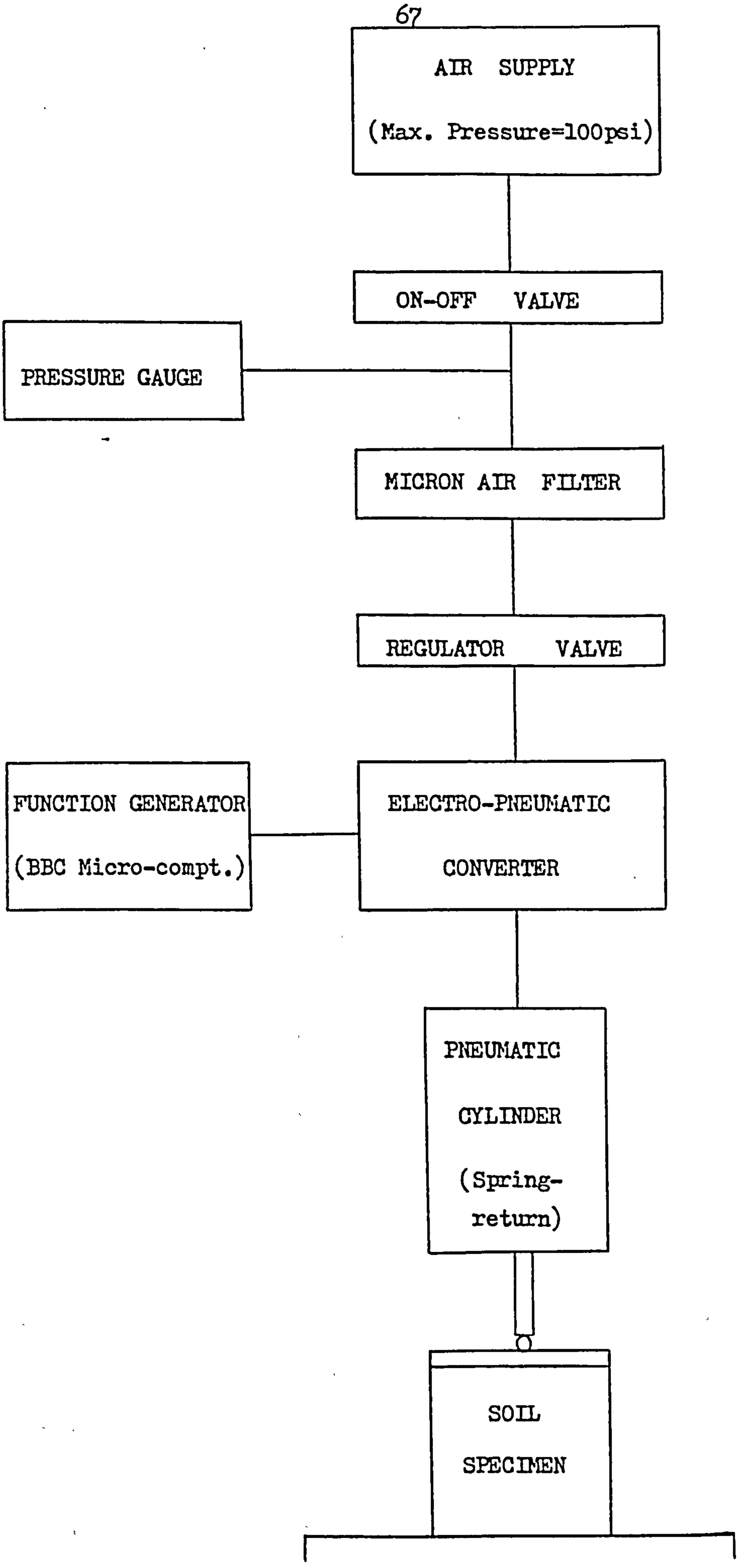

FIGURE 2.10 Schematic diagram of the cyclic and monotonic loading system.

the driven shafts were turned which allowed the side walls to move outwards. The amount of total movement of the side walls was measured by the dial gauges. These dial gauges had a resolution of 0.002 mm which is equivalent to 0.001% lateral strain.

The vertical strain could not be measured by a dial gauge since cyclic loads were applied to the sample as well as monotonic. Therefore a linear variable differential transducer (LVDT) was used (D2/100 model from RDP Electronics Ltd., manufactured in the UK). The LVDT was mounted on a special platform near the container in contact with the loading plate and was able to measure up to ± 12 mm of vertical movement. It was carefully calibrated using the micrometer calibration table in the laboratory. The resolution of the LVDT was found to be 0.02 mm which allows measurement of the vertical strain to 0.01%. Finally a d.c power supply (PL-320 model, made by Thurlby Ltd.) capable of supplying a constant and stable voltage was used to power the LVDT during operation.

2.7.2 STRESS MEASUREMENT DEVICES

The total forces acting upon the three independent faces of the container were measured by three load cells. Knowing these forces the principal stresses can easily be calculated. The principles of design and performance of the three load cells were the same the only difference being in the maximum design load for the vertical and horizontal load cells. As the ratio of lateral to vertical stress was not expected to exceed 0.5 [El-Gammel, 22] the design load for the lateral load cells was 5 kN and that for the vertical

load cell 10 kN.

Each load cell consists of a hollow aluminium cylinder with a pair of loading caps which fit into the ends of the cylinder. The caps are recessed at one end to accommodate ball bearings and have the same internal diameter as the hollow cylinder at the other end to fix into the cylinder. The reason for using caps is to avoid damaging the load cell body and to distribute the load uniformly over the cross-section of the cylinder.

The load cells operate by using electrical resistance strain gauges bonded to their bodies. The strain gauges form a Wheatstone bridge and as the cylinder compresses under load their resistance changes and this changes the output voltage of the bridge which has a constant input voltage. The output voltages can be related to the applied load by calibrating the load cell.

The type of strain gauges used are rosette PC 5-11, 5 mm length, 120±0.3 Ohm resistance and gauge factor 2, manufactured by Tokyo Sokki Kenkyuio Co. Ltd. Two rosette strain gauges were fitted on opposite sides of the cylinder to form the full Wheatstone bridge which compensates for temperature fluctuations. The surface of the cylinder was first degreased and cleaned with Chlorothene SM solvent then the strain gauges were glued using Ultra Superglue. Next they were clamped in position on the cells while the Superglue cured in the oven at 120° C for 2 hours. The strain gauges were then wired so that they formed a full bridge circuit. The cell bodies were coated using a special rubber compound (Sealing Compound 2114-5) to protect the strain

gauges.

The load cells were calibrated using an oedometer apparatus. Forces upto the design loads were applied to the load cells in increments and the resulting output voltages were recorded at each step. A number of loading and unloading cycles were carried out to eliminate any hysteresis effects and to ensure a linear response from the load cells. These procedures were repeated after each main series of tests in order to check the performance of the load cells. No significant drifting in the output voltages and changes of the calibration factor were observed. The calibration graphs are linear and the response was repeatable to about 1%.

Using the calibration factor, as the resolution of the data logger unit was ±0.003 mV, the sensitivities of the lateral load cells were found to be ±0.45 kN/m^2 and that of the vertical load cell ±0.9 kN/m^2 . These results for the measurement of the lateral stresses, which change approximately from 0 to 200 kN/m^2 ,and for the vertical stress which ranges from 0 to 450 kN/m^2 are quite acceptable.

Finally a d.c power supply similar to that used for the LVDT was employed to energise the three load cells. Typical circuits and the dimensions of the load cells with end caps are shown in figure 2.11.

2.7.3 THE DATA ACQUISITION SYSTEM

The data acquisition system is based on a data logger controlled by a micro-computer. The output voltages from the load cells and the LVDT. are sent to the data logger unit. They are converted from analogue to digital forms

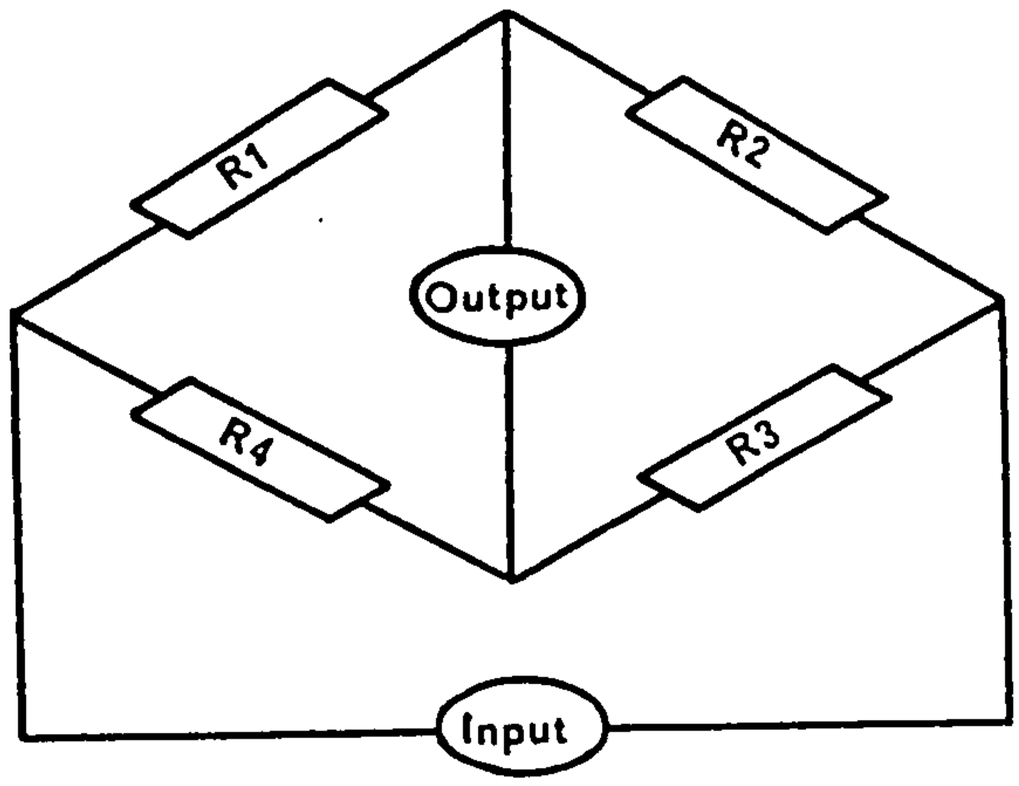

Typical circuit used in the load cells.

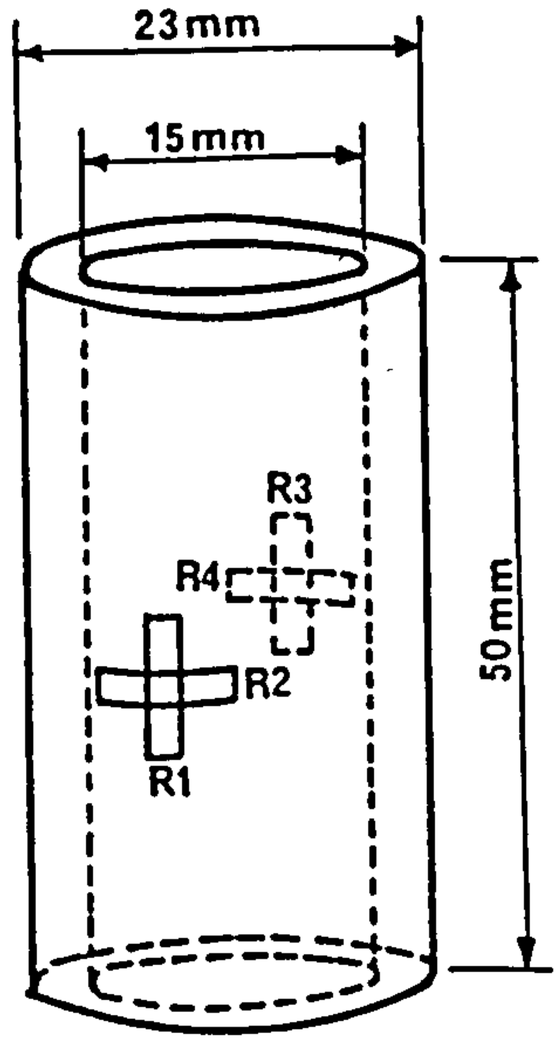

Body of the vertical load cell.

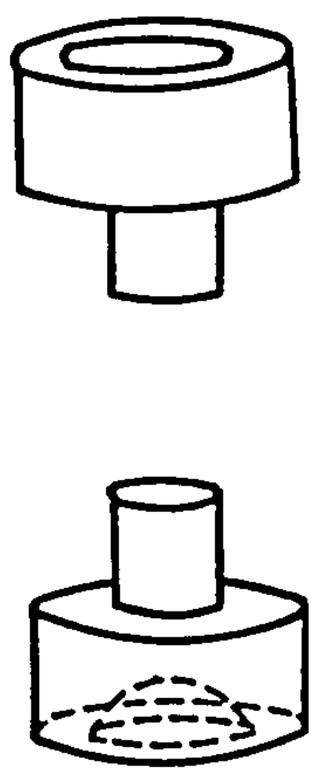

The end caps.

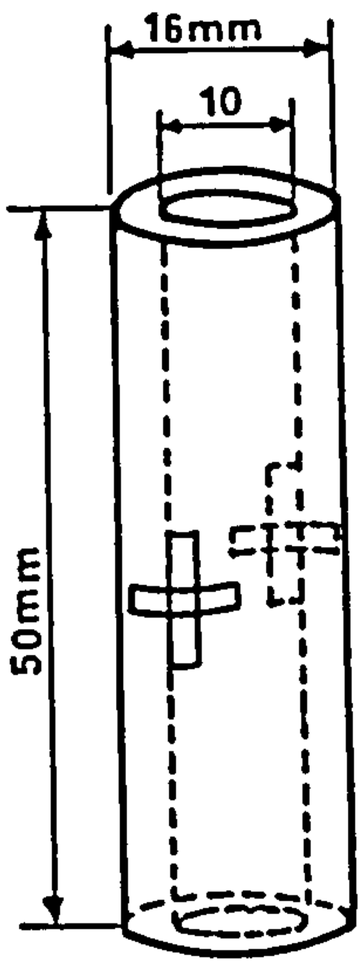

Body of the lateral load cells.

FIGURE 2.11 Typical circuit and load cell dimensions.

by the data logger. The digital results are then read by a micro-computer and saved on floppy disks. The results could be directly analysed by the micro-computer or transmitted to the university's main frame computer. During this investigation the second method was used to allow the use of other plotting facilities.

The data logger used in this research is a multi functional instrument (MFI), model 1010, manufactured by CIL Electronics Ltd.(UK). It has twelve channels and can be expanded. The MFI is a programmable unit which can communicate with the micro-computer. A special programme was written by which the whole data reading procedure; scan intervals, number of channels in use, filtration of scan etc., could easily be monitored. The resolution of the MFI is ±0.003 mV and the fastest scan rate is 1 sec. for each channel.

The micro-computer linked to the MFI is an Apricot model F1 made by ACT Ltd.(UK). It has 128K memory and accepts both single and double sided floppy disks. Although it can be fitted to any electronic interface easily (a delicate operation) complex and lengthy technical support were required to join the whole system together to achieve a satisfactory result. A schematic diagram of the data acquisition system is shown in figure 2.12.

2.8 SUMMARY AND CONCLUSIONS

The apparatus used in this investigation is a true triaxial device with fully rigid (lubricated) boundaries, originally developed by El-Gammel [22] for monotonic stress-strain studies of the sand. It has been further developed

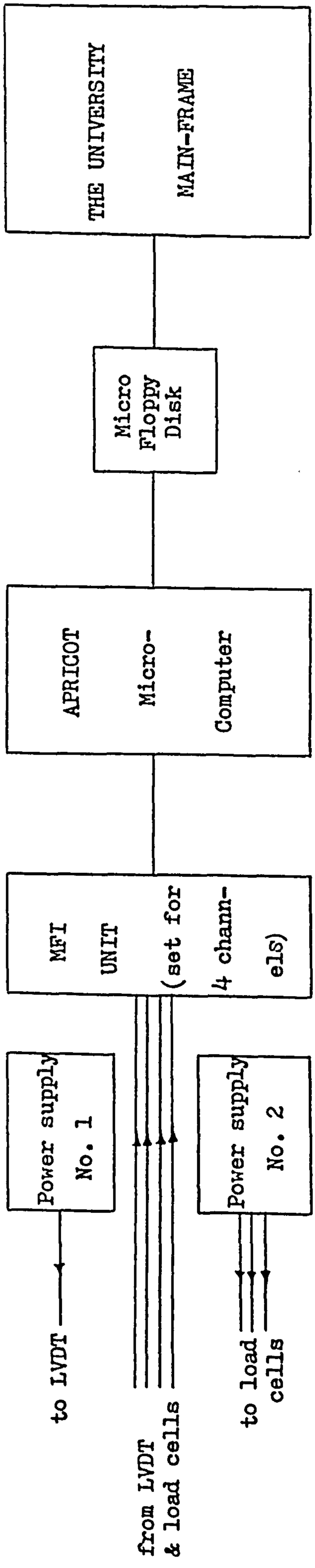

FIGURE 2.12 Schematic diagram of the data acquisition system

for both monotonic and cyclic loading conditions. The performance of the equipment was carefully checked and some problems were identified. The sources of errors were studied and the necessary modifications were carried out which improved the performance of the equipment.

A pneumatic computer controlled loading system was constructed which allowed monotonic and cyclic loads to be applied to the specimen. The measurement system was designed to enable automatic logging of the test results. The data were read by a data logger linked to a micro-computer and saved using floppy disks. They were then transferred to the university's main frame for analysing the tests results. The general view of the whole testing equipment used is shown in figure 2.13.

FIGURE 2.13 The general view of the SCTA modified for both monotonic and cyclic tests, with load controlling system and the data acquisition unit.

CHAPTER THREE

TEST MATERIALS AND SAMPLE PREPARATION

3.1 INTRODUCTION

The stress-strain behaviour of granular materials, as mentioned in chapter one, is highly complex and affected by several factors. These factors must be controlled but without limiting the applicability of the results obtained. The sand particle size distribution is one of the most important factors which needs to be accurately reproduced in laboratory studies. Experiments performed on homogeneous samples of uniformly graded granular materials will help to clarify the effect of other factors such as the porosity of the sample, confining pressure, stress history, drainage conditions, etc, on their stress-strain behaviour. The experiments can then be repeated with the same test conditions but using other sized sands in order to study the influence of particle size. The uniformity of such samples in the laboratory has to be controlled carefully, otherwise erratic results are inevitable.

In this investigation homogeneous samples of various sized uniform sands were prepared with different porosities. The method of preparation was based on the work of Kolbuszewski [50] on uniform sand samples in the laboratory which is described later in section 3.3.

3.2 TEST MATERIALS

Different grades of Leighton Buzzard sand ranging from coarse to very fine were used in order to study the stress-strain behaviour of sands over the whole size range. These materials are prepared and classified from a natural silica sand by the David Ball Company Ltd. in the UK.

The first group(A) is a very fine sand quite close to coarse silt in the soil classification system. The particles of this sand have an angular shape and are between 0.024 mm and 0.15 mm in size with an average of 0.085 mm. Their specific gravity is 2.67 and the maximum and minimum porosities obtained in the laboratory were 51% (e=1.04) and 42% (e=0.72) respectively. Group B is a medium sand with sub-angular particles of between 0.12 mm and 0.84 mm in size, an average of 0.48 mm and specific gravity of 2.65. This material is the same as that which El-Gammel [22] used in his investigation on the static stress-strain behaviour of sand. The maximum and minimum porosities of this sand were 44% (e=0.78) and 33% (e=0.49) respectively. The third group(C) is a coarse sand with the same particle shape as B and between 0.32 mm and 2.0 mm in size. The average particle size is 1.1 mm with a specific gravity of 2.68. The maximum and minimum porosities were 45% (e=0.81) and 34% (e=0.51) respectively.

The specific gravity of the materials was measured in the laboratory according to the method defined in B.S. 1377 [134]. The minimum porosity given above is the densest condition of the sand produced by the raining technique(this is explained in the next section) and the maximum is the

loosest case produced by pouring into a container using a scoop. As the stress-strain response of sand B under monotonic loads was studied by El-Gammel [22], this material was mainly used for cyclic tests in this investigation. The other two groups(A and C) were subjected to monotonic loadings to complete the stress-strain data over the complete sand size range. All three types of sands tested were in an air dried and clean condition. Particle size distributions and micrographs of the materials are given in figures 3.1 and 3.2 respectively.

3.3 THE SAMPLE PREPARATION TECHNIQUE

Different techniques can be used to prepare dry sand samples in the laboratory e.g. by compaction, vibration, raining, etc. What was required in this research was a method which will produce a uniform dry sample of the desired porosity. Compaction and vibration could not produce a sample with an acceptable degree of uniformity as some preliminary tests showed. In these tests each sample was prepared in 5 layers each 3 cm thick and the porosity of each layer was measured and compared (figure 3.3). Therefore the raining technique was used to deposit sand in the sample container of the SCTA. The general principles of this method are based on the fundamental work carried out by Kolbuszewski [50] in 1961. In this , he established a new method for preparing sand samples for laboratory testing.

In this method the sample container is filled by allowing the sand to fall from a certain height at a certain flow rate. Increasing the height of fall will lead to an

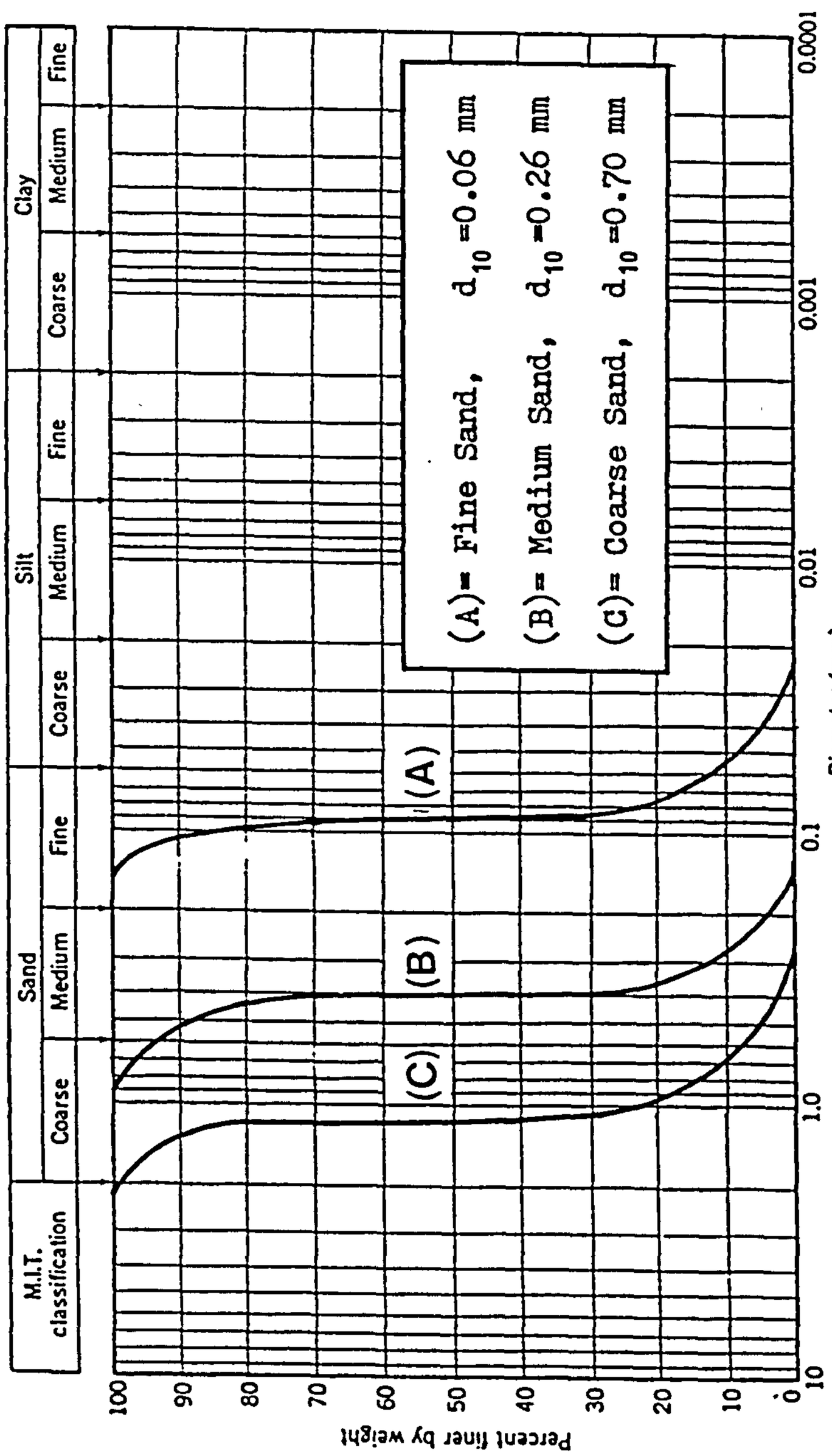

FIGURE 3.1 Particle Size Distribution of the Test Materials.

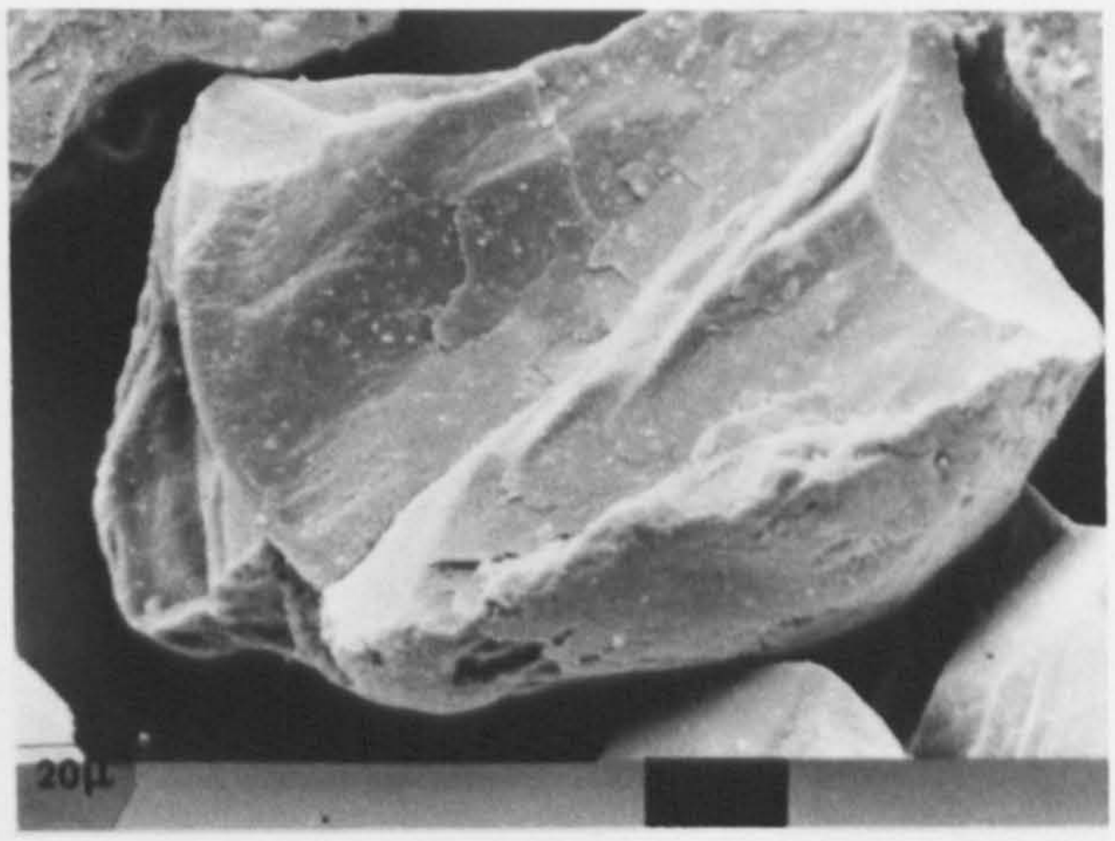

Fine sand (group A)

Medium sand (group B)

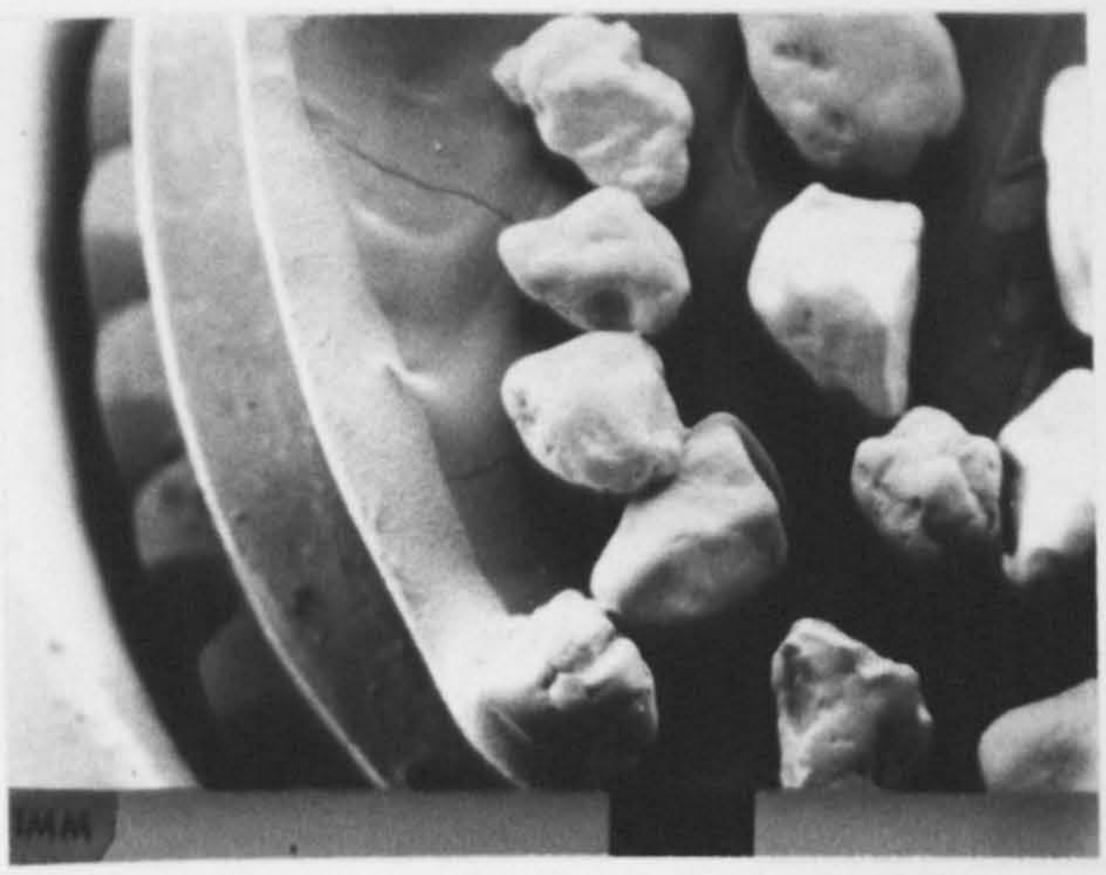

Coarse sand (group C)

FIGURE 3.2 Micrographs of the test materials.

e=0.76	n=43.2 %	5th layer	e=0.67 n=40.1 %
e=0.69	n=40.8 %	4th "	e=0.89 n=47.0 %
e=0.58	n=36.7 %	3rd "	e=0.96 n=48.9 %
e=0.64	n=39.0 %	2nd "	e=0.75 n=42.8 %
e=0.51	n=33.7 %	1st "	e=0.82 n=45.0 %

Sample of fine sand (A), compacted by a 1 kg weight (40 blows/layer).

Sample of fine sand(A),vibrated by a plate vibrator(20 sec./layer).

e=0.56	n=35.8 %	5th layer	e=0.61 n=37.9 %
e=0.52	n=34.2 %	4th "	e=0.53 n=34.6 %
e=0.60	n=37.5 %	3rd "	e=0.58 n=36.7 %
e=0.58	n=36.7 %	2nd "	e=0.62 n=38.3 %
e=0.62	n=38.3 %	1st "	e=0.55 n=35.5 %

Sample of coarse sand (C), compacted by a 1 kg weight (40 blows/layer).

Sample of coarse sand (C),vibrated by a plate vibrator (20 sec. per layer).

FIGURE 3.3 Measurement of the uniformity of the cubic samples of 150 mm dimensions prepared in 5 layers of 3 mm thick by compaction and vibration.

increase of the density of the sample, while increasing the intensity of the mass flow rate will result in a decrease of the density. Consequently different densities can be obtained by altering the height of fall and/or rate of flow as appropriate. The uniformity of the sand samples prepared in this manner for this project were found to be acceptable and repeatable (see section 3.5).

3.4 THE SAND RAINING DEVICE

The sand raining apparatus used in this investigation follows the principles outlined in section 3.3. and is similar to that built and used by El-Gammel [22]. It consists of a hopper, sand tray and a mounting system (figure 3.4).

The hopper is a wooden box 240x240x300 mm internal dimensions, open at its upper and lower ends. It is designed to contain sufficient sand to fill the sample container without refilling and to hold a plate perforated with circular holes at the lower end. The plate is made of 20 mm thick plywood with a regular square network of holes. Different perforated plates were made with 2, 3, 5 and 8 mm diameter holes. A shutter plate of fiberglass 3 mm thick is used under the perforated plate to control the release of the sand. The shutter plate has the same pattern of holes as the perforated plate, but with a larger hole size. By displacing the shutter plate relative to the perforated plate flow could be controlled. A diffusion screen made from wire mesh is placed horizontally in the path of the falling sand to produce a uniform rain of sand by breaking up the falling columns of sand. An aluminium frame to which a plastic

curtain is attached is fixed to the outer circumference of the hopper. The curtain rests on the sand tray fixed to the top of the sample container and was used when samples of sand A were prepared, to prevent dust spreading onto other parts of the SCTA.

As the volume of the hopper is greater than the volume of the sample container, to ensure the filling of the container in a single pour a sand tray is used to collect the excess sand. This is a 500x500 mm wooden plate with side walls 150 mm high. The tray has a square hole in the middle (150x150 mm) which fits around the sample container. An inside wall of sharp edged steel surrounds the square hole to prevent sand falling back from the tray into the container which might affect the sample uniformity. The sand tray is designed to rest on top of the sample container during filling.

The support system of the sand pouring apparatus allows the hopper to be set at the desired height on the vertical centre line of the sample container. It consists of a 200 cm long, 60 mm diameter steel tube fixed to a corner of the supporting table of the SCTA. The hopper is connected to this column by a cantilever arm. The cantilever arm has an adjustable support on the column so that it can be moved up and down. The hopper can be fixed at any height up to 170 cm above the sample container. The sand raining apparatus is shown in figure 3.4.

3.5 CALIBRATION OF THE SAND RAINING DEVICE

A cubical wooden container with the same internal surfaces (i.e. covered with PTFE and rubber membranes) and

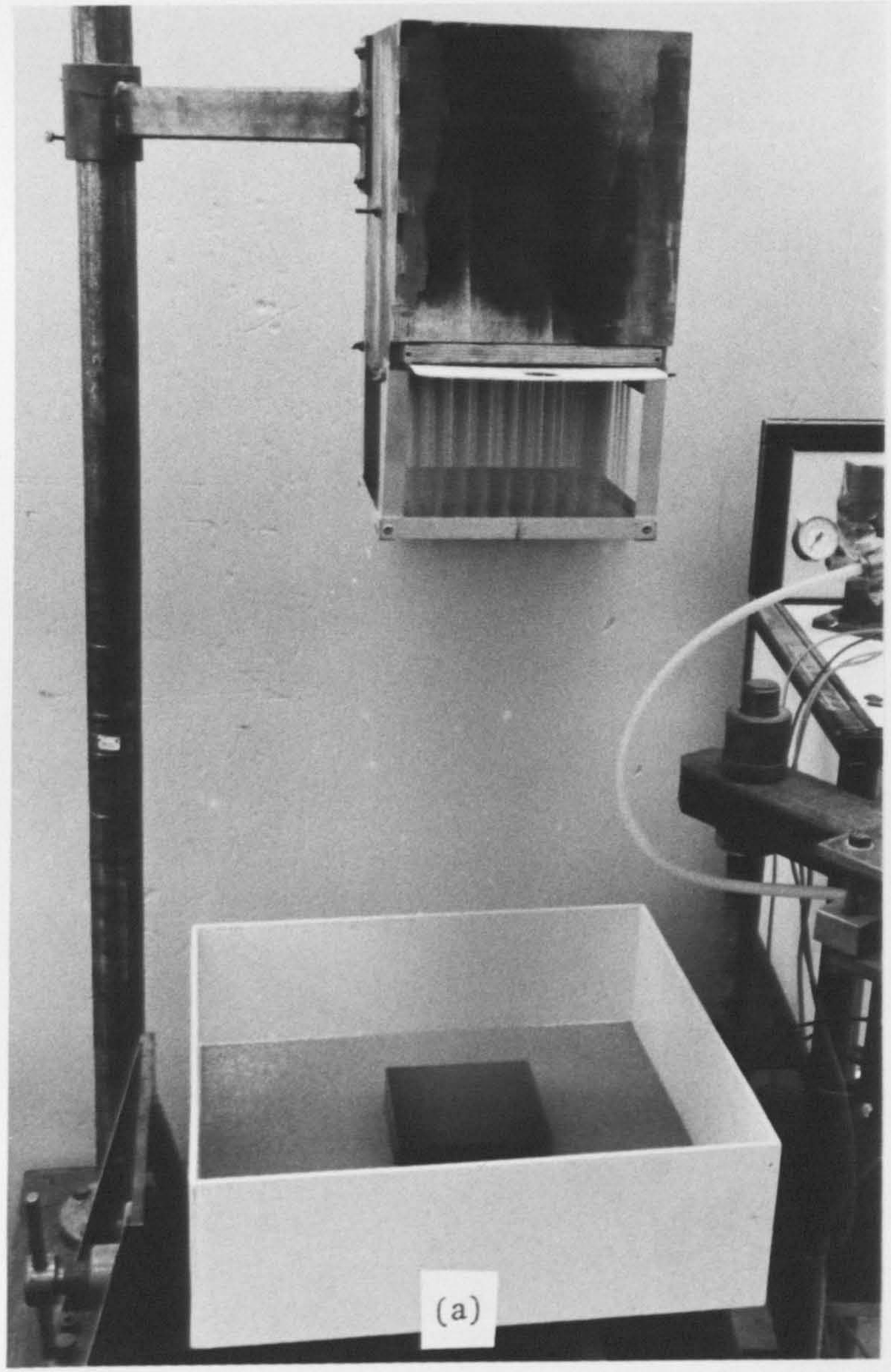

FIGURE 3.4 The sand raining device (a) with its attachment (b) for preparing fine material.

the same dimensions as the sample container of the SCTA (150x150x150 mm), was used to assess the reliability and repeatability of the sample preparation process and also to calibrate it for the different sands used in this investigation. The sand was deposited in the wooden container and the porosity of the sample was determined by measuring the mass of the sand inside the container. For each sand type different perforated plates were used and the samples were prepared allowing the sand to fall into the wooden container from different heights. In order to assess the repeatability of the apparatus each test was carried out three times. A few tests were also carried out to check the uniformity of the sample. In these tests the wooden container was filled with sand in five layers. The porosities of the layers of sand were obtained and compared. Less than 0.3% difference in porosity of the layers was found (figure 3.5).

The height of fall of the sand was measured from the base of the hopper to the middle of the container. Initially it was measured from the base of the hopper to the top of the sample inside the container and an attempt was made to keep this constant by lifting the hopper up while the pouring process was in progress. However as this did not have a significant effect for the ranges of heights used (less than 0.2%), it was abandoned as being an unnecessary complication in the preparation stage.

In figure 3.6 the results of the calibration tests on the medium size sand (group B) are shown. Depending on the particles size, different perforated plates with aperture diameters of 3, 5, and 8 mm were used and the height of

5th layer	e=0.794	n=44.25 %
4th "	e=0.799	n=44.41 %
3rd "	e=0.790	n=44.15 %
2nd "	e=0.793	n=44.23 %
1st "	e=0.792	n=44.19 %

Sample of fine sand (group A), prepared by pouring through the hopper (2 mm. aperture) from 30 cm. height.

5th layer	e=0.571	n=36.33 %
4th "	e=0.565	n=36.11 %
3rd "	e=0.568	n=36.23 %
2nd "	e=0.567	n=36.18 %
1st "	e=0.569	n=36.28 %

Sample of coarse sand (group C), prepared by pouring through the hopper (8 mm. aperture with mesh) from 80 cm. height.

FIGURE 3.5 Measurement of the uniformity of the cubic samples of 150 mm dimensions (sands A and C) prepared in 5 layers of 3 mm thick by the raining technique.

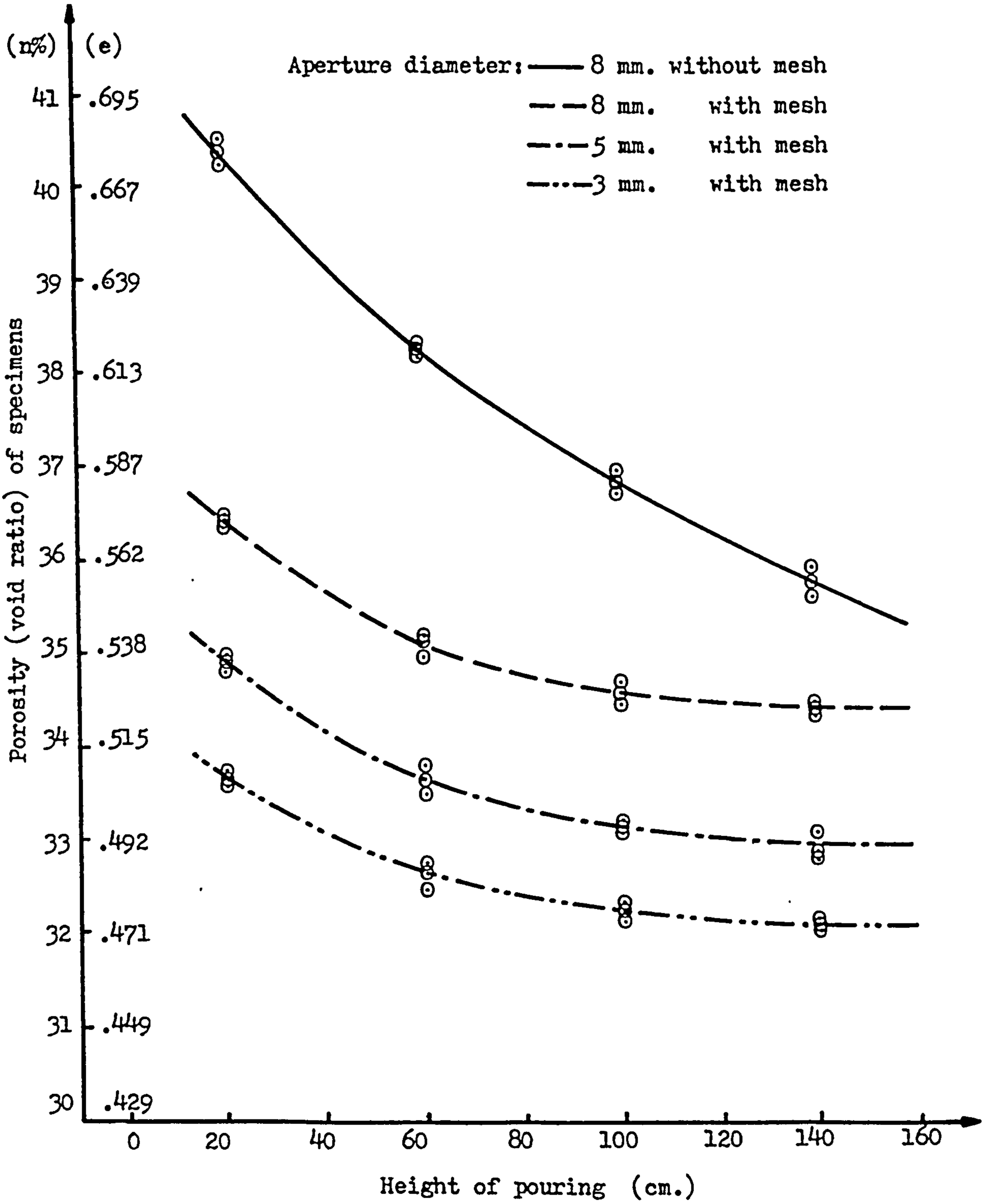

FIGURE 3.6 The variation of porosity (void ratio) with different heights of fall with fixed aperture for medium sand (B).

pouring was altered for each test. Each test was repeated three times and the best curve fitted to the points.

The calibration graphs for the coarse sand (group C) are shown in figure 3.7. Perforated plates with apertures of 5 and 8 mm were used and different heights of pouring were tried in an attempt to cover a wide range of porosities. Each test was repeated three times and the best fit curves are drawn on the graphs.

The samples of fine sand (group A) were prepared by using both a single aperture (3 mm outlet diameter funnel) and the hopper with a perforated plate with 2 mm diameter apertures. These were found to be best after trying different plates. Due to its very fine and light weight grains, preparation of this material was not as easy as the others. The particles soon reach their ultimate velocity, which is quite low, and the flow is uncontrollable unless great care is taken to provide adequate conditions as turbulent flow of the sand can easily occur resulting in a very uneven surface of the sample. In addition the flow is easily disturbed by air currents in the laboratory. It was also likely that the wide dispersion of the very fine sand might damage the apparatus. Samples prepared using other methods such as compaction and vibration to avoid the problems described above proved unacceptable, therefore two variations of the raining method were used. The first was using a funnel of 3 mm outlet diameter. In this method the sand was poured through the funnel at a certain height while moving it around the container to give a level surface. The second was using the hopper with a perforated plate of 2 mm diame-

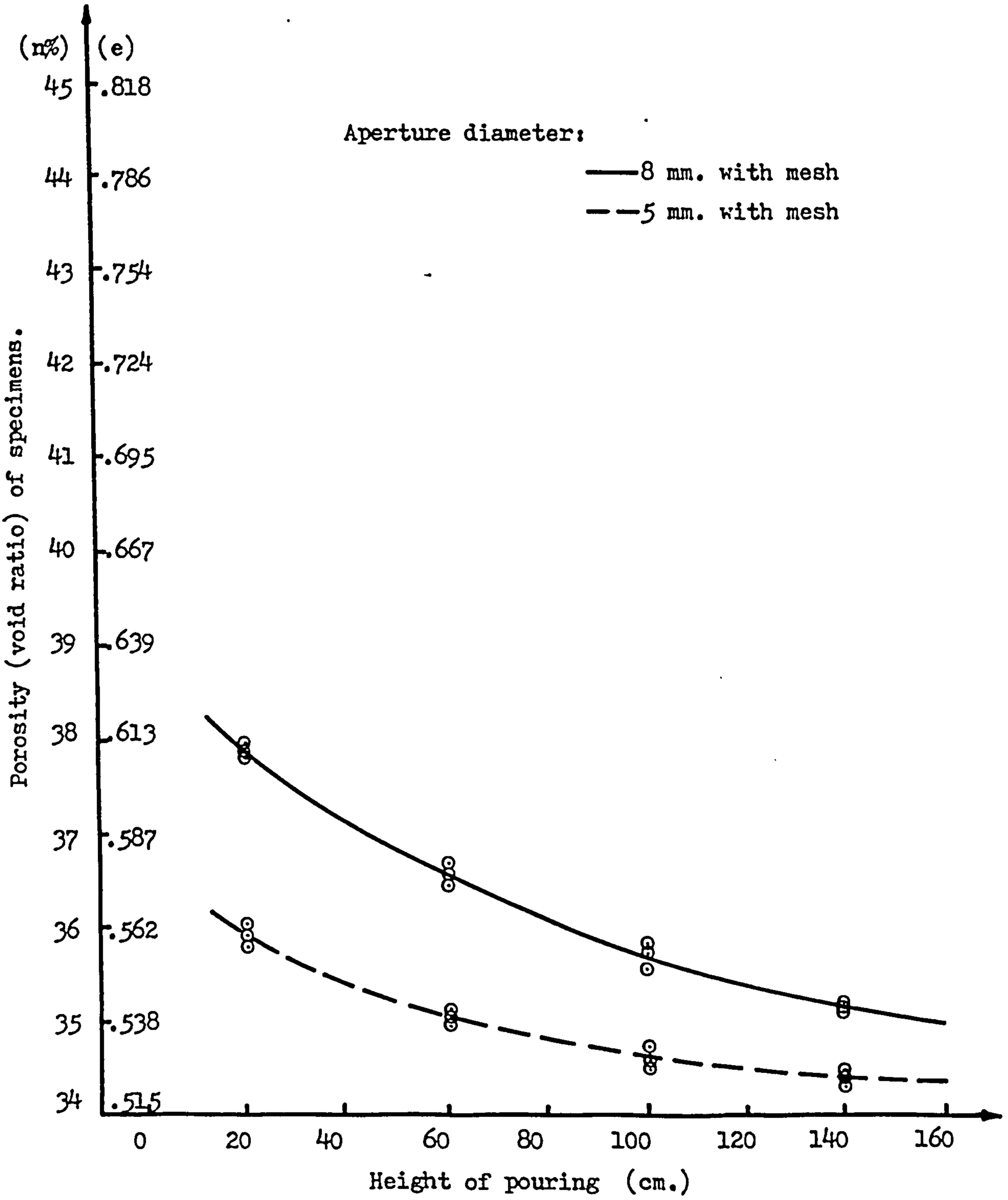

FIGURE 3.7 The variation of porosity (void ratio) with different heights of fall with fixed aperture for coarse sand (C).

ter. This was the same technique as used for the other types of sand. The samples were prepared using different heights of pouring and again each test was repeated three times. The results are plotted in figure 3.8. To control the dust produced with this sand the plastic curtain described in section 3.4 was used.

Using all three types of sand, raining was stopped to give a final surface just above the top edge of the container. The surface of the sample was then levelled using a very sharp steel straight edge. The excess grains were carefully removed by sliding the straight edge over the top of the container in order to avoid disturbing the upper zone of the sand.

Having calibrated the sand raining device for the different groups of sand, it was possible to prepare samples with the desired porosity by choosing the appropriate height of fall and outlet plate and the results show that a fairly precise degree of control is possible.

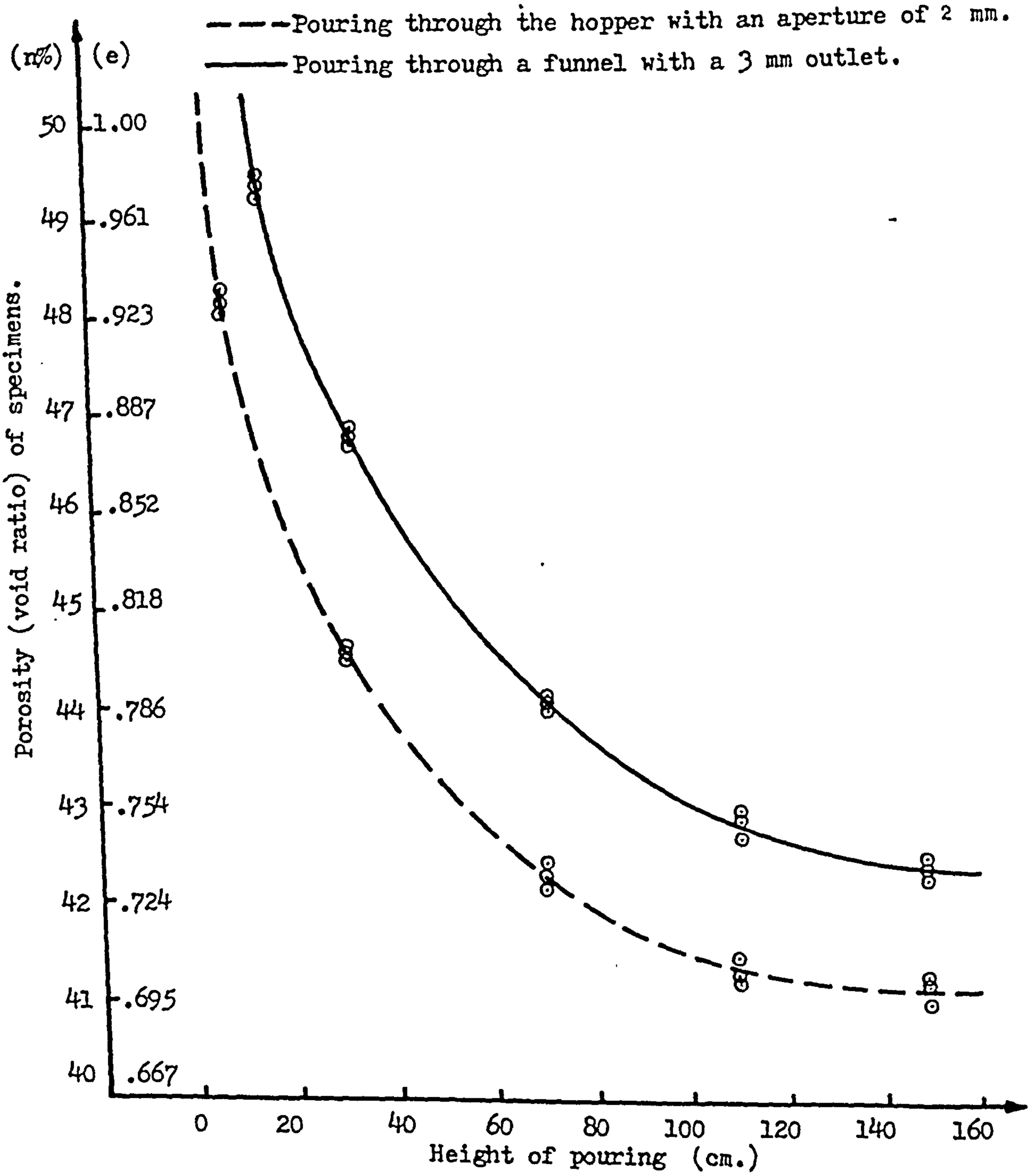

FIGURE 3.8 The variation of porosity (void ratio) with different heights of fall with fixed aperture for fine sand (A).

CHAPTER FOUR

MONOTONIC TESTS

4.1 INTRODUCTION

In order to obtain a better understanding of the stress-strain characteristics of granular soils at small deformations before failure occurs under monotonic loading conditions, a series of tests were performed on both fine and coarse Leighton Buzzard sands. The dry cubic specimens of 15x15x15 cm were prepared as described in chapter three. A large number of samples with different initial porosities were tested under vertical stresses of up to 400 kN/m^2.

During the tests the vertical stress was applied by the loading system in steps up to the maximum desired stress level. The vertical strain and two lateral stresses were regularly measured while the two lateral strains were controlled to give the desired confining conditions.

The apparatus and particularly the soil container were designed so that the principal strains could be controlled. Although the shear stresses induced on the faces of the specimen were not zero, they were small enough to ignore when analysing the results (see section 2.3).

In this chapter only the results of the experiments are described. Discussion and comments on the data are given separately in chapter six.

4.2 THE GENERAL TEST PROCEDURE

The general experimental procedure for monotonic loading is the same as that used by El-Gammel [22] during his investigation. Only a brief outline is given below to identify the most important features of the procedure.

Initially the soil container is dismantled, cleaned and any sand particles removed. It is then assembled for the confined condition. The six interior faces of the container are covered with a thin layer of silicon grease and a latex rubber membrane is applied carefully to each greased face. The soil is rained into the container from a height required to obtain the desired porosity and the sample is prepared following the method described in chapter 3. Next the top loading plate is put in place. Having positioned the vertical load cell and loading shaft on the centre of the loading plate, the LVDT is mounted on the top of the loading plate to record the vertical strain. The lateral load cells are already fixed in place. The first increment of vertical load is applied and the vertical strain and the lateral stresses are measured. At this point the test can be continued either in the confined condition by simply applying the next increment of vertical load, or in the other test confinement conditions under which the sample can move laterally to a certain degree. Having completed the test, the frame is removed and the container is emptied and cleaned for the next test.

As the constraint conditions under which the specimens are tested have a significant effect on the behaviour of the soils and as the apparatus is capable of applying a

range of conditions, ninety tests were carried out using three different constraint conditions to cover the most commonly considered situations. In the first series specimens were tested under conditions of no lateral strain or fully confined situations. The second series was of plane strain condition tests $\varepsilon_2=0$, ε_3 controlled and finally in the third series, strains were allowed in all three directions, i.e. triaxial strain tests in which $\varepsilon_2=\varepsilon_3$.

4.3 CONFINED TESTS

The main objective of this series of tests was to study the stress-strain behaviour of different grades of sand under no-lateral strain conditions. Therefore during these experiments the two lateral moveable walls of the container were fixed, hence $\varepsilon_2=\varepsilon_3=0$.

In each test the vertical stress was applied in incremental steps up to 400 kN/m^2 and the values of vertical strain ε_1 and lateral stresses σ_2 and σ_3 were measured for each step.

For the fine sand the samples were tested at different initial porosities ranging from 42% (Dr=100%) to 49% (Dr=22%), while for the coarse sand the range was between 34% and 45% corresponding to relative densities of 100% and 0% respectively. To check the repeatability of the apparatus and test procedure each experiment was carried out twice under the same condition. The results obtained show the tests are quite repeatable. In order to assess the behaviour of the apparatus after the modifications (chapter three), some confined tests were performed also on the same sand

(group B) as was used before by El-Gammel [22].

The testing programme in confined conditions including the number of tests, initial porosity, relative densities and the type of sand used are summarized in table 4.1.

4.3.1 THE RELATIONSHIP BETWEEN VERTICAL STRESS AND VERTICAL STRAIN

The most common way of representing data in stress-strain studies of soils is to plot the relationship between σ_1 and ε_1 which shows the magnitude and rate of change of the vertical deformations of the sample as the applied σ_1 increases.

Figures 4.1 to 4.3 show the relationship between σ_1 and ε_1. In figure 4.1 the curves show the variation of vertical strain versus vertical stress for sand A for different initial porosities while in figure 4.2 the same relationships for sand C are shown. In order to be able to compare the results of the two different sizes of sand figure 4.3 plots all the curves for both sand A and C on one graph.

The relationship between σ_1 and ε_1 for many materials is linear, especially at low stress levels but for soils, as can be seen from the figures this does not hold. The curves begin with large strains initially and as the vertical stress increases, the rate of increase of vertical strain becomes smaller and the relationship between stress and strain tends towards a straight line. For denser samples this tendency is more noticeable than for loose samples. Also the amount of initial vertical strain for the coarse material is significantly smaller than for the fine one. The maximum vertical strains under the maximum applied vertical

type of sand	test number	initial porosity(%)	relative density(%)	vertical stress(kN/m^2)
fine(A)	1 & 2	42	100	0-400 in increments of 25
	3 & 4	43	89	
	5 & 6	45	67	
	7 & 8	47	44	
	9 & 10	49	22	
coarse(C)	11 & 12	34	100	0-400 in increments of 25
	13 & 14	35	91	
	15 & 16	36	82	
	17 & 18	38	64	
	19 & 20	45	0	

TABLE 4.1 Test programme in confined conditions under monotonic loading.

stress for the coarse sand are considerably smaller in comparison with those of the fine sand, and it seems that the fine material is more deformable and 'softer' than the coarse one. In figure 4.2 there is a large gap between the curve of the loosest sample (porosity of 45%) and the rest of the curves. This is probably because a different method of preparation was necessary for this case and the container was filled using a scoop. The uniformity of such a sample is doubtful.

To assess the behaviour of the apparatus after the modifications, some confined tests on sand B were carried out repeating some of those performed by El-Gammel [22]. The results of these tests together with those obtained by El-Gammel are shown in figure 4.4. It is clear that the vertical strains generally are smaller than those reported before. Although the difference for dense samples is small, as the porosity increases it becomes noticeable (maximum increase of 10%). This value for the fine sand which has relatively large strain could have been even greater. The reduction in ε_1 may be due to the increased support and stiffening of the free side walls which had undesirable movements before.

4.3.2 THE RELATIONSHIP BETWEEN VERTICAL STRESS AND LATERAL STRESS

The resultant lateral stresses are plotted against the applied vertical stresses in figure 4.5. In fact for each increment of $\Delta\sigma_1$ there are two lateral stresses σ_2 and σ_3 which should be equal but, due to practical limitations such as the impossibility of setting up the two free side

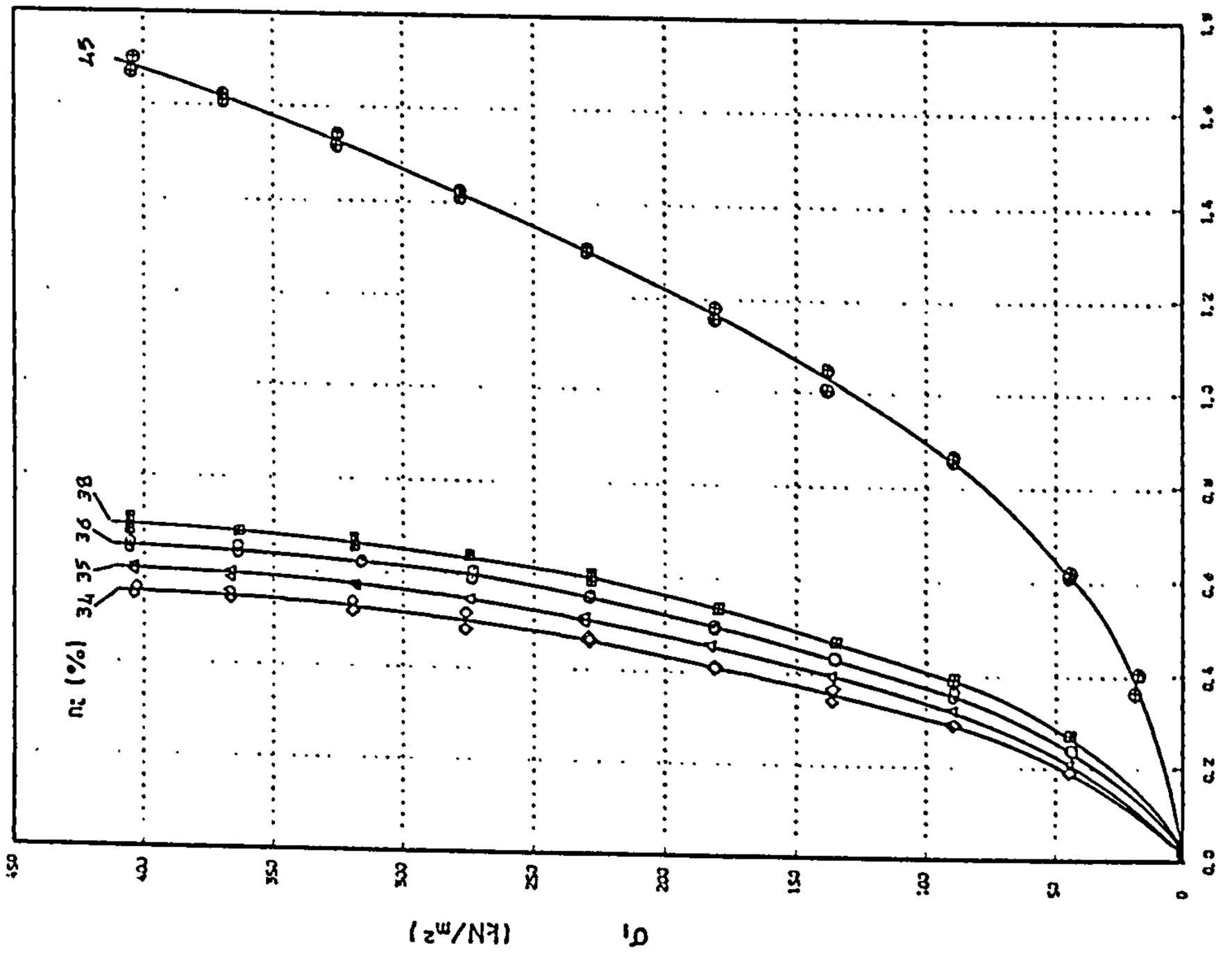

FIGURE 4.2 Relationship between ε_1 and σ_1 for different initial porosities for sand C under confined conditions.

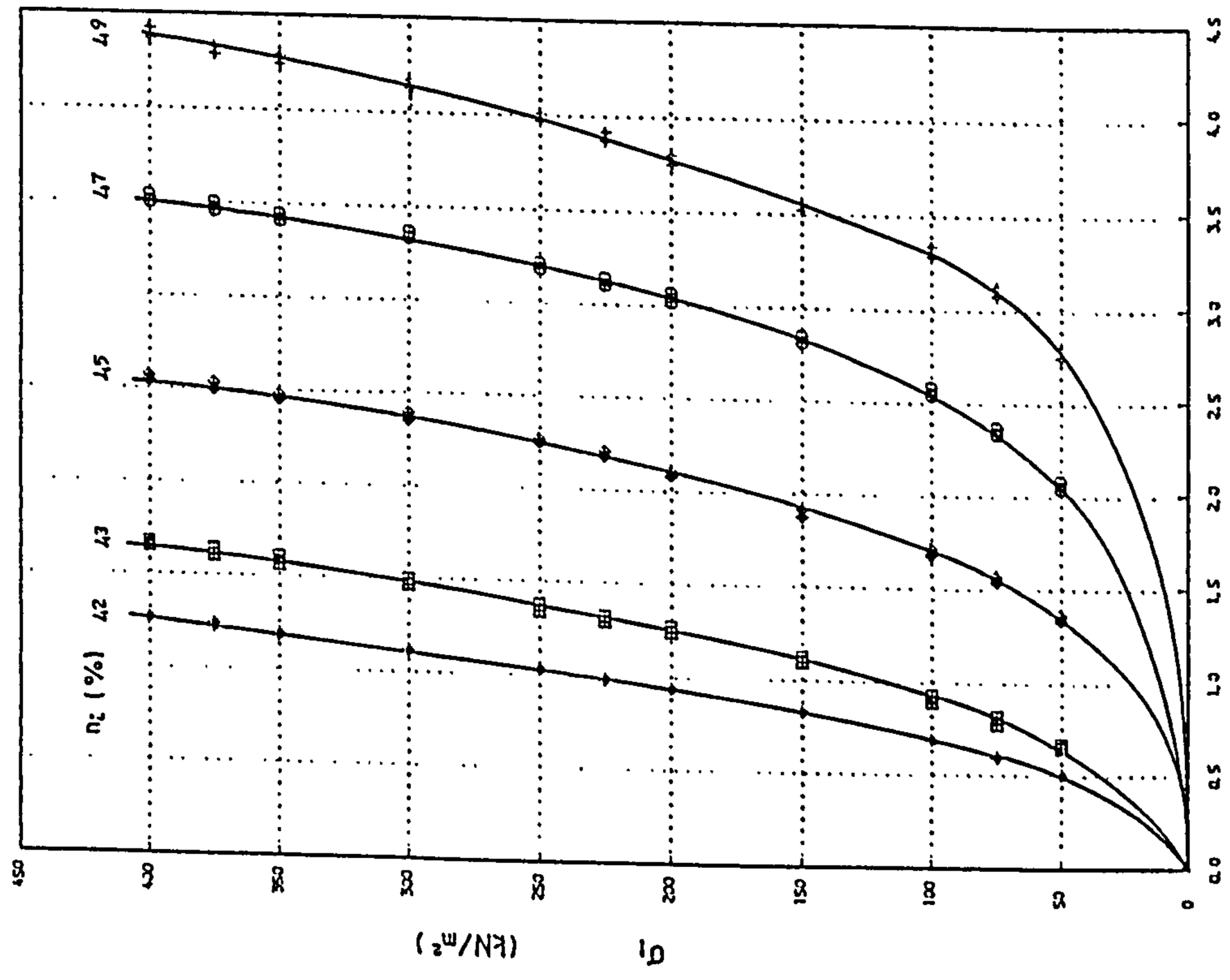

FIGURE 4.1 Relationship between ε_1 and σ_1 for different initial porosities for sand A under confined conditions.

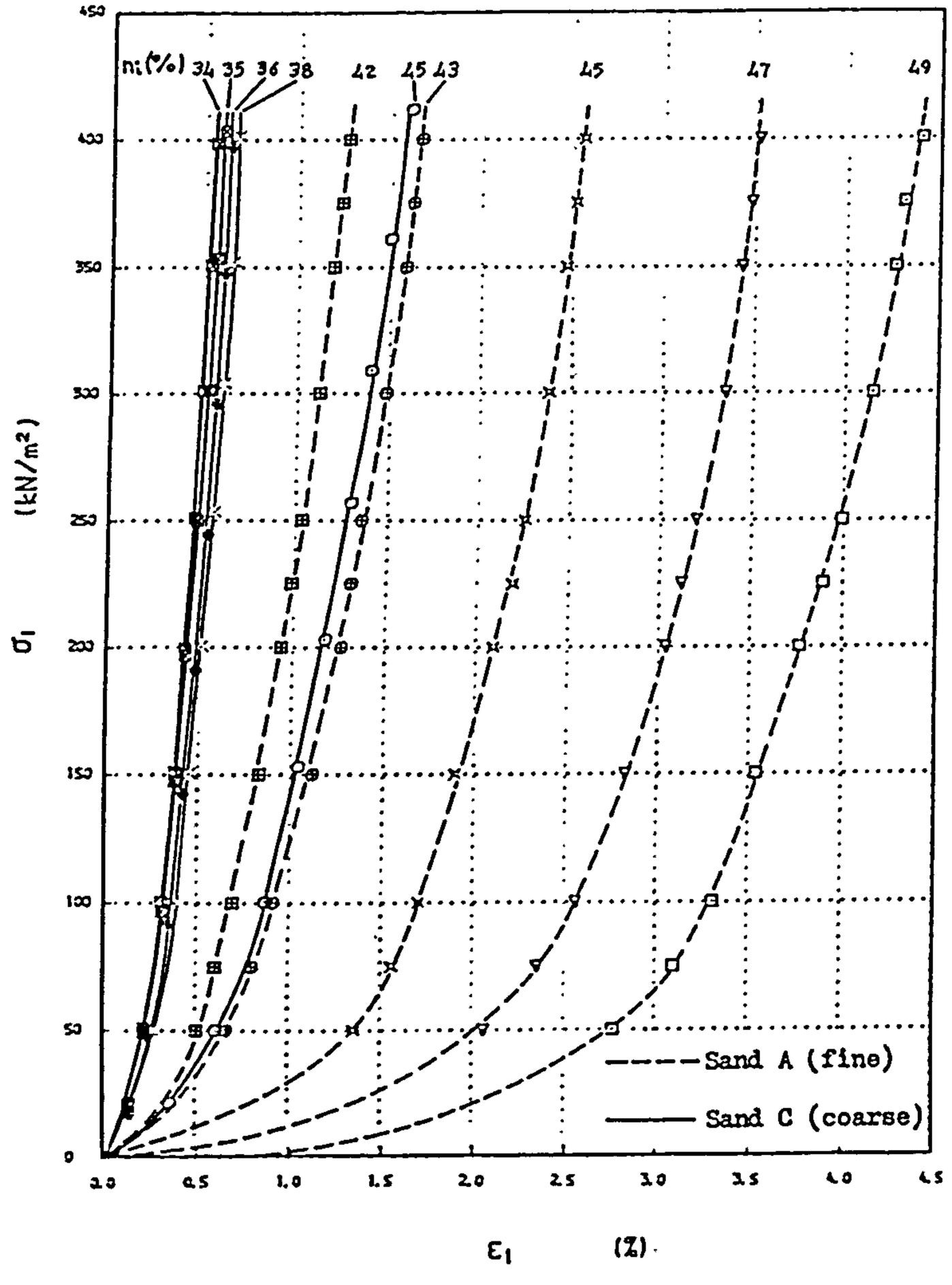

FIGURE 4.3 Relationship between ε_1 and σ_1 for different initial porosities for sands A and C under confined conditions.

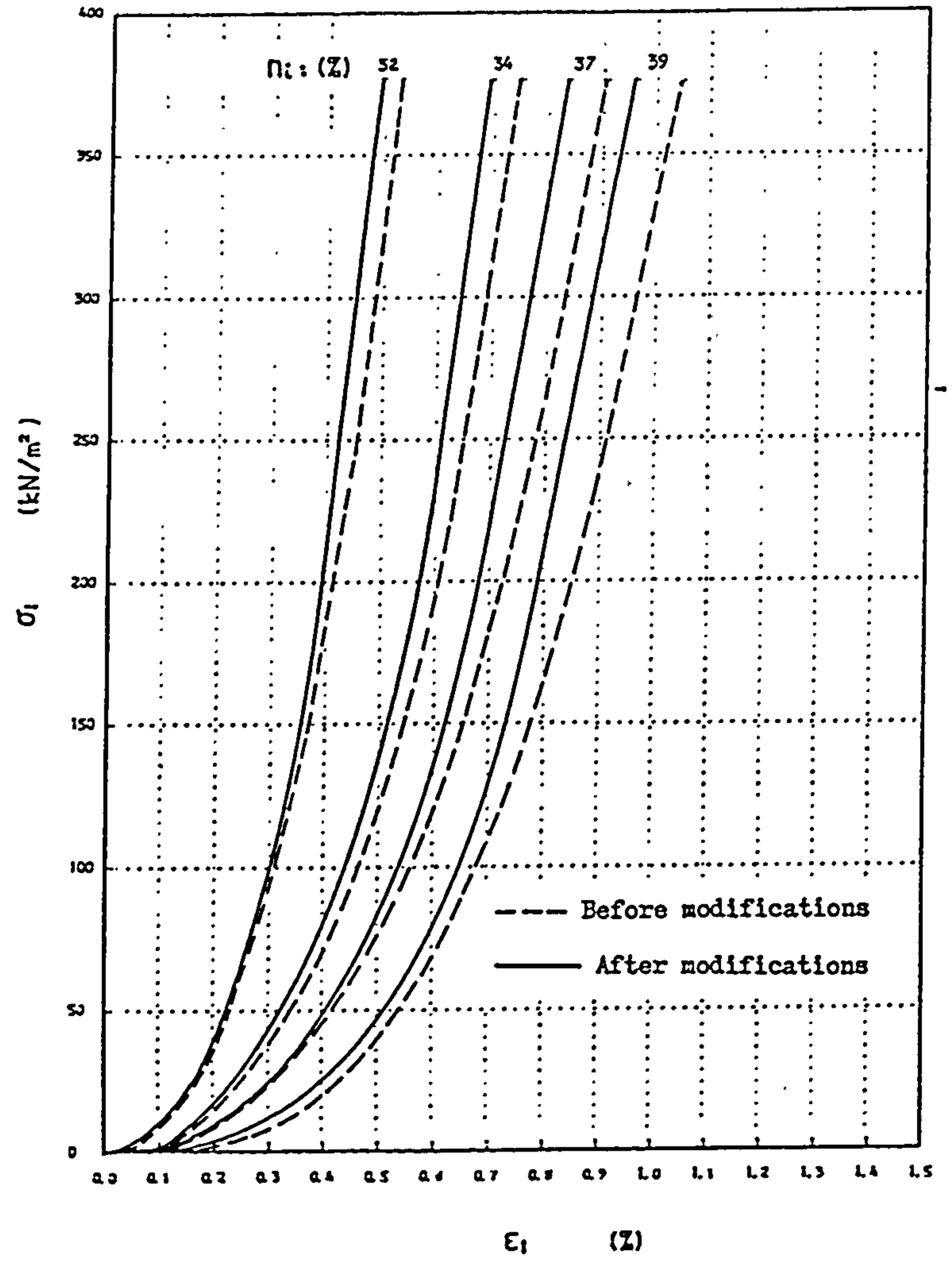

FIGURE 4.4 Comparison between the confined test results before and after modifications of the apparatus.

walls so that the base friction developed over their contact areas are exactly identical (and the same difficulties apply to the two guide shafts inside the support bearing) etc, there is some difference between the two lateral stresses for both confined and triaxial tests in which $\varepsilon_2 = \varepsilon_3$. However the difference between σ_2 and σ_3 is never more than 2% of their average value which is not significant. For this reason, in figure 4.5, the average value of the lateral stresses is plotted as:

$$\sigma_h = \frac{\sigma_2 + \sigma_3}{2} \qquad (4.1)$$

As can be seen in figure 4.5 the relationship between vertical stress and lateral stress is nearly linear for each specimen but as the sand becomes looser the gradient of the lines decreases and it is a minimum for the loosest case. This general pattern is valid for both coarse and fine sand, but on the whole the slopes of the lines for the coarse sand are greater than those for the fine sand which means that for the same initial porosities and vertical stress, lower lateral stresses are induced in the coarse sand. Again the gap between the last line of coarse sand (porosity 45%) and the other lines is due to the use of a different method for preparing this sample.

4.3.3 THE RELATIONSHIP BETWEEN THE COEFFICIENT OF EARTH PRESSURE AT REST (Ko) AND THE VERTICAL STRESS

The ratio of the lateral stress to vertical stress in confined conditions is called the coefficient of earth pressure at rest (Ko) and has been the subject of interest and study for many years. The ratio of average values of lateral

stress (σ_h) to vertical stress is plotted against vertical stress in figures 4.6 to 4.8.

The curves in figure 4.6 show the relationship between Ko and σ_1 for fine sand while figure 4.7 shows the results for coarse sand and the results for both sands are illustrated in figure 4.8 so that they may be compared easily.

From the figures it is apparent that the assumption that Ko is a constant for soils, whatever the stress or strain conditions, is not true. It can be seen that Ko depends on the stress level and the initial porosity of the sample. For a certain initial porosity, as the vertical stress increases the value of Ko decreases and under a constant level of vertical stress Ko increases as the porosity of the specimen increases. The rate of decrease in Ko due to increasing vertical stress is initially great but it drops at higher stress levels.

Although the general trend of variation of Ko for both fine and coarse sand is the same, from figure 4.8 it is quite clear that the values of Ko for the coarse sand are significantly smaller than those for the fine sand.

4.3.4 THE EFFECT OF VERTICAL STRESS ON THE CONSTRAINED SECANT MODULUS (D)

When soils are studied under confined conditions, the constrained secant modulus (D) is a parameter characterising the behaviour of soil which is commonly calculated and used. D characterizes the deformability of a soil and is given by the slope of the line connecting two points of the stress strain curve together, hence:

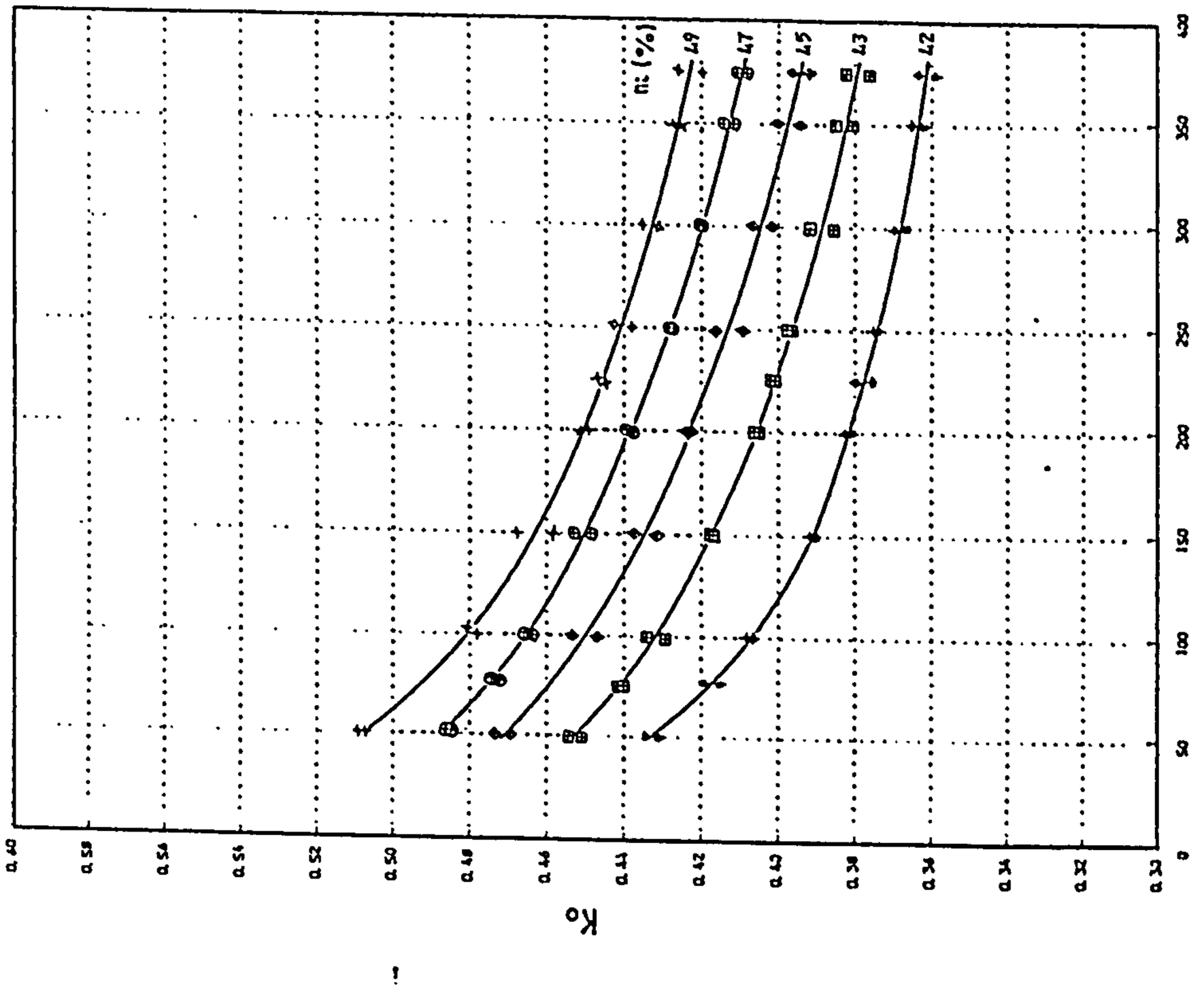

FIGURE 4.6 Variation of Ko with σ_1 for different initial porosities for sand A.

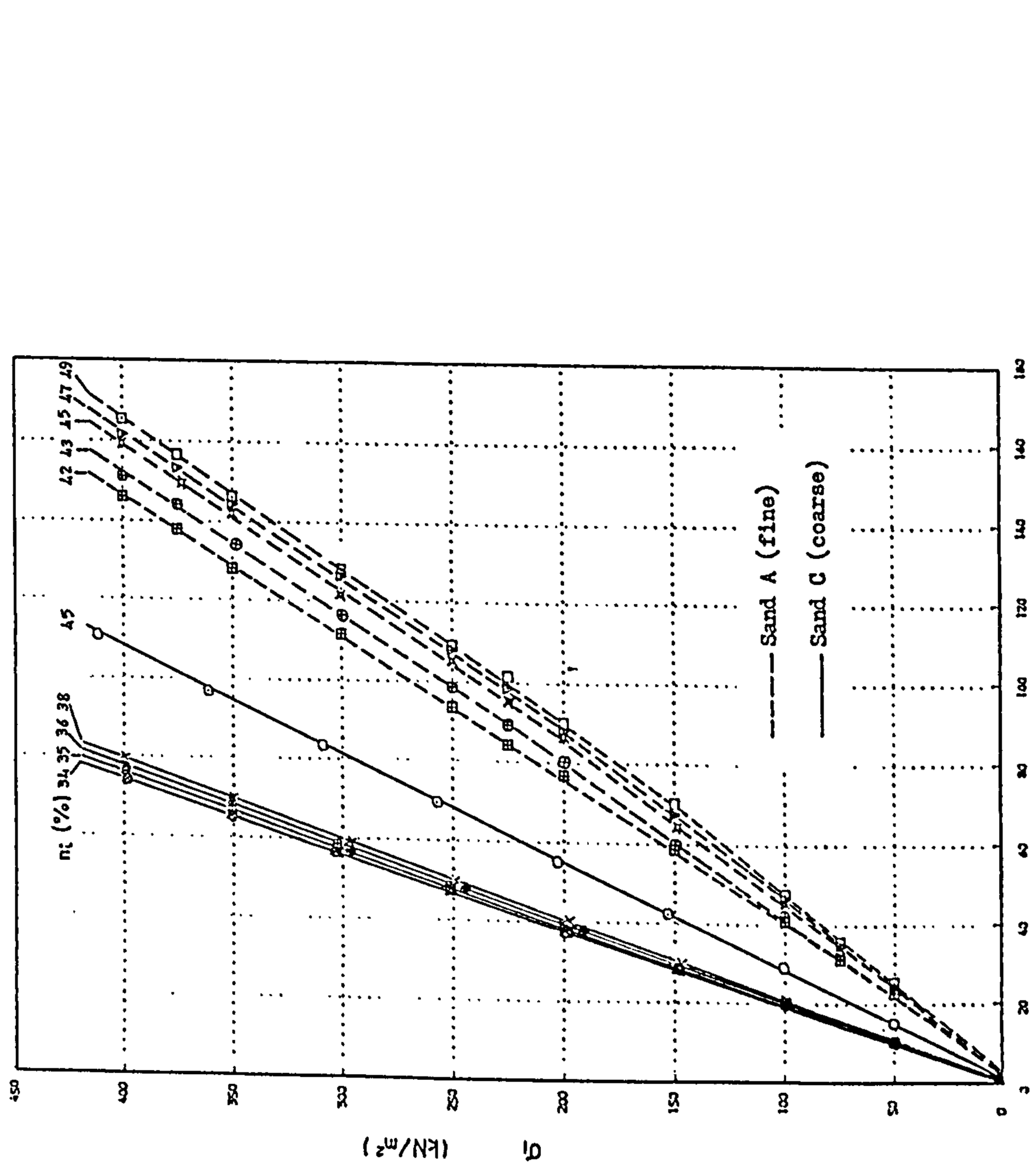

FIGURE 4.5 Relationship between σ_1 and average of the lateral stresses (σ_h) for different initial porosities for sands A and C under confined conditions.

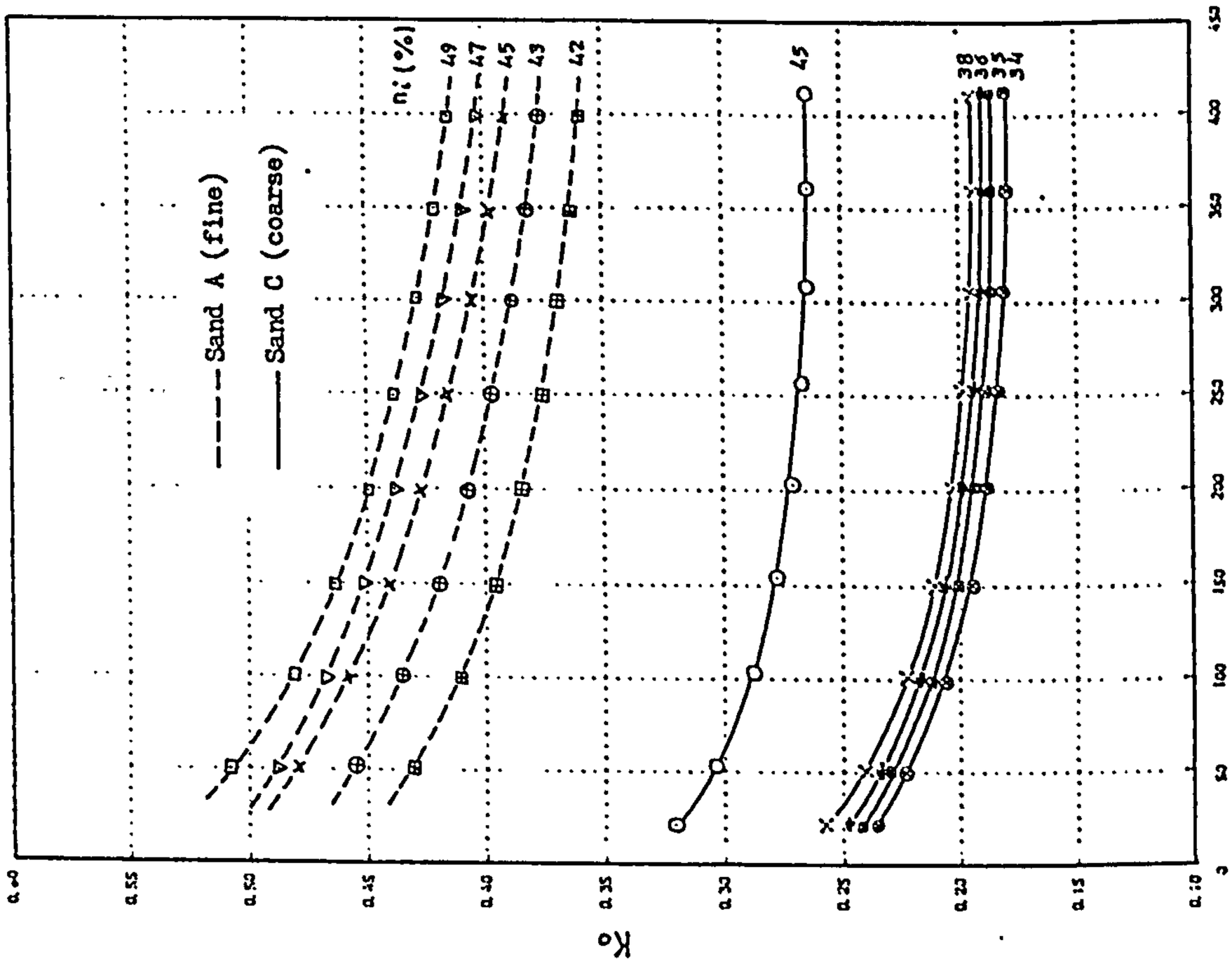

FIGURE 4.8 Variation of Ko with σ_1 for different initial porosities for sands A and C.

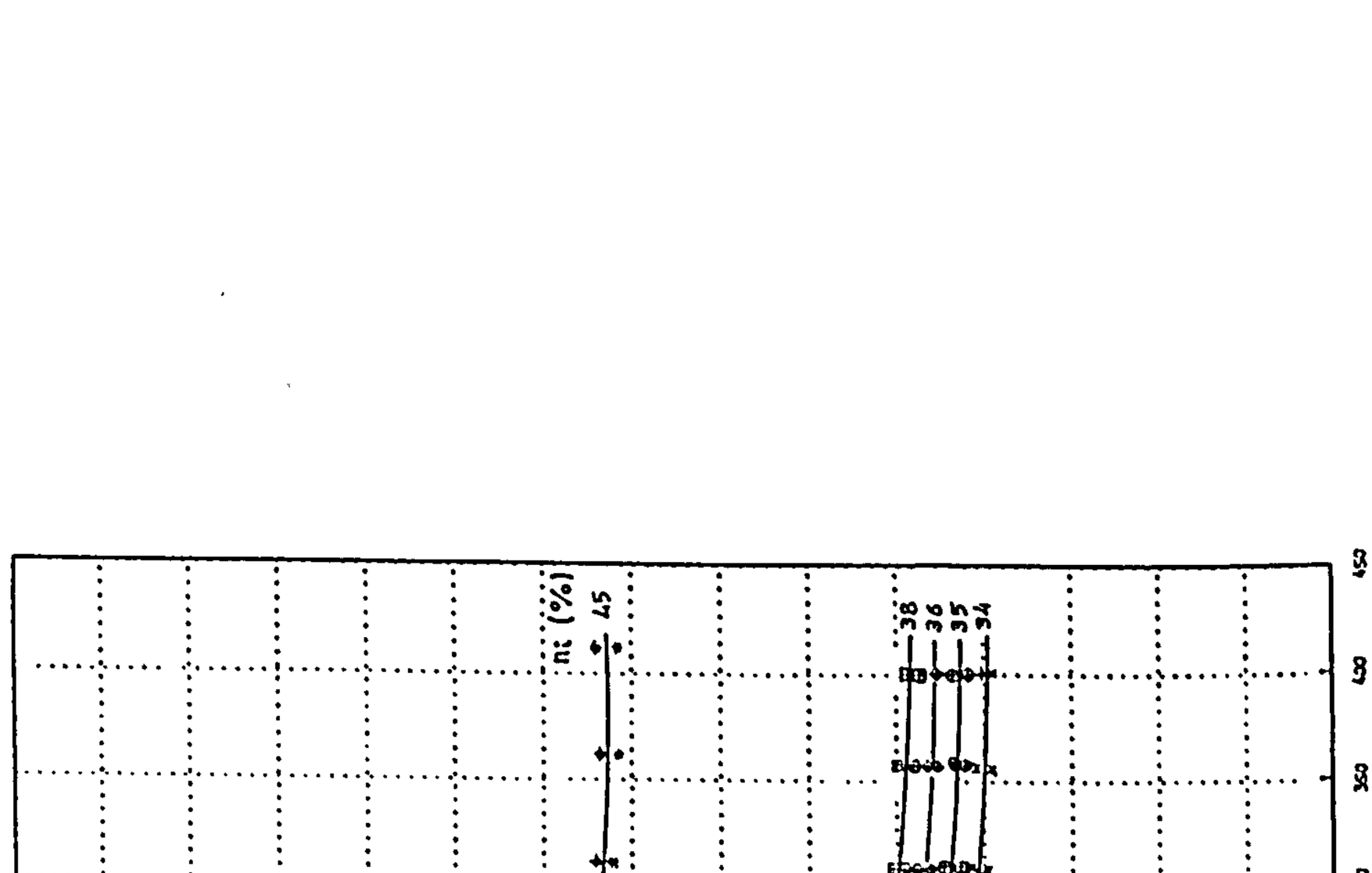

FIGURE 4.7 Variation of Ko with σ_1 for different initial porosities for sand C.

$$D = \frac{\Delta\sigma_1}{\Delta\varepsilon_1} \qquad (4.2)$$

It is quite obvious that if the stress strain relationship of the soil is linear, the secant modulus will be a constant equal to the slope of the line (i.e.the modulus of elasticity). However, due to the non-linear behaviour of sands the secant modulus will usually change as the vertical stress increases.

In figures 4.9 to 4.11 the variation of constrained secant modulus with vertical stress for fine and coarse sands are shown separately and then together. In these figures the values of D are calculated using the differences between the point of interest and the origin point on the $\sigma_1 - \varepsilon_1$ curve.

It can be seen in figure 4.9 that the relationship between D and vertical stress is approximately linear for the loose samples of fine sand but as the samples get denser it tends to become curved concave upwards. This tendency is quite clear for the densest specimen (of 42% porosity).

In figure 4.10 the variation of D against σ_1 for coarse sand shows a non-linear relationship even for loose samples. It is apparent from figure 4.11 that the constrained secant modulus for both fine and coarse sand increases with increasing σ_1 ,but the rate of increase for dense samples is greater than loose samples and also greater for coarse sand than fine sand.

4.3.5 THE VARIATION OF VOIDS RATIO WITH VERTICAL STRESS

As the vertical stress is applied to the specimen it strains vertically and the volume of voids will decrease. The particles move to a denser packing and the voids ratio decreases.

The variation of the voids ratio of soils, during confined compression tests, with vertical stress follows typical patterns in most cases. This type of data, usually from an oedometer test is commonly used for settlement calculations for clays. The great advantage of this type of representation of data is that when using semi-logarithmic axes, the relationship between voids ratio (e) and the vertical stress for non-prestressed samples is usually linear. The slope of this line is called the compression index (Cc) and is given by:

$$C_c = \frac{\Delta e}{\Delta(\log \sigma_1)} \qquad (4.3)$$

which is the change in voids ratio per logarithmic cycle of stress.

In figures 4.12 to 4.14 the variation of voids ratio with the logarithm of the vertical stress for both fine and coarse sand are shown. From the figures it is apparent that the curves plotted are straight lines and Cc for each type of sand is almost constant and dependent on the initial porosity. The other factors influencing the compression index seem to be the size and shape of the grains. Cc for the fine sand is greater than that for the coarse sand.

4.4 PLANE STRAIN TESTS

A series of experiments on both fine and coarse sands

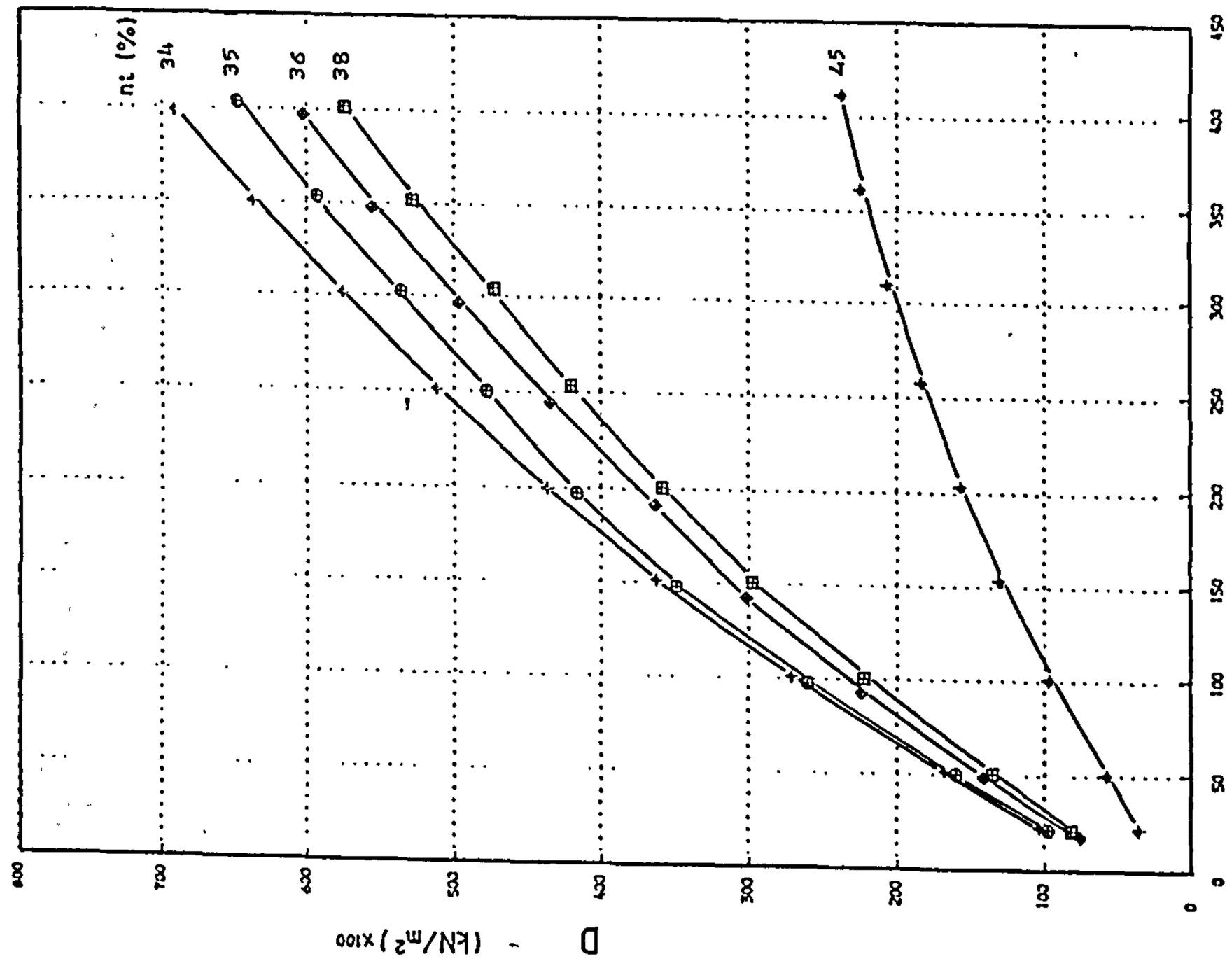

FIGURE 4.10 Variation of the constrained secant modulus (D) with σ_1 for different initial porosities for sand C.

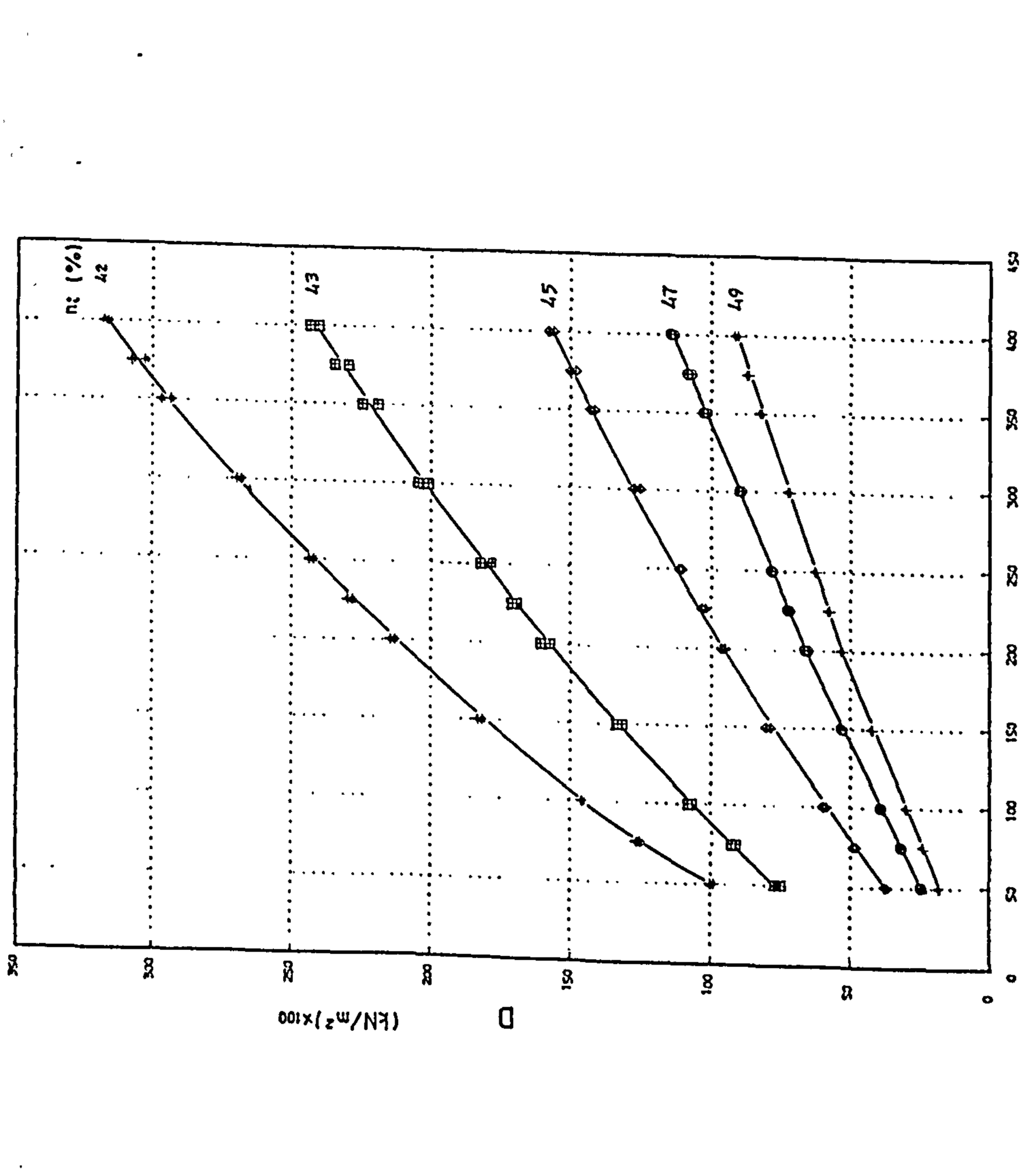

FIGURE 4.9 Variation of the constrained secant modulus (D) with σ_1 for different initial porosities for sand A.

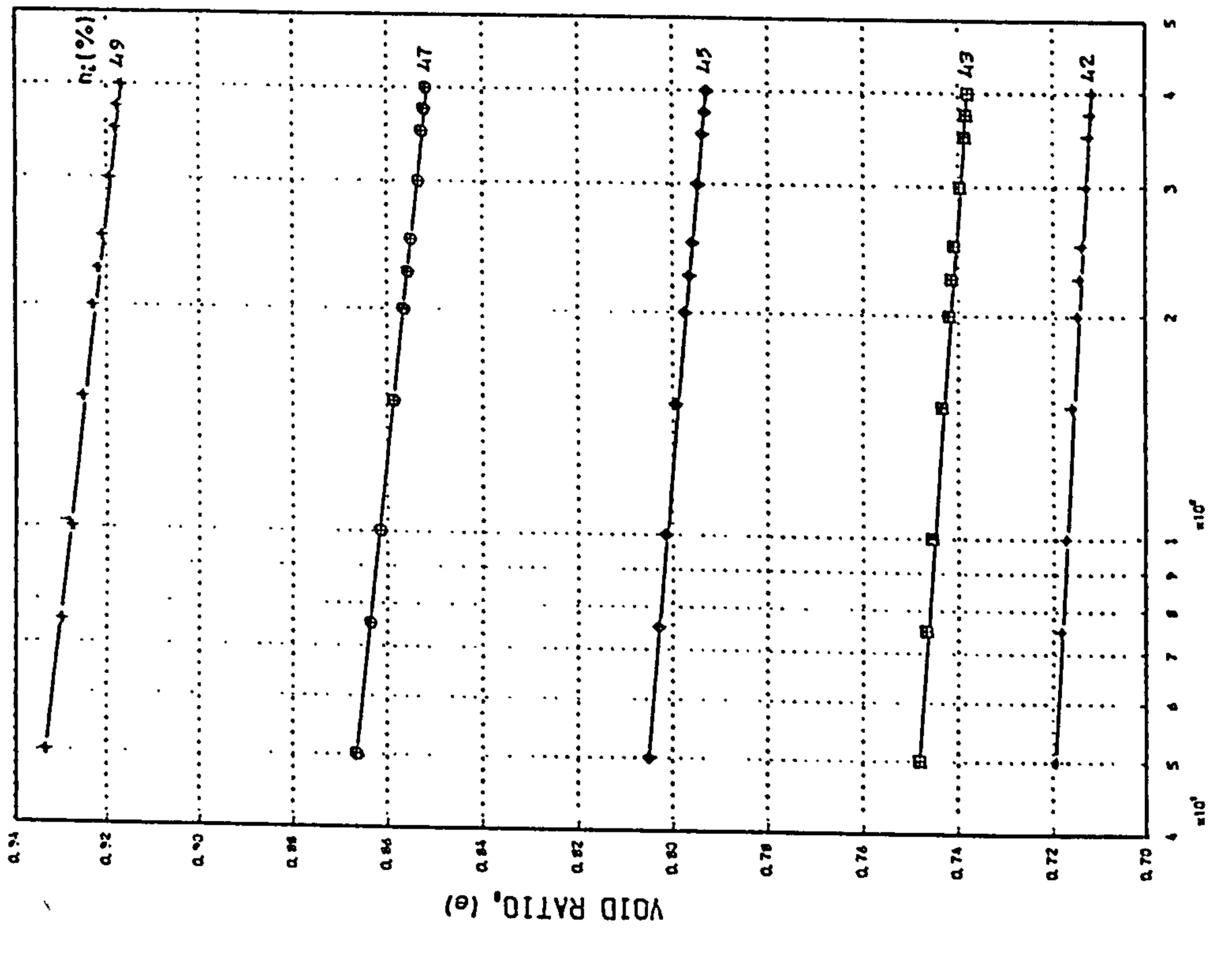

FIGURE 4.12 Variation of the void ratio of the sample with σ_1 for sand A under confined conditions.

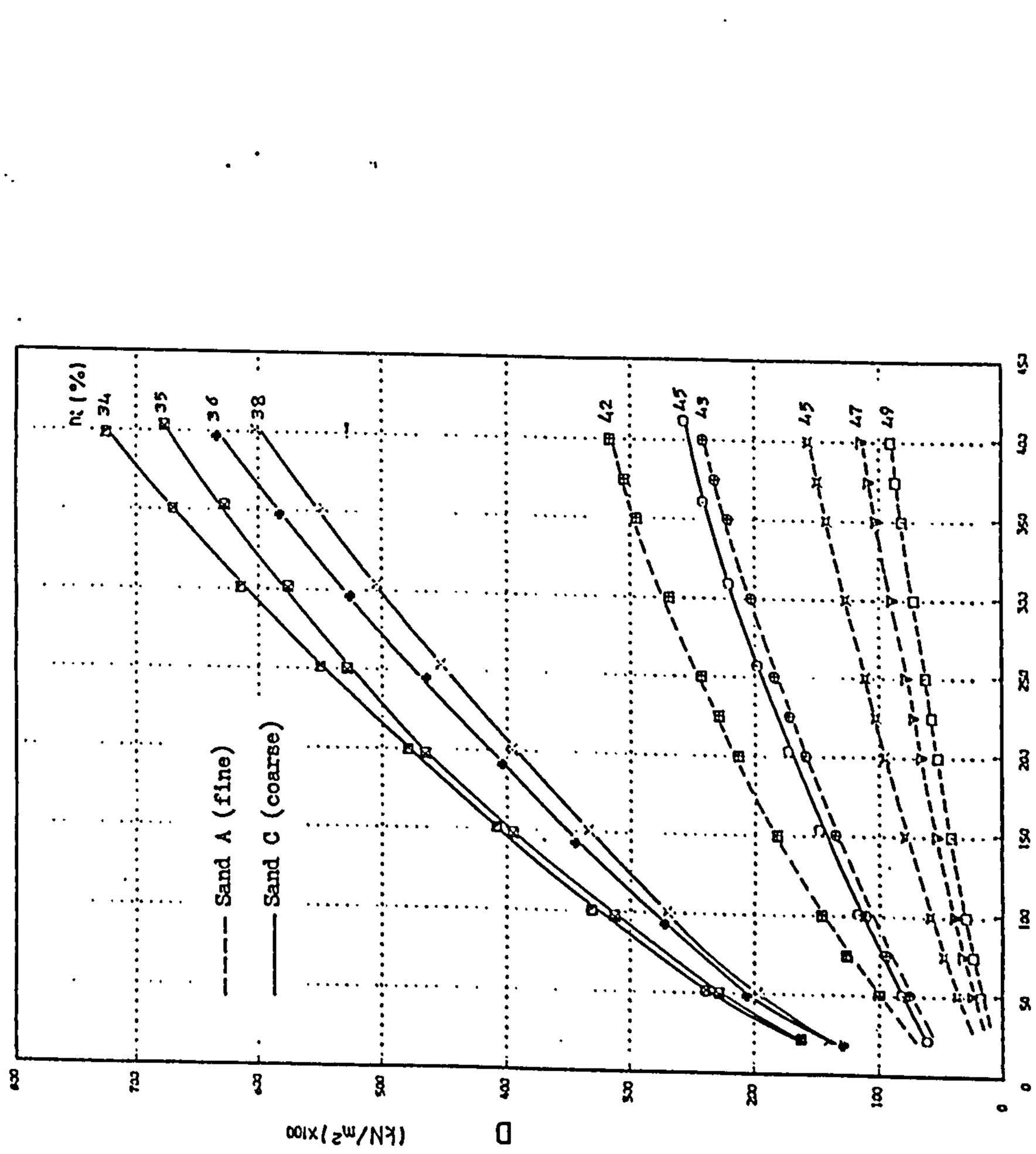

FIGURE 4.11 Variation of the constrained secant modulus (D) with σ_1 for different initial porosities for sands A and C.

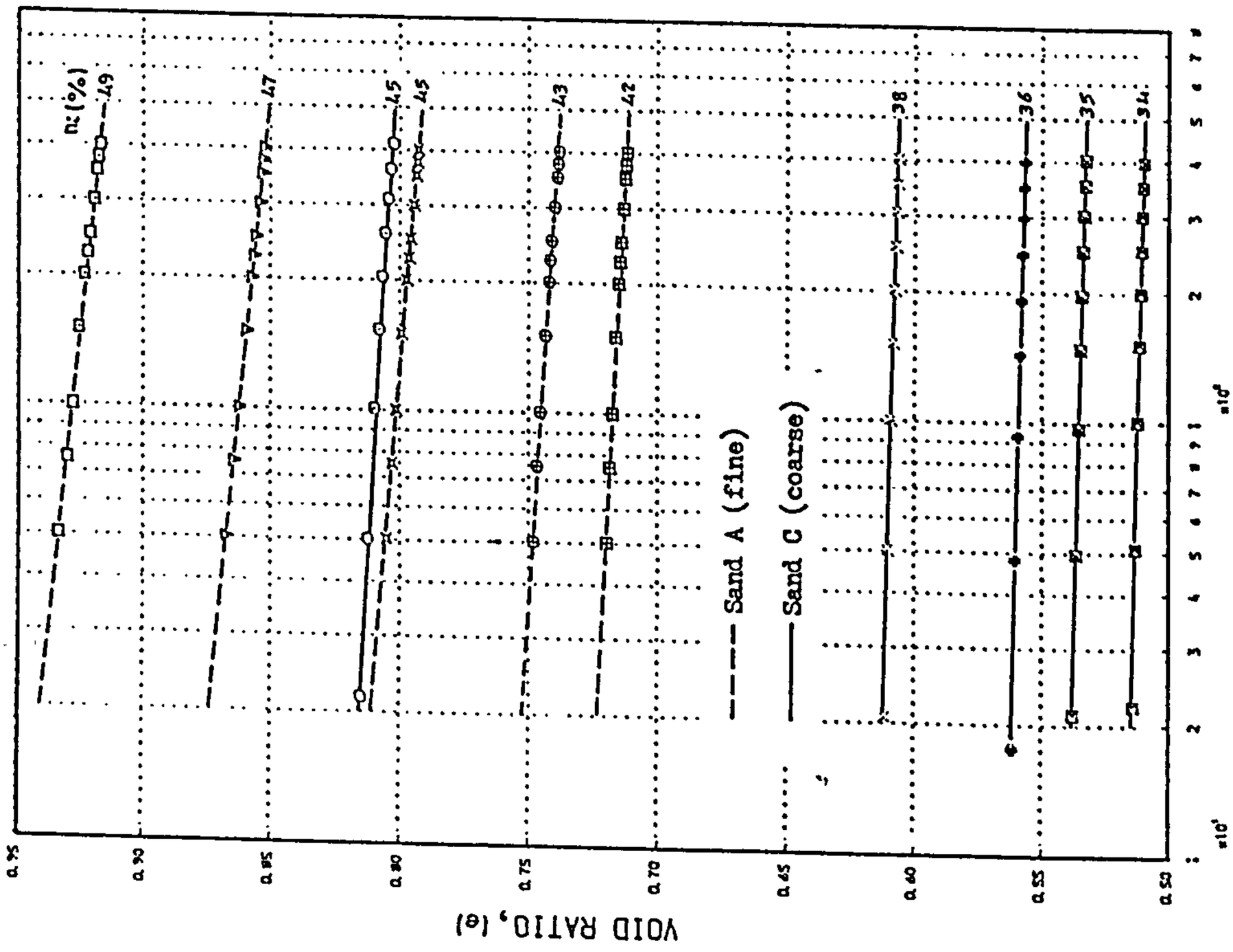

FIGURE 4.14 Variation of the void ratio of the sample with σ_1 for sands A and C under confined conditions.

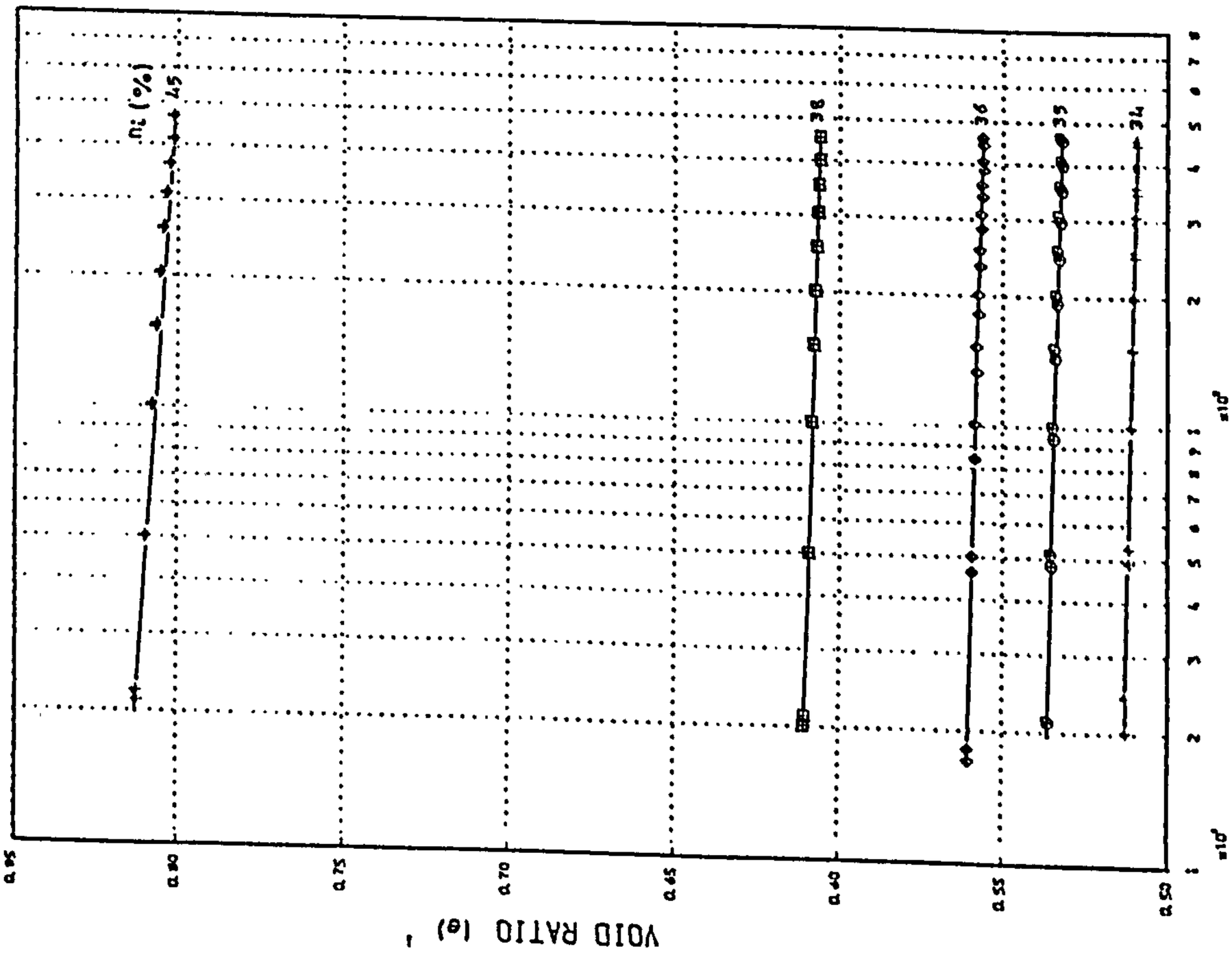

FIGURE 4.13 Variation of the void ratio of the sample with σ_1 for sand C under confined conditions.

were carried out under plane strain conditions. This condition was produced in the SCTA by allowing lateral strain in one direction (ε_3), and keeping ε_2 at zero all the time in the other horizontal direction.

4.4.1 TEST PROCEDURE AND OBJECTIVES

The test procedure for the plane strain experiments is generally the same as described in section 4.2 for confined tests. The only important difference is the way of producing plane strain conditions. After applying the required vertical stress and measuring ε_1, σ_2, and σ_3, the first increment of lateral strain is applied along one axis by means of the control handle, while in the other direction no lateral strain is permitted. Therefore the sample is allowed to strain in one horizontal direction, ε_3, but there is no lateral strain in the other direction ($\varepsilon_2=0$). Having done this the resulting vertical strain (ε_1) and the two lateral stresses were recorded and under the same σ_1 the lateral strain was increased and so on to the required ultimate value of the lateral strain. The incremental step of the lateral movement was 0.05 mm which is equal to 0.033% strain for the 150 mm cubic specimen.

The main objective of this series of experiments was to investigate the stress-strain behaviour of granular soils under plane strain conditions including:

a) the effect of lateral strain on the minor and intermediate principal stresses (σ_2 and σ_3)

b) the effect of the lateral strain on the vertical strain (ε_1)

c) the volume change of the sand in the plane strain

condition

d) the effect of the porosity of the sample and the level of vertical stress on the plane strain behaviour.

e) the effect of the lateral strain on the coefficient of earth pressure.

4.4.2 THE TEST PROGRAMME

Two series of plane strain tests were carried out in this part of the investigation. The first series was on the fine sand and included some 25 experiments with different initial porosities and different levels of vertical stress. The values of porosity tested were the same as those used for the confined tests (i.e. 42%, 43%, 45%, 47%, and 49%) and the maximum values of vertical stress for each new test were 75, 150 , 225, 300, and 375 kN/m^2.

The second series of tests was on the coarse sand and included some 10 tests. The results of the tests on this type of sand with different initial porosities in the confined conditions had shown that the variations of behaviour are small and it was therefore decided to test only the upper and lower limits of porosity, i.e. the densest and loosest cases achieved in the laboratory, equivalent to 34% (Dr=100%) and 38% (Dr=64%). The levels of applied vertical stress were the same as for the fine sand.

The testing programme including the number of experiments, levels of vertical stress, porosity of the specimens, relative densities and the type of sand used are given in table 4.2.

4.4.3 THE RELATIONSHIP BETWEEN σ_3 AND ε_3

type of sand	test number	initial porosity (%)	relative density (%)	vertical stress (kN/m^2)
fine(A)	21	42	100	75
	22	43	89	
	23	45	67	
	24	47	44	
	25	49	22	
	26	42	100	150
	27	43	89	
	28	45	67	
	29	47	44	
	30	49	22	
	31	42	100	225
	32	43	89	
	33	45	67	
	34	47	44	
	35	49	22	
	36	42	100	300
	37	43	89	
	38	45	67	
	39	47	44	
	40	49	22	
	41	42	100	375
	42	43	89	
	43	45	67	
	44	47	44	
	45	49	22	
coarse(C)	46	34	100	75
	47	38	64	
	48	34	100	150
	49	38	64	
	50	34	100	225
	51	38	64	
	52	34	100	300
	53	38	64	
	54	34	100	375
	55	38	64	

TABLE 4.2 Test programme for plane strain experiments.

In figures 4.15 to 4.19 the variation of lateral stress (σ_3) is plotted against lateral strain. The solid lines denote the coarse sand response while the dotted lines the fine sand. Each figure shows the results of tests under one value of σ_1. From the figures it can be seen that all the curves start from the values of lateral stress equal to no-lateral strain conditions. As the lateral strain is increased all σ_3 drop sharply and increasing ε_3 leads to a further decrease in σ_3. As ε_3 increases the rate of decrease of the lateral stress in most of the samples falls and after some increment of lateral strain σ_3 tends to become constant.

At low levels of σ_1, σ_3 becomes constant more quickly than at high values. For example, in figure 4.15 which shows the response of both fine and coarse sand in plane strain tests under σ_1=75 kN/m^2, there is little if any change in σ_3 after ε_3=0.3% for both materials, while in figure 4.19 for which σ_1=375 kN/m^2, there is still some change in σ_3 even after ε_3=0.60%. It is also evident that for samples with greater porosity, σ_3 tends to become stable more rapidly than for those at lower porosity.

Although the general trend for both sands is similar, for the coarse sand variations of σ_3 seem to be less dependent on the initial porosity than for fine sand. Also, for coarse sand σ_3 stabilizes more clearly at around ε_3=0.40% after which no significant decrease is discernible.

4.4.4 THE EFFECT OF ε_3 ON σ_2

In the SCTA when a sample is initially confined and subjected to a vertical stress, the two lateral stresses

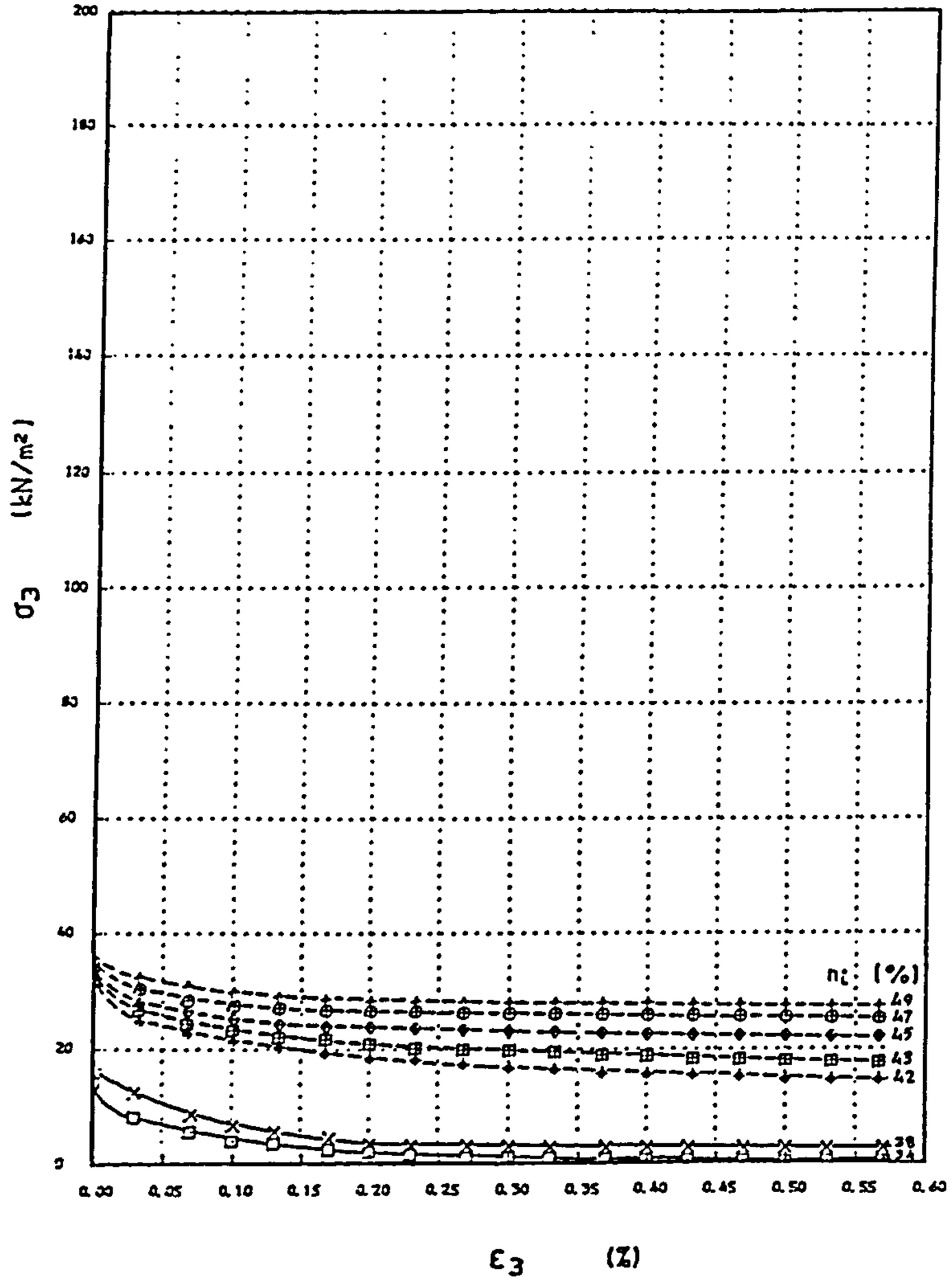

FIGURE 4.15 Relationship between σ_3 and ε_3 for different initial porosities for sands A and C under plane strain conditions with. $\sigma_1 = 75$ kN/m².

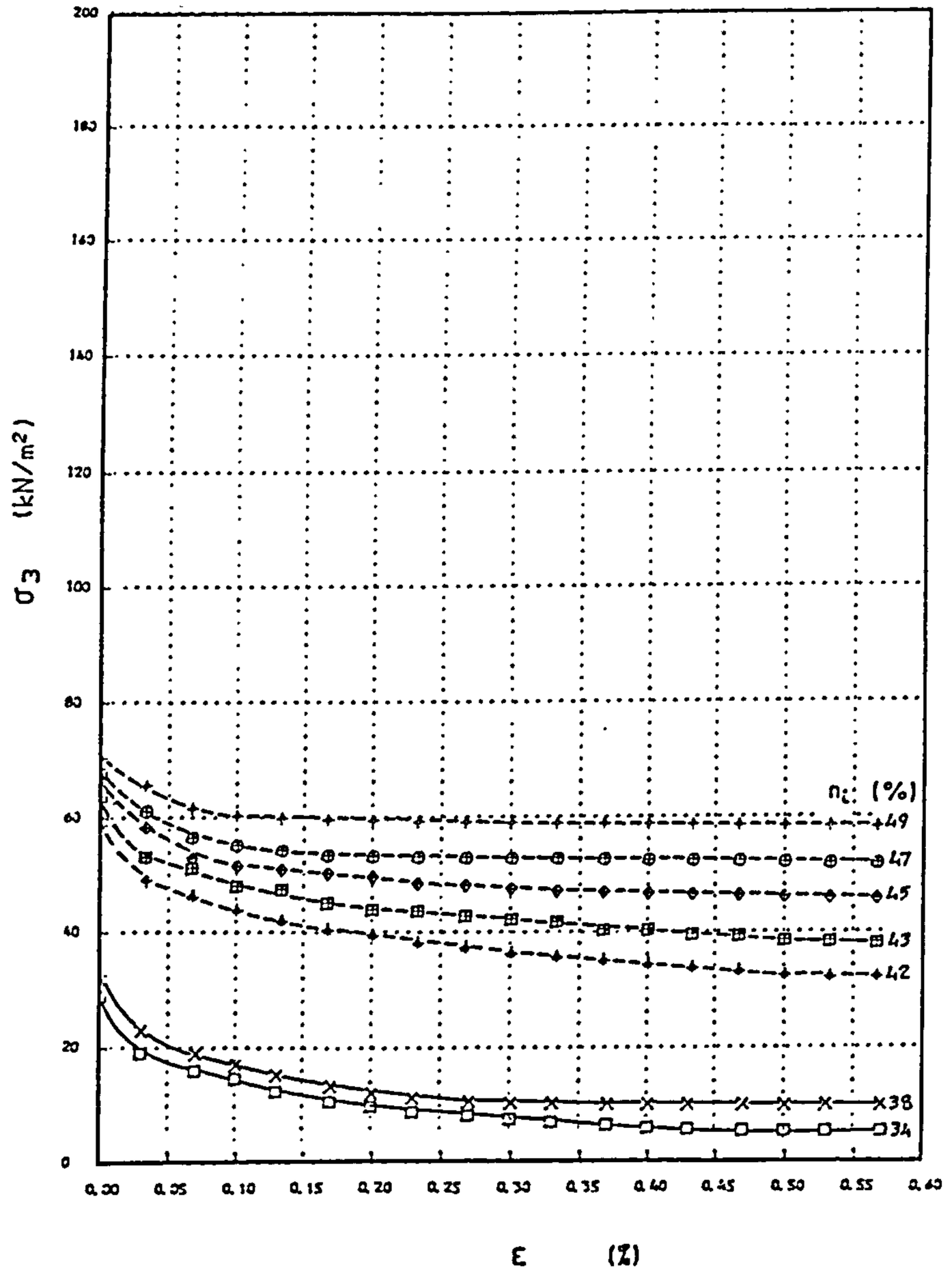

FIGURE 4.16 Relationship between σ_3 and ε_3 for different initial porosities for sands A and C under plane strain conditions with $\sigma_1 = 150$ kN/m².

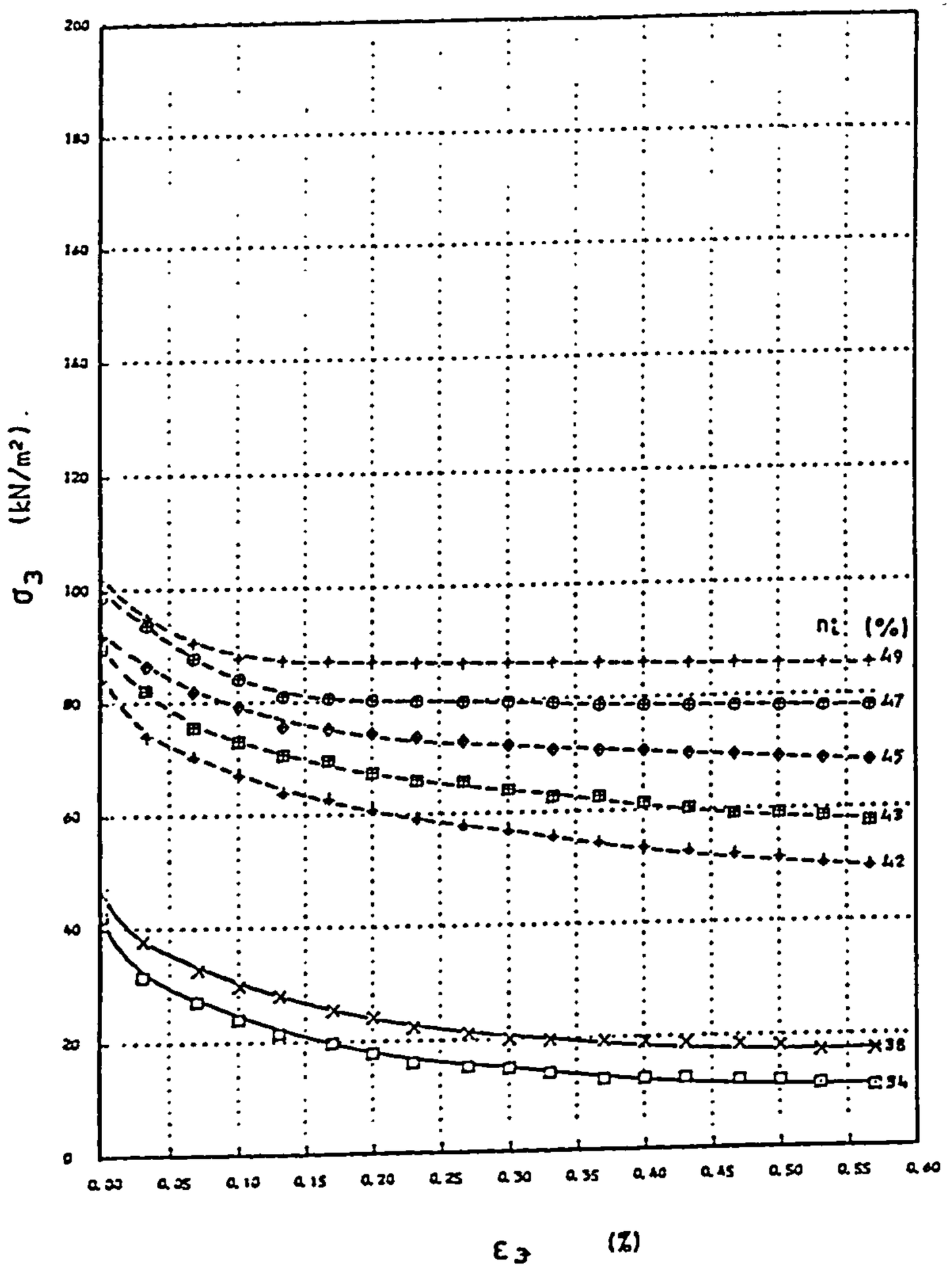

-----Sand A (fine)

——— Sand C (coarse)

FIGURE 4.17 Relationship between σ_3 and ε_3 for different initial porosities for sands A and C under plane strain conditions with $\sigma_1 = 225$ kN/m².

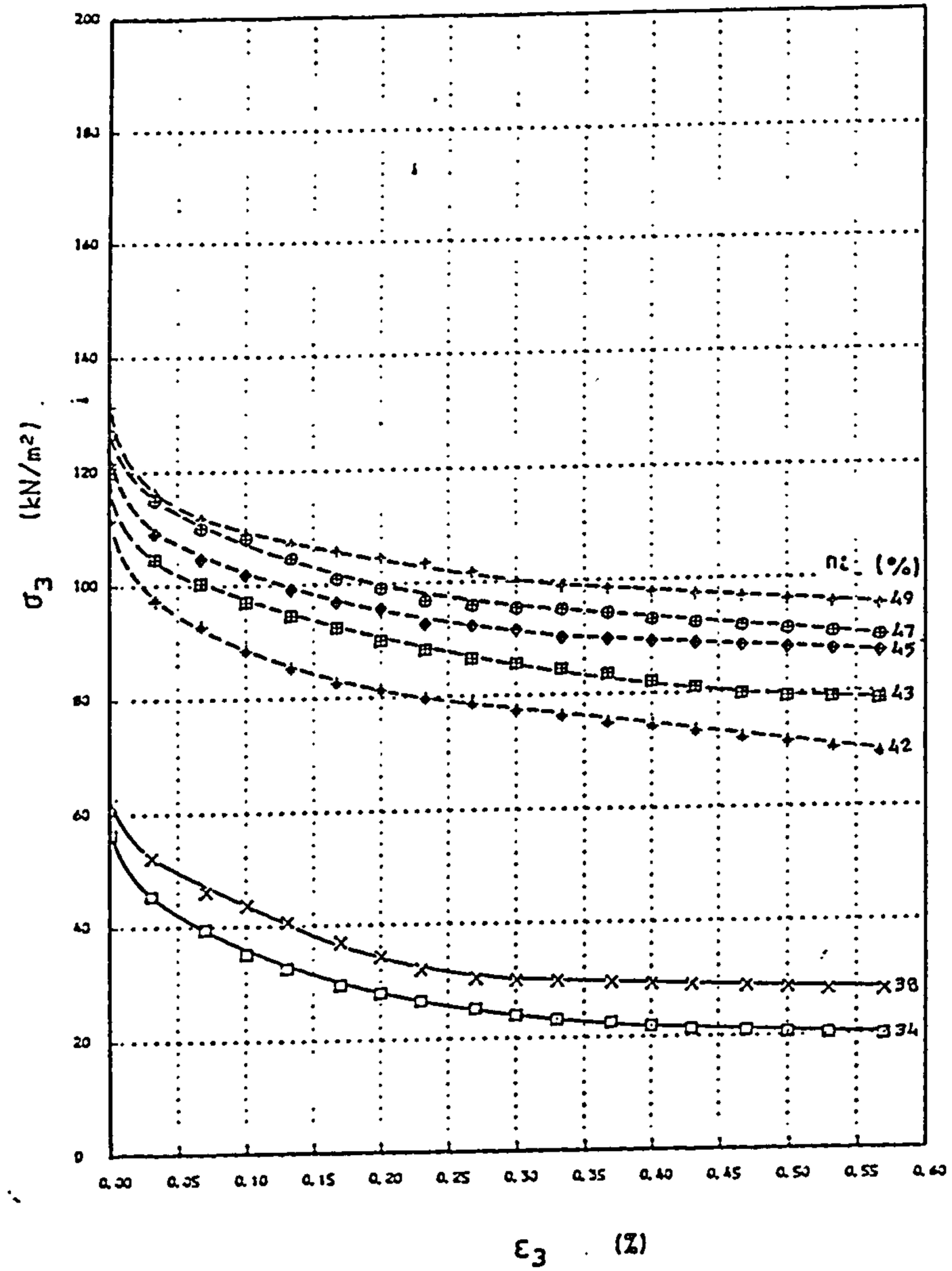

FIGURE 4.18 Relationship between σ_3 and ε_3 for different initial porosities for sands A and C under plane strain conditions with $\sigma_1 = 300$ kN/m².

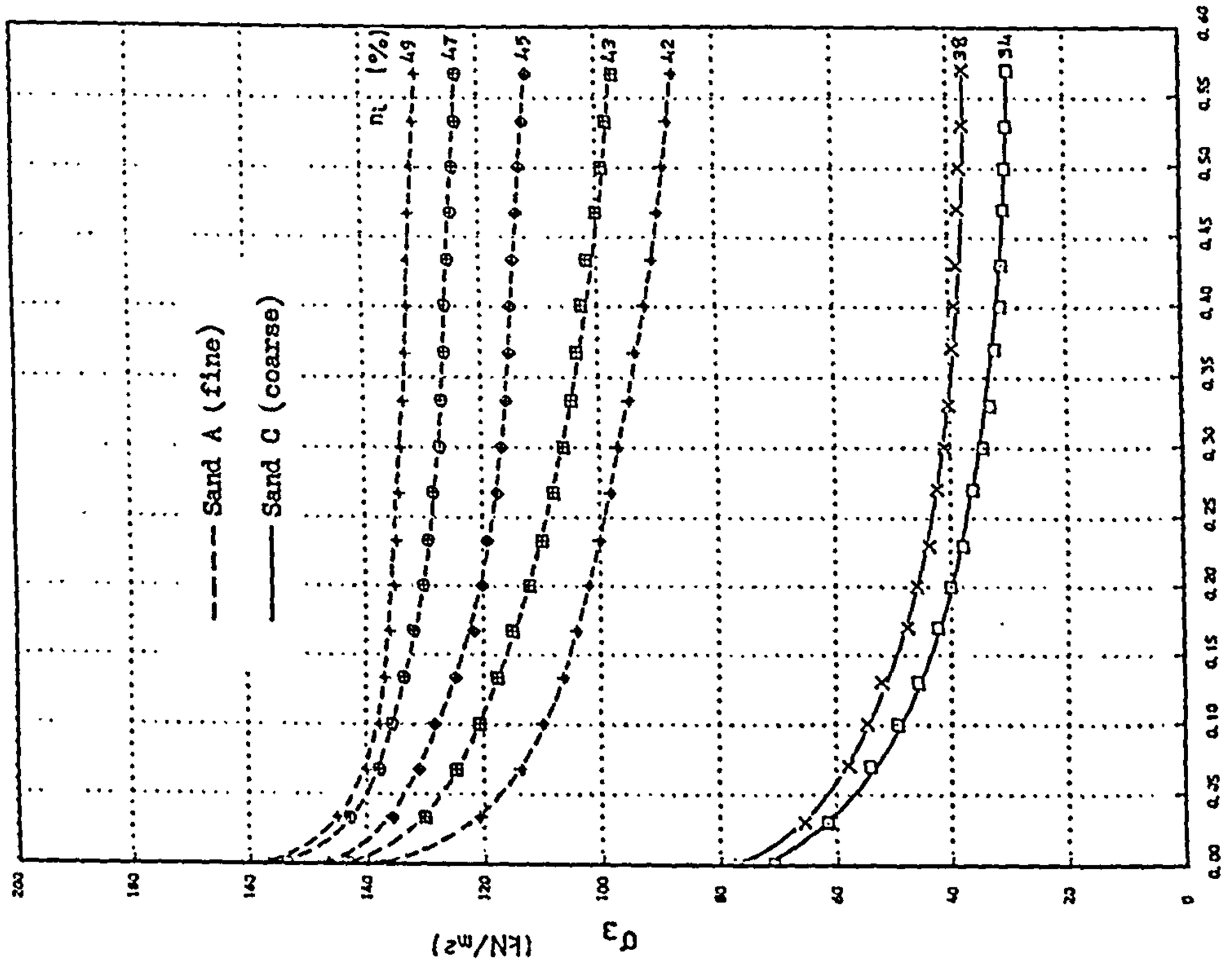

FIGURE 4.19 Relationship between σ_3 and ε_3 for different initial porosities for sands A and C under plane strain conditions with σ_1= 375 kN/m².

(minor and intermediate principal stresses) induced are equal (see section 4.3.2). Allowing lateral strain in one direction, giving the plane strain condition, will lead to a rapid fall of the lateral stress in that direction, but in the other principal direction with no-lateral strain the lateral stress will not drop. Therefore the induced lateral stress in the direction of lateral strain will be the minor principal stress (σ_3) and in the other horizontal direction will be the intermediate principal stress (σ_2).

Since the majority of the stress strain investigations carried out to date have used variations of the standard triaxial apparatus in which the lateral stresses are equal, there is limited information available on the role of the intermediate principal stress in soil behaviour.

In figures 4.20 to 4.24 the variation of σ_2 with ε_3 for different initial porosities for both fine and coarse sand are shown. It can be seen from the figures that at certain values of σ_1, σ_2 starts initially at the same values as found in the confined tests, σ_2 increases as ε_3 increases while σ_3 decreases as shown in figure 4.19. These increments for the fine sand are negligible except for the samples under maximum σ_1 but for coarse sand are significant and the medium sand response as reported by El-Gammel [22] is intermediate. The important point is that without applying any lateral strain in the direction of the intermediate principal stress it starts increasing due to the application of lateral strain in the other direction.

The increase of σ_2 seems to be dependent on vertical stress. It is apparent that at low levels of σ_1 it is small,

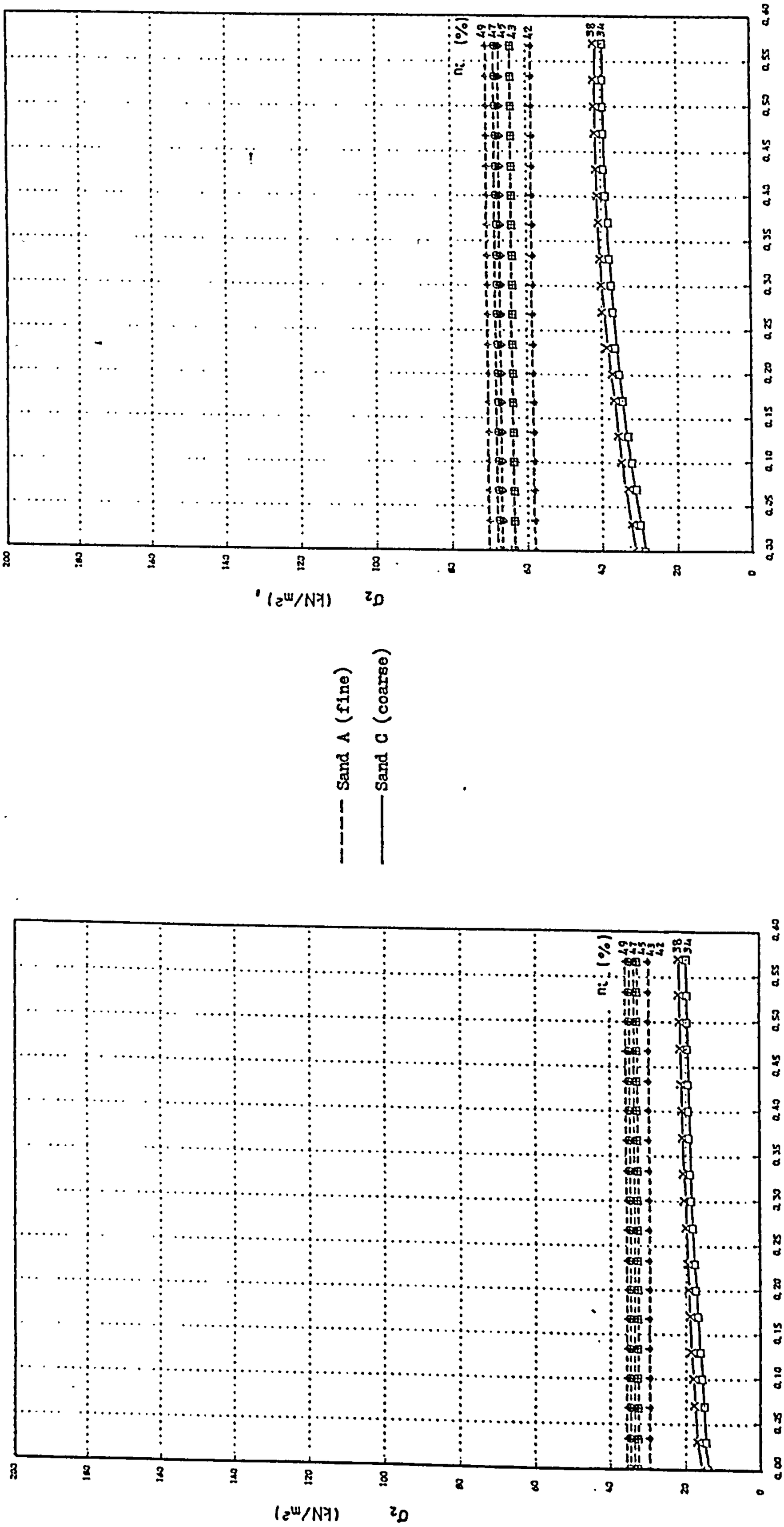

FIGURE 4.21 Relationship between σ_2 and ε_3 for different initial porosities for sands A and C under plane strain conditions with σ_1 = 150 kN/m².

FIGURE 4.20 Relationship between σ_2 and ε_3 for different initial porosities for sands A and C under plane strain conditions with σ_1 = 75 kN/m².

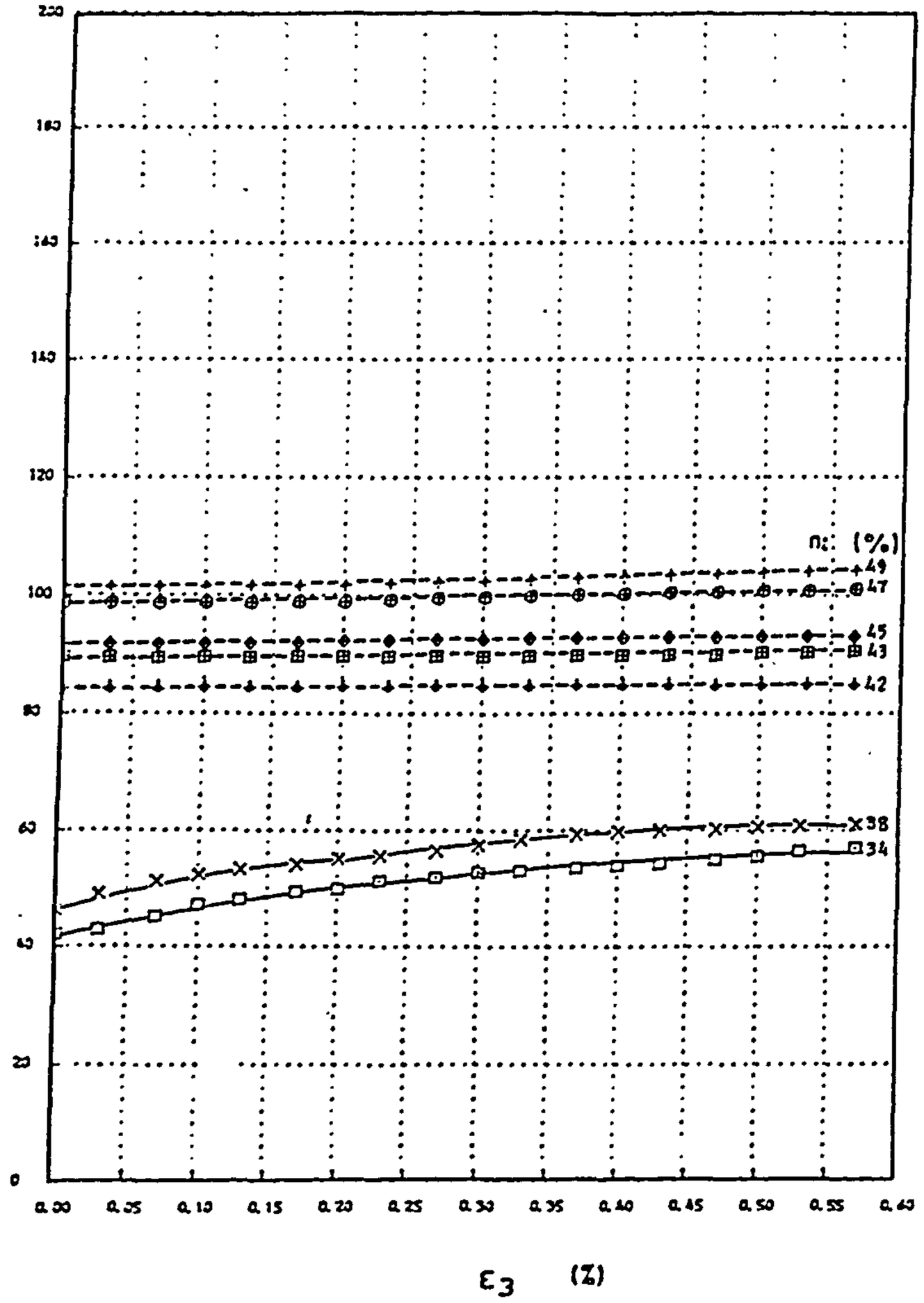

FIGURE 4.22 Relationship between σ_2 and ε_3 for different initial porosities for sands A and C under plane strain conditions with $\sigma_1 = 225$ kN/m².

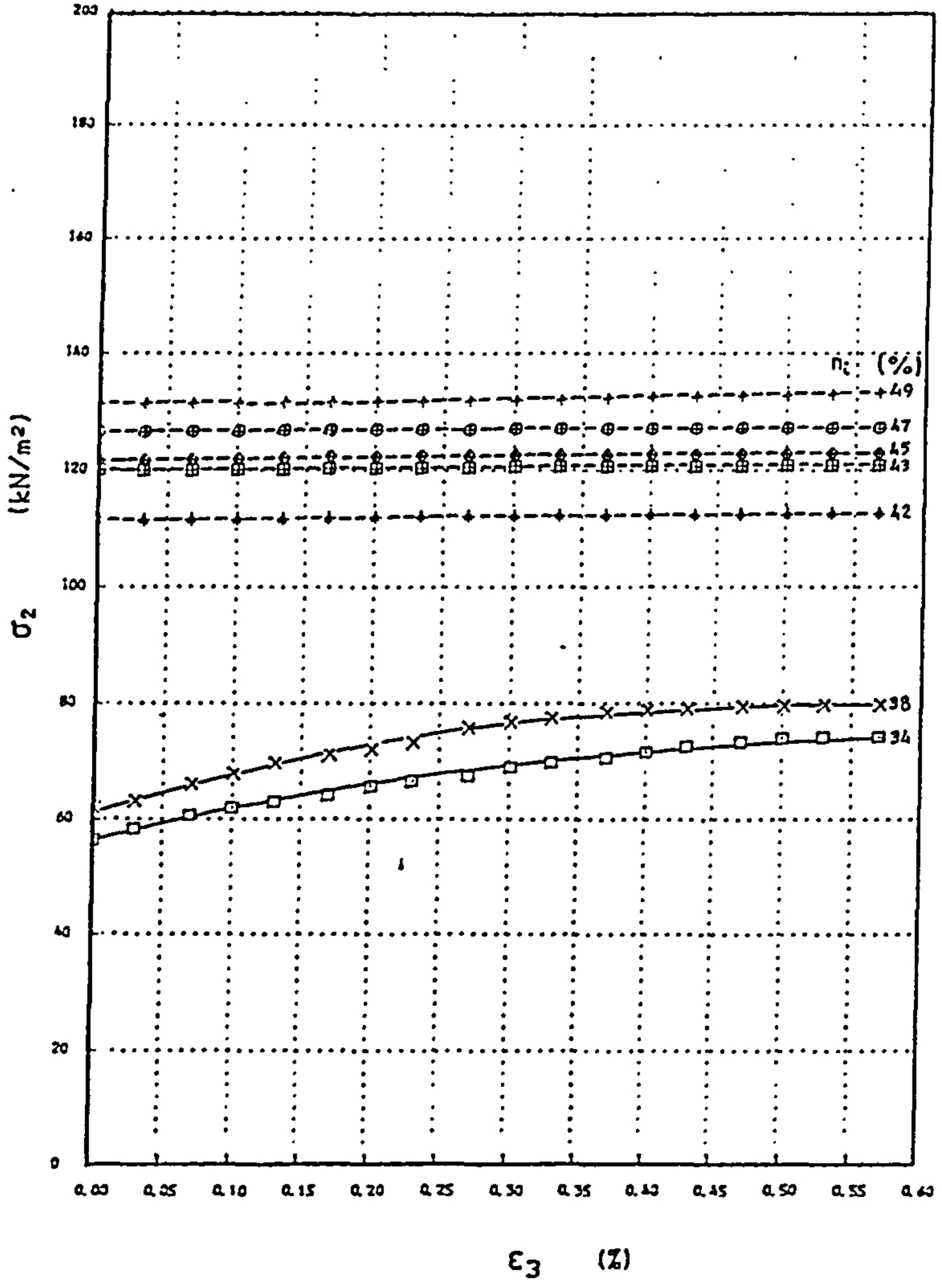

FIGURE 4.23 Relationship between σ_2 and ε_3 for different initial porosities for sands A and C under plane strain conditions with $\sigma_1 = 300$ kN/m².

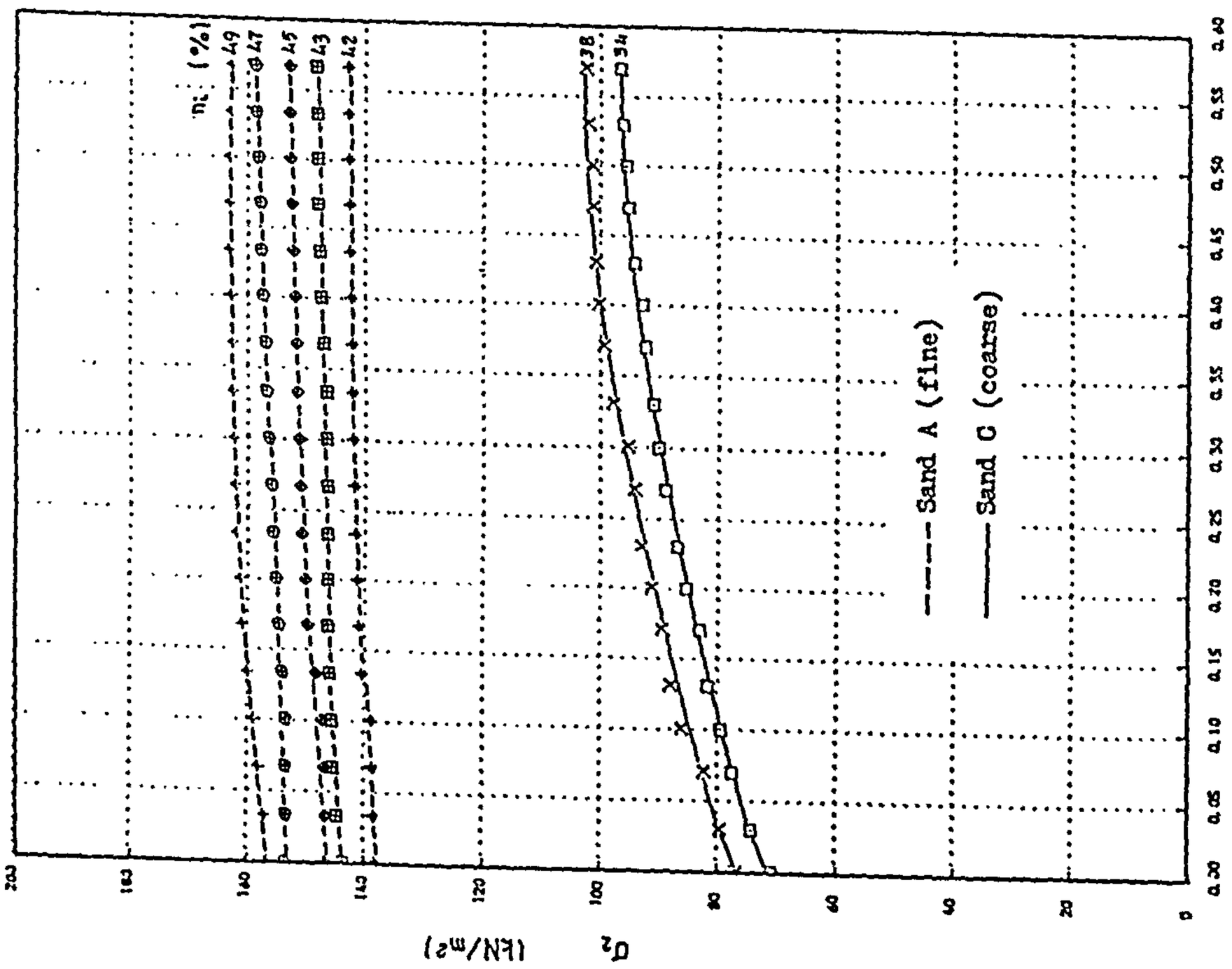

FIGURE 4.24 Relationship between σ_2 and ε_3 for different initial porosities for sands A and C under plane strain conditions with σ_1 = 375 kN/m².

but when σ_1 reaches its maximum level (375 kN/m^2) figure 4.24, it becomes marked. These variations are quite clear for the coarse sand. It is also discernible that σ_2 for the coarse sand tends to level off as the lateral strain increases and it becomes almost constant as σ_3 becomes constant. These conditions for sands are usually called the active state which means the interparticle frictional resistance has been fully mobilized.

Finally from the figures it seems that the porosity of the sand has no major effect on the response of σ_2.

4.4.5 THE RELATIONSHIP BETWEEN VERTICAL STRAIN AND LATERAL STRAIN

In figures. 4.25 to 4.29 the variation of ε_1 with ε_3 at different levels of constant σ_1 and different initial porosities for both fine and coarse sand are plotted. Having $\varepsilon_1 - \varepsilon_3$ graphs, the volume change behaviour of the samples can easily be studied. The volumetric strain can be calculated as follows:

$$\frac{\Delta V}{V} = \frac{\varepsilon_3 \cdot d^3 - \varepsilon_1 \cdot d^3}{d^3} = \varepsilon_3 - \varepsilon_1 \qquad (4.4)$$

where: Δv= sample volume change

V= initial volume of the sample

d= side dimension of the cubical samples

and ε_3 and ε_1 = minor and major principal strains.

According to the above equation , in plane strain tests if there is no volume change the vertical strain should be equal to the lateral strain and hence the curves should be straight lines at 45 degrees to the horizontal. If there is some negative volume change, i.e. $|\varepsilon_1| > |\varepsilon_3|$, the

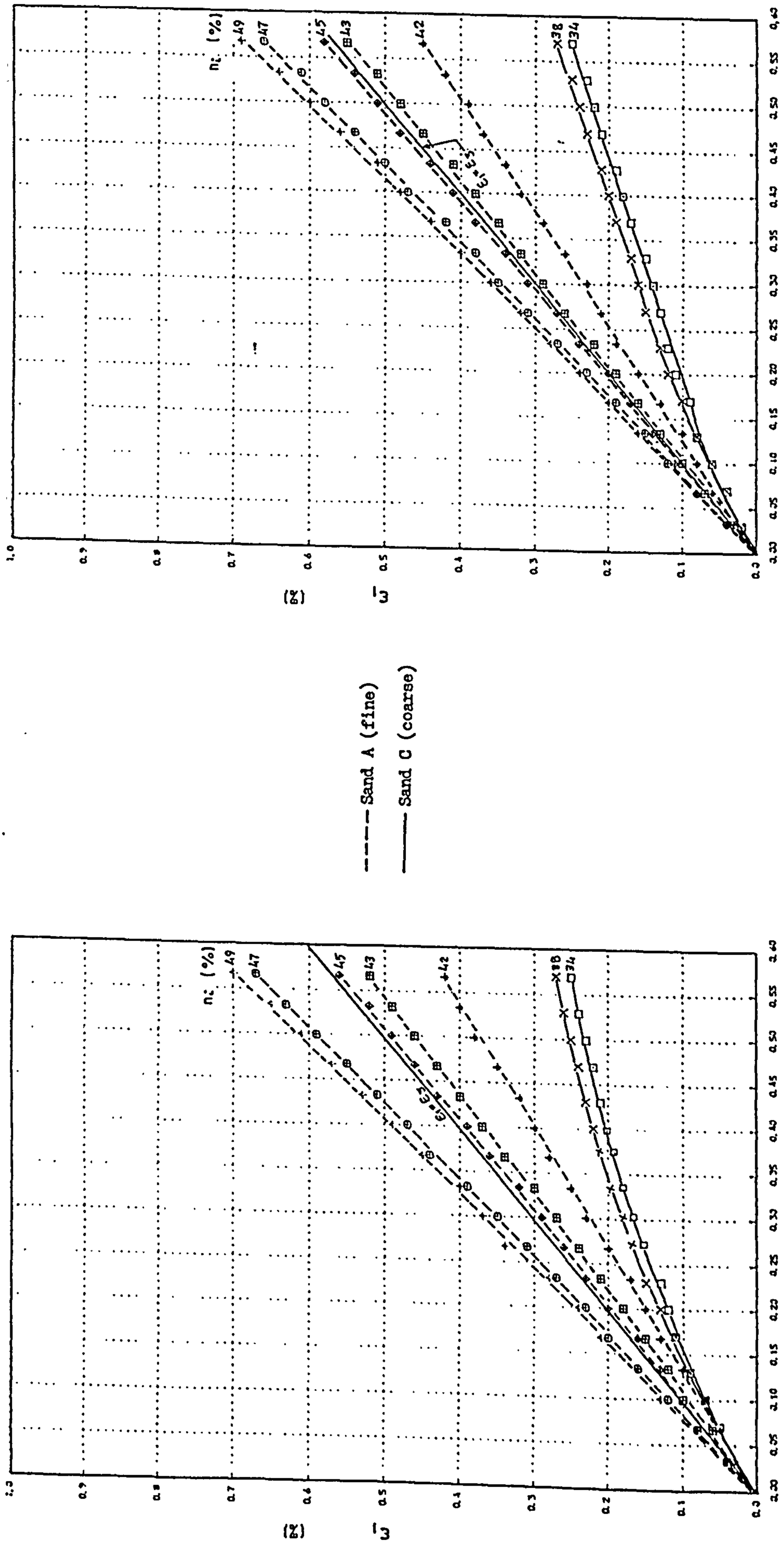

FIGURE 4.26 Relationship between ε_1 and ε_3 for different initial porosities for sands A and C under plane strain conditions with $\sigma_1 = 150$ kN/m^2.

FIGURE 4.25 Relationship between ε_1 and ε_3 for different initial porosities for sands A and C under plane strain conditions with $\sigma_1 = 75$ kN/m^2.

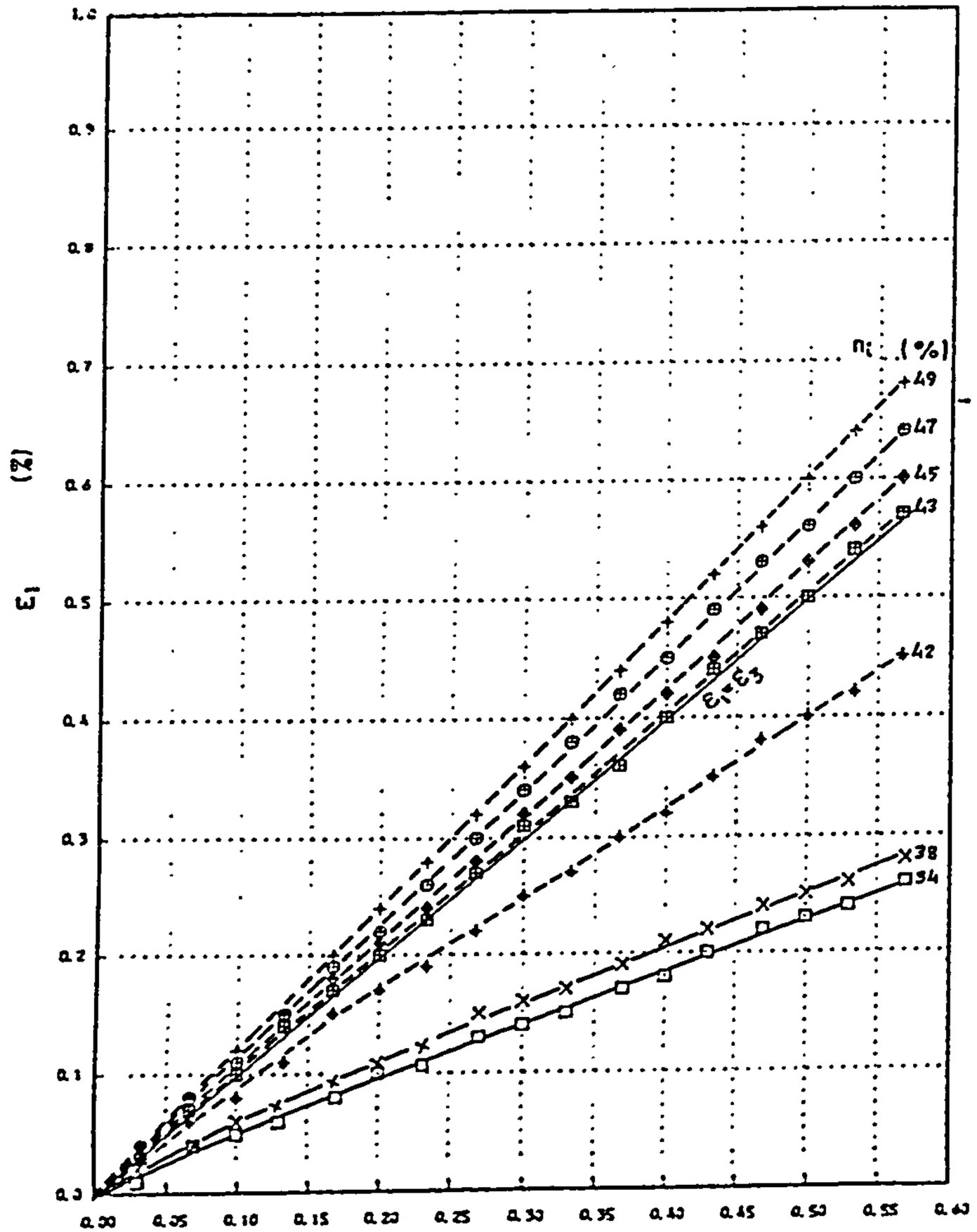

Sand A (fine)

Sand C (coarse)

FIGURE 4.27 Relationship between ε_1 and ε_3 for different initial porosities for sands A and C under plane strain conditions with $\sigma_1 = 225$ kN/m^2.

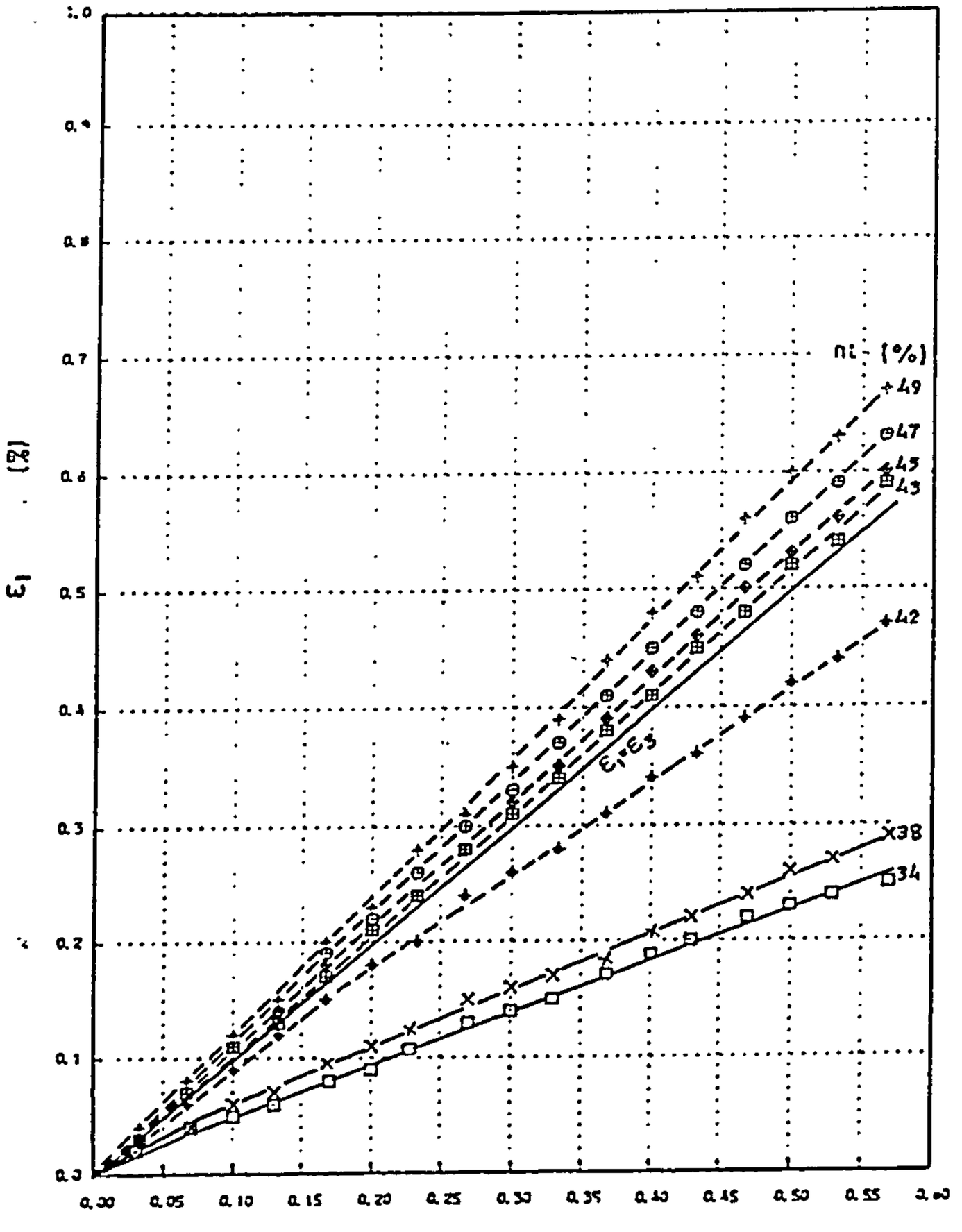

FIGURE 4.28 Relationship between ε_1 and ε_3 for different initial porosities for sands A and C under plane strain conditions with $\sigma_1 = 300$ kN/m^2.

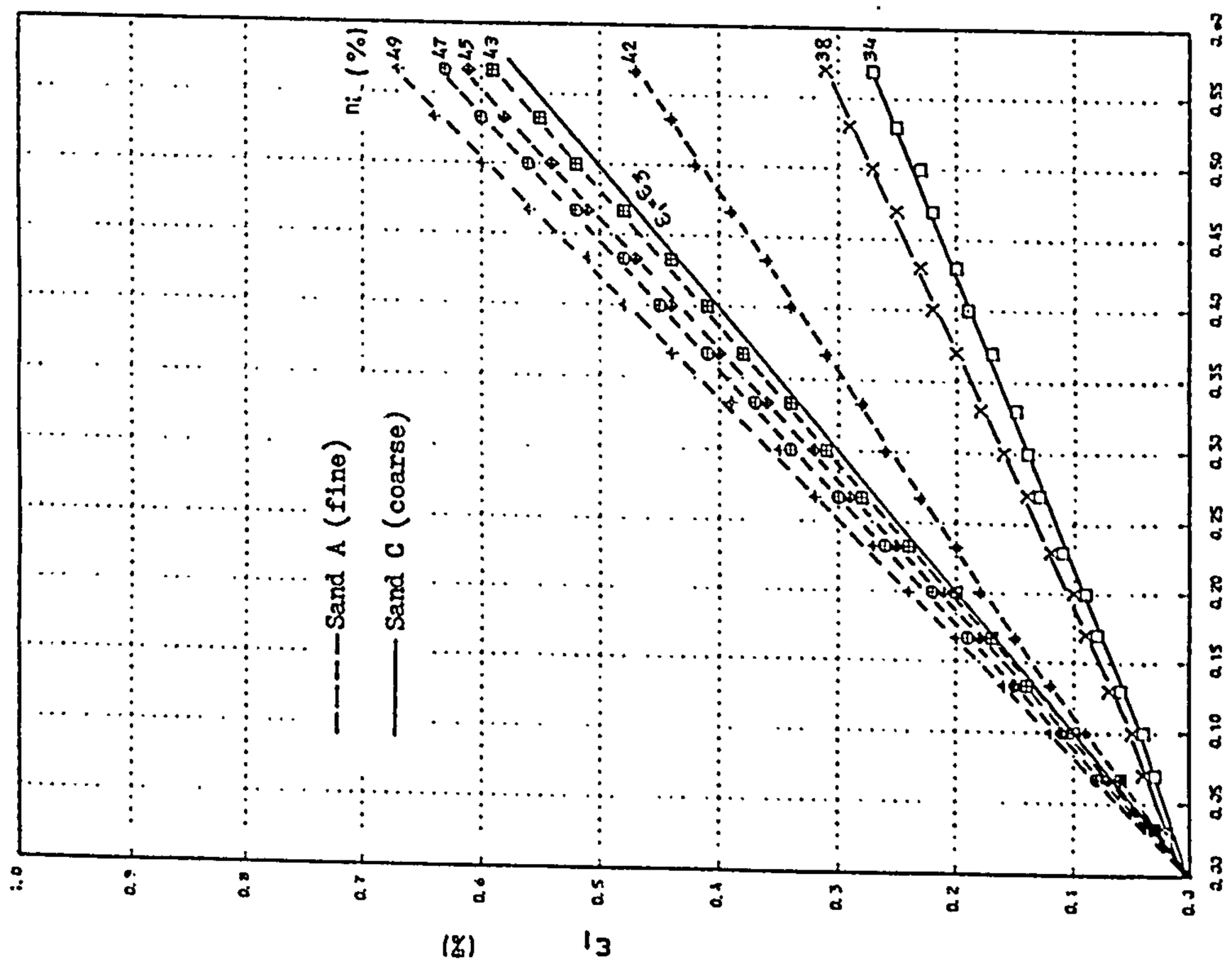

FIGURE 4.29 Relationship between ε_1 and ε_3 for different initial porosities for sands A and C under plane strain conditions with $\sigma_1 = 375$ kN/m^2.

experimental curve will be above the 45 degrees line on the $\varepsilon_1 - \varepsilon_3$ plot. In this case the sand compresses and its porosity decreases. For positive volume change, i.e. $|\varepsilon_1| < |\varepsilon_3|$ the experimental curve would lie under the 45 degrees line on the $\varepsilon_1 - \varepsilon_3$ plot. The sand in this case is dilating and its porosity will increase. In the case in which no change in porosity takes place i.e. neither contraction nor dilation occurs, the sand is said to be at its critical voids ratio.

From the figures it can be observed that for the coarse sand dilation takes place in all tests, while for the fine sand often there is notable compression and only for very dense samples (porosities=42% and 43%)is there either some dilation or no volume change.

Refering to the figures some other points can be noted:

a) The vertical strain increases as the lateral strain increases. The variation is nearly linear for fine sand, but for coarse sand there is some non-linearity initially, but after this the relationship is linear.

b) For both coarse and fine sands the increase in vertical strains for loose samples is more than that for the dense ones.

c) As the level of σ_1 increases the vertical strains for the coarse sand gradually increase but for the fine sand it happens only in the dénse condition. For the samples prepared in loose conditions (porosities=47% and 49%) there is either no change or a small decrease on increasing the vertical stress.

d) In spite of preparing the specimens of both fine

and coarse sands for ranges of initial porosities i.e. from very loose to very dense, it seems that the general state of packing of the fine samples is loose in comparison with its critical voids ratio , while for the coarse sand it is quite dense with initial porosities below critical.

4.4.6 THE RELATIONSHIP BETWEEN THE COEFFICIENT OF LATERAL STRESS AND LATERAL STRAIN

The variations of the ratio of σ_3/σ_1 with the lateral strain for different initial porosities and different levels of constant vertical stress for both fine and coarse sand are shown in figures 4.30 to 4.34.

From the figures it is evident that the coefficient of lateral stress for each series of graphs starts from Ko values, but as the first step of lateral strain is applied it decreases. Increasing the lateral strain the coefficient keeps decreasing but at a decreasing rate, and finally the value becomes almost constant. The state after which no further significant change takes place is called the active state and the coefficient of lateral stress at this stage is said to be the coefficient of active earth pressure (Ka).

It can be seen that Ka depends on the level of the vertical stress, porosity of the sand, and type of the sand. The effect of the porosity of the sample decreases as the level of vertical stress increases. For loose samples the sand reaches its active state at lower strains than for dense samples.

In figures 4.35 to 4.39 the variation of the ratio of σ_2/σ_1 against ε_3 are plotted. The coefficients of lateral stress (σ_2 / σ_1) in this case begin from the same points as

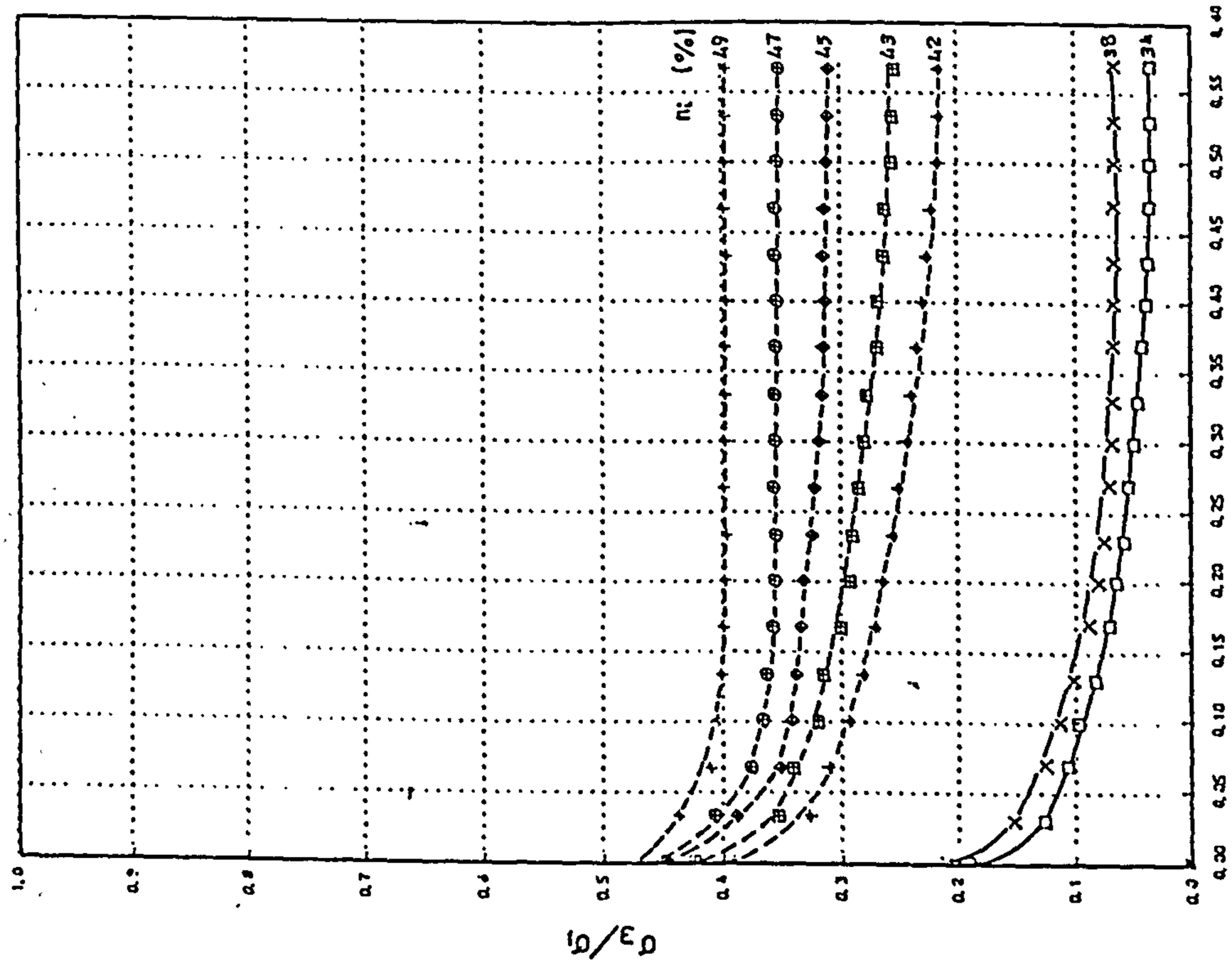

FIGURE 4.31 Variation of the ratio of σ_3/σ_1 with ε_3 for different initial porosities for sands A and C under plane strain conditions with $\sigma_1 = 150$ KN/m².

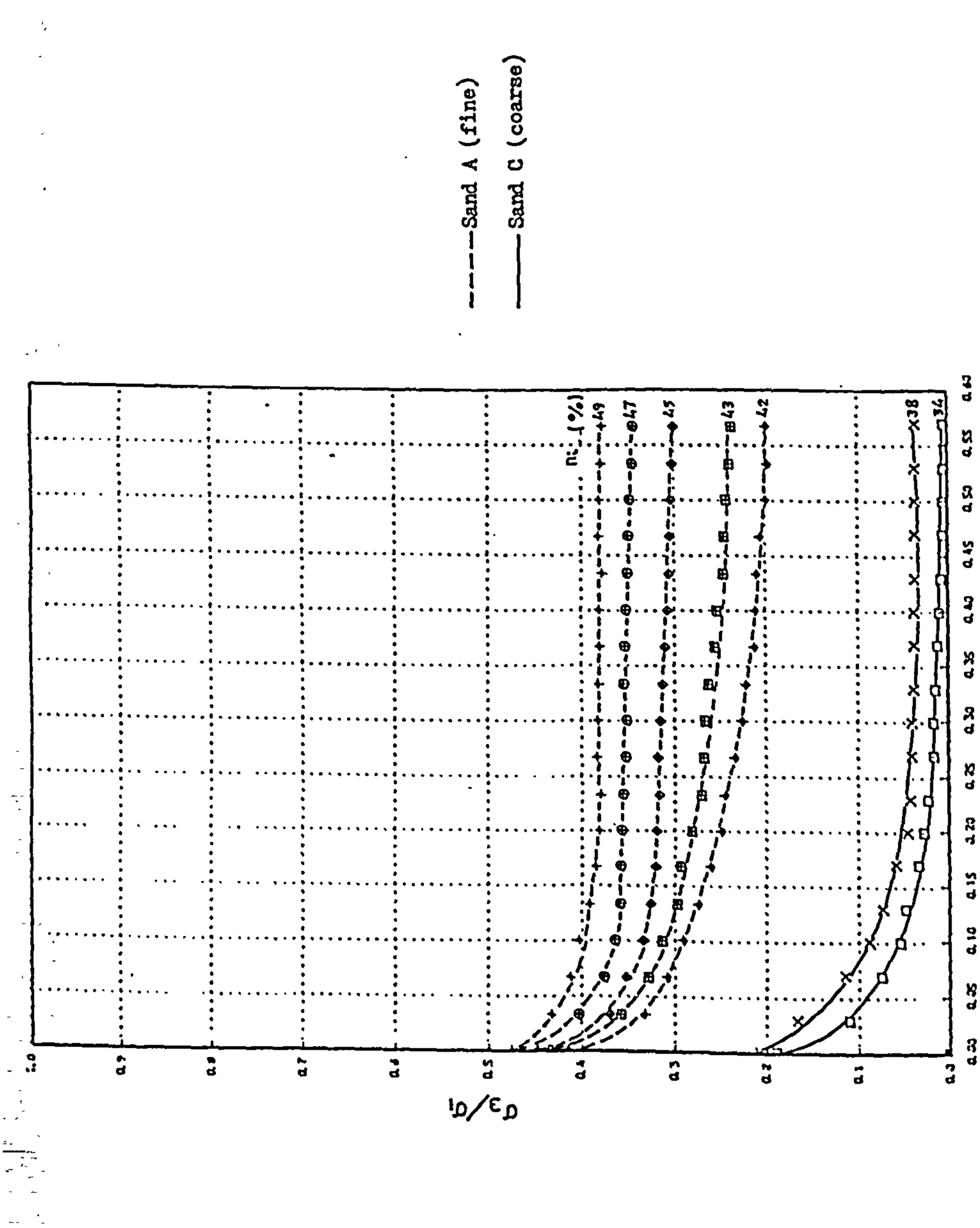

FIGURE 4.30 Variation of the ratio of σ_3/σ_1 with ε_3 for different initial porosities for sands A and C under plane strain conditions with $\sigma_1 = 75$ KN/m².

---Sand A (fine)
——Sand C (coarse)

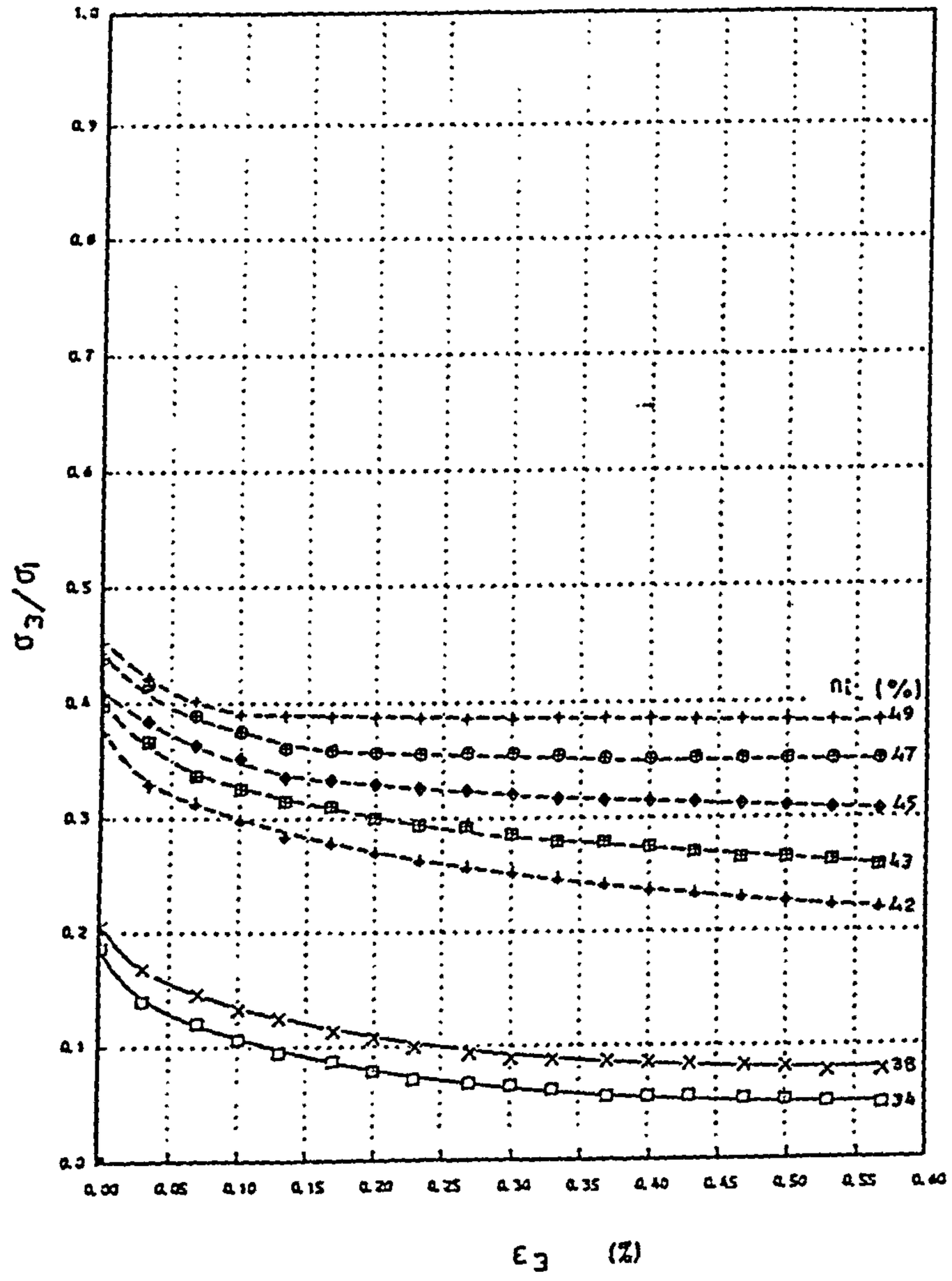

FIGURE 4.32 Variation of the ratio of σ_3/σ_1 with ε_3 for different initial porosities for sands A and C under plane strain conditions with $\sigma_1 = 225$ kN/m^2.

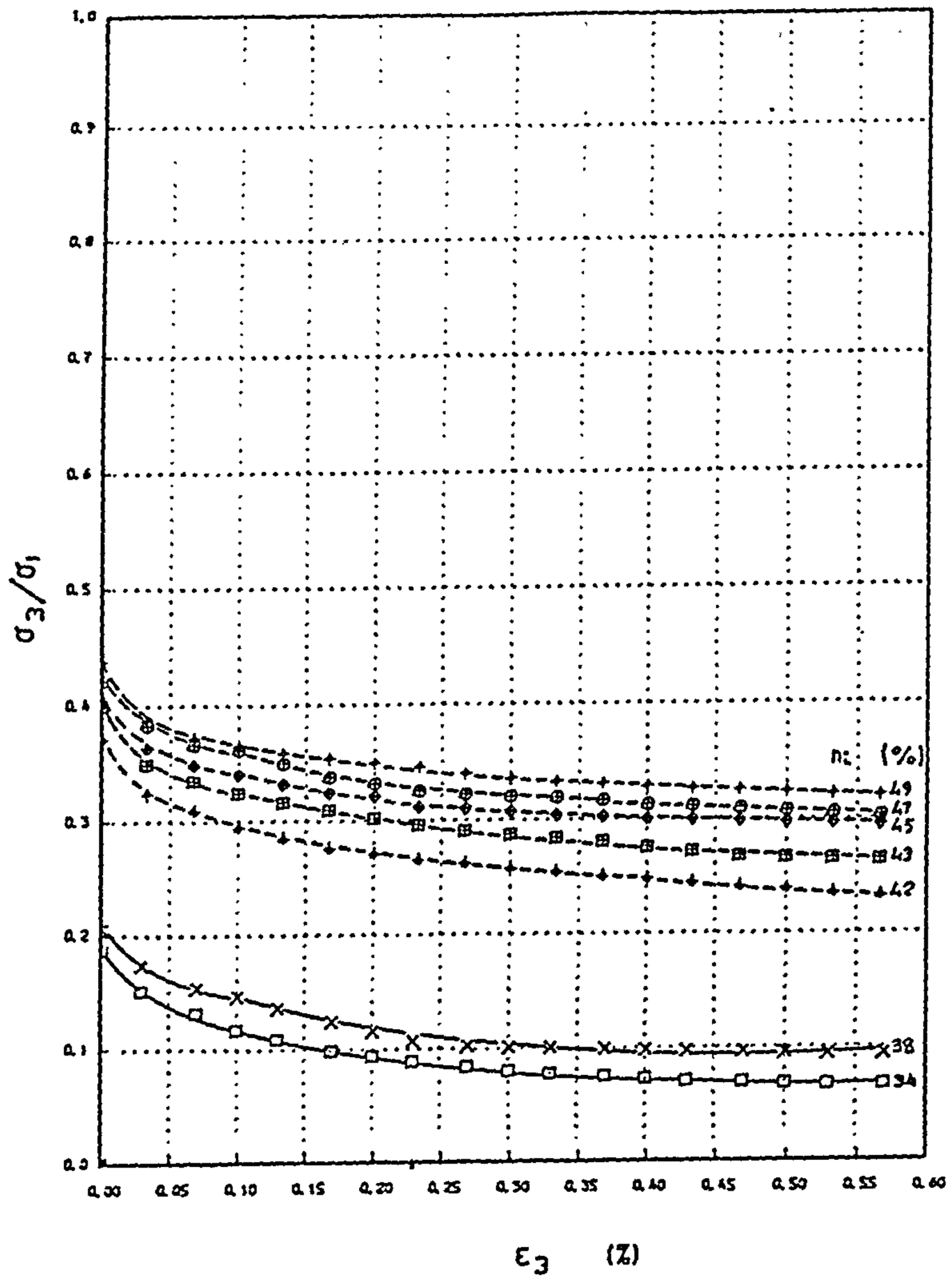

FIGURE 4.33 Variation of the ratio of σ_3/σ_1 with ε_3 for different initial porosities for sands A and C under plane strain conditions with $\sigma_1 = 300$ kN/m^2.

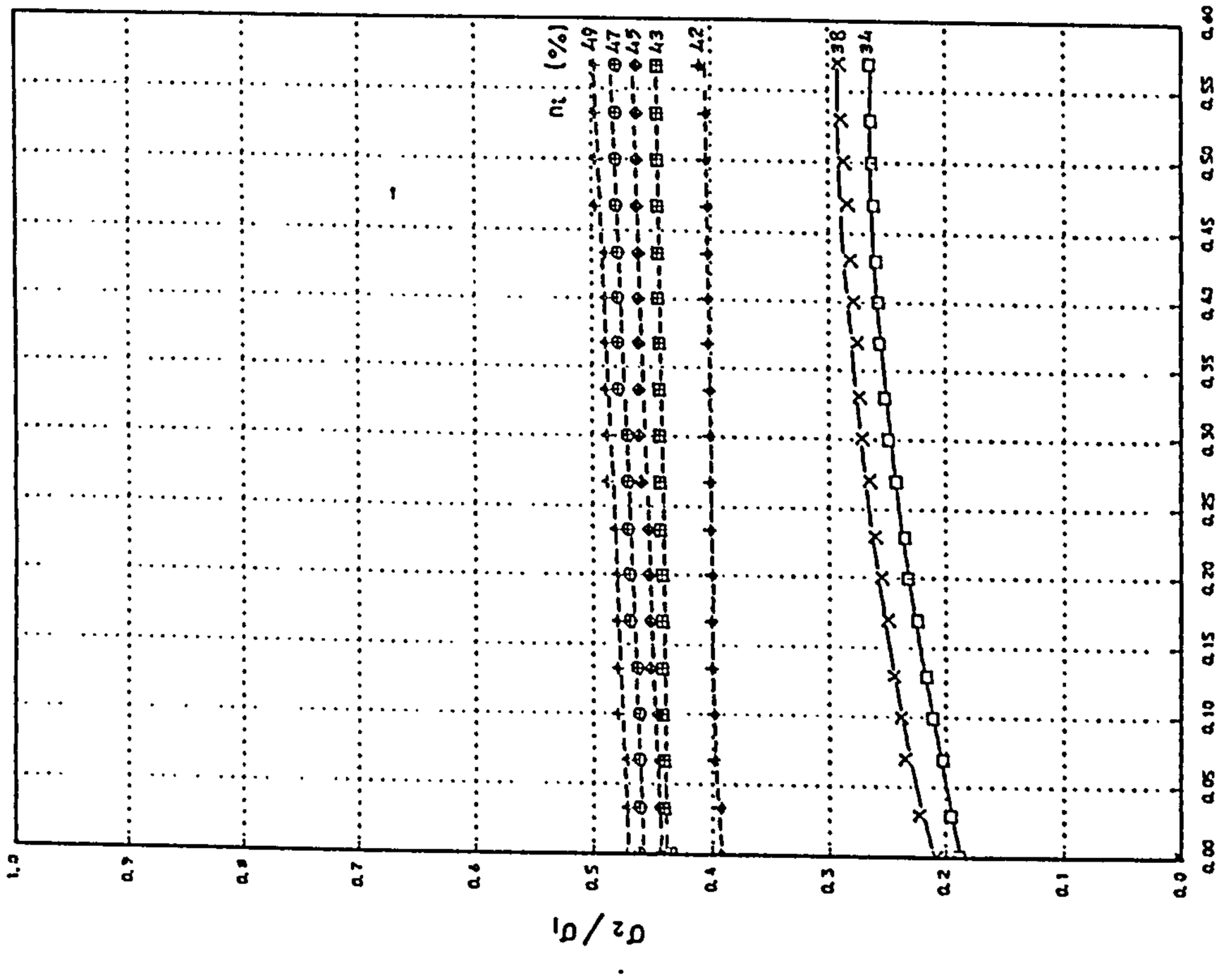

FIGURE 4.35 Variation of the ratio of σ_2/σ_1 with ε_3 for different initial porosities for sands A and C under plane strain conditions with σ_1 = 75 kN/m^2.

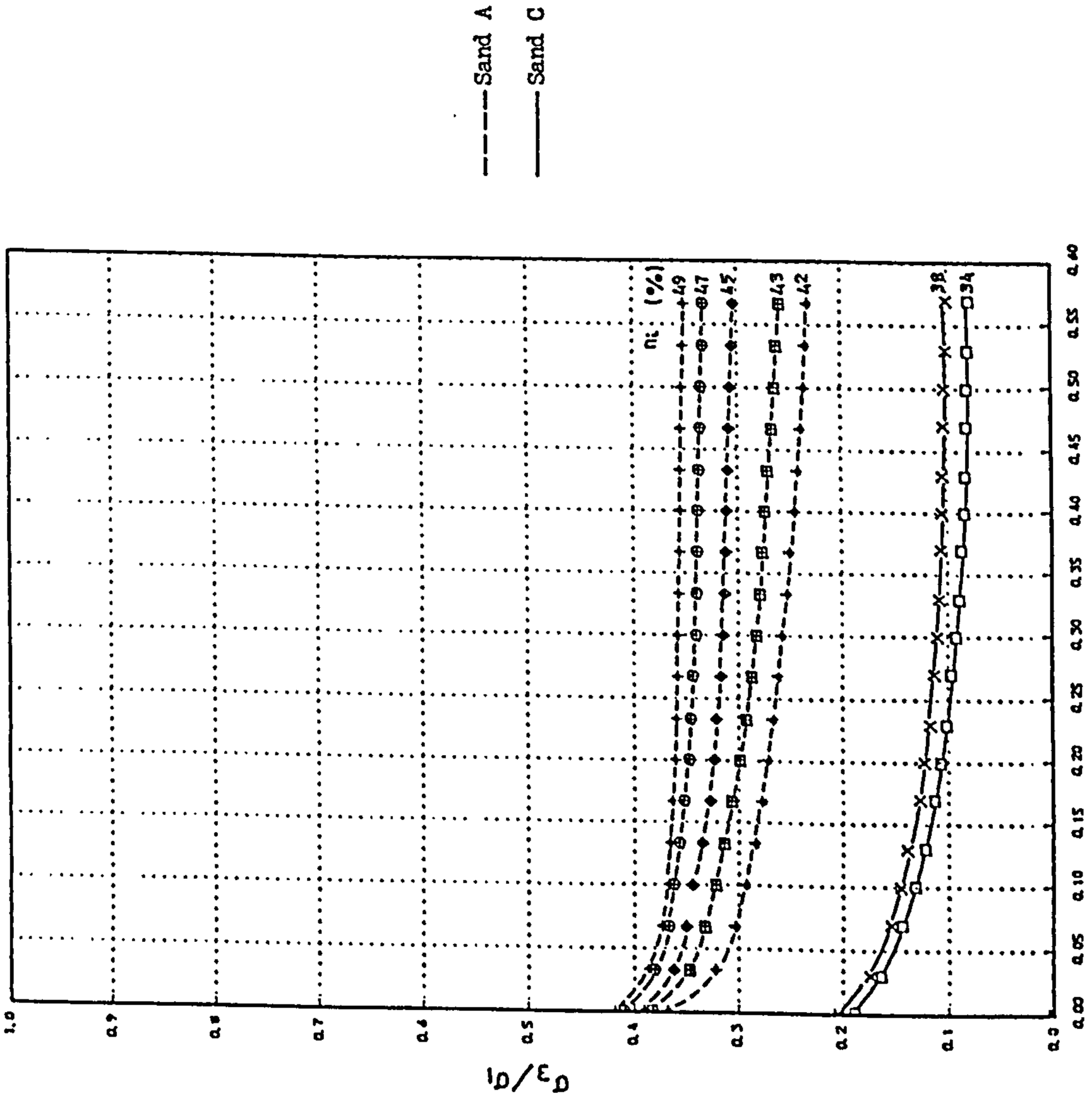

FIGURE 4.34 Variation of the ratio of σ_3/σ_1 with ε_3 for different initial porosities for sands A and C under plane strain conditions with σ_1 = 375 kN/m^2.

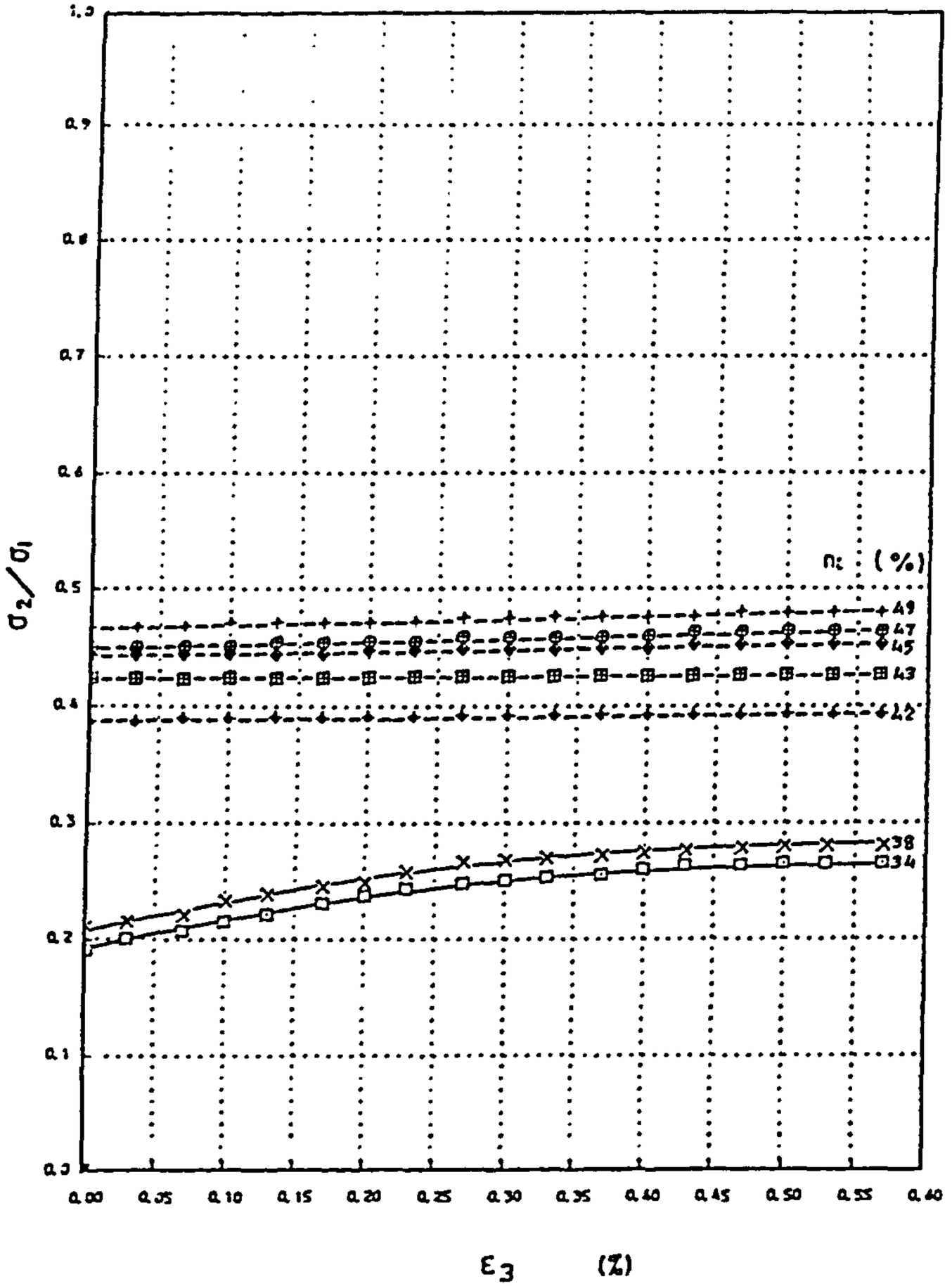

FIGURE 4.36 Variation of the ratio of σ_2/σ_1 with ε_3 for different initial porosities for sands A and C under plane strain conditions with $\sigma_1 = 150$ kN/m².

----- Sand A (fine)

——— Sand C (coarse)

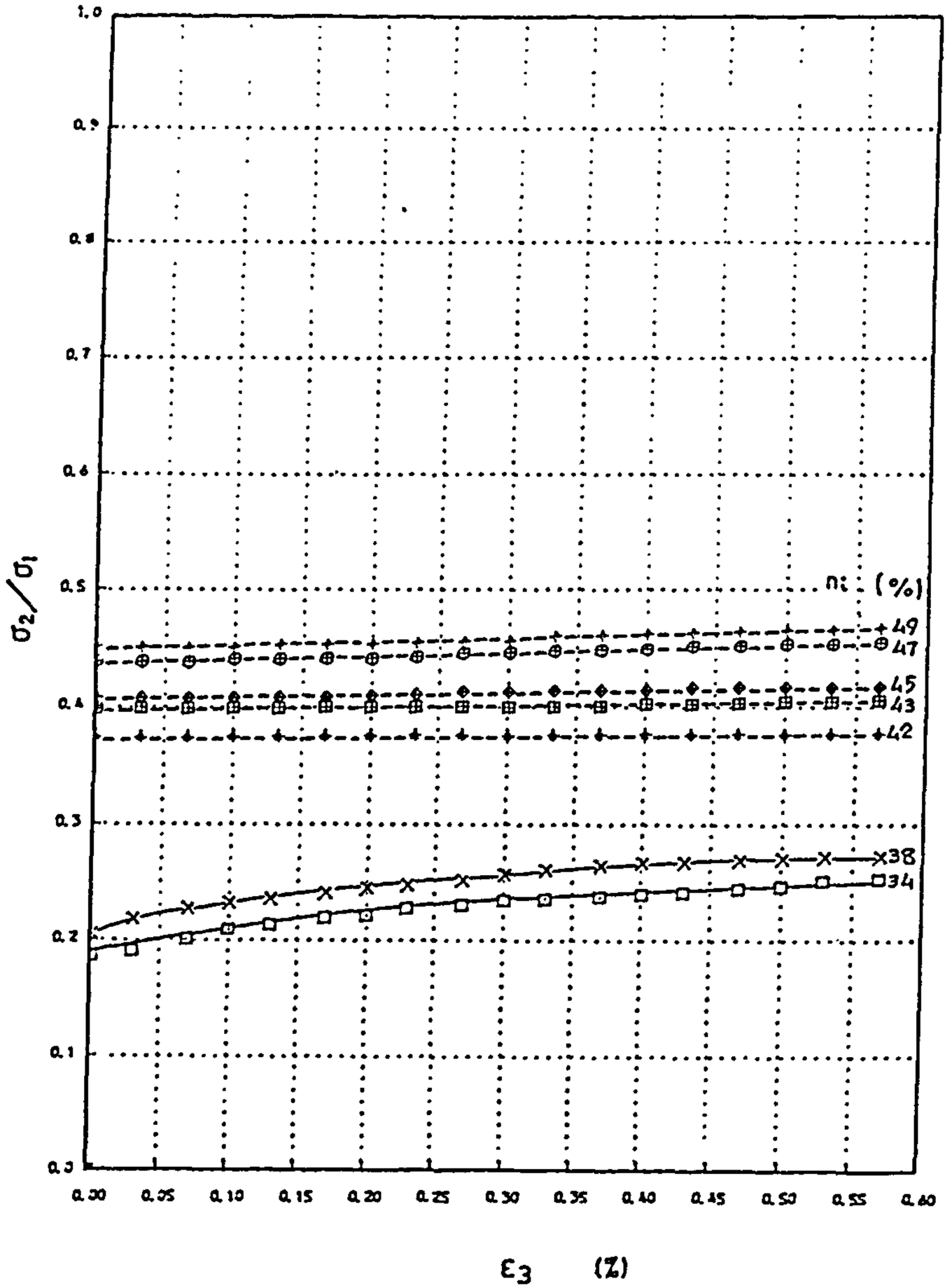

FIGURE 4.37 Variation of the ratio of σ_2/σ_1 with ε_3 for different initial porosities for sands A and C under plane strain conditions with $\sigma_1 = 225$ kN/m².

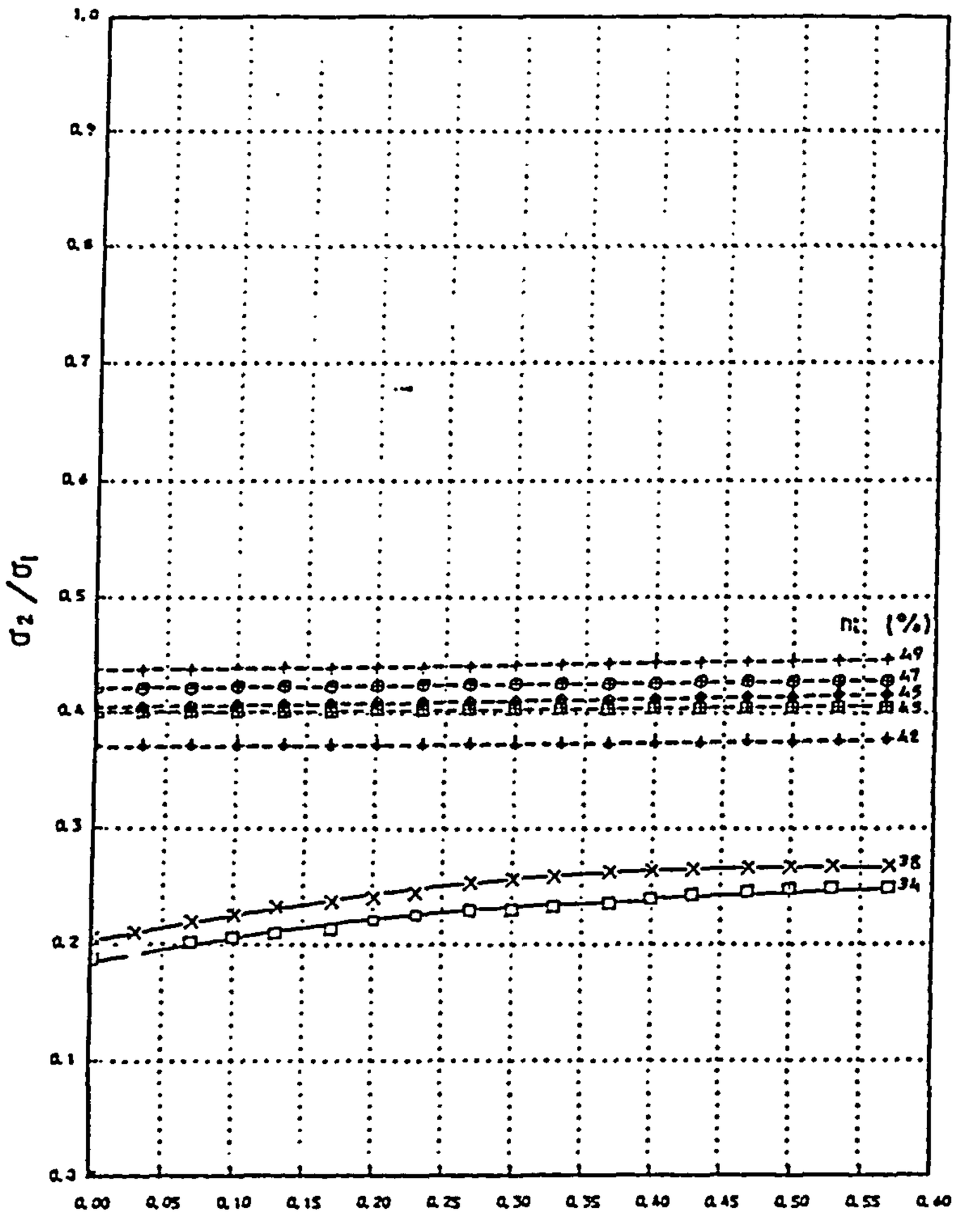

Sand A (fine)

Sand C (coarse)

FIGURE 4.38 Variation of the ratio of σ_2/σ_1 with ε_3 for different initial porosities for sands A and C under plane strain conditions with $\sigma_1 = 300$ kN/m^2.

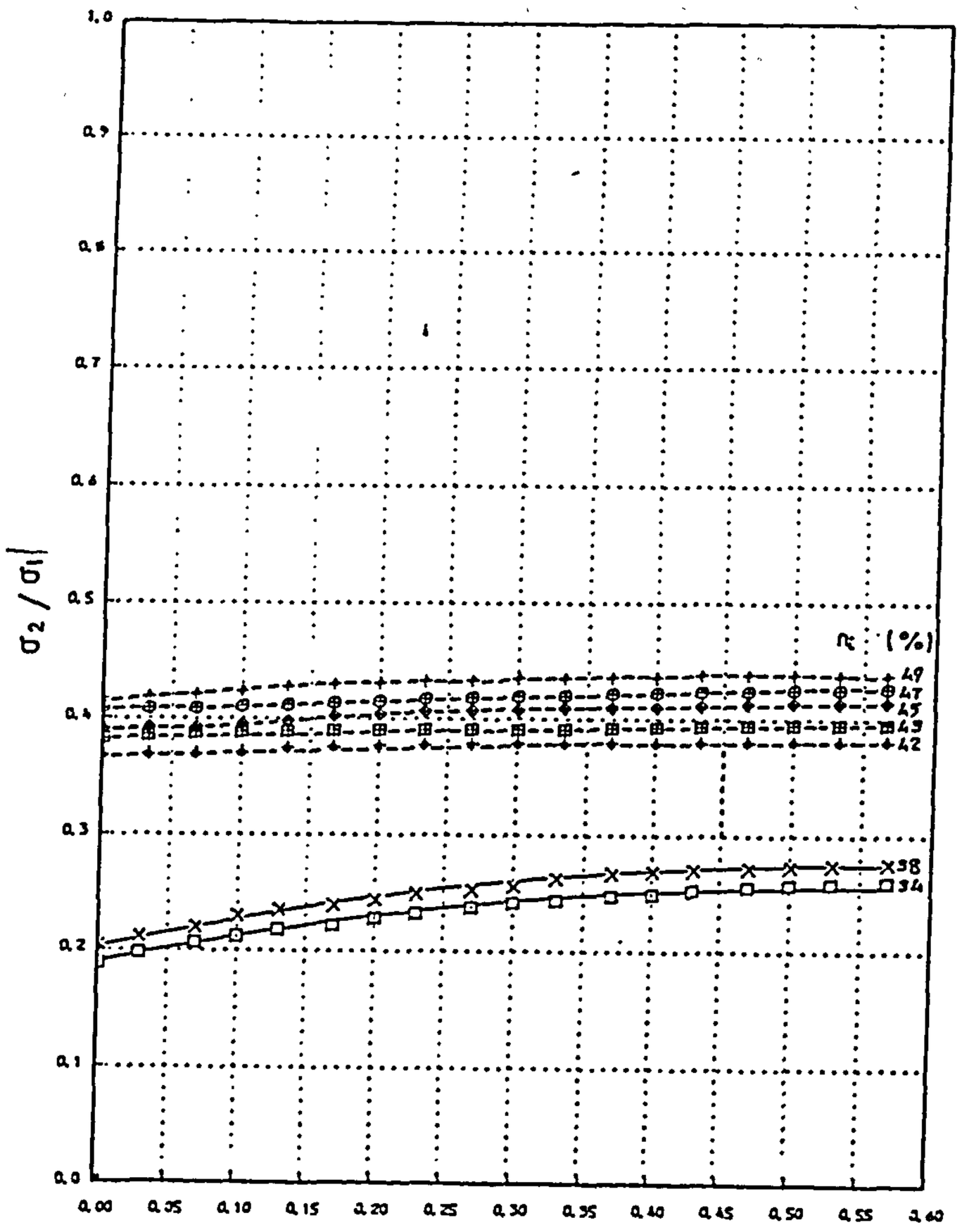

FIGURE 4.39 Variation of the ratio of σ_2 / σ_1 with ε_3 for different initial porosities for sands A and C under plane strain conditions with $\sigma_1 = 375$ kN/m^2.

mentioned above (i.e. Ko). but they increase with increasing lateral strain. The increase for the fine sand is not so marked but for coarse sand it is quite discernible. The rate of increase of the coefficients drops as ε_3 keeps increasing and finally they become more or less stable as the sand reaches its active state.

4.5 TRIAXIAL TESTS

The vast majority of triaxial stress-strain experiments that have been carried out on sand so.far have used some kind of standard triaxial apparatus in which the confining pressure on the sample is applied by means of water pressure on a cylindrical specimen and the vertical stress is applied along the axis of the sample. In the SCTA triaxial tests are different in that the cubical samples are subjected to two independent lateral strains (ε_2 and ε_3) simultaneously while the specimen is under a constant vertical stress (σ_1). If the applied lateral strains are equal, $\varepsilon_2=\varepsilon_3$, the lateral stresses should also be equal but usually, due to practical difficulties, there are small differences between the two lateral stresses which, however, can be neglected in analysis (see section 4.3.2).

The triaxial tests carried out on the SCTA in this investigation can be assumed to be similar to those carried out on the standard triaxial apparatus in which the vertical stress on the sample (σ_1) is kept constant and the confining pressure (σ_3) is gradually decreased, except that the sample here is in a symmetric rather than axi-symmetric condition, which is the case in the standard triaxial apparatus.

4.5.1 THE OBJECTIVES OF THE TESTS

The reason for performing triaxial tests in the SCTA was to study the behaviour of cubic samples under different levels of vertical stress and different initial porosities while they were allowed to strain in the three principal directions, the lateral strains being equal. The information obtained in the other monotonic tests covers only the behaviour of sands subjected to confined and plane strain conditions. The detailed objectives of this series of tests are:

a) To study the effect of the lateral strains on the lateral stresses.

b) To study the effect of the lateral strains on the vertical strain.

c) To study the volume changes of the sample in this condition.

d) To study the variations of the ratios of the lateral stress to the vertical stress of the sand.

e) to compare the results with those obtained in plane strain conditions.

4.5.2 TEST PROCEDURE AND TEST PROGRAMME

The test procedure is similar to that of the plane strain tests (section 4.4.1). The only difference here is the application of lateral strain in two directions instead of only one. Independent and different lateral strains can be applied to specimens but in this research project in order to compare the results with plane strain tests, the lateral strains were kept equal ($\varepsilon_2 = \varepsilon_3$) and applied

simultaneously.

In a similar manner to the plane strain tests the cubic samples of both fine and coarse sand with different initial porosities were subjected to different constant levels of vertical stress from 75 to 375 kN/m^2. For each test the lateral strains were applied in both directions in steps of 0.033% up to 0.60% equally. The lateral stresses (σ_2 and σ_3) and the vertical strain (ε_1) after applying σ_1 at the begining of the tests, and after each step of increasing lateral strains were measured and recorded.

Some 25 tests on the fine sand and 10 tests on the coarse sand were carried out in order to cover the required range of conditions. The test programme including the test numbers, the initial porosity of the samples, relative densities, the levels of vertical stress and finally, the type of sand used are given in table 4.3.

4.5.3 THE RELATIONSHIP BETWEEN LATERAL STRAINS AND LATERAL STRESSES

The variation of σ_2 and σ_3 with lateral strains for different initial porosities and different levels of σ_1 are plotted in figures 4.40 to 4.44.

As mentioned in section 4.5 on applying equal lateral strains to the samples the resulting lateral stresses should be equal ($\sigma_2 = \sigma_3$), but during the experiments they exhibited some small differences which were (less than 2% of the average) and so the differences have been neglected. To demonstrate the differences between σ_2 and σ_3 in each figure both have been marked and then the best curve fitting their average values is plotted. It can be seen that the values of σ_2

type of sand	test number	initial porosity (%)	relative density (%)	vertical stress (kN/m^2)
Fine(A)	56	42	100	75
	57	43	89	
	58	45	67	
	59	47	44	
	60	49	22	
	61	42	100	150
	62	43	89	
	63	45	67	
	64	47	44	
	65	49	22	
	66	42	100	225
	67	43	89	
	68	45	67	
	69	47	44	
	70	49	22	
	71	42	100	300
	72	43	89	
	73	45	67	
	74	47	44	
	75	49	22	
	76	42	100	375
	77	43	89	
	78	45	67	
	79	47	44	
	80	49	22	
Coarse(C)	81	34	100	75
	82	38	64	
	83	34	100	150
	84	38	64	
	85	34	100	225
	86	38	64	
	87	34	100	300
	88	38	64	
	89	34	100	375
	90	38	64	

TABLE 4.3 Test programme for triaxial strain experiments.

and σ_3 are close.

From the figures it can be seen that the lateral stresses in each test start from the values corresponding to the confined condition and, as the lateral strains are applied in the first step, they drop rapidly. On increasing the lateral strains they keep falling but with a decreasing rate and they eventually become constant i.e. after this point increasing the lateral strains causes no further significant decrease in σ_2 or σ_3 . This trend is the same for both fine and coarse sand but the values of the lateral stresses for the fine sand are, on the whole, much greater than those of the coarse sand repeating the pattern seen in the other tests (i.e. confined and plane strain).

It is evident from the figures that under a particular value of σ_1 the lateral stresses tend to become constant earlier in loose samples than dense ones. In other words under a constant σ_1 as the porosity of the specimen increases, the rate of decrease of the lateral stresses reduces. This reduction is more obvious for fine sand than coarse sand.

At lower levels of σ_1 the lateral stresses tend to become constant at lower lateral strains e.g. in figure. 4.40 which shows the variation of the lateral stresses under σ_1= 75 kN/m^2, after 0.35% lateral strains there is no marked change in σ_2 or σ_3 , while in figure 4.44 (σ_1=375 kN/m^2) even after applying 0.60% lateral strains, in some cases, the lateral stresses show a tendency to drop and they have not levelled out completely.

4.5.4 THE RELATIONSHIP BETWEEN VERTICAL STRAIN AND LATERAL

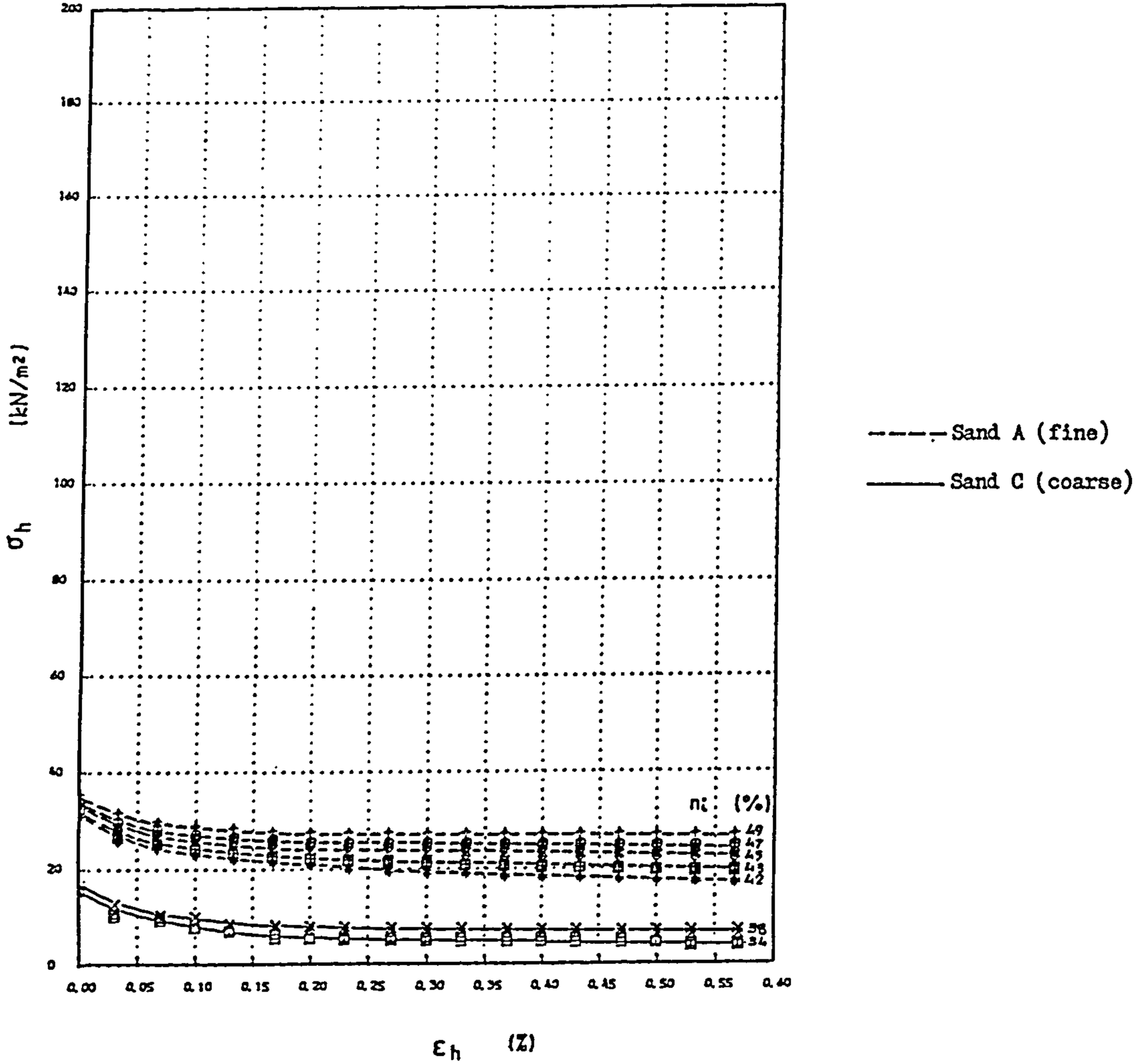

FIGURE 4.40 Relationship between σ_h and ε_h for different initial porosities for sands A and C under triaxial conditions with $\sigma_l = 75$ kN/m².

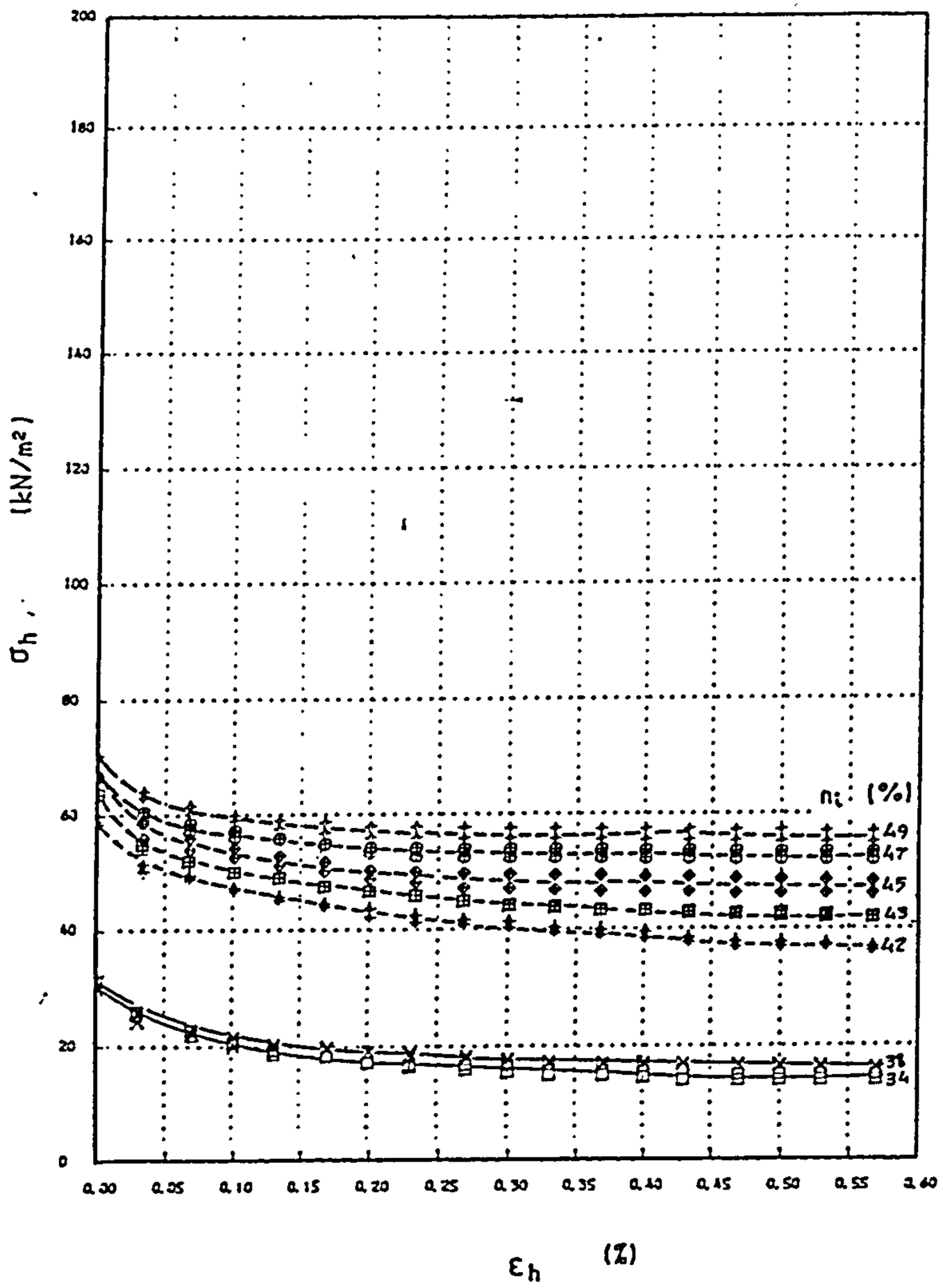

FIGURE 4.41 Relationship between σ_h and ε_h for different initial porosities for sands A and C under triaxial conditions with $\sigma_l = 150$ kN/m².

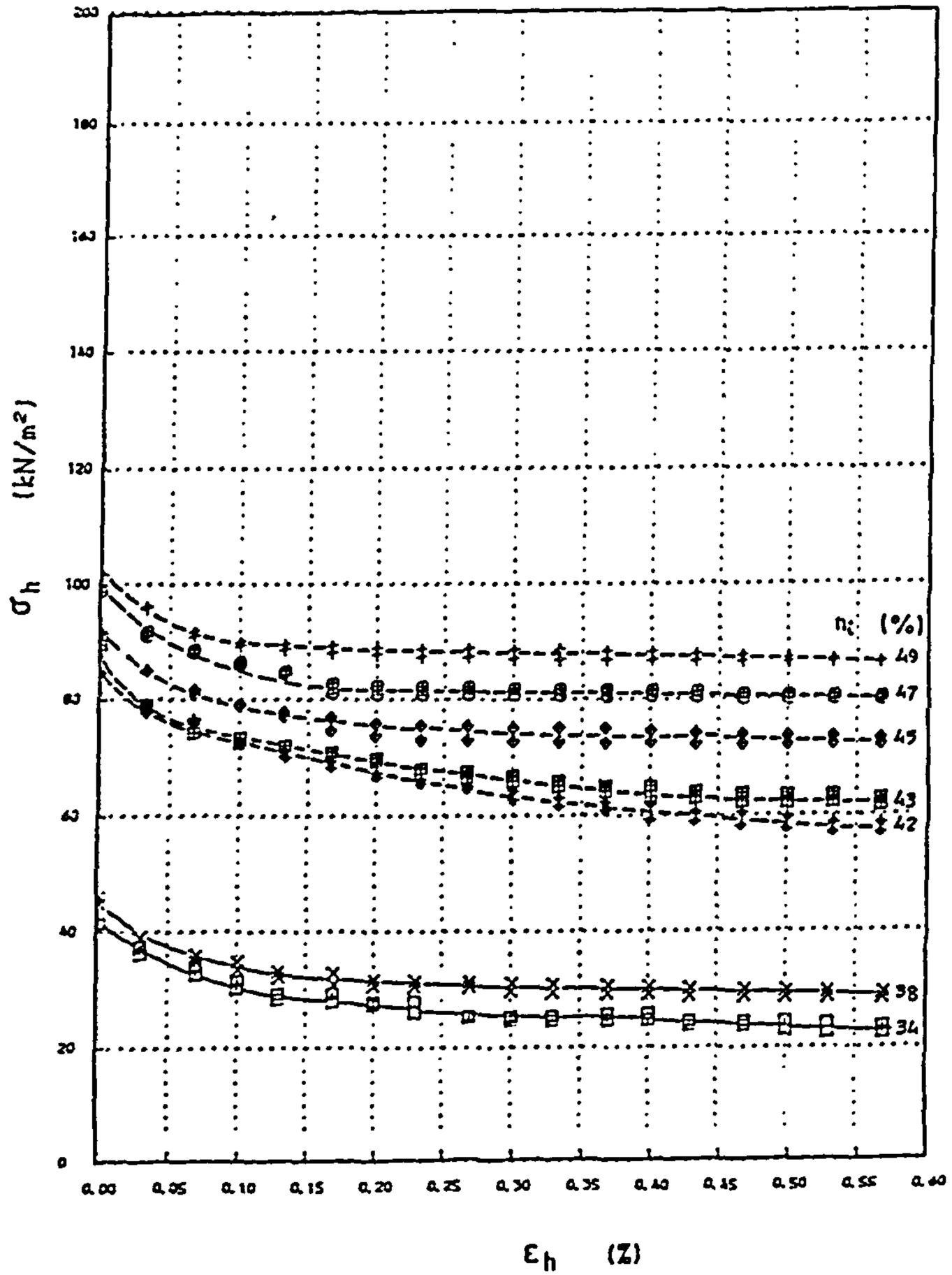

FIGURE 4.42 Relationship between σ_h and ε_h for different initial porosities for sands A and C under triaxial conditions with $\sigma_l = 225$ kN/m².

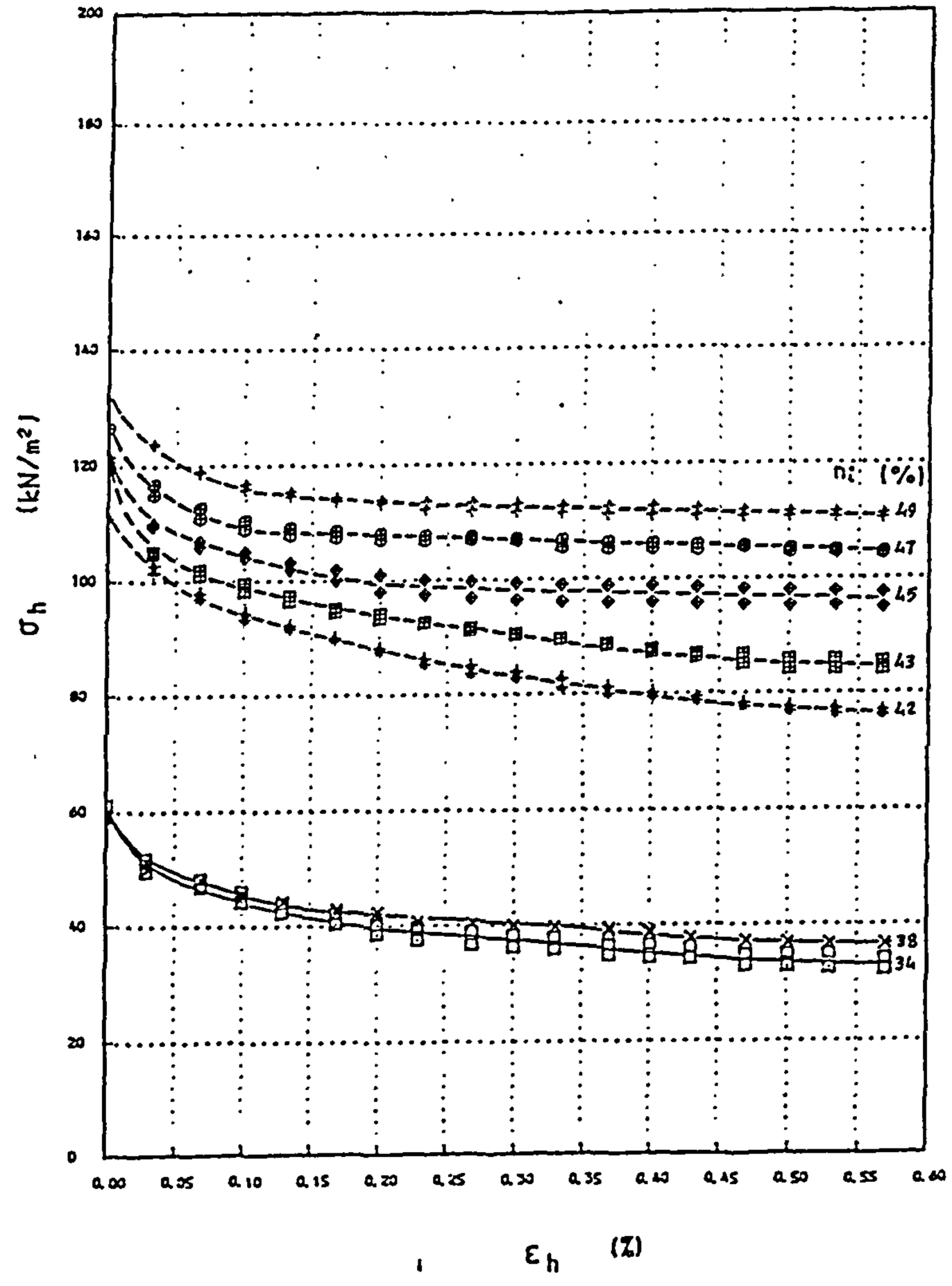

FIGURE 4.43 Relationship between σ_h and ε_h for different initial porosities for sands A and C under triaxial conditions with $\sigma_l = 300$ kN/m².

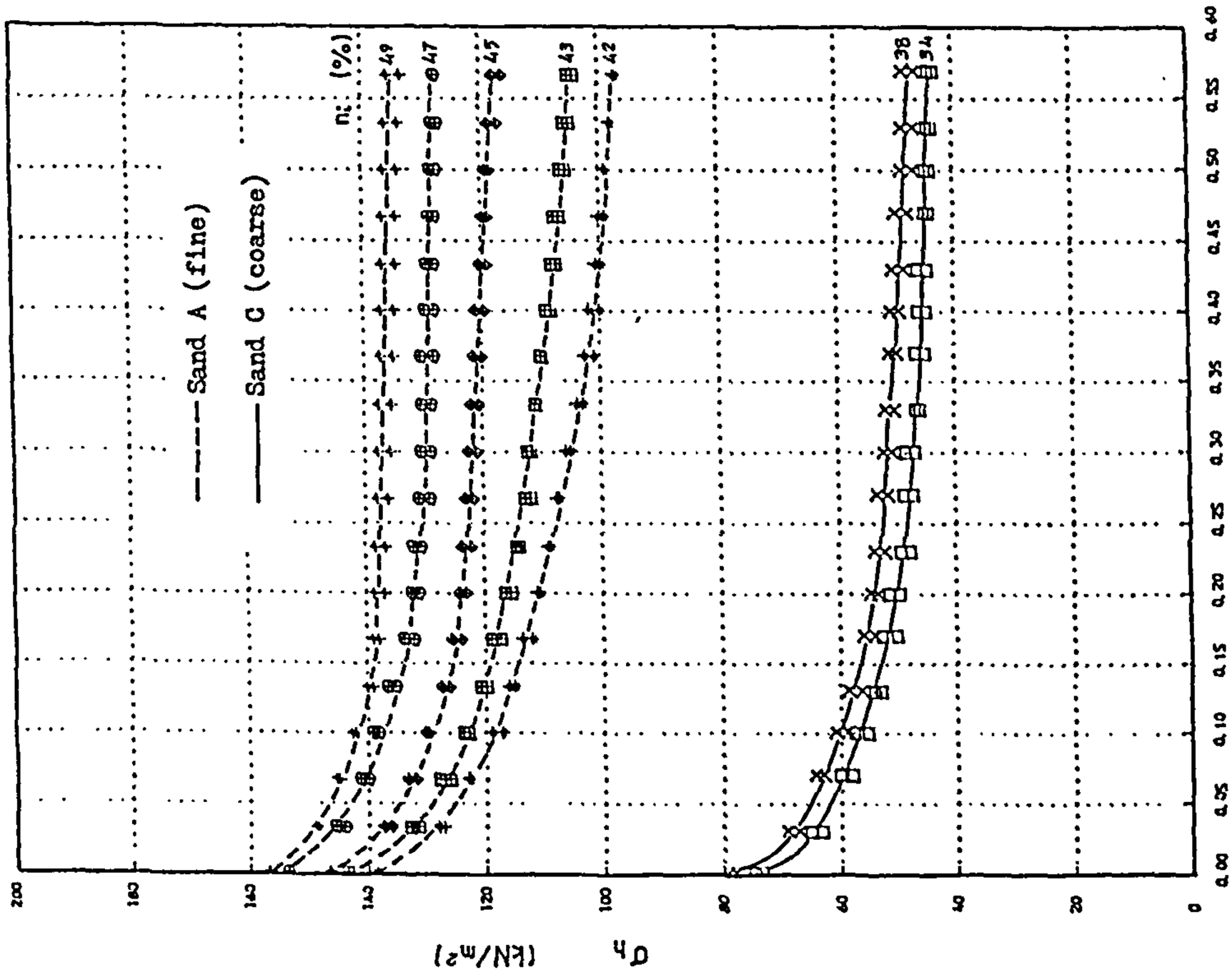

FIGURE 4.44 Relationship between σ_h and ε_h for different initial porosities for sands A and C under triaxial conditions with σ_1 = 375 kN/m².

STRAINS:

The variation of ε_1 with lateral strains at different levels of σ_1, for various initial porosities and for both fine and coarse sands are shown in figures 4.45 to 4.49. From the figures it can be seen that the relationships between ε_1 and lateral strains are nearly linear. If some small initial non-linearity of the curves is ignored, the relationships for the rest of the points are quite linear. This is more marked for the coarse sand than for the fine sand.

At a constant level of σ_1, as the porosity of the sample increases, ε_1 increases. For samples with the same porosity, as the level of σ_1 increases ε_1 increases as well.

The specimens' volume change can also be easily studied while the vertical-lateral strain relationships are under consideration. If the lateral strain is denoted by ε_h, vertical strain by ε_1, volume change by Δv, and the dimensions of the cubic sample by d, then the volumetric strain can be calculated as below:

$$\frac{\Delta V}{V} = \frac{2\varepsilon_h \cdot d^3 - \varepsilon_1 \cdot d^3}{d^3} = 2\varepsilon_h - \varepsilon_1 \qquad (4.5)$$

In comparison with the plane strain data in which the volumetric strain was $\varepsilon_h - \varepsilon_1$, here the coefficient of 2 is due to the application of lateral strain in two directions. The lines of $\varepsilon_1 = \varepsilon_h$ and $\varepsilon_1 = 2\varepsilon_h$ are plotted using a solid line in each figure in order to determine whether the volume change is positive (dilation) or negative (compression).

From all the figures it is evident that the coarse samples show positive volumetric strain, which means they

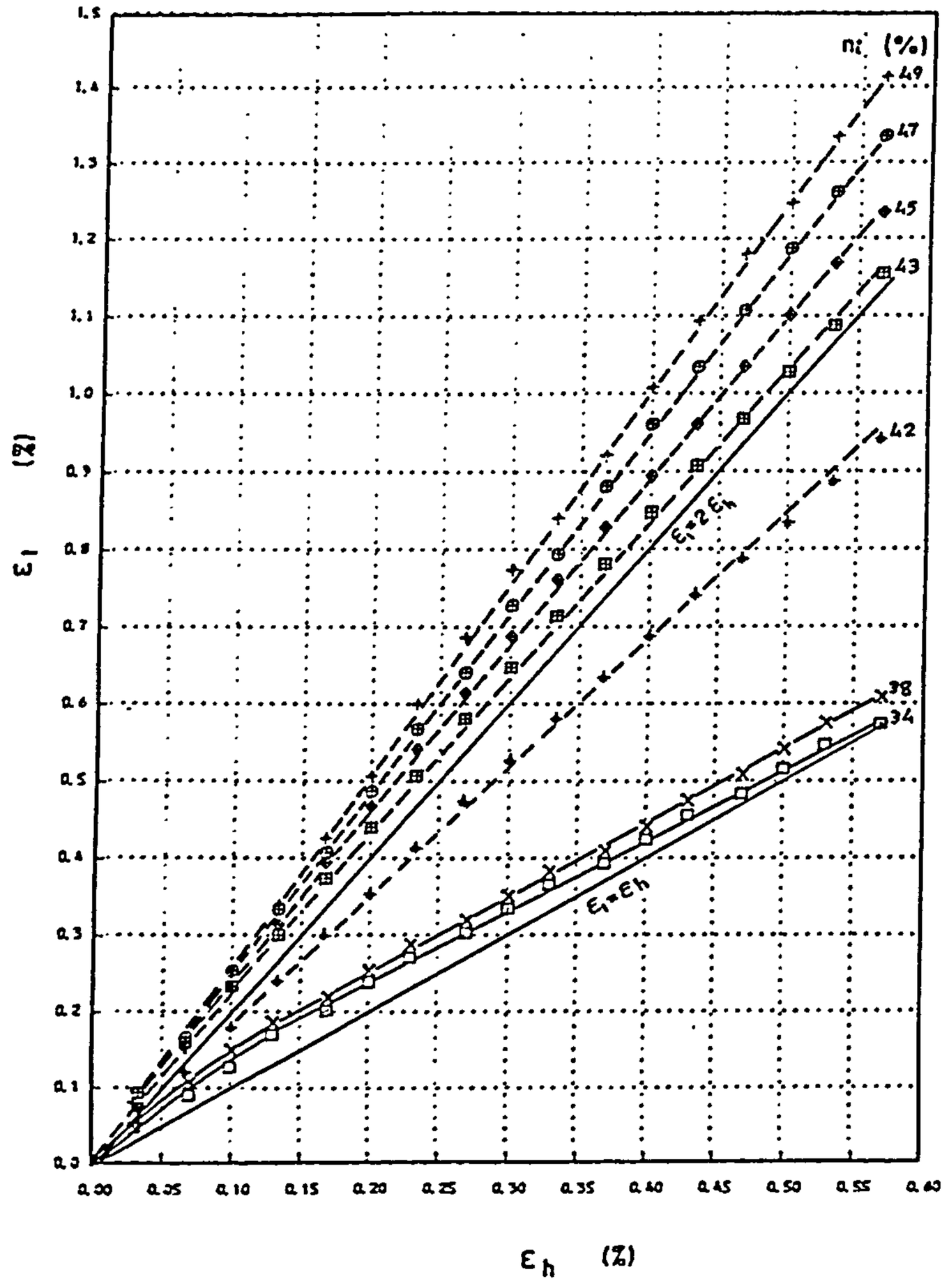

FIGURE 4.45 Relationship between ε_l and ε_h for different initial porosities for sands A and C under triaxial conditions with $\sigma_l = 75$ kN/m^2.

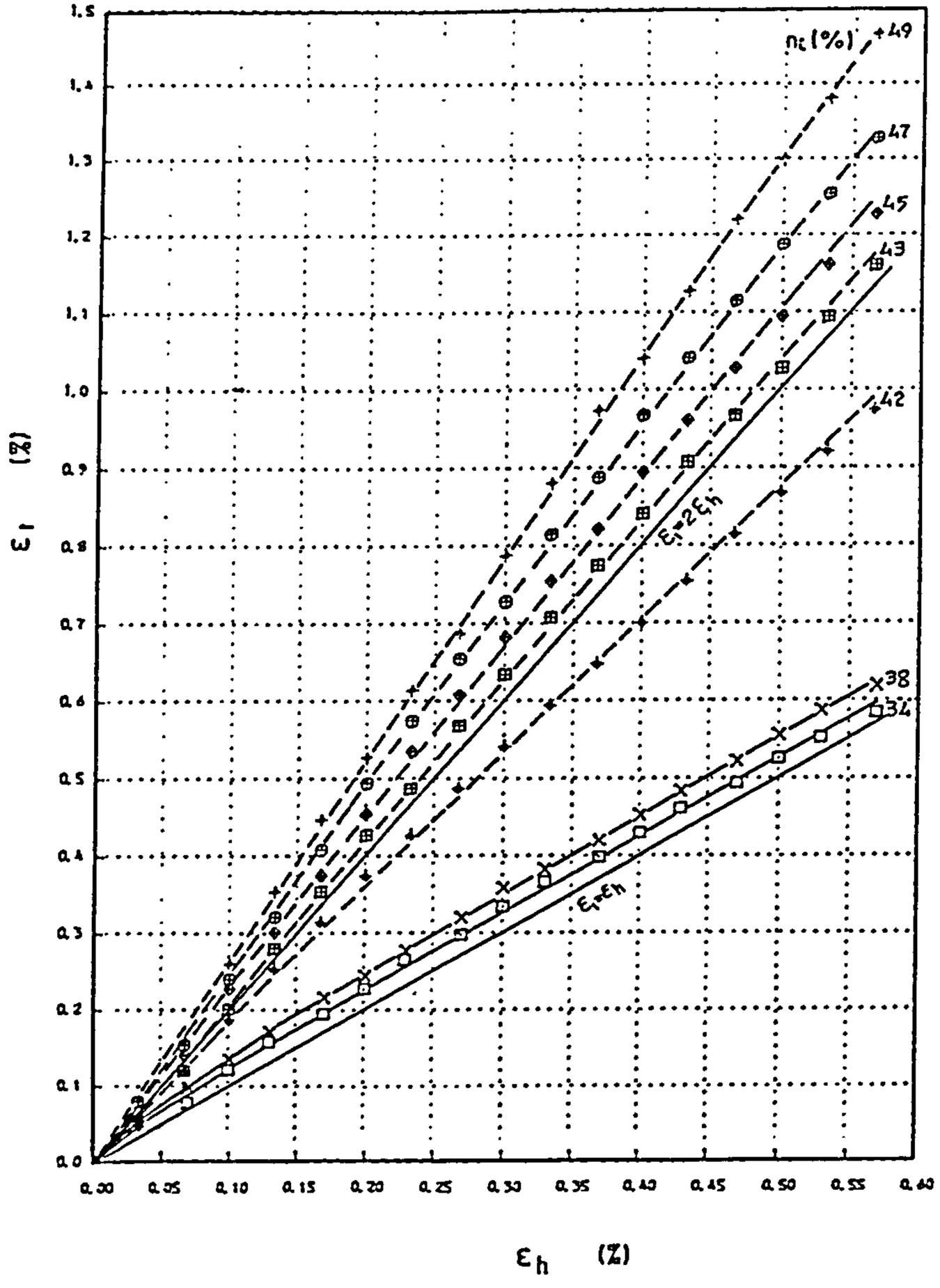

FIGURE 4.46 Relationship between ε_l and ε_h for different initial porosities for sands A and C under triaxial conditions with $\sigma_l = 150$ kN/m^2.

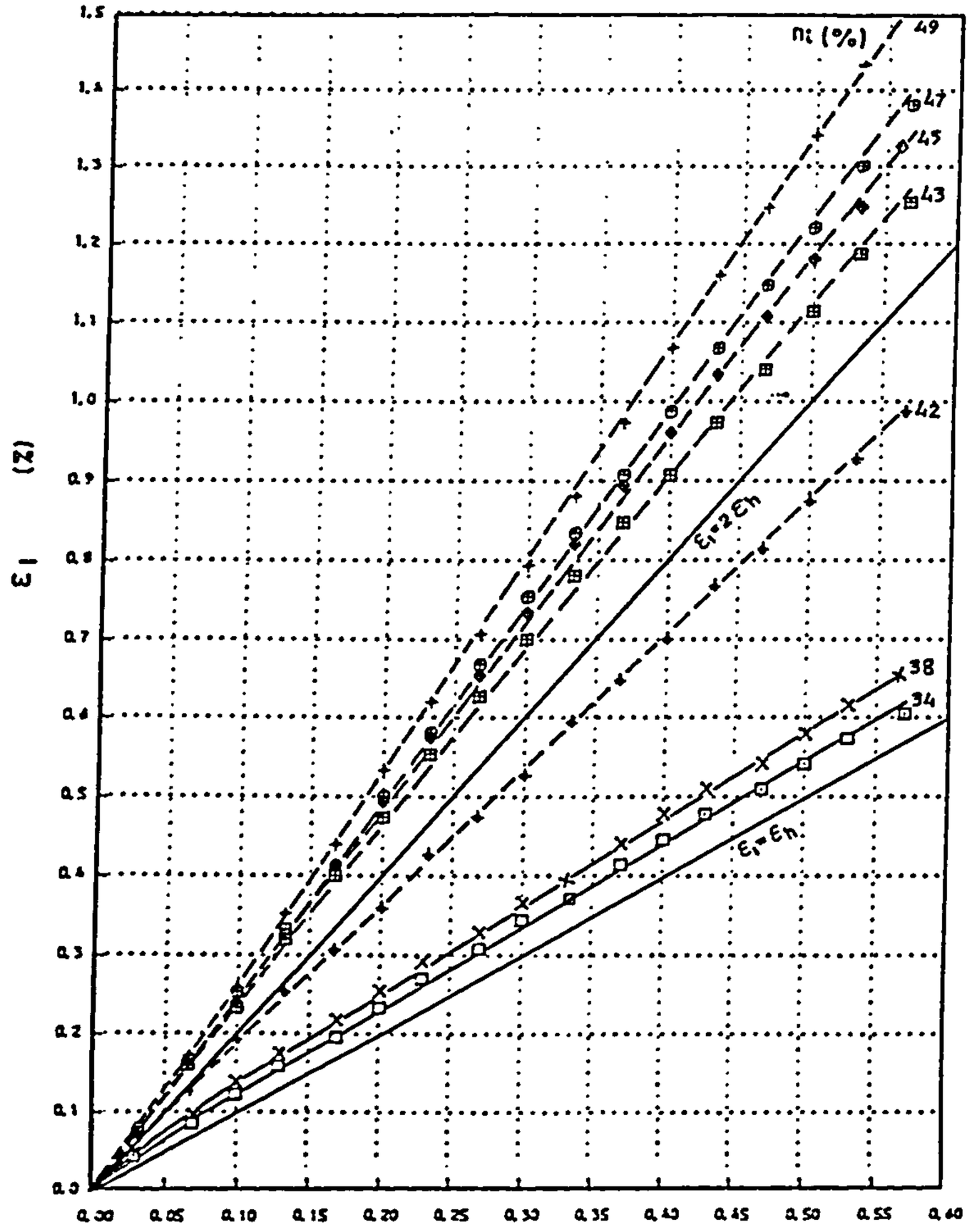

Sand A (fine)

Sand C (coarse)

FIGURE 4.47 Relationship between ε_1 and ε_h for different initial porosities for sands A and C under triaxial conditions with $\sigma_1 = 225\ kN/m^2$.

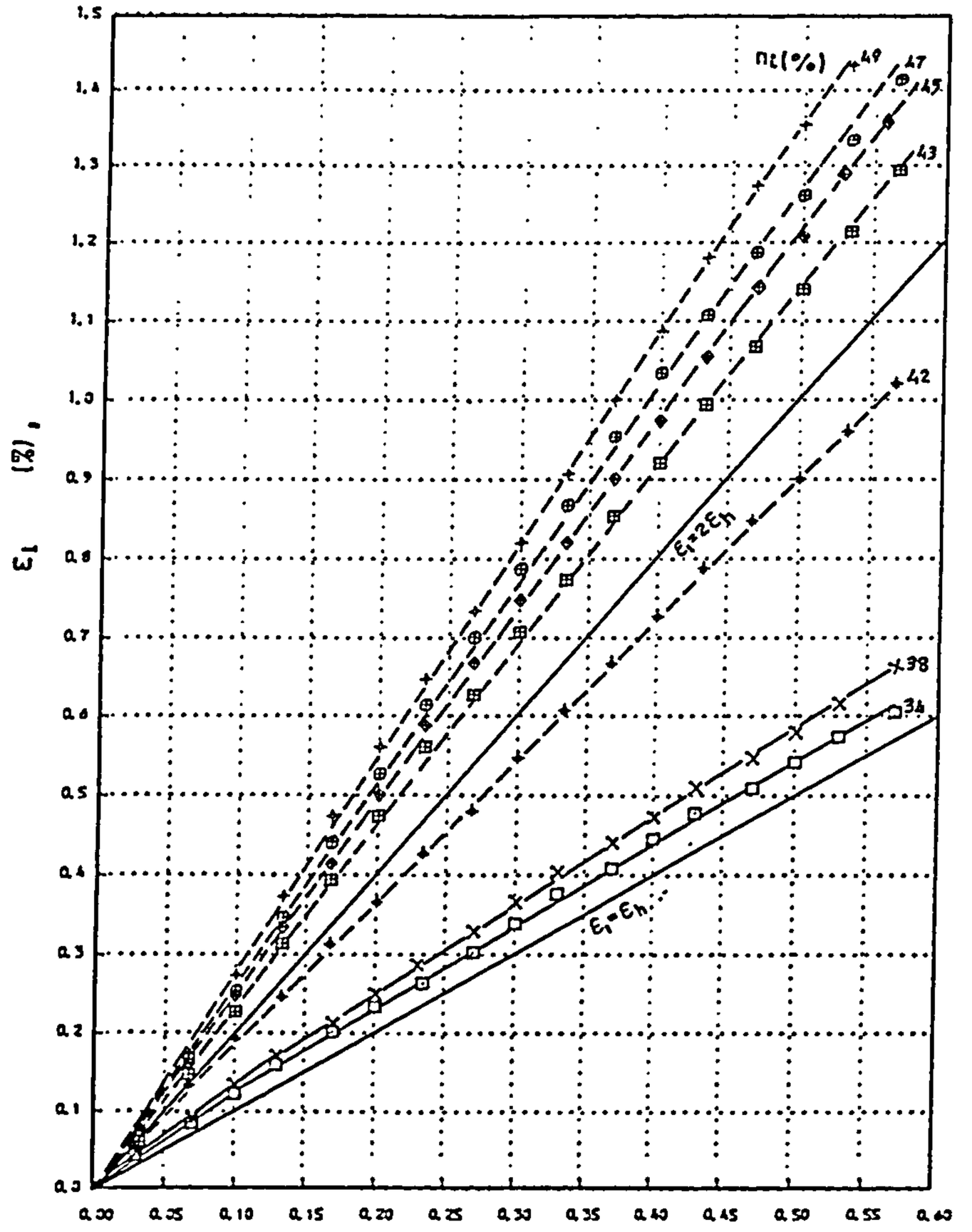

FIGURE 4.48 Relationship between ε_1 and ε_h for different initial porosities for sands A and C under triaxial conditions with $\sigma_1 = 300\ kN/m^2$.

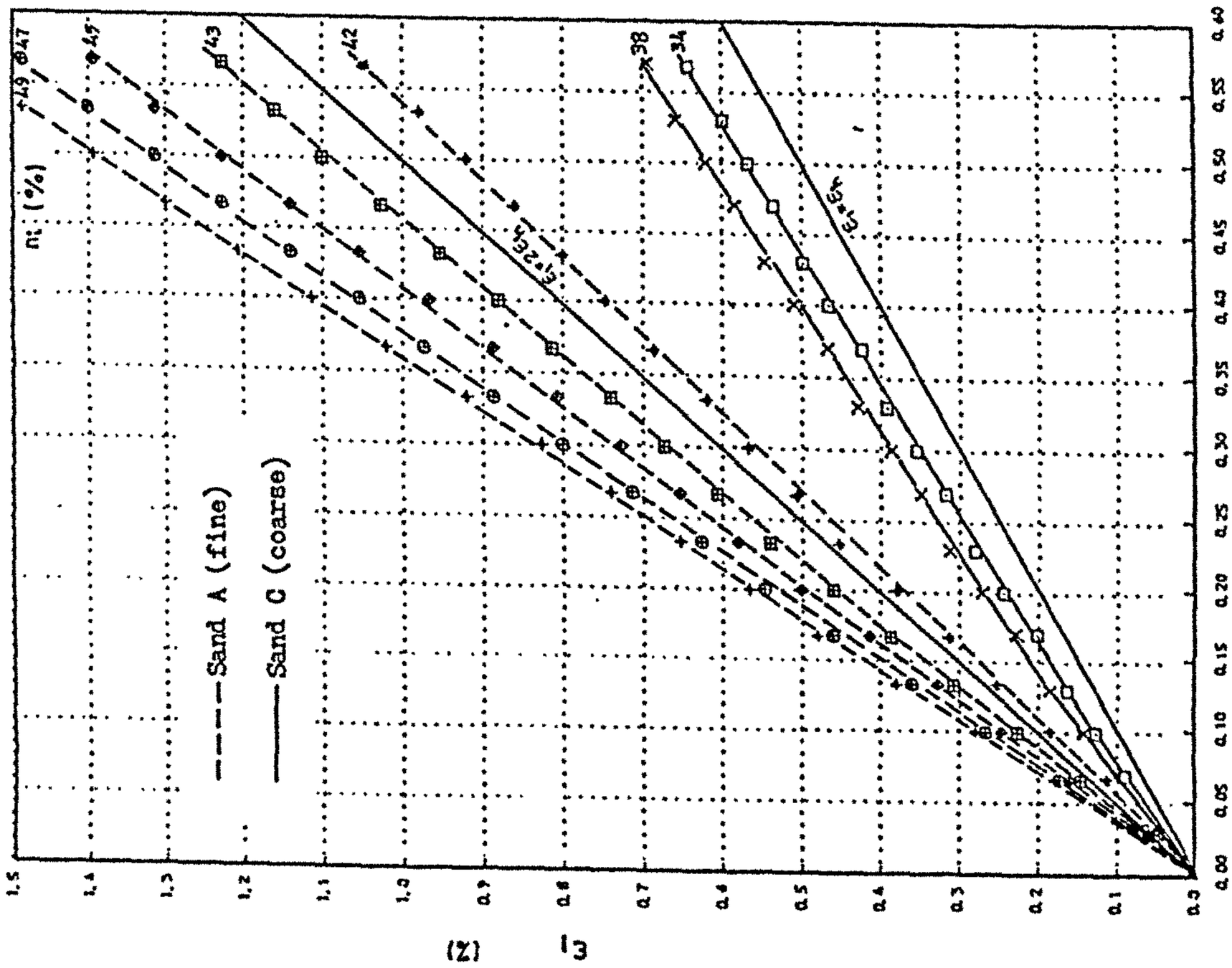

FIGURE 4.49 Relationship between ε_1 and ε_h for different initial porosities for sands A and C under triaxial conditions with $\sigma_1 = 375$ kN/m^2.

are dilating as the lateral strains are applied. For the fine samples negative volume change (compression) always occurs except for those samples which were prepared in the densest state (porosity of 42%), in which dilation has taken place. The amounts of volumetric strain for coarse sand are located between the two lines ($\varepsilon_l = \varepsilon_h$ and $\varepsilon_l = 2\varepsilon_h$), but as the porosity of the samples increases the volumetric strain decreases. For fine sand however, the volumetric strains increase as the porosity increases.

It can also be noted from the figures that the volumetric strains for the coarse sand, and for the fine sand in the densest case (porosity=42%), decrease as σ_l increases but for the fine sand in all other cases it increases on increasing σ_l.

4.5.5 THE RELATIONSHIP BETWEEN THE RATIO OF LATERAL TO VERTICAL STRESS AND LATERAL STRAIN

The ratios of lateral to vertical stress versus lateral strains are plotted in figures 4.50 to 4.54. Each graph is for a series of samples with different initial porosities at a constant σ_l and shows both fine and coarse data. As mentioned previously because of small differences between σ_2 and σ_3, their average values [$\sigma_h = (\sigma_2 + \sigma_3)/2$] have been used for calculating the coefficient of lateral stress.

From the figures it can be observed that, for each level of σ_l, the coefficients of lateral stress start from the value equal to that of the confined tests (Ko). As the lateral strains are applied they drop sharply and on increasing the lateral strains they keep falling but the

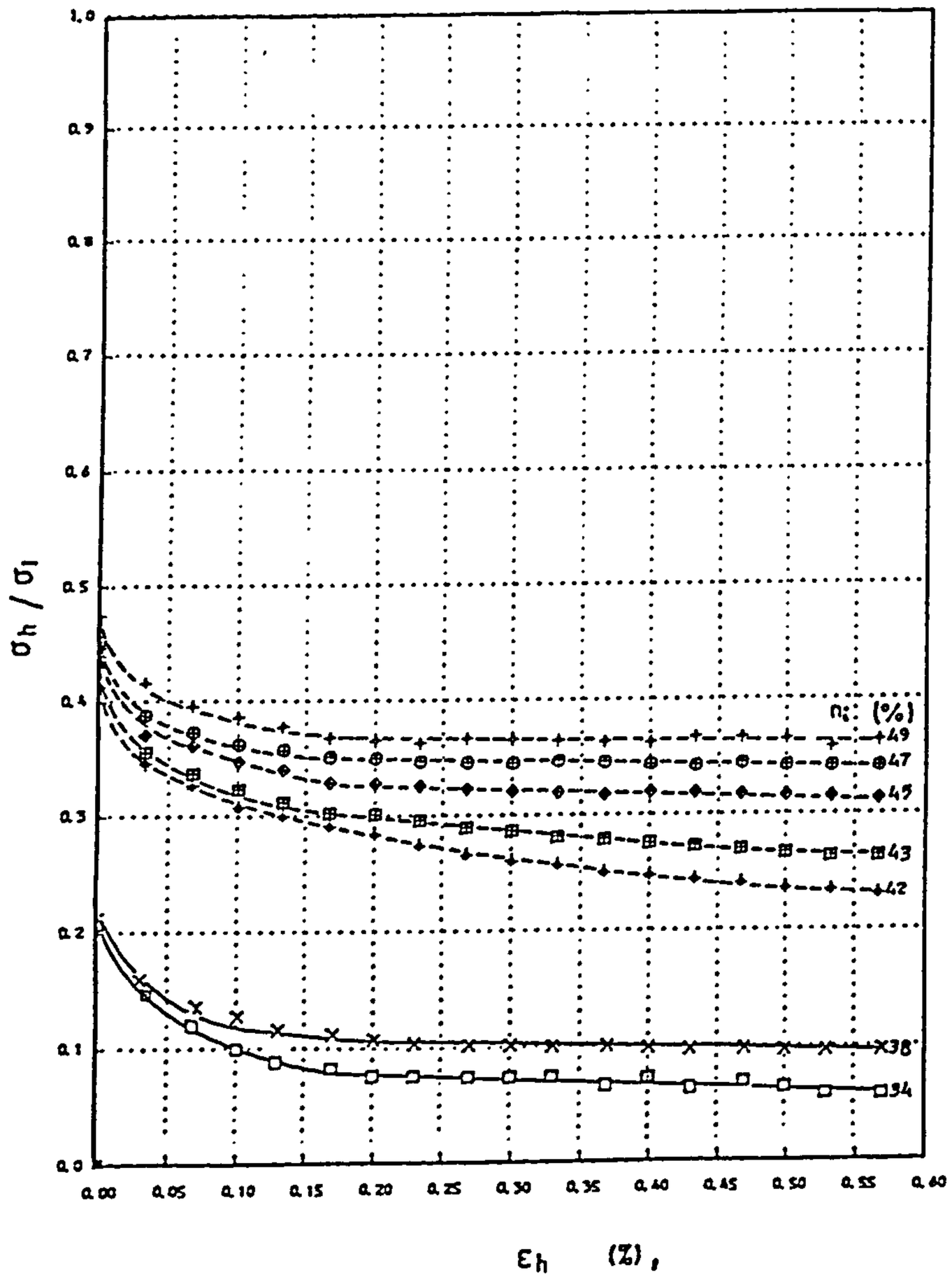

FIGURE 4.50 Variation of the ratio of σ_h / σ_1 with ε_h for different initial porosities for sands A and C under triaxial conditions with $\sigma_1 = 75$ kN/m^2.

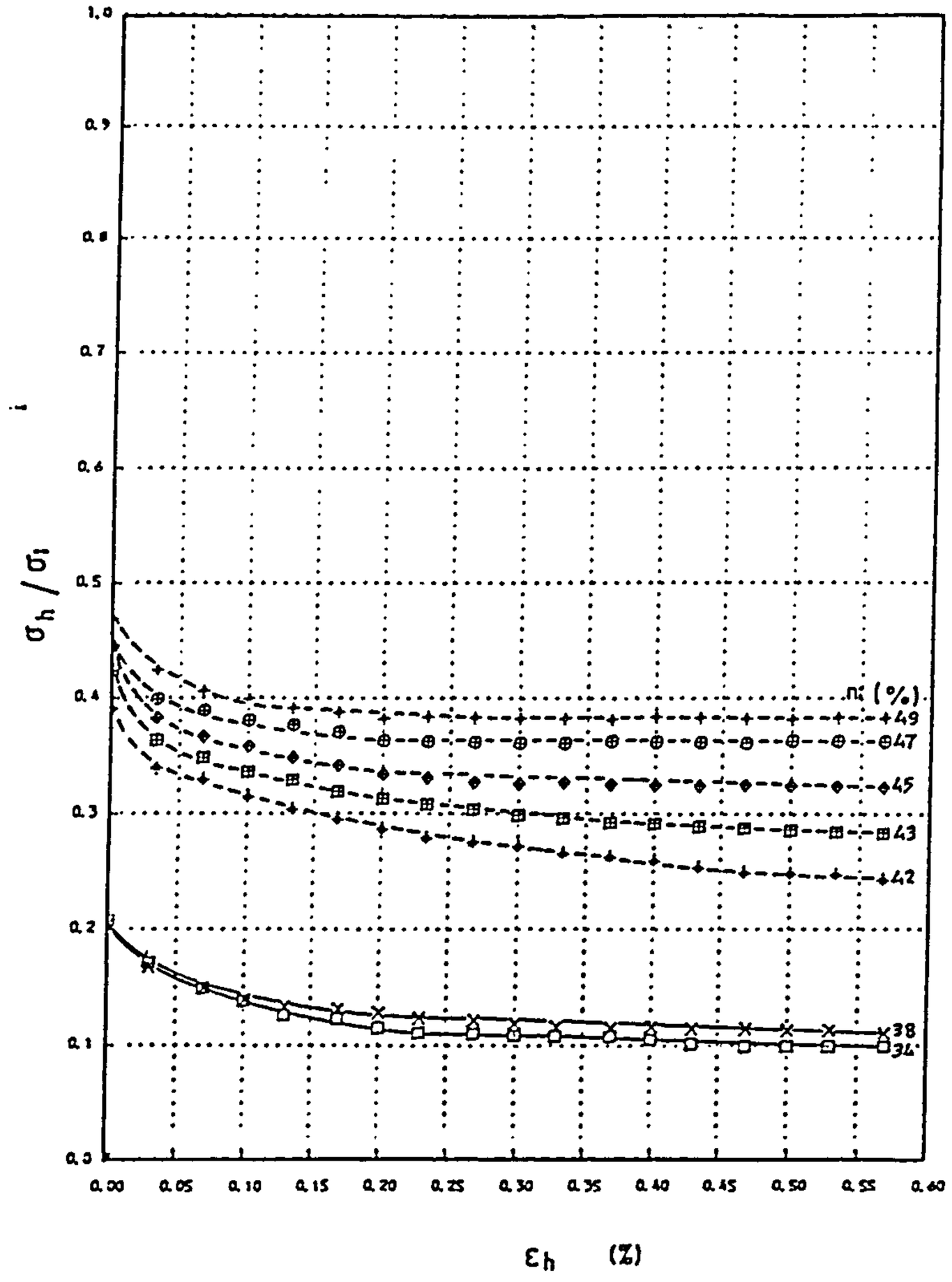

FIGURE 4.51 Variation of the ratio of σ_h / σ_1 with ε_h for different initial porosities for sands A and C under triaxial conditions with $\sigma_1 = 150$ kN/m^2.

Sand A (fine)

Sand C (coarse)

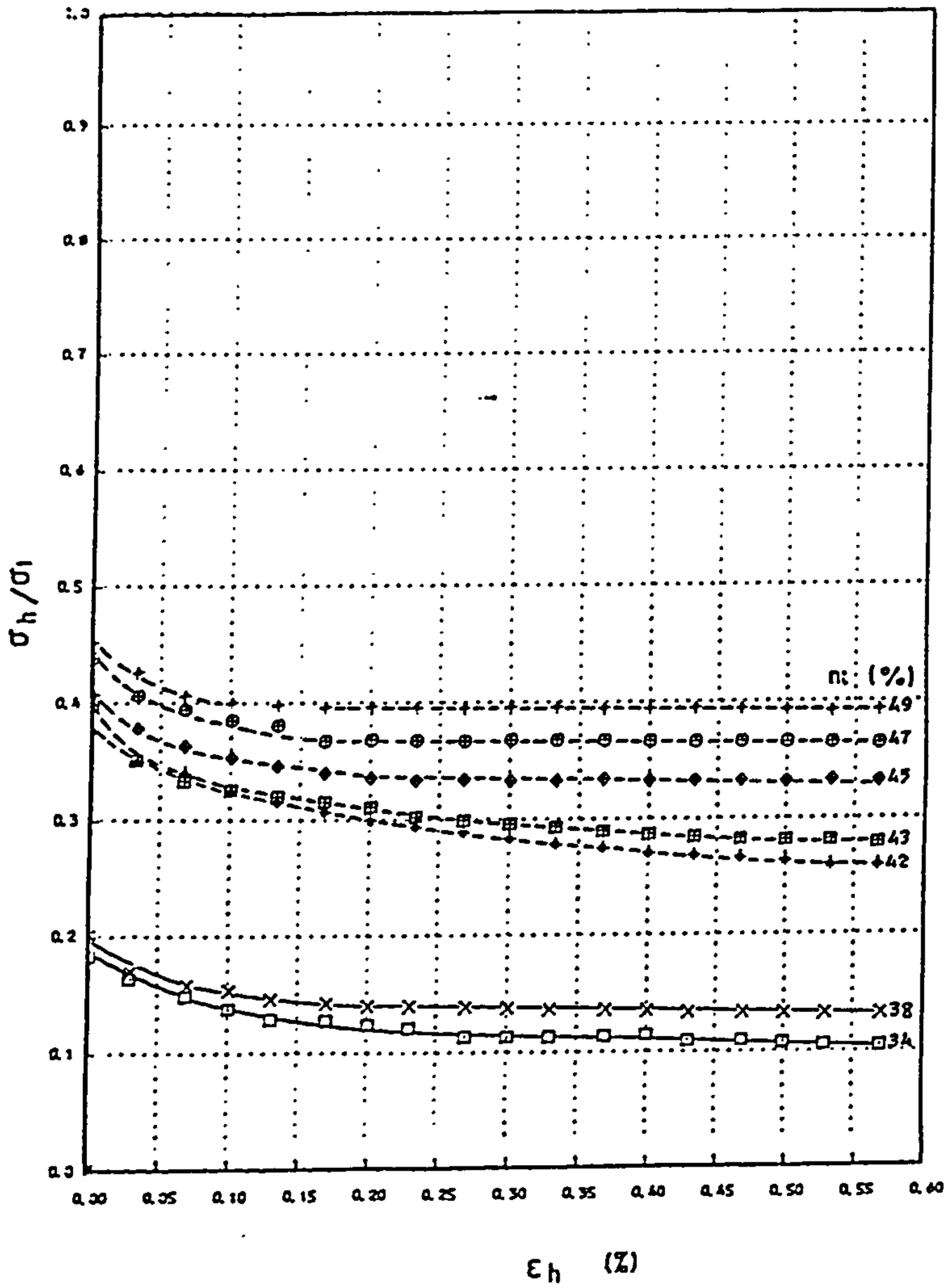

Sand A (fine)

Sand C (coarse)

FIGURE 4.52 Variation of the ratio of σ_h/σ_1 with ε_h for different initial porosities for sands A and C under triaxial conditions with $\sigma_1 = 225\ kN/m^2$.

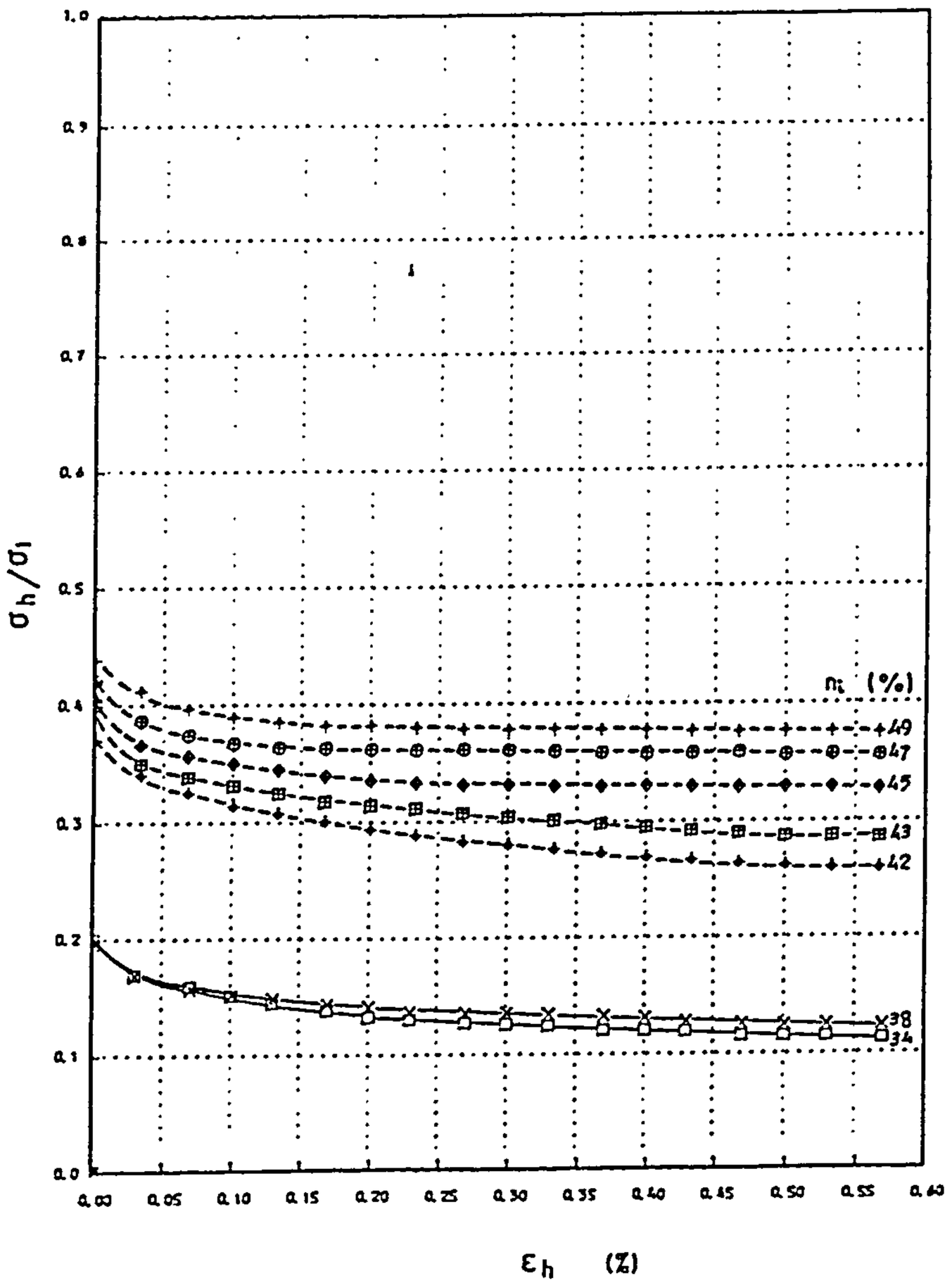

FIGURE 4.53 Variation of the ratio of σ_h/σ_1 with ε_h for different initial porosities for sands A and C under triaxial conditions with $\sigma_1 = 300\ kN/m^2$.

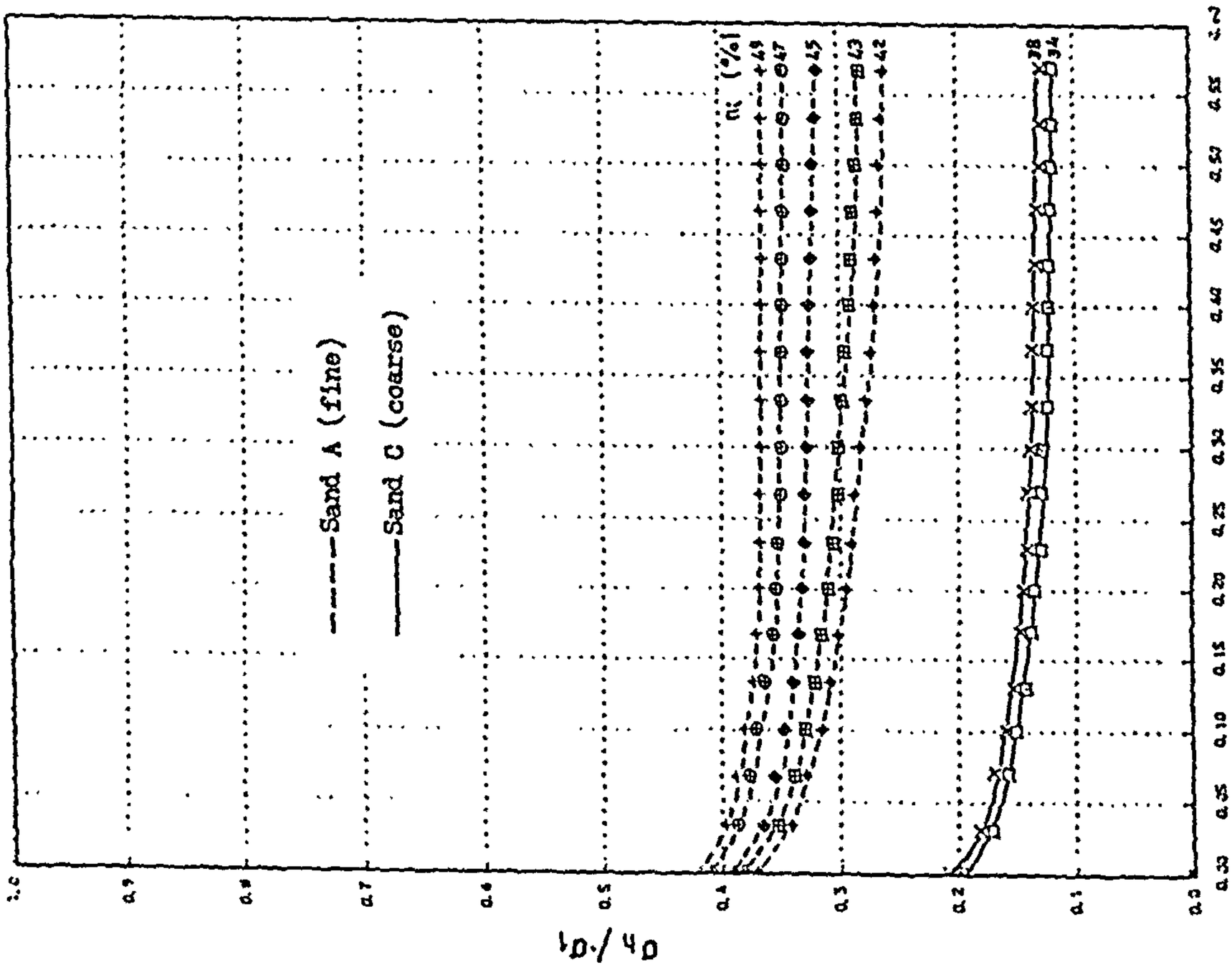

FIGURE 4.54 Variation of the principal stress ratio of σ_h/σ_1 with ε_h for different initial porosities for sands A and C under triaxial conditions with $\sigma_1 = 375$ kN/m^2.

rate of change decreases and gradually they tend to become constant. This is when the frictional strength of the sand has been fully mobilized and the sand is said to reach its active state and so the ratio of lateral to vertical stresses in this case is called the coefficient of active pressure (Ka). The discussion about Ka and comparison between the values obtained in plane strain and triaxial tests are given in chapter six.

According to the figures Ka increases on increasing the initial porosity of the sample. Also it is apparent that the loose samples reach their active states sooner than dense ones. This means that at a constant value of σ_1, less lateral movement is required to mobilize the frictional strength of the sand. This fact is more marked for the fine sand than for the coarse. The effect of porosity on the coefficient of active pressure decreases as the level of vertical stress increases.

CHAPTER FIVE

CYCLIC TESTS

5.1 INTRODUCTION

Stress-strain data obtained from tests using monotonic loading is limited in application and in the information it gives on the behaviour of sand under more general loading conditions. The elastic and plastic properties of sand can only be examined when unloading takes place after initial loading , and further cyclic loading enables the relationship between these properties to be studied.

In recent years a large number of researchers have concentrated on the behaviour of sand under cyclic loading, but most of them have focused their studies on the strength and failure of the material under cyclic loading conditions in which large deformations are involved (see section 1.3). As a result there is a lack of knowledge on the cyclic stress-strain behaviour of sand at small deformations before reaching failure, a condition which is likely to occur in most practical cases.

Therefore a programme of cyclic tests under controlled strain conditions on one of the test sands has been performed in an attempt to fill this gap and also for comparison with the monotonic tests. In these experiments, which were performed on dry medium size Leighton Buzzard sand (group B), the stress-strain behaviour of the 150 mm cubic

specimens under cyclic loading at various frequencies, amplitudes and total number of cycles was studied. Using a similar technique to that used for the monotonic tests, the samples were tested under confined , plane strain and triaxial strain conditions. All the experiments were carried out at two different porosities : the densest and the loosest cases which can be prepared by the raining method (chapter 3).

During these experiments the vertical stress was applied cyclically to the top of the sample. The lateral stresses and the vertical strains induced were measured continuously and the lateral strains set to give the required test conditions. Due to the change of the principal stress and strain directions during cycles of load the three principal stresses and strains acting upon the faces of the samples in these tests are denoted in this chapter as shown below:

σ_v and ε_v = vertical stress and strain ,

σ_{h1} and ε_{h1} = lateral stress and strain in one direction,

σ_{h2} and ε_{h2} = lateral stress and strain in the other direction.

5.2 THE TEST PROCEDURE

The test procedure for the cyclic loading tests is similar to that of the monotonic tests described in section 4.2. The only additional detail which needs to be explained is the way in which vertical load was applied to the specimen. After completing the preparation of the sample (see section 4.2), the desired loading programme including the shape , amplitude, frequency and number of load cycles was

loaded into the BBC micro computer linked to the loading system. Hence on running the programme the appropriate cyclic loading was applied to the specimen. A sinusoidal wave form was used for the cyclic load tests. The data acquisition system , prepared by loading the appropriate programme , reads the forces acting on the sample faces and the vertical - displacement at specified periods. After the last loading cycle the data acquisition and loading systems are stopped and the sample container is emptied and cleaned for the next test. During the tests lateral strains may be applied to the sample as detailed below.

The specimens were tested under confined ,plane strain and triaxial conditions. Each test was initially carried out under confined conditions (no-lateral strain permitted) until a certain number of cycles had been reached. In the case of plane strain or triaxial tests further cycles of load were then applied after some small lateral strain had been applied to one side (plane strain) or simultaneously to two sides (triaxial tests). This procedure was continued for the required number of steps of lateral strain.

5.3 CONFINED TESTS

The main objective of this series of tests was to study the cyclic stress-strain behaviour of sand B when $\varepsilon_{h1} = \varepsilon_{h2}=0$. Therefore during these experiments the two moveable sides of the sample container were fixed so that no lateral strains were allowed.

During these experiments the vertical stress was cycled between its minimum and maximum values while the two

lateral stresses and the vertical strain were measured and recorded continuously by the data acquisition unit.

In order to study the effect of the frequency of loading, frequencies ranging from 0.1 Hz (i.e. one cycle per 10 sec) to 0.0033 Hz (i.e. one cycle per 300 sec) were used. The maximum vertical stress applied was also varied up to its maximum level of 425 kN/m^2 . Although the number of cycles applied in most tests was about 60, in order to study the effect of this parameter some tests were carried out in which up to 215 cycles for the dense and 360 cycles for the loose samples were applied. These figures were chosen in an attempt to achieve stable conditions of stress and strain in the sample.

To assess the reliability of the apparatus and the repeatability of the tests under cyclic loading conditions some of the initial experiments were performed twice. The test programme, including the number of experiments, the frequency of loading, the amplitude and number of cycles and finally the initial porosity of samples is summarized in table 5.1.

5.3.1 THE GENERAL BEHAVIOUR OF CONFINED SAMPLES UNDER CYCLIC LOADING

Typical results of the confined tests are shown in figures 5.1 and 5.2. As can be seen the behaviour of the sand under this condition of loading is as follows.

1- As σ_v cycles between its minimum and maximum values ,the lateral stresses (σ_{h1} and σ_{h2}) vary between minimum and maximum values as well.

2- Although the minimum and maximum values of σ_v, as

test number	Frequency (Hz.)	Period (Sec.)	Amplitude (kN/m^2)	No. of cycles	Initial porosity (%)
1 & 2	0.1000	10	212.5	60	33
3 & 4	0.1000	10	212.5	60	41
5 & 6	0.0333	30	212.5	40	33
7 & 8	0.0333	30	212.5	40	41
9 & 10	0.0167	60	212.5	60	33
11 & 12	0.1000	10	112.5	60	33
13 & 14	0.1000	10	112.5	60	41
15 & 16	0.0333	30	112.5	40	33
17 & 18	0.0333	30	112.5	40	41
19 & 20	0.0167	60	112.5	60	41
21	0.0167	60	112.5	60	33
22	0.0167	60	212.5	60	41
23	0.0333	300	212.5	50	33
24	0.0333	300	212.5	50	41
25	0.0667	15	212.5	215	33
26	0.0667	15	212.5	360	41
27	0.0667	15	62.5	70	33
28	0.0667	15	62.5	70	41
29	0.0667	15	112.5	70	33
30	0.0667	15	112.5	70	41
31	0.0667	15	162.5	70	33
32	0.0667	15	162.5	70	41
33	0.0667	15	50.0	70	33
34	0.0667	15	50.0	70	41
35	0.0667	15	100.0	70	33
36	0.0667	15	100.0	70	41
37	0.0667	15	150.0	70	33
38	0.0667	15	150.0	70	41
39	0.0667	15	100.0	70	33
40	0.0667	15	100.0	70	41
41	0.0667	15	50.0	70	33
42	0.0667	15	50.0	70	41
43	0.0667	15	50.0	70	33
44	0.0667	15	50.0	70	41

TABLE 5.1 Test programme in confined conditions under cyclic loading.

STRESS-STRAIN CURVES FOR CONFINED TESTS UNDER CYCLIC LOADING CONDITIONS

Initial porosity=41%, Frequency=0.016 Hz. Period=60Sec., Amplitude=215 kN/m^2 ,Number of cycles= 60

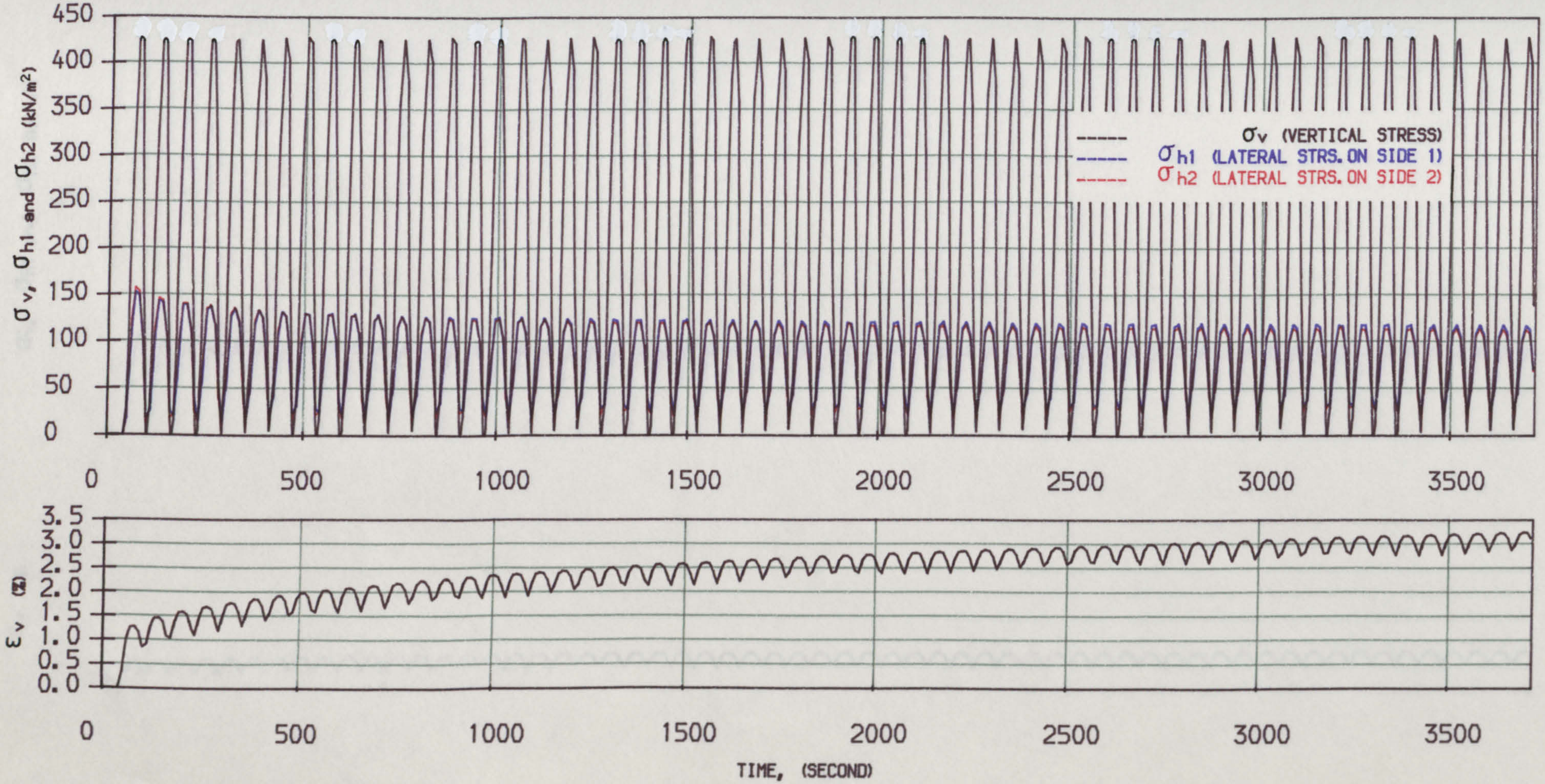

FIGURE 5.1 Typical variations of σ_v, σ_{h1} , σ_{h2} and ε_v for loose samples under cyclic loading conditions.

STRESS-STRAIN CURVES FOR CONFINED TESTS UNDER CYCLIC LOADING CONDITIONS

Initial porosity=33%, Frequency=0.016 Hz. Period=60 Sec., Amplitude=215 kN/m^2, Number of cycles= 60

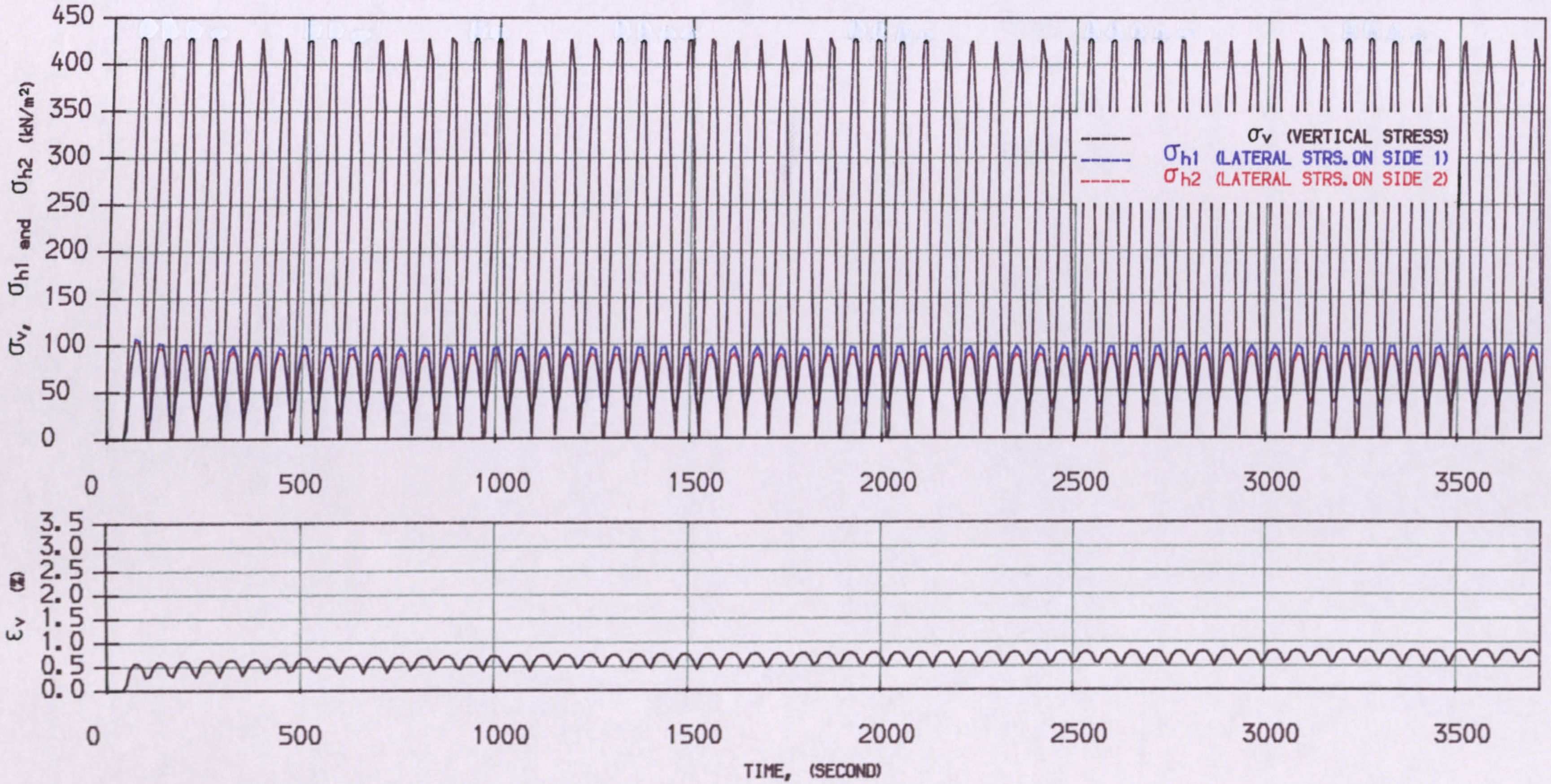

FIGURE 5.2 Typical variations of σ_v, σ_{h1}, σ_{h2} and ε_v for dense samples under cyclic loading conditions.

controlled by the loading system, are constant, the minimum and maximum values of the lateral stresses change.

3- The maximum values of the lateral stresses decrease while their minima increase as the number of cycles increases.

4- The rates of decrease of the maximum and increase of the minimum values decrease and the lateral stresses tend to stabilize after a certain number of load cycles (i.e. the maxima and minima become constant).

5- As the samples are in symmetric test conditions σ_{h1} and σ_{h2} should be equal as found before (chapter 4) there are some small differences.

6- As the first cycle of σ_v is applied to the specimen the vertical strain increases until the peak of the load cycle, but on unloading it does not return to zero and some plastic strain remains.

7- For the next cycle of σ_v, ε_v starts from the value it had at the end of the previous cycle (i.e. the maximum plastic strain) and then fluctuates between minimum and maximum values which increase as the number of cycles increases.

8- The rate of increase of the minimum and maximum values of the vertical strain decreases as the cyclic loading continues.

9- The percentage of the changes of the minimum and maximum values of ε_v over a certain number of load cycles is greater than that of σ_h.

The general behaviour of sand samples under confined cyclic loading conditions as described above is the same for both loose and dense samples. However the difference between

the minimum and maximum values of the vertical strain and lateral stresses induced are greater for loose samples than for dense samples. Also in loose samples the maximum values of the lateral stresses and the amount of plastic strain induced in the first cycle of load are greater than those of dense samples.

5.3.2 THE EFFECT OF FREQUENCY ON CYCLIC BEHAVIOUR

In order to assess the influence of the frequency of the cyclic load on the response of sand samples, a series of cyclic tests were carried out on both dense and loose specimens in which the test conditions were the same except for the frequency of the load. The frequency of the cyclic loads used were 0.1 Hz (one cycle per 10 sec), 0.033 Hz (one cycle per 30 sec), 0.016 Hz (one cycle per 60 sec) and, 0.003 Hz (one cycle per 300 sec).

The variations of σ_v, σ_{h1}, σ_{h2} and ε_v for the different frequencies are shown in figures 5.3 to 5.10. In these graphs only the minimum and maximum points of the stresses and strains are plotted, the other points of the cycles are omitted to clarify the graphs.

From figures 5.3 to 5.6, which are of test data on dense samples, it can be seen that the results are very similar for the different frequencies applied. The maximum lateral stresses are initially marginally above 100 k/m^2 and then decrease quite gradually to values under 100 kN/m^2, and finally after about 40 cycles stabilize. The minimum lateral stresses are initially nearly 20 kN/m^2 and increase gradually to about 40 kN/m^2 after 40 cycles of load, and still seem to be increasing. The maximum values of the vertical

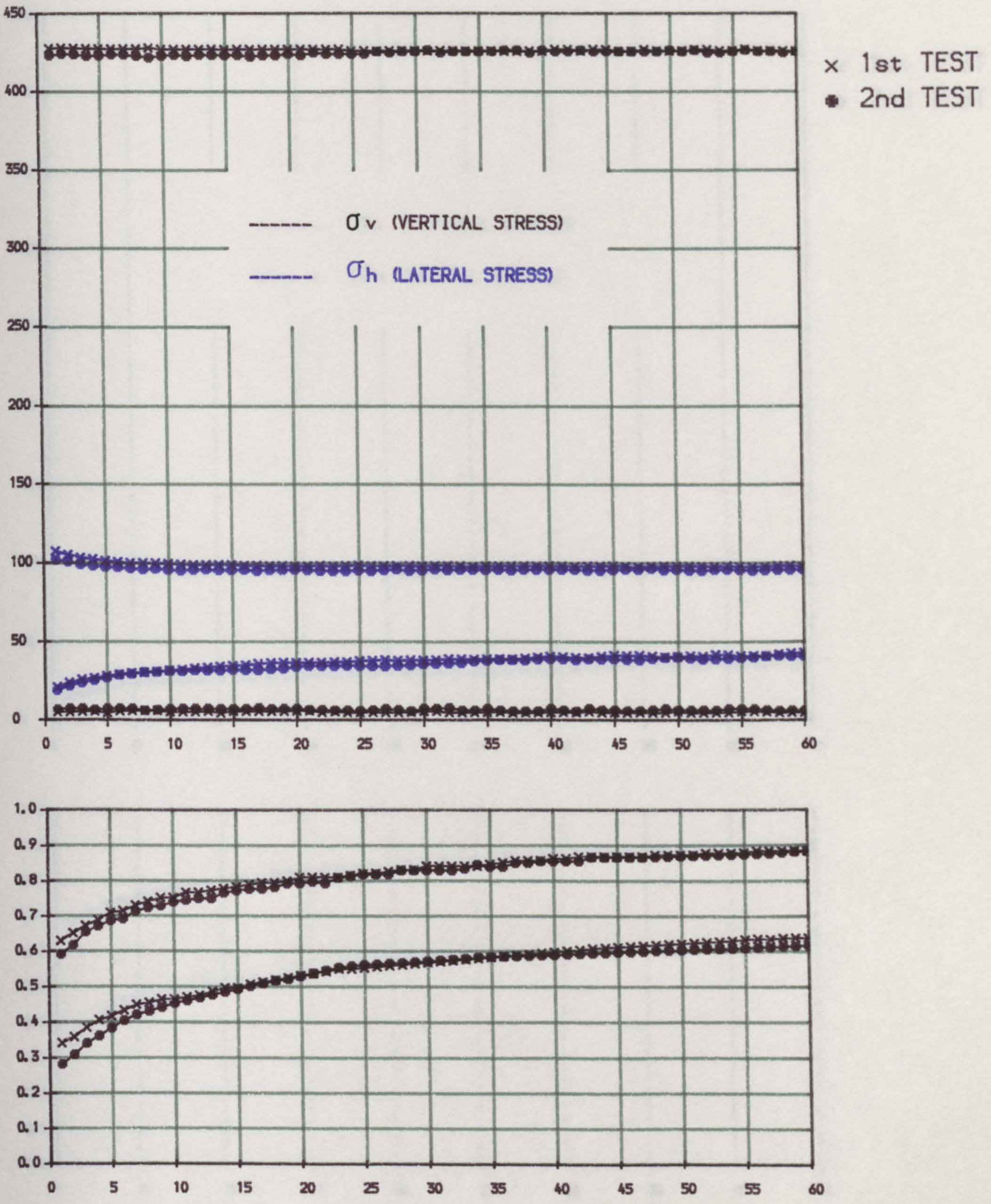

FIGURE 5.3 Variations of the maximum and minimum values of σ_v, σ_h and ε_v for confined dense samples under the cyclic load with 0.100 Hz frequency.

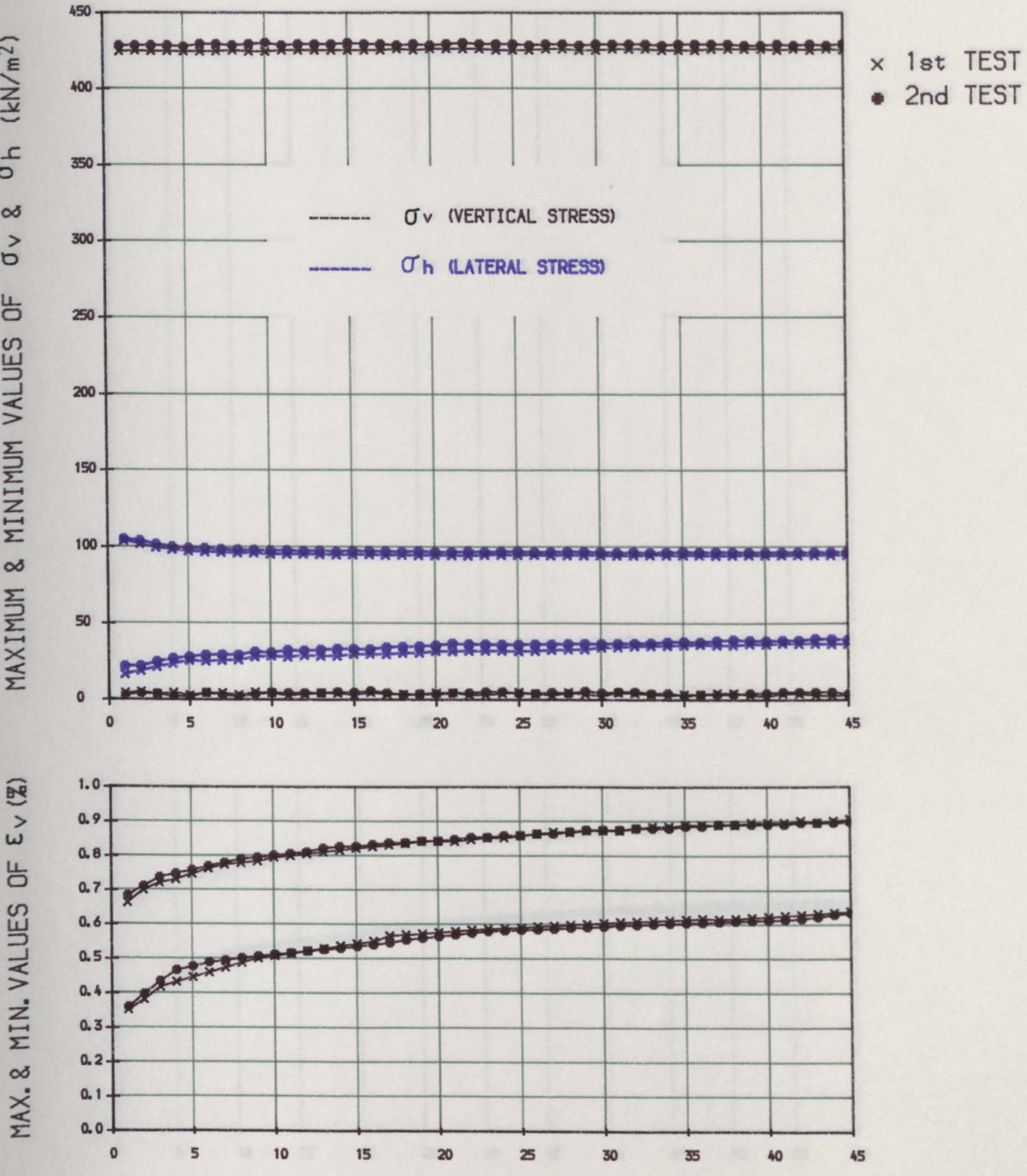

FIGURE 5.4 Variations of the maximum and minimum values of σ_v , σ_h and ε_v for confined dense samples under the cyclic load with 0.033 Hz frequency.

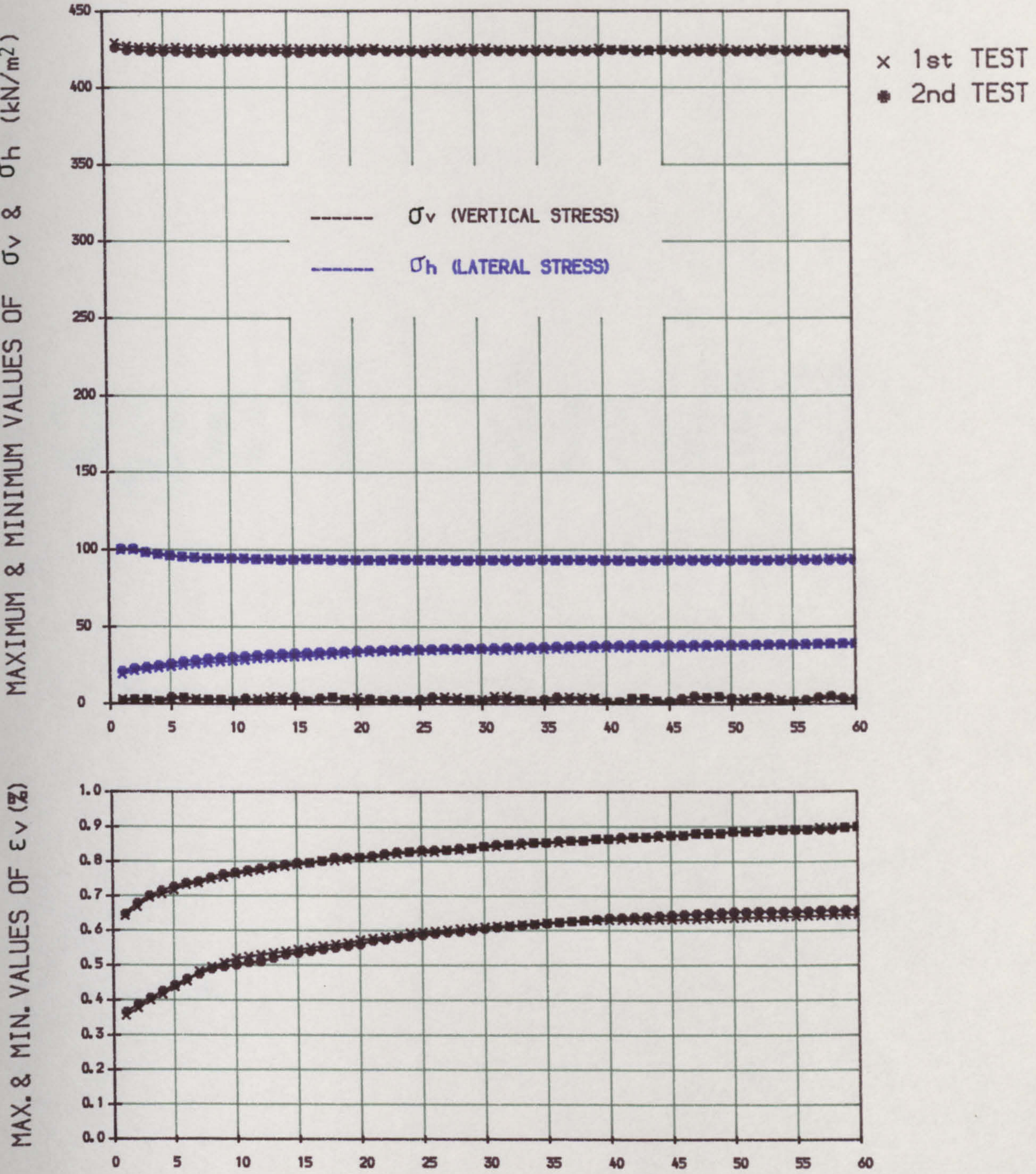

FIGURE 5.5 Variations of the maximum and minimum values of σ_v, σ_h and ε_v for confined dense samples under the cyclic load with 0.016 Hz frequency.

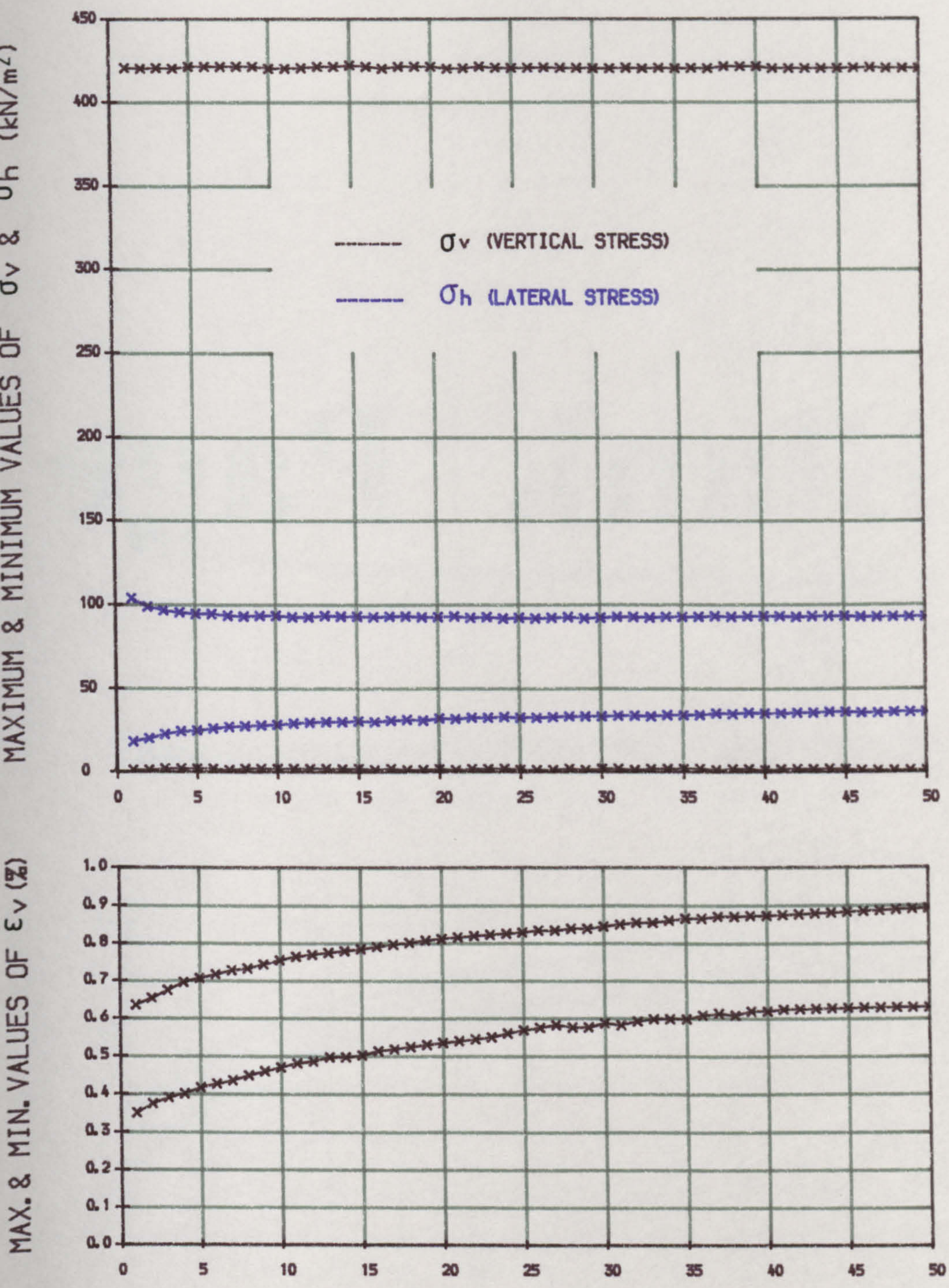

FIGURE 5.6 Variation of the maximum and minimum values of σ_v, σ_h and ε_v for confined dense samples under the cyclic load with 0.003 Hz frequency.

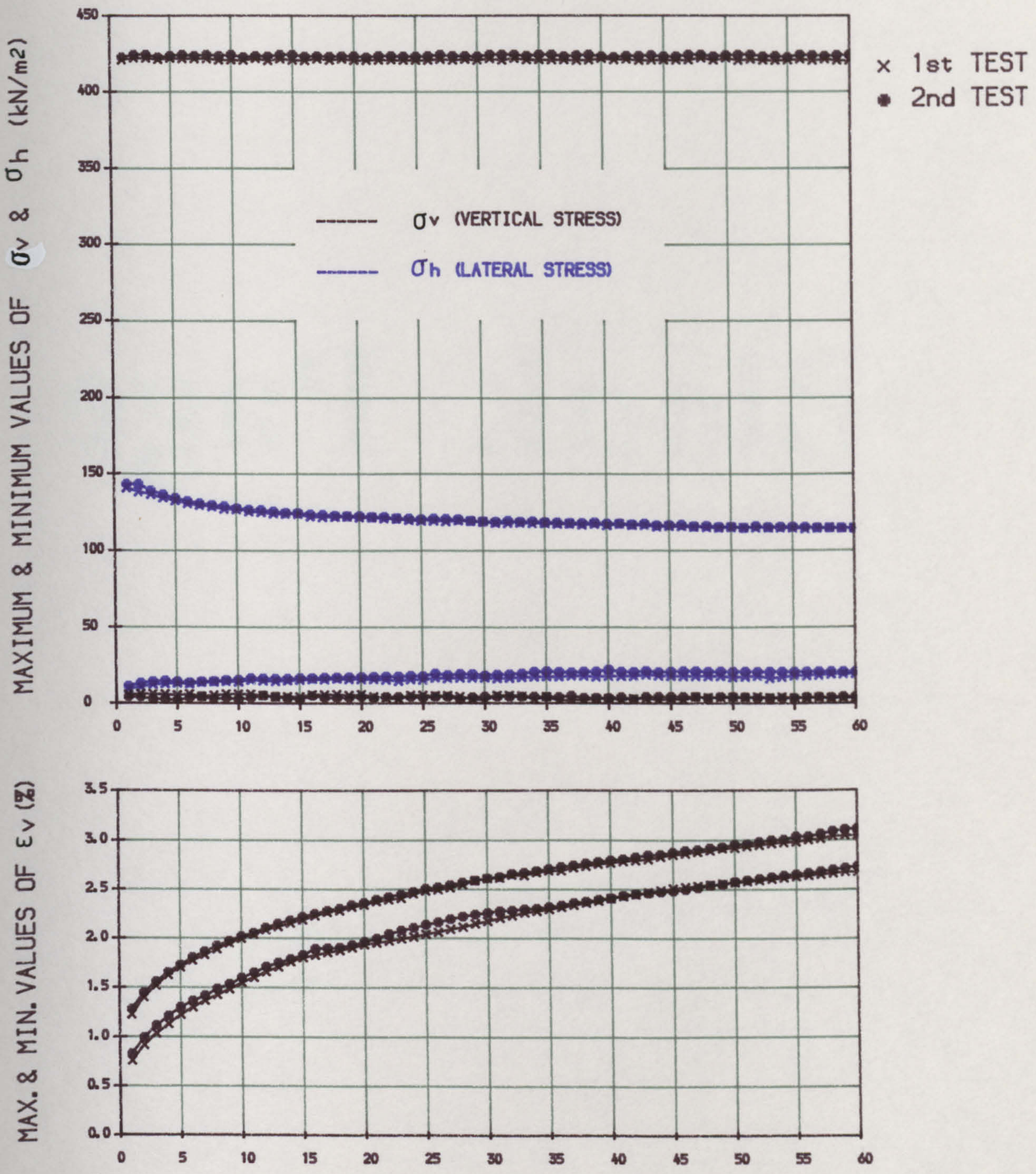

FIGURE 5.7 Variations of the maximum amd minimum values of σv , σh and εv for confined loose samples under the cyclic load with 0.100 Hz frequency.

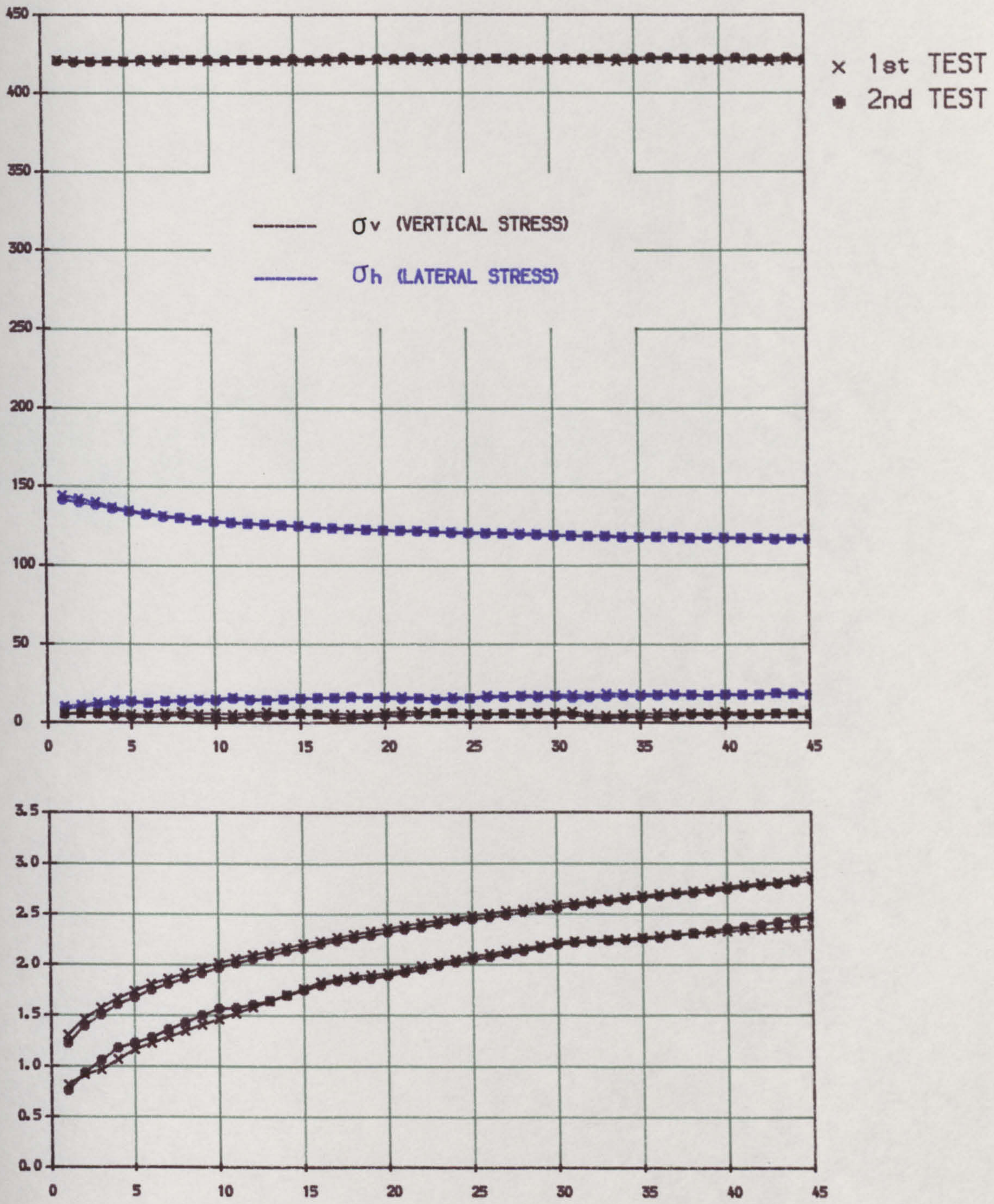

FIGURE 5.8 Variations of the maximum and minimum values of σv , σh and εv for confined loose samples under the cyclic load with 0.033 Hz frequency.

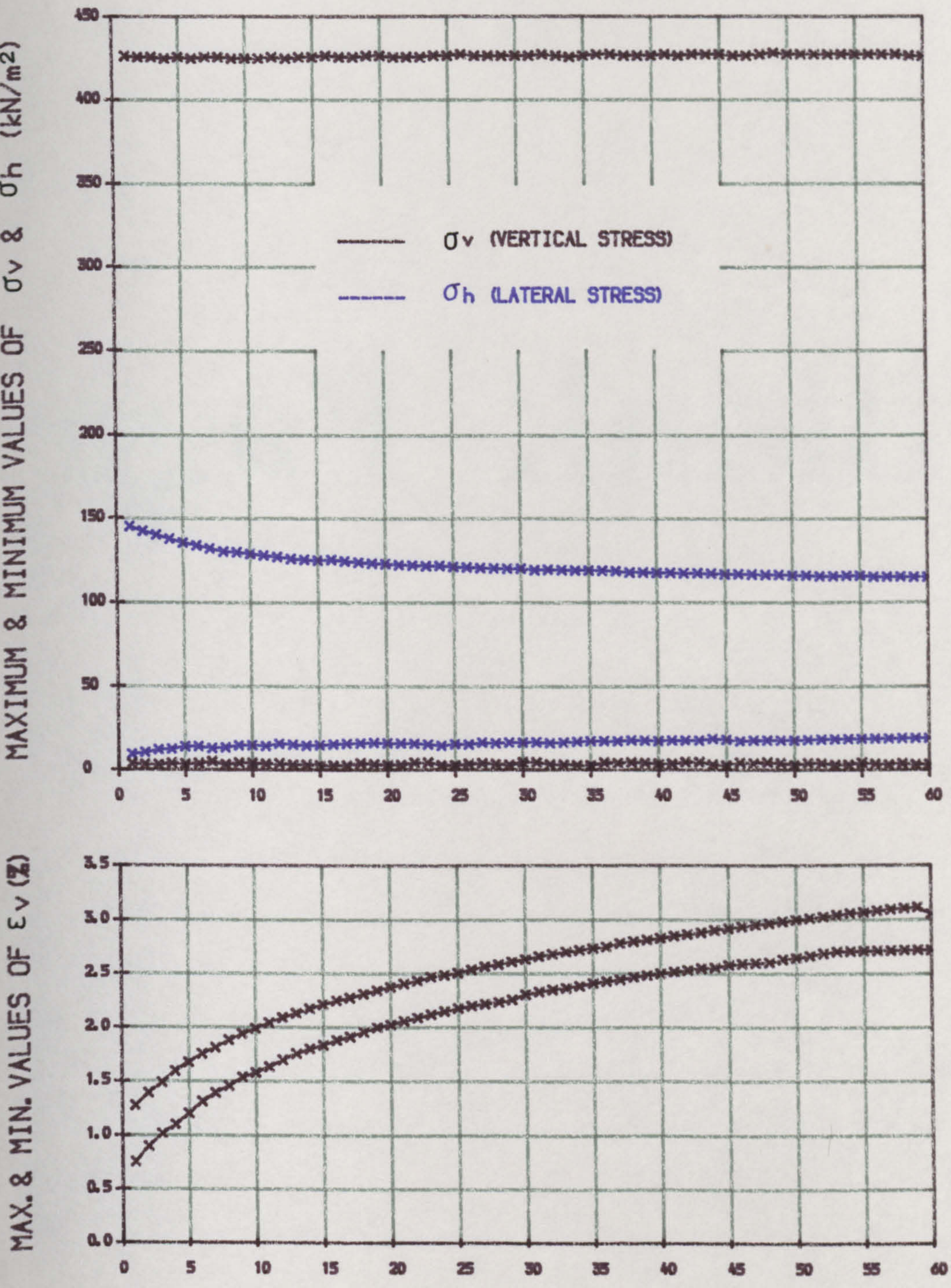

FIGURE 5.9 Variations of the maximum and minimum values of σ_v, σ_h and ε_v for confined loose samples under the cyclic load with 0.016 Hz frequency.

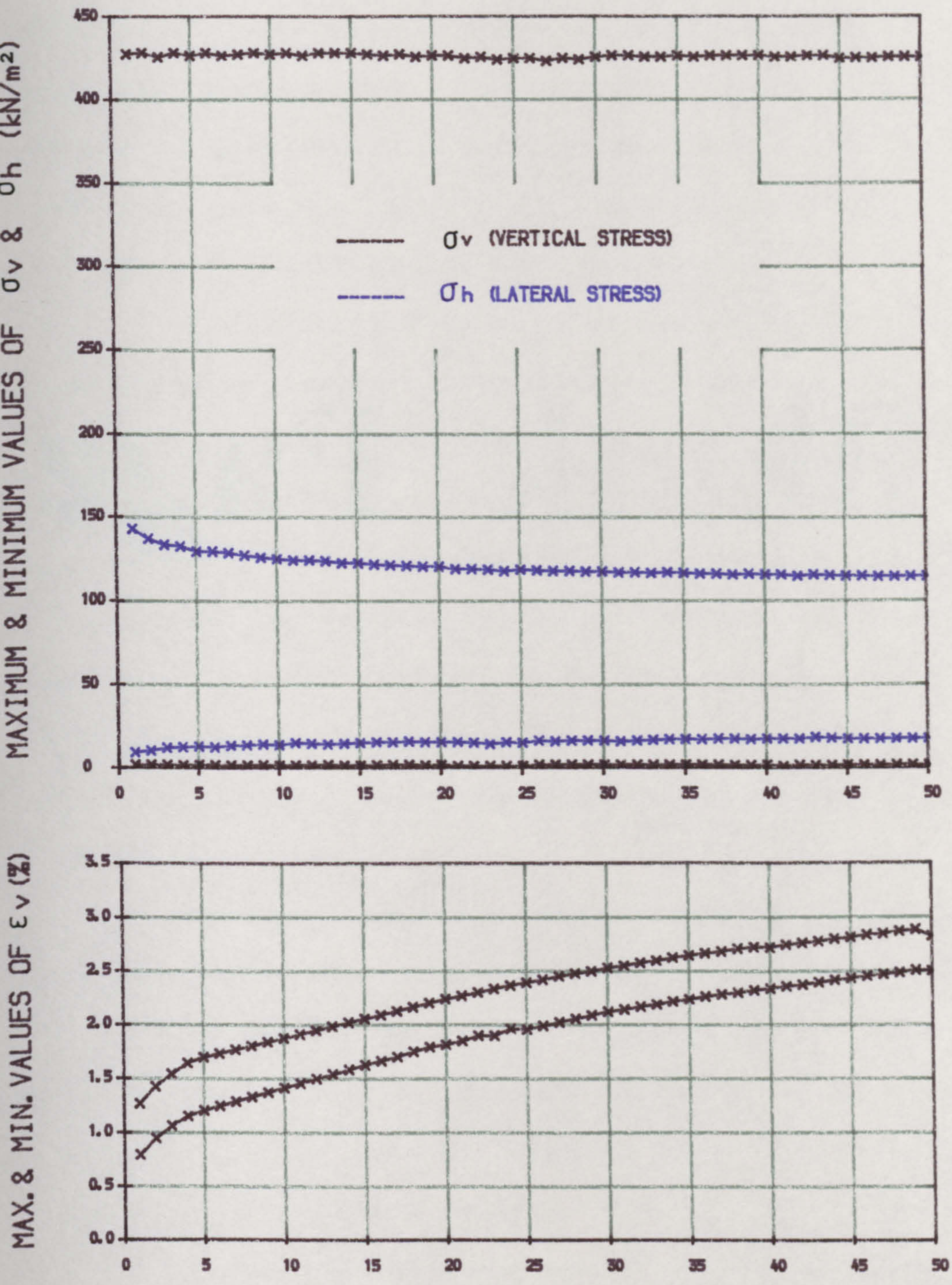

FIGURE 5.10 Variations of the maximum and minimum values of σv , σh and εv for confined loose samples under the cyclic load with 0.003 Hz frequency.

strain are approximately 0.65%, increase sharply during the first 25 cycles, then keep increasing at a slower rate and reach values of about 0.88% at 45 and of 0.90% at 60 cycles. However they are still increasing significantly at 45 cycles when the tests ended. The minimum value of the vertical strain is approximately 0.35% at the end of the first cycle and then with the same trend as for the maximum values, increases to 0.65% at the 60th cycle.

In figures 5.7 to 5.10 of data from tests on loose samples under similar conditions to those of the dense sand tests, the same general trends in variations of the vertical strain and lateral stresses for all different frequencies are evident. The only significant differences for the loose samples are the initial values of minima and maxima of σ_{h1}, σ_{h2} and ε_v which are not equal to those of dense samples. Also the distances between the minimum and maximum points of these parameters for loose samples are greater than those for dense samples.

From the results of this series of tests it can be concluded that the frequency of cyclic loading does not have a major effect on the general response of dry sand, and that variations of lateral stresses and vertical strain are independent of the rate of loading and unloading within the ranges of frequencies tested. For this reason the frequency of cyclic loading for the rest of the cyclic tests performed was fixed at 0.067 Hz (i.e. one cycle in 15 sec). This rate is fast enough to minimize the time of experiments on the one hand and to allow the data to be scanned at the most effective rate by the data acquisition unit on the other

hand.

5.3.3 THE EFFECT OF THE NUMBER OF LOADING CYCLES ON THE RESPONSE OF THE SAND

As mentioned in section 5.3.1 for the confined samples, under successive cycles of load the maximum and minimum lateral stresses and vertical strains appear to tend to a constant value. These general trends were found after applying approximately 60 cycles of load to the samples. However it is not clear from the data how many cycles are needed to reach a constant value, if indeed a constant value is reached, or what the constant values will be.

To answer the questions raised above, two additional series of confined tests on dense (n=33%) and loose (n=41%) samples were carried out in which the number of cycles was increased to 360 for the loose specimen and to 215 for the dense sample. Both experiments were performed at a frequency of 0.067 Hz and an amplitude of 215 kN/m^2.

The results of these tests are shown in figures 5.11 and 5.12. In these figures the variations of the minimum and maximum values of σ_v, σ_{h1}, σ_{h2} and ε_v are plotted.

In fig 5.11, test on a dense sample, the minimum and maximum values of lateral stresses stabilize after approximately 120 cycles of load, while the vertical strain does not become constant even after 215 cycles. In fig 5.12 the results of the test on the loose sample show much more variation in σ_{h1},σ_{h2} and, ε_v than those of the test on the dense sample. The maximum values of the lateral stresses stabilize after almost 200 cycles, whereas the minimum values still keep increasing up to 360 cycles, the limit of the

STRESS-STRAIN CURVES FOR CONFINED TESTS UNDER CYCLIC LOADING CONDITIONS

INITIAL POROSITY=33%, FREQUENCY=0.067 Hz, PERIOD=15Sec., AMPLITUDE=215 kN/m^2, NUMBER OF CYCLES=215

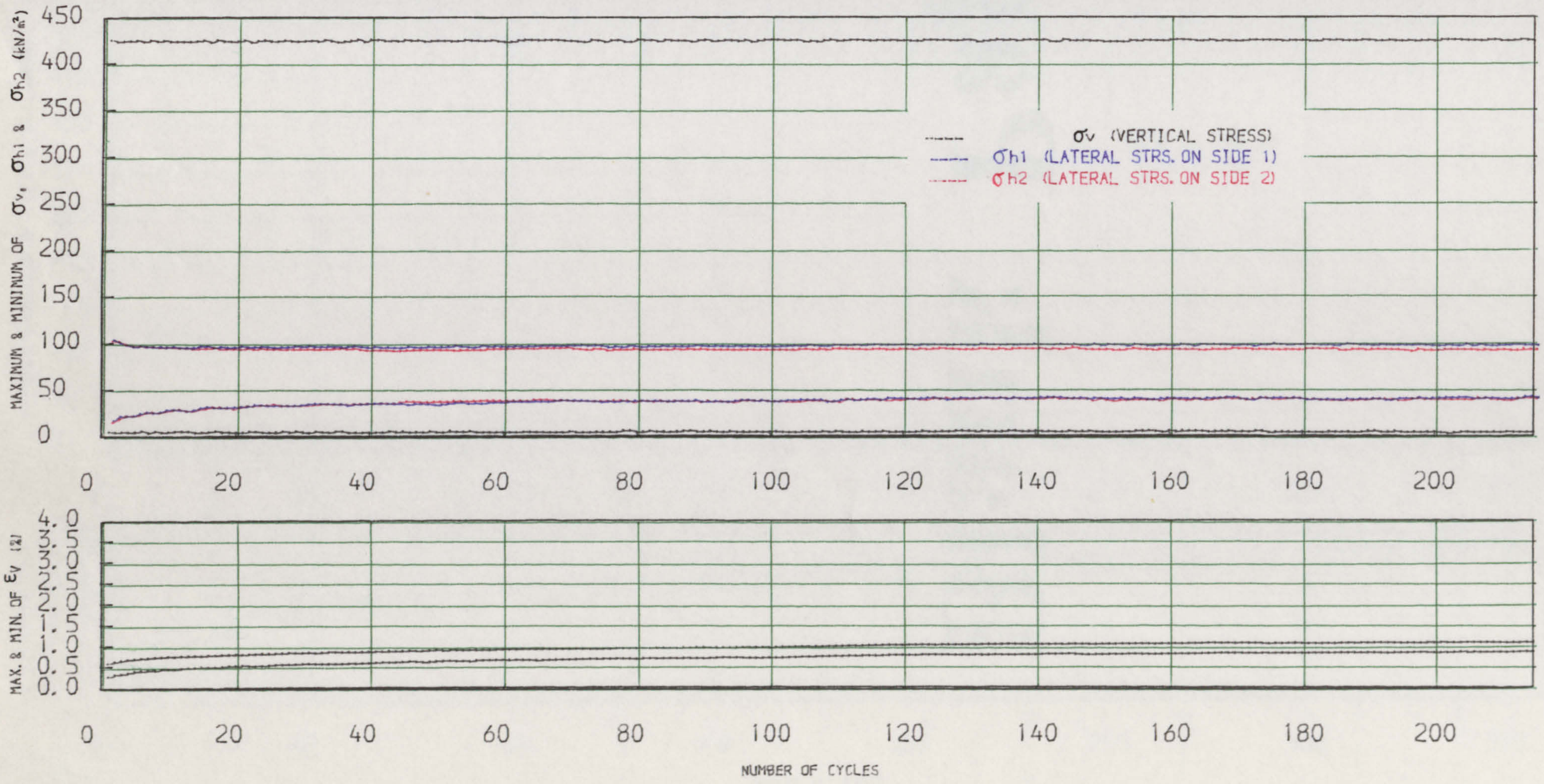

FIGURE 5.11 VARIATIONS OF THE MAXIMUM AND MINIMUM VALUES OF σ_v, σ_{h1} , σ_{h2} AND ε_v FOR DENSE SAMPLES UNDER CYCLIC LOAD UP TO 215 CYCLES OF THE LOAD.

STRESS-STRAIN CURVES FOR CONFINED TESTS UNDER CYCLIC LOADING CONDITIONS

INITIAL POROSITY=41%, FREQUENCY=0.067 Hz, PERIOD=15Sec., AMPLITUDE=215 kN/m^2 , NUMBER OF CYCLES=360

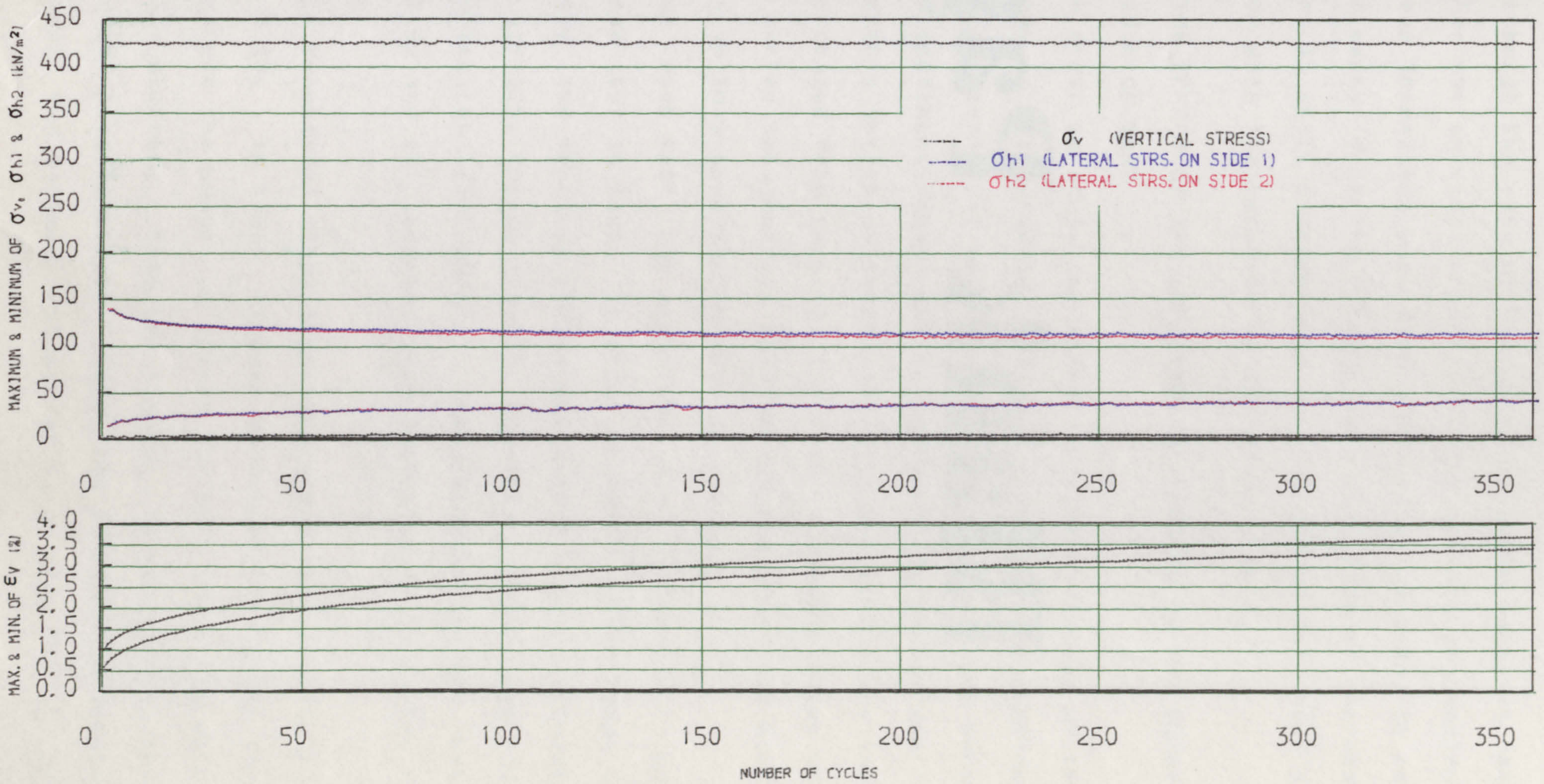

FIGURE 5.12 VARIATIONS OF THE MAXIMUM AND MINIMUM VALUES OF σ_v, σ_{h1}, σ_{h2} AND ε_v FOR LOOSE SAMPLES UNDER CYCLIC LOAD UP TO 360 CYCLES OF THE LOAD.

test, although the rate of increase is quite small at this stage. For the vertical strain both the minimum and maximum values keep increasing even after 360 cycles of load. It can be seen clearly from the figures that the rate of increase in strain is still considerable at the end of the test in comparison with the response of the dense sample.

5.3.4 THE EFFECT OF THE AMPLITUDE OF LOADING ON THE BEHAVIOUR OF SAND

In order to study the effect of the amplitude of the cyclic load on the behaviour of sand samples under confined conditions, a series of tests were carried out on both dense and loose specimens under cyclic loads at different amplitudes. In this series of tests, the vertical stress was initially increased from zero to the desired maximum value and was then cycled between this maximum and the specified minimum value up to a specified number of cycles.

For each test the amplitude was constant but was varied from test to test. In order to cover a wide range of amplitudes, the vertical stress was cycled between 425-325, 425-225, 425-125, 425-0, 325-225, 325-125, 325-0, 225-125, 225-0 and finally 125-0 kN/m^2. The frequency for all tests was 0.067 Hz and all samples were subjected to 70 cycles of loadings.

The results of these experiments are shown in figures 5.13 to 5.19. In these figures variations of σ_v, σ_{h1}, σ_{h2} and ε_v against the number of cycles for both loose and dense samples are plotted. From the figures it can be seen that the amount of elastic strain (i.e. the differences between the maximum and minimum values of ε_v) depends on the

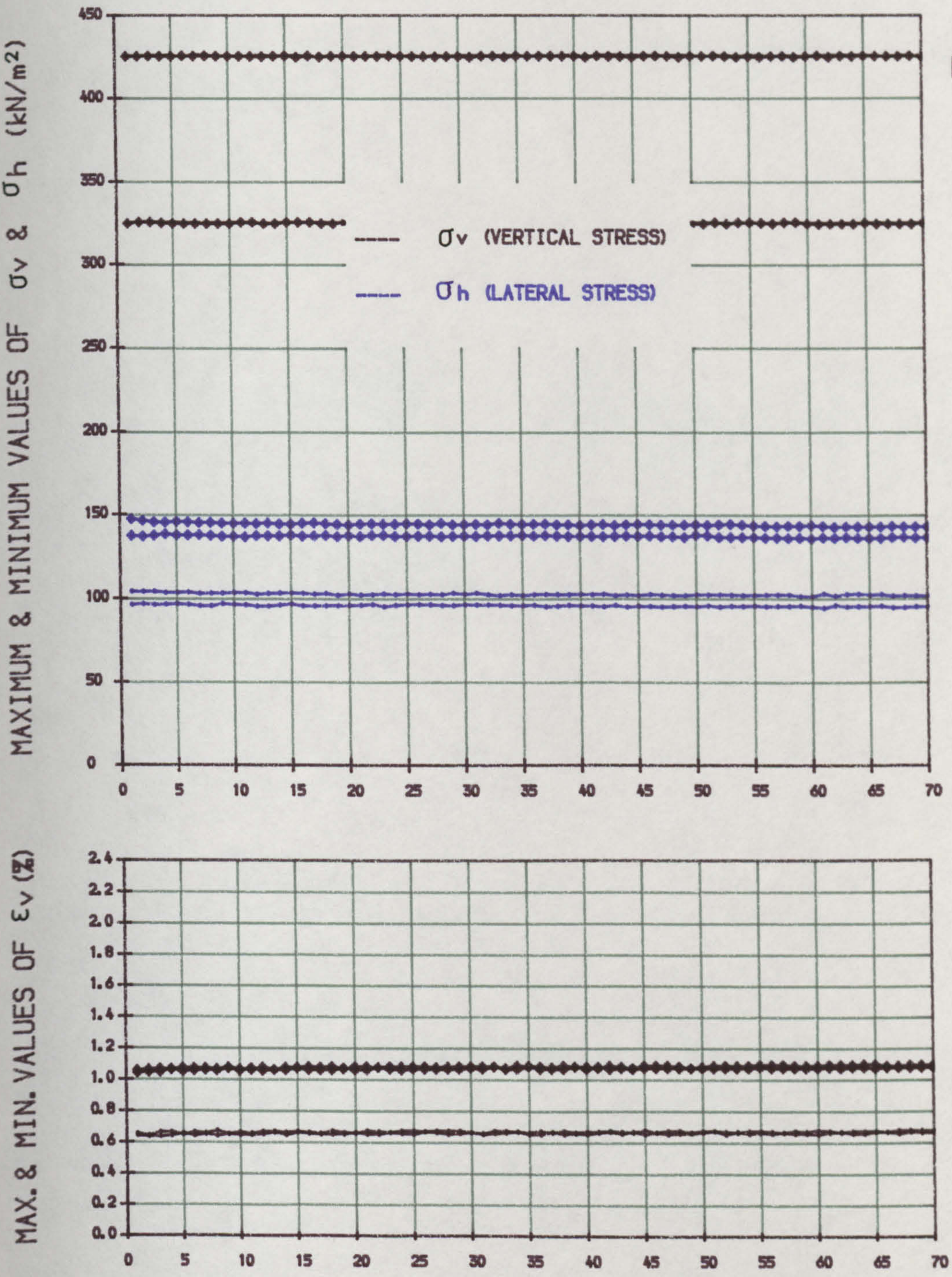

FIGURE 5.13 Variations of the maximum and minimum values of σ_h and ε_v for confined samples when σ_v cycles between 325 and 425 kN/m² with the frequency of 0.067 Hz.

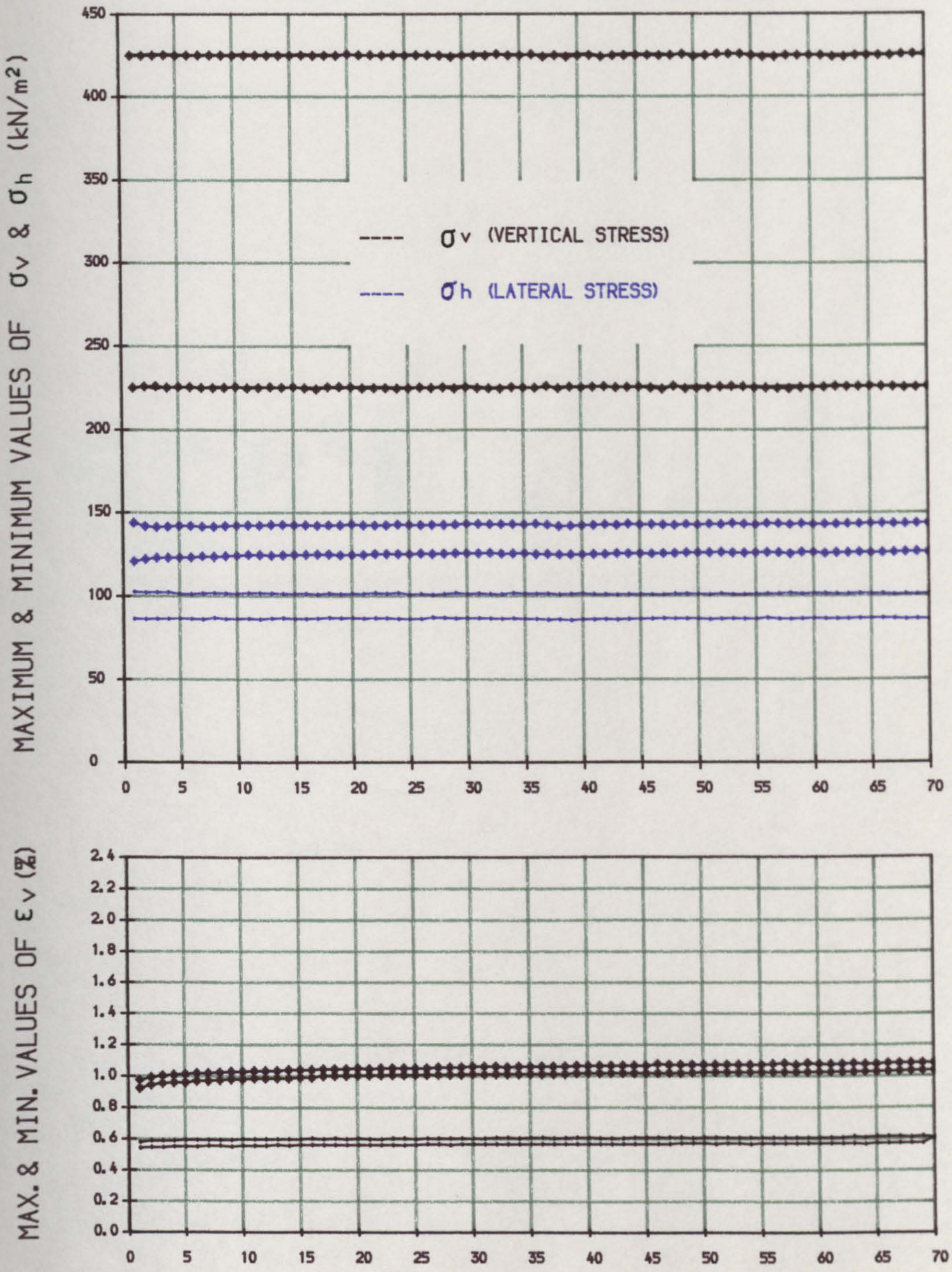

FIGURE 5.14 Variations of the maximum and minimum values of σ_h and ε_v for confined samples when σ_v cycles between 225 and 425 kN/m² with the frequency of 0.067 Hz.

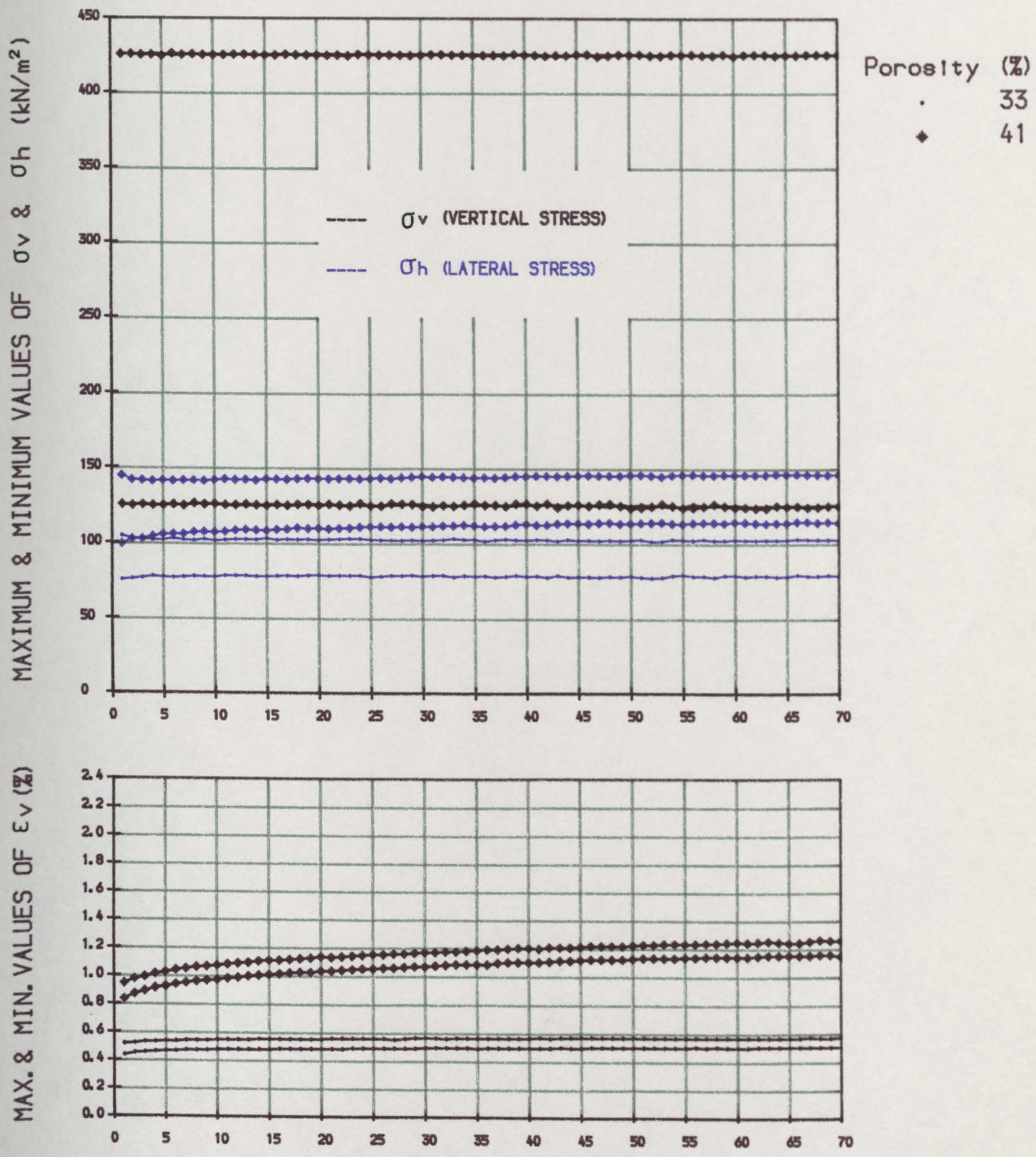

FIGURE 5.15 Variations of the maximum and minimum values of σ_h and ε_v for confined samples when σv cycles between 125 and 425 kN/m² with the frequency of 0.067 Hz.

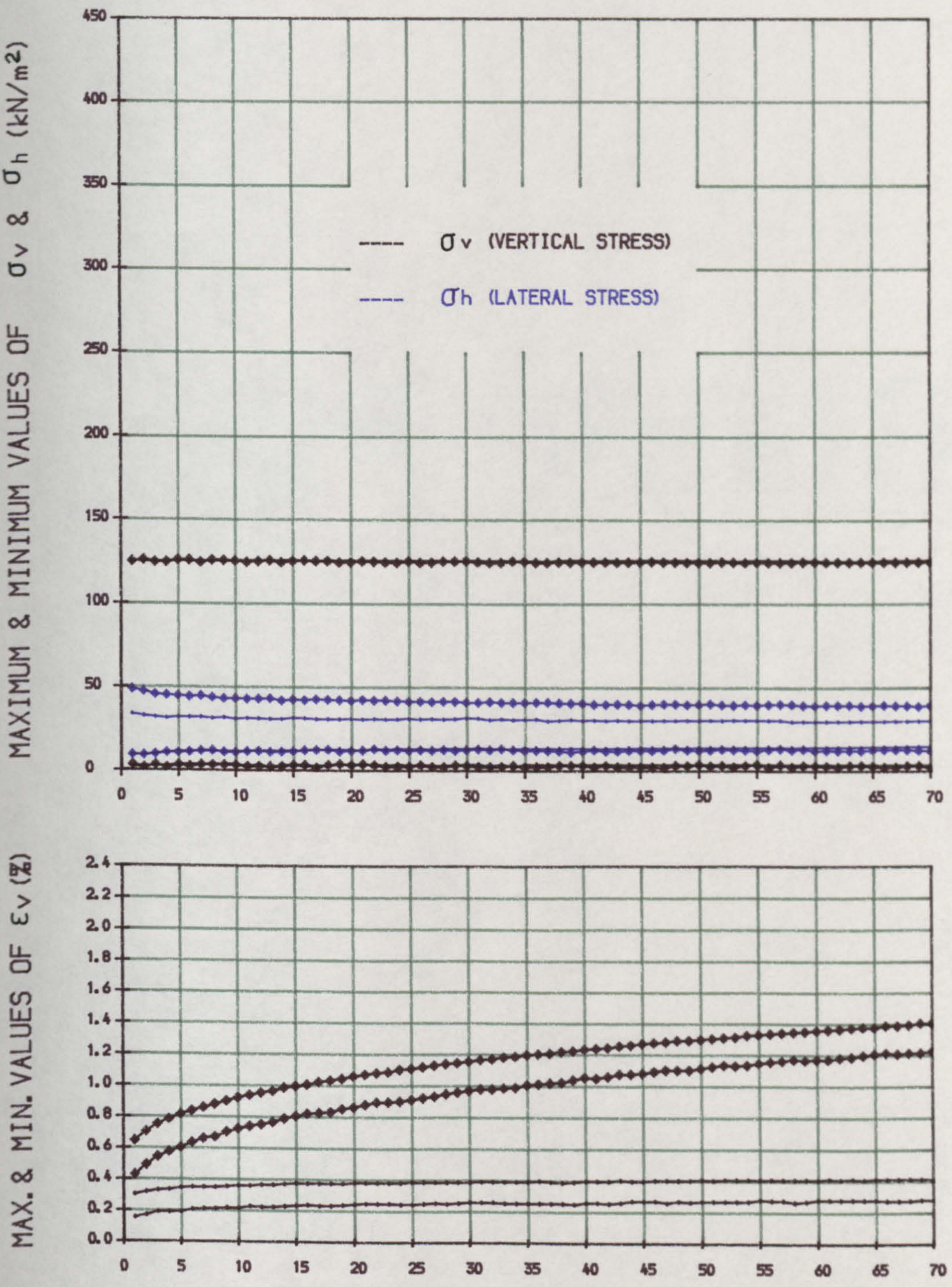

FIGURE 5.16 Variations of the maximum and minimum values of σ_h and ε_v for confined samples when σ_v cycles between 0 and 125 kN/m² with the frequency of 0.067 Hz.

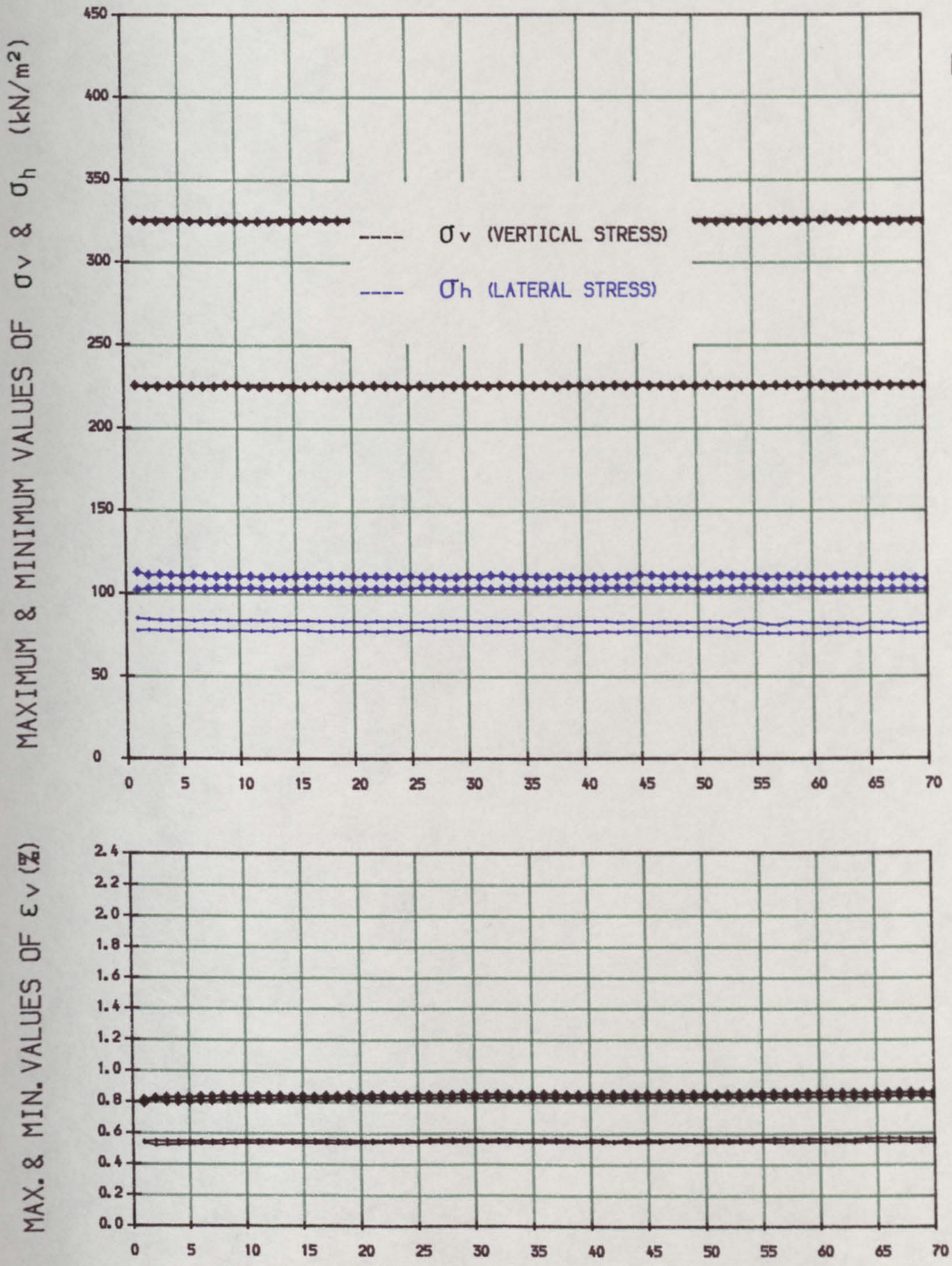

FIGURE 5.17 Variations of the maximum and minimum values of σ_h and ε_v for confined samples when σv cycles between 225 and 325 kN/m² with the frequency of 0.067 Hz.

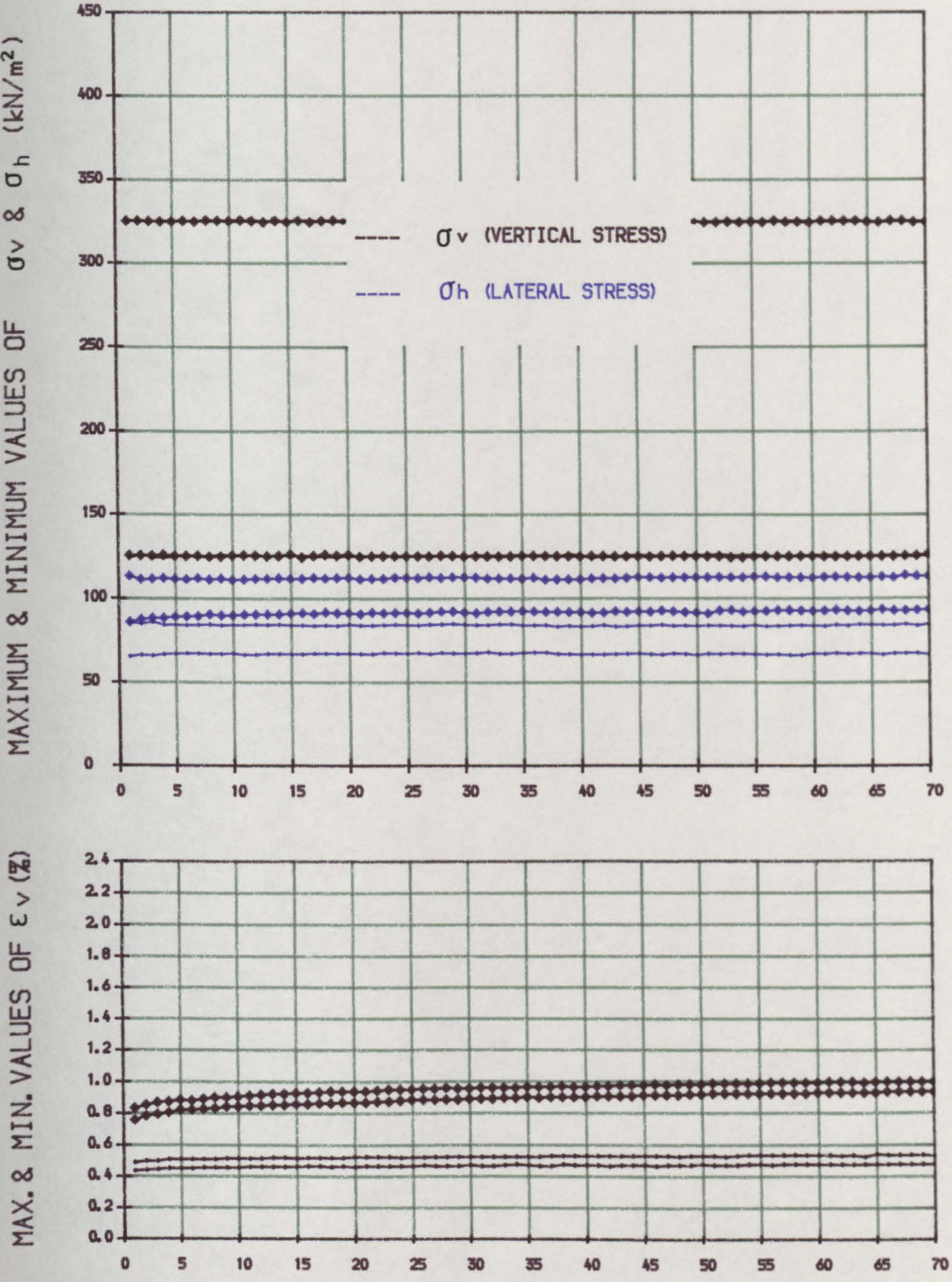

FIGURE 5.18 Variations of the maximum and minimum values of σ_h and ε_v for confined samples when σ_v cycles between 125 and 325 kN/m² with the frequency of 0.067 Hz.

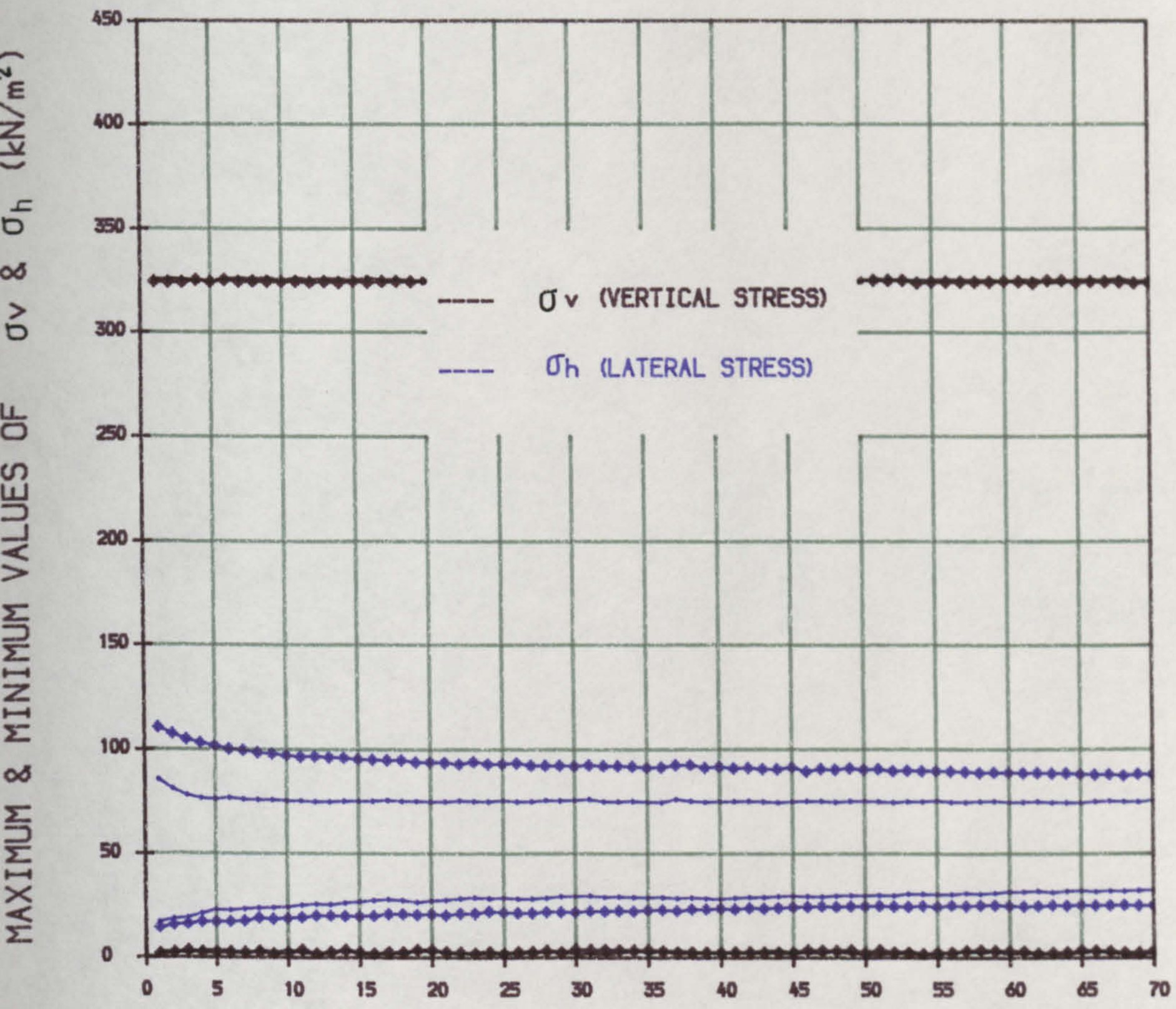

FIGURE 5.19 Variations of the maximum and minimum values of σ_h and ε_v for confined samples when σ_v cycles between 0 and 325 kN/m² with the frequency of 0.067 Hz.

amplitude of the load. When the amplitude of the cycle increases the elastic vertical strain increases as well. The other factor affecting the elastic strain is the percentage of unloading in each cycle. The greater this percentage, the larger the elastic vertical strain. From figure 5.13 it is clear that for variations of vertical stress less than 25% of the maximum applied stress, there is no appreciable change of elastic strain on cyclic loading for both loose and dense samples. For a cyclic load with full unloading, maximum elastic vertical strain takes place (figures 5.16 and 5.19). The same trend for the variation of plastic strain (i.e. the maximum values of ε_v) can be seen from the figures. The differences here are the threshold values for amplitude effects. For loose samples, cycling of the vertical stresses at less than 30% of the maximum applied stress (figure 5.17) does not have any effect on σ_h and ε_v, and for values greater than this the plastic strains begin to increase. For dense samples this limit is about 60% (figure 5.18). This means that cyclic loads with variations of vertical stress less than 60% of the maximum applied stress do not have any major effect on the plastic vertical strain of the dense samples. Generally, under full unloading conditions the elastic and plastic vertical strains increase on increasing the peak load value (figures 5.16 and 5.19). When a comparison is made between two amplitudes with different percentages of unloading, this factor should be taken into account otherwise the results cannot be justified. E.g. the values of elastic strains (for both dense and loose samples) and plastic strains (for only loose sample) in fig 5.16 are

greater than those in figure 5.15 in spite of having smaller amplitude.

Although the minimum and maximum values of the lateral stresses directly depend on the minimum and maximum values of the vertical stress applied to the samples, the percentage of unloading is again a key factor on the changes of these values over the cycles of load. For loose samples the cyclic loadings with unloading percentage less than 45% do not cause any change in σ_{hmin} and σ_{hmax} (figure 5.14), whereas for dense samples this percentage increases to about 70%. It means that only the cyclic loadings with amplitude greater than these ranges will cause changes in the minimum and maximum values of the lateral stresses.

5.3.5 THE RELATIONSHIP BETWEEN VERTICAL STRESS AND VERTICAL STRAIN AND NUMBER OF CYCLES

Vertical stress versus vertical strain for both dense and loose samples under confined conditions for different cycles of load are shown in figures 5.20 and 5.21. For loose samples the stress-strain curves are plotted for the 1st, 10th, 50th, 100th, 150th, 200th, 250th, 300th, 350th and, 360th cycles and for dense samples they are illustrated for the 1st, 5th, 10th, 20th, 50th, 100th, 150th, 200th and 215th cycles. The amplitude (212 kN/m^2) and frequency (0.067 Hz) are the same for all experiments.

From the figures it can be seen that for both dense and loose samples elastic and plastic strains occur from the first cycle of load. In the first cycle the plastic and elastic strains, particularly for dense samples, are nearly equal but as the number of cycles increases the total

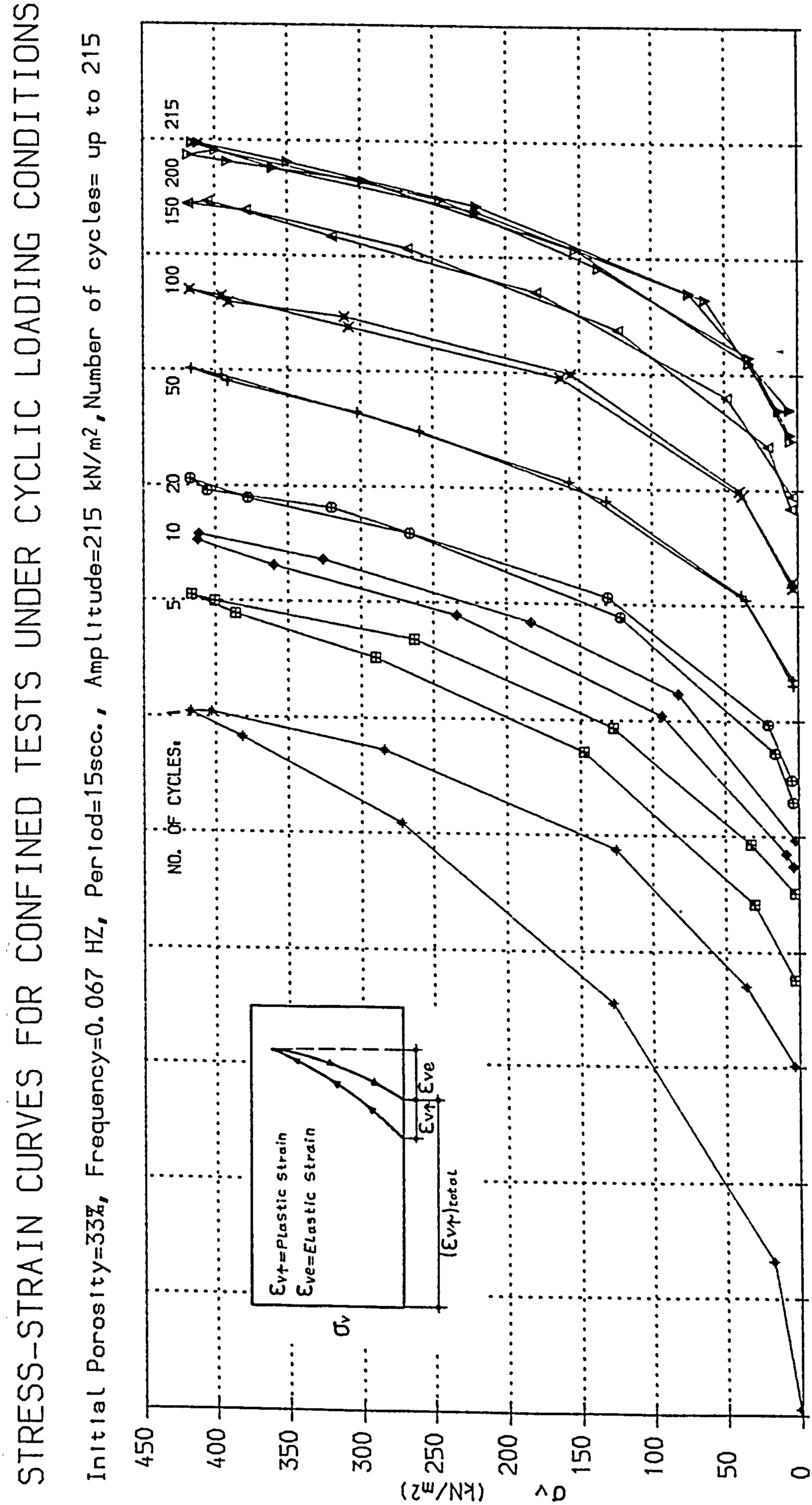

FIGURE 5.20 Relationship between vertical stress and vertical strain for dense samples at different load cycles.

STRESS-STRAIN CURVES FOR CONFINED TESTS UNDER CYCLIC LOADING CONDITIONS

Initial Porosity=41%, Frequency=0.067 Hz, Period=15Sec., Amplitude=215 kN/m², Number of cycles= up to 360

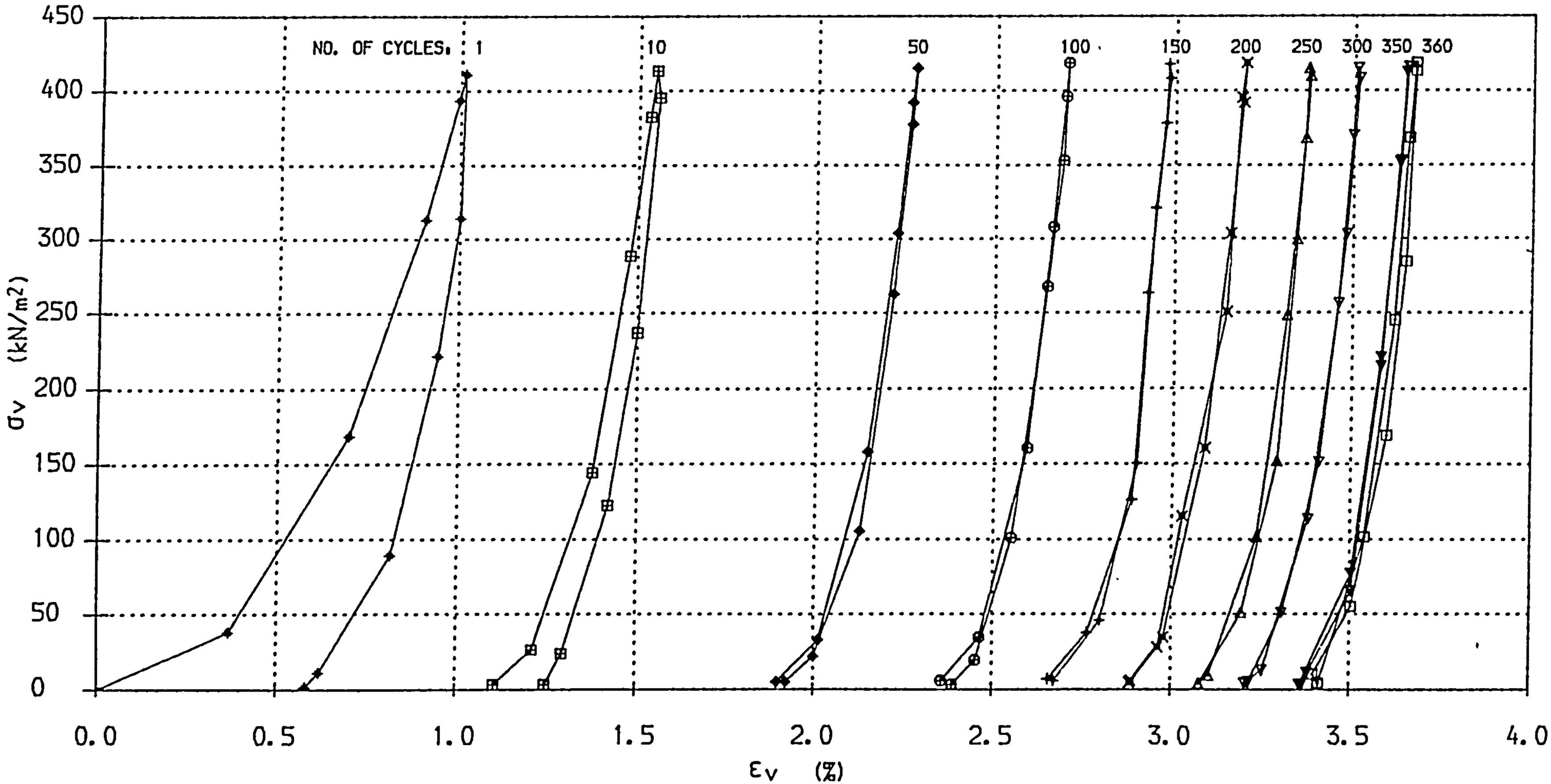

FIGURE 5.21 Relationship between vertical stress and vertical strain for loose samples at different load cycles.

plastic strains dominate. The elastic strains for both densities are initially large but as the cycling continues they become marginally smaller and after some cycles (10 for dense and 100 for loose) they become nearly constant. However the total plastic strain increases on increasing the number of cycles. Although the rate of increase in plastic strain gradually decreases, there is no sign of stability after 215 cycles on dense and 360 cycles on loose samples. The hysteresis loops of the stress-strain curves for the early load cycles are quite large but they become smaller as the number of cycles increases and after a certain number of cycles they become small and negligible. From these results it is seen that after a number of load cycles the sand will behave as a non-linear elastic material with nearly constant elastic properties.

5.3.6 THE RELATIONSHIP BETWEEN VERTICAL STRESS, LATERAL STRESS AND NUMBER OF LOADING CYCLES

In figures 5.22 and 5.23 the lateral stress versus vertical stress under cyclic loading at different numbers of cycles are shown for dense and loose samples respectively. As there are small differences between σ_{h1} and σ_{h2}, their average values are plotted on these graphs. The same amplitude and frequency of loading were used for each test. In order to show the trend of the results the curves for 1st, 5th, 10th, 15th, 20th, 25th, 30th, 40th and 50th cycles of load are given.

It can be seen from the figures for both dense and loose samples that the loading portions of the curves are similar to those for monotonic loading and are generally

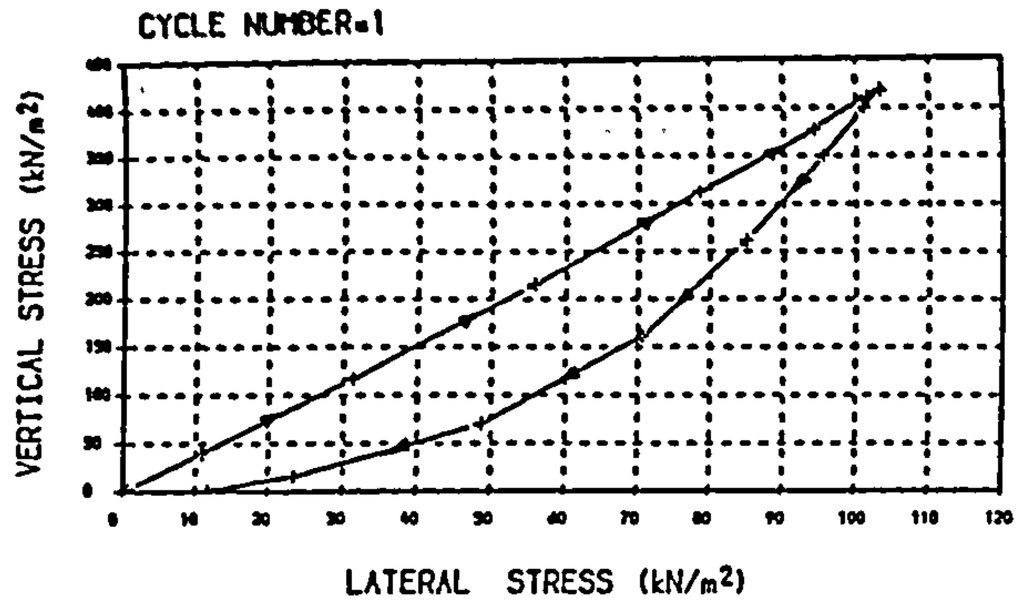

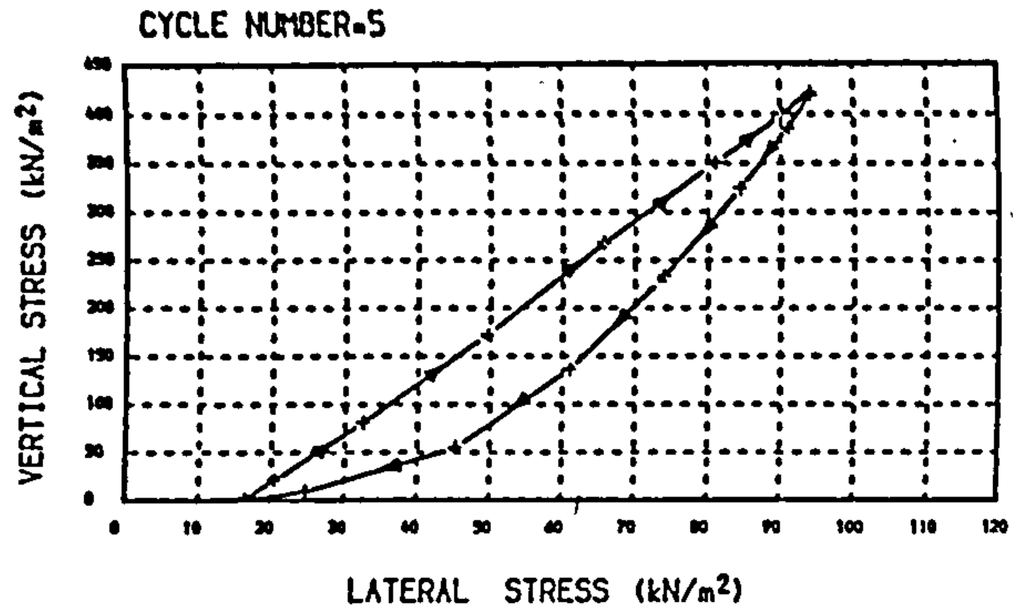

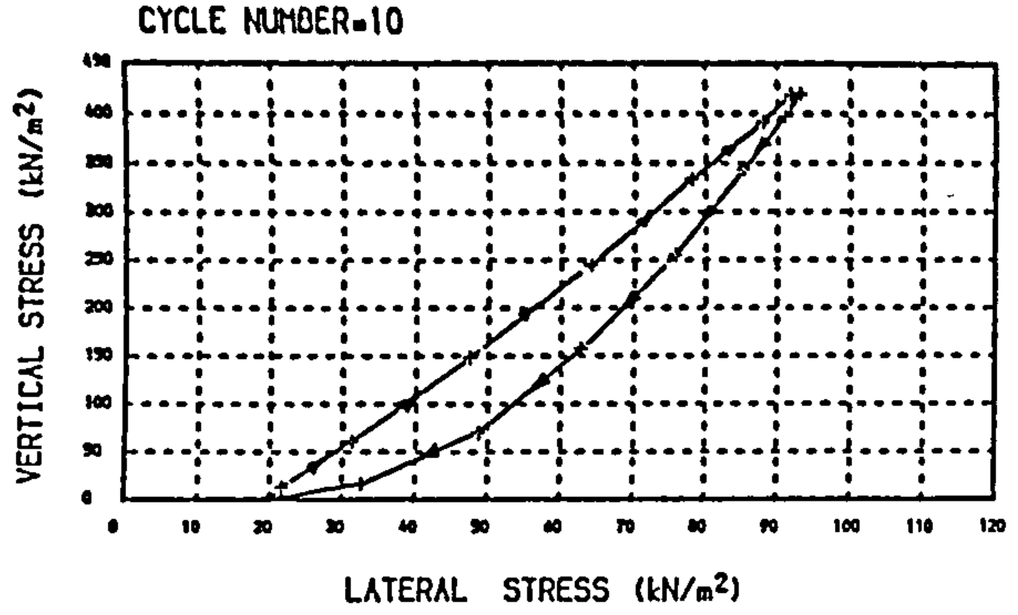

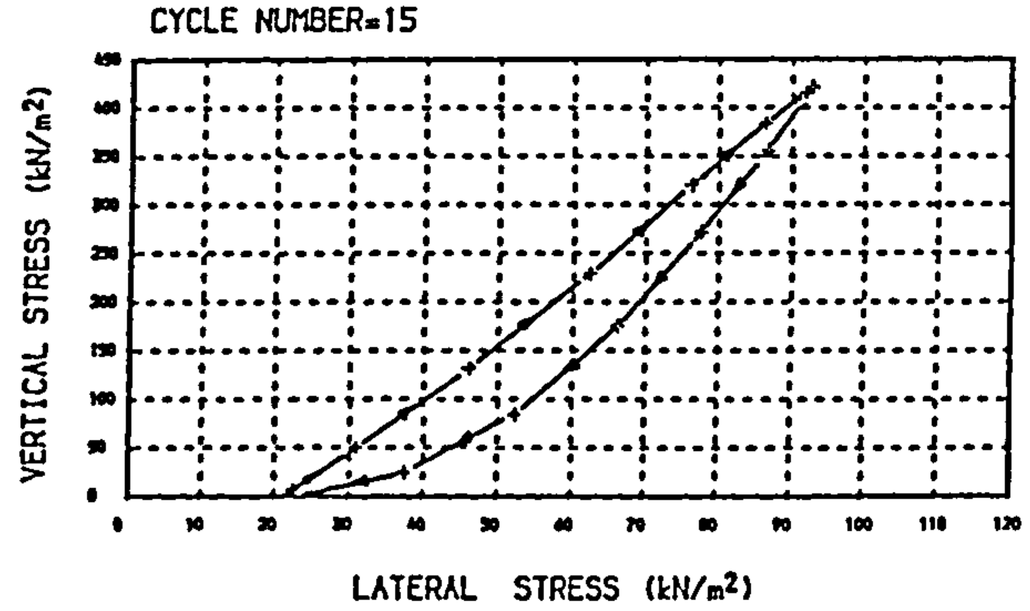

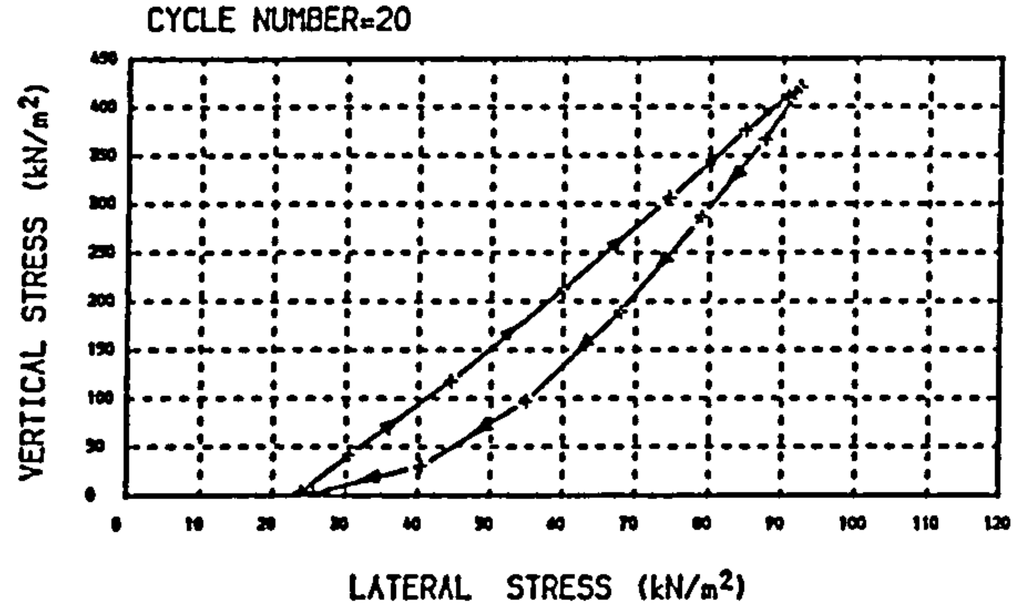

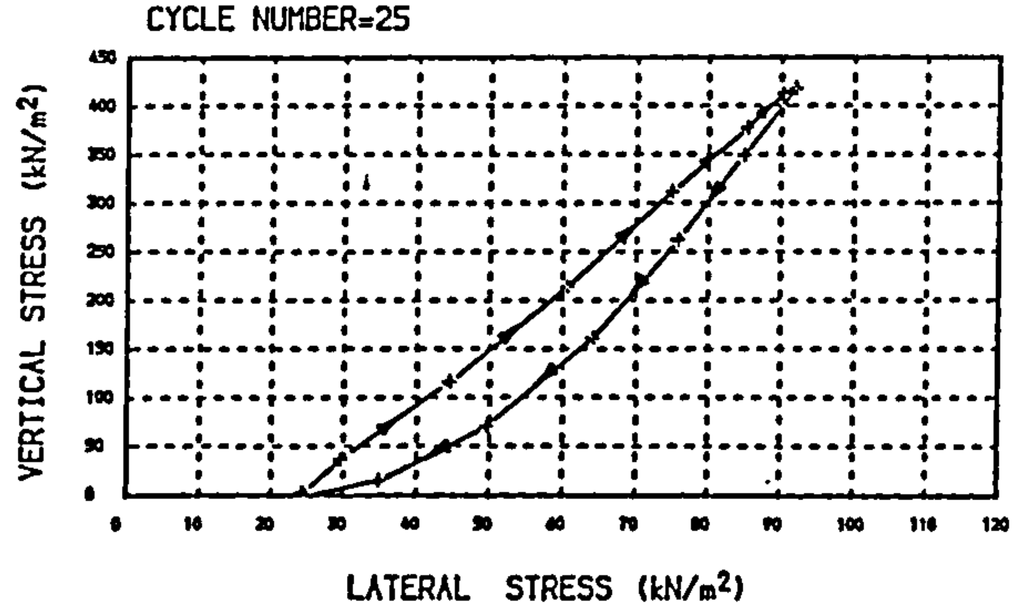

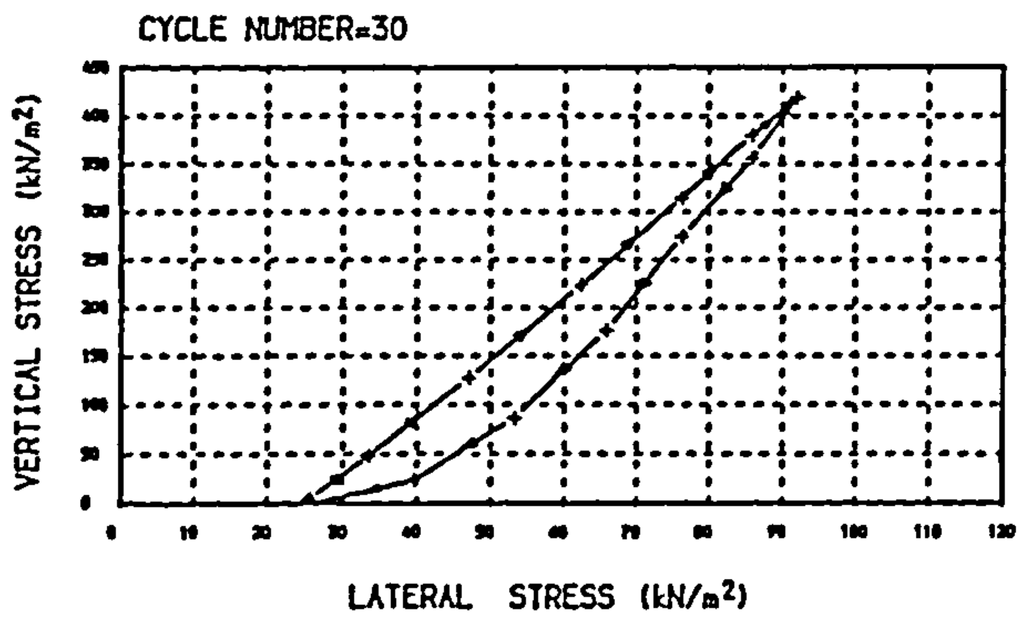

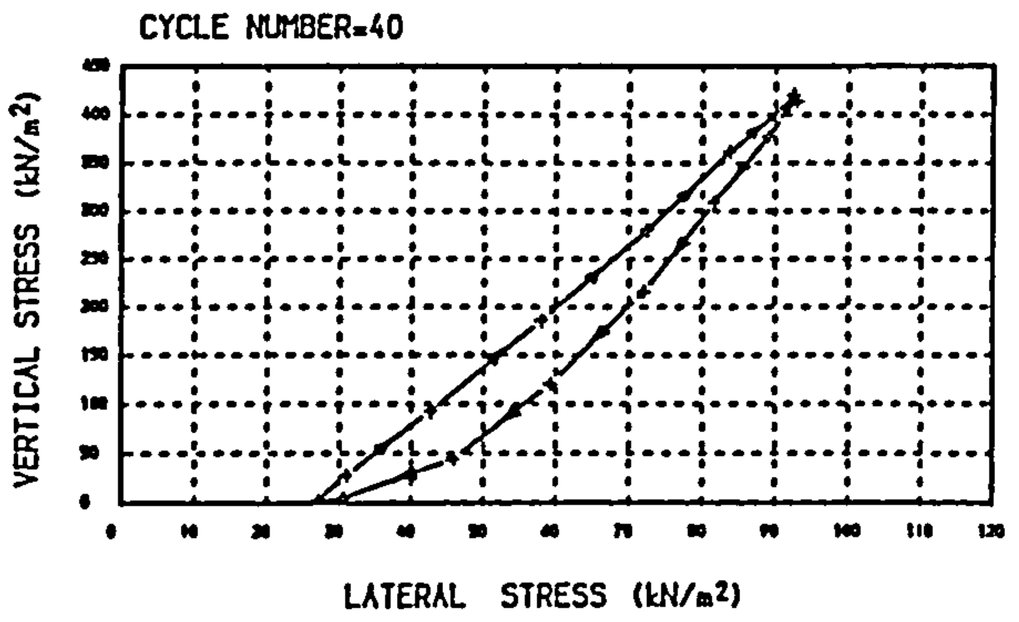

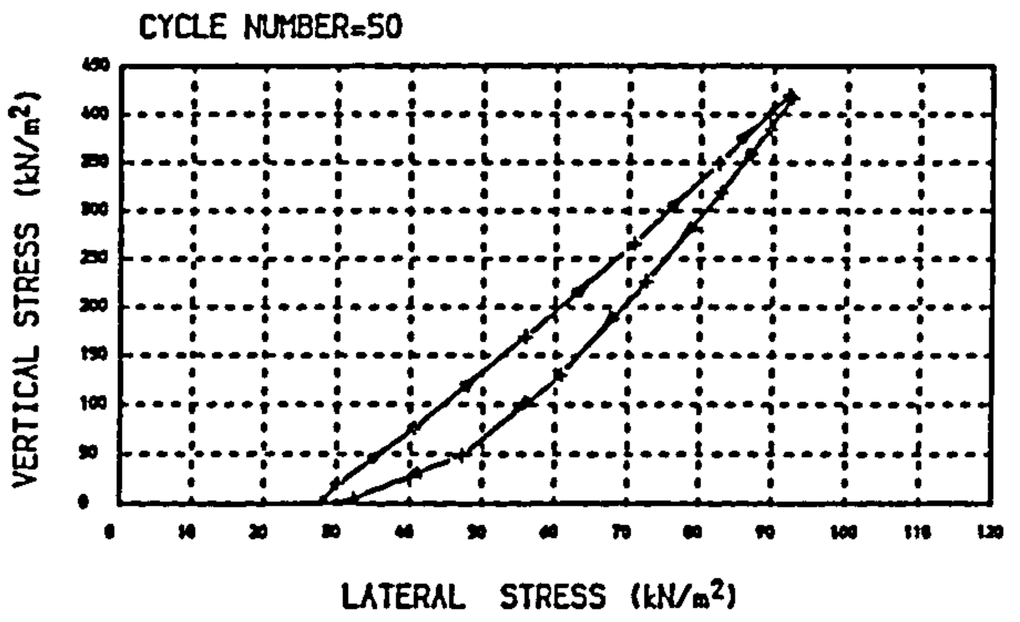

FIGURE: 5.22 RELATIONSHIP BETWEEN VERTICAL STRESS AND LATERAL STRESS FOR DENSE SAMPLES UNDER CONFINED CONDITION AT DIFFERENT CYCLES OF LOAD.

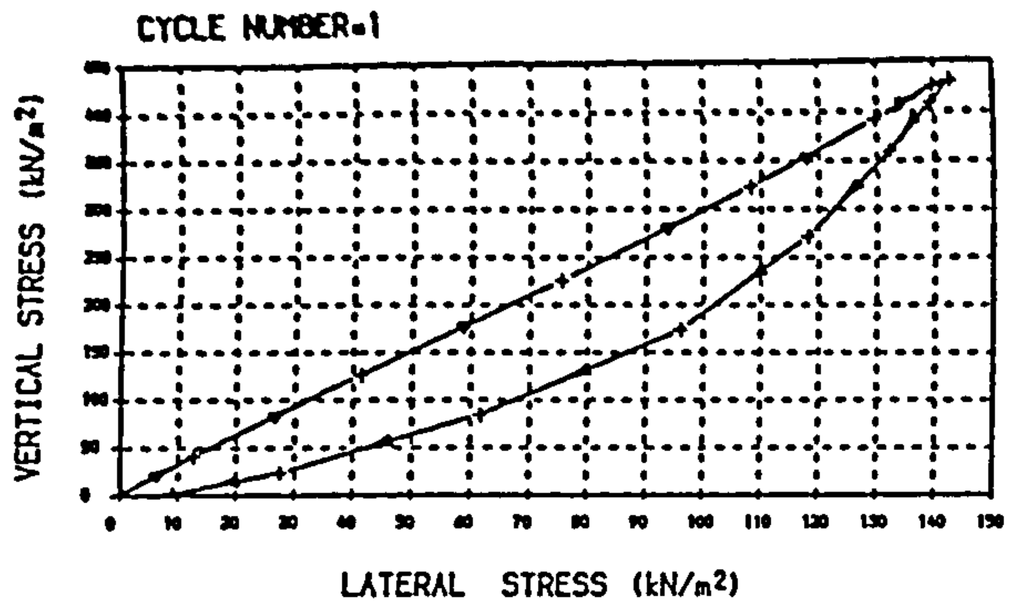

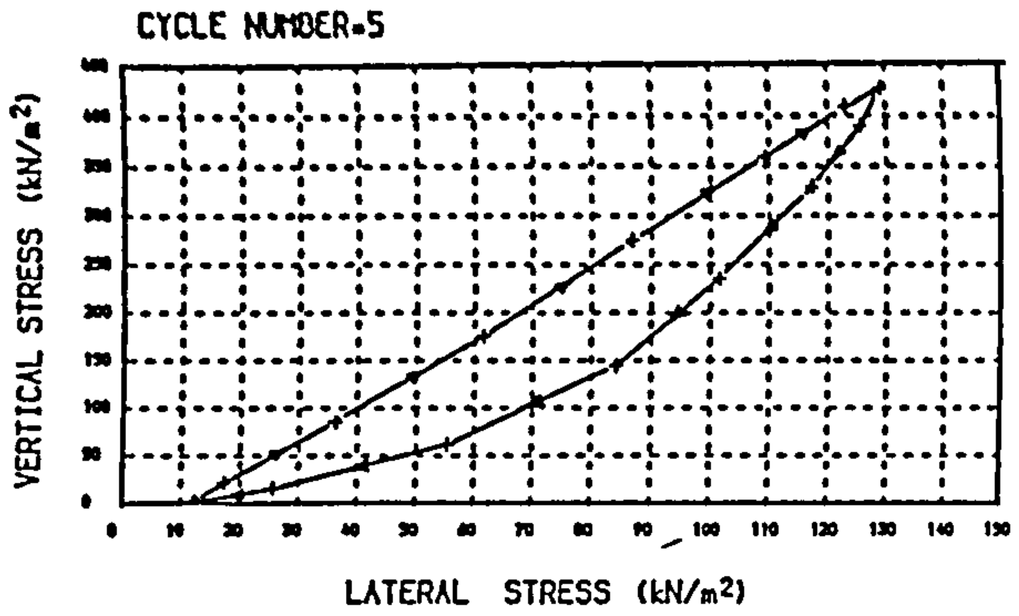

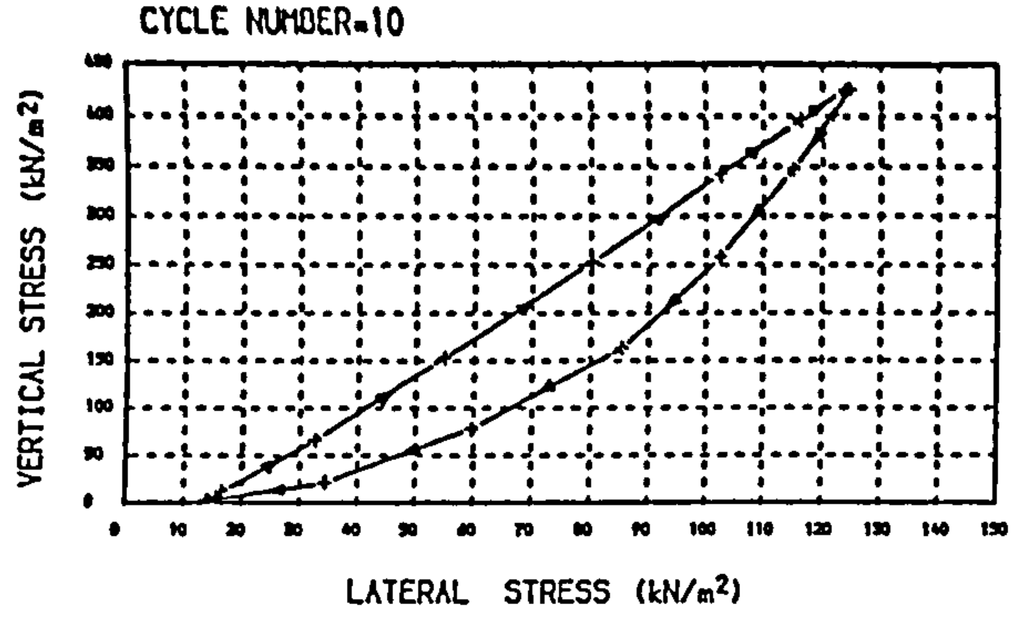

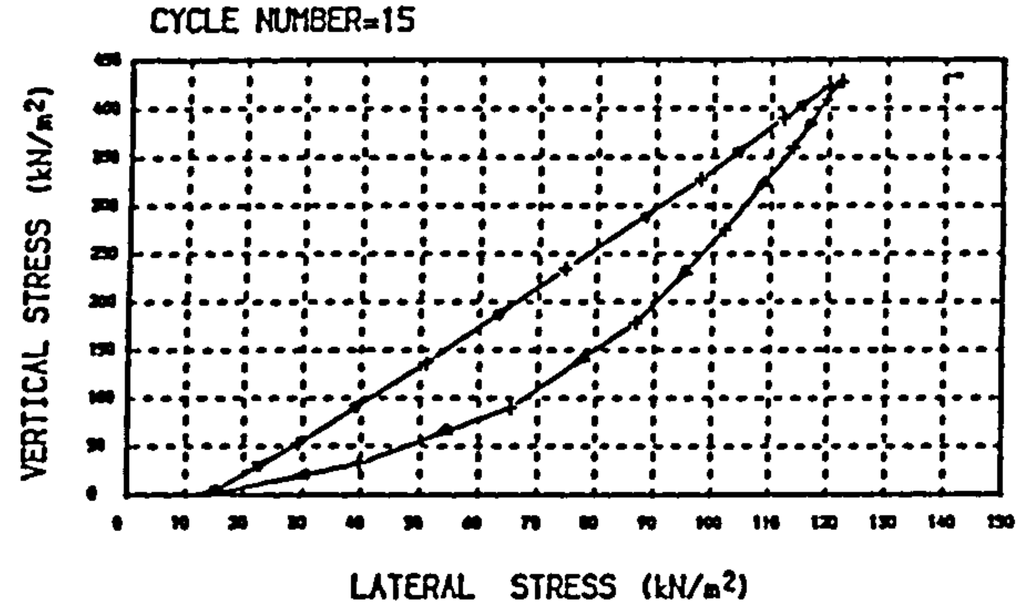

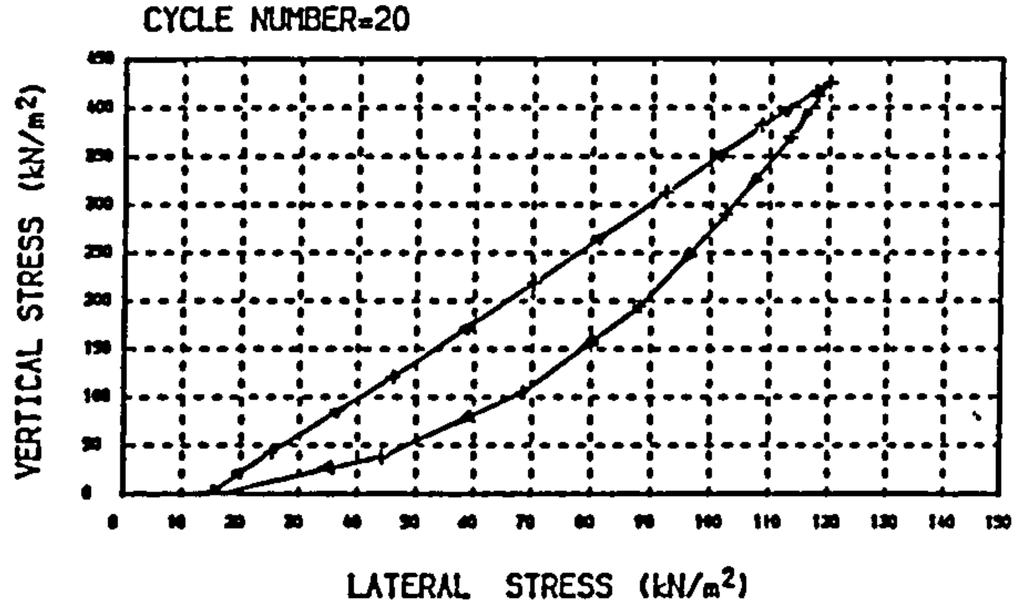

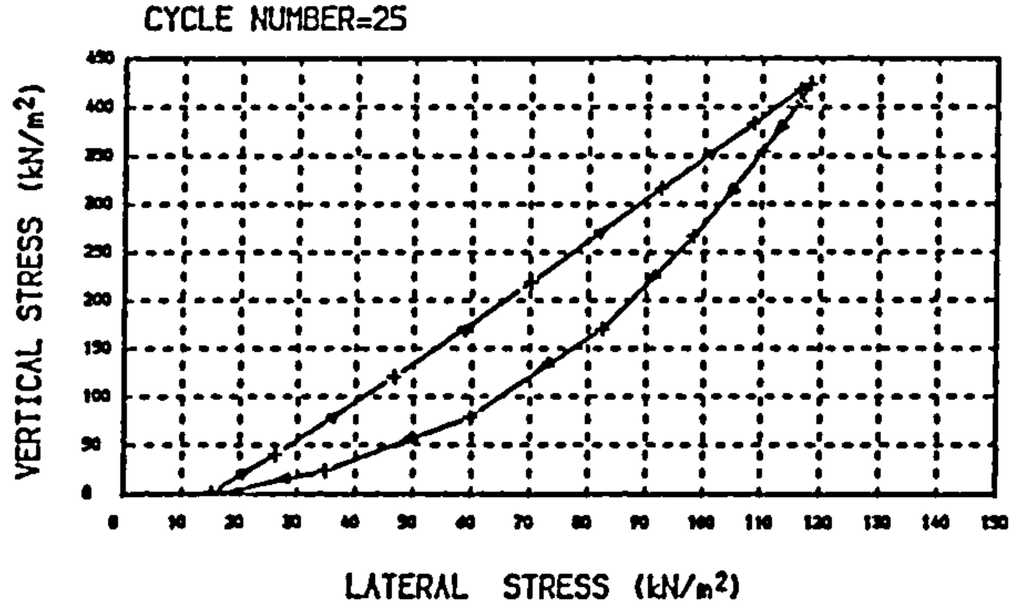

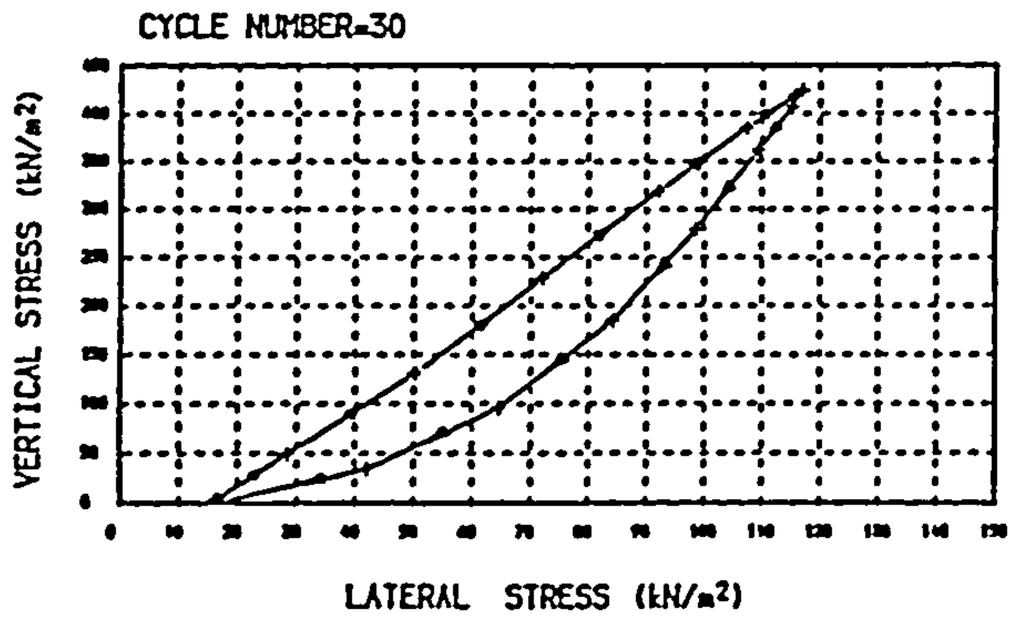

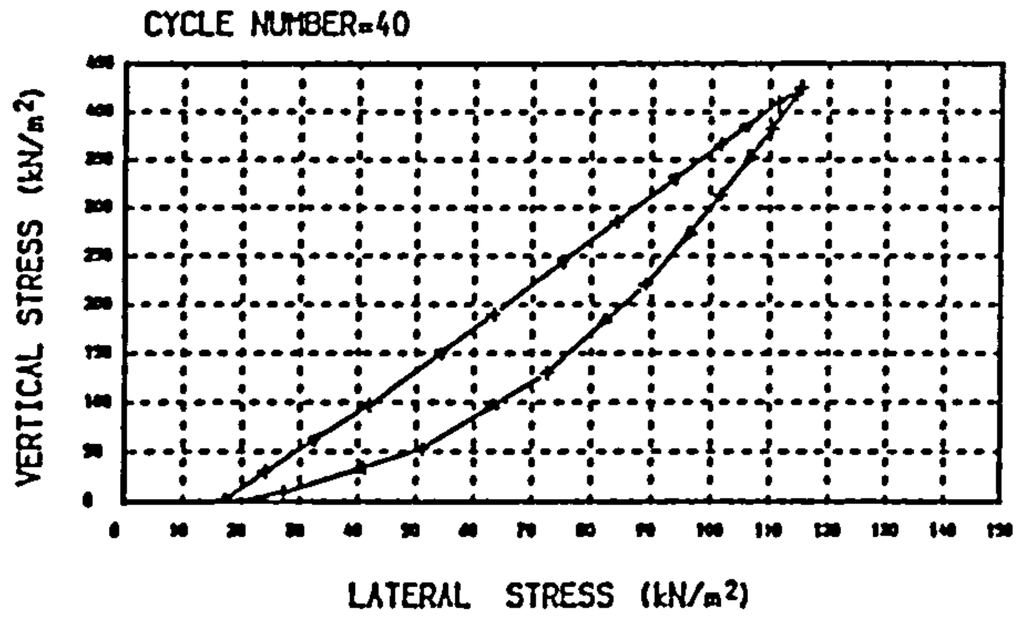

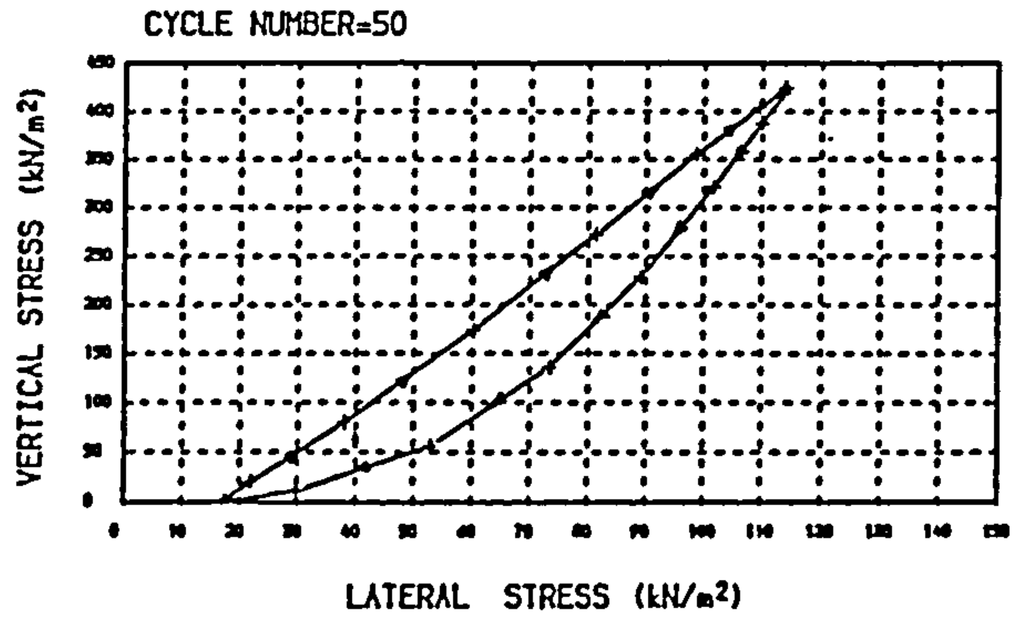

FIGURE: 5.23 RELATIONSHIP BETWEEN VERTICAL STRESS AND LATERAL STRESS FOR LOOSE SAMPLES UNDER CONFINED CONDITION AT DIFFERENT CYCLES OF LOAD.

reasonably linear, while the unloading portions are curves which are concave downwards. As a result, from the first cycle of load, hysteresis loops develop which are initially large but as the number of cycles increase they become smaller.

For the first cycle of loading, on increasing the vertical stress the lateral stress increases until peak of the loading. When unloading commences the lateral stress decreases but at a smaller rate than on loading. After complete unloading ($\sigma_v=0$) the lateral stress does not return to zero and some irrecoverable stress remains. In the second cycle of loading, the lateral stress begins to increase again linearly from this point and after complete unloading, the residual lateral stress is higher than at the end of the previous cycle. Therefore as the cycling continues the values of residual lateral stress increase. This means that the minimum point of the lateral stress on the curve (i.e. when $\sigma_v=0$) increases. The rate of increase of the minimum values of the lateral stress decreases as the loading continues, so that after about 30 cycles of load for dense samples and 40 cycles for loose samples no appreciable changes are observed.

The values of lateral stress corresponding to the peak points of the loading cycles decreases on increasing the number of cycles. In other words the maximum values of lateral stress (i.e. where $\sigma_v=425$ kN/m^2) decrease as the loading continues. Again the rate of decrease in the maximum values of lateral stress decreases on increasing the number of cycles. After about 20 cycles the maximum values of lat-

eral stress in dense sample become constant (figure 5.22). The figure for the loose sample increases to 30 cycles (figure 5.23).

From the above results it is clear that as the cycling on the samples continues the resulting lateral stress in the loading portions of each cycle initially -decreases but finally stabilizes. It means that the coefficient of earth pressure at rest for cyclic loading reaches a new stable value proportional to the characteristics of the loading and initial porosity of the material.

5.4 PLANE STRAIN TESTS

There are many practical instances in which a sand mass is free to move in one direction and hence the confined condition will not be applicable. In these cases the sand is said to be in a plane strain condition and the two lateral stresses induced by loading the sand will not be equal.

In an attempt to study the behaviour of sand under cyclic loading conditions where there is some degree of freedom in one direction, two series of plane strain tests on loose and dense samples were carried out.

In these tests the specimens were initially subjected to 36 cycles of load under confined conditions ($\varepsilon_{h1} = \varepsilon_{h2} = 0$), then another cycle of load was applied and when it reached its peak a small increment of lateral strain was applied to one side (ε_{h1}), while the other side was fixed ($\varepsilon_{h2} = 0$). Then the vertical stress was cycled for another 36 cycles after which the whole procedure was repeated for the new increment of ε_{h1} . This was continued up to twelve increments of

lateral strain.

The increment of lateral strain applied at each step was .067% equal to 0.10 mm movement of the side wall. This value was chosen so that neither too large a sudden change nor only negligible changes in the lateral stresses took place. The 36 load cycles applied in each step was the maximum number which could be applied to the sample for a single run of the loading programme and for which the data obtained could be recorded by the data acquisition unit without any break in the operations. Furthermore it was found that changes in the maximum and minimum values of the lateral stresses were very small by the end of this number of loading cycles.

The tests were carried out under the same amplitude (215 kN/m^2) and frequency (0.067 Hz) as used previously for confined tests. A schematic diagram of the test procedure is shown in figure 5.24.

5.4.1 THE GENERAL RESPONSE OF SAND IN PLANE STRAIN CONDITIONS UNDER CYCLIC LOADING

The variations of the maximum and minimum values of σ_v, σ_{h1}, σ_{h2} and ε_v with the number of loading cycles for dense (n=33%) and loose (n=41%) samples are shown in figures 5.25 and 5.26 respectively.

The first 36 cycles of loading are applied to the sample in confined conditions ($\varepsilon_{h1}=\varepsilon_{h2}=0$) and it can be seen from the figures that the variations of σ_{h1}, σ_{h2} and, ε_v in this stage are the same as described earlier (section 5.3). At the peak point of the 37th cycle, when the first increment of ε_{h1} is applied, there is a sudden drop in both the

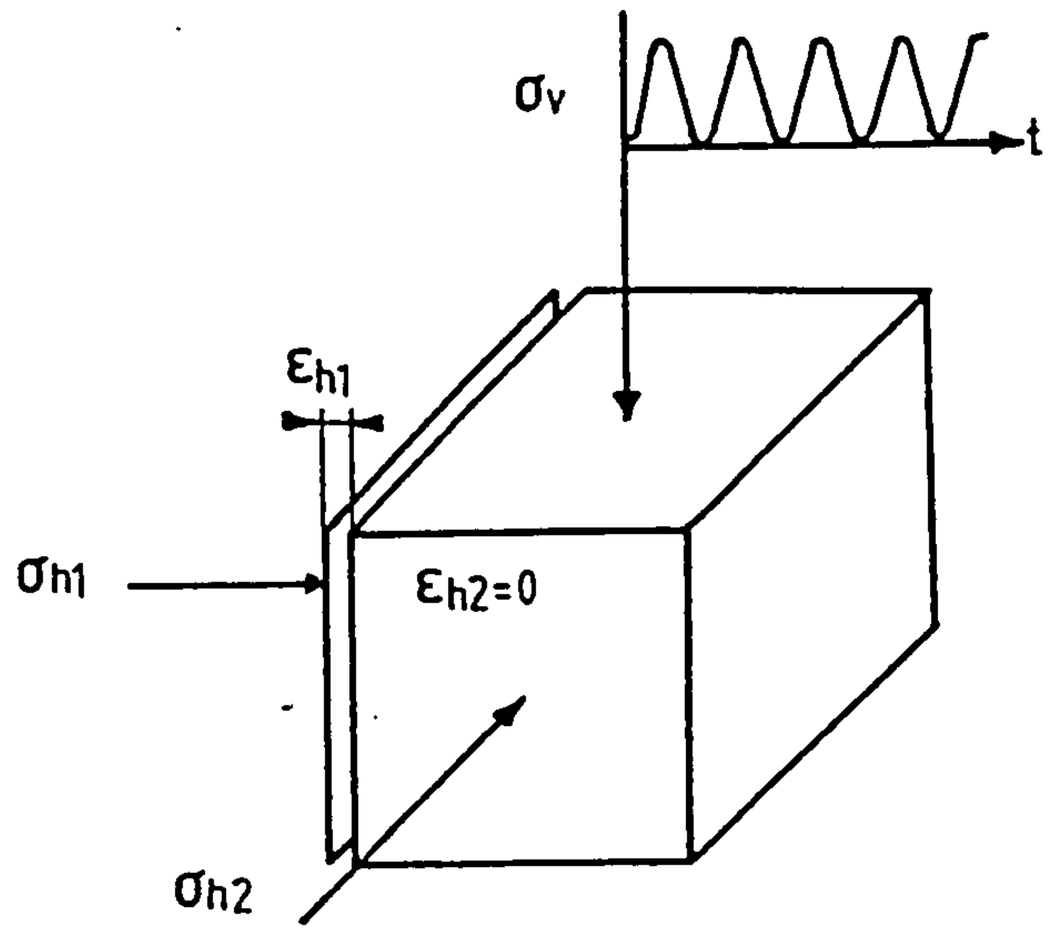

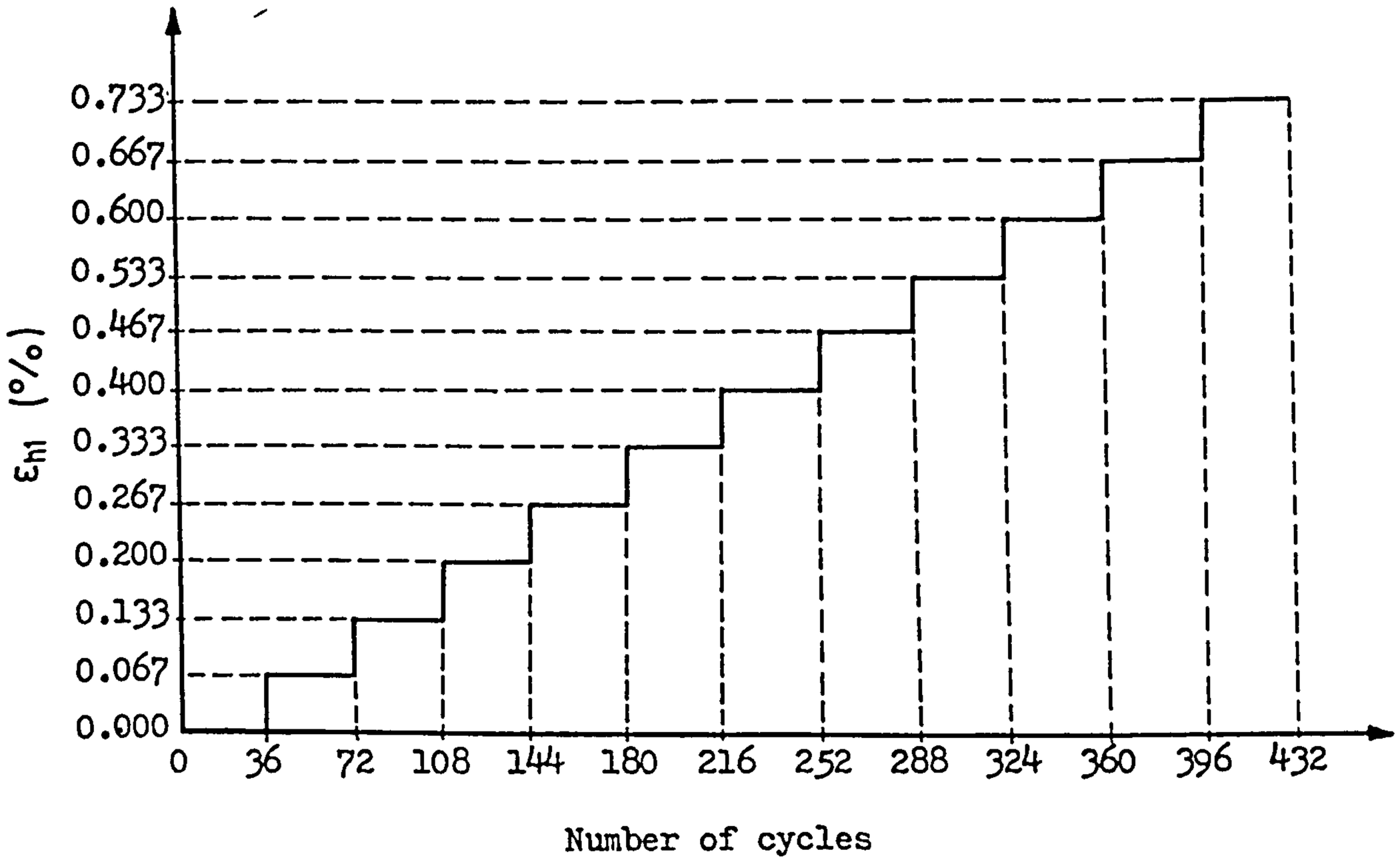

FIGURE 5.24 Schematic diagram of the test procedure in the cyclic plane strain experiments.

STRESS-STRAIN CURVES FOR PLANE-STRAIN TESTS UNDER CYCLIC LOADING CONDITIONS

INITIAL POROSITY=33%, FREQUENCY=0.067 HZ , AMPLITUDE=215 kN/m2 , TOTAL LATERAL STRAIN APPLIED=0.73%

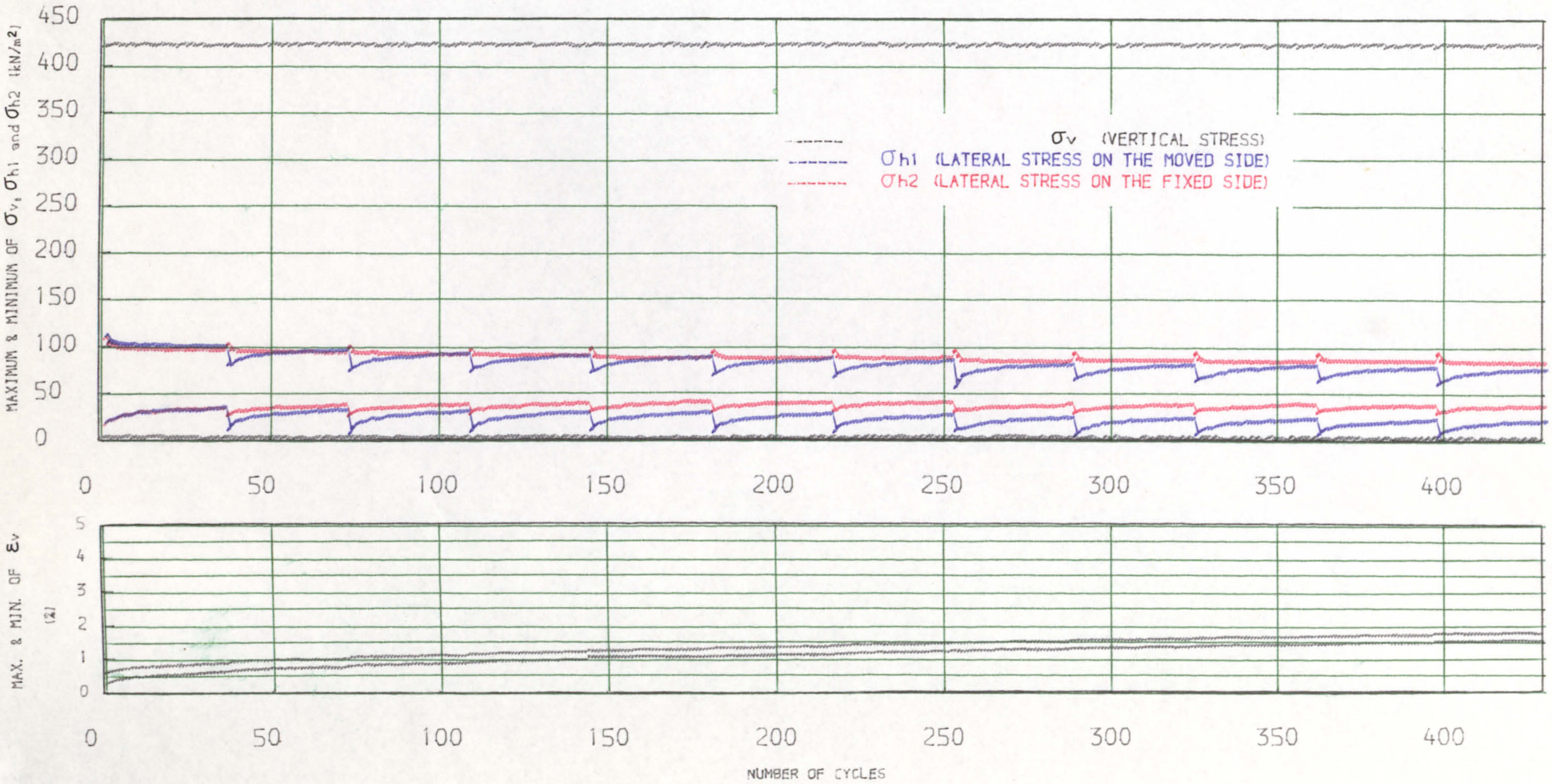

FIGURE 5.25 VARIATIONS OF THE MAXIMUM AND MINIMUM VALUES OF σ_v, σ_{h1}, σ_{h2} and ε_v FOR DENSE SAMPLES UNDER CYCLIC PLANE STRAIN TEST>

STRESS-STRAIN CURVES FOR PLANE-STRAIN TESTS UNDER CYCLIC LOADING CONDITION

INITIAL POROSITY=41%, FREQUENCY=0.067 HZ, AMPLITUDE=215 kN/m^2, TOTAL LATERAL STRAIN APPLIED=0.73%

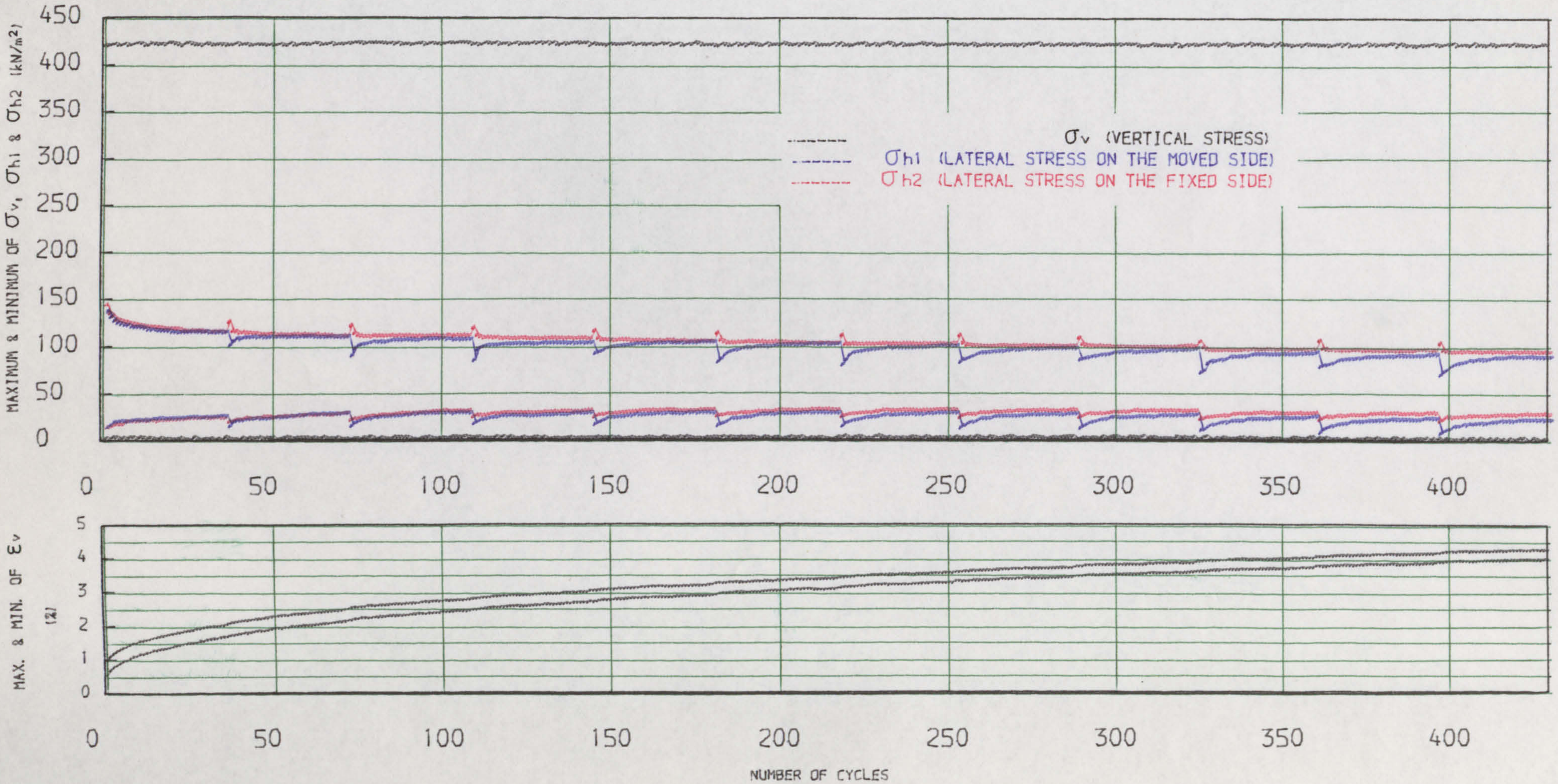

FIGURE 5.26 VARIATIONS OF THE MAXIMUM AND MINIMUM VALUES OF σ_v, σ_{h1}, σ_{h2} AND ε_v FOR LOOSE SAMPLES UNDER THE CYCLIC PLANE STRAIN TEST.

maximum and minimum values of σ_{h1} and a sudden increase in both the maximum and minimum values of ε_v. But the variation of the lateral stress in the direction of no-lateral strain (σ_{h2}) is somewhat different. The minimum values of σ_{h2} drop suddenly by a relatively small amount whereas its maximum values show some increase at this stage.

As the cycling continues, for the first few cycles the maximum and minimum values of σ_{h1} build up sharply and then keep increasing at a slower rate. Their variations become very small towards the end of the second series of cycles. For σ_{h2}, the maximum values drop while the minimum values increase as the cycling goes on. The variations of the maximum and minimum values of this lateral stress are relatively small and they tend to stabilize sooner than the other lateral stress. The maximum and minimum values of both σ_{h1} and σ_{h2} tend to become approximately equal when they reach the end of the second series of load cycles.

After the peak point of the second series of 37 cycles, where the second increment of lateral strain is applied, the same trend of variation in the lateral stresses takes place. The important point is that besides the typical variations of the maximum and minimum values of lateral stresses in each step, the general trend of their variation over all twelve steps of test shows that the maximum values of lateral stresses, particularly for σ_{h1}, gradually decrease. But the minimum values of lateral stresses in the loose sample are nearly constant, whereas for the dense sample this is only true for σ_{h2}. For σ_{h1} an overall decrease is evident.

As far as the vertical strain is concerned, it is clear from the figures that in both loose and dense samples, there are sudden and small increases at the time of application of the lateral strain. After that the vertical strain keeps increasing until the next step of the lateral strain. The plastic strain builds up continuously and there is no sign of stability over any of the twelve increments of lateral strain application. However the elastic strain shows only a very small decrease during the tests and can be assumed to be constant.

5.5 TRIAXIAL TESTS

In order to study the cyclic response of sand samples when the particles have some degree of freedom to move in both horizontal directions, triaxial tests on dense (n=33%) and loose (n=41%) sand samples were carried out. In both tests the same amplitude (215 kN/m^2) and frequency (0.067 Hz) were used as the plane strain tests.

The procedure for these tests is similar to that described for plane strain tests, the only difference being the application of the lateral strains. In these tests instead of applying lateral strain in only one direction ($\varepsilon_{h1} \neq 0$ and $\varepsilon_{h2} = 0$) it was applied to both directions equally and simultaneously ($\varepsilon_{h1} = \varepsilon_{h2} \neq 0$). Therefore the samples were under symmetric conditions which should result in equal lateral stresses.

The lateral strain increments in each step, the number of cycles of load applied after each increment of lateral strain and the number of steps for these tests were

exactly the same as for the plane strain experiments. This allows a comparison of the test results obtained under different constraint conditions.

5.5.1 THE GENERAL RESPONSE OF SAND IN TRIAXIAL CONDITIONS UNDER CYCLIC LOADING

The maximum and minimum values of σ_v , σ_{h1} , σ_{h2} and ε_v versus the number of cycles for both dense and loose samples are shown in figures 5.27 and 5.28.

It can be seen from the figures that the values of σ_{h1} and σ_{h2} are very similar. The maximum and minimum values of the lateral stresses for the first 36 cycles of load are the same as those obtained in the confined tests. At the peak of the 37th cycle, on the application of the first increment of the lateral strains, a sudden drop in both the maximum and minimum values of lateral stresses occurs. As the cycling continues the lateral stresses recover relatively sharply over the first few cycles and then keep increasing at a much slower rate. At the end of the second series of 36 cycles of load their variations become very small but there is an appreciable drop in the maximum and minimum values of σ_{h1} and σ_{h2} for dense samples, in comparison to the first series of loading. In the loose samples this total drop occurs only for the maximum values of the lateral stresses.

After the second increment of lateral strain there is again a sudden drop in both the maximum and minimum values of the lateral stresses followed by a partial recovery. The same trend as described for the first increment is seen. Therefore, for dense samples, as the steps of test continue

STRESS-STRAIN CURVES FOR TRIAXIAL TESTS UNDER CYCLIC LOADING CONDITIONS

INITIAL POROSITY=33%, FREQUENCY=0.067 Hz , AMPLITUDE=215 kN/m^2, TOTAL LATERAL STRAINS APPLIED=0.73%

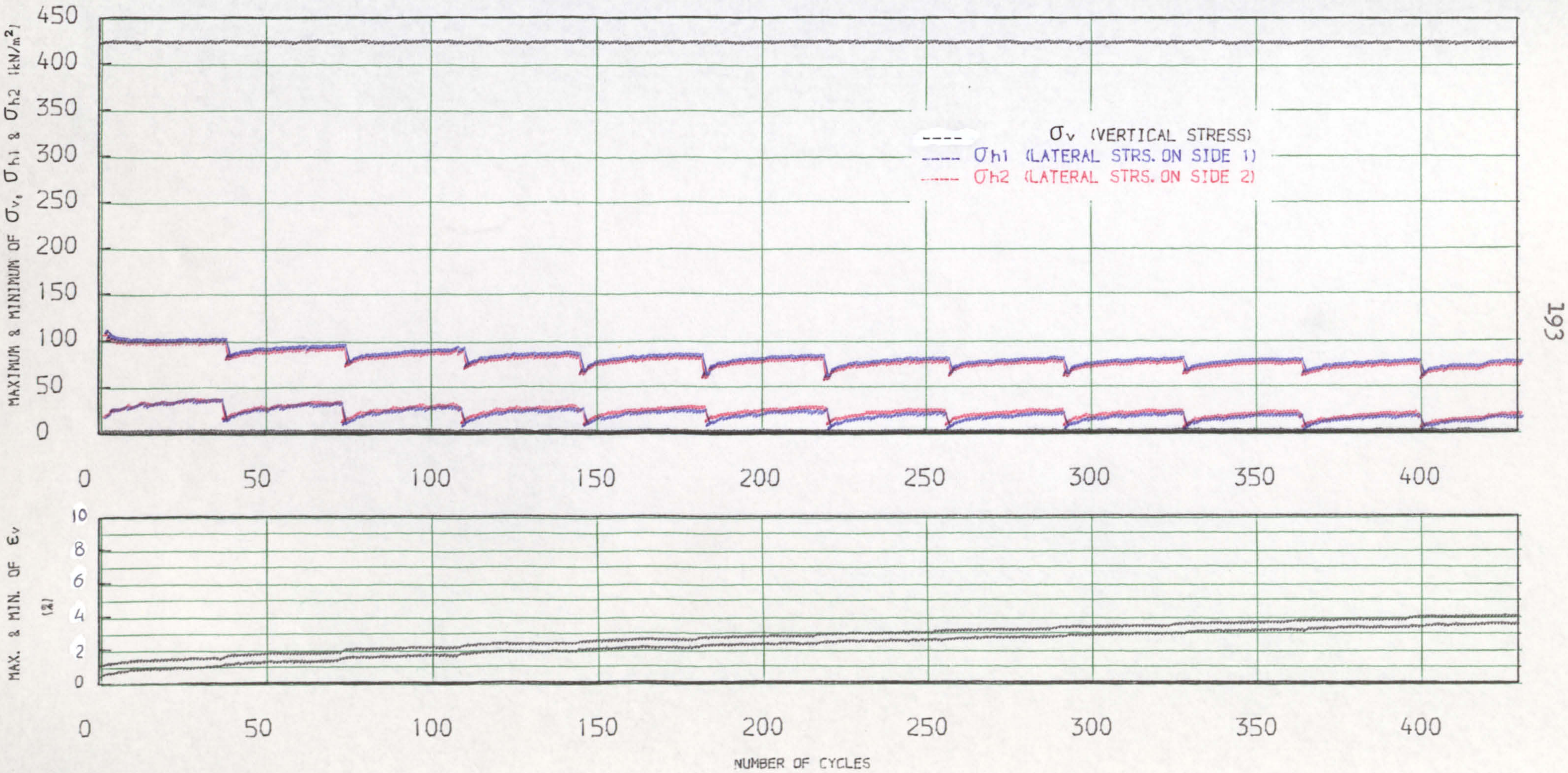

FIGURE 5.27 VARIATIONS OF THE MAXIMUM AND MINIMUM VALUES OF σ_v, σ_{h1}, σ_{h2} AND ε_v FOR DENSE SAMPLES UNDER THE CYCLIC TRIAXIAL TEST.

STRESS-STRAIN CURVES FOR TRIAXIAL TESTS UNDER CYCLIC LOADING CONDITION

INITIAL POROSITY=41%, FREQUENCY=0.067 Hz , AMPLITUDE=215 kN/m2, TOTAL LATERAL STRAINS APPLIED=0.73%

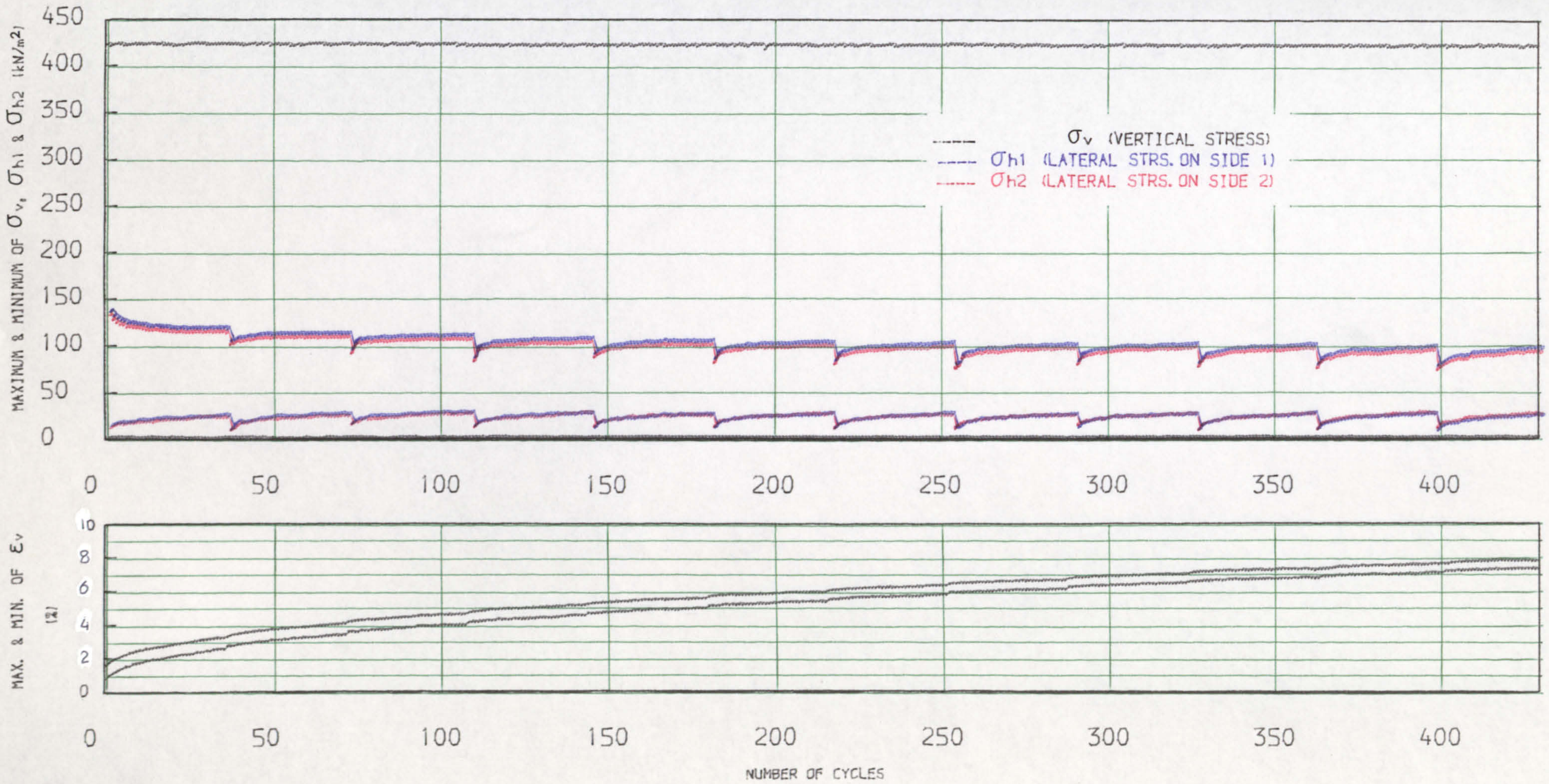

FIGURE 5.28 VARIATIONS OF THE MAXIMUM AND MINIMUM VALUES OF σ_v, σ_{h1} , σ_{h2} and ε_v FOR LOOSE SAMPLES UNDER THE CYCLIC TRIAXIAL TEST.

both σ_h minimum and maximum decrease although over a single step the maximum and minimum values of the lateral stresses increase. This can be seen only in the maximum values for loose samples. The minimum values of the lateral stresses for the loose sample seem to reach the same value at the end of each step of the test.

The maximum and minimum values of the vertical strain (figures 5.27 and 5.28) show a continuous increase in plastic strain which is very marked for the loose samples. There is a sudden increase in both the maximum and minimum values of the vertical strain on application of the increments of lateral strain. The elastic strain does not show a significant change during experiments. As a result it can be assumed to be constant over all the 12 steps of each test. However the plastic strain jumps in value at the beginning of each step and then keeps increasing at a nearly constant rate without showing any sign of stability.

5.6 SUMMARY AND CONCLUSIONS

The stress-strain behaviour of dry sand samples under cyclic loading conditions is significantly different from that found under monotonic loading. The elastic and plastic properties of the sand can be investigated more easily under this condition. Although the elastic strain of sand under cyclic loading was found to be nearly constant, the plastic strain kept increasing as the number of load cycles increased. Up to a maximum of 360 cycles of load on loose samples and 215 on dense no signs of stability were observed in the plastic strain. Both elastic and plastic strains increase as the porosity of the sand increases.

During the application of the cyclic vertical stress, the lateral stresses in both horizontal directions cycle between some minimum and maximum values. While the maximum values of the lateral stresses decrease on increasing the number of load cycles, their minimum values increase. The rate of decrease in the maximum values and increase in the minimum values decreases as the cycling continues and the lateral stresses finally cycle between constant values.

The frequency of the cyclic loads seems to have no significant effect on the stress-strain behaviour of the dry sand samples within the ranges tested (from 0.1 to 0.003 Hz), whereas the amplitude of the loads has a marked influence on the response of the dry sand. The key factor affecting the lateral stresses and ε_v apart from the level of the vertical stress, was found to be the percentage of unloading in each cycle. The cyclic loads with full unloading cycles have the maximum effect on the samples and as σ_{vmin} increases the effect of the cyclic loading decreases.

In a similar way to that found for monotonic loading the constraint conditions of the sample have a great effect on the behaviour of the sand sample under cyclic loading. In plane strain conditions the lateral stress in the direction of the applied lateral strain suddenly drops, but as the cycling continues, it recovers part of its loss relatively quickly in the first few cycles. Then it keeps increasing at a smaller rate and after several more cycles becomes nearly constant. The maximum values of the lateral stress in the other direction increases at the time of applying the lateral strain. On increasing the number of

cycles, it sharply decreases over the first few cycles and then keeps decreasing at a smaller rate until it becomes constant. In triaxial conditions both lateral stresses change in a similar manner. The general trend is the same as the lateral stress changes in the direction of the applied lateral strain in the plane strain tests. Although the elastic vertical strains induced are equal in both plane strain and triaxial test conditions, the total vertical plastic strains produced in triaxial conditions are greater than those in plane strain tests.

CHAPTER SIX

DISCUSSION OF THE MONOTONIC TEST RESULTS

6.1 INTRODUCTION

The vertical strain caused by the application of a load under confined conditions is indicated by the subscript o , the additional vertical strains due to the application of plane or triaxial lateral displacements of the sample box by the subscripts p and t. The total strain in the plane strain and triaxial tests is given by $\varepsilon_1 = \varepsilon_{1o} + \varepsilon_{1p}$ or $\varepsilon_1 = \varepsilon_{1o} + \varepsilon_{1t}$ respectively depending on the test procedures.

Similar subscripts are used to differentiate the volumetric strains , lateral stresses and the coefficients of lateral to vertical stress induced under different constraint conditions.

6.2 CONFINED TESTS

The data obtained from the confined tests are in fact the principal stresses and strains at the boundaries of a cubic sample under Ko conditions. In these tests the vertical stress was applied to the sample in incremental steps while the sides of the sample container were fixed so that no lateral strains occurred ($\varepsilon_2 = \varepsilon_3 = 0$). The vertical strain and lateral stresses induced were measured at the boundaries.

Using the results of this series of tests the funda-

mental properties of the material under fully confined conditions can be studied. For example the modulus of elasticity and Poisson's ratio of the sand can be calculated assuming the concepts of elasticity are valid. The coefficients of earth pressure at rest (Ko) can be compared with those found by other investigators and the effects of particle size and porosity of the sand on its behaviour may be assessed.

6.2.1 VERTICAL STRAIN IN Ko CONDITIONS

As described earlier (chapter 4, figure 4.3) when the vertical stress applied to the sample is increased , the vertical strain increases by relatively large amounts during the first steps of loading but the rate of change becomes smaller over further steps. This behaviour may be attributed to the degree of freedom of the grains to move into a denser packing under a vertical stress. Initially the particles can move relatively easily but as the loading continues the new packing of the grains does not have the same degree of freedom as before and proportionally higher stresses are required to cause equal movement.

The initial porosity of the sample is a major factor determining the degree of freedom of the particles and it has a large influence on the stress strain behaviour of the sand. From figure 4.3 it is quite evident that on increasing the initial porosity of the sample the rate of change of the vertical strain increases significantly.

The total vertical strains induced in the fine samples are considerably larger than those measured for the coarse sand. From figure 4.3 it can be seen that under 400

kN/m^2 vertical stress , the fine sample with a relative density of 67% has a vertical strain of 2.5% while for the same conditions the coarse sand has only 0.6% vertical strain, less than a quarter of the fine sand value. The stress strain curves for the coarse sand are also steeper than those of the fine sand.

To assess the effect of the particle size on the stress strain behaviour of granular soils the complete series of $\sigma_1 - \varepsilon_1$ curves for the three types of sands (A , B and C) are shown in figure 6.1. It is clear that the medium sand (B) curves fit well into the gap between the fine (A) and coarse (C) sands curves. Although the general trend of stress strain behaviour for all three sands is the same , the strains of the fine sand are much greater than those of the medium and coarse sands. This may be due to the cumulative effects of both particle size and shape of this type of sand. These results are in good agreement with those obtained by Kolbuszewski and Frederick [135]. In an experimental study of the significance of particle size and shape on the mechanical behaviour of sands , they found that the more angular the sand the higher the minimum porosity. They also noted that the minimum porosity of the sand increases on decreasing the size of particles. In case of sand A which has fine angular particles the state of packing , in even the densest case , is still loose in comparison to those of sands B and C. Therefore the resulting vertical strains under the same levels of vertical stress are relatively large.

The variation of vertical strain with initial poros-

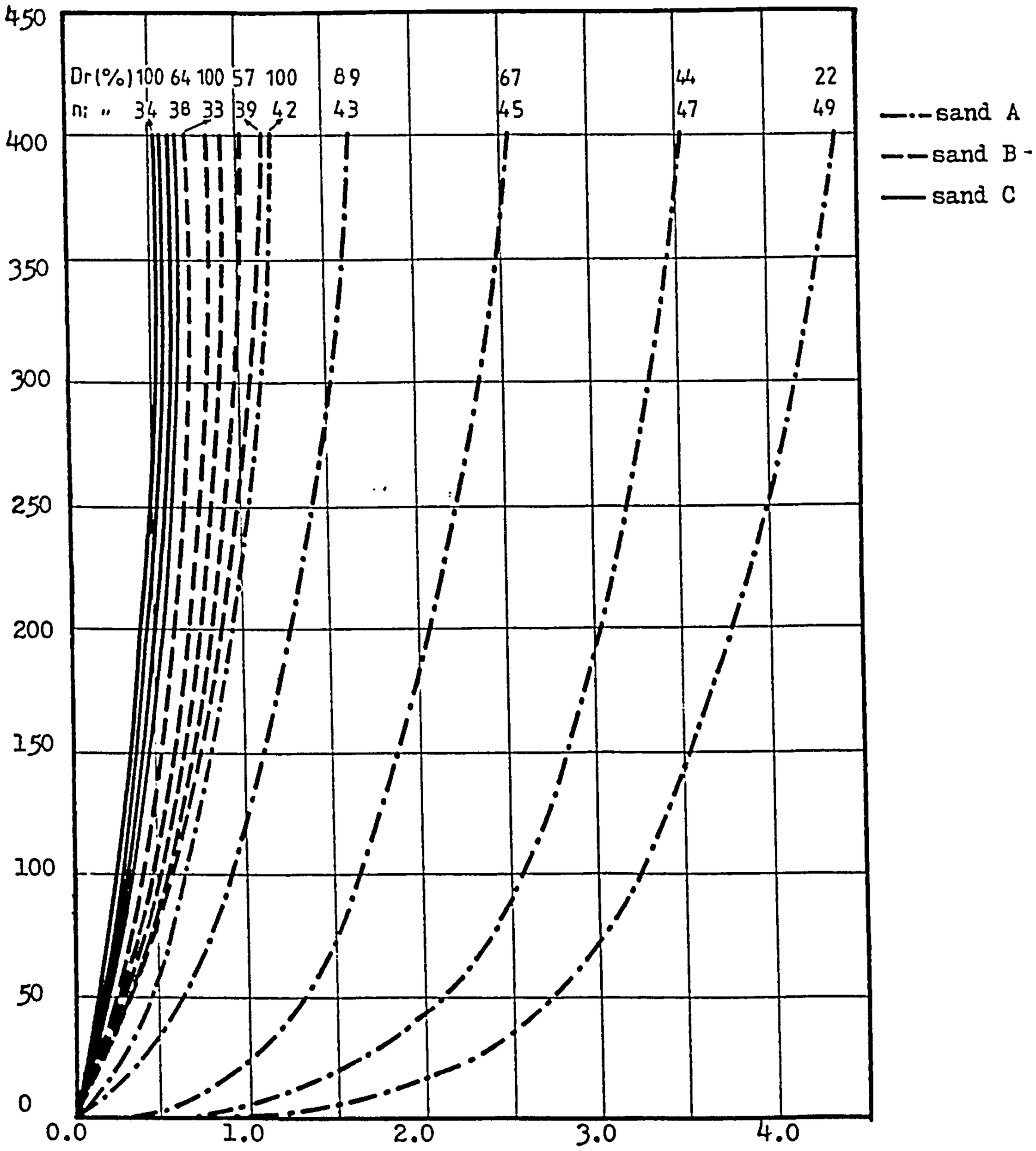

FIGURE 6.1 Relationship between σ_1 and ε_1 for sands A, B and C under confined conditions.

ity of the samples and the changes in the porosity due to 400 kN/m^2 vertical stress are shown in figure 6.2. It can be seen that ε_1 increases almost linearly on increasing n; but the effect of the initial porosity on ε_1 in the fine sand is more significant than in the coarse sand.

6.2.2 THE MODULUS OF ELASTICITY (E) AND POISSON'S RATIO (V) UNDER Ko CONDITIONS

In a perfect elastic and isotropic material whose properties are independent of the direction of loading, the stress strain characteristics can be identified by two constant parameters, namely the modulus of elasticity (E) and Poisson's ratio (V) or the bulk and shear moduli (K and G). The stress strain relationships for such a material are:

$$\varepsilon_1 = \frac{1}{E}[\sigma_1 - \nu(\sigma_2 + \sigma_3)] \qquad (6.1)$$

$$\varepsilon_2 = \frac{1}{E}[\sigma_2 - \nu(\sigma_1 + \sigma_3)] \qquad (6.2)$$

$$\varepsilon_3 = \frac{1}{E}[\sigma_3 - \nu(\sigma_1 + \sigma_2)] \qquad (6.3)$$

In this research project as mentioned earlier (section 3.5) the specimens tested were uniform and homogeneous as far as practicable. Although sand does not display elastic behaviour in general , at small strains and for increasing loading the theory of elasticity may be applicable. The modulus of elasticity and Poisson's ratio can easily be calculated under confined conditions where $\varepsilon_2 = \varepsilon_3 = 0$ and $\sigma_2 = \sigma_3 = \sigma_h$:

$$\nu = \frac{\sigma_h}{\sigma_1 + \sigma_h} = \frac{K_o}{1 + K_o} \qquad (6.4)$$

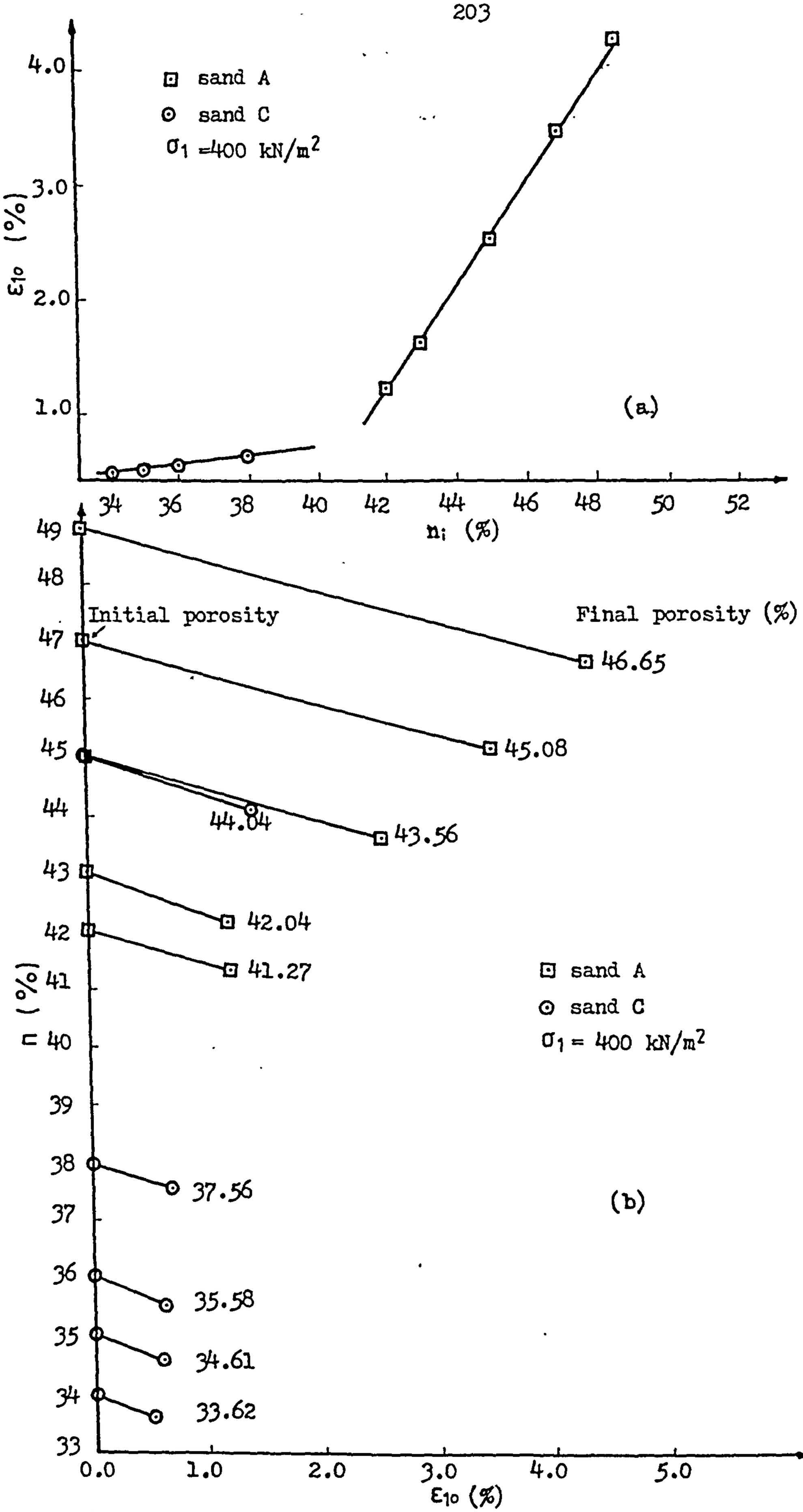

FIGURE 6.2 Variation of the total vertical strain with initial porosity(a) and the change in porosity under confined compressin (b).

$$E=\frac{(\sigma_1-\sigma_h)(\sigma_1+2\sigma_h)}{\varepsilon_1(\sigma_1+\sigma_h)} \qquad (6.5)$$

The variations of E and ν with vertical stress are plotted in figures 6.3 and 6.4. While the Poisson's ratios for all three sands are nearly constant (a small decrease on increasing σ_1 and n_i) , the moduli of elasticity show significant increases as a result of increasing the vertical stress. They also increase as the initial porosity of the samples decreases. It can be concluded that as the sand becomes finer its Poisson's ratio increases but the modulus of elasticity decreases.

6.2.3 THE COEFFICIENT OF EARTH PRESSURE AT REST (Ko)

The variations of Ko for both fine and coarse sands with initial porosity and vertical stress are shown in figure 4.7 and described in chapter 4. The changes of Ko can be related to the degree of freedom of the grains to move and the shearing resistance between them. For a certain level of the vertical load if the friction between particles is low and the grains can move to a denser packing easily more horizontal pressure is induced. Therefore Ko will be higher. From figure 4.7 it is quite obvious that , with increasing initial porosity , Ko increases. Also when the applied vertical load increases, which results in more interlocking of the grains , Ko decreases. As was discussed earlier , section 6.2.1 , the stiffer and more stable structure of the coarse sand means that Ko for this material is considerably smaller than that for the fine sand.

The results of the confined tests carried out by

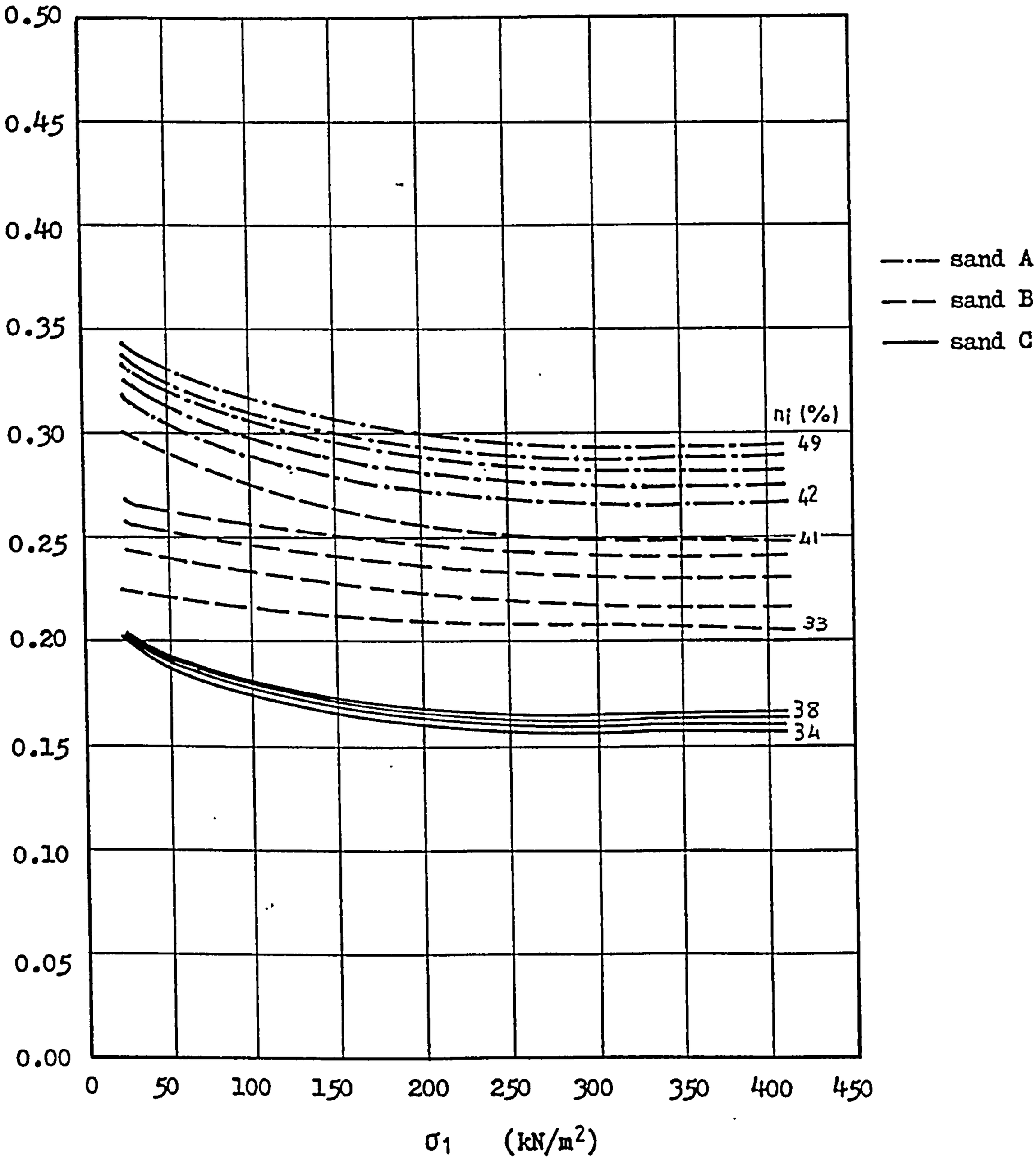

FIGURE 6.3 Variation of Poisson's ratio (ν) with σ_1 for different initial porosity for sands A, B and C.

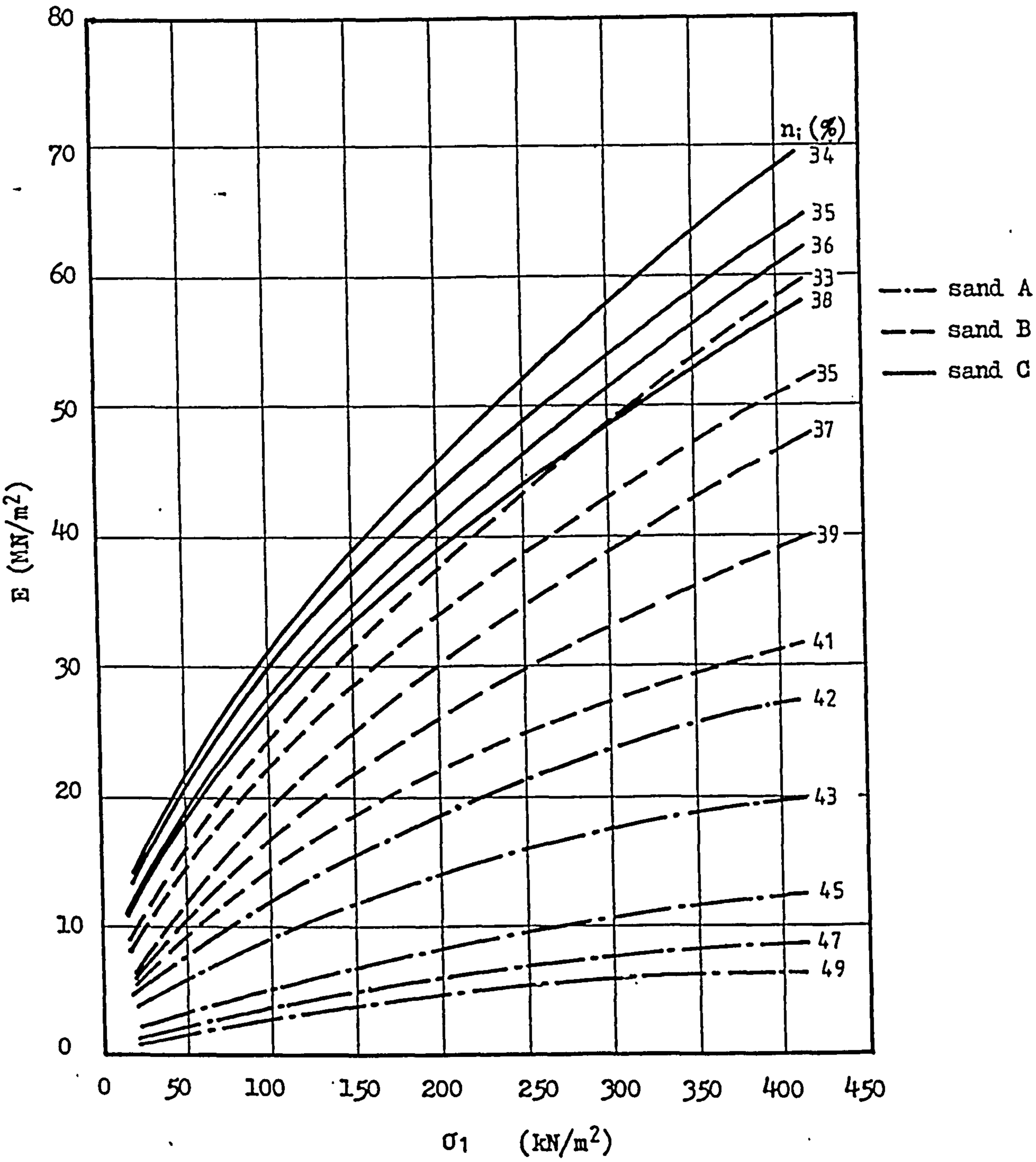

FIGURE 6.4. Variation of elastic modulus (E) with σ_1 for different initial porosities for sands A, B and C.

El-Gammel [22] on group B sand lie in the gap between the results of the tests on fine and coarse sands. In figure 6.5 the variation of Ko with vertical stress for the three types of Leighton Buzzard sands at different initial porosities is plotted. It is quite clear that Ko for the densest case of each group of sand is nearly equal to the loosest case of the next coarser sand. Although the general trend of Ko variations for the three sands is similar, as the grains become coarser Ko decreases remarkably which implies that the frictional forces between particles increase and a more stable and stiffer structure is formed. The higher rate of decrease of Ko for sand A compared to the other two sands may be related to the angular shape of its grains in contrast with the more rounded particles of sands B and C. As discussed in section 6.2.1, the angularity may cause a generally looser state of packing and this might result in a higher rate of decrease in the porosity of the sample and hence in the lateral stresses. Therefore, under the same increment of the vertical stress Ko for this sand can be higher than those for the coarser sands.

A comparison between values of Ko obtained from confined tests on the SCTA and those found or suggested by other investigators is made in table 6.1. Since values of Ko obtained from the SCTA change with the vertical stress, the minimum and maximum values for each porosity are given in the table. From this table it can be seen that for sand A the well known equation introduced by Jaky [142] underestimates (Ko)min (obtained from the SCTA) whereas the Seidek equation overestimates them. Using the De Wet equation

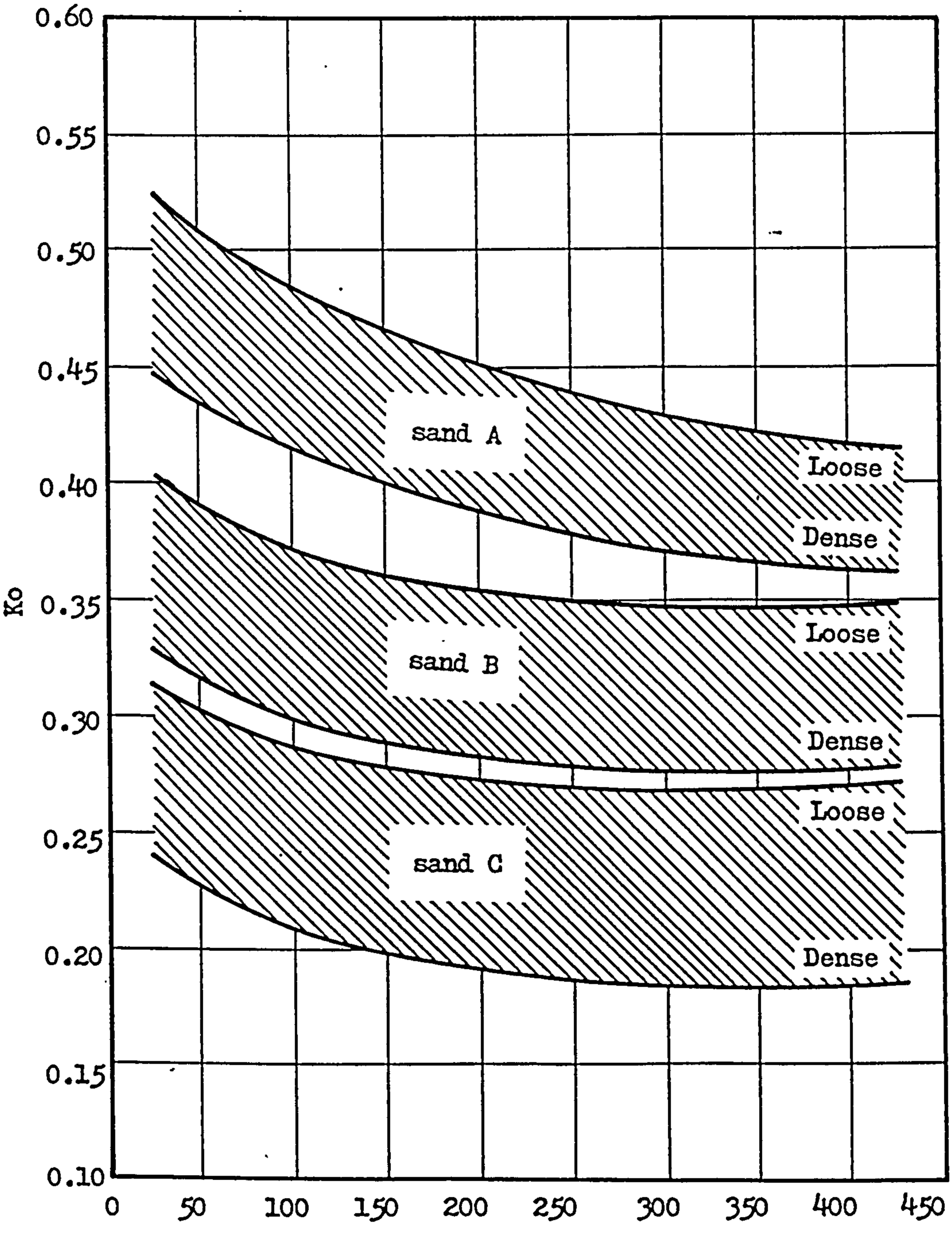

FIGURE 6.5 Variation of the coefficient of lateral earth pressure (Ko) with σ_1 for sands A, B and C.

Type of the sand		Fine sand (group A)					Medium sand (group B)					Coarse sand (group C)				
Initial porosity of the sample n_i (%)		42	43	45	47	49	33	35	37	39	41	34	35	36	38	45
Friction angle from shear box test, φ (o)		44	42	39	36	34	43	40	37	33	31	40	35	32	30	28
Ko from SCTA	Ko(minimum)	.36	.38	.39	.40	.42	.26	.28	.29	.33	.36	.18	.185	.19	.195	.27
	Ko(maximum)	.44	.46	.48	.49	.51	.34	.35	.36	.39	.41	.24	.245	.25	.26	.36
Ko from other experimental data	Bjerrum et. al (1961), standard triaxial apparatus, fine sand. Yound & Craven (1975), simple shear apparatus, medium sand.	.50	.53	.60	.67	.76	.28	.31	.35	.38	.42	—	—	—	—	—
Ko from empirical and theoretical equations	Jaky (1944) $Ko=1-\sin\varphi$	.31	.33	.37	.41	.47	.32	.36	.40	.46	.48	.36	.43	.47	.50	.53
	Brooker and Ireland(1965) $Ko=0.95-\sin\varphi$	.26	.28	.32	.36	.39	.27	.31	.35	.41	.43	.31	.38	.42	.45	.48
	De Wet $Ko=\frac{1-\sin^2\varphi}{1+2\sin^2\varphi}$	.35	.38	.43	.48	.52	.37	.42	.47	.50	.57	.42	.50	.56	.60	.64
	Seidek $Ko=0.75\,Ka+0.25$	.39	.40	.42	.44	.39	.39	.41	.44	.47	.49	.41	.45	.48	.50	.52
	Hendron (1963): $Ko=\frac{1}{2}\left[\frac{1+\sqrt{6}/8(1-3\sin\varphi)}{1-\sqrt{6}/8(1-3\sin\varphi)}\right]$	.25	.27	.29	.31	.33	.26	.28	.31	.34	.36	.28	.32	.35	.37	.39

TABLE 6.1 Comparison of Ko for three sands obtained from different experimental, empirical and theoretical works.

gives (Ko)min in the dense condition but as the sample becomes loose the values approximate to (Ko)max. For sand B (Ko)min is given if the equation suggested by Hendron [138] is used. The results of tests carried out by Youd and Craven [36] on medium Ottawa sand and also the values calculated from the equation introduced by Jaky (1944) (Ko=1-SinØ) are in relatively good agreement with the maximum values of Ko obtained by the SCTA on sand B. For sand C only the minimum values of Ko from the SCTA are close to those calculated from the Hendron equation.

On the whole the previous works are more realistic in predicting Ko for the medium size sand rather than finer or coarser sands. The differences in Ko from different experimental works may be due to the use of different types of sands and different testing apparatus e.g. shear box , standard triaxial, etc., in which the testing conditions are not identical. However the differences between Ko obtained from the SCTA and the empirical or theoretical works can be attributed to the simple expressions offered by most researchers introducing Ko as a function of the angle of internal friction.

6.3 PLANE STRAIN TESTS

The samples tested in the SCTA under plane strain conditions were in fact subjected to two sequential loadings. In the first step the vertical stress is applied incrementally up to the desired maximum level while the sample is under confined conditions. Then the sample is allowed to move in one lateral direction while the maximum vertical stress is applied. This point should be noted when the

results of this series of tests are discussed.

6.3.1 VERTICAL STRAIN IN PLANE STRAIN CONDITIONS

Variations of ε_{1p} with ε_3 are shown on figures 4.25 to 4.29 and these were described in chapter 4. As the initial porosity of the samples increases ε_{1p} increases as well. This behaviour may be related to the degree of freedom of the particles to move into a new packing. Under the same vertical stress when the sample is sheared the grains of a loose sample can slide more easily than those of a dense sample because they are not so well interlocked. This argument is applicable for both fine and coarse sands. In the case of the fine sand in which the samples are relatively loose compared to the coarse and medium sands the resulting ε_{1p} is much greater than that for the other sands under similar conditions.

To compare the deformational behaviour of sand with different particle sizes under plane strain conditions, the values of ε_{1o} and ε_{1p} for the loosest and densest cases of sands A and C and also the total vertical strain ($\varepsilon_{1o} + \varepsilon_{1p}$) of the three types of sands at a lateral strain of $\varepsilon_3 = 0.57\%$ against vertical stress are plotted in figure 6.6. This lateral strain is the maximum value applied to the samples and causes the main part of the mass to achieve the active state. From the figure it is clear that not only the general trend of the variation of ($\varepsilon_{1o} + \varepsilon_{1p}$) for the three sands is the same but the values of the total vertical strain of the sand B fit between the results of other two sands. It can also be concluded that as the particles become finer the effect of the porosity of the mass on the deformational

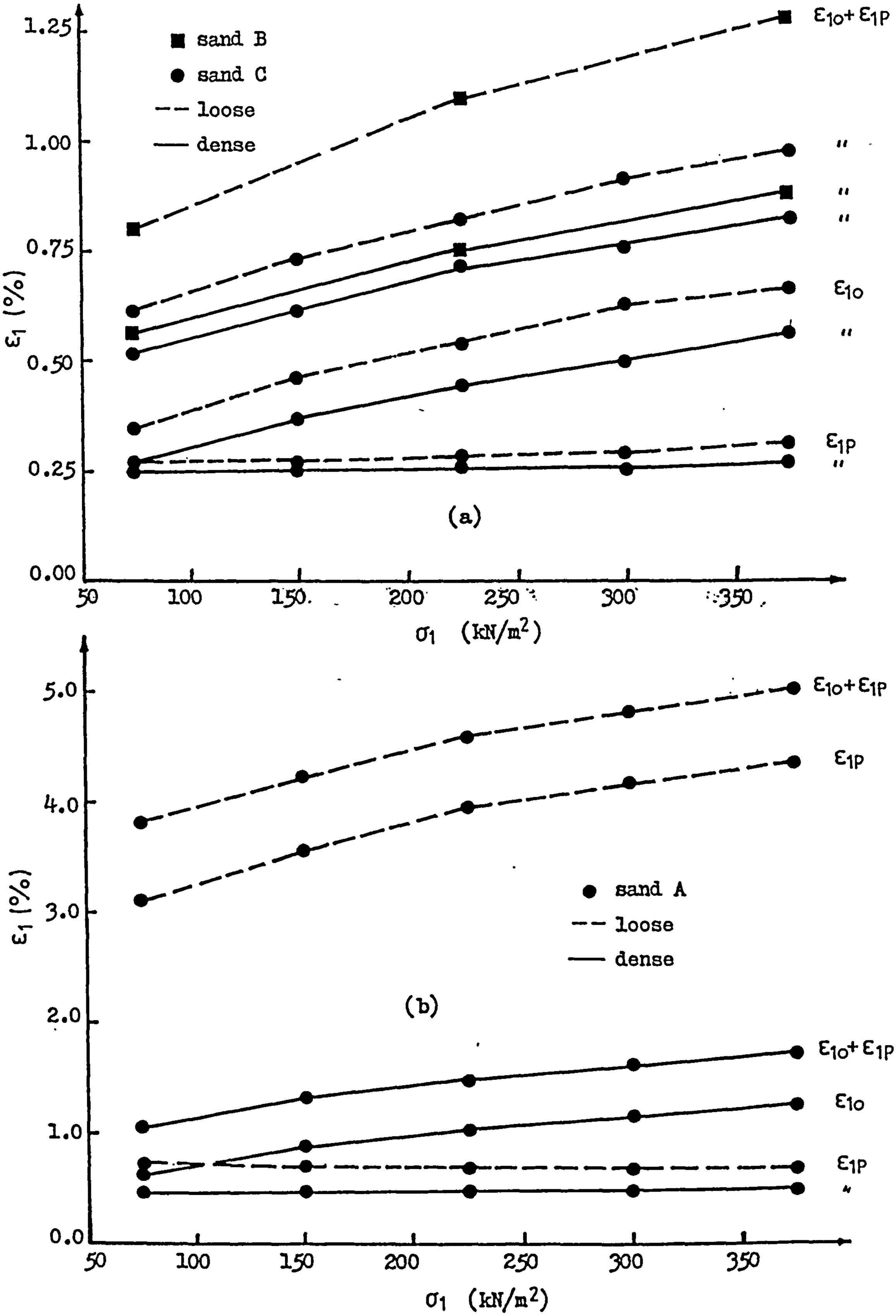

FIGURE 6.6 Variation of the vertical strains(ε_{1o} , ε_{1p} & $\varepsilon_{1o}+\varepsilon_{1p}$) with σ_1 under plane strain conditions at ε_3=0.57% for sands A, B and C.

behaviour of the sand increases. The difference between the total vertical strain of the densest and loosest samples for σ_1=375 kN/m² and at ε_3=0.57% for the sand C is about 0.15% while for the sand B is 0.40% and for the sand C it increases sharply to about 3.3%.

6.3.2 VOLUME CHANGES OF SAND IN PLANE STRAIN

The volumetric strains in plane strain tests carried out on the SCTA are defined by:

$(\Delta V/V)o = \varepsilon_{1o}$ due to the compression of the sample under Ko conditions initially and,

$(\Delta V/V)p = \varepsilon_3 - \varepsilon_{1p}$ due to the straining of the sample while it is subjected to a constant vertical stress.

If $(\Delta V/V)p$ is positive the sample dilates and if it is negative the sample compresses during application of the lateral strain. The change of $(\Delta V/V)p$ with ε_3 under σ_1 =375 kN/m² is shown in figure 6.7(a). It can be seen from the figure that $(\Delta V/V)p$ increases almost linearly with increasing ε_3 for sands A and C. Although the volumetric strain for the sand C is always positive, for the sand A only the densest sample (n_i = 42%) has a positive volumetric strain. For the other cases $(\Delta V/V)p$ is negative. The response is related to the state of packing of the specimens. When a dense sample, in which there is a high degree of interlocking between the grains, is subjected to a shear stress any sliding which occurs between the particles will result in dilation of the sample and hence the positive volumetric strain. Development of shear stresses inside the loose samples will cause the grains to move into a denser packing and the volume of the samples to decrease, and as a result the volumetric

strain will be negative. According to this argument only the sample of sand A with an initial porosity of 42% (the densest case) is dense enough to dilate when shear stresses develop due to application of the lateral strain. This interpretation is in good agreement with that proposed earlier for the results of the confined tests (section 6.1.1) in which it was concluded that in spite of preparing the fine samples over a range of initial porosities , from very dense to the very loose , their overall state of packing compared to sands B and C is loose. The volumetric strains obtained in a similar series of plane strain tests on sand B carried out by El-Gammel [22] were reported to be positive.

In figure 6.7(b) the variation of $(\Delta V/V)p$ with σ_1 for sands A and C are shown. It can be seen that when σ_1 increases $(\Delta V/V)p$ decreases gradually. This reduction may be due to the effect of the intermediate principal stress (σ_2). During straining of the samples σ_2 increases somewhat on increasing σ_1 (this is discussed in section 6.3.3). This may restrain the particles and decrease the volume change of the sample. Otherwise as the total decrease in $(\Delta V/V)p$ is not significant (less than 0.0004 strain) it might be due to errors occuring in the measurement of the vertical strain.

In figure 6.7(c) variations of $(\Delta V/V)p$ with initial porosity of the samples for sands A and C at $\varepsilon_3 = 0.57\%$ under minimum (75 kN/m^2) and maximum (375 kN/m^2) σ_1 are shown. It is clear that as the initial porosity increases , dilation of the samples decreases and compression increases. Samples of sand C , which are relatively dense, display small decreases in $(\Delta V/V)p$ and still dilate. Samples of sand

A which are generally relatively loose, in the densest conditions (n_i=42% and 43%), exhibit dilation which does not occur on increasing the initial porosity.

Changes in the porosity of the samples due to volume changes of the sands while compressing at Ko conditions (n_o) and to the additional volume change when ε_3 is applied (n_p) are calculated and given in table 6.2. From this table and figure 6.7(c) it can be seen that the critical porosity of the sand is not constant. It depends on the level of the vertical stress as well as the type of the sand. For the sand A which reached this state during plane strain tests, under σ_1 = 75 kN/m^2 n_{cv}=44.13% while under σ_1 = 375 kN/m^2 it decreases to n_{cv}=42.04%. Changes in the porosity of the samples subjected to σ_1= 375 kN/m^2 at ε_3= 0.57% for both sands A and C are shown in figure 6.8.

6.3.3 LATERAL STRESSES IN PLANE STRAIN CONDITIONS

Variations of σ_2 and σ_3 with ε_3 for sands A and C are shown in figures 4.15 to 4.24. According to the data both σ_2 and σ_3 initially start from the same value as that found in the confined tests. When ε_3 is applied σ_3 drops sharply and on increasing ε_3 it keeps falling but at a slower rate until it reaches an approximately constant value. Under the initial application of σ_1 under Ko conditions the sand is compressed. When the first increment of ε_3 is applied the particles start moving towards the free side. The shear stresses produced by the friction between particles are mobilized in the opposite direction to ε_3. As a result σ_3 acting upon the free face of the sample decreases. This reduction in σ_3 continues until the frictional forces are

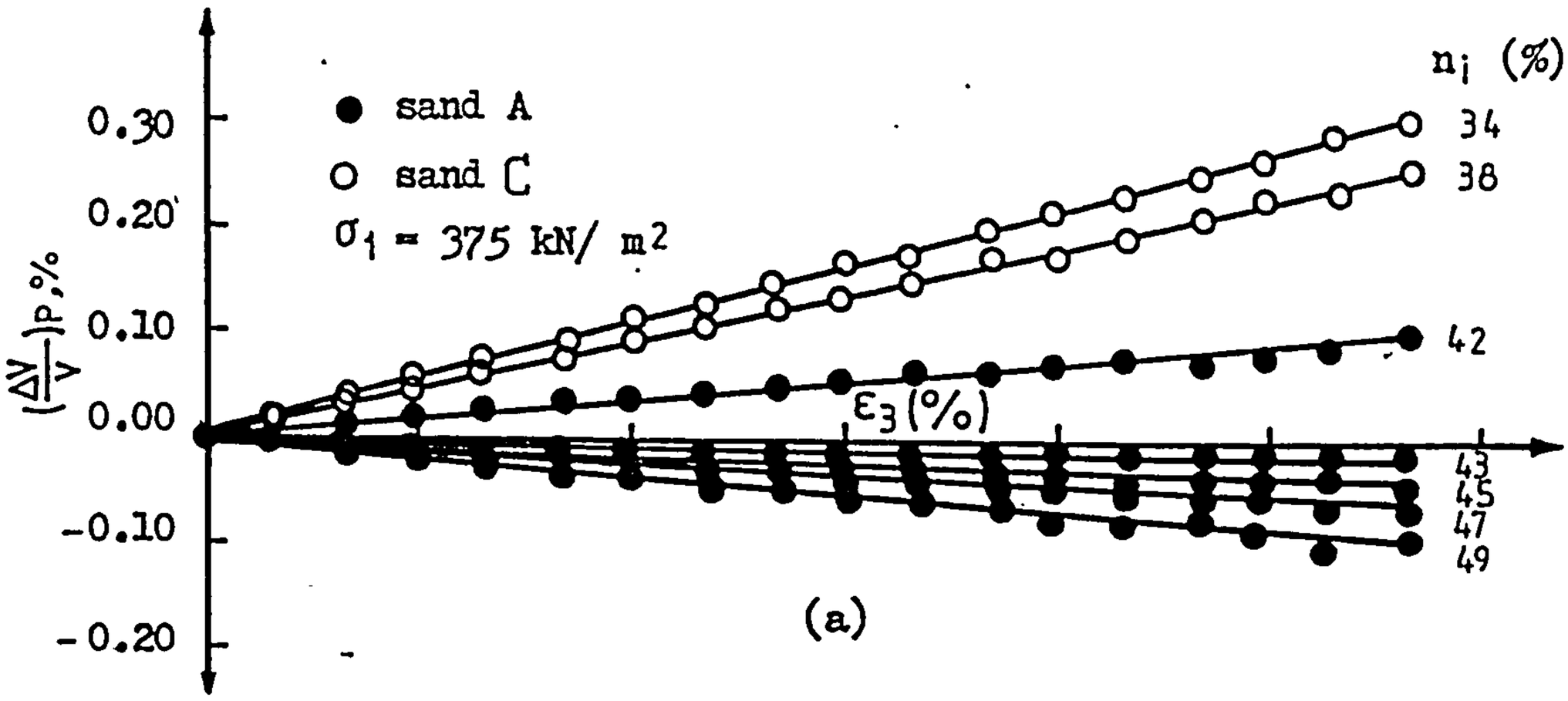

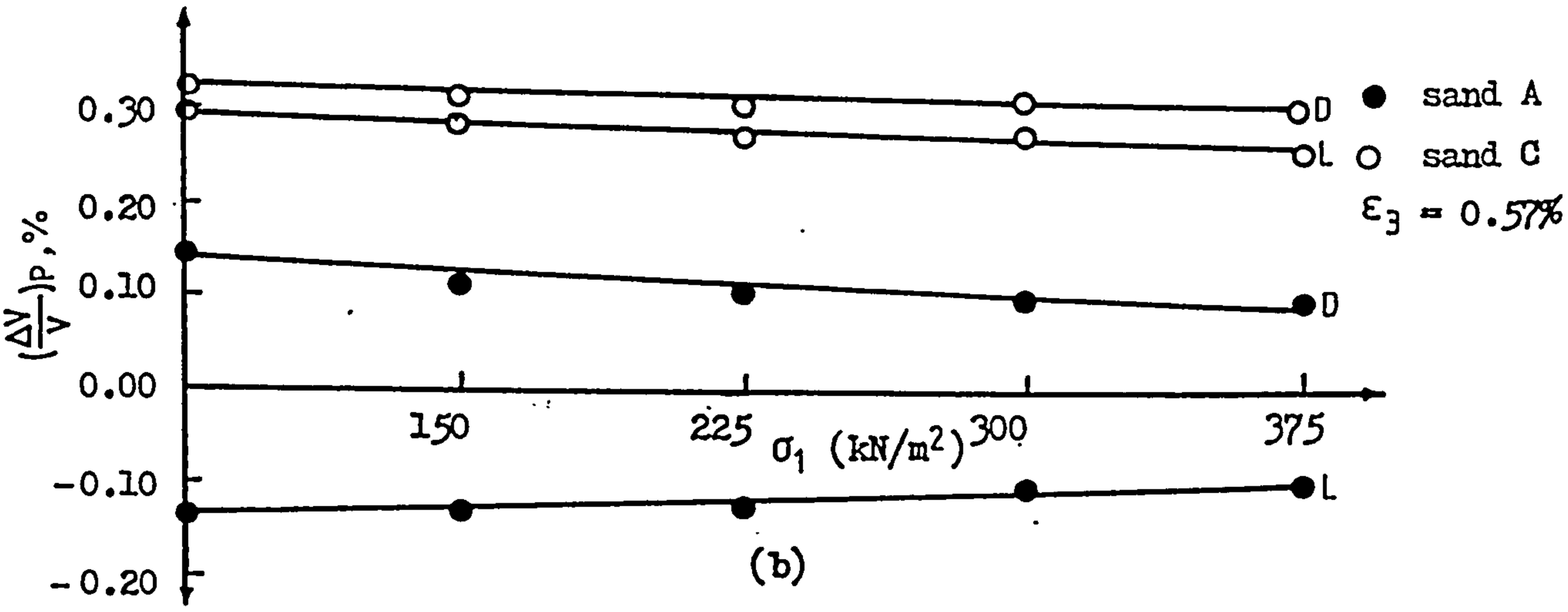

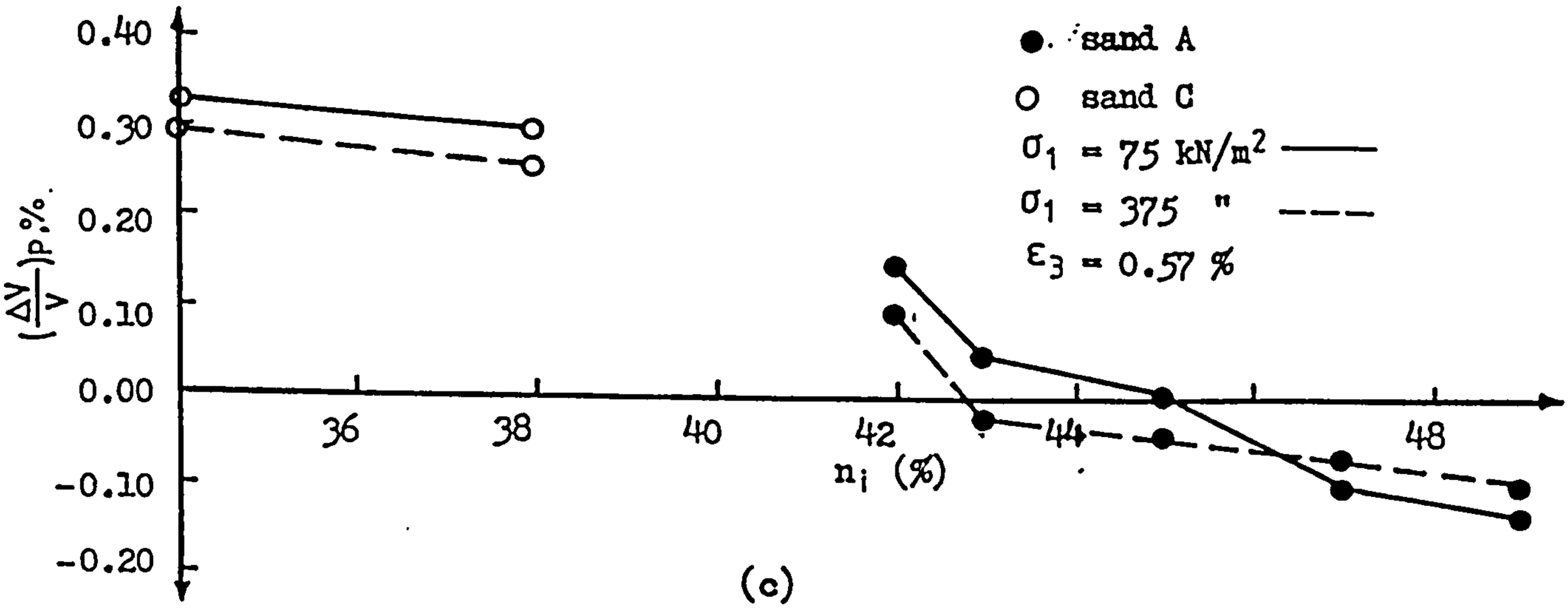

FIGURE 6.7 Variation of $(\frac{\Delta V}{V})_P$ with lateral strain (a), vertical stress (b) and initial porosity of the sample for sands A and C.

—— Change in the initial porosity due to application of incremental vertical stress up to 375 kN/m^2 on the sample under Ko condition.

—— Change in the porosity due to straining the sample in one of the lateral directions up to 0.57 %, while 375 kN/m^2 vertical stress is applied.

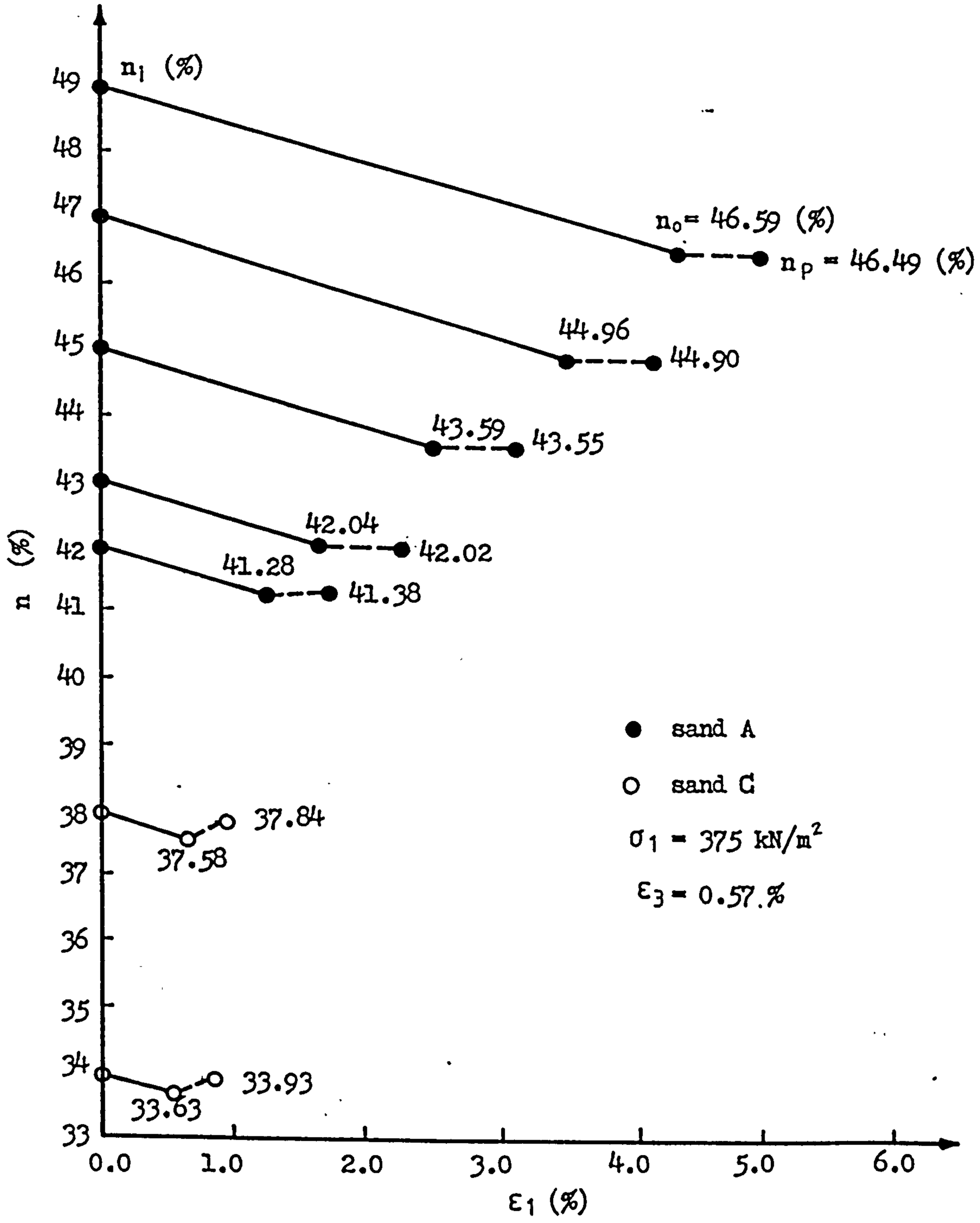

FIGURE 6.8 Changes in the porosity of the samples during plane strain tests for sands A and C.

Sand type	Initial porosity (%)	σ_1=75 kN/m²		σ_1=150 kN/m²		σ_1=225 kN/m²		σ_1=300 kN/m²		σ_1=375 kN/m²		max. change in n	
		n_o(%)	n_p(%)	n_o(%)	n_p(%)	n_o(%)	n_p(%)	n_o(%)	n_p(%)	n_o(%)	n_p(%)	Δn_o(%)	Δn_p(%)
Fine (%)	42	41.65	41.80	41.50	41.62	41.41	41.52	41.34	41.44	41.28	41.38	- 0.37	+ 0.15
	43	42.57	42.62	42.35	42.37	42.24	42.23	42.13	42.11	42.04	42.02	- 0.54	+ 0.05
	45	44.13	44.14	43.93	43.92	43.77	43.73	43.66	43.62	43.59	43.55	- 0.54	- 0.04
	47	45.72	45.62	45.45	45.35	45.29	45.21	45.15	45.08	44.96	44.90	- 0.76	- 0.10
	49	47.37	47.24	47.14	47.01	46.92	46.80	46.79	46.69	46.59	46.49	- 0.78	- 0.13
Coarse (%)	34	33.82	34.15	33.75	34.07	33.71	34.02	33.67	33.99	33.63	33.93	- 0.19	+ 0.36
	38	37.79	38.09	37.71	38.00	37.66	37.94	37.61	37.89	37.58	37.84	- 0.21	+ 0.36

n_o= porosity of the samples after application of σ_1 under confined conditions.

n_p= porosity of the samples after straining them in one of the lateral directions upto 0.57 % while σ_1 is applied.

TABLE 6.2 Final values of the porosity of the samples under plane strain tests for both coarse and fine sands.

fully mobilized after which further decreases in ε_3 do not have a significant effect on σ_3 and it becomes nearly constant.

The amount of lateral strain which is required to mobilize the active state of the sand varies with the initial porosity of the sample, level of the vertical stress and type of the sand. There are conflicting views about the exact value of this strain, probably due to different testing conditions, but according to many investigators it does not exceed 1%. Different values of the required lateral strain to develop the active state of cohesionless soils obtained from the SCTA and other researchers are given in the following table. In this table the values of strains introduced by Kirk [137] and Terzaghi [141] are those calculated from the ratio of the movement of a retaining wall to the height of the wall.

lateral strains (%)					
sources		from SCTA	by Kirk	Lambe & Whitman	Terzaghi
fine sand	loose	0.35	0.50	0.50	0.13
	dense	0.57	0.33	0.50	0.87
medium sand	loose	>0.33	0.33	0.50	0.13
	dense	>0.33	0.33	0.50	0.87
coarse sand	loose	0.57	0.50	0.50	0.13
	dense	>0.57	0.33	0.50	0.87

TABLE 6.3 Lateral strains required to mobilize the active state.

The principal intermediate stress (σ_2) was found to increase marginally for fine samples and considerably for coarse samples while the lateral strain in the other direc-

tion (ε_3) was increased. The rate of this increase decreases with increasing ε_3 and when σ_3 becomes constant σ_2 also becomes constant. This behaviour may be due to the effect of the movements of the particles in the direction of ε_3 on the other direction (ε_2). As ε_3 is applied, the grains which are stressed and interlocked start moving towards the free face. When a particle tries to move in the ε_3 direction, due to interlocking with others there is inevitably some effect in the other direction. However as the sample in this direction is confined ($\varepsilon_2 = 0$) this results in an increase in the lateral stress acting upon this face probably due to the new distribution of stresses inside the mass.

In figure 6.9 the average lateral stresses before lateral straining of the sample [ie. $\sigma_h = (\sigma_2 + \sigma_3)/2$] and also σ_2 and σ_3 after lateral straining to $\varepsilon_3 = 0.57\%$ for both sands A and C are plotted against σ_1. It can be seen that the values of σ_2 and σ_3 increase approximately linearly with increasing the vertical stress. Also they increase as the porosity of the sample increases. The effect of the initial porosity of the sample on σ_3 for sand A is more significant than for sand C, e.g. comparison of the values of σ_3 under $\sigma_1 = 375$ kN/m^2 (figure 6.9 a and b) for the densest and loosest cases shows an increase of about 50% for the sand A compared to about 28% for the sand C. In order to differentiate between the effect of the initial compression of the sample under Ko conditions on the lateral stresses from that of the lateral straining the sample, in figure 6.10 variation of $\sigma_2 - \sigma_h$ and $\sigma_h - \sigma_3$ with σ_1 are shown. It is clear from

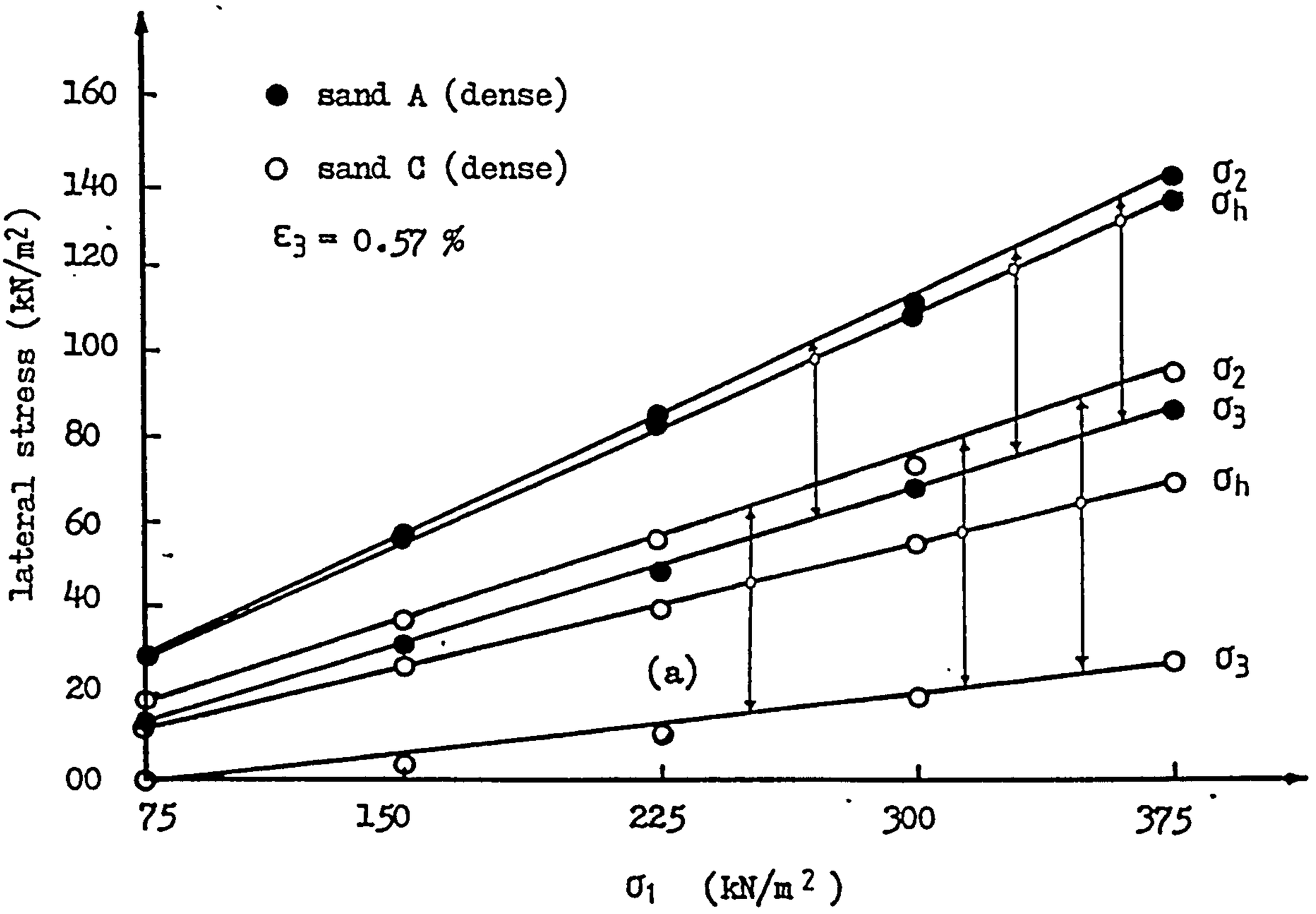

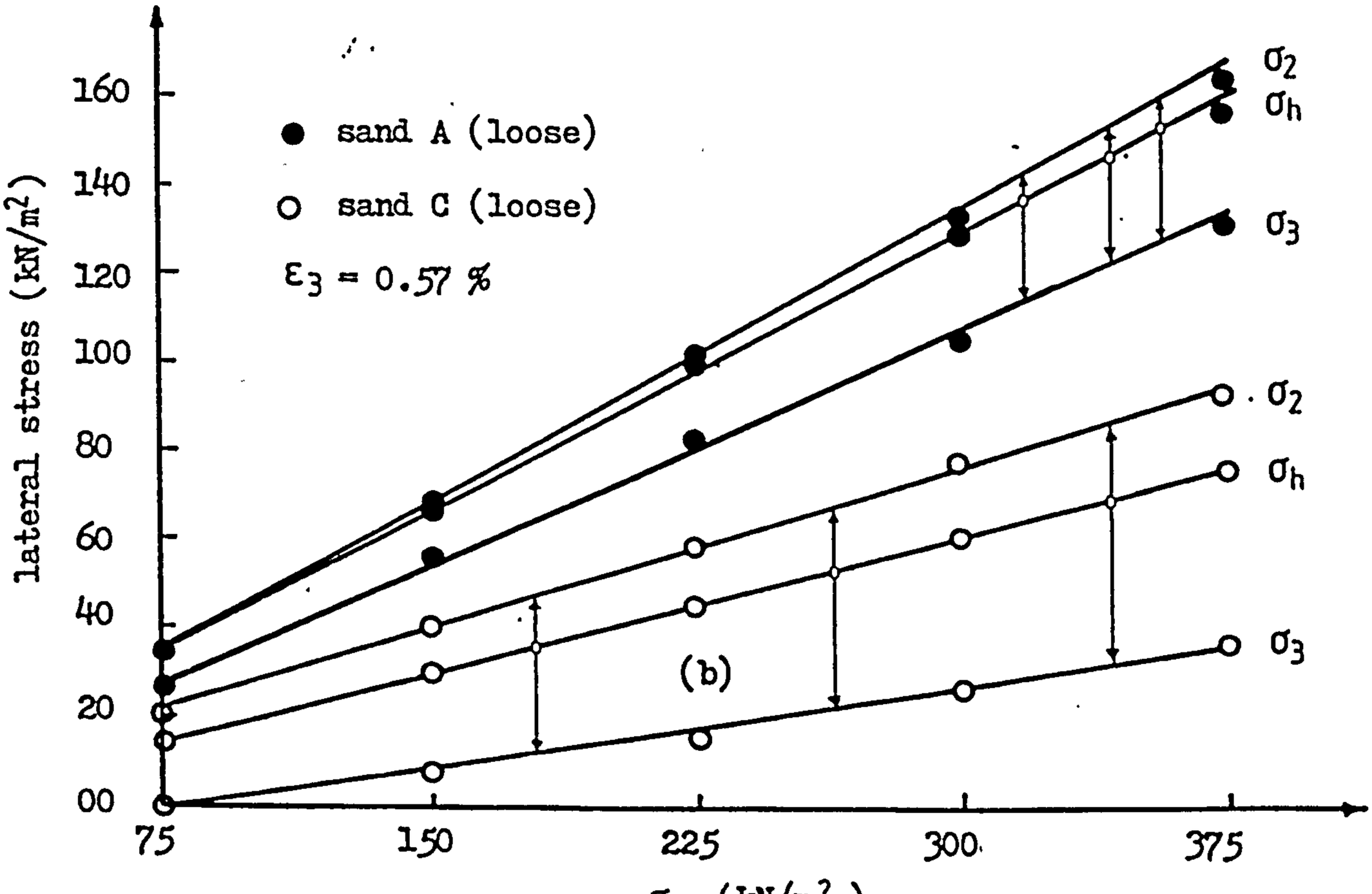

FIGURE 6.9 Variation of the lateral stresses (σ_2 and σ_3) with σ_1 under plane strain conditions (at ε_3 = 0.57 %) compared with that under confined conditions for sands A and C.

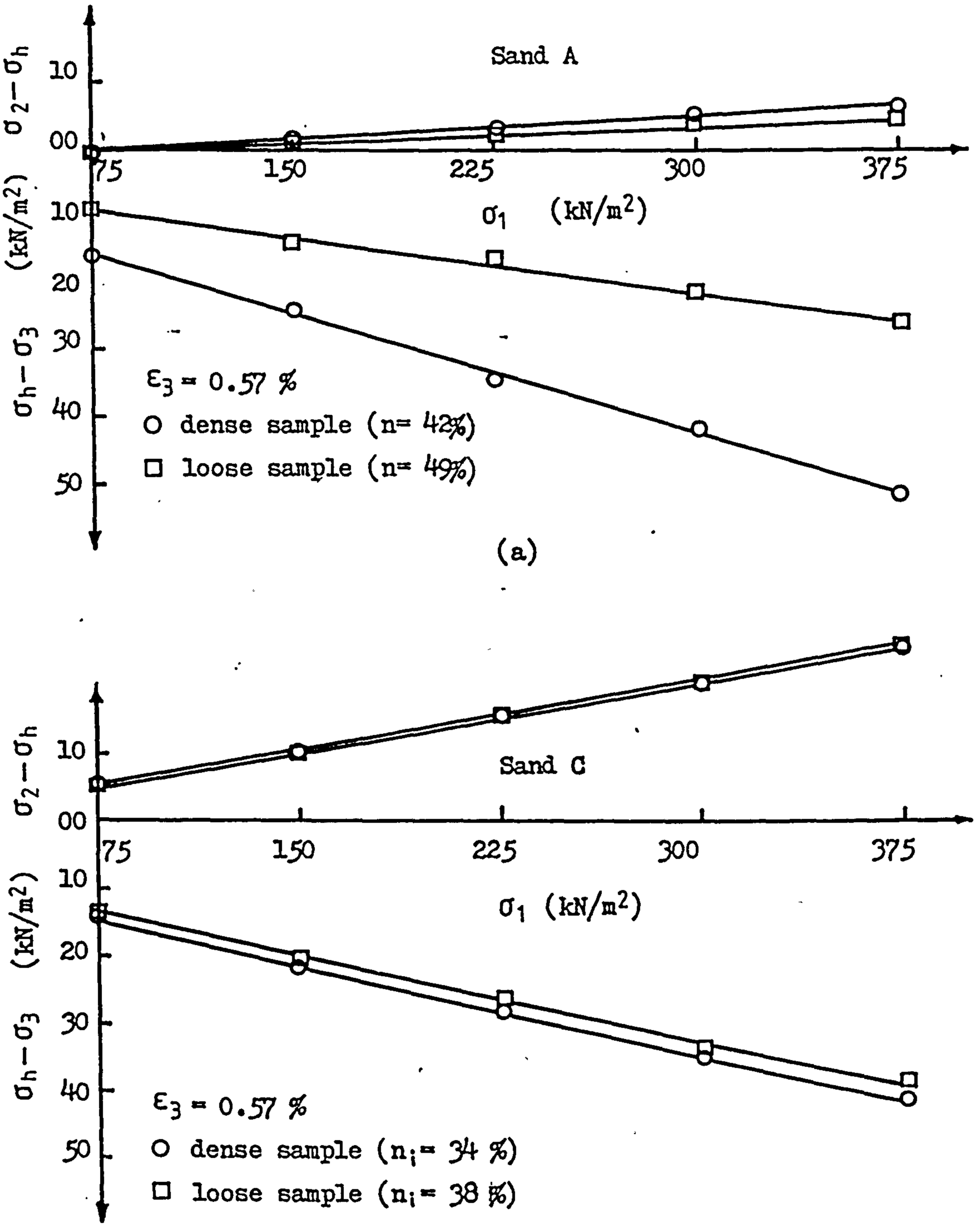

FIGURE 6.10 Variation of both $(\sigma_2-\sigma_h)$ and $(\sigma_h-\sigma_3)$ with σ_1 due to application of 0.57 % lateral strain for sanda A and C.

the figure that the increase in σ_2 and decrease in σ_3 increase on increasing the vertical stress. Applying a greater σ_1 to the sample increases interlocking of the grains. When the sample is strained in one lateral direction the frictional forces increase faster in the sample subjected to a greater σ_1 than that subjected to smaller σ_1. As the frictional forces act to decrease σ_3 the sample which is subjected to the greater σ_1 shows a greater decrease in σ_3. The same argument can be applied to the effect of the porosity on σ_3 in which the denser the sample, the more decrease takes place in σ_3. The increase in σ_2 is higher in the samples having a higher degree of interlocking than for those in a loose condition as the effect of particle movements in the ε_3 direction on the other direction diminishes since particles become freer to move independently in a looser packing.

6.3.4 COEFFICIENT OF EARTH PRESSURE IN PLANE STRAIN CONDITIONS

The relationship between ε_3 and ratios of σ_3/σ_1 and σ_2/σ_1 are shown in figures 4.30 to 4.39. When σ_1 is applied to the sample under confined conditions before straining the sample, the ratio of σ_3/σ_1 and σ_2/σ_1 are equal and represent the coefficient of earth pressure at rest (Ko).

When the samples are strained in one direction (ε_3) while σ_1 is applied, the ratio of σ_3/σ_1 decreases to a nearly constant value at which point the whole shear strength of the sand is mobilized. The ratio at this stage is called the coefficient of active earth pressure and is denoted by Ka. The ratio of σ_2/σ_1 increases above the

original value (Ko) by a relatively small amount for sand A (max. 6.5%) and by a quite remarkable amount for sand C (max. 45%). The increase for sand B was reported to be 10.30% maximum [El-Gammel, 22]. The ratio of σ_2/σ_1 tends to become constant when no further decrease occurs in the other ratio.

Since the vertical stress is constant during the straining of the samples, variations of σ_2/σ_1 and σ_3/σ_1 are only due to changes in σ_2 and σ_3 and similar arguments to those proposed to explain the changes of lateral stresses can be applied to the variations of these ratios. However because of the importance and frequent use of the coefficient of active earth pressure in practice, values of Ka obtained for the three types of sands under plane strain conditions are calculated and compared briefly. Further comparisons between Ka values obtained in plane strain and triaxial tests and also by the other investigators are given in section 6.4.5.1.

In figure 6.11 variation of Ka and Ko for sands A, B and C at different initial porosities under σ_1=375 kN/m^2 are shown. As the initial porosity of the samples increases both Ka and Ko for three sands increase approximately linearly. But the rate of increase is lower if the sand is coarser. In sands A and B the rate of increase in Ka is more than that in Ko while sand C shows the same rate for both Ko and Ka. The average values of Ka are 0.294, 0.163 and 0.09 for sands A, B and C respectively.

In figure 6.12 the variation of Ka with σ_1 for the densest and loosest cases of the three sands is shown. It

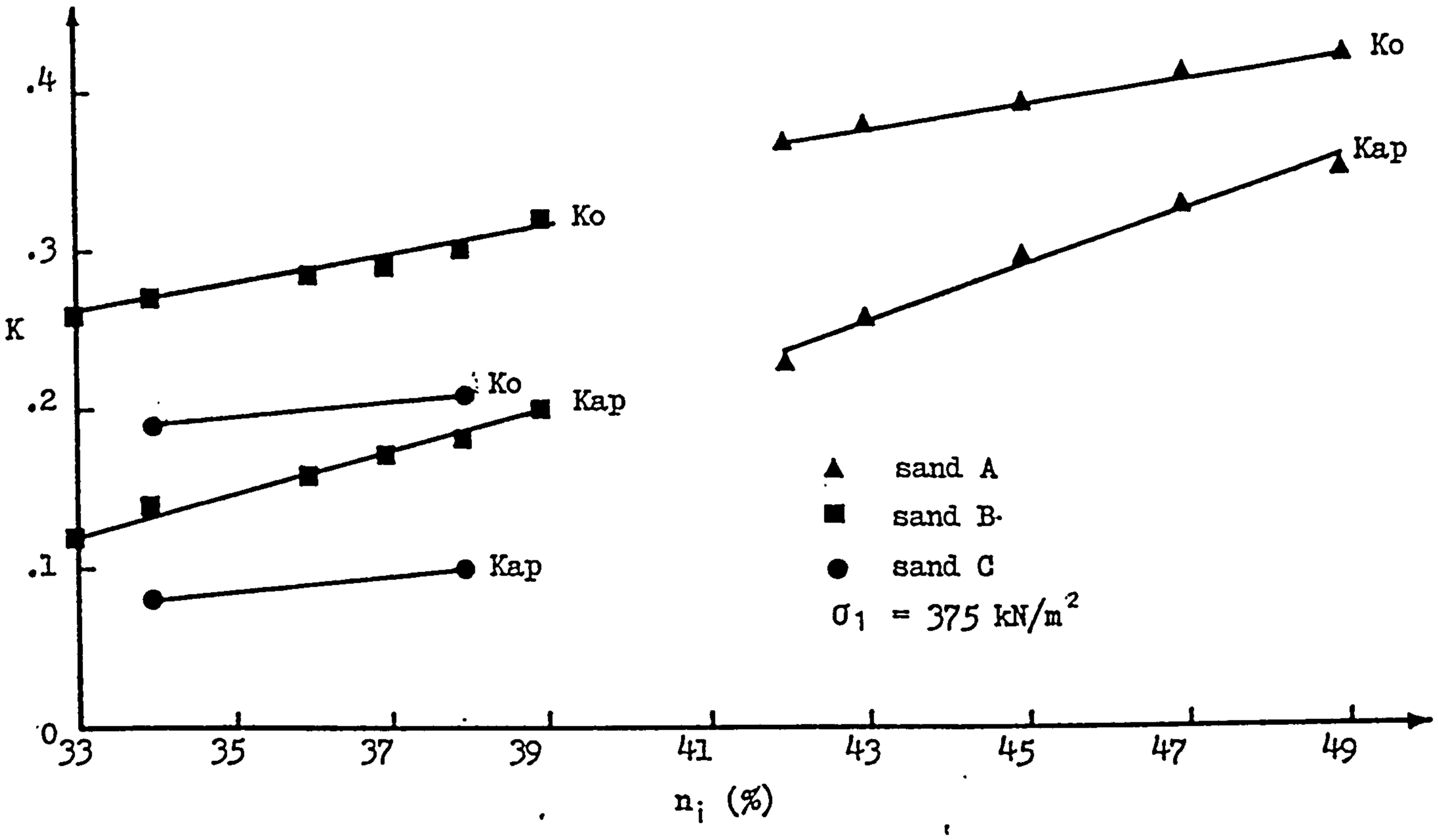

FIGURE 6.11 Variation of Ko and Ka (from plane strain tests) with initial porosity of the samples for sands A, B and C.

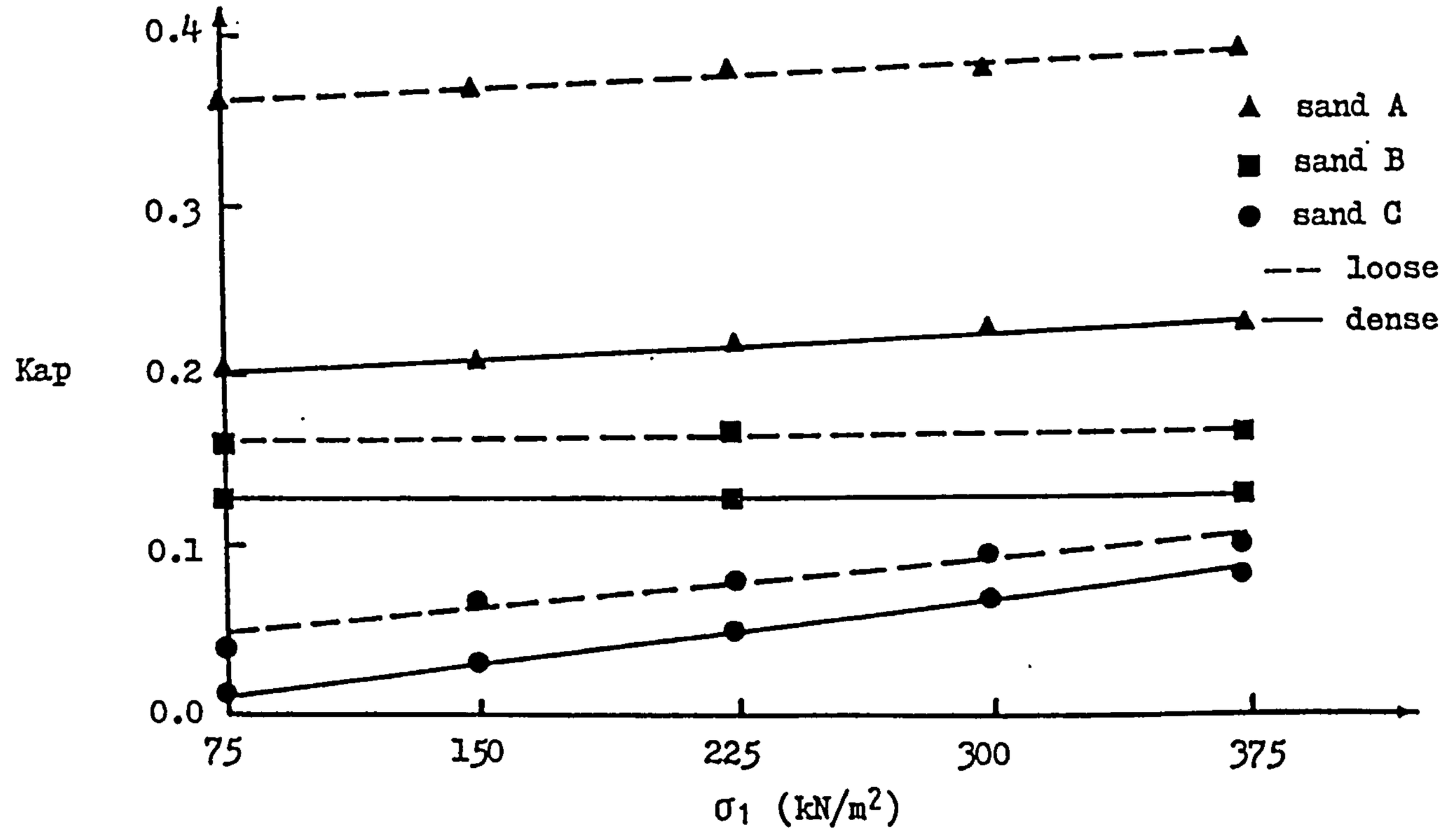

FIGURE 6.12 Variation of Ka (from plane strain tests) with σ_1 for the densest and loosest samples of the test sands.

can be seen that as σ_1 increases Ka for all sands increases. But the rate of increase decreases as the sand becomes finer. Although the values of Ka for sand B over the ranges of σ_1 tested fit well between the results of sands A and C, the trend of the curves are different from the other sands ,although there is not sufficient data reported by El-Gammel to enable fine conclusions to be drawn.

6.4 TRIAXIAL TEST DATA AND COMPARISON WITH PLANE STRAIN BEHAVIOUR

In the triaxial tests carried out on the SCTA the sample is initially subjected to a vertical stress under Ko conditions and is then allowed to strain in the two lateral directions equally. Therefore the sample should behave similarly in the two lateral directions, where $\varepsilon_2 = \varepsilon_3 = \varepsilon_h$ and theoretically $\sigma_2 = \sigma_3 = \sigma_h$.

6.4.1 VERTICAL STRAIN UNDER TRIAXIAL CONDITIONS

Curves of $\varepsilon_1 t$ against ε_h for different initial porosities under different levels of σ_1 for both sands A and C are shown in figures 4.45 to 4.49. The greater $\varepsilon_1 t$ for fine samples compared to that for coarse samples under the same conditions of σ_1 and ε_h may be explained by their states of packing which are loose compared to the coarse sand in spite of the same relative density. Increasing $\varepsilon_1 t$ with increasing the initial porosity of the samples can be similarly explained.

In figures 6.13 and 6.14 the effects of the initial porosity of the samples on $\varepsilon_1 t$ are shown. In these figures $\varepsilon_1 t$ under $\sigma_1 = 375$ kN/m^2 at lateral strains needed to develop

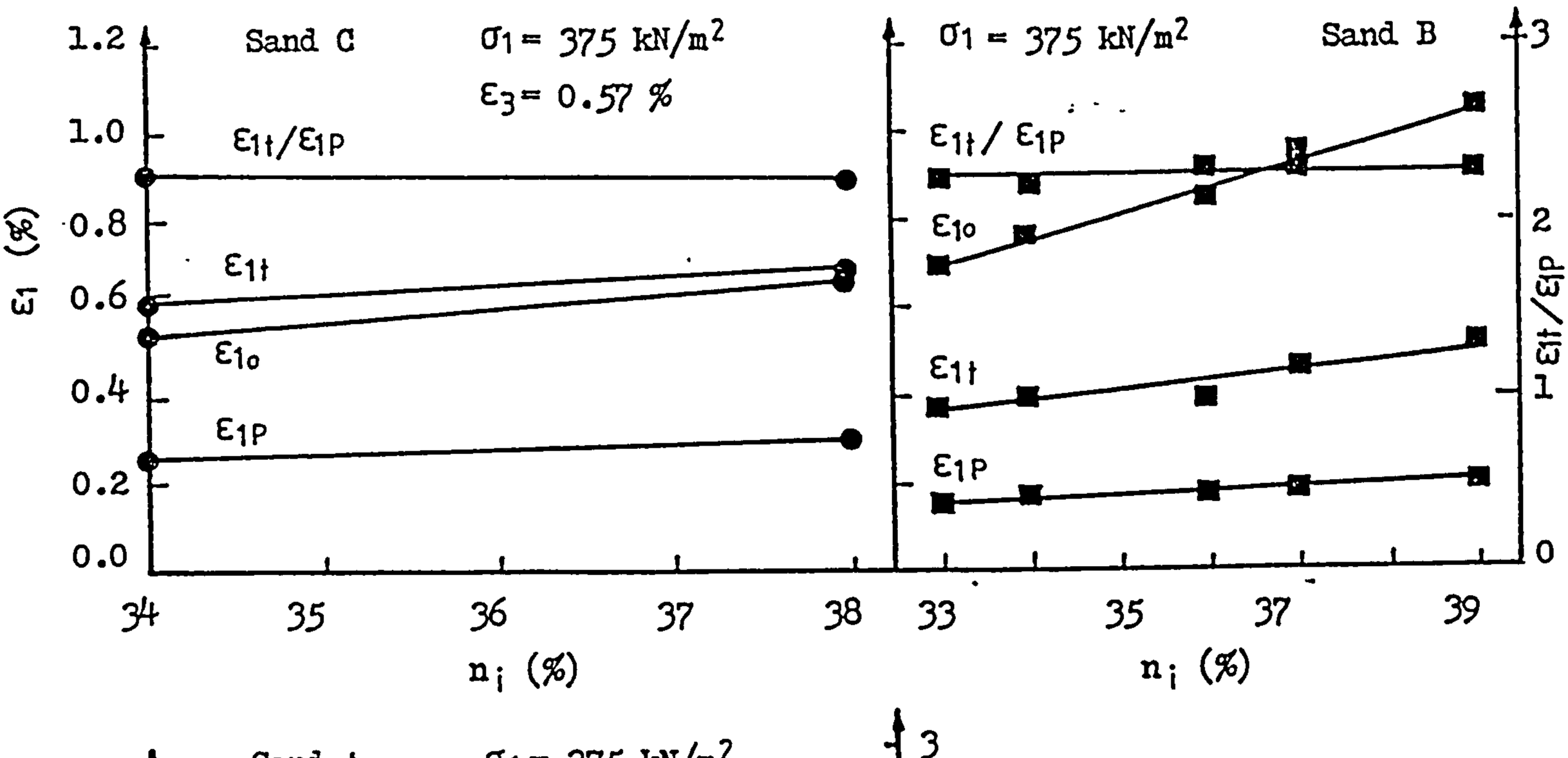

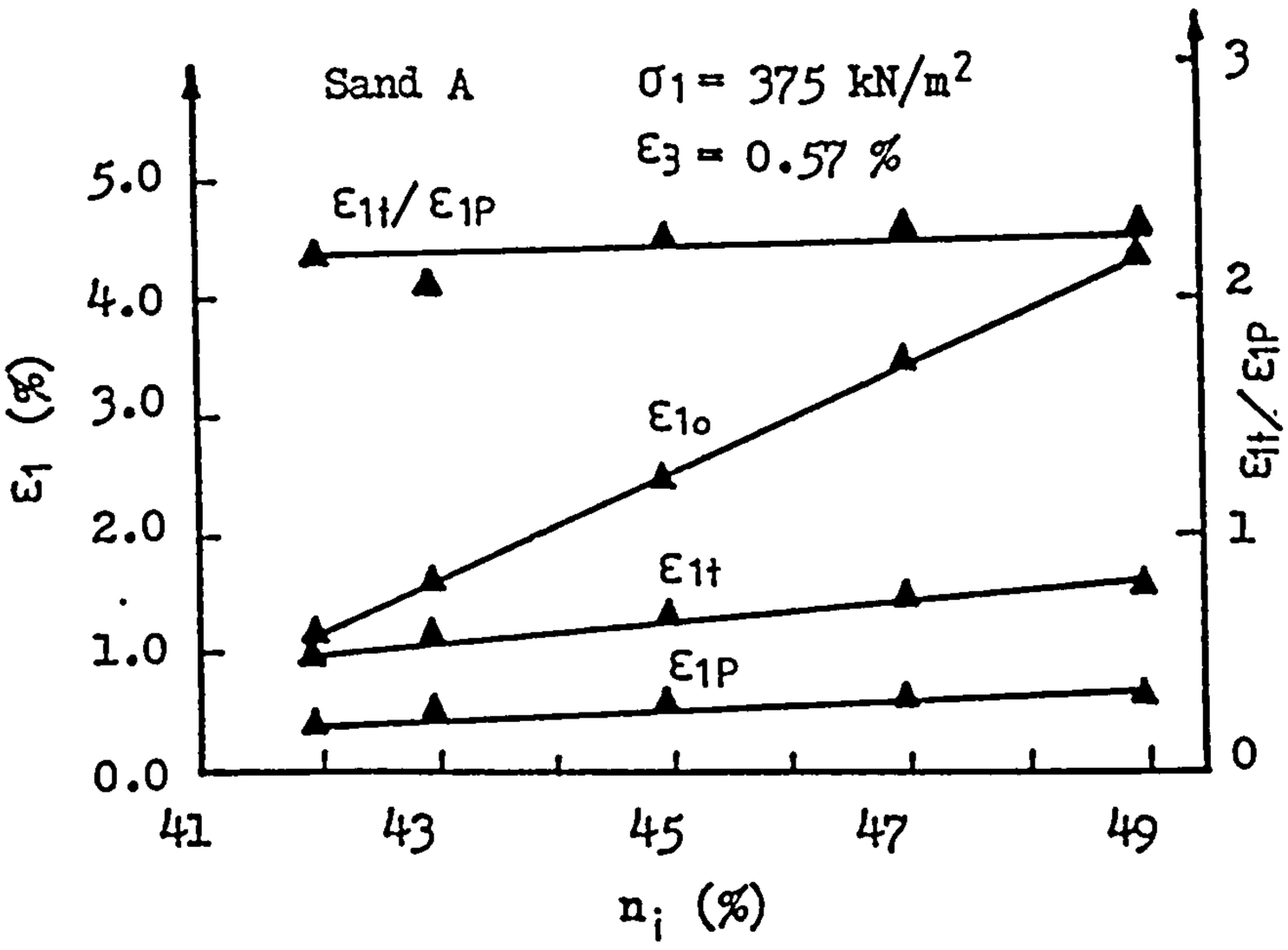

FIGURE 6.13 Variation of ε_{1o} ε_{1P} and ε_{1t} with initial porosity of the samples for sands A, B and C.

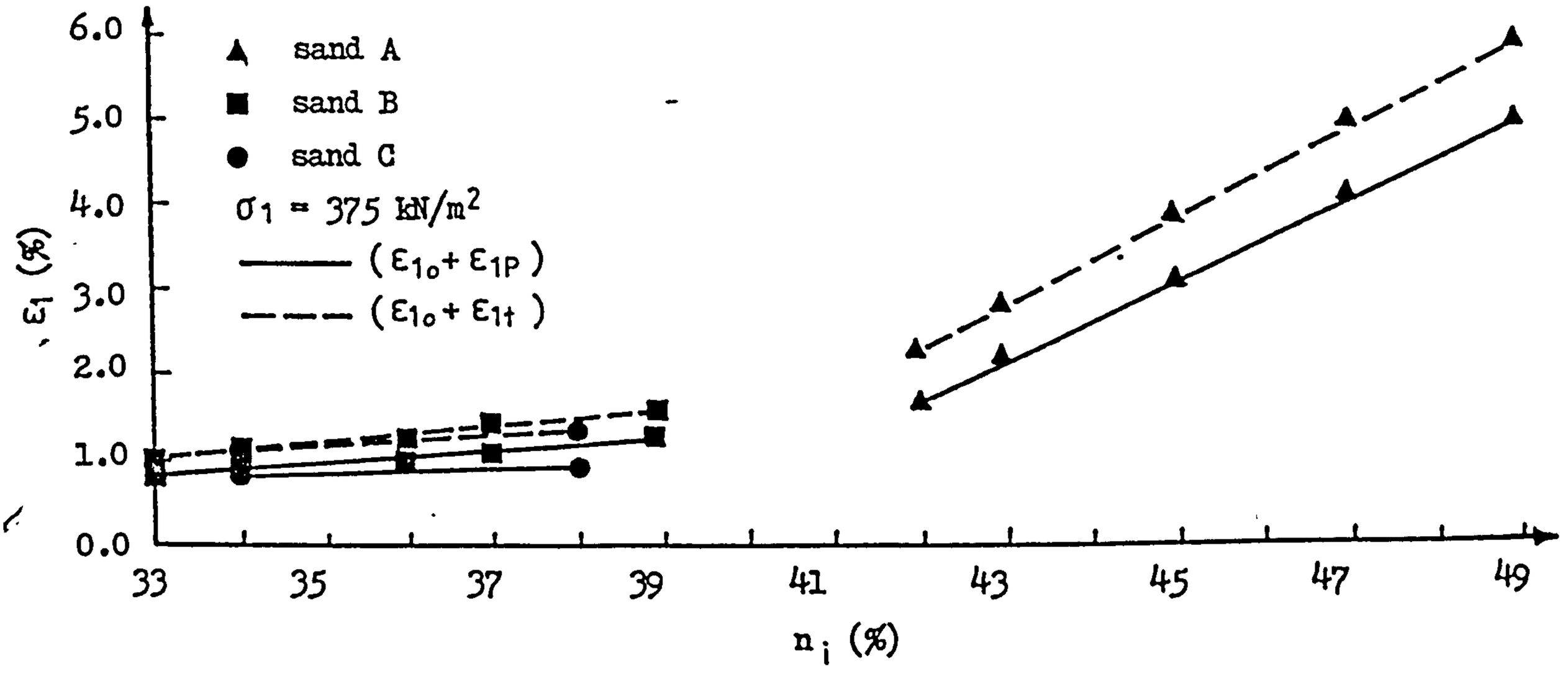

FIGURE 6.14 Variation of both total vertical strains ($\varepsilon_{1o}+\varepsilon_{1P}$) and ($\varepsilon_{1o}+\varepsilon_{1t}$) with initial porosity of the sample for sands A, B and C.

the active state of the sands are plotted against n_i. It can be seen that ε_{1t} increases almost linearly on increasing the initial porosity for all three sands, but the rate of increase decreases as the sand becomes coarser. This trend is quite clear in figure 6.14 which shows the variation of the total vertical strain ($\varepsilon_{1o} + \varepsilon_{1t}$)with initial porosity. At the same vertical stress the effect of the initial porosity of the sample on $\varepsilon_{1o} + \varepsilon_{1t}$ becomes greater as the sand becomes finer.

The effect of σ_1 on ε_{1t} and on $\varepsilon_{1o}+ \varepsilon_{1t}$ is shown in figures 6.15 and 6.16 respectively. From these figures, which show the changes in vertical strains in the loosest and densest conditions, it is evident that ε_{1t} increases almost linearly on increasing the vertical stress. As σ_1 increases the sand is more compressed and the degree of interlocking is increased. When the lateral strains are applied, the samples which are subjected to the greater σ_1 tend to shear more than those which are subjected to smaller σ_1. As a result ε_{1t} builds up as σ_1 increases. The total increase of ε_{1t} for loose samples is more than that for dense samples (the ratio is about 1.5 for sand C and 1.7 for sand A). Although the trend of variation of ε_{1t} for sand B is the same as that of A and C, its values, which are taken from El-Gammels' work do not fit well between values of sands A and B. This may be due to using a different maximum lateral strain of 0.33% at which point sand B seems has not yet attained its active state.

6.4.1.1 COMPARISON OF TRIAXIAL AND PLANE STRAIN VERTICAL STRAIN

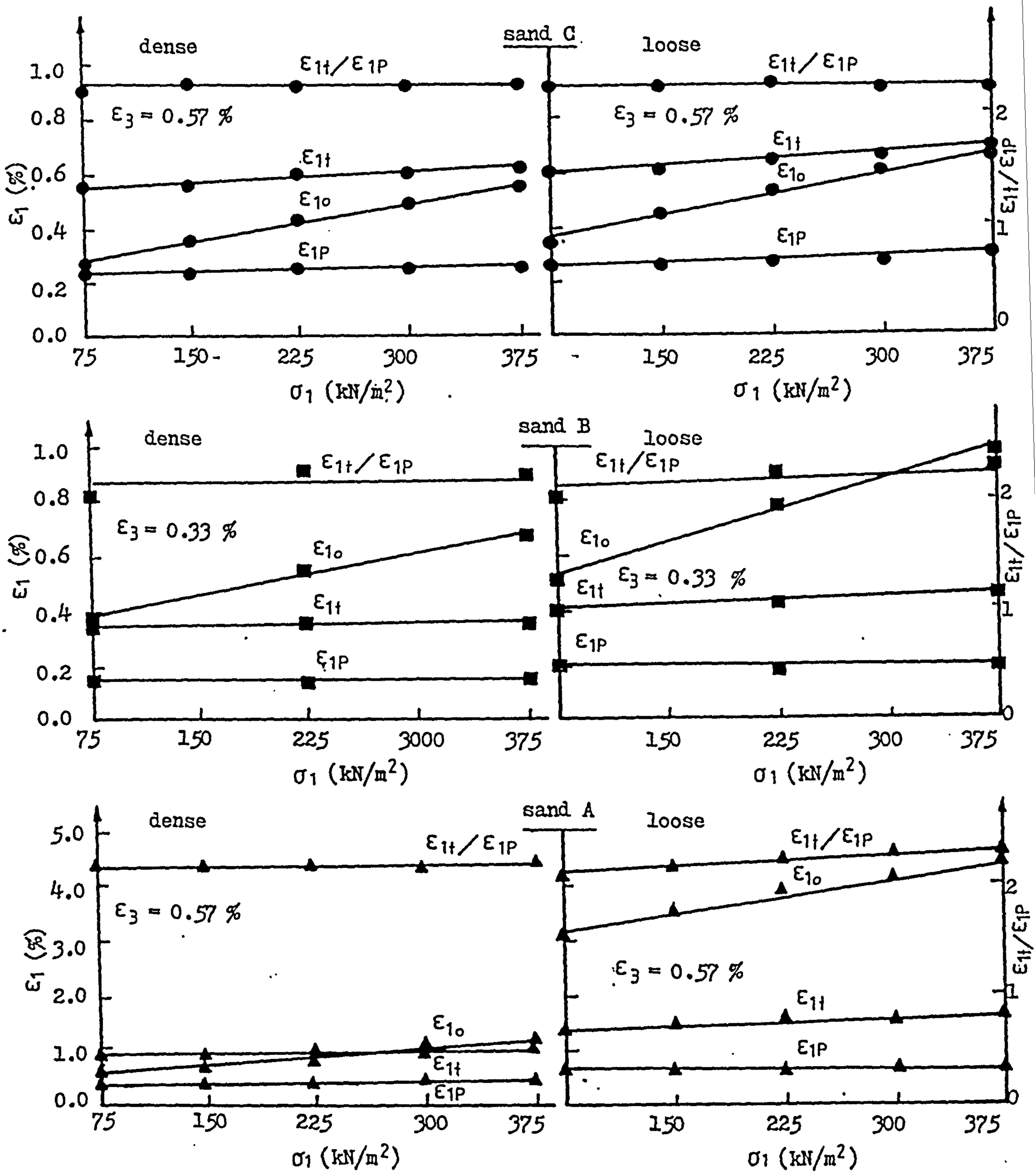

FIGURE 6.15 Variation of vertical strains ε_{1o} , ε_{1P} and ε_{1t} with σ_1 for the densest and loosest samples for sands A, B and C.

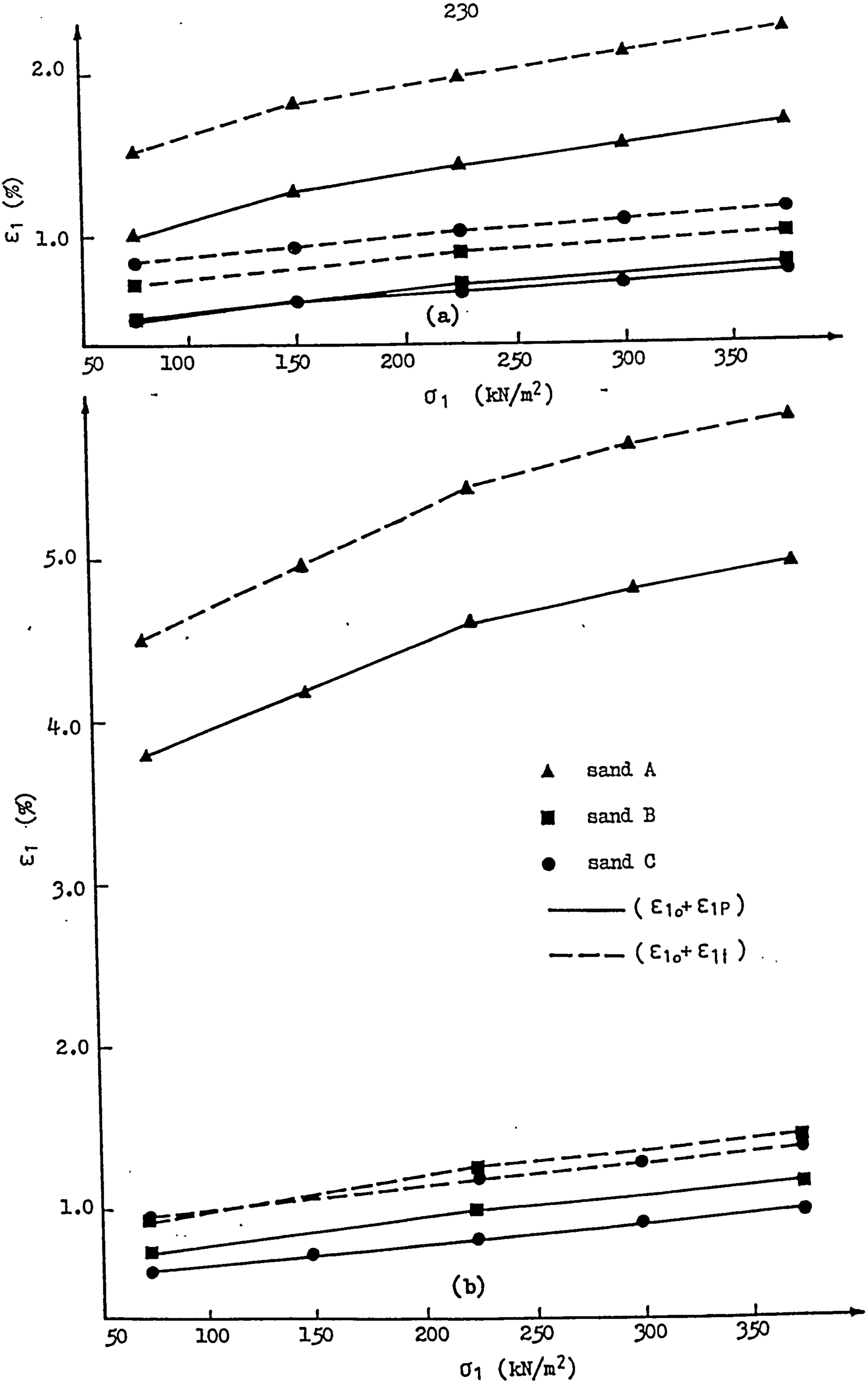

FIGURE 6.16 Variation of both vertical strains ($\varepsilon_{1o}+\varepsilon_{1P}$) and ($\varepsilon_{1o}+\varepsilon_{1l}$) with σ_1 in the densest (a) and loosest (b) cases of test sands.

ε_{1p} and $\varepsilon_{1o}+\varepsilon_{1p}$ against initial porosities and vertical stresses are plotted for all three sands together with ε_{1t} and $\varepsilon_{1o}+\varepsilon_{1t}$ in figures 6.13 to 6.16. Under similar conditions of vertical stress and lateral strain it can be seen that ε_{1t} and ε_{1p} show the same trend with initial porosity but ε_{1t} is always greater than ε_{1p}. The ratio of $\varepsilon_{1t}/\varepsilon_{1p}$ is almost constant and equals 2.25 for the three sands.

Also from figure 6.15 and 6.16 it is evident that ε_{1p} and ε_{1t} under the same conditions of initial porosity and lateral strain follow similar patterns, but in the case of triaxial tests the resulting vertical strain (ε_{1t}) is again greater than that in the plane strain tests. The ratio of $\varepsilon_{1t}/\varepsilon_{1p}$ is almost constant and nearly equal to 2.25 for all three sands.

Although it was expected that a greater vertical strain would occur in the triaxial tests than in plane strain tests , the ratio of $\varepsilon_{1t}/\varepsilon_{1p}$ shows something more. It was initially expected that ε_{1t} induced in the triaxial tests would be about twice that induced in the plane strain tests under the same test conditions since in the triaxial tests the samples are strained in two lateral directions rather than one. However during the experiments ε_{1t} was found to be about $2.25 \times \varepsilon_{1p}$. The reason may be the effect of the intermediate principal stress which restrains the samples in the direction of no-lateral strain and reduces the vertical strain. Therefore the sand under plane strain conditions would show a higher strength than that under triaxial conditions. This argument can be applied to the compari-

son of the angles of internal friction obtained from standard triaxial and different plane strain tests made by Lee [140] who concluded that under drained conditions the plane strain angle of internal friction exceeds the value obtained from triaxial tests by about 6 to 8 degrees.

6.4.2 THE VOLUME CHANGE BEHAVIOUR OF SAND UNDER TRIAXIAL CONDITIONS

AS mentioned earlier (section 4.5.4) the volumetric strain of the samples in the triaxial tests is given by:

$$(\Delta V/V)t = 2\varepsilon_h - \varepsilon_{1t} \qquad (6.6)$$

where $\varepsilon_h = \varepsilon_2 = \varepsilon_3$ represents the applied lateral strain.

If the vertical strain caused by the lateral straining of the sample is equal to the sum of the lateral strains applied in two directions (i.e. $\varepsilon_{1t} = \varepsilon_2 + \varepsilon_3 = 2\varepsilon_h$), $(\Delta v/v)t=0$ and on the $\varepsilon_{1t}-\varepsilon_h$ plot the line of $\varepsilon_{1t}=2\varepsilon_h$ represents this condition. For samples with $\varepsilon_{1t} < 2\varepsilon_h$ there is positive volumetric strain or dilation and for those with $\varepsilon_{1t} > 2\varepsilon_h$ there would be negative volume change or compression. From figures 4.45 to 4.48 it can be seen that sand C always dilates while sand A undergoes compression except for the densest sample (n_i=42%) where a small amount of dilation occurs. As discussed previously for the plane strain tests this behaviour may be related to the state of packing of the samples.

In figure 6.17 the variations of $(\Delta V/V)t$ with lateral strain for the three sands are plotted. It can be seen that as the initial porosity of the samples decreases the dilation caused by the lateral straining of the samples of sands

B and C, and the compression of the samples of sand A, increase. Between the porosities of 42% and 43% for sand A there is a critical state at which neither dilation nor compression happens (i.e. zero volume change).

In figures 6.18 and 6.19 $(\Delta V/V)t$ and $(\Delta V/V)t + (\Delta V/V)o$ against vertical stress for the densest and loosest cases of three sands are plotted. For the sands B and C $(\Delta V/V)t$ decreases gradually as σ_l increases, but for sand A the decrease happens only in the densest case. The total volumetric strain of the samples, $(\Delta V/V)t + (\Delta V/V)o$, are nearly all negative except for the sand C. This is due to considerable compression which happens as a result of the application of σ_l in Ko conditions before straining the samples. In the case of sand C especially when it is dense, the dilation that occurs when lateral strain is applied dominates the vertical strain.

The variations of $(\Delta V/V)t$ with initial porosity of the samples for the three sands are shown in figure 6.20(b). From the figure it can be seen that as the initial porosity of the sample increases $(\Delta V/V)t$ decreases. Within the ranges of porosities achieveable in the laboratory, sands B and C always dilate, but sand A initially dilates (at n_i=42%) and as the initial porosity increases the dilation decreases. At some value of the initial porosity $(\Delta V/V)t$ becomes zero after which compression begins. The amount of compression increases on further increasing the initial porosity.

The values of porosity of the samples after initial compression (n_o) and also after straining them to 0.57% (n_t) at different σ_l up to 375 kN/m^2 for sands A and C are shown

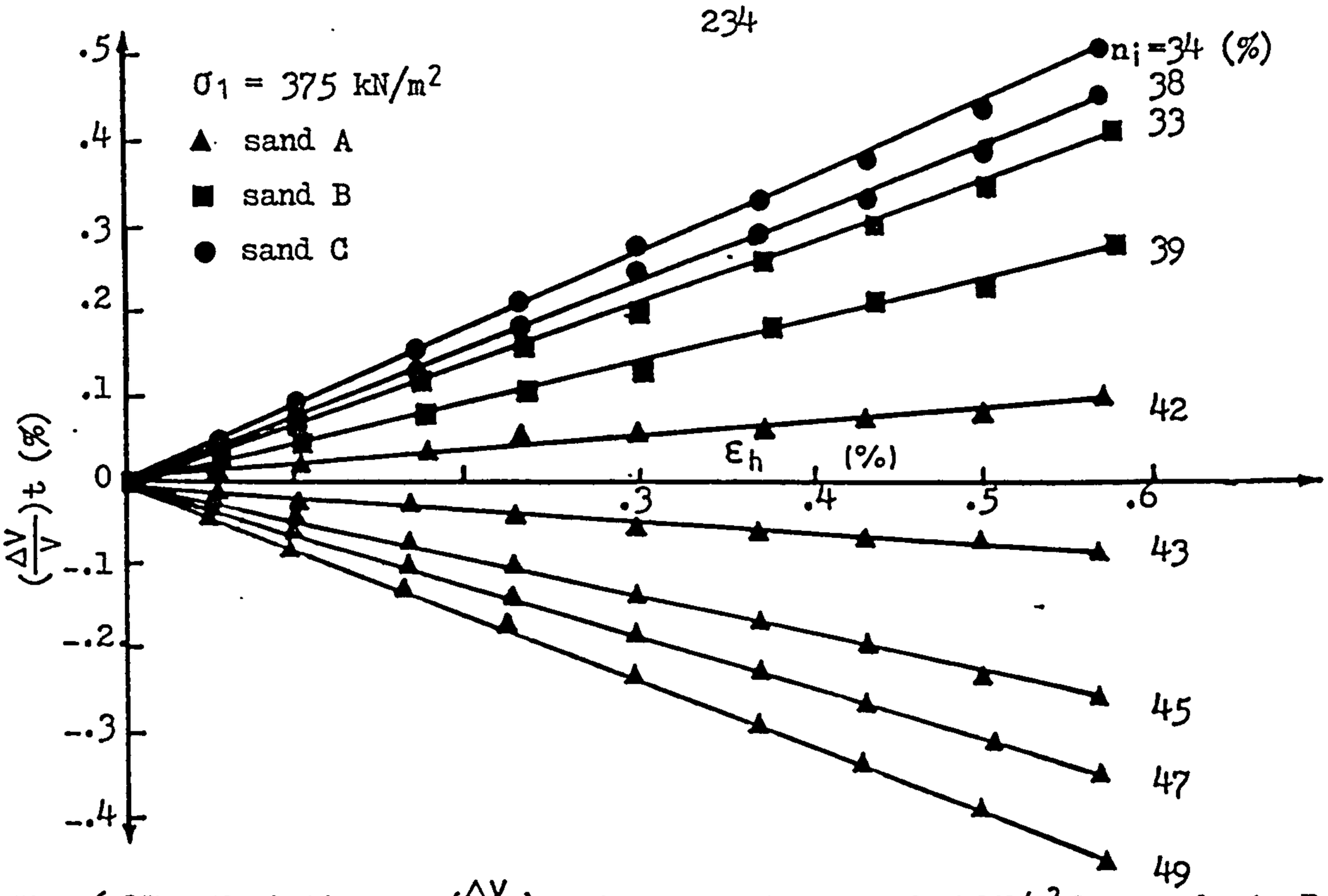

FIGURE 6.17 Variation of $(\frac{\Delta V}{V})t$ with ε_h under σ_1 = 375 kN/m² for sands A, B and C.

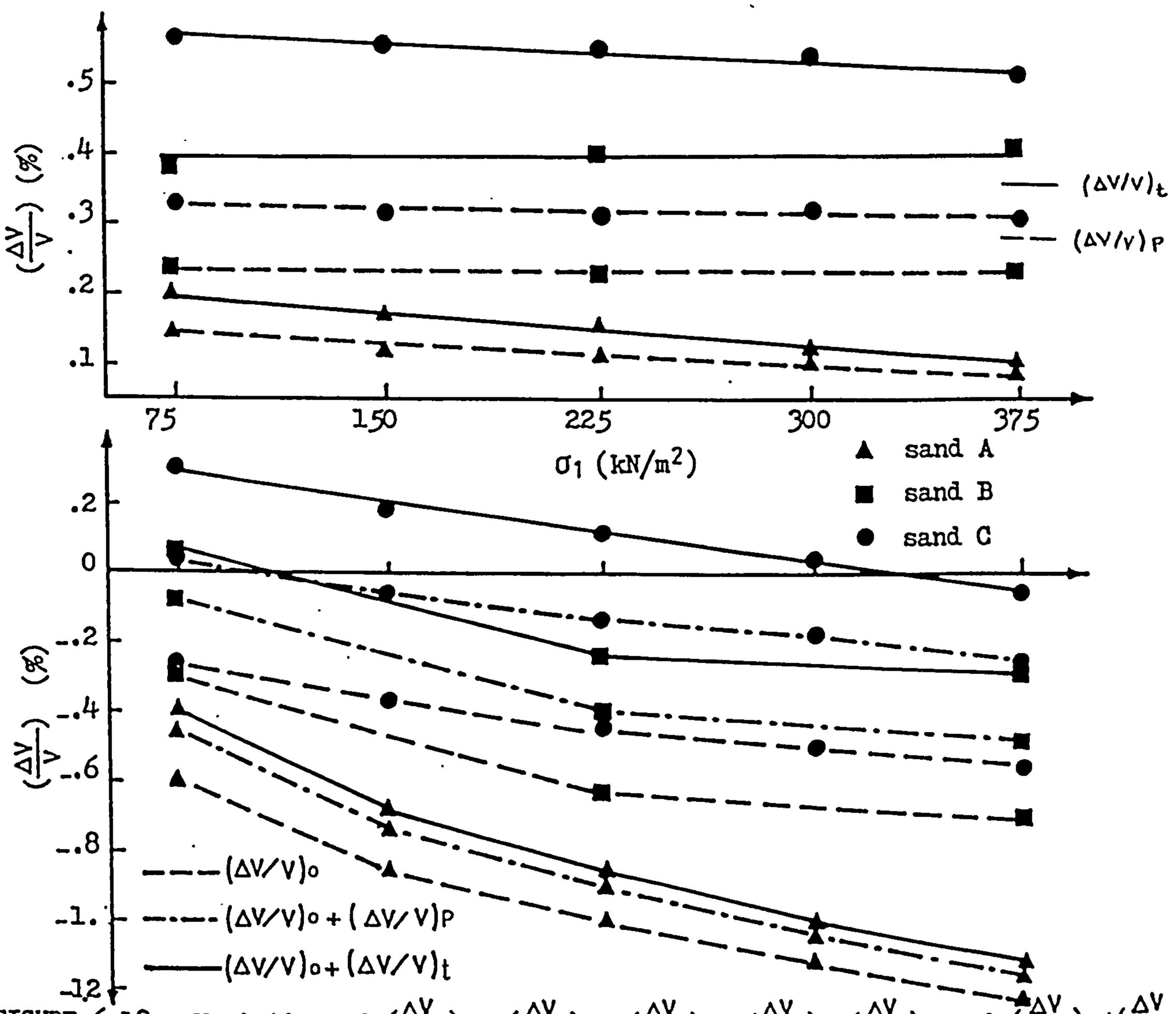

FIGURE 6.18 Variation of $(\frac{\Delta V}{V})t$, $(\frac{\Delta V}{V})p$, $(\frac{\Delta V}{V})o$, $(\frac{\Delta V}{V})t+(\frac{\Delta V}{V})o$ and $(\frac{\Delta V}{V})p+(\frac{\Delta V}{V})o$ with σ_1 for the densest case of sands A, B and C.

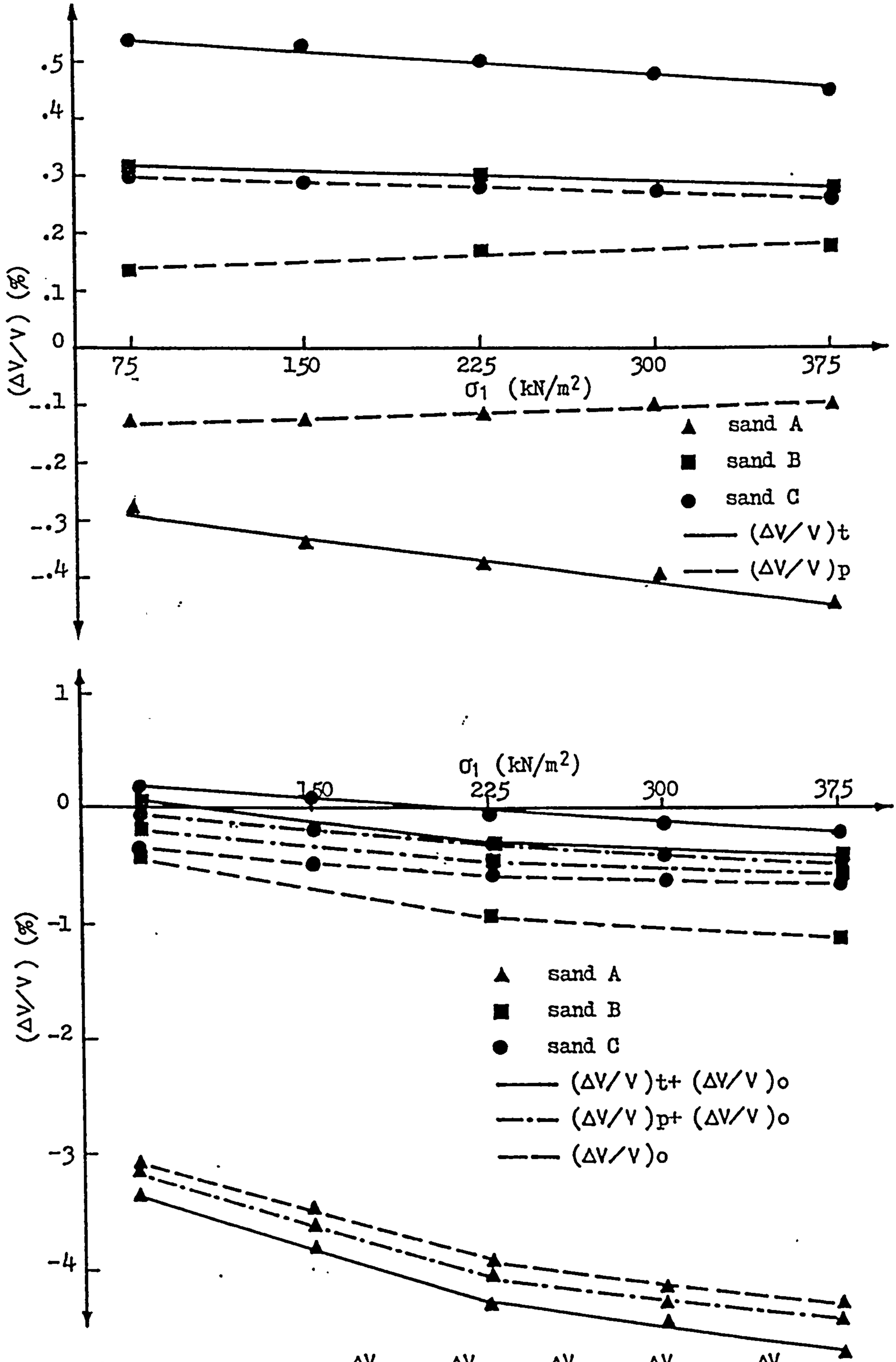

FIGURE 6.19 Variation of $(\frac{\Delta V}{V})t$, $(\frac{\Delta V}{V})p$, $(\frac{\Delta V}{V})o$, $(\frac{\Delta V}{V})t + (\frac{\Delta V}{V})o$ and $(\frac{\Delta V}{V})p + (\frac{\Delta V}{V})o$ with σ_1 for the loosest case of sands A, B and C.

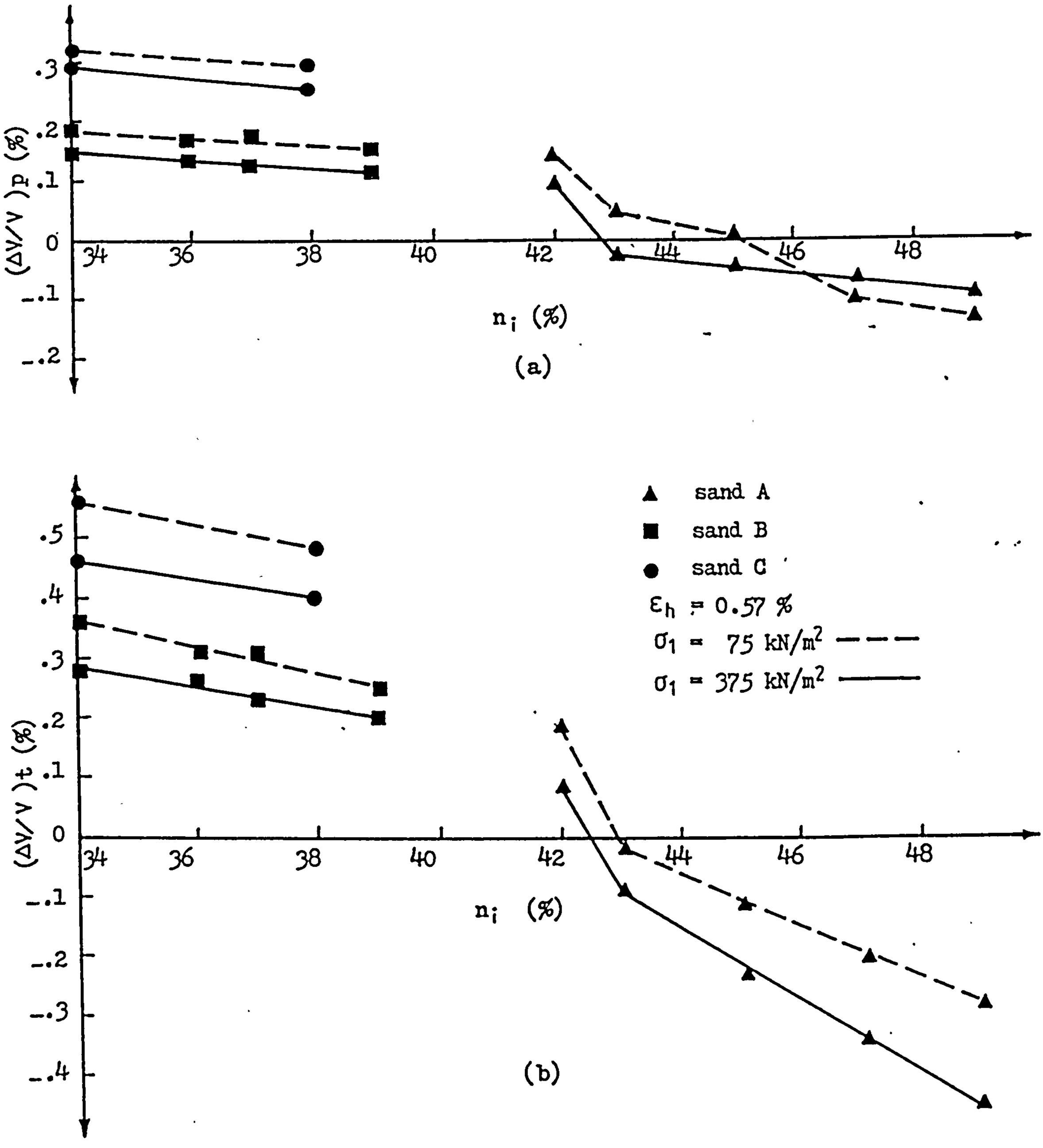

FIGURE 6.20 Variation of $(\Delta V/V)_p$ and $(\Delta V/V)_t$ with the initial porosity of the samples under the same testing conditions for sands A, B and C.

—— Change in the initial porosity due to application of incremental vertical stress up to 375 kN/m^2 on the sample under confined conditions.

—— Change in the porosity due to straining the sample in both lateral directions up to 0.57 %, while σ_1 = 375 kN/m^2 is applied.

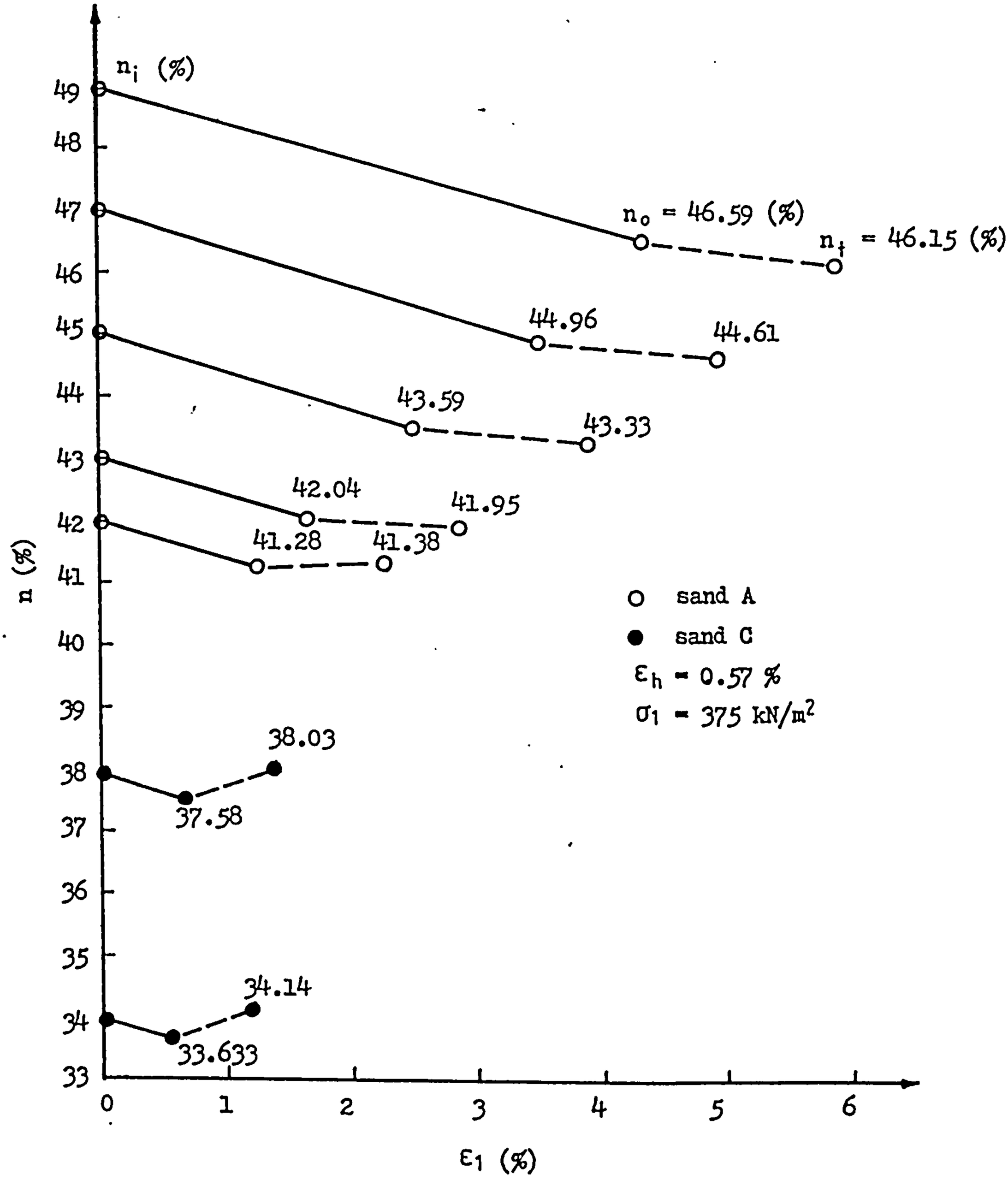

FIGURE 6.21 Changes in the porosity of the samples during triaxial tests for sands A and C.

Sand type	Initial Porosity (%)	σ_1=75 kN/m²		σ_1=150 kN/m²		σ_1=225 kN/m²		σ_1=300 kN/m²		σ_1=375 kN/m²		max. change in n	
		n_o(%)	n_t(%)	n_o(%)	n_t(%)	n_o(%)	n_t(%)	n_o(%)	n_t(%)	n_o(%)	n_t(%)	Δn_o(%)	Δn_t(%)
Fine (A)	42	41.65	41.85	41.50	41.67	41.41	41.56	41.34	41.46	41.28	41.38	- 0.37	+ 0.20
	43	42.57	42.55	42.35	42.32	42.24	42.12	42.13	41.98	42.04	41.95	- 0.54	- 0.15
	45	44.13	44.03	43.93	43.83	43.77	43.59	43.66	43.44	43.59	43.33	- 0.54	- 0.26
	47	45.72	45.52	45.45	45.25	45.29	45.24	45.15	44.88	44.96	44.61	- 0.76	- 0.35
	49	47.37	47.09	47.14	46.80	46.92	46.54	46.79	46.39	46.59	46.15	- 0.78	- 0.45
Coarse (C)	34	33.82	34.39	33.75	34.31	33.71	34.26	33.67	34.21	33.63	34.14	- 0.19	+ 0.57
	38	37.79	38.33	37.71	38.24	37.66	38.16	37.61	38.09	37.58	38.03	- 0.21	+ 0.54

n_o= porosity of the samples after application of σ_1 under confined conditions.

n_t= porosity of the samples after straining them in both lateral directions up to 0.57 % while σ_1 is applied.

TABLE 6.4 Final values of the porosity of the samples under triaxial tests for both coarse and fine sands.

in table 6.4. From this table the critical porosity of sand A under σ_1 =75 kN/m^2 is n_{cv} =42.57% , while under σ_1=375 kN/m^2 it decreases to about n_{cv} =41.66%. The changes in the initial porosity of the samples under σ_1=375 kN/m^2 and ε_h=0.57% for sands A and C are plotted in figure 6.21. The dilation of sand C and compression of sand A (except for n_i =42%) are quite clear from this figure.

6.4.2.1 COMPARISON BETWEEN PLANE STRAIN AND TRIAXIAL VOLUMETRIC STRAINS

Figures 6.18 and 6.19 show the variation of $(\Delta V/V)p$ and $(\Delta V/V)o + (\Delta V/V)p$ together with $(\Delta V/V)t$ and $(\Delta V/V)o + (\Delta V/V)t$ for the three sands in the densest and loosest states respectively. It can be seen that the volumetric strains for all three sands under similar testing conditions in triaxial tests are greater than those in plane strain tests. The ratios of , $(\Delta V/V)t/(\Delta V/V)p$ for sands B and C are nearly constant. They are very close and no significant differences between the densest and loosest cases are noted. The ratio for sand C changes from 1.7 to 1.8 and for sand B varies between 1.65 to 1.78. For sand A there is a significant difference between the ratio of $(\Delta V/V)t/(\Delta V/V)p$ for the densest and loosest cases. The ratio for the densest case changes from 1.33 to 1.43 , while for the loosest case it starts from 2.15 (under σ_1=75 kN/m^2) and increases to 4.5 (under σ_1 =375 kN/m^2). The larger volume change of this sand in triaxial conditions compared with that in plane strain conditions may be attributed to the very loose packing of this type of sand as well as the different shape of its particles.

Comparison between the results of the triaxial and plane strain tests can be also made from the figures 6.20(a) and (b) in which the volumetric strains of three sands are plotted against the initial porosity of the samples. Comparing graphs a and b it can be seen that the values of $(\Delta V/V)$ in triaxial tests for sands B and C are greater (at least 50%) than those obtained in plane strain tests. For sand A this difference starts from 30% (in the densest case) and increases to 450%. The values of the critical porosities which have already been shown to be a function of the vertical stress (see section 6.3.1), seem to depend also on the constraint conditions as well. It can be seen from the figures that the critical porosities of sand A obtained from plane strain tests are greater than those obtained from triaxial tests. The differences between these values under σ_1=75 kN/m^2 is about 4% whereas under σ_1=375 kN/m^2 it decreases to about 1%.

6.4.3 THE MODULUS OF ELASTICITY (E) AND POISSON'S RATIO (ν) UNDER TRIAXIAL AND PLANE STRAIN CONDITIONS

The modulus of elasticity and Poisson's ratio for calculating the elastic deformations of granular soils are still used in many engineering projects. It is known that these parameters for a real soil are not constants and they change as the stress-strain condition of the mass changes and the lack of a simple and realistic method to find these parameters is evident. Since most soil projects involve plane strain or triaxial conditions, e.g. retaining walls, earth dams, large embankments, etc, it seems to be important to calculate these parameters from triaxial and

plane strain tests and compare them with those obtained in confined conditions.

In figures 6.22 and 6.23 the values of ν and E obtained from plane strain and triaxial tests are plotted against vertical stress for the test sands. From figure 6.22 it can be seen that the Poisson's ratio of the sands in tri-axial conditions is greater than that in plane strain conditions. Comparing this figure with figure 6.3 it is evident that the Poisson's ratio of the sands obtained from confined tests is even smaller than that obtained from plane strain tests. However, the modulus of elasticity of the sands changes in the opposite way to that of ν. From figures 6.23 and 6.24 it is clear that the values of E obtained from confined tests are greater than those obtained from plane strain tests and the plane strain values of E are greater than the triaxial values.

To compare the values of E obtained from different constraint conditions with the constrained secant modulus ($D=\Delta\sigma_1/\Delta\varepsilon_1$) and also with those calculated using the following equation suggested by Duncan and Chang [2] for the conventional triaxial tests, table 6.5 was compiled.

$$E_t=\left[1-\frac{R_f(1-\sin\varphi)(\sigma_1-\sigma_3)}{2\sigma_3\sin\varphi}\right]^2 k\cdot P_a\cdot\left(\frac{\sigma_3}{P_a}\right)^n \qquad (6.7)$$

where Pa is the atmospheric pressure and R_f, k and n are constants which should be found experimentally.

This equation is based on the hyperbolic stress strain relationship of soils and is used in many finite ele-

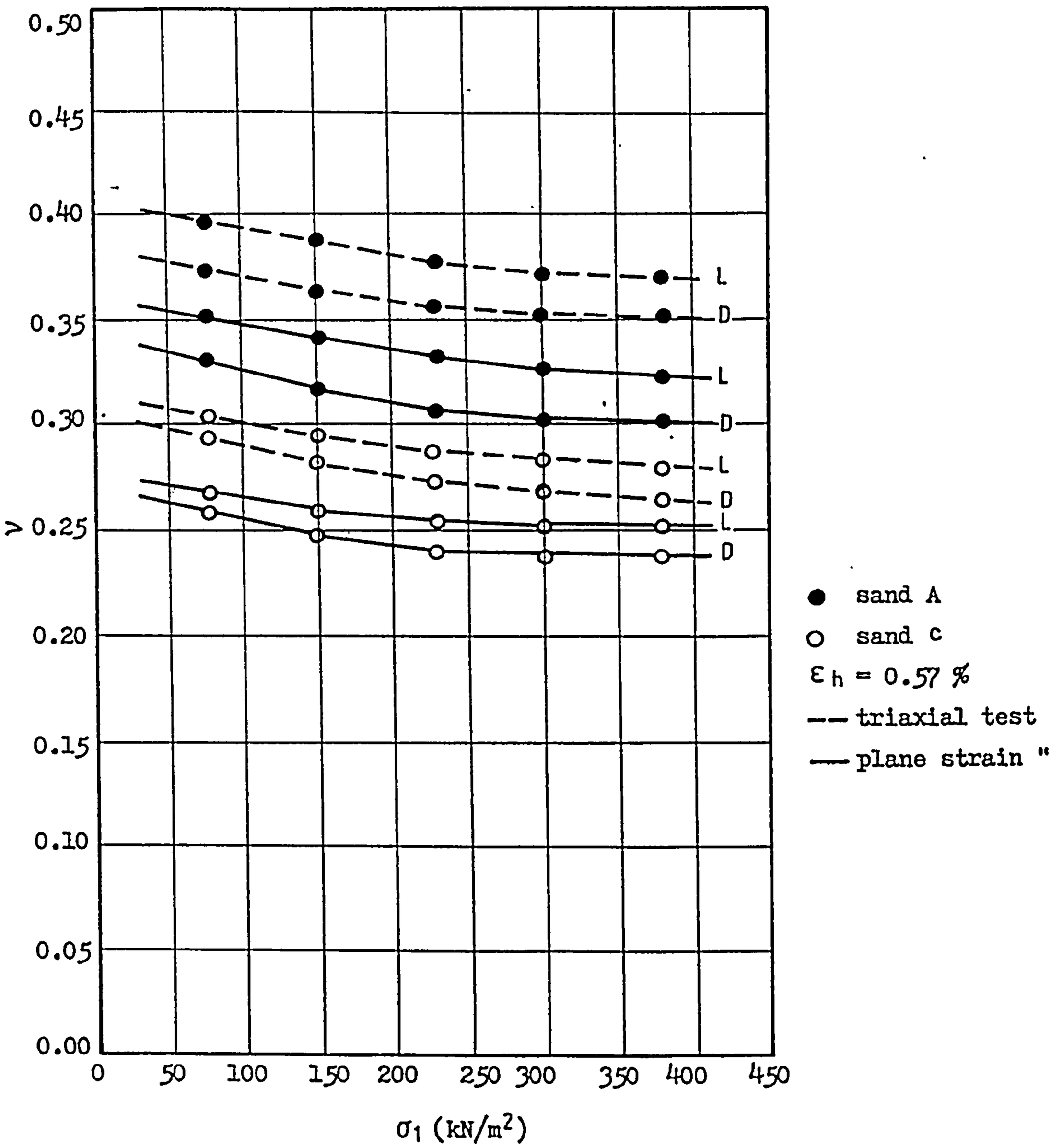

FIGURE 6.22 Poisson's ratio of the test sands in the densest and loosest conditions obtained from triaxial and plane strain tests.

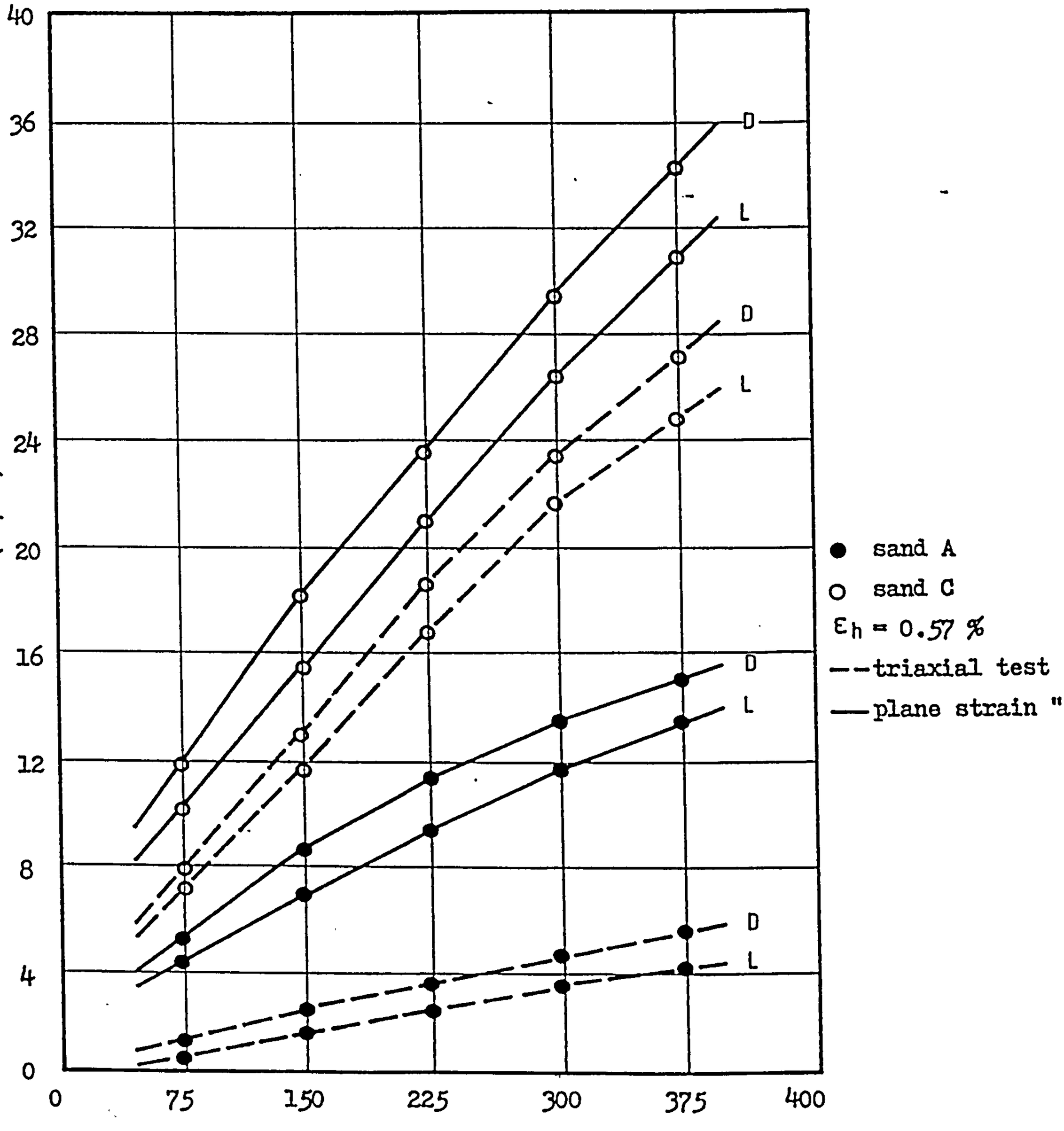

FIGURE 6.23 Modulus of elasticity (E) of the test sands in the densest and loosest conditions obtained from triaxial and plane strain tests.

elastic modulus (MN/m^2)		Sand A		Sand B		Sand C	
		loose	dense	loose	dense	loose	dense
$\sigma_1 = 75$ (kN/m^2)	Secant modulus	2.40	12.30	11.30	22.50	23.80	28.60
	Confined test	1.50	9.50	10.00	18.50	21.50	26.00
	Plane strain "	1.25	5.25	5.63	10.25	10.25	12.00
	Triaxial "	0.75	4.25	4.10	7.50	7.10	8.20
	Duncan & Chang	0.54	3.11	2.93	4.67	4.98	5.18
$\sigma_1 = 150$ (kN/m^2)	Secant modulus	4.11	18.41	19.40	34.75	33.45	41.25
	Confined test	2.75	14.20	17.12	30.13	31.50	38.60
	Plane strain "	2.75	9.10	10.15	15.25	16.20	17.75
	Triaxial test	1.75	7.25	9.17	12.82	12.50	13.88
	Duncan & Chang	1.09	5.89	7.45	10.17	9.21	10.12
$\sigma_1 = 225$ (kN/m^2)	Secant modulus	5.73	22.81	25.84	44.35	42.30	51.15
	Confined test	4.10	18.15	22.50	40.17	39.52	48.10
	Plane strain "	3.63	11.75	14.13	21.20	22.17	24.31
	Triaxial test	2.88	10.11	12.10	17.25	17.75	19.50
	Duncan & Chang	2.17	8.09	10.63	14.93	13.30	15.42
$\sigma_1 = 300$ (kN/m^2)	Secant modulus	7.16	26.91	31.42	54.12	50.80	61.72
	Confined test	5.11	21.50	26.51	48.31	48.11	58.17
	Plane strain "	4.80	14.10	17.25	25.75	27.51	31.10
	Triaxial test	3.75	12.11	14.75	21.20	22.60	24.70
	Duncan & Chang	2.93	10.13	12.31	18.38	19.61	20.98
$\sigma_1 = 375$ (kN/m^2)	Secant modulus	8.52	30.11	36.30	60.51	57.78	70.40
	Confined test	6.50	24.15	30.10	56.70	55.14	66.32
	Plane strain "	5.75	15.75	20.30	30.31	32.50	36.20
	Triaxial test	4.38	14.25	16.75	24.17	26.25	28.50
	Duncan & Chang	3.64	11.62	13.42	20.19	22.10	23.92

TABLE 6.5 Elastic moduli of the sands obtained from the SCTA and Duncan's equation under the same condition ($\varepsilon_h = 0.57\ \%$).

ments calculations. From table 6.5 it is quite clear that the modulus of elasticity of sands varies over a wide range from about 1 to 70 MN/m^2 depending on the level of the vertical stress, porosity of the sample and constraint conditions. The constrained secant modulus which can be easily measured from the slope of the line joining the origin and any point of the $\sigma_1 - \varepsilon_1$ curve of the confined tests offers the highest values and cannot be used for accurate calculations. The values of E obtained from confined tests are also greater than those obtained from plane strain and triaxial tests and the importance of using the right value of E for each condition is quite evident. However, the equation suggested by Duncan and Chang for E to enable non-linear incremental stress-strain calculations to be carried out does not seem to be accurate. Values of E calculated form this equation, for the same σ_1 and ε_h of triaxial tests, are always smaller (max. 37%) than those obtained from direct calculation using the elasticity equations (6.1 to 6.3). The differences may be due to either the hyperbolic assumption of the stress strain relationship of the soil or the exponential effect of the confining pressure on the initial tangent modulus suggested by Janbu which the Duncan and Chang equation is based on.

6.4.4 LATERAL STRESSES IN TRIAXIAL CONDITIONS

Variations of the lateral stresses with ε_h for sands A and C are shown in figures 4.40 to 4.44. The same argument developed while discussing the plane strain tests to explain the decreasing σ_3 with increasing ε_3, can be applied to the decrease of σ_h with ε_h. In this condition, as ε_h is applied

to both lateral directions, the shearing resistance of the sand is mobilized in the both directions. In a similar way to plane strain tests when ε_h reaches about 0.57% lateral stresses become almost constant which means at this point the shearing resistance of the sand has been fully mobilized.

Variations of lateral stresses with the vertical stress at ε_h=0.57% for the three test sands in the densest and loosest cases are plotted in figure 6.24. It can be seen that as σ_l increases σ_{ht} increases almost linearly for all three sands. But the rate of increase of σ_{ht} for sand A is approximately twice that for sands B and C. This may be related to the general state of packing of sand A which is loose compared with sands B and C.

Variations of σ_{ht} with initial porosity under σ_l=375 kN/m^2 and at ε_h=0.57% for the three sands are shown in figure 6.25. Again it can be seen that σ_{ht} increases approximately linearly with increasing initial porosity of the samples over the ranges of porosities achieveable in the laboratory. The total increase in σ_{ht} for sand A is about twice that of sand B and about nine times that occurring for sand C within the range of their porosities. It can be concluded that the initial porosity has a major effect on the response of sand A in contrast to sands B and C.

6.4.4.1 COMPARISON BETWEEN LATERAL STRESSES IN THE TRIAXIAL AND PLANE STRAIN CONDITIONS

The lateral stresses (σ_{3p}) are plotted against the vertical stress and initial porosity of the samples together with σ_{ht} in figures 6.24 and 6.25 for all the test sands.

From the figures it is clear that the lateral stresses in the triaxial condition are greater than those in plane strain conditions. To compare these results the ratio of σ_{ht}/σ_{3p} for all cases are plotted in these figures. It can be seen that the ratio of σ_{ht}/σ_{3p} for each sand is nearly constant. From figure 6.24 this ratio for sand A is about 1.05, while for sand B is 1.37 and for sand C 1.5. These values are the averages obtained from the densest and loosest values for each sand since there is only a small difference between them. According to these results there is not a significant difference between the results of plane strain and triaxial tests for sand A. However for sand B there is about 37% increase in lateral stresses obtained in triaxial compared with plane strain tests and for sand C this difference becomes about 50%.

This outcome from a direct comparison of test results in triaxial and plane strain conditions carried out on the SCTA is in good agreement with that reported by Lee [140] comparing the values of the angle of internal friction obtained from conventional triaxial and plane strain tests. He found that as the initial porosity of the sample increases the differences between values of ϕ obtained from triaxial and plane strain tests becomes smaller and for the very loose sample this difference becomes negligible. As discussed before in section 6.1.1, for sands C to A as the overall state of the samples changes from very dense to very loose the ratio of σ_{ht}/σ_{3p} changes from 1.5 to 1.05 which agrees well with that found by Lee.

Variation of σ_{ht} and σ_{3p} with initial porosity of the

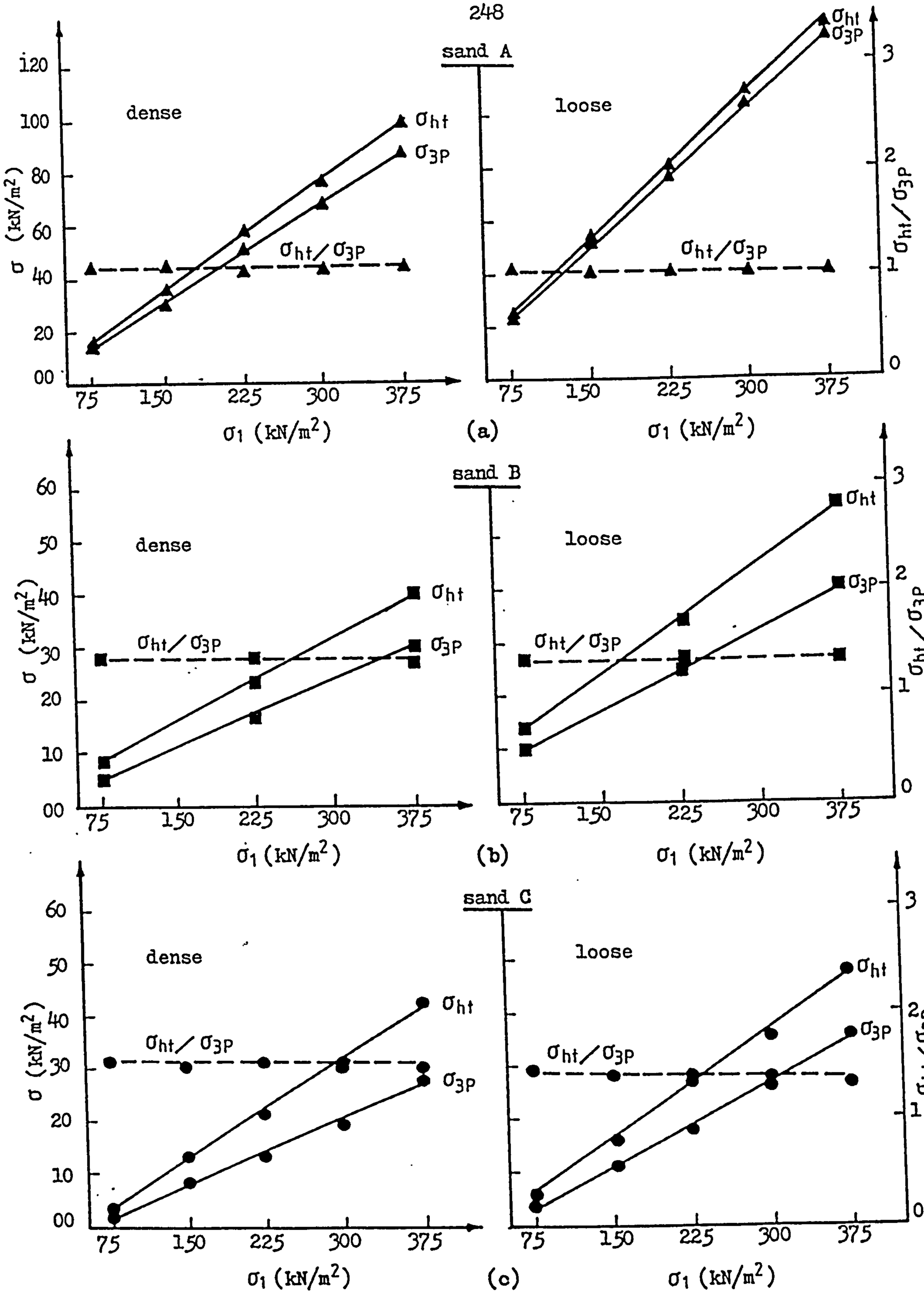

FIGURE 6.24 Variation of the lateral stress with σ_1 in triaxial and plane strain tests for dense and loose samples of sands A, B and C.

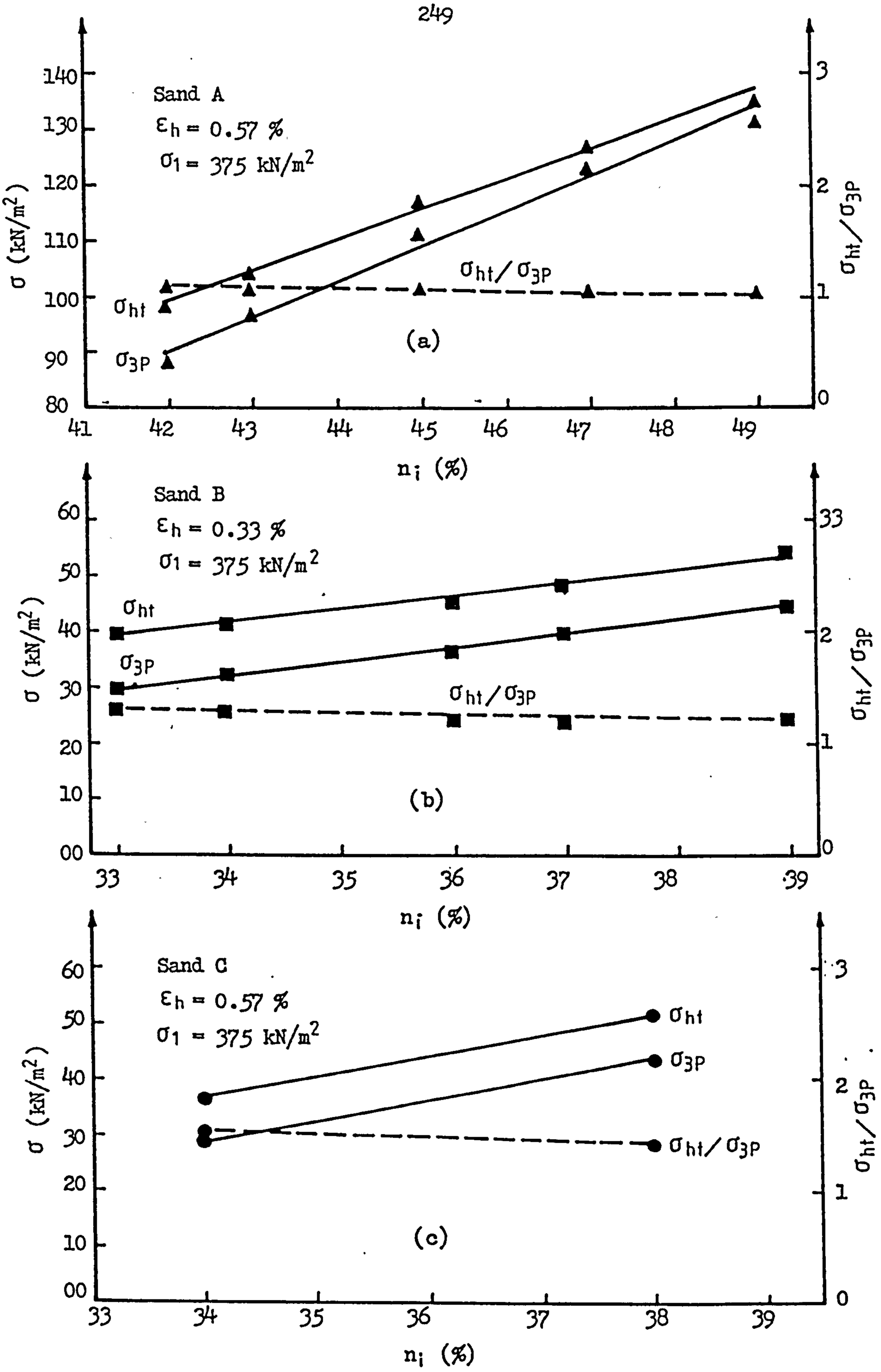

FIGURE 6.25 Variation of the lateral stress with the initial porosity of the sample in triaxial (σ_{ht}) and plane strain (σ_{3p}) tests for test sands.

samples for the three test sands are plotted in figure 6.25. It is evident that the ratio of σ_{ht}/σ_{3p} decreases gradually as the initial porosity of the sample increases.

6.4.5 COEFFICIENT OF EARTH PRESSURE IN TRIAXIAL CONDITIONS

The ratio of $K= \sigma_{ht}/\sigma_1$ against ε_h for sands A and C is plotted in figures 4.50 to 4.54. As explained earlier in chapter 4 for both sands A and C K starts from values equal to Ko in each test and then as ε_h is applied it decreases. At some value of ε_h when there is no significant decrease in the lateral stress K becomes nearly constant and equal to Ka. To differentiate between Ka obtained from plane strain tests from that obtained from triaxial tests they are denoted by Kap and Kat respectively.

Variations of Kat with σ_1 in the loosest and densest cases for the three test sands are shown in figure 6.26. From this figure Kat increases approximately linearly as σ_1 increases. The values of Kat over the ranges of vertical stresses used decreases as the sand becomes coarser.

Variations of Kat with the initial porosity of the samples under σ_1=375 kN/m^2 for the three sands are plotted in figure 6.27. From this figure it can be seen that Kat increases almost linearly as the initial porosity of the samples increases for all test sands. But the total increase of Kat over the ranges of porosities achieveable decreases as the sand becomes coarser.

6.4.5.1 COMPARISON OF Ka FROM TRIAXIAL AND PLANE STRAIN TESTS

Figures 6.26 and 6.27 also show the variations of Kap and Ko as well as Kat in each case for the three sands in

order to allow a comparison of the results obtained from different constraint conditions. According to these figures Ka obtained from triaxial tests is always greater than those obtained from plane strain tests. The ratios between these two values (R = Kat/Kap) are calculated and plotted on figures 6.26 and 6.27 as well. It can be seen that for sand A, R is about 1 whereas for sand B is about 1.37 and for sand C 1.5.

Variations of R for each sand over the ranges of initial porosities are shown in figure 6.27. There is a small decrease in R from the densest to the loosest cases of each sand. Variation of Ko with σ_1, as can be seen from figure 6.26 is in the opposite direction of Kat and Kap, while Ko, Kap and Kat change in the same way with the initial porosity of the samples. The overall values of Ko, Kap and Kat decrease as the sand becomes coarser.

To compare Ka obtained from triaxial and plane strain tests on the SCTA with those obtained or suggested by other investigators table 6.6 is given. As Ka obtained from the SCTA varies with the level of the vertical stress, the minimum and maximum values are used. From this table it can be seen that the values of Ka suggested by other researchers for the medium sand in many cases are close to those obtained on the SCTA, but for the fine and coarse sands some differences are evident. While Ka suggested by other investigators for the fine sand are smaller than those obtained in this research, for the coarse sand they are greater. All Ka values given in this table from the previous works are those found actording to the retaining wall studies [after

Kirk, 137], thus the above differences may be due to the different assumptions taken for the wall effects on the sand response as well as to the different types of sand used.

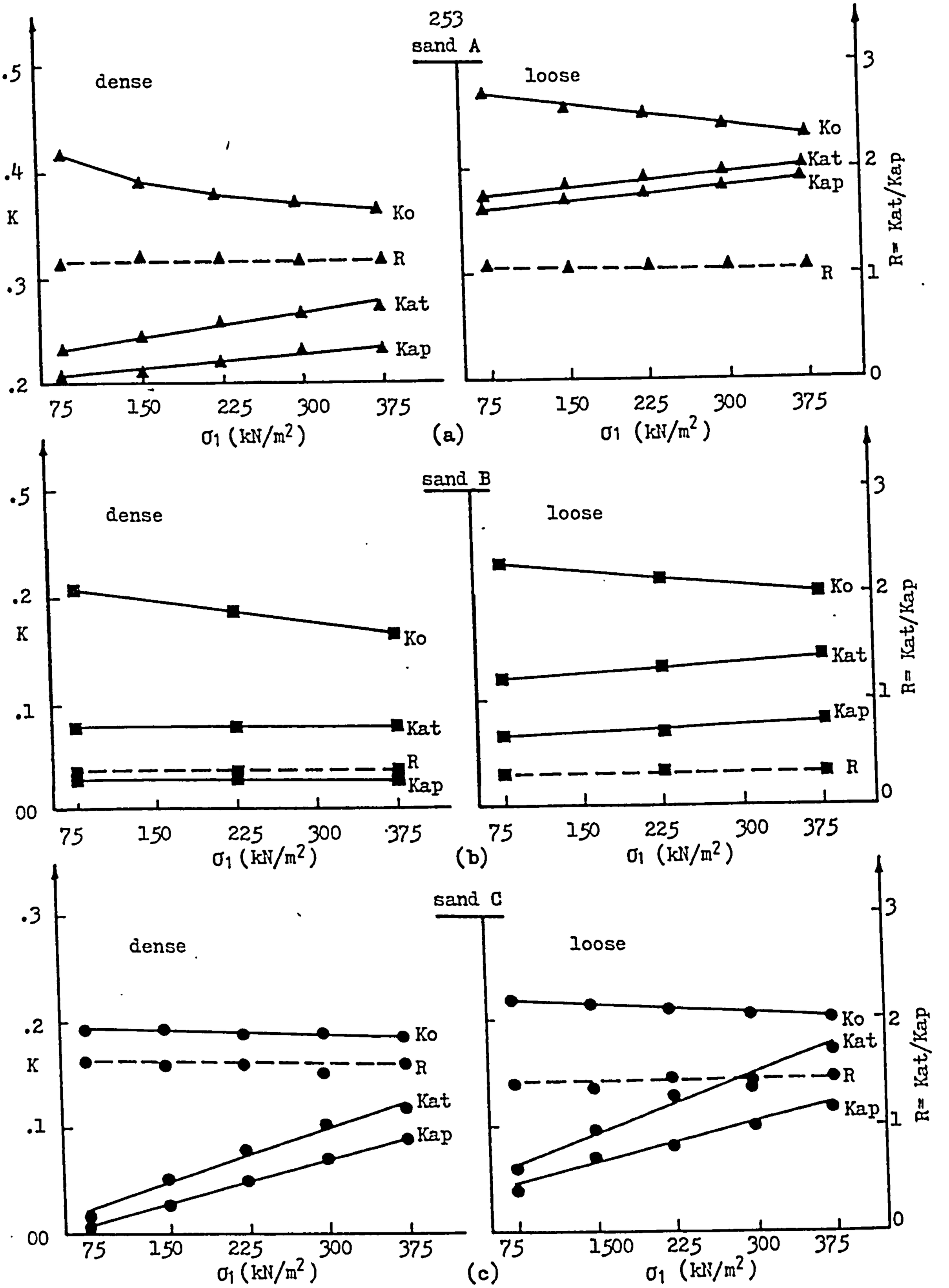

FIGURE 6.26 Variation of Ko, Kat and Kap with σ_1 in the densest and loosest conditions for sands A, B and C.

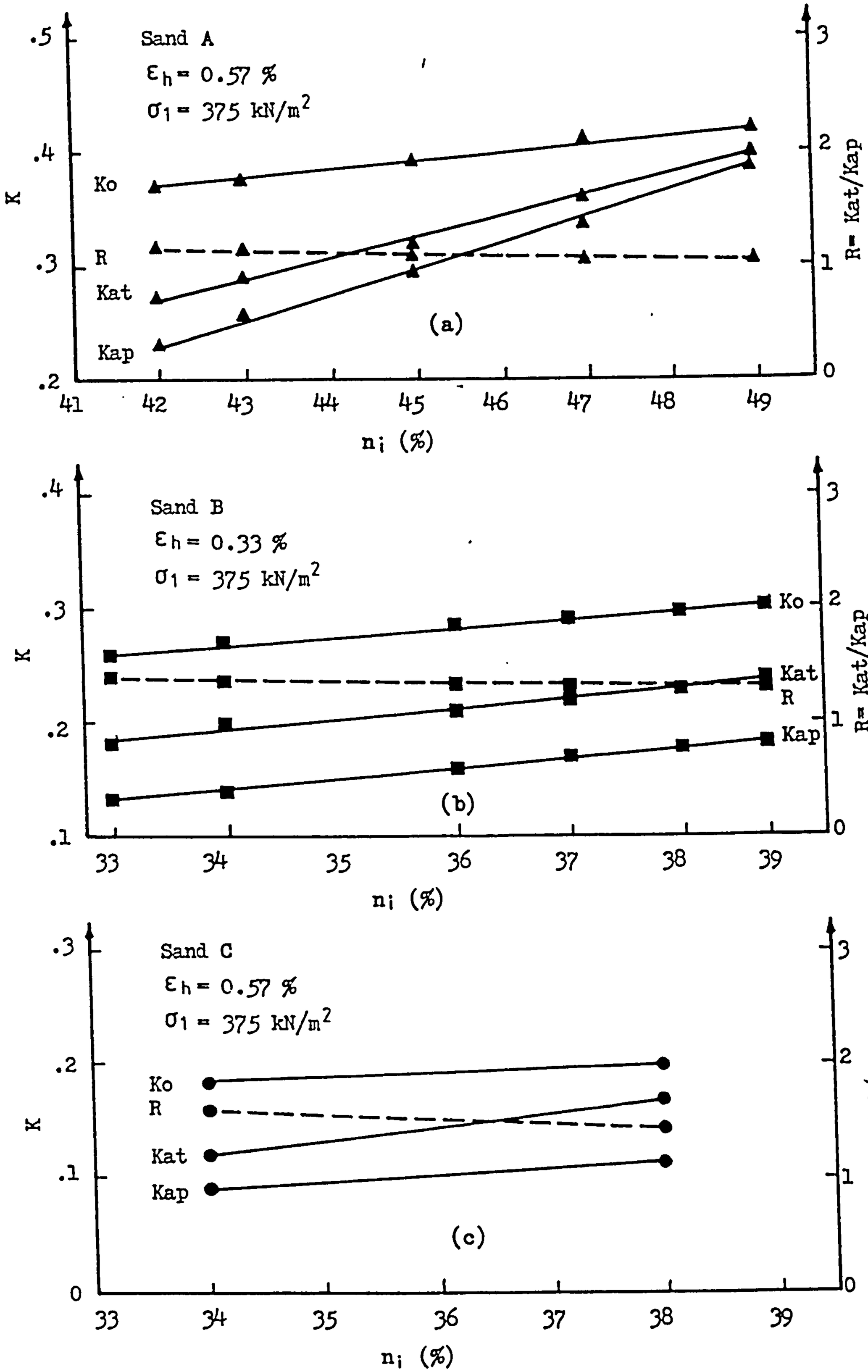

FIGURE 6.27 Variation of Ko, Kat and Kap with initial porosity of the sample under σ_1 = 375 kN/m^2 for sands A, B and C.

Type of sand			Fine (A)		Medium (B)		Coarse (C)	
States of packing			loose	dense	loose	dense	loose	dense
Ka from SCTA	Plane strain test	Ka(minimum)	0.36	0.20	0.16	0.13	0.04	0.01
		Ka(maximum)	0.39	0.23	0.18	0.13	0.11	0.09
	Triaxial test	Ka(minimum)	0.37	0.23	0.22	0.18	0.06	0.02
		Ka(maximum)	0.40	0.27	0.24	0.18	0.17	0.12
Ka from a model study of the retaining wall, Kirk (1967)			0.22	0.29	0.19	0.27	0.17	0.25
Ka from empirical and theoretical works	Coulomb (1773)		0.28	0.18	0.31	0.18	0.35	0.21
	Rankine (1857)		0.28	0.18	0.29	0.19	0.36	0.22
	Ohde (1938)		0.26	0.21	0.25	0.21	0.21	0.19
	Rowe (1954)		0.21	0.16	0.21	0.16	0.21	0.16
	Janbu (1957)		0.27	0.12	0.22	0.13	0.18	0.13
	Caquot and Kerisel (1966)		0.25	0.13	0.23	0.14	0.19	0.13
	Reimbert (1974)		0.20	0.12	0.21	0.12	0.25	0.15

TABLE 6.6 Ka obtained from the SCTA and other experimental, empirical and theoretical works.

CHAPTER SEVEN

DISCUSSION OF THE CYCLIC TEST RESULTS

7.1 INTRODUCTION

The cyclic tests carried out in the SCTA are similar to the monotonic tests in the preparation of the test specimen, application of the different constraint conditions and measurements of the stresses and strains at the boundaries of the sample. The only difference is in the application of the vertical stress on the sample. In this series of tests, as described in chapter 5, instead of applying the vertical stress up to a maximum level as in the monotonic tests, it is applied cyclically at a constant frequency and amplitude in each test for a certain number of cycles.

As described before, the direction of the principal stresses and strains change during this series of tests and so σ_v, σ_{h1}, σ_{h2}, ε_v, ε_{h1} and ε_{h2} are used to denote the principal stresses and strains rather than σ_1 etc.. In the confined and triaxial tests in which $\varepsilon_{h1} = \varepsilon_{h2}$ and as a result $\sigma_{h1} = \sigma_{h2}$ the lateral strains and stresses are denoted by ε_h and σ_h.

The cyclic tests were carried out on the medium sand (group B) only and so a comparison can only be made between the results of these tests and the monotonic tests carried out on the same sand although it would be reasonable to expect the general pattern of behaviour to apply to the

other sands.

7.2 CONFINED TESTS

In this series of tests 150 mm cubic samples were tested under a sinusoidal loading at different frequencies, amplitudes and number of cycles under Ko conditions. Lateral stresses and vertical strains of the samples were continuously measured during the experiment. The tests were carried out at the two states of packing of the sand i.e. the densest (n_i=33%) and the loosest (n_i=41%) conditions possible for this sand in the laboratory using the raining technique.

The elastic and plastic deformations of the sand during loading can easily be measured and detailed information on the behaviour of the sand obtained is discussed in the following sections.

7.2.1 VERTICAL STRAINS IN Ko CONDITIONS

Typical variations of the vertical strains of the samples under cyclic confined tests are shown in figures 5.1 and 5.2 for the densest and loosest conditions and the general response was discussed in chapter 5. As described in section 5.3.1, within the first cycle of the vertical stress, ε_v cycles as well but it never returns to its initial value and some irrecoverable strain occurs. That part of the total vertical strain which is recovered after the removal of the load is the elastic strain and is denoted by ε_{ve}, and that part which is permanent is the plastic strain and is denoted by ε_{vp}.

7.2.1.1 THE EFFECT OF THE FREQUENCY OF THE LOAD ON ε_v

The influence of the frequency of the cyclic loads on

the vertical strain of the samples was investigated in chapter 5 by comparing the tests results on the densest and loosest samples of the sand at different frequencies (figures 5.3 to 5.10). In figure 7.1 the variations of the maximum and minimum values of the vertical strain are plotted against the frequency of the cyclic loads for the densest and loosest conditions. These values are those measured after the application of the first and 45th cycles of the load on the samples at a constant amplitude.

From figure 7.1 it is clear that ε_v does not depend on the frequency of the loading. The vertical strains are expected to be independent of the frequency of the loads within the ranges tested in this research as the tests are performed on dry samples. The main factor that determines whether the rate of loading is a critical parameter is the time taken for the soil skeleton to respond to a change in load and for the sand grains to move to a new stable position. For saturated samples under drained conditions the rate of loading has a great influence on the vertical strain of the sand particularly if the material consists of fine particles and consequently has a low permeability. Nevertheless when the samples are dry, except for the loads with high frequency which impact the soil or for vibrations, as the load is applied the grains move to a denser packing and pore air pressure effects are negligible. The creep of the sand under such loadings, i.e. with low frequency, does not seem to be considerable although the evidence is limited.

7.2.1.2 THE EFFECT OF THE AMPLITUDE OF THE LOAD ON ε_v

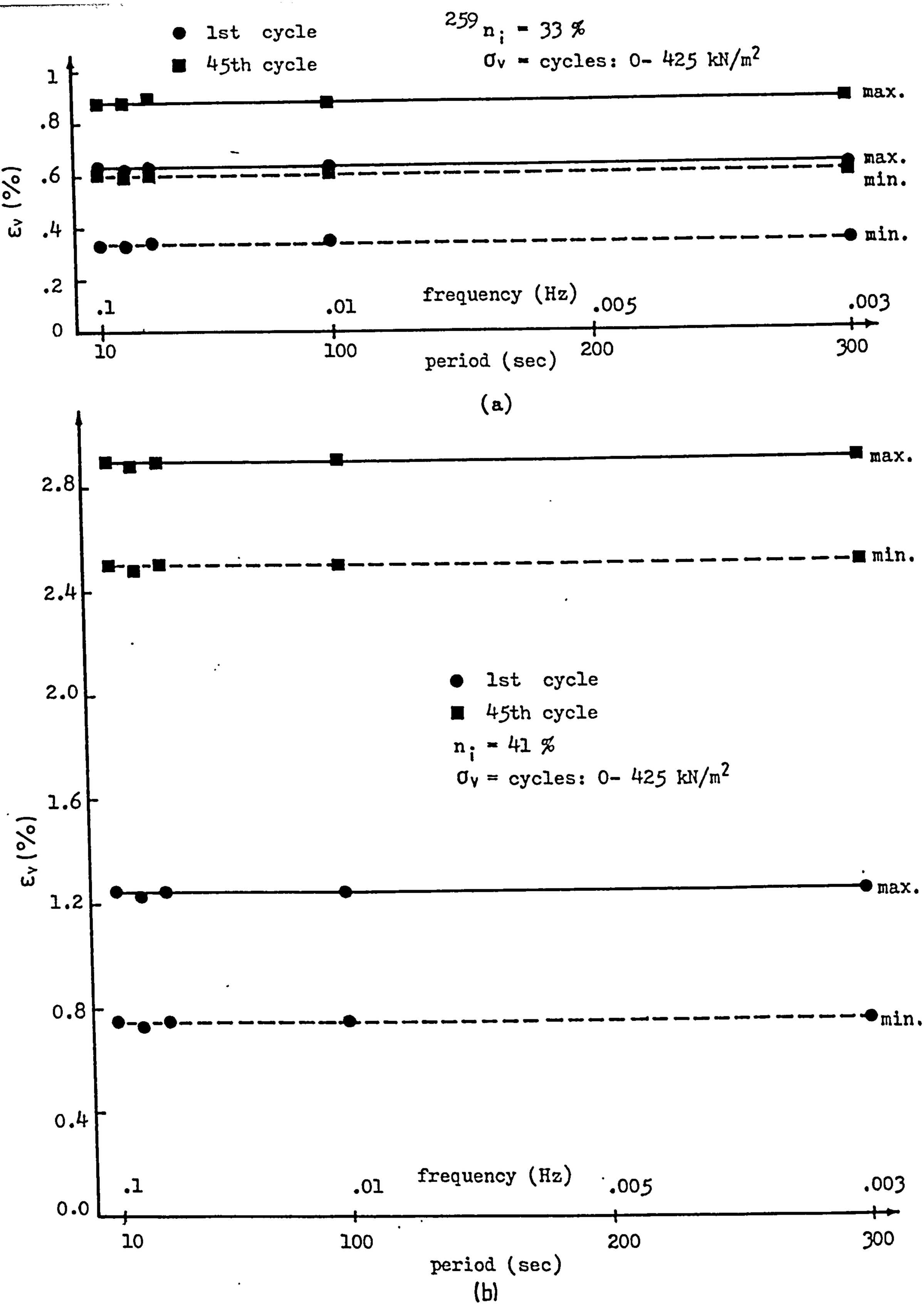

FIGURE 7.1 Variation of the maximum and minimum values of ε_v with frequency of the load cycles at the end of the 1st and 45th cycles for dense (a) and loose (b) samples.

In chapter 5 it was found that the percentage of unloading as well as the amplitude of the cycles has a major effect on the vertical strain and both of these factors have to be taken into account when considering cyclic loadings. If the vertical stress applied to the sample cycles between $\sigma v min.$ and $\sigma v max.$ the percentage of unloading is defined as follows:

$$\text{percentage of unloading} = \frac{\sigma v max. - \sigma v min.}{\sigma v max.} \times 100$$

In figure 7.2 the differences between the maximum and minimum values of the Vertical Strain, are plotted against the percentage of unloading at a constant amplitude (a and b) and also against the amplitude for a constant unloading percentage (c). From this figure it is clear that the effect of the cyclic loads on the vertical strain increases with both increasing amplitude and unloading percentage. The effect is greater on the loose samples than on the dense samples.

When a sample is loaded the sand grains are compressed and forced to move into a denser packing. As a result the vertical strain increases from zero to a maximum level depending on the peak value of the vertical stress. When unloading commences due to the compressibility of the grains, part of the vertical strain recovers. The greater the percentage of unloading, the more grains are free to recover. Increasing the amplitude of loading at a constant unloading percentage, which means increasing $\sigma v max.$, causes the particles to be compressed more. Therefore when unloading takes place $\varepsilon v max. - \varepsilon v min.$ for the sample subjected to a greater amplitude of loading is higher than in those sub-

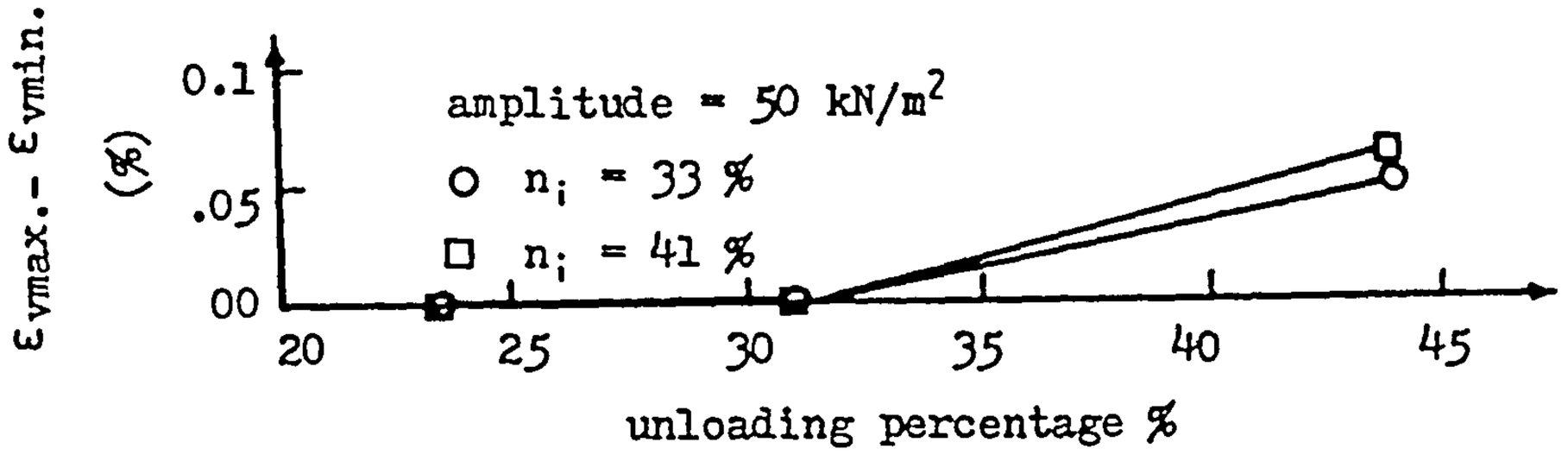

(a)

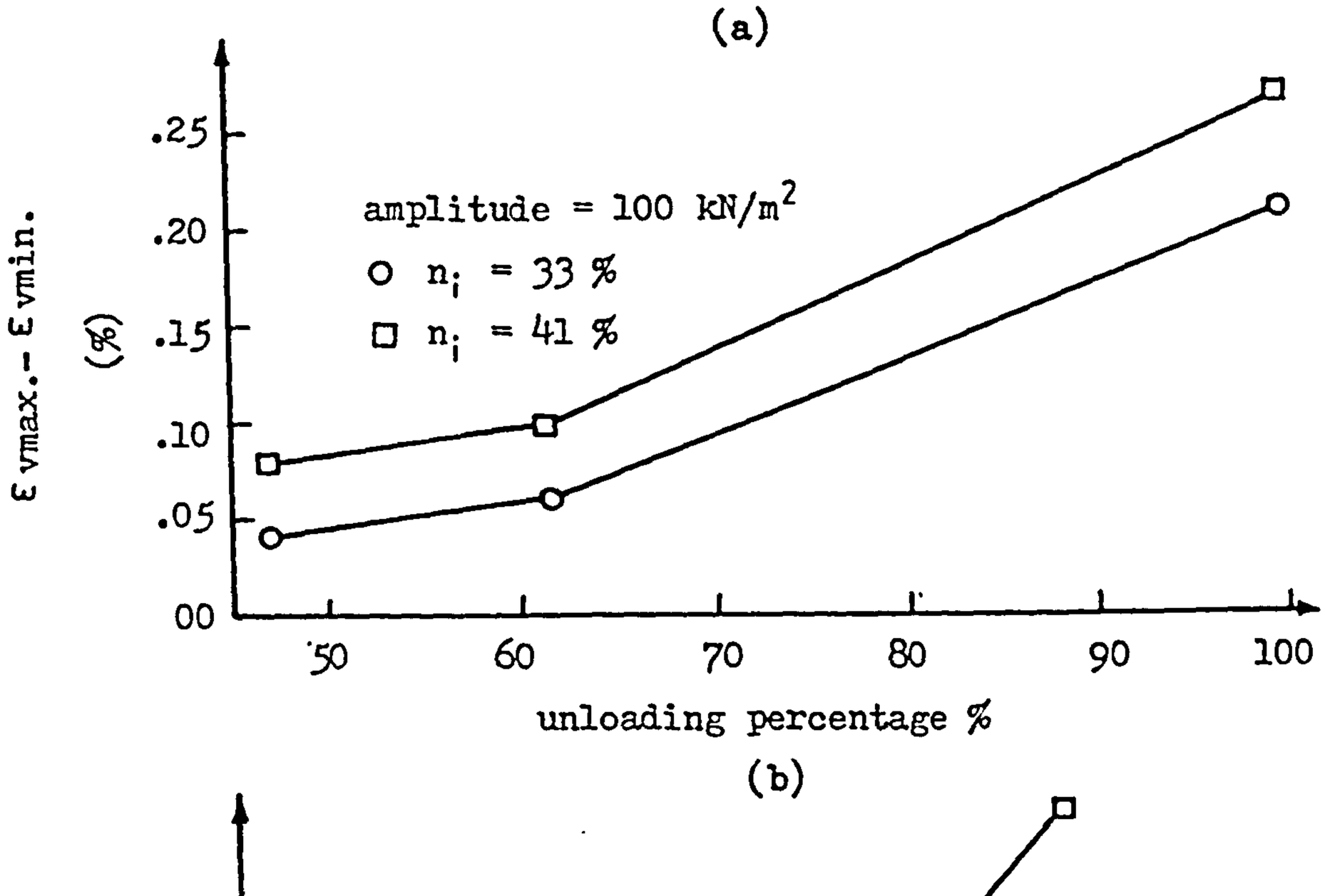

(b)

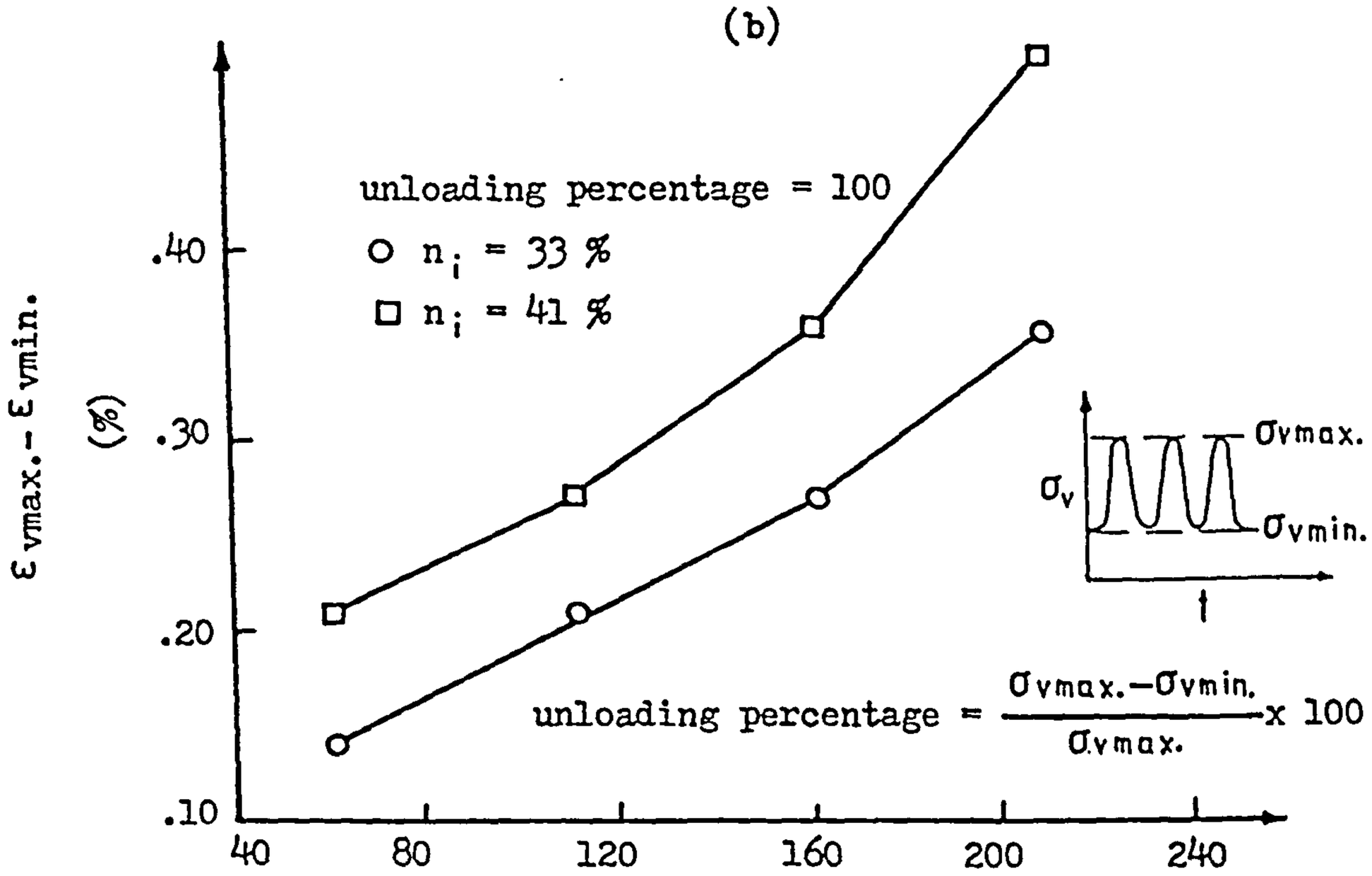

(c)

FIGURE 7.2 Variation of ($\varepsilon_{vmax.} - \varepsilon_{vmin.}$) with unloading percentage (a & b) and amplitude (c) of the cyclic loads for dense and loose samples.

jected to lower amplitude.

7.2.1.3 ELASTIC AND PLASTIC COMPONENTS OF THE VERTICAL STRAIN IN Ko CONDITIONS

The effects of the number of load cycles on Ev are shown in figures 5.20 and 5.21 which were discussed in chapter five. In figure 7.3 the elastic and plastic components of the vertical strain and also the total plastic strain are plotted against the number of load cycles for both dense and loose samples. From the figure it is evident that the elastic and plastic strains are initially approximately equal. However, as the cycling continues the incremental plastic strain decreases sharply while the elastic strain remains nearly constant. Eventually the plastic strain per cycle becomes almost negligible. It can be seen from figure 7.3 (a and b) that after a series of cycles, the incremental plastic strain for both dense and loose samples becomes nearly zero, whereas the elastic strain stabilizes at about 0.24% and 0.28% for the dense and loose samples respectively. This behaviour can be explained as follows.

When sand samples are subjected to a vertical stress under Ko conditions , the individual particles are compressed and deformed while the whole mass is forced to move into a denser packing by the grains sliding relative to each other. These two phenomena which occur simultaneously result in an increase in the vertical strain proportional to the maximum value of the vertical stress and the initial porosity of the sample. When unloading takes place the individual particles return to their initial shape as much as possible depending on the unloading percentage and elastic

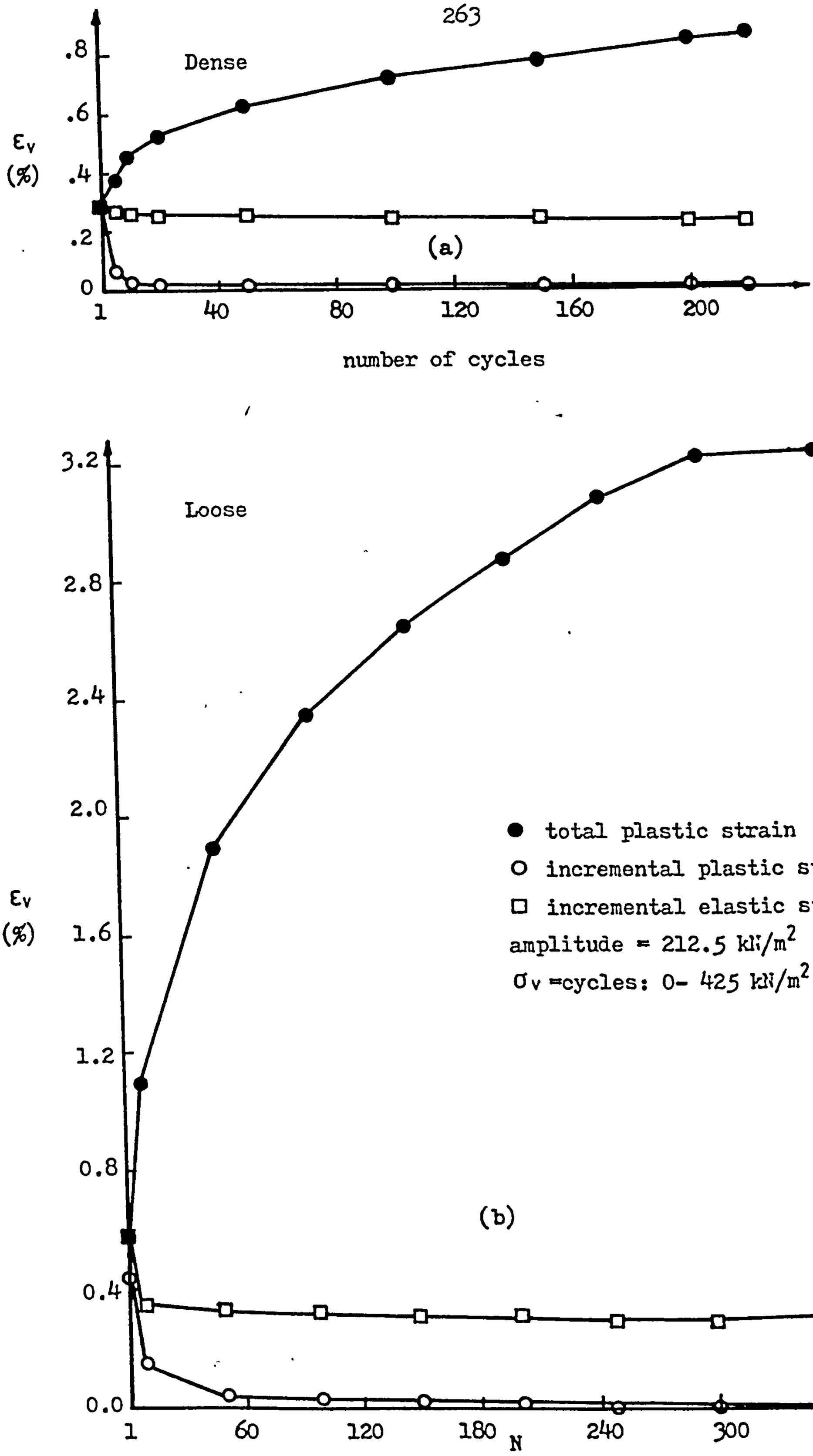

FIGURE 7.3 Variation of the elastic and plastic components of the vertical strain with number of load cycles for dense (a) & loose (b) samples.

properties of the grains. This will cause a recovery of part of the vertical strain. This part which is attributed to the elastic deformations of the sand is called the elastic component (ε_{ve}). The other part of the vertical strain which is due to the sliding of the grains is permanent and is called plastic strain (ε_{vp}). This component can also be caused by the crushing or plastic deformation of the particles. However under the ranges of the vertical stress (0-450 kN/m^2) applied in this investigation it is unlikely to happen. When the sample is reloaded the new increment of the elastic strain is of almost the same magnitude as before while the incremental plastic strain decreases sharply due to the new denser packing of the mass after the previous cycle. On the second unloading the elastic strain is recovered but the new increment of the plastic strain remains and is additional to the previous increment. As a result the sample becomes even denser and the total plastic strain builds up. As the cycling continues, in each cycle of the load the elastic component of the vertical strain is approximately constant but the incremental plastic strain decreases sharply. The total plastic strain of the sample increases particularly for the loose sample but the rate decreases as the sample becomes denser.

Although the elastic strain increment of the sample usually depends on the level of the vertical stress and on the compressibility of the grains for a particular sand, according to the results of this series of cyclic tests, the initial porosity of the sample seems to have some considerable effect as well. For the same sand under the same cyclic

load the elastic strain of the loose sample is found to be 17% greater than that of the dense sample. This increase may be attributed to the smaller number of contact points of the particles in the loose sample which causes greater stresses on the grains. On the other hand when the sample is dense the number of contact points increases and the stresses on these points of contacts are smaller. Therefore the grains are less deformed and the elastic strain is smaller. This argument can be applied to explain the small decrease which occurs in the elastic strain of each sample over cycles of the load.

7.2.1.4 SECANT MODULUS OF THE SAND IN Ko CONDITIONS

The secant modulus (D) of the stress strain curves of the sand under confined conditions at different cycles of load are plotted in figures 7.4 and 7.5 for dense and loose samples. These values are calculated from the slopes of lines joining the desired point and the $\sigma v=0$ point of each curve. As can be seen from the figures, in the first cycle of the load, values of D during loading are significantly smaller than those during unloading. However, the differences between unloading and loading values of D decrease as the number of cycles increases. After application of 50 cycles of load to the dense sample and about 100 cycles to the loose sample the secant modulus for both loading and unloading becomes equal and the sand behaves like an elastic material.

Although the behaviour of the samples after the application of several cycles of load is quite elastic, the stress strain relationship can not be approximated by a

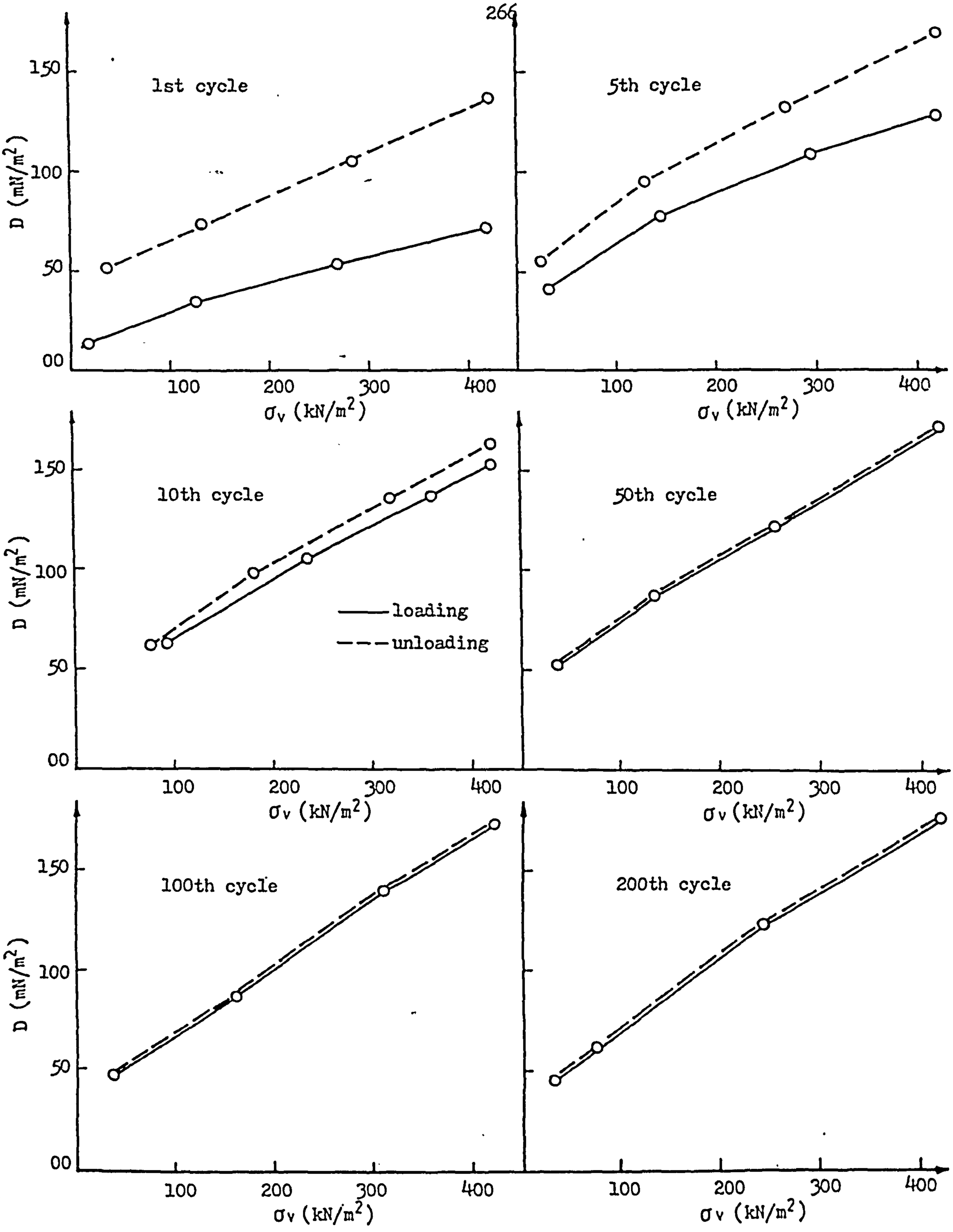

FIGURE 7.4 Variation of the Secant modulus with the vertical stress and number of load cycles for the dense sample of sand B.

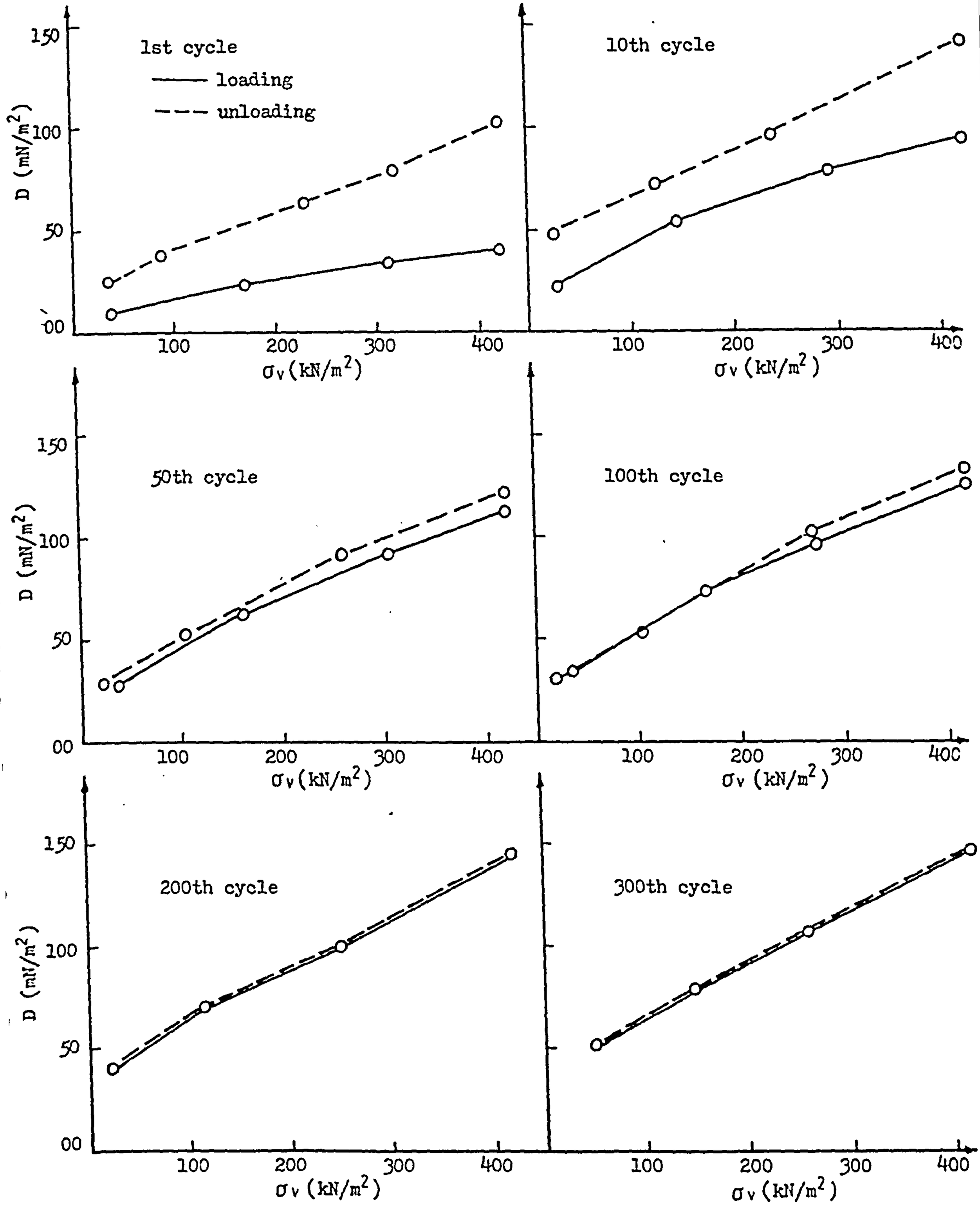

FIGURE 7.5 Variation of the Secant modulus with the vertical stress and number of load cycles for the loose sample of sand B.

linear model even at this stage because of significant changes that occur in the secant modulus. Instead, the values of D seem to increase almost linearly on increasing the vertical stress for σv above 50 kN/m^2, and can be related to σv by the following equation:

$$D = a + b\,\sigma v \qquad (7.1)$$

a and b are constants that can be found from the test data at this stage (pure elastic response). For the medium sand used in these tests a and b are found to be 38.0 and 0.35 for the dense and 37.5 and 0.27 for the loose conditions, where σv is in kN/m^2 and D in MN/m^2. According to this result the sand can be defined as a material which has non-linear elasto-plastic behaviour under primary loading but becomes non-linear elastic under successive cyclic loadings.

7.2.1.5 THE CHANGES OF POROSITY OF THE SAMPLES IN Ko CONDITIONS

The change in volume of the sand samples under Ko conditions is similar to the vertical strain response since no lateral strains are permitted in these experiments. Therefore the changes in the porosity of the samples which occur can be directly calculated from the vertical strains. In the cyclic confined tests the volume of the specimen decreases due to an increase in the total plastic strain after the application of a certain number of load cycles.

In figure 7.6 the changes in the porosity of the dense (a) and loose (b) samples with load cycles are shown. The porosity of the dense sample changes from 33% to 32.4%, a decrease of 1.8% after the application of 215 cycles of

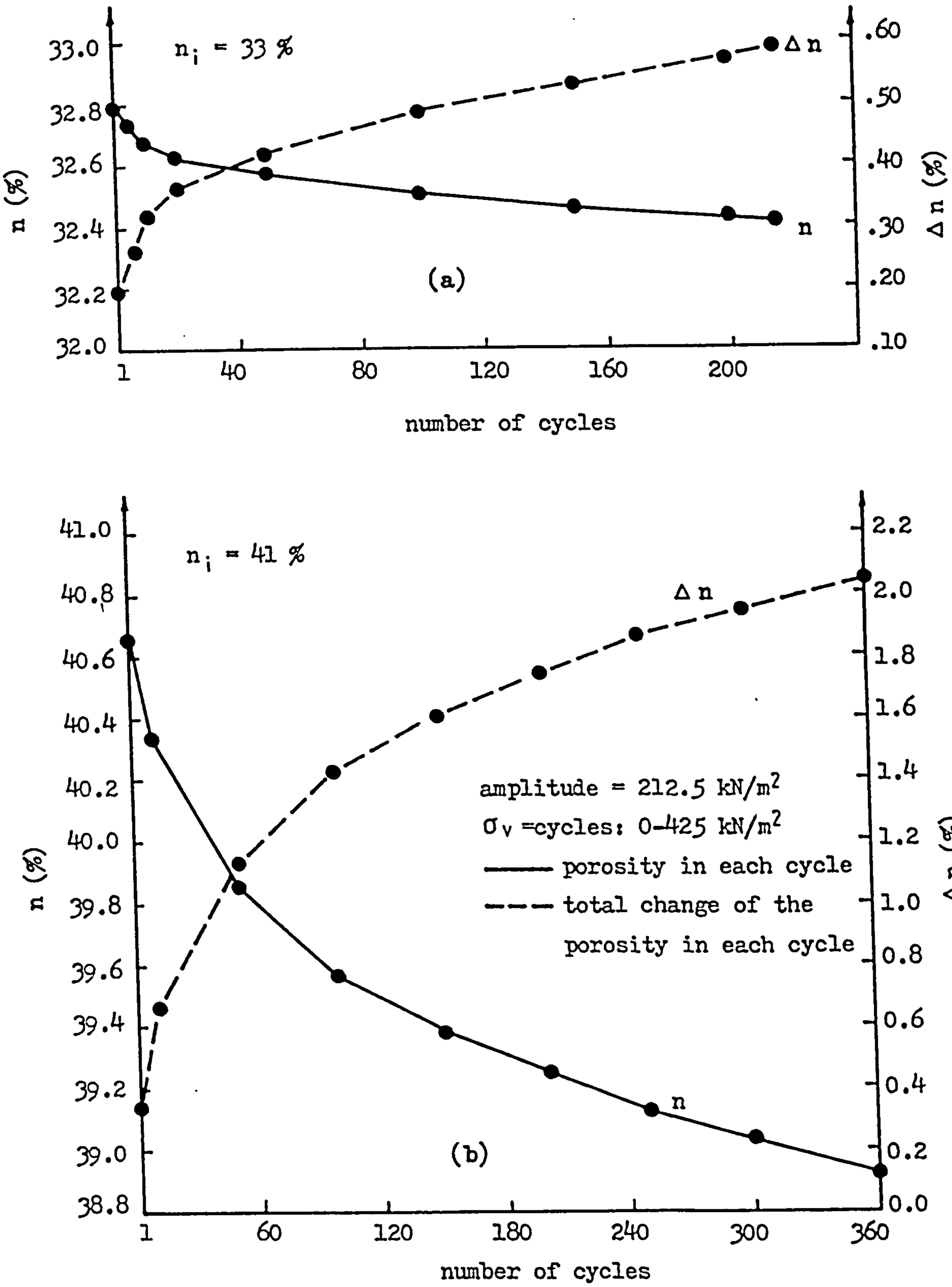

FIGURE 7.6 Changes in the porosity of the sample due to application of cyclic vertical loads in confined conditions for both dense (a) and loose (b) samples.

load while the porosity of the loose sample over the same number of cycles changes from 41% to 39.2%,a decrease of 4.4%. Continuing the application of the cyclic loads on the loose sample up to 360 cycles results in a further decrease of 1.6% , a total decrease of about 6% over 360 cycles of load.

It was thought that the loose sample may achieve the same density as the initially dense sample given a sufficient number of load cycles. During this series of tests it was found that the porosity of the sample does not change so rapidly and that the rate of change significantly decreases as the number of cycles increases. This behaviour is due to the decreasing rate of increase of the total plastic strain as discussed in the previous section. Thus it seems to be very difficult to achieve the same density as the initially dense sample by the application of cyclic vertical stresses only. The major factor in causing compaction in sand has been found to be cyclic shear stresses [65 and 66] rather than vertical stress.

7.2.1.6 COMPARISON OF CYCLIC AND MONOTONIC Ko TEST RESULTS

To compare the vertical strains of cyclic confined tests with those of monotonic tests under the same level of vertical stress the results of both types of test are shown in figure 7.7. In this figure the maximum values of the vertical strain in the first and also 70th cycles of load are plotted against the peak values of the applied vertical stress. The results are from tests carried out on the densest and loosest samples under monotonic and cyclic loadings. From the figure it can be seen that the maximum

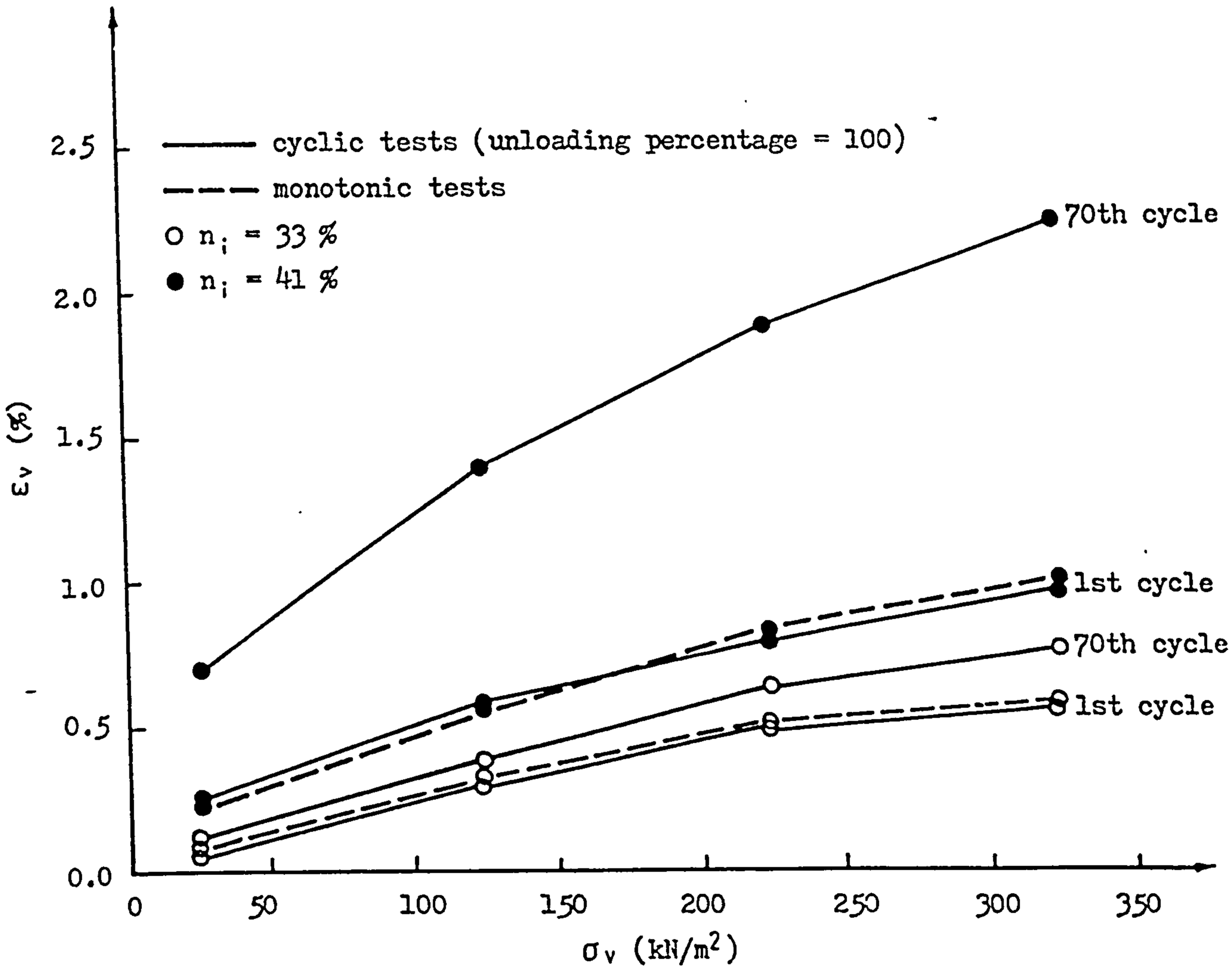

FIGURE 7.7 Comparison between the monotonic and cyclic test results under the same level of the vertical stress for dense and loose samples.

values of the vertical strain in the first cycle of loading are nearly the same as those of the monotonic tests. However, as the cycling continues on the sample, the strains in the cyclic tests increase and exceed those of the monotonic tests. The differences between monotonic and cyclic tests results increase on increasing the number of cycles and also on increasing the level of the vertical stress. From the figure it is also clear that the initial porosity of the sample has a great effect on the differences induced between the results of the monotonic and cyclic tests at higher numbers of cycles. The differences between ε_v induced under $\sigma_1=325\ kN/m^2$ in the monotonic tests and the 70th cycle of the cyclic tests for dense samples is about 0.15% strain. This figure for the loose sample increases to about 1.25%, i.e. it becomes about 8 times greater than that in the dense sample.

7.2.2 LATERAL STRESSES IN Ko CYCLIC TESTS

Typical variations of the lateral stresses under cyclic vertical stress loading in confined conditions are shown in figures 5.1 and 5.2. As described in section 5.3.1 the lateral stresses of the sand samples vary between maximum and minimum values in each cycle of load. As the number of cycles increases these maximum and minimum values get closer and after a series of cycles they become virtually constant. The various factors affecting the lateral stresses of the samples under cyclic loading conditions and also explanations of the sand response are discussed in the following sections.

7.2.2.1 THE EFFECT OF THE FREQUENCY OF THE LOAD CYCLES ON σ_h

In figure 7.8 the maximum and minimum values of the lateral stresses at the end of the 1st and also 45th cycles of the loads are plotted against the frequencies used in these tests for dense (a) and loose (b) samples (full results are given in figures 5.3 to 5.10). As can be seen there are no significant changes in the maximum and minimum values of the lateral stresses over the ranges of frequencies used in these experiments.

Since the frequency of the loading used also had no effect on ε_v (section 7.2.1.1) it can be concluded that the stress strain behaviour of dry sand is independent of the frequency of the loads over the ranges tested.

7.2.2.2 THE EFFECT OF THE NUMBER OF THE LOAD CYCLES ON σ_h

Variations of the lateral stresses with the number of load cycles for dense and loose samples are shown in figures 5.11 and 5.12. In figure 7.8 maximum and minimum values of the lateral stresses at the end of the 1st and 45th cycles are plotted. It was explained in section 5.3.3 that the maximum values of the lateral stresses decrease whereas their minimum values increase on increasing the number of load cycles.

In section 7.2.1.3 it was shown that as the cycling continues the total plastic strain increases and causes the sample to become denser. In the monotonic confined tests it was found that when the porosity of the sample decreases the lateral stress for a particular vertical stress decreases as well. As a result the decrease in the maximum values of the lateral stresses may be attributed to the decrease in the

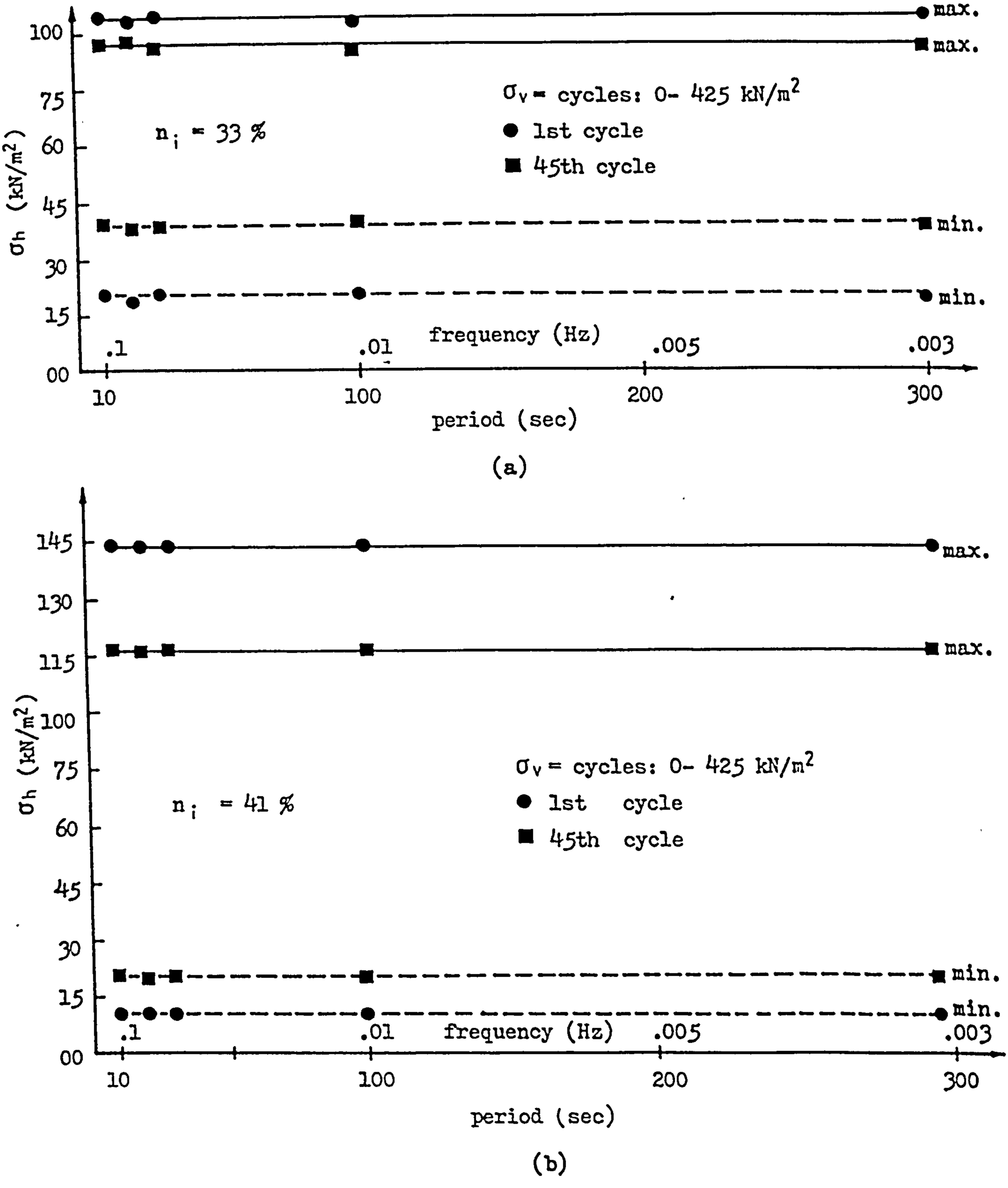

FIGURE 7.8 Variation of the maximum and minimum values of σ_h with frequency of the load cycles at the end of the 1st and 45th cycles for dense (a) and loose (b) samples.

porosity of the sample which occurs as the number of cycles increases.

For the increase in the minimum values of the lateral stresses another argument may be used. On the application of the first cycle of the vertical stress, the lateral stresses increase almost linearly from zero up to a maximum value proportional to the peak value of the vertical stress in the loading portion of the cycle. When unloading commences, the lateral stresses recover with a slower rate than on loading. At complete unloading ($\sigma v=0$) some lateral stresses still remain in the mass ($\sigma_h \neq 0$). This may be due to reversal of the direction of the frictional forces occurring during unloading at the contact points between the particles. As cycling continues the sample becomes denser, as a result the contact areas and the frictional forces increase and the locked in lateral stresses thus increase.

The change in the maximum values of the lateral stresses over 45 cycles of loads shown in figure 7.8 for the loose sample is about 4.4 times greater than that for the dense sample. This can be attributed to the greater compressibility of the loose sample. However, the change in the minimum values of the lateral stresses is in the opposite direction to that of the maxima. This change for the dense sand is twice that for the loose sand over 45 cycles of load application.

7.2.2.3 THE EFFECT OF THE AMPLITUDE OF THE LOAD CYCLE ON σ_h

The influence of the amplitude of the cyclic load on the lateral stresses of sand samples under Ko conditions has been discussed in section 5.3.4 and figures 5.13 to 5.19.

The differences between maximum and minimum values of the lateral stresses are plotted against amplitude and also against unloading percentage in figure 7.9.

From this figure it can be seen that at a constant amplitude as the unloading percentage increases the effect of the cyclic loads increases as well. Also for a constant unloading percentage [figure 7.9(c)] as the amplitude of the cyclic loads increases, the values of $\sigma_{hmax.}-\sigma_{hmin.}$ increase approximately linearly for both dense and loose samples. The effect of the cyclic loads on the lateral stresses in loose samples is always greater than in dense samples.

It can be concluded that, in a similar manner to the response of the vertical strain, both unloading percentage and amplitude of the cycles should be taken into account when the behaviour of the lateral stresses under cyclic loading are investigated. Comparing figures 7.9(a) and 7.2(a) shows that cyclic loads with an unloading percentage of less than 30% do not have any effect on the vertical strain, whereas they do have a remarkable effect on the lateral stresses. This may be argued in terms of the nature of these parameters (i.e. ε_v and σ_h). For the vertical strain $\varepsilon_{vmax.}-\varepsilon_{vmin.}$ represents the elastic strain resulting from the application of a load cycle and this depends on the elastic properties of the sand. However, the lateral stresses are the horizontal components of the resultants of the distributed σ_v and developed shear stresses between particles. Therefore it is conceivable that there will be some fluctuation in the lateral stresses even when there is only a small unloading percentage in the applied cyclic vertical

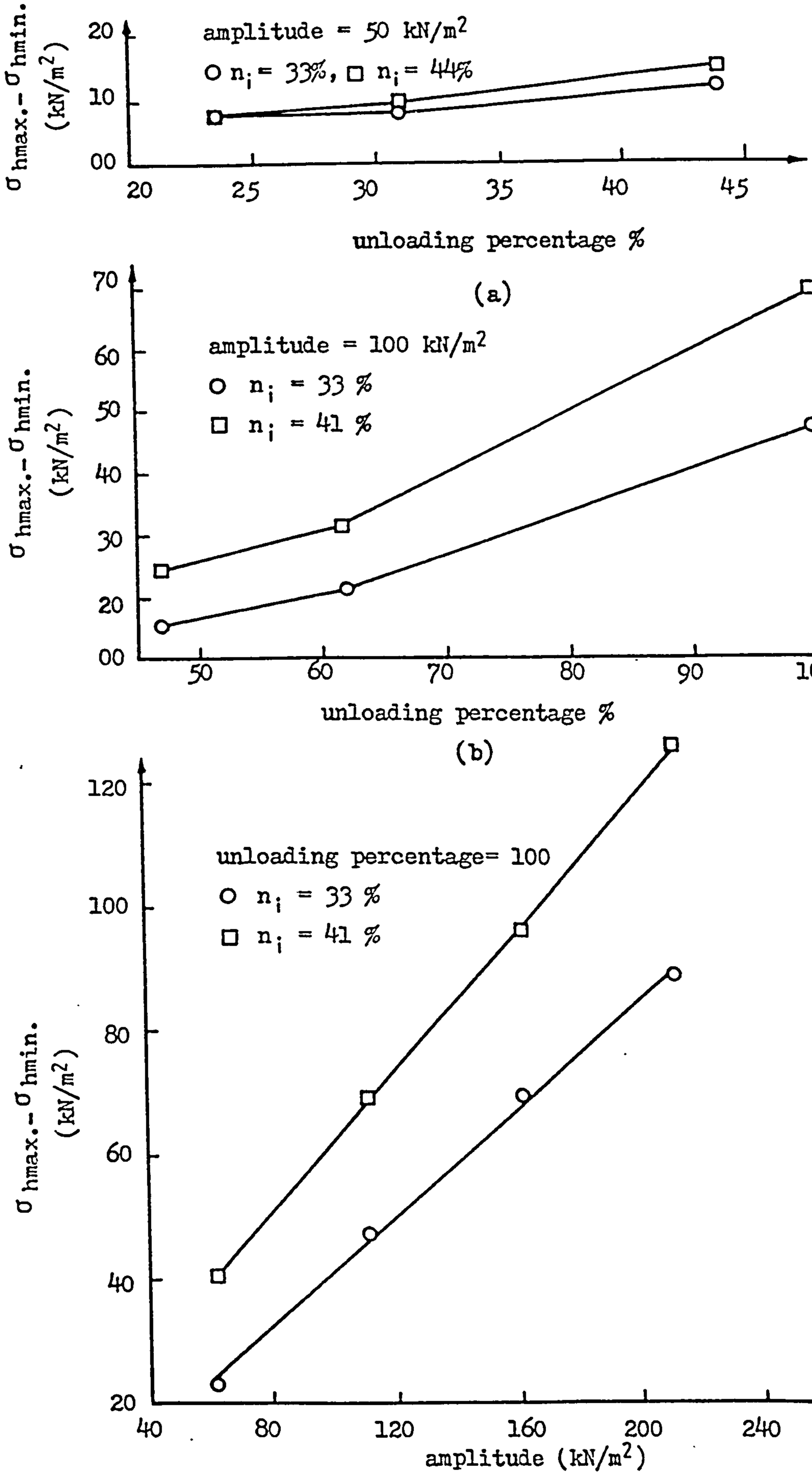

FIGURE 7.9 Variation of ($\sigma_{hmax.}-\sigma_{hmin.}$) with unloading percentage (a & b) and with amplitude (c) of the cyclic loads for dense and loose samples.

stress.

7.2.2.4 COMPARISON OF σ_h FROM CYCLIC AND MONOTONIC TESTS

To compare the lateral stresses from cyclic loading and monotonic loading tests under Ko conditions, the results of tests are plotted in figure 7.10 for the dense and loose samples. In this figure the maximum values of the lateral stresses in the 1st and 70th cycles of the load are plotted against the peak values of the applied vertical stress.

From the figure it can be seen that the maximum values of the lateral stresses in the first cycle of load for both dense and loose samples are equal to those measured ,under the same level of the vertical stress, in the monotonic tests. They all increase linearly with increasing vertical stress. The difference between the lateral stresses in cyclic and monotonic tests begins as cycling continues. In this case the maximum values of the lateral stresses for both dense and loose sample decrease as the number of cycles increases. This decrease increases on increasing the peak value of the vertical stress and on increasing the initial porosity of the sample.

7.3 CYCLIC PLANE STRAIN TESTS

As a result of the test conditions in the SCTA the samples tested are not in a continuous plane strain state (see section 5.4.1). At the begining of each step of the test, after the application of the vertical stress, a constant increment of the lateral strain is applied to one face but as the cycling on the sample continues the situation quickly changes and approximates the confined condition.

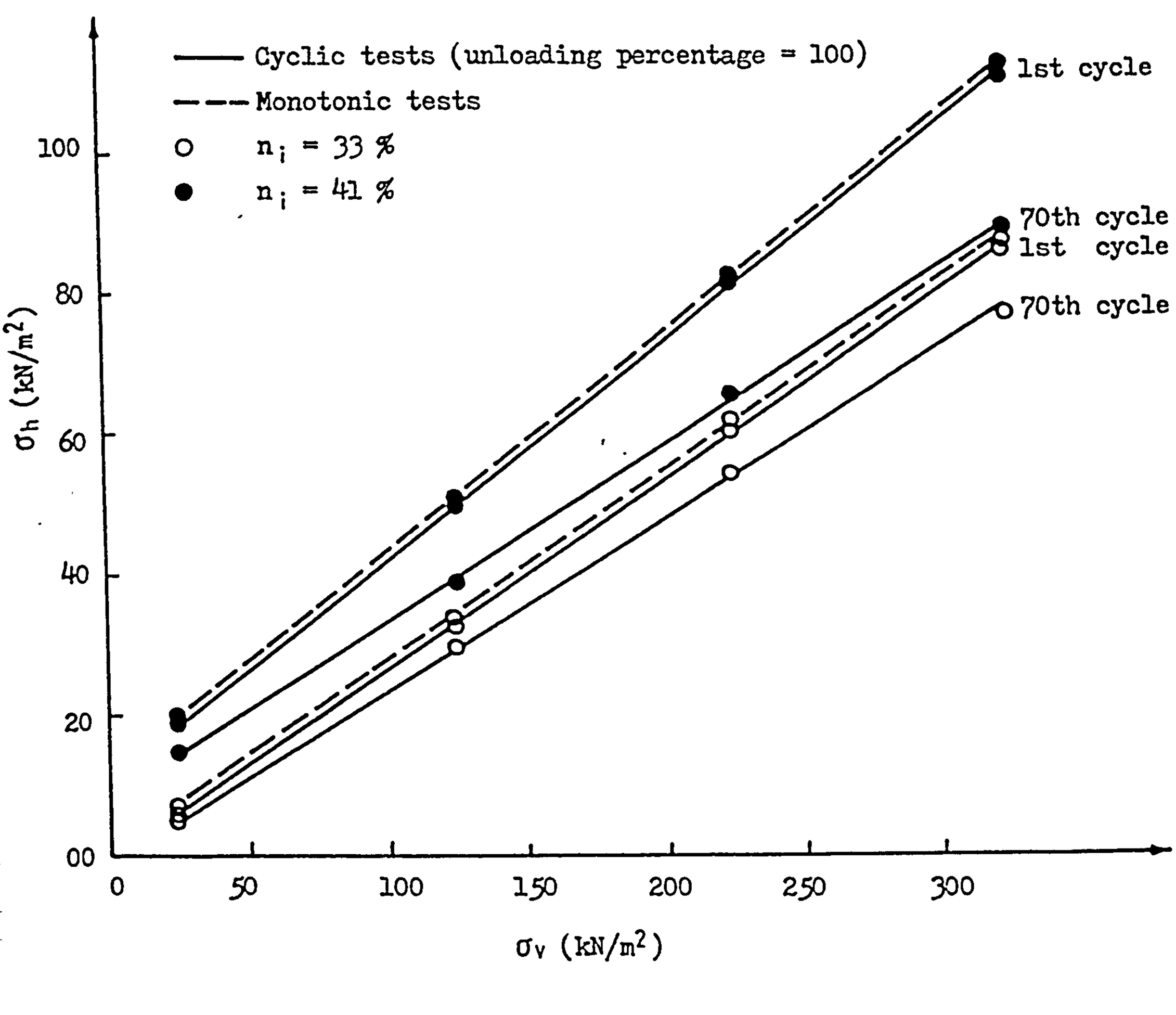

FIGURE 7.10 Comparison of monotonic and cyclic test results under the same level of the vertical stress for dense and loose samples.

This should be taken into account during the discussion of the results.

7.3.1 VERTICAL STRAIN UNDER PLANE STRAIN CONDITIONS

Vertical strains due to the application of 36 cycles of vertical stress and 0.067% lateral strain in each of the 12 steps of the cyclic plane strain test are shown in figures 5.25 and 5.26. In figure 7.11 changes in the vertical strain due to the application of the lateral strain increment for each step of the test ($\Delta\varepsilon_{vp}$) and also the porosity of the sample at these points are plotted against number of steps of tests during cyclic plane strain experiments.

From the figure it can be seen that $\Delta\varepsilon_{vp}$ decreases as the number of steps increases. The values of $\Delta\varepsilon_{vp}$ are always less than the constant increment of the lateral strain in each step. This means that when the samples are strained dilation takes place. This result is in good agreement with that obtained in the monotonic tests on the same sand in which the samples always dilated when subjected to the lateral strain.

The total decrease in $\Delta\varepsilon_{vp}$ of about 50% for dense and 60% for loose samples may be due to the decrease in the porosity of the specimens over the 12 steps of the test. This change in the porosity is about 1.8% and 4.4% for the dense and loose sample respectively. Also the greater $\Delta\varepsilon_{vp}$ induced in the loose sample compared to that in the dense sample may be due to the state of packing of the specimens.

7.3.2 LATERAL STRESSES UNDER PLANE STRAIN CONDITIONS

The variation of the lateral stresses with the number

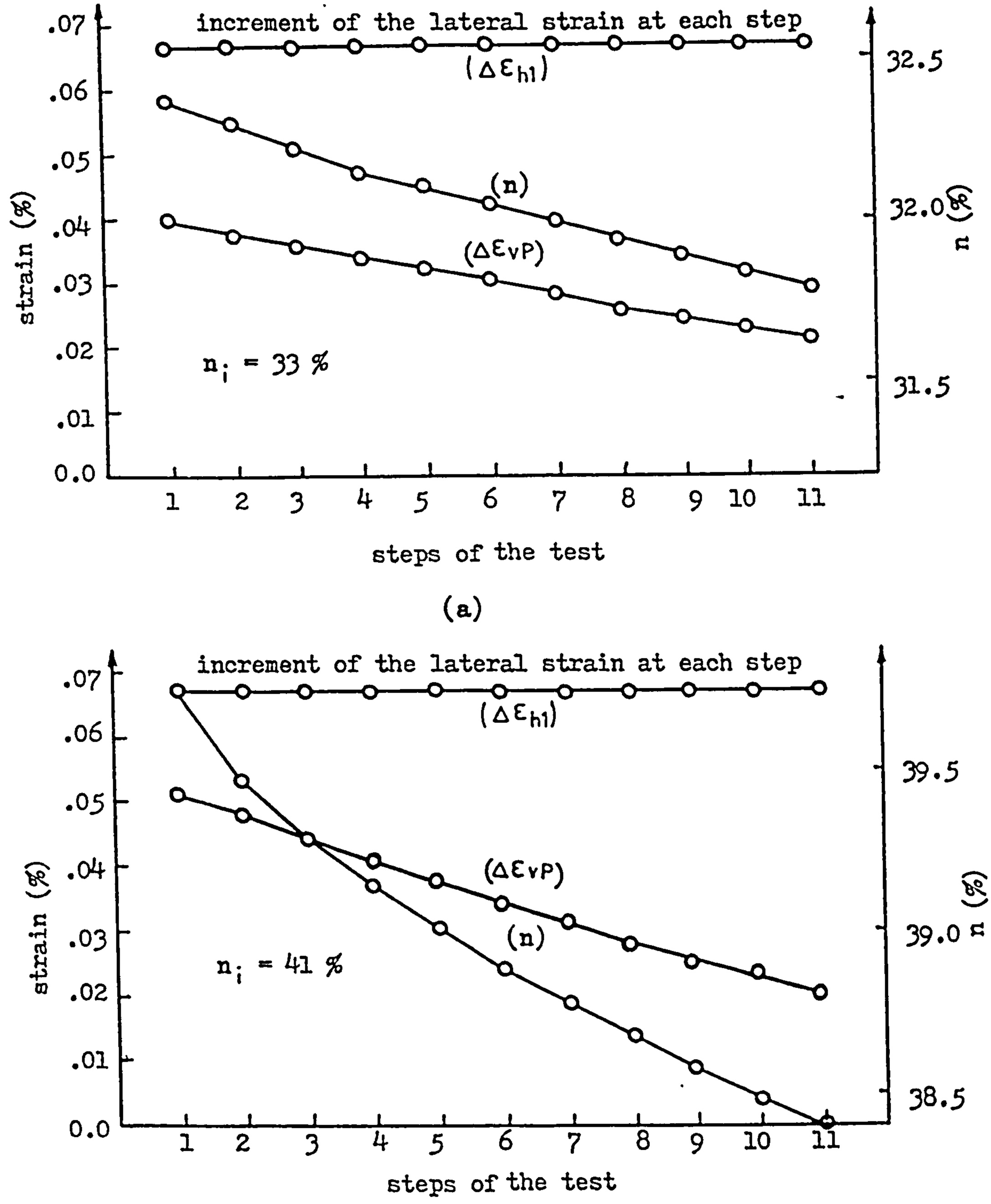

FIGURE 7.11 Porosity of the sample and the incremental vertical strain in each step of the cyclic plane strain test for dense (a) and loose (b) samples.

of cycles due to the application of the increments of the lateral strain are shown in figures 5.25 and 5.26. As explained in section 5.4.3, applying the 36 cycles of vertical stress to the samples with fixed side walls in each step of the test, results in nearly equal lateral stresses ($\sigma_{h1}=\sigma_{h2}=\sigma_h$). The maximum and minimum values of the lateral stresses before and after straining the sample at each step are plotted against the number of steps in figure 7.12 for dense and loose samples.

From this figure it can be seen that, in a similar manner to the monotonic plane strain tests, as the lateral strain is applied ($\varepsilon_h=0.\bar{0}67\%$) the maximum values of σ_{h1} decrease while the maximum values of σ_{h2} increase. This phenomenon is repeated in all steps and the amounts of decrease in σ_{h1} and increase in σ_{h2} are nearly constant over the 12 steps. As the values of the lateral stress, before straining the sample, decrease continuously the percentages decrease in σ_{h1} and increase in σ_{h2} due to the application of a constant $\varepsilon_{h1}=0.067$ % increase while the test steps are carried on.

Similar arguments to those given for the monotonic plane strain tests for the decrease of σ_3 and increase of σ_2 due to straining the samples, can be applied here for describing the cause of this phenomenon which happens in the loading portion of the cycle. The increase in the percentage decrease of σ_{h1} (from 16% to about 19% for loose and from 18% to 24% for dense samples) and in the percentage increase of σ_{h2} (from 7% to about 8.5% for dense and from 6.5% to about 7.5% for loose samples) may be attributed to the

decrease in the porosity of the samples over the 12 steps of the tests..

The values of σ_{h1min} and σ_{h2min} shown in figure 7.12 represent the variation of σ_{h1} and σ_{h2} under plane strain conditions when unloading occurs. As it can be seen both σ_{h1min} and σ_{h2min} decrease to some minimum level in each step, but σ_{h1} decreases more than σ_{h2}. This behaviour of lateral stresses in the unloading portion of the cycles can be explained as follows. As discussed in the confined cyclic tests, the lateral stresses induced due to loading the sample under Ko conditions do not recover completely when unloading occurs. For dense samples the recovery of 'locked in' lateral stresses is less than that for loose samples. In the plane strain test as the lateral strain is applied in one side, the grains tend to move towards this side but this movement cannot be done in isolation without any effect, although small, on the other side. Therefore, in this condition the locked in lateral stresses decrease sharply in the direction of straining the sample and suffer a relatively smaller decrease in the other direction. Due to this effect the minimum values of the lateral stresses become different. They might become equal if further load cycles were applied to the sample.

7.4 CYCLIC TRIAXIAL TESTS

In this series of tests carried out on the SCTA, in a similar manner to the plane strain tests, the experiments were performed in 12 steps. In each step the sample was initially subjected to 36 cycles of the vertical stress and then at the peak of the 37th cycle a constant increment of

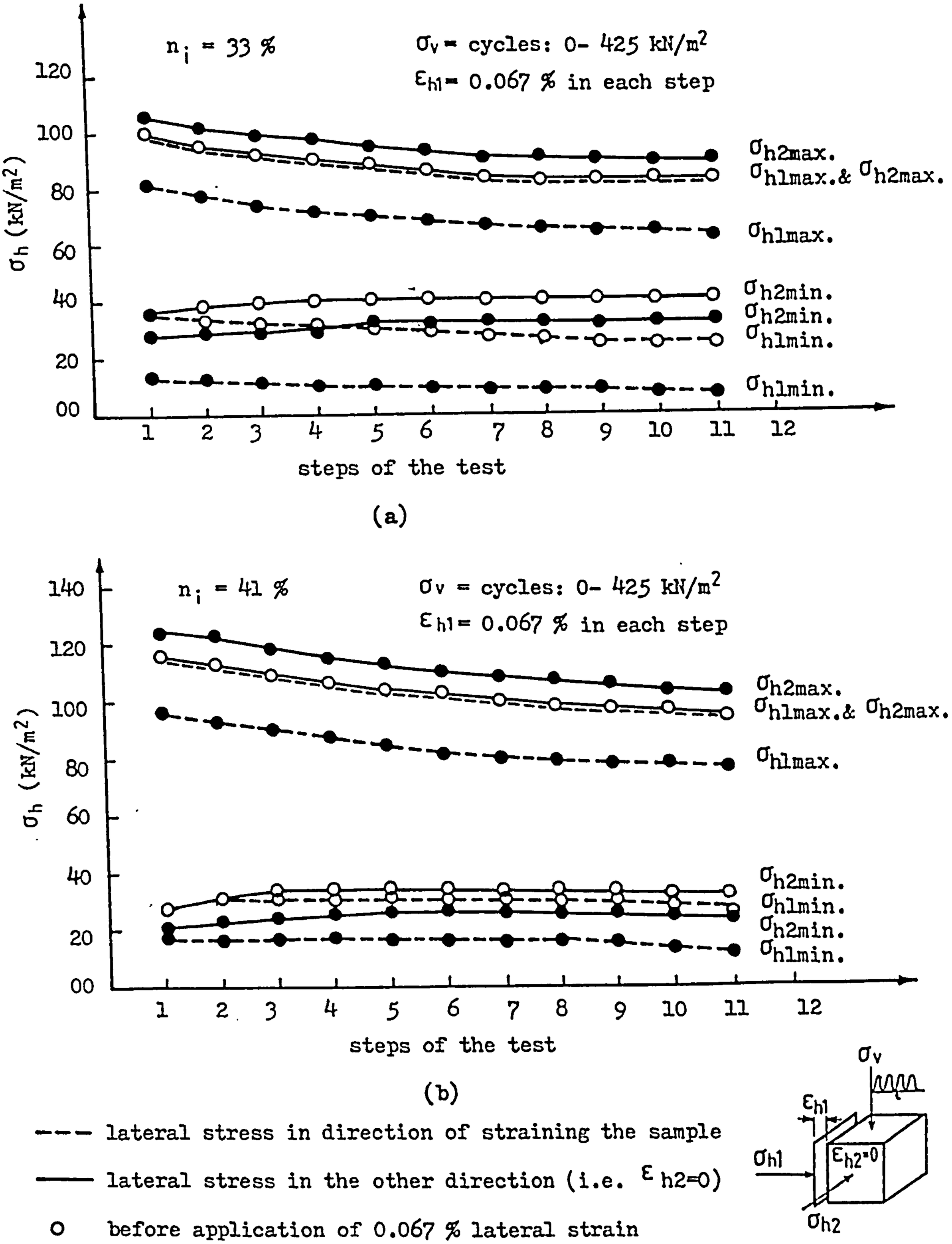

FIGURE 7.12 Lateral stress in each step of the cyclic plane strain test before and after straining the sample.

the lateral strain of 0.067% was applied in both horizontal directions. Thus the specimens should behave similarly in both lateral directions where $\varepsilon_{h1}=\varepsilon_{h2}=\varepsilon_h=0.067\%$ and theoretically $\sigma_{h1}=\sigma_{h2}=\sigma_h$.

To differentiate the vertical strains due to straining the sample in triaxial conditions from those due to plane strain conditions they are denoted by ε_{vt}, and ε_{vp} respectively. Similar suffixes are used to differentiate the lateral stresses from different constraint conditions, i.e. σ_{ht}, and σ_{hp}.

7.4.1 VERTICAL STRAIN UNDER CYCLIC TRIAXIAL CONDITIONS

Variation of the vertical strain due to the application of 36 cycles of load and straining the samples are shown in figures 5.27 and 5.28. Concentrating on the vertical strains due to the lateral straining of the samples, variations of $\Delta\varepsilon_{vt}$ with the number of steps of triaxial tests are plotted in figure 7.13 for both dense and loose samples.

From this figure it can be seen that for both dense and loose samples $\Delta\varepsilon_{vt}$ decreases approximately linearly as the number of steps increases. The horizontal line of $\Delta\varepsilon_{vt}=2\Delta\varepsilon_h$ represents the no-volume change condition due to straining the sample since a constant $\Delta\varepsilon_h$ (0.067%) was applied in each step of the test. As is apparent from the figure, for both dense and loose samples $\Delta\varepsilon_{vt}$ is below this line. This means that when the samples are strained dilation occurs. Values of $\Delta\varepsilon_{vt}$ for dense samples are smaller than those for loose samples. Thus the dilation of dense samples is greater than that of loose samples. Also the amount of

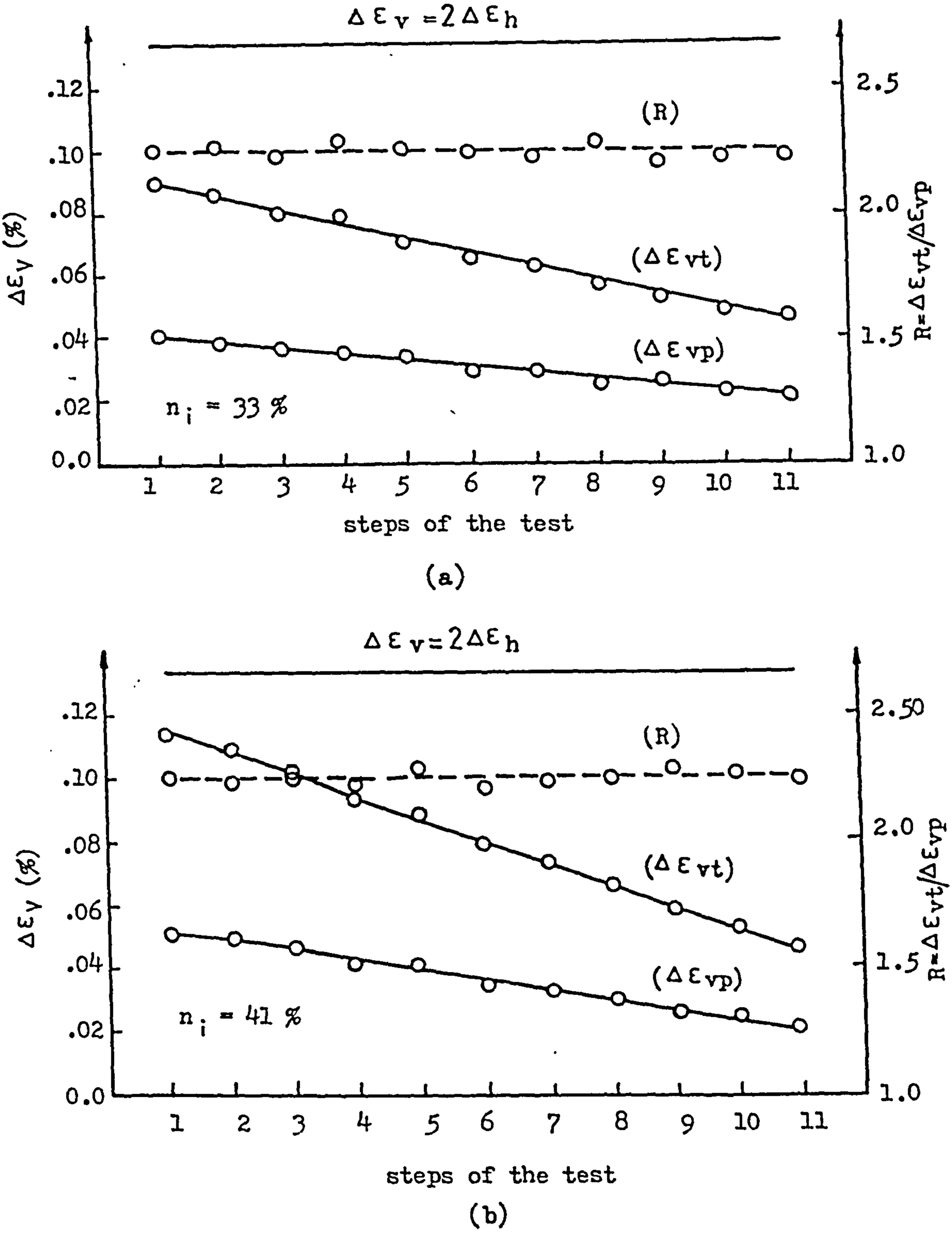

FIGURE 7.13 The incremental vertical strain in each step of the cyclic triaxial ($\Delta\varepsilon_{vt}$) and cyclic plane strain ($\Delta\varepsilon_{vp}$) tests under the same testing conditions for dense (a) and loose (b) samples.

dilation of each sample increases as the number of steps increases. This increase in dilation or decrease in the vertical strain may be related to the appreciable decrease which occurs in the porosity of the specimen over the 12 steps of triaxial tests.

7.4.1.1 COMPARISON OF ε_v FROM CYCLIC PLANE STRAIN AND CYCLIC TRIAXIAL TESTS

Figure 7.13 also shows the variation of $\Delta\varepsilon vp$ and the ratio of $\Delta\varepsilon vt/\Delta\varepsilon vp$ with the number of steps of the test for both dense and loose samples. From this figure it can be seen that the values of the vertical strain under cyclic triaxial conditions are greater than those under plane strain conditions. The ratio of $R=\Delta\varepsilon vt/\Delta\varepsilon vp$ is nearly constant at approximately 2.25 for all cases. This means that the increment of the vertical strain, in the loading portion of a cycle, due to application of a certain ε_h, in the case of triaxial is about 2.25 times greater than that in the plane strain tests. As discussed in chapter 6, the greater vertical strain than was expected (i.e. 2.25 times instead of 2 times) in the triaxial tests may be due to the effect of the lateral stress in the direction of no-lateral strain in case of plane strain test.

7.4.2 THE LATERAL STRESSES IN CYCLIC TRIAXIAL TESTS

The lateral stresses in the cyclic triaxial tests due to the application of 36 cycles of load and 0.067% lateral strain are shown in figures 5.27 and 5.28. In figure 7.14 the values of σ_h before and after straining the sample in each step are plotted against the number of test steps for

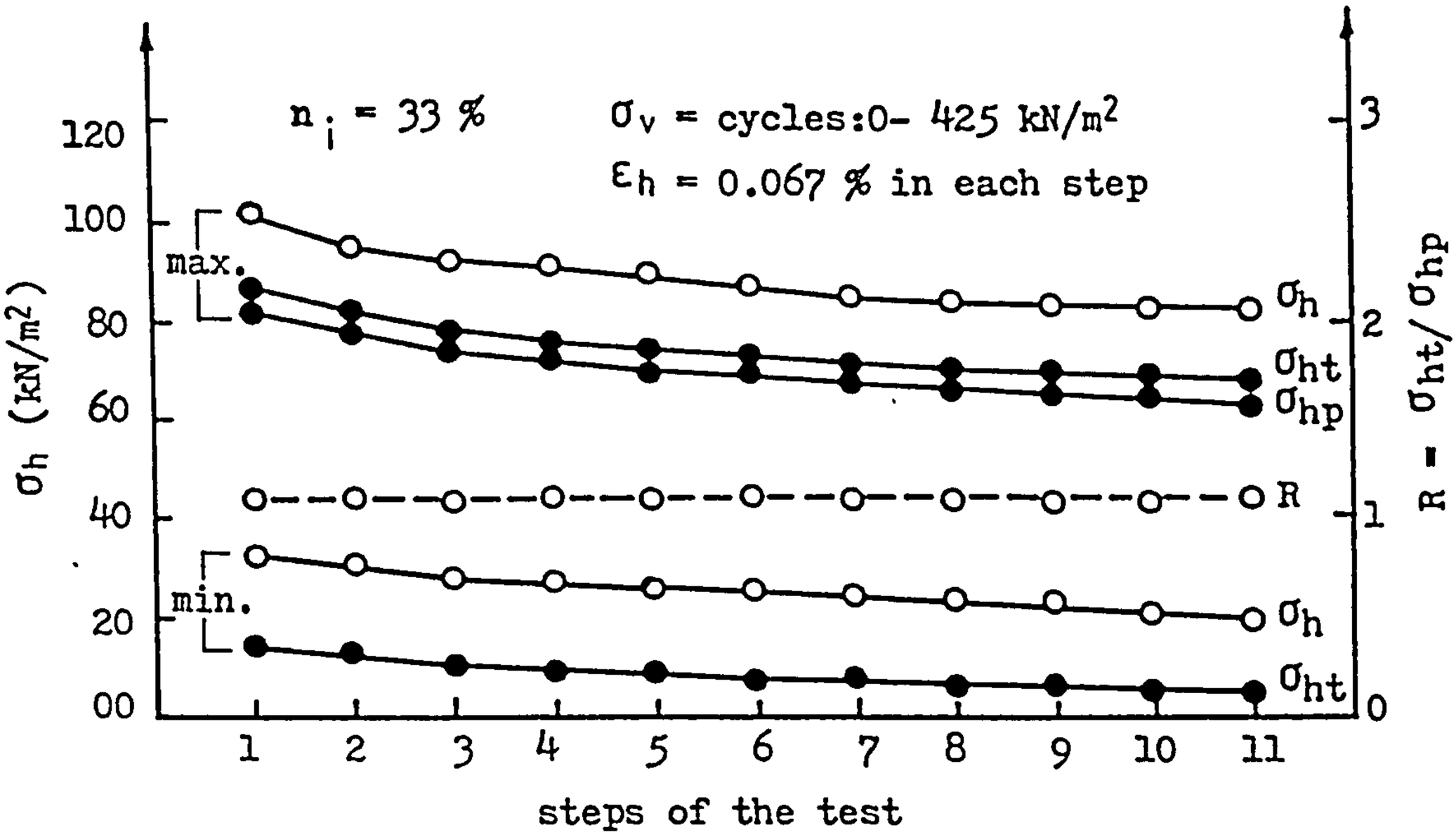

(a)

○ before application of 0.067 % lateral strain

● after application of 0.067 % lateral strain

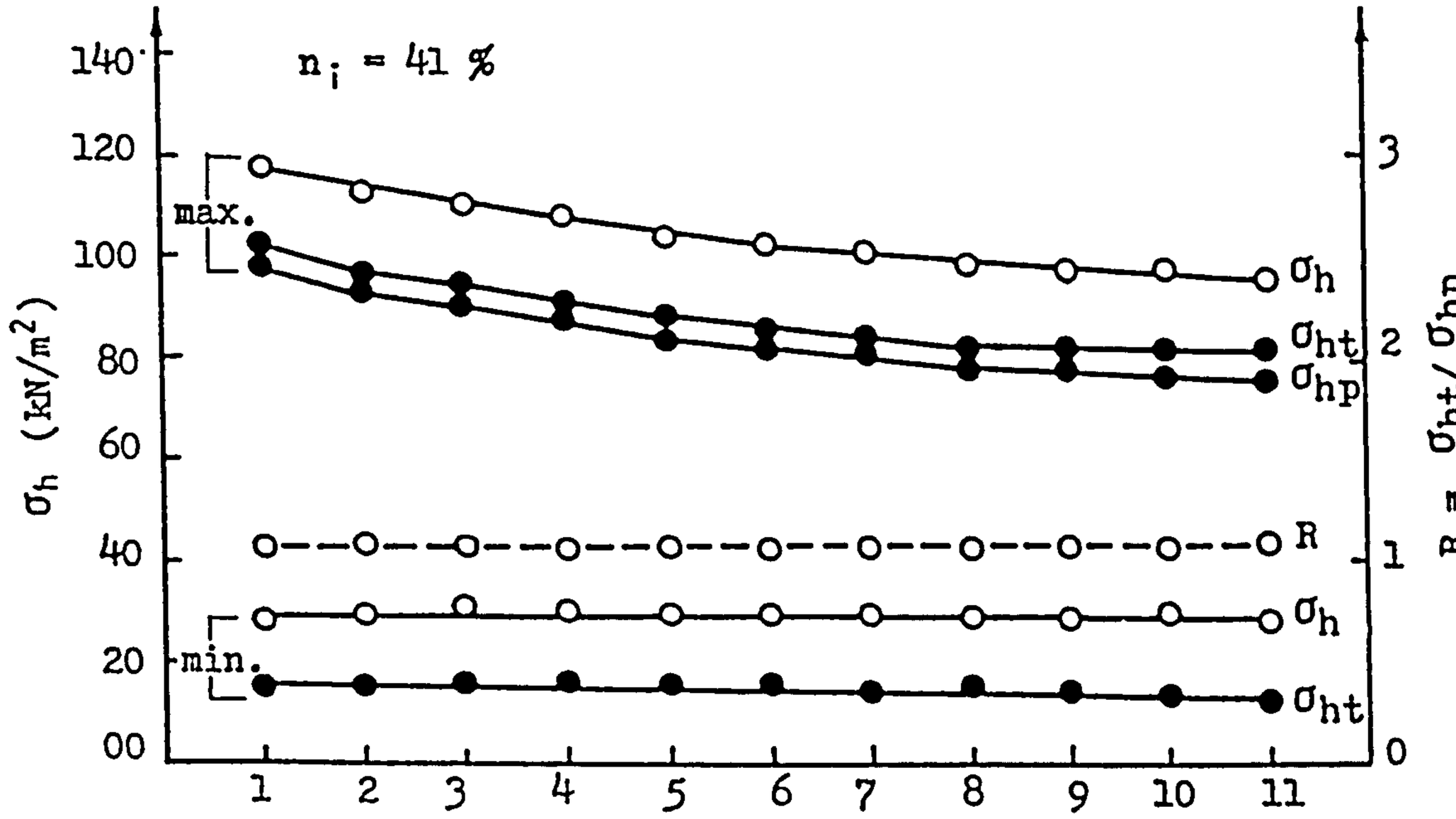

(b)

FIGURE 7.14 Lateral stress in each step of the cyclic triaxial test before (σ_h) and after (σ_{ht}) straining the sample compared with that in cyclic plane strain tests (σ_{hp}) for dense (a) and loose (b) samples.

both loose and dense samples. As σ_{h1} and σ_{h2} in these tests are quite close, their average values (σ_h) are used in this figure.

From this figure it can be seen that for both dense and loose specimens values of σ_h before straining the sample decreases as the test continues. This reduction, which is about 20% over the 12 steps of the test, may be related to the appreciable decrease in the porosity of the samples which occurs due to the application of 36 cycles of load in each step. The sudden drop which happens in the lateral stresses on the loading portion of the cycle due to the application of the 0.067% lateral strain increment is approximately constant in all steps. As a result the percentage decrease of the lateral stresses increases from 15% to about 17% for the dense and from 12% to 15% for the loose sample over the 12 steps of the test.

It was expected that an increase in the minimum values of σ_h before straining the sample would occur as the number of steps increases. This expectation is based on the cyclic confined tests which show that the minimum values of the lateral stresses increase as the number of cycles increases. But during the cyclic triaxial tests, as is clear from figure 7.14, these minimum values of σ_h for the loose sample were found to be constant in spite of a decrease in the porosity of the sample. This behaviour in the minimum values of the lateral stresses may be related to the insufficient number of cycles applied after straining the samples. Different trends of variations of the minimum values of the lateral stresses in dense and loose samples may be

due to the same reason that the number of cycles has a greater effect on loose sample than that on dense.

7.4.2.1 COMPARISON OF σ_h IN CYCLIC PLANE STRAIN AND CYCLIC TRIAXIAL TESTS

Variations of σ_h at the peak of the cycles (ie. maximum values) and the ratio of σ_{ht}/σ_{hp} with the number of test steps are shown if figure 7.14. It can be seen from the figure that σ_{ht} for both dense and loose samples are greater than σ_{hp} under the same testing condition. This means that under the same cycle of load and at the same lateral strain when the sample is tested in plane strain condition the lateral stress drops more than that in the triaxial condition. As discussed for the monotonic tests, this may be related to the lower freedom of the soil in the plane strain condition than triaxial condition. As a result greater frictional forces develop between the particles and this causes less stress to be transfered to the side compared with the triaxial condition. The ratio of σ_{ht}/σ_{hp} for both dense and loose samples is nearly constant and equal to 1.07.

CHAPTER EIGHT

CONCLUSIONS AND RECOMMENDATIONS FOR FURTHER WORK

8.1 INTRODUCTION

The stress-strain behaviour of granular soils under monotonic and cyclic loading in different constraint conditions was investigated in this research project. A simple cubic triaxial apparatus (SCTA), developed at Leeds University, was used in the study. The SCTA uses 150 mm cubical samples. A vertical principal stress is applied to the specimen and the two lateral principal stresses are measured. The resulting vertical strain is also measured and the two lateral strains can be controlled to provide the desired constraint conditions i.e. confined, plane strain or triaxial conditions.

The performance of the SCTA was checked and some areas of weakness were identified. These were studied and the necessary rectifications made. The SCTA was modified so that cyclic loading tests could be carried out as well as monotonic tests. A new computer controlled loading system using a pneumatic cylinder was constructed. Vertical stresses of upto 450 kN/m^2 can be applied to the samples by this system. Cyclic loads of various shapes, amplitude, frequency (to a maximum of 0.1 Hz) and number of cycles can be specified. A data acquisition system based on a programmable data logger unit linked to a micro-computer was

developed which reads the principal stresses and the vertical strains and stores the data on floppy discs for later analysis.

Samples of different porosities were prepared using the raining technique described by Kolbuszewski [55]. Three types of sand, namely fine (A), medium (B) and coarse (C) were used. Two main types of experiment were carried out. Monotonic loading tests similar to those performed by El-Gammel on the medium sand were carried out on the fine and coarse sands to extend the stress-strain information in this area. Cyclic loading tests were also performed on the medium sand. The results of both types of tests show a satisfactory degree of repeatability and consistency. A summary of the main findings and conclusions from the experiments in each area are given below.

8.2 MONOTONIC LOADING

When a cubical sand sample is subjected to an increased vertical stress (up to 375 kN/m^2), the following characteristics can be identified.

1- The particle size and the initial porosity of the sand have a significant effect on the vertical strain.
The vertical strain of the sample increases sharply as the initial porosity increases and also as the particle size decreases.

2- Under vertical stresses when the sample is strained laterally, the incremental vertical strain in the triaxial conditions is about 2.25 times greater than that in the plane strain conditions.

3- There is a small decrease in the incremental vertical strain as the vertical stress applied to the sample increases.

4- The volume change of the coarse and medium sands due to straining the sample in plane strain or triaxial tests are always positive (dilation) but the fine sand, except for the samples prepared at the densest conditions, has negative volume changes (compression). The critical porosity of this sand was found to be a function of the vertical stress and the constraint condition of the sample. From the plane strain tests the critical porosity was between 1% to 4% greater than that from the triaxial tests.

5- The Poisson's ratio of the sand was found to vary over a small range under different levels of the vertical stress, initial porosity and different constraint conditions.

6- The modulus of elasticity changes significantly as the stress-strain conditions of the sand change. For the ranges of particle size, vertical stress, and constraint conditions studied in this project, it was found to vary between 750 and 70000 kN/m^2.

7- The lateral stresses of sand in confined conditions were found to increase approximately linearly on increasing the vertical stress.

8- The particle size and the initial porosity of the sand have a considerable effect on the lateral stresses.

9- Decreasing the particle size and increasing the initial porosity of the sand both increase the lateral stresses.

10- Under a fixed vertical stress when the sample is strained laterally the lateral stresses decrease but the rate of decrease drops as the lateral strain increases.

11- At some value of the lateral strain the lateral stresses become nearly constant. This is when the shearing resistance of the sand is fully mobilized and the sand is said to achieve its active state.

12- The ratio of the lateral to vertical stress in confined conditions, which is called the coefficient of earth pressure at rest (Ko), decreases on increasing the vertical stress, particle size and density of the sand.

13- As the sample is laterally strained the ratio of lateral to vertical stress decreases but the rate of decrease falls as the lateral strain is increased. When sand achieves its active state the ratio becomes nearly constant. It is denoted by Ka the active pressure coefficient at this stage.

14- Values of Ka obtained from triaxial tests are greater than those obtained from the plane strain tests (from 5% for the fine sand up to 50% for the coarse sand).

15- Ka decreases on increasing the particle size and density of the sand. It increases on increasing the vertical stress.

16- Over ranges of particle size, vertical stress, initial porosity and constraint conditions tested in this project Ko

was found to vary between 0.20 and 0.50 and Ka between 0.04 and 0.39.

8.3 CYCLIC LOADING

When a cubical sand sample is subjected to a number of cyclic vertical loadings under different constraint conditions the following pattern of behaviour emerges.

1- As the vertical load, applied to the confined sample, cycles between constant minimum and maximum values, the vertical strain cycles as well but its maximum and minimum values continuously increase on increasing the number of load cycles.

2- The elastic strain per cycle , which is the recoverable part of the vertical strain, decreases in the first few cycles but finally becomes constant. Its ultimate value was found to be about 0.24% for the dense and 0.28% for the loose samples.

3- The plastic strain per cycle, which is the irrecoverable part of the vertical strain, continuously decreases as the number of cycles increases but the total plastic strain increases as the cycling continues. After the application of a series of load cycles the incremental plastic strain becomes almost negligible.

4- Both the elastic and plastic vertical strain per cycle increase as the porosity of the sample increases.

5- The frequency of the cyclic loads within the range tested (0.003 to 0.1 Hz) does not have a significant effect on the

vertical strain probably because the sand is dry.

6- The unloading percentage which is defined as below, as well as the amplitude of cyclic loads, has a great effect on the vertical strain.

$$\text{unloading percentage} = \frac{\sigma_{vmax.} - \sigma_{vmin.}}{\sigma_{vmax.}} \times 100$$

7- The higher this percentage the greater the elastic strain induced per cycle. In the cyclic loads with the same unloading percentage when the amplitude increases the incremental plastic strain increases as well.

8- The constrained secant modulus of the sand (D) during unloading is greater than that during loading for the first few cycles, but as the cycling continues they become close to each other. After several load cycles (50 for dense and 100 for loose samples) they become equal. At this stage the sand shows an elastic behaviour and the values of D can be related to the vertical stress by a linear equation. For the sand tested in this project (for $\sigma_v > 50$ kN/m^2) it was found:

$$D = 38 + 0.35\,\sigma_v \quad \text{(dense condition)}$$

$$D = 37.5 + 0.27\sigma_v \quad \text{(loose condition)}$$

where σv is in kN/m^2 and D in MN/m^2.

9- Therefore, the sand can be defined as a material which has a non-linear elasto-plastic behaviour on primary loading and has a non-linear elastic response when is subjected to several cycles of load under confined conditions.

10- If the initially confined sample after a series of

cyclic vertical loads is strained laterally, the incremental vertical strain due to straining the sample, in the case of triaxial conditions is greater (2.25 times) than that measured in the plane strain conditions. On further application of the vertical load, the vertical strain keeps increasing after the sudden jump due to straining the sample and the confined condition gradually dominates.

11- When a cyclic vertical load with constant amplitude and frequency is applied to a confined sample the lateral stresses cycle between some maximum and minimum values. On increasing the number of cycles, while maximum values of the lateral stresses decrease, their minimum values increase. The rate of decrease in the maxima and increase in the minima decreases as cycling continues. After the application of several load cycles they become almost constant. The maximum changes in the minimum and maximum values of the lateral stresses over a certain number of load cycles are associated with the initial porosity of the sample.

12- The frequency of the cyclic load over the range tested does not have a significant effect on the lateral stresses of dry samples.

13- Applying a certain increment of lateral strain to a confined sample which is under cyclic vertical load causes the maximum and minimum values of the lateral stresses to drop suddenly at the time of straining the sample. However, as the cycling continues they recover quickly and then behave as described for the confined condition.

14- In the plane strain tests, the maximum values of the lateral stress in the fixed direction increase by relatively small amounts compared to the other lateral stress. The minimum values of this stress drops but less than that occurring for the lateral stress in the direction of straining the sample.

8.4 RECOMMENDATIONS

As far as the stress-strain behaviour of granular soils is concerned there are some other areas of interest which can be studied using the apparatus used in this investigation. For some of them the SCTA would need to be modified and developed, and for the other it can be used directly. The points which are recommended for further investigations in this area are as follows.

1- Studying the effect of the particle size and shape on the cyclic behaviour of the sand.

2- Studying the uniformity and isotropy of the samples prepared in the laboratory, using the raining technique, in the lateral directions by rotating the axes of the principal stresses 90 degrees.

3- Doing a series of drained and undrained tests on saturated samples with pore pressure measurement and comparing the results with the dry tests results obtained from monotonic and cyclic loading conditions.

4- Performing cyclic tests with higher frequency and transient amplitude in order to study the effects of earthquake loadings on the stress-strain response of the sand.

5- Studying the stress-strain behaviour of the sand when it is subjected to the passive conditions by pushing

one or two moveable faces of the sample container towards the specimen (passive plane strain or triaxial tests).

6- Undertake a theoretical study of all experimental data obtained so far in order to find a mathematical model which covers the monotonic and cyclic stress-strain behaviour of granular soils more realistically.

REFERENCES

1. Pyke, R.M.(1975):" The behaviour of sands under cyclic loading"; 2nd Aust-New Zealand Conf.on Geomech. , Brishane, Australia.

2. Duncan, J.M. & Chang, C.Y.(1970):" Nonlinear analysis of stress and strain in soils ";J. soil mech. & found. div., ASCE, vol.96, No. SM5, Proc. paper 7513, pp. 1629-1653.

3. Griffith (1929): " The pressure under substructures"; Eng. & contracting, vol.68 , pp. 113-119.

4. Timoshenko, S. (1955) :" Strength of materials"; Third edition, McGraw-Hill Book Co., New York.

5. Wilson, G. & Sutton, J.L.E.(1948): " A contribution to the study of the elastic properties of sand "; Proc. 2nd Int. Conf. on soil Mech., Rotterdam , vol.1 pp. 197-202.

6. Jackobson, B.(1957): " Some fundamental properties of sand"; Proc. 4th Int. Conf., London, vol.1, pp. 167-171.

7. Janbu, N.(1963): " Soil compressability as determined by oedometer and triaxial tests"; Proc. Europaische Baugrundtagung (Wiesbaden).

8. Ohde, J.(1939): " Zur theorie der Druckverteilung in Baugrund"; Der Bauingenieur 20, Heft 33/34, p. 451.

9. Janbu, N. & Hjeldnes, E.I.(1965): " Principal stress ratios and their influence on the compressibility of soils"; Proc. 6th Int. Conf. on soil Mech.& Found. Eng., Montreal, vol.1, pp. 249-253.

10. Kondner, R.L. & Zelasko, S.(1963): " A hyperbolic stress-strain formulation for sands"; Proc. 2nd. pan American Conf. on soil Mech. & Found. Eng., Vol.1, Brazil, pp. 289-324.

11. Hansen, J.B.(1963): Discussion of " Hyperbolic stress -strain response: cohesive soils"; J. Soil Mech. & Found. Div., ASCE, Vol.89, No. SM4, Proc. paper 3578, pp. 241-242.

12. Ko, H.Y. & Scott, R.F.(1967): " Deformation of sand in shear"; J. Soil Mech. & Found. Div., ASCE, Vol. 93, No. SM5, Proc. paper 5470, pp. 283-310.

13. Holubec, I.(1968): " Elastic behaviour of cohesionless

soil"; J. Soil Mech. & Found. Div., Proc. ASCE, Vol.94, No. SM6. pp.1215-1231.

14. El-Sohby, M.A.(1969): " Elastic behaviour of sand"; J. Soil. Mech. & Found. Div., Proc. ASCE, Vol.95 , No. SM6, pp. 1393-1409.

15. Foppl (1897):" Vesuche uber die elastizitat des erdb-odens"; Zentrabblat der Bauverviltung.

16. Diamagio, F.L. & Sandler, I.(1971): " Material model for granular soils"; Proc. ASCE, Eng. Mech. Div. EM6.

17. Roscoe, K.H. & Burland, J.B.(1968): " On generalized stress-strain behaviour of wet clay"; Eng. Plasticity, J. Heyman., & F.A. Leckie., eds. Camridge University press, Cambridge, England.

18. Duncan, J.M. & Lade, P.V.(1973): " Cubical triaxial tests on cohesionless soil"; Proc. ASCE, Soil Mech. & Found. Div., Vol.99, No. SM10.

19. Burley, E., Harvey, R.C., and Daniel, A.W.T.(1975): " Stress-strain characteristics of sand"; Proc. , ASCE, Geot. Eng. Div. Vol.101, No. GT5.

20. Kii, L.G.(1978): " Stress-strain characteristics of cohesionless soil"; M.Phil. Thesis, Faculty of Eng., University of London.

21. Al-Hussaini, M.(1981): " Comparison of various methods for determining K_o"; Laboratory shear strength of soil, ASTM, STP 740, pp. 78-93.

22. El-Gammel, M.A.G.(1984): " Elastic stress and strain in cohesionless soils"; Ph.D. thesis, Civil Eng. dept., Leeds University.

23. Seed, H.B., Chan, C.K., & Monismith, C.L.(1955): "Effects of repeated loading on the strength and deformation of compacted clay"; Proc. HRB, Vol. 34, pp. 541-558.

24. Seed, H.B. & McNeil, R.L.(1956): "Soil deformation in normal compression and repeated loading tests"; Highway research road, Bull. 141, p.44.

25. Seed, H.B. and Chan, C.K.(1958): " Effect of stress-history and frequency of stress application on deformation of clay subgraded under repeated loading"; Proc. Highway Research Board, Vol.37 , pp. 555-575.

26. Converse, F.J.(1962): " Stress deformation relation for soft saturated silt under low frequency oscillating direct shear forces"; Special technical publication, No.305, ASTM, pp. 15-19.

27. Larew, H.G. & Leonards, G.A.(1962): " A strength criterion for repeated loads"; Proc. Highway Research Board, Bull. 41.

28. Taylor, P.W. & Menzies, B.K.(1963) " The damping characteristics of dynamically-stressed clay"; 4th Austr.-New Zealand Conf. on Soil Mech. & Found. Eng..

29. Astbury, N.P. & Moore, F.(1965): " Torsional hysteresis in plastic clay"; Material research and standards, ASTM, pp. 178-183.

30. Seed, H.B. & Lee, K.L.(1966): " Liquefaction of saturated sands during cyclic loading"; J. Soil Mech. & Found. Div., ASCE, Vol.92, No.SM6, pp.105-134.

31. Park, T.(1975): " Dynamic soil behaviour under cyclic loading conditions"; Ph.D. Thesis, University of Illinois.

32. Youd, T.L.(1967) " The engineering properties of cohesionless materials during vibration " ; Ph.D. Thesis, Iowa state, University of Science and Technology.

33. Timmerman, D.H. & Wu, T.H.(1969): " Behaviour of dry sand under cyclic loading"; J. Soil Mech. & Found. Div.,ASCE, Vol.95ii, No.SM4, pp.1097-1115.

34. Silver, M.L. & Seed, H.B.(1971): " Deformation characterestics of sand under cyclic loading";J.Soil Mech. & Found. Div., ASCE, Vol. 97, No.SM8, pp. 1081-1098.

35. Khosla, V.K.(1972):" Behaviour of dry Ottawa sand under cyclic loading"; Ph.D. Thesis, The Ohio State University.

36. Youd, T.L. & Craven, T.N.(1975): " Lateral stress in sands during cyclic loading"; J. Geot.Eng. Div. ASCE, Vol.101, No. GT2, pp.217-221.

37. Boussinesq,J. (1876):"Essai theorique sur 1' equilibre d'elastic des massifs pulvurents compare' a celui de massifs solids et sur la pousse des terres sans cohesion"; Memories couronnes et memorise des savants extranges publice's par 1' academie...de Belgique. Tome XL, Bruxelles.

38. Oh-Oka, H.(1976): " Drained and undrained stress-strain behaviour of sands subjected to cyclic shear stress under nearly plane-strain condition"; Soils & found., Vol.16, No.3, pp.19-31.

39. Ladd, R.S.(1977) " Specimen preparation and cyclic

stability of sands"; J. Geot. Eng. Div., ASCE, Vol. 103, No. GT6, pp.535-547.

40. Schappener, B.(1977): " Some aspects of the testing procedures for cyclic loading of sand samples"; Proc. of DMSR 77/Karlsruhe/5-16, Sept.77,Vol.2.

41. Banerjee, N.G.(1979): " Cyclic behaviour of dense coarse-grained materials in relation to the seismic stability of dams"; Ph.D. Thesis, University of California, Berkeley.

42. Ghaboussi, J. & Momen, H.(1979) " Modeling and analysis of cyclic behaviour of sands"; Int. Symp.on soil under cyclic & transient loading/ Swansea, 7-11 January 1980.

43. Sangrey, A.D., Castro, G., Polous, S.J., and France , J.W.(1978): " Cyclic loading of sands, silts, and clays"; Proc., ASCE, special Conf.,Earthquake Eng. & Soil Dynamic, Pasadena, pp.836-851.

44. Shaw, P.(1980): " Stress-strain relationship for granular materials under repeated loading"; Ph.D. Thesis, University of Nottingham.

45. Ting, C.S.(1981): " Elastic and plastic strain properties of sand"; J. Geot. Eng. Div., Proc.,ASCE, Vol. 108, No. GT5, pp. 787-793.

46. Drnvich, V.P. & Richart, F.E.(1970): " Dynamic prestraining of dry sand"; J. Soil Mech.& Found.Div. Proc., ASCE, Vol.96i, No.SM2, pp. 453-469.

47. Macky, T.A.(1982): " Behaviour of anisotropic clays subjected to cyclic loading"; Ph.D. Thesis,Case Western Reserve University.

48. Shen, C.K., Ker, C.C., Wang, Z., and Li, X.S.(1985):" Dynamic response of silt"; Proc. of 2nd. Int. Conf. on board the liner The Queen Elizabeth2 , New York to Southampton, June/July 1985.

49. Isenhower, W.M.(1978): " Torsional simple shear resonant column properties of San Francisco Bay-mud "; M.Sc. Thesis, University of Texas at Austin.

50. Kolbuszewski, J.J.(1961): " The preparation of sand samples for laboratory testing"; Proc. of the Midland soil Mech. & Found. Eng. Soc., Vol. 4.

51. Kolbuszewski, J.J.(1948): " An experimental study of the maximum and minimum porosities of sands " ; Proc. of the 2nd Int. Conf.on Soil Mech.& Found. Eng., Rotterdam, Netherland, pp.158-165.

52. Dantu, P.(1961): " Etude mechanique d'un milieu pulverulent forme' de sphere egales de compacite'

maxima"; Proc. 5th Int. Conf. Soil Mech. & found. Eng., Paris, Vol.1, pp.61-70.

53. Frohlich (1934):"Druckverteilung in Baugrunde";Vienna.

54. Boussinesq (1885): " Application des potentials a 1' etude de 1' equilibre et du mouvement des solides elastiques"; Paris.

55. Ko, H.Y. & Scott, R.F.(1967b): " Deformation of sand in hydrostatic compression" ; J. Soil Mech. and Found. Div. Proc. ASCE, Vol.93, No.SM3, pp.137-156.

56. Smith, I.M.(1971):"Plane plastic deformation of soil" ; Proc. Roscoe Memo. Symp., Cambridge.

57. Huang, Y.H.(1968): " Stresses and displacements in non-linear soil media"; J. Soil Mech. & Found. Div., ASCE, Vol.94, No. SM1.

58. Coon, M.D. & Evans, R.J.(1971): " Recoverable deformation of cohesionless soils"; J. Soil Mech. and Found. Div., ASCE, Vol.97, No. SM2.

59. Drucker, C.D., Prager, W., and Greenberg, H.J.(1952): " Extend limit design theorems for continuous media"; Quart. Applied Math. Vol.9, No.4.

60. Drucker, D.C., Gibson, R.E., and Henkel, D.J.(1957):" Soil mechanics and work-hardening theories of plasticity"; Trans., ASCE, Vol.122, pp.338-348.

61. Poorooshasb, H.B., Holubec, I., and Sherbourne, A.N.(1966): " Yielding and flow of sand in triaxial compression"; Part 1, Canadian Geot. J., Vol.3, No. 4.

62. Barden, L. & Khayatt, A.J.(1966): "Incremental strain rate ratios and strength of sand in the triaxial test"; Geot., Vol.16, No.4.

63. Daniel, A.W.T.(1953): " A study of the stress-strain characteristics of granular materials " ; Ph.D. Thesis, University of London.

64. Shackel, B.(1973) " Repeated loading of soils"; J. of Aust. Road Res., Vol.5, No.1.

65. Pyke, R.M.(1973): " Settlement and liquefaction of sands under multi directional loading"; Ph.D.Thesis, University of California, Berkeley.

66. Youd, T.L.(1972): " Compaction of sands by repeated shear straining"; Proc. ASCE, Vol.98, No.SM7.

67. Atkinson, G.M., Finn, W.D.L., & Charlwood, R.G.(1984) : " Simple computation of liquefaction probabi-

lity for seismic hazard applications";Earthquake Eng.,Research Institute,Berkeley,California.

68. Finn, W.D. Liam & Atkinson, G.M.(1985): " Probability of seismically induced liquefaction in British sector of North sea";Earthquakes and Earthquake Eng. in Britain,Thomas Telford Ltd.,London, pp. 285-297.

69. Desai, C.S.(1971): " Non-linear analysis using spline functions"; Proc. ASCE, Soil Mech. & Found. Div , Vol. 97, No. SM10.

70. Breth, H., Schuster, E. and Pise, P.(1973): " Axial stress-strain characteristics of sand"; Proc., ASCE, Soil Mech. & Found. Div., Vol.99, No.SM8.

71. Hill, R.(1950): " The mathematical theory of plasticity"; Oxford University Press.

72. Rowe, P.W.(1962):" The stress-dilatancy relation for static equilibrium of an assembly of particles in contact";Proc. Roy. Soc.,A.269, pp.500-527.

73. Khosla, V.K., & Tien, H.Wu. (1976): " Stress-strain behaviour of sand"; Proc. ASCE, Geot. Eng.Div. , Vol.102, No. GT4.

74. Vesica, A.S. and Clough, G.W.(1968): " Behaviour of granular material under high stresses"; Proc. Am. Soc. civil Engrs.94, No.SM3, pp.661-688.

75. Schofield, A.N. & Worth, C.P.(1968): " Critical State Soil Mechanics"; Mc Graw_Hill (London).

76. Atkinson, J.H. & Bransby, P.L.(1978): " The mechanics of soil"; Mc Graw-Hill (London).

77. Kirkpatrick, W.M.(1957): " The condition of failure for sands"; Proc. 4th Int. Conf. Soil Mech.and Found. Eng., Vol.1.

78. Vermeer, P.A.(1978) : " A double hardening model for sand"; Geotechnique, 28.

79. Naylor, D.J.(1978): " Stress-strain laws for soil";In developments in soil mechanics.(Ed.Scott, C.R.) Applied Science Publ. (London).

80. Scott, C.R.(1980): " An introduction to soil mechanics and foundations"; 3rd Ed. Applied Science Publ.(London).

81. Wroth, C.P. & Bassett, R.H.(1965): " A stress-strain relationship for the shearing behaviour of sand "; Geotechnique, Vol.15, No.1.

82. Roscoe, K.H., Schofield, A.N. & Thurairajah, A.(1963)

: " Yielding of clays in states wetter than critical"; Geotechnique, Vol.13, No.3.

83. Barden, L. & Khayatt, A.J.(1968): " Incremental stress-strain relations for sand"; Research Report No.5, Univ. of Manchester, Dept. of civil Eng..

84. Horne, M.R.(1965): " The behaviour of an assembly of rotund rigid cohesionless particles";Part I and II, Proc. Roy.Soc. A.,Vol.286, pp.62-97.

85. Bardet, J.P.(1985): " Application of bounding surface plasticity to cyclic sand behaviour"; Proc. of the 2nd Int. Conf.on board the liner, the Queen Elizabet II, New York to Southampton, June/July 1985,Session II,pp.2-3 to 2-16.

86. Lambe, T.W. and Whitman, R.V.(1969): " Soil mechanics"; Series in soil Eng., John Wiley and sons, New York.

87. Bjerrum, L. & Landva, A.(1966): "Direct simple shear tests on Norwegian quick clay"; Geotechnique , Vol.16, No.1, pp.1-20.

88. Broms, B.B. & Gásbarian, A.O.(1965):" Effects of the rotation of the principal stress axes and the intermediate principal stress on the shear strength"; Proc. 6th Int. Conf. soil Mech.& Found. Eng., Montreal, Vol.I, pp.179-183.

89. Roscoe, K.H.(1953): " An apparatus for the application of simple shear to soil samples"; Ph.D. Thesis, Cambridge University.

90. Arthur, J.R.F.,etal.(1981): " Stress path tests with controlled rotation of principal stress directions"; Lab. shear strength of soil, ASTM, STP , 740, pp.516-540.

91. Rodriguez del Camino, J.I. & Dunstan, T.(1981):" The directional shearing cell"; Proc. of Int. Conf. on soil Mech. and Found. Eng.,10th, Stockholm, pp. 756-770.

92. Henkel, D.J. & Bishop, A.W.(1957): " The measurement of soil properties in the triaxial test";First Ed., William Clowes and sons, Ltd., London.

93. Reads, D.W. (1972): " Stress-strain characteristics of sand under three dimensional loading"; Ph.D. Thesis, Imperial College, Univ. of London.

94. Kjellman, W.(1936): " Report on apparatus for the consumate investigation of the mechanical properties of soils"; Proc. 1st. Int. Conf. of soil Mech. & Found. Eng., Vol.2 , pp.16-20.

95. Buisson, M.(1948): " Tassement 'evalues' d'apre's les essais oedometrique, comparison des hypothe'ses-apparil triaxial"; Travaux, No.164, Juin, pp. 319-320.

96. Mesdary, M.S.(1969): " The shearing behaviour of the granular material under a general stress system "; Ph.D. Thesis, Glasgow University.

97. Green, G.E.(1969): " Strength and compressability of granular materials under generalized strain conditions"; Ph.D.Thesis, University of London (2 Vols.).

98. Dyson, S.(1970): " The strength and deformation behaviour of a cohesionless soil under generalized stress conditions"; Ph.D. Thesis, University of Aston in Birmingham.

99. Rawat, P.C.(1976): " Shear behaviour of cohesionless materials under generalized conditions of stress and strain"; Ph.D. Thesis, Indian Institute of Technology, Delhi.

100. Hambly, E.C.(1969): " A new true triaxial apparatus" ; Geotechnique, Vol.19, No.2 , pp.307-309.

101. Pearce, J.A.(1971): " A new true triaxial apparatus" ; Proc. Roscoe Memo. Symp., Cambridge, pp. 303-339.

102. Gudehus, G.(1971): Discussion to session 3," The meaning and measurement of basic soil parameters" ; Proc. Roscoe Memo. Symp., Cambridge, pp. 373-375.

103. Wood, D.M.(1975): " Explorations of principal stress space with Kaolin in a true triaxial apparatus" ; Geotechnique, Vol.25, No.4, pp. 783-797.

104. Fardis, E. & Fridman, S.(1977): " Stress-strain behaviour of sand under generalized stress conditions"; Proc. of the Int. Conf.on soil Mech. and Found. Eng., 9th., Tokyo, Japan, pp.57-64.

105. Sture, S. & Desai, C.S.(1979): " Fluid cushion truly triaxial on multiaxial testing device"; Geotechnical Testing Journal, Vol.2, No.1, pp.20-33.

106. Bell, J.M.(1965): " Stress-strain characteristics of cohesionless granular materials subjected to statically applied homogenous loads in an open system"; Ph.D. Thesis, Califonia Inst. of Tech. , Pasadena, California.

107. Ko, H.Y.(1966): " Static stress-deformation characteristics of sand";Ph.D.Thesis, California Inst. of Tech., Pasadena, California.

108. Ko, H.Y. & Scott, R.F.(1967): " A new soil testing apparatus"; Geotechnique, Vol.17, No.1, pp. 40-57.

109. Lomize, G.M. & Kruzhanovsky, A.L.(1967): " On the strength of sand";Proc. Geot. Conf. Oslo., Vol.1, pp. 215-219.

110. Lomize, G.M., Kruzhanovsky, A.L., Voronstov, E.I., & Goldin, A.L.(1969): " Study on deformation and strength of soils under three dimensional state of stresses";Proc. 7th. Int. Conf.on soil Mech. and Found. Eng., Vol.1, pp.257-265.

111. Arthur, J.R.F. & Menzies, B.K.(1972): " Inherent anisotropy in a sand"; Geotechnique, Vol.22, No.1 pp. 115-128.

112. Menzies, B.K.(1970): " Stress-strain anisotropy in a sand"; Ph.D. Thesis, London University.

113. Lewin, P.I.(1971): " A new apparatus for testing a one dimensionally consolidated clay cube with independent stress control";Proc. Roscoe, Memo. Symp., Cambridge, pp. 324-329.

114. Ko, H.Y. & Masson, R.M.(1976): " Non-linear characterization and analysis of sand"; 2nd. Int. Conf on numerical methods in geomechanics, Vol.1,pp 294-305.

115. Brends, B.E.(1977): " Development of multiaxial testing cell for cohesive soils"; M.Sc. Thesis, University of Colorado, Boulder, Colorado.

116. Yamada, Y. & Ishihara, K.(1979): " Anisotropic deformation characteristics of sand under three dimensional stress conditions"; Japaneas Soc. of soil Mech. and Found. Eng., Soils & Foundation, Vol.19, No.2, pp.79-94.

117. Brends, B.E. & Ko, H.Y.(1980): " Cubical multiaxial cell for testing cohesive soils";J.of the Geot. Eng. Div., ASCE, Vol. 106, No.GT1, pp.106-111.

118. Green, G.E.(1971): Correspondence on " A new soil testing device", by H.Y. Ko & R.F. Scott, Geotechnique, Vol.17, No.3, p.295.

119. Arthur, J.R.F. & Menzies, B.K.(1968): Correspondence on " A new soil testing apparatus";by H.Y. Ko & R.F. Scott, Geotechnique, Vol.18, No.2, pp.271-272.

120. Bell, J.M.(1968): Correspondence on " A new soil testing apparatus"; by H.Y. Ko & R.F. Scott, Geotechnique, Vol.18, No.2, pp.267-271.

121. Shibata, T. & Karube, D.(1965): " Influence of the vibration of the intermediate principal stress on the mechanical properties of normally consolidated clays"; Proc. 6th. Int. Conf. on soil Mech. and Found. Eng., Vol.1, pp.359-363.

122. Lenoe, E.M.(1966): " Deformation and failure of granular media under three dimensional stresses"; Experimental mechanics, Feb.66, pp.99-104.

123. Young, R.M. & Mckyes, E.(1971): " Yield and failure of clay under triaxial stresses"; J. of soil Mech. and Found. Div., ASCE, Vol.97, SM1, pp.159-176.

124. Sutherland, H.B. and Mesdary, M.S.(1969): " The influence of the intermediate principal stress on the strength of sand"; Proc. 7th. Int. Conf. in soil Mech. & Found. Eng.,Vol.1, pp. 391-399.

125. Ramamurthy, T.(1970): " A universal triaxial apparatus"; J. of Indian Nat. Soc. SMFE, Vol.9, No.3, pp. 251-269.

126. Barden, L. & Procter, D.C.(1971): " The drained strength of granular material"; Canadian Geot. J., Vol.8, No.3, pp. 372-383.

127. Ramamurthy, T. & Rawat, P.C.(1973): " Shear strength of sand under general stress system"; Proc. 8th Int. Conf. SMFE, Vol.1, pp. 339-342.

128. Lade, P.V. & Duncan, J.M.(1973): " Cubical triaxial tests on a cohesionless soil "; J. SMFD, ASCE, Vol.99, SM10, pp. 793-812.

129. Green, G.E. & Reads, D.W.(1975): " Boundary conditions anisotropy and sample shape effects on the stress-strain behaviour of sand in triaxial compression and plane strain"; Geotechnique, Vol. 25, No.2, pp. 333-356.

130. Somashekar, B.V.(1977): " Studies on stress deformation and strength of soils under general stress state"; Ph.D. Thesis, Indian Inst. of Science , Bangalor.

131. Rawat, P.C. & Ramamurthy, T.(1978): " Shear behaviour of sand under generalized conditions of stress and strain "; Indian Geotechnical Journal, Vol. III, No.4.

132. Parry,G.H.R.(1972):"Stress-strain behaviour of soils" ; Proc. of the Roscoe memorial symposium, Cambridge University, 29-31 March 1971.

133. Seaman, L. Bycroft, G.N.& Kriebel, H.W.(196):"Stress

propagation in soils-part III"; Report by Standford Institute to defence atomic support agency, DASA-1266-3.

134. B.S. 1377(1975): "Methods of testing soils fo civil engineering purposes " ;British standard Inst., British Standard 1377.

135. Kolbuszewski, J.& Frederick, M.R.(1963): "The significance of particle shape and size on the mechanical behaviour of granular materials"; Europ. Conf. on soil mech. & found. eng., section 4, paper 9, pp. 253-263.

136. Bjerrum, L., Kringstad, S.& Kummeneje, O.(1961);"The shear strength of fine sand"; Proc. 5th Inter. Conf on soil mech. & found. eng.(London), vol 1 , pp. 29-37.

137. Kirk, D. P. (1967) :" The earth pressure in granular soils";Ph.D. thesis, civil engineering department, Leeds University.

138. Hendron, A.J.(1963):"Behaviour of sand in one dimensional compression";Ph.D. thesis, university of Illinoise, 285 pp.

139. Brooker, E.W. & Ireland, H.O.(1965): "Earth pressure at rest related to stress history"; Cana. Geot. journal, vol 2, part1, p 1-15.

140. Lee, K.L.(1970):"Comparison of plane strain and triaxial tests on sand"; J. of soil mech. & found. eng. Div.,vol 96, No. SM3, May 1970.

141. Terzaghi, K. (1934): " Large retaining wall tests "; E.N.R., 1934.

142. Jaky, J.(1944):"The coefficient of earth pressure at rest"; J. Soc. of Hungarian architects and engineers, Budapest, Hungary, pp. 355-358.

143. Reimbert,M.L.& Reimbert,A.M.(1974):"Retaining walls, anchorage and sheet piling, theory and practice" ; vol 1, 1st edition, Trans.Tech. publications, Claustbal, Germany.

145. Caquot, A. & Kerisel, J.(1966):" Tables for calculation of passive pressure, active pressure, and bearing capacity of foundations";Gauther-Villas , Paris.

146. Rankine, W.J.M. (1857): " Theory on the stability of loose earth, based on the ellipse of stress " ; Phil. Trans. Royal Soc., vol 147.

147. Ohde, J.(1938) :" Zur theories des erddruckers unter besonder berucksichtigung der erddruck venteil-

ung"; Die Bautechnik, vol 16.

148. Coulomb,(1773):"Essai sur une application des regles de maximis et minimis a quelques problems des statique, relatifs a l'architecture"; In mathematical memories presented to the academic royal des sciences, vol 7.

149. Rowe, P.W.(1954):" A stress-strain theory for cohesionless soils, with application to earth pressure at rest and moving walls " ; Geotechnique, vol 4.

150. Janbu, N.(1957):"earth pressure and bearing capacity calculations by generalized procedure of slices" ; Proc. 4th Inter. conf. soil mech., vol II.